UNIVERSIDAD NACIONAL AUTONÓMA DE MÉXICO
DOCTORADO EN CIENCIAS BIOMÉDICAS
INSTITUTO DE ECOLOGÍA

MODELO DINÁMICO DE LA RED GENÉTICA DEL NICHO DE CÉLULAS MADRE DE LA RAÍZ DE *Arabidopsis thaliana*

TESIS
QUE PARA OPTAR POR EL GRADO DE:
DOCTOR EN CIENCIAS

PRESENTA:
EUGENIO MARTÍN AZPEITIA ESPINOSA

DIRECTOR DE TESIS
DRA. MARÍA ELENA ALVAREZ-BUYLLA ROCES
INSTITUTO DE ECOLOGÍA
COMITÉ TUTOR
DRA. ADRIANA GARAY ARROYO
INSTITUTO DE ECOLOGÍA
DR. LUIS ANTONIO MENDOZA SIERRE
INSTITUTO DE INVESTIGACIONES BIOMÉDICAS

MÉXICO, D.F. NOVIEMBRE DE 2013

A mi familia (Jimena, Joni y mi Amá)

Agradecimientos

A mi familia (Jimena, Joni y mi amá), la cual me ha apoyado incondicionalmente a lo largo de todo el doctorado y en todos los aspectos de mi vida. Su cariño ha sido fundamental en mi vida, he aprendido constantemente a su lado y son un pilar en mi día a día. A mi tía Locha que también ha estado a mi lado a lo largo de estos años y todos mis tíos, primos y sobrinos. A mi papá, con quien me hubiera gustado poder compartir esta experiencia.

A mi Urs que me conoció cuando comenzaba el doctorado y desde entonces me ha acompañado y apoyado dentro y fuera del laboratorio. Creo que hemos ido creciendo juntos en muchos aspectos y que gracias a ella he podido llegar a donde estoy ahora.

A mis amigos Meming, Dani, Fer, Mariana rana, Pili, Chac, Diez, Lynna, Marianiux, Chac y Ana con quienes he compartido muchas cosas a lo largo de muchos años bajo muchas circunstancias. Tal vez casi nadie me conozca como ellos, quienes a pesar de mis constantes salidas, siempre me han recibido con una sonrisa cuando regreso.

A mis amigos y compañeros del C3, Eli, Moni, Mariana E, Liber, Checo, Emilio, Vale, Marianiux. Junto con ellos discutí y aprendí un sin fin de cosas, compartí cursos y congresos. Igualmente a los demás compañeros del labo, Karl, Pao, Rigo, Alma, David, José Dávila, José Díaz, Aurora, Andréa, Jerry. A las investigadoras del laboratorio, Adriana, Bere, Maripaz y Elena. A Dianita y Kahorik, que nos apoyan en todo siempre. A todos los asistentes al seminario de biología teórica del C3, donde siempre hubo una gran apertura a la discusión interdisciplinaria. A los del labo que compartimos, Chio (Dra. Cora), la Dra. Falcón, Carla, Yis, Mario, Osiris. A toda la gente de Francia que me apoyo durante la estancia, en especial a Christophe Godin.

A mi asesora, Elena quien me apoyo dándome libertad para desarrollarme y desarrollar el proyecto en todo momento de todas las formas posibles y aun lo sigue haciendo. A mis tutores Luis y Adriana, quienes retroalimentaron la investigación desde un punto de vista biológico y computacional. A mis sinodales de la tesis Gladys, Pedro, Carlos, Mariana y Elena a quienes agradezco todos los comentarios hechos a este escrito.

A la gente con la que compartí proyectos, David Rosenblueth, Pablo Padilla, Carlos Villarreal, Iliusi Vega, Rafa Barrio, Roberto, José, Nathan, Alfredo, Stalin, Yuriria, Roberto Romero, Marco Noguez, Vale, Eli, Moni, José Dávila, Julián Argil y espero no olvidar a nadie más

A mis grandes amigos, que aunque tal vez ya vea poco a algunos de ellos, siguen siendo parte importante de mi vida, como Mariana rana, Memelas, Dani, Fer, Diez, Lynna, Pili, Lai, Urs, Toño, Maria, Phil (Oscar), Abraham, Malacara, Karlita, Eleonora, Germán, Erika, Robert, Daniela, Carlitos y espero no olvidar a ninguno más.

Son tantas las personas que quiero agradecer que espero no haber olvidado a alguno y si lo he hecho le pido una disculpa.

Gracias a todos los que han compartido de alguna forma este proyecto conmigo.

Índice

1. Resumen

Arabidopsis thaliana es uno de los organismos modelo para el estudio de la genética molecular de multicelulares con un genoma pequeño totalmente secuenciado. La raíz de *A. thaliana* presenta varias características que la hacen especialmente útil para estudios celulares y experimentales. Es un órgano transparente con pocos tipos celulares y una organización celular bastante simple. En particular la anatomía, organización y mecanismos involucrados en el desarrollo y mantenimiento del nicho de células troncales de raíz han sido ampliamente estudiado en el último par de décadas. Esto ha permitido describir los principales mecanismos involucrados.

A pesar de los grandes avances experimentales, la información había permanecido fragmentada, imposibilitando una explicación integral y sistémica de los procesos involucrados en el desarrollo y mantenimiento del nicho. Las aproximaciones matemático-computacionales han demostrado ser excelentes para integrar y analizar los mecanismos moleculares a diferentes niveles. En particular, las redes genéticas son una herramienta útil para integrar componentes genéticos y no genéticos en el estudio de procesos de diferenciación celular y morfogénesis. Las redes pueden usarse para llevar a cabo análisis estructurales y dinámicos, y con ellas se puede establecer la suficiencia de los componentes y sus interacciones para explicar los comportamientos observados experimentalmente.

En este proyecto, hice uso de herramientas computacionales, especialmente del formalismo de redes dinámicas, para estudiar los procesos involucrados en el establecimiento y mantenimiento de los patrones celulares en el nicho de células troncales de la raíz de *A. thaliana*. Con el uso de estas herramientas integramos la información experimental disponible y brindamos una explicación sistémica de los procesos de diferenciación celular y de la emergencia del patrón espacial de los distintos tipos de células madre dentro del nicho. Los modelos propuestos en esta tesis fueron validados con datos experimentales para los mutantes disponibles. A su vez, generamos predicciones e hipótesis de información faltante, así como también detectamos información o interpretaciones erróneas de los datos moleculares. Además, con el formalismo de redes generamos análisis de las

propiedades genéricas de las redes dinámicas y propusimos un conjunto de procedimientos para detectar de forma sistemática posible información faltante en una red genética dada. El proyecto ha dejado un modelo a partir del cual se han empezado a contestar una gran cantidad de preguntas, relacionadas con la integración de fuerzas físicas, gradientes químicos y dinámicas celulares acopladas a la dinámica de la red genética, para explorar los procesos dinámicos que subyacen tras el patrón del nicho de células troncales de raíz..

1. Abstract

Arabidopsis thaliana is one of the most important model organisms with a completely sequenced genome. Its root is especially useful for experimental research because it is a transparent organ with only a few cell types and a simple cellular organization. In last few decades, the anatomy, cellular organization and the molecular mechanisms involved in its development and maintenance have been widely studied and described.

Anyhow, part of this information has remained fragmented, preventing a systemic and an integral explanation of the processes involved in its maintenance and development. Computational and mathematical models, especially gene regulatory networks, have proved to be excellent tools to integrate and analyze molecular mechanisms involved in morphogenetic and cellular differentiation processes. Networks can be used to make structural and dynamical analyses, and to study the sufficiency of experimental data to explain experimentally observed behaviors.

In this project, I used computational and mathematical tools, including gene regulatory networks, to study the molecular mechanisms involved in the maintenance and development of the *A. thaliana* root stem cell niche. With these tools we integrate the available information to give a systemic explanation of the behaviors observed in the niche, like the mutant phenotypes. We also generate predictions about putative missing and wrong experimental information. Finally, we the project generated new tools for the analyses of biomolecular networks.

2.- Introducción general

2.1.- El desarrollo y el desarrollo de raíz

La biología del desarrollo se ha encargado de estudiar los procesos por medio de los cuales los organismos pasan de una célula fecundada, y un cúmulo de células relativamente homogéneas, a un organismo adulto. De acuerdo con Scott G. Gilbert (2000), la biología del desarrollo tiene dos grandes preguntas: ¿cómo es que un huevo fertilizado da origen a un organismo adulto? y ¿cómo es que un organismo adulto produce otro organismo?. Ambos procesos implican procesos de diferenciación celular y morfogénesis. Los estudios sobre estos temas comenzaron hace siglos, pues al menos existen registro de ello desde la época de Aristóteles, quien ya se preguntaba si los organismos se encuentran preformados desde un inicio o si las diferentes estructuras que se observan se forman poco a poco durante el ciclo de vida de los organismos (Van Speybroeck et al., 2002).

Actualmente la biología del desarrollo se ha dividido en varias subdisciplinas que estudian como es que las células se diferencian en distintos tipos celulares, cómo es que estos tipos celulares se organizan para generar los distintos órganos y tejidos de un organismo, cómo es que un organismo crece y como sabe cuando debe dejar de crecer, cómo transmite las "instrucciones" para que un nuevo organismo se desarrolle, cómo es que estos procesos del desarrollo han ido evolucionando y cómo responden y modifican el ambiente (Gilbert 2000). Sin embargo, aún no hay una respuesta completa a estas preguntas, por lo que grandes discusiones se dieron, se dan y probablemente se seguirán dando sobre estos temas (e.g., Purnell 2013).

En un inicio, los estudios de la biología del desarrollo se hacían a escalas macroscópicas (Van Speybroeck et al., 2002). Sin embargo, con el avance tecnológico ha sido posible llegar a analizar los mecanismos moleculares involucrados en el desarrollo (Weaver y Hogan 2001). Aun más, hoy en día sabemos que en el desarrollo se encuentran involucrados no sólo los procesos moleculares, sino que también son importantes los procesos a nivel celular (Newman y Bath 2009), las fuerzas físicas (Mirabet et al., 2011; Heisenberg y Bellaïche 2013; Routier-Kierzkowska y Smith 2013) e inclusive las condiciones

ambientales (Müller 2007; Benitez et al., 2013), todos los cuales interactúan entre sí (Lander 2011; Jaeger et al., 2012). Aunque actualmente se ha podido conocer a mucho mayor detalle estos procesos, generando una mejor comprensión de ellos, también ha quedado al descubierto su complejidad.

El desarrollo en plantas no es la excepción a esto y los estudios del desarrollo de plantas han dejado ver con claridad la gran complejidad de los procesos de desarrollo en los vegetales también (Meyerowitz 1997; Traas y Hamant 2009; Azpeitia y Alvarez-Buylla 2012). En las plantas el desarrollo se da a lo largo de todo su ciclo de vida debido a la presencia de meristemos activos a partir de los cuales se producen nuevos órganos de forma continua. Las plantas cuentan con dos meristemos principales, el meristemo de raíz y el del vástago aéreo (Sablowski 2011).

Arabidopsis thaliana ha sido el modelo en estudios de genética molecular más importante en plantas, por presentar ciclo de vida corto y un genoma compacto y bien caracterizado, lo que ha llevado a tener una gran cantidad de información sobre ella y la biología de las plantas en general (Meyerowitz 2001). En *A. thaliana*, al igual que en la mayoría de las plantas, el meristemo o los meristemos aéreos producen todos los órganos que se encuentran en la parte aérea de las plantas, mientras que el meristemo de raíz se encarga del desarrollo de toda la raíz.

La raíz es un órgano simple y transparente, el cual está dividido de manera longitudinal en zona de proliferación, zona de elongación, zona de diferenciación y nicho de células troncales (Perilli et al., 2012). La zona de proliferación se distingue por tener una alta tasa de división celular y una baja tasa de elongación, la zona de elongación por no tener división celular y una alta tasa de elongación y la zona de diferenciación por ser la zona donde las células se diferencían a su destino final (Benfey y Scheres 2000).

Todas las zonas están compuestas por los siguientes tipos celulares en el eje radial de afuera hacia el centro de la raíz: Epidermis, cortex, endodermis, periciclo y haz vascular, y hacia la punta de la raíz se localiza la columnela y cubriéndo todos los tejidos a partir de este órgano apical y hasta una porción de la zona meristemática, se encuentra la cofia lateral. Las hileras de cada de uno de los tipos de células

pueden rastrearse a células iniciales en el nicho de células troncales. El nicho se localiza en la punta de la raíz y está compuesto por 4 diferentes tipos de células iniciales (i.e., iniciales de cortex-endodermis, iniciales de cofia lateral-epidermis, iniciales de columnela e iniciales de tejido vascular) (Perilli et al., 2012, Scheres y Benfey 2000). Las células iniciales rodean al centro quiescente, el cual es un pequeño grupo de células que por medio de señales de corto alcance, mantiene indiferenciadas a las células iniciales (van den Berg et al., 1995 y 1997).

Hay varios procesos moleculares implicados en el desarrollo de raíz, pero tres de estos han mostrado ser especialmente importantes. Estos mecanismos son:

1) Los factores de transcripción de la familia GRAS *SHORTROOT* (*SHR*) y *SCARECROW* (*SCR*), así como algunos de sus genes blanco y genes que interactúan con ellos (Sabatini et al., 2003; Levesque et al., 2006).
2) Los genes *PLETHORA* (*PLT*), de la familia AP2/EREBP de factores de transcripción. Los genes *PLT* regulan y son regulados por las auxinas, las cuales son hormonas vegetales fundamentales para el desarrollo de las plantas (Aida et al., 2004; Galinha et al., 2007).
3) El péptidos móvil CLE40 y las proteínas que lo regulan, como ACR4 y CLV1 (Stahl et al., 2009 y 2013).

Así como se mencionó, estos mecanismos presentan comportamientos complejos, en gran medida debidos a la no linearidad de sus interacciones y a la interconectividad de los elementos. A continuación presentamos una copia del artículo Azpeitia y Alvarez-Buylla (2012), donde revisamos con mayor detalle los mecanismos involucrados en el desarrollo y mantenimiento del nicho de raíz, así como varios de los comportamientos complejos que presentan, como lo son su capacidad de auto organización, modularidad y robustez, entre varios otros. Algunos detalles mucho más finos de los procesos moleculares involucrados en el desarrollo y mantenimiento, no sólo del nicho, sino de la raíz en general, se pueden encontrar en Garay-Arroyo y colaboradores (2012), publicación en donde colaboré durante mi formación doctoral, la cual se presenta en el apéndice de la tesis.

Plant Mol Biol
DOI 10.1007/s11103-012-9954-6

REVIEW

A complex systems approach to Arabidopsis root stem-cell niche developmental mechanisms: from molecules, to networks, to morphogenesis

Eugenio Azpeitia · Elena R. Alvarez-Buylla

Received: 5 June 2012 / Accepted: 15 August 2012

Abstract Recent reports have shown that the molecular mechanisms involved in root stem-cell niche development in *Arabidopsis thaliana* are complex and contain several feedback loops and non-additive interactions that need to be analyzed using computational and formal approaches. Complex systems cannot be understood in terms of the behavior of their isolated components, but they emerge as a consequence of largely non-linear interactions among their components. The study of complex systems has provided a useful approach for the exploration of system-level characteristics and behaviors of the molecular networks involved in cell differentiation and morphogenesis during development. We analyzed the complex molecular networks underlying stem-cell niche patterning in the *A. thaliana* root in terms of some of the key dynamic traits of complex systems: self-organization, modularity and structural properties. We use these analyses to integrate the available root stem-cell niche molecular mechanisms data and postulate novel hypotheses, missing components and interactions and explain apparent contradictions in the literature.

Keywords Root stem-cell niche · *Arabidopsis thaliana* · Gene regulatory networks · Complex systems · Self-organization · Modularity

E. Azpeitia · E. R. Alvarez-Buylla (✉)
Laboratorio de Genética Molecular, Desarrollo y Evolución de Plantas, Instituto de Ecología, Centro de Ciencias de la Complejidad (C3), Universidad Nacional Autónoma de México, Ciudad Universitaria, 04510 Coyoacán, Mexico, D.F., Mexico
e-mail: eabuylla@gmail.com

Introduction

Located at the tip of the root, the root stem-cell niche (RSCN) sustains the development and growth of all below-ground tissues. Given its anatomical simplicity and accessibility, the *Arabidopsis thaliana* RSCN has become an excellent model system. The RSCN has been amenable to cellular and molecular genetic analyses unraveling a plethora of molecular regulatory mechanisms (MRMs) involved in maintaining its pattern and functionality. Partially due to the lack of data, until recently, most of the RSCN MRMs were understood as fragmented and isolated processes that were many times assumed to exhibit a linear relationship between genotype and phenotype. For example, currently, the identity and location of the RSCN is explained by the intersection of the expression patterns of a small set of transcription factors (Aida et al. 2004). However, recent findings reveal that a complex network composed of many interacting elements underlie RSCN patterning.

In her great introductory book to complexity, Mitchell (2009) described a complex system as "…a system that exhibits nontrivial emergent and self-organizing behaviors". Indeed, complex systems comprise feedback loops and other non-linear interactions that produce the emergence of often non-intuitive behaviors that without the use of theoretical approaches seem impenetrable and many times preclude clear interpretations of the experimental data. The RSCN regulatory network involves several components interacting in non-linear ways. This does not mean that actual approaches are not useful; instead, systematic and integrative approaches can complement detailed analyses of particular molecular components, improving our understanding of the system. Such integrative approaches become more relevant if we consider that complex networks have systemic key structural and dynamic properties, such as self-organization

Published online: 04 September 2012

and modularity, which cannot be understood by characterizations of isolated components.

Theoretical and computational approaches are necessary to study complex systems, like biological systems, affording the verification, prediction, and deeper understanding of experimental data with a more integral and systemic view (Strogatz 2001; Kitano 2002). While we will not review the many different tools available (But see: Alvarez-Buylla et al. 2007; Ay and Arnosti 2011), we will focus on the conceptual integration of experimental and theoretical approaches while analyzing the MRMs of RSCN patterning. To do this, we will describe some key properties, namely self-organization, modularity, and some structural and dynamic network properties, to guide the integrative description of the RSCN MRMs, detect missing components and interactions and provide novel hypotheses and plausible explanations for apparently contradictory data. Importantly, apart from the functional modularity and auxin-transport self-organization properties (Azpeitia et al. 2010; Mironova et al. 2010; Leyser 2011), the properties that we will describe have not been explicitly tested in the RSCN. However, the available data suggest that a robust complex molecular network with certain structural and dynamic characteristics, which are typical of complex networks, underlies RSCN patterning. Moreover, some of these properties appear to be generic to previously characterized MRMs (Barabási and Oltvai 2004; Kitano 2007).

In this review, first, we briefly describe the RSCN and the current explanation of how the RSCN is maintained. We then analyze the structural and dynamic characteristics of the RSCN MRMs with regard to complex systems approaches with a particular focus on network theory. Our analysis enabled us to propose novel explanations and propose experimentally verifiable predictions. For example, this approach is useful for uncovering and understanding the specific mechanisms of cell patterning, regenerative capacity and the maintenance of stem cells (SC) in the system under study. Finally, we discuss the implications and future directions of the ideas presented here.

The RSCN

All primary tissues of the root develop from the RSCN. The RSCN consists of a small group of cells with low division rates called the quiescent center (QC), which are surrounded by a cell layer composed of four different cell types of initial or SCs (Fig. 1; Dolan et al. 1993). The QC is necessary for SC maintenance because its ablation or malfunction produces premature SC differentiation, RSCN consumption, and, finally, if not reestablished, root determinacy (van den Berg et al. 1995; van den Berg et al. 1997; Xu et al. 2006; Sarkar et al. 2007).

Multiple MRMs are involved in RSCN maintenance, and the most important MRMs identified thus far include the following: (1) The regulatory interactions sustained among the GRAS family transcription factors *SHORTROOT* (*SHR*) and *SCARECROW* (*SCR*) and a few additional genes, (2) the interplay between the redundant transcription factors *PLETHORA1* (*PLT1*), *2*, *3, BBM*, and the auxin signaling pathway, (3) the *CLAVATA LIKE40* (*CLE40*) and *WUSCHEL RELATED HOMEOBOX5* (*WOX5*) MRM, (4) many hormonal signaling pathways in addition to the auxin signaling pathway and (5) epigenetic mechanisms (reviewed in Scheres 2007; Benková and Hejátko 2009; Shen and Xu 2009; Sablowski 2011).

Molecular genetic approaches have suggested that the identity and location of the RSCN depends on the intersection of the SHR, SCR and PLT protein domains (Aida et al. 2004) and the negative regulation of the *WOX5* QC identity marker by CLE40 (Stahl et al. 2009). Because the PLT transcriptional and protein domains depend on the auxin concentration (Aida et al. 2004; Zhou et al. 2010), the maximum auxin concentration coincides with the QC location (Brunoud et al. 2012), and auxin signaling, transport and metabolism modifications alter the RSCN (Ding and Friml 2010), auxin is assumed to have a fundamental role in RSCN specification. Finally, epigenetic mechanisms modulate the expression location and level of, at least, the *SCR* and *PLT* genes (Shen and Xu 2009). We recently published a model that demonstrated that the concerted action of at least the first three MRMs mentioned above, and not the isolated activity of any such MRMs, is necessary to understand how the RSCN is specified and maintained (Azpeitia et al. 2010). Importantly, our results suggested that the characterized RSCN regulatory network is incomplete because the model was not capable of reproducing important processes observed in the RSCN such as its robustness. We believe that a complex systems perspective such as the one used here may be used to propose the missing components and interactions necessary for the production of the RSCN observed systemic behaviors and aid in the achievement of a better understanding of the properties of the MRMs underlying the RSCN.

Complex system approaches to RSCN patterning

We now use a complex systems-based approach to analyze the integrated action of the above mentioned MRMs during RSCN patterning and study some systems-level traits and behaviors of the integrated network. We also discuss whether such a systematic and integrative approach reveals novel predictions to be tested experimentally or innovative approaches towards understanding how the cellular patterns and organization of the RSCN emerge.

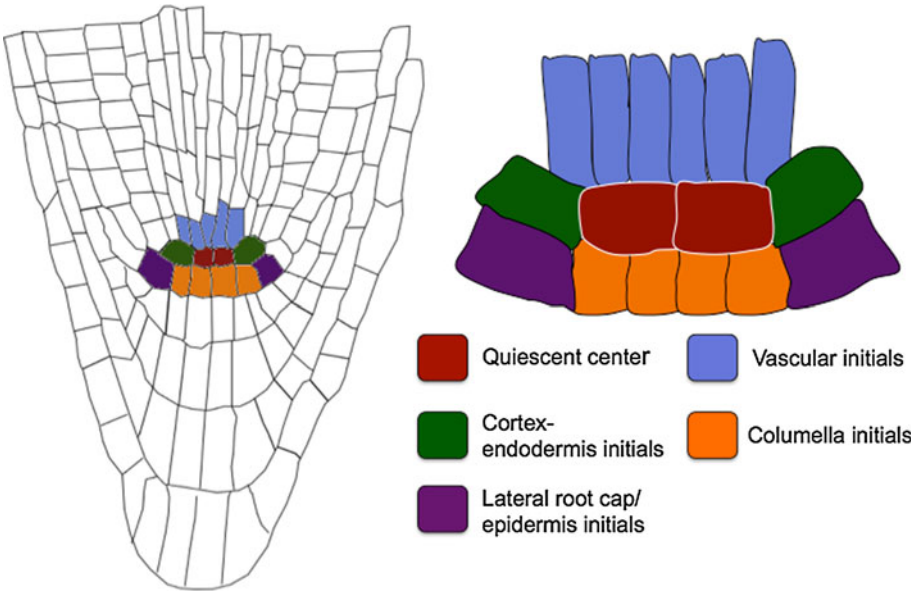

Fig. 1 *Arabidopsis thaliana* root meristen and zoom to the root stem-cell niche (RSCN). The RSCN is located at the tip of the root meristem, here colored. The different colors stand for the different initial or stem cell types that compose the RSCN and two quiescent cells revealed in a longitudinal section

Structural network-based study of the RSCN MRM

A network is composed of components called nodes that are connected through edges. In molecular regulatory networks, the nodes usually represent genes, proteins or molecules (e.g., hormones), while the edges represent regulatory interactions (reviewed in Barabási and Oltvai 2004; Albert 2007).

The most basic structural features of networks are their degree (also called connectivity) and degree distribution. The connectivity or degree k refers to the number of direct links that one node has with the other nodes of the network, while the degree distribution $P(k)$ refers to the probability that a randomly selected node has a specific degree k. Many biological networks follow a power law degree distribution (Babu et al. 2004) or a similar long-tail distribution. A power law degree distribution means that $P(k) \approx Ak^{-\lambda}$, where A is a normalization constant and λ is the degree exponent. Networks with a power law degree distribution are also known as scale-free networks. As observed with the degree distribution, in scale-free networks, there are many low degree nodes, while a few of the nodes, known as hubs, have high degrees (Barabási and Oltvai 2004; Albert 2007). Because of their high connectivity, hubs have been proposed as important nodes for network functionality, connecting nodes that can participate in different processes and bringing together the network as a whole (Barabási and Oltvai 2004).

Although we lack a large enough network structure or architecture for RSCN patterning to allow for statistical analyses of the degree distribution, more than one of the genes involved in RSCN maintenance are probably hubs. For example, *SHR* and *SCR* regulate hundreds of genes (Sozzani et al. 2010), a fact that is reflected by the many processes in which they are involved apart from RSCN maintenance such as root regeneration (Xu et al. 2006; Sena et al. 2009), lateral root development (Lucas et al. 2011), cell cycle (Sozzani et al. 2010), root radial patterning (Helariutta et al. 2000), middle cortex formation (Cui and Benfey 2009), vascular development (Carlsbecker et al. 2010; Cui et al. 2011) and stress response (Cui et al. 2012).

Scale-free networks present the small-world propertiy. The small-world property refers to the shortest possible path to travel from a node to any other node using only directly linked network nodes (Watts and Strogatz 1998). In small-world networks, nodes are connected to each other through a short path. Importantly, the small-world property has been reported in biological networks (Wagner and Fell 2001). Most of the MRMs involved in RSCN maintenance were initially characterized as independent of each other; however, recent work has discovered some links among them, creating short communication paths. For example, the SHR/SCR and PLT/auxin MRM were first described as independent MRMs (Aida et al. 2004). However, Lucas et al. (2011) recently reported that *shr* single mutants have an excessive accumulation and synthesis of auxin during the first 6 days after germination and have a progressive reduction in the auxin transport facilitators *PINFORMED* (*PIN*) expression in the root tip, likely regulating *PIN* abundance at the posttranscriptional level or indirectly regulating their expression, as suggested by Levesque et al. (2006). Moreover, SHR and SCR up-regulate the expression of miR165a, miRNA166a and miR166b (collectively referred as miR165/6). miR165/6 can diffuse from its site of expression and negatively regulate the post transcriptional expression of the HD-ZIP III gene PHABULOSA

(*PHB*) (Carlsbecker et al. 2010; Miyashima et al. 2011). HD-ZIP III genes apparently act by antagonizing the *PLT* genes in the RSCN (Smith and Long 2010). Moreover, during embryogenesis, HD-ZIP III genes regulate auxin flow (Izhaki and Bowman 2007), a fact that needs to be tested in the case of the root. Importantly, the PLT/auxin MRM feeds back to the SHR/SCR MRM. An analysis of whole seedlings revealed that HD-ZIP III genes expression is induced by auxin (Zhou et al. 2007), and the inhibition of *PHB* and its redundant gene *PHAVOLUTA* in the basal pole during embryogenesis is necessary for *SCR* and *WOX5* expression and thus proper RSCN development (Grigg et al. 2009; Fig. 2).

The last example is not the only example of the communication of MRMs through short paths. Many hormones are important for the RSCN including auxin, cytokinins (CK), ethylene, brassinosteroids (BR), jasmonate and abscisic acid, all of which alter the RSCN pattern, functionality or development (Ortega-Martínez et al. 2007; Müller and Sheen 2008; Ding and Friml 2010; Zhang et al. 2010; Chen et al. 2011a; González-García et al. 2011). However, hormones do not act trough isolated pathways or MRMs; they instead regulate each other at the biosynthesis, signal transduction and transport levels. For example, ethylene, CK and auxin regulate the synthesis of each other (Nordström et al. 2004; Tsuchisaka and Theologis 2004; Stepanova et al. 2005; Swarup et al. 2007; Stepanova et al. 2008; Jones et al. 2010; Zhou et al. 2011), PIN auxin transporter expression is affected by CK, BR, ethylene and auxin itself (Blilou et al. 2005; Vieten et al. 2005; Ruzicka et al. 2007; Dello Ioio et al. 2008; Ruzicka et al. 2009; Zhang et al. 2011), and the effects of ethylene on cell elongation are dependent on the auxin signaling pathway (Swarup et al. 2007; Stepanova et al. 2007; Fig. 3). Indeed, hormonal cross-talk is important for root patterning (reviewed in Benková and Hejátko 2009). The evidence reviewed here suggests that the small-world property is present in the whole RSCN network and demonstrates that the SHR/SCR, the PLT/auxin MRMs, and the hormone signaling pathways, which were originally reported as independent MRMs, are interconnected through short and most likely multiple pathways.

Importantly, due to the presence of short communication paths, the small-world property proposes that modifications in one MRM can have unexpected effects in other MRMs (Watts and Strogatz 1998), while, at the same time, allowing for simpler and direct explanations of such effects. For example, the *PIN* genes and *WOX5* expression are affected in *scr* and *shr* single mutant backgrounds, even though neither *PIN* nor *WOX5* appear to be direct target genes of SHR or SCR (Levesque et al. 2006; Sarkar et al. 2007; Sozzani et al. 2010). Based on the fact that SHR directly up-regulates the expression of cytokinin oxidase 3 (CKX3; Cui et al. 2011), a CK catabolism enzyme, and that CK represses *PIN* expression (Ruzicka et al. 2009; Zhang et al. 2011), one possible explanation is that SHR indirectly regulates *PIN* expression through its down-regulation of CK synthesis. Other possible explanations are (1) that SHR and SCR regulate *PIN* expression through its effect on auxin, as *shr* mutants accumulate auxin and high concentrations of auxin reduce the PIN protein levels (Vieten et al. 2005; Lucas et al. 2011), or (2) through an effect of SHR and SCR on PHB (Carlsbecker et al. 2010) given that the

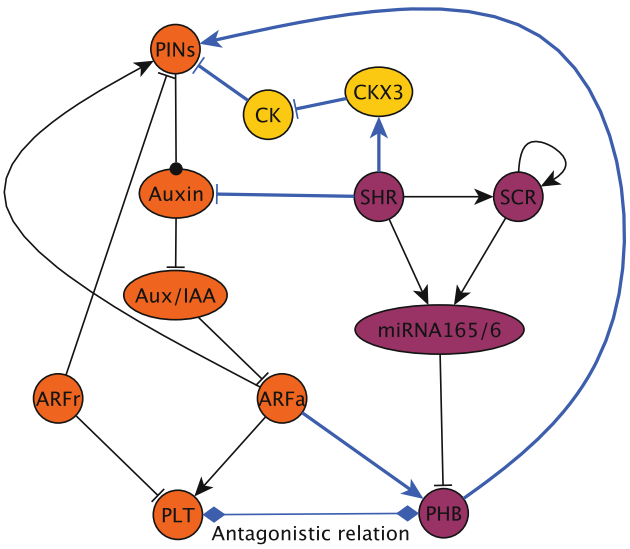

Fig. 2 Shortest paths connecting the SHR/SCR (*purple*) and the PLT/Auxin (*orange*) modules as described in the main text. Simplified versions of these modules are depicted. *Blue* edges highlight the short paths that connect both modules. As observed, even when these were characterized as independent pathways or modules, they have multiple short communication paths. *Arrowheads* represent positive interactions, *T arrowheads* represent negative interactions, *doted arrowhead* auxin transport facilitation and *diamond arrowhead* antagonistic probably non-regulatory interactions. *ARFa* ARF activator, *ARFr* ARF repressor, *CK* cytokinin

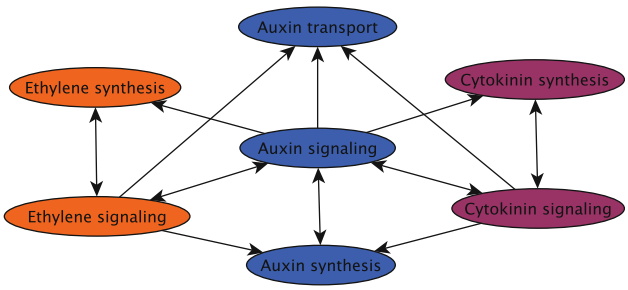

Fig. 3 Cross-talk among auxin, cytokinin and ethylene pathways involved in RSCN patterning as described in the main text. As observed, these hormones pathways have multiple interactions or crosstalk connections at the signaling, synthesis and transport levels demonstrating that they are part of an integrated complex network with short communicating paths

HD-ZIP III genes regulate auxin flow (Izhaki and Bowman 2007; Fig. 2). SHR and SCR could modulate WOX5 through its regulation of the HD-ZIP III genes or through another indirect mechanism. For example, *CLE10* was recently reported as a putative SHR target gene (Cui et al. 2011). However, CLE10 has been described as a peptide involved in protoxylem vessel formation and not in RSCN maintenance (Kondo et al. 2011).

Interestingly, neither hub importance nor small-world properties are rules in biological networks. The deletion of the more connected genes does not necessarily lead to the most drastic phenotypes (e.g., Espinosa-Soto et al. 2004), and the perturbation of a MRM does not alter all other MRMs. Why does this happen in biological networks? High connectivity is not necessarily directly related to functionality in a network. Other measurements, such as betweenness (i.e., the number of shortest paths that pass through a node), may also determine the functionality of a node (Goh et al. 2002). In addition, positive feedback loops appear to make biological networks more robust against mutations in highly connected nodes (Espinosa-Soto et al. 2004). However, understanding how structure and function are related is a difficult task and entails different approaches. Theoretical biology has proposed other properties of biomolecular networks, such as modularity, which may help explain why neither hub importance nor small-world properties are rules in biological networks.

The RSCN as a modular system

Recent research suggests that biological networks usually have modular organization. At a structural level, network modules are usually defined as a subset of network components that are more connected with each other than with other components of the network (Fig. 4; Wagner et al. 2007; Espinosa-Soto and Wagner 2010). Modular organization may reduce the pleiotropic effects of perturbations (such as mutants) in the network (von Dassow and Munro 1999; Wagner et al. 2007) because modules have a relatively autonomous behavior with respect to the rest of the network. Hence, such modularity may help explain why, in biological networks, mutations of highly interconnected nodes may not alter the phenotype, or they do not necessarily behave as expected for small-world networks.

As previously mentioned, some interactions occur between the SHR/SCR MRM and the PLT/auxin MRM. However, there are multiple interactions within PLT/auxin and SHR/SCR MRMs (Figs. 2, 5, 6). *PLT* genes expression patterns are altered by auxin addition, transport inhibition and signaling pathway mutants (Aida et al. 2004; Blilou et al. 2005; Galinha et al. 2007). The PLTs response to auxin is partially dependent on tyrosylprotein sulfotransferase (TPST). TPST controls the activity of the secreted

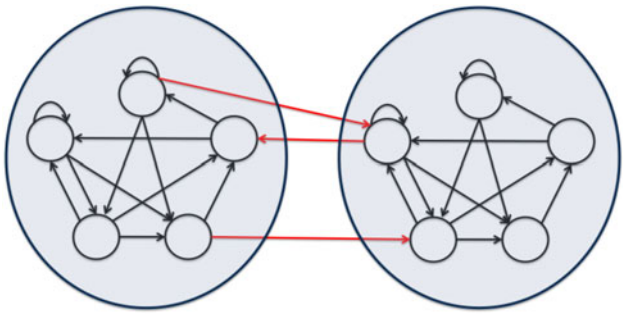

Fig. 4 Structural modularity of gene regulatory networks where there are many more within-module interactions than between module interconnections. This property can reduce pleiotropic effects of mutants, due to the relative independence of different modules

peptide portion of the root meristem growth factors 1 (RGF1), 2 and 3 (herein RGFs) by Tyr sulfation (Matsuzaki et al. 2010). RGFs expression is auxin-independent, while TPST expression is auxin-dependent. Matsuzaki et al. (2010) proposed that RGFs probably stabilize PLT proteins based on the fact that wild-type seedlings treated with RGF1 expand PLT1 and 2 protein domains but not *PLT1* or *PLT2* transcriptional domains. However, other results demonstrated that *tpst* mutants reduce PLT at the transcriptional and protein levels, demonstrating that TPST can control PLT expression at both levels (Zhou et al. 2010). Interestingly, *PLT* genes control auxin transport, which is indispensable for the observed auxin graded concentration in the root, creating a loop in which PLT genes simultaneously control and are controlled by auxin distribution (Aida et al. 2004; Blilou et al. 2005; Galinha et al. 2007). The RopGEF7 gene is positively regulated by auxin and acts as a positive regulator of *PLT* expression. Interestingly, RopGEF7 also affects the auxin transport and response in the RSCN (Chen et al. 2011b). Moreover, as described below, there are multiple feedback loops within the auxin signaling pathway, greatly increasing the connectivity of the MRM (Fig. 5).

On the other hand, SCR and SHR form a dimer, and they together directly up-regulate *MAGPIE* (*MGP*) expression and JACKDAW (*JKD*) postembryonic expression (Levesque et al. 2006; Welch et al. 2007; Cui et al. 2011). Mutations in *JKD* diminish *SCR* expression in the QC and cortex-endodermis initials (CEI), causing a misspecification of the QC and ectopic periclinal divisions of the CEI. The double mutant *jkd mgp* restores *SCR* expression in the QC and CEI, suggesting that MGP is a negative regulator of *SCR*. Yeast two-hybrid and transient assays have shown that SHR, SCR, JKD, and MGP can physically interact and modulate the expression of and transcriptional activity of each other (Welch et al. 2007; Ogasawara et al. 2011). SCR also acts as a negative regulator of *MGP* when it forms a dimer with like heterochromatin protein1 (LHP1) (Cui and

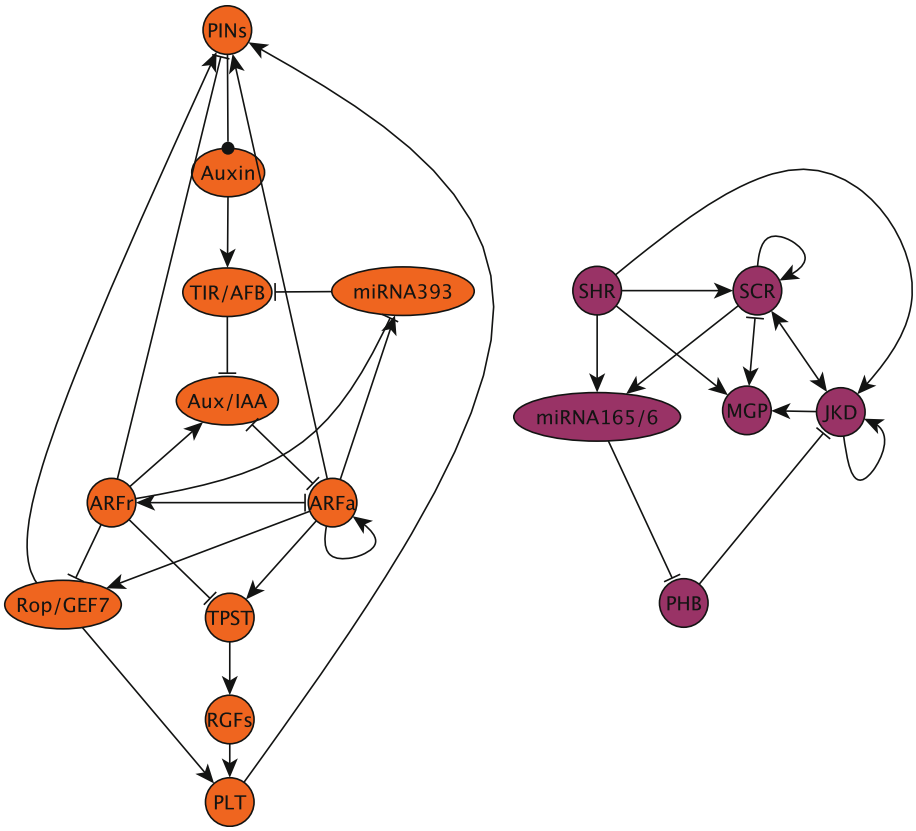

Fig. 5 The PLT/Auxin (*orange*) and the SHR/SCR (*purple*) structural modules. The whole RSCN network is probably divided into several structural modules, based on their relative intra-module versus inter-module interactions: in these two modules there are many more within-module interactions than between-module connections (see also Fig. 2). *Arrowheads* as in Fig. 2

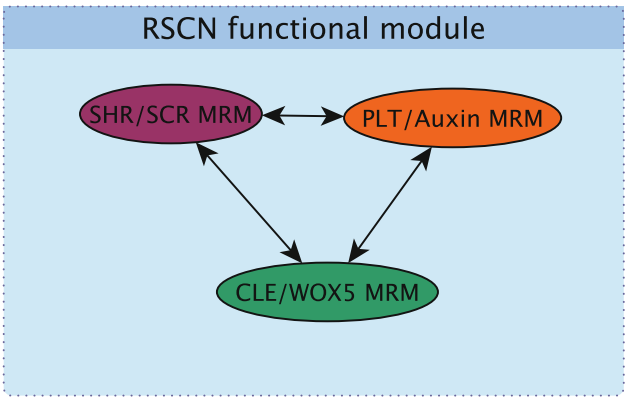

Fig. 6 The root stem-cell niche functional module. As observed, the RSCN functional module is composed of several structural modules, indicating that structural and functional modules do not always coincide

Benfey 2009). LHP1 is a candidate protein for the histone trimethylation that is necessary for PcG repression activity (Exner et al. 2009). As mentioned above, SHR and SCR negatively regulate PHB through miR165/6. Recently, Miyashima et al. (2011) demonstrated that the restriction of *PHB* to the stele is necessary for maintaining *JKD* expression. Consistent with this result, the gain-of-function allele *phd-1d* has a similar ground tissue phenotype as the *jkd* single mutant with low *SCR* expression levels, which may explain why PHB repressed SCR expression in a previous study (Grigg et al. 2009; Fig. 5).

Until now, we have considered a structural definition of modularity. However, dynamic regulatory network models may be used to test whether a set of interacting genes or other molecular components constitute a functional module that is sufficient and necessary to recover an observed gene-state configuration and its spatial pattern. Importantly, structural and functional modules may not coincide (Ten Tusscher and Hogeweg 2011). For example, in Azpeitia et al. (2010), we aimed to analyze whether PLT/auxin, SHR/SCR, and CLE/WOX5 MRMs were sufficient to reproduce the stable gene configurations that characterize each cell type within the RSCN and their observed spatial distribution. We found that some important interactions are missing, but by adding a few predictions, our RSCN regulatory network model constitutes a functional module that incorporates the necessary and sufficient MRMs required to recover the genetic configurations that have been described for the main cell types of the RSCN and their observed qualitative spatial patterning. However, as mentioned above, each of the MRMs considered in the proposed RSCN network may constitute a different structural module (Fig. 6). Thus, dynamic analyses are fundamental to the understanding of how the MRM structure and function are related.

Once a dynamic model is developed, the model can be validated with experimental evidence. For example, our model is capable of reproducing most of the mutant phenotypes observed, but it is not as robust as expected from experimental observations and from comparison with other biomolecular networks (Azpeitia et al. 2010). This indicates that the uncovered regulatory module is incomplete. Additional components, interactions or complete modules may be necessary to recover the observed robustness and overall RSCN behavior. For example, epigenetic MRMs were not considered in our model and are fundamental to RSCN maintenance because *SCR* or *PLT* have an altered expression in mutants of the *TONSOKU* (*TSK*), *TEBICHI* (*TEB*), *FASCIATA1* (*FAS1*) and *FAS2*, NAP1-related protein1 (NRP1) and NRP2, Polycomb group (PcG), general control nonderepressible protein5 (GCN5) and Pickle (PKL) genes, which are all involved in epigenetic regulation (reviewed in Shen and Xu 2009). Moreover, all mutants of these genes have alterations in RSCN patterning, the expression of QC markers, and/or columella SC differentiation (Shen and Xu 2009). These epigenetic MRMs, which are part of structural modules that are different than the ones incorporated thus far, may be required to recover observed dynamic behaviors in the RSCN patterning and the regulatory networks involved within it. Thus, such epigenetic mechanisms should be an important part of the RSCN functional module even when they are likely a part of different structural modules. However, we believe that one of the most interesting and important properties of the dynamic analysis of complex networks is self-organization. This may also provide important biological insights into such networks, e.g., in terms of uncovering missing components or interactions.

The RSCN as a self-organized system

Self-organization refers to the emergence of patterns or behaviors at the global system level as a consequence of non-linear interactions among system components without depending upon the action of a central controller (Seeley 2002). For example, the stable gene-state configurations (attractors) that characterize each cell type within a RSCN constitute a self-organized property of the complex regulatory module. These attractors emerge as a consequence of the concerted action of all of the molecular interactions considered in the particular network under consideration. At a different level of organization, the spatial cellular arrangement that characterizes the RSCN may also be considered as a self-organized pattern resulting from the coupled dynamics of intracellular networks in a multicellular spatial domain. In the case under consideration, the coupling of the dynamics of the intracellular networks occurs via the intercellular movement of some of the network components (Azpeitia et al. 2010).

The lack of a central controller means that self-organization arises from the local interactions of the system components and not from an individual component at any level of organization that works as a "guiding" unit. In this sense, it is relevant to uncover the structure and dynamics of intracellular biological networks and their coupling mechanisms among cells, rather than only concentrating on the role of so-called "key" genes. In contrast, we should understand, in terms of integrated regulatory networks, what makes a "key" gene key and why the mutation of such genes are sometimes sufficient to take the system from one multigenic and multicellular configuration to another one in contrast to mutations in other genes that are not "key".

In the root, there are many traits and behaviors that suggest the existence of self-organizing processes at the macro and micro levels. The regeneration process is perhaps one of the most obvious and best examples of self-organization in the RSCN. Normally, the RSCN develops from early embryonic stages (Dolan et al. 1993); however, when the root tip is excised or the QC ablated, a new RSCN is formed (Xu et al. 2006; Sena et al. 2009). The process of root and RSCN regeneration follows an ordered sequence of events. It begins with the formation of a new auxin maximum, which induces *PLT* expression and, later, SHR nuclear localization and *SCR* expression where the new RSCN will be relocated. *SHR*, *SCR*, *PLT* genes and the auxin maximum are all necessary for the RSCN regeneration process (Xu et al. 2006). After the root tip is excised, the RSCN is completely eliminated, and the root tip pattern is severely affected. However, even in the absence of the original pattern, RSCN regeneration proceeds (Sena et al. 2009). Moreover, callus regeneration from root, cotyledon, and petals, all of which have completely different morphologies, resemble the root regeneration process (Sugimoto et al. 2010). The fact that the RSCN can regenerate without a specific pre-established pattern and employ multiple molecular components strongly suggests that no single molecular component, module, external agent or pre-pattern directs the RSCN regeneration and patterning process. The process is instead due to the self-organizing capability of the molecular regulatory network involved, and it is likely that additional coupling constraints such as physical and chemical (e.g., hormone) fields are also involved.

The root auxin gradient is another excellent example of a self-organizing process involved in RSCN maintenance (Leyser 2011). Theoretical and experimental studies have suggested that the graded distribution of auxin along the root longitudinal axis depends on the polar localization of the PIN proteins (Blilou et al. 2005; Vieten et al. 2005; Grieneisen et al. 2007; Mironova et al. 2010) and on auxin metabolism (synthesis and degradation; Stepanova et al. 2008; Petersson et al. 2009). However, the polar localization of the PIN transporters is, in turn, regulated by the auxin-signaling pathway (Vieten et al. 2005; Sauer et al.

2006), which partly depends on the auxin cell concentration that at the same time, depends on the auxin gradient (Tiwari et al. 2001; Kepinski and Leyser 2005; Fig. 5). Hence, the auxin gradient is at the same time a cause and effect through its interdependences with the auxin signaling and transport mechanisms and not a process directed by any specific fixed force.

Self-organizing systems have a dissipative structure behavior, meaning that they are far from thermodynamic equilibrium. Interestingly, dissipative structures are maintained in steady states or attractors (Prigogine 1978), which can adapt and adjust to internal and external changes, allowing them to maintain coherent patterns or functions under a wide range of conditions and several types of perturbations (Heylighen 2001) that could include genetic loss or gain of function mutations. The latter behaviors are observed in the above examples of RSCN regeneration because it occurs in different types of RSCN lesions and different organs (Xu et al. 2006; Sena et al. 2009; Sugimoto et al. 2010). The auxin gradient is maintained even under some PIN and auxin signaling mutant backgrounds and during auxin addition or overproduction (Blilou et al. 2005; Vieten et al. 2005; Grieneisen et al. 2007). Finally, the overall multigenic RSCN configurations and cellular patterns are maintained in the presence of several mutations. However, without understanding how such apparently dispensable nodes are connected to the "key" nodes, we cannot understand the molecular regulatory basis of the overall behavior of the system.

Hormone signaling pathways are probably better examples of self-organizing, dissipative, and adaptable systems, i.e., they return to a basal state or attractor after perturbation. Such attractors are usually the inactive state of the pathway when the hormone is absent or present at low concentrations. Such systems also modulate and stabilize (adapt) their response when their inputs, usually hormone concentrations, change. There are multiple ways in which hormone pathways can reach this adaptable behavior (e.g., Dreher and Callis 2007).

As previously mentioned, one of the best-studied pathways during RSCN patterning is the auxin pathway. Auxin signaling can be modulated by adjusting the auxin concentration. As stated above, the auxin concentration depends on its transport, which is a self-organizing process, but it is also dependent on auxin metabolism. Auxin metabolism is regulated by multiple signals. Interestingly, auxin signaling also regulates some of these signals. For example, auxin inhibits CK synthesis (Nordström et al. 2004) and promotes ethylene synthesis (Rahman et al. 2001), while both CK and ethylene promote auxin synthesis (Stepanova et al. 2008; Jones et al. 2010; Zhou et al. 2011; Fig. 3). The internal components of the auxin pathway are also regulated to maintain a coherent adaptive response. Receptors of the transport inhibitor response1/auxin signaling f-box protein1–5 (TIR1/AFB) detect auxin. TIR/AFB are components of the SKP1/Cullin/F-box protein $(SCF)^{TIR1/AFB}$ ubiquitin ligase complex (Mockaitis and Estelle 2008) and are negatively regulated post-transcriptionally by miR393. The $SCF^{TIR1/AFB}$ complex promotes Aux/IAA degradation in the presence of auxin (Tiwari et al. 2001; Kepinski and Leyser 2005). Interestingly, Aux/IAAs act as an auxin co-receptor because TIR/AFB cannot readily bind auxin in the absence of Aux/IAA proteins (Calderón Villalobos et al. 2012). The Aux/IAA proteins form heterodimers with the Auxin Response Factor (ARF) proteins that mediate auxin transcriptional regulation (Tiwari et al. 2001). Some ARFs act as transcriptional activators (ARFa), while others act as transcriptional repressors (ARFr; Guilfoyle and Hagen 2007), and all compete for the regulation of the same target genes (Ulmasov et al. 1999); thus, the ARFa/ARFr ratio also modulates the auxin signaling response (Vernoux et al. 2011). Through its transcriptional activity, ARFa generates many feedback loops inducing the induction of *Aux/IAA* expression, and probably miR393 and some ARF family members (Wang et al. 2005; Paponov et al. 2008; Parry et al. 2009; Chen et al. 2011c; Fig. 3).

Importantly, the auxin signaling pathway can differentially modulate its response, depending on the Aux/IAA, ARF and TIR/AFB members involved in each specific process, because the members of these gene families have partially redundant functions, but also have specific characteristics that are involved in different responses (Hardtke et al. 2004; Parry et al. 2009; Calderón Villalobos et al. 2012; Rademacher et al. 2012). For example, the members of the TIR/AFB family have different strengths of interaction with Aux/IAAs, and different Aux/IAA-TIR/AFB complexes have different sensitivities to the auxin concentration (Parry et al. 2009; Calderón Villalobos et al. 2012). Thus, auxin signaling can adapt to several conditions, modulating the auxin concentration, adjusting the expression level and activity of the different receptors and proteins involved in the pathway through many feedback loops, adjusting the ARFa/ARFr ratio and selecting specific members of the Aux/IAA, ARF and TIR/AFB gene families that are involved in each response and condition.

Explicitly considering the self-organizing properties of a complex dynamic system could help resolve some apparently conflicting points regarding the MRMs involved in RSCN patterning. For example, some reports have shown that auxin promotes the expression of *WOX5* (Gonzali et al. 2005; Sarkar et al. 2007; Sena et al. 2009; Sugimoto et al. 2010). In contrast, a recent manuscript by Ding and Friml (2010) demonstrated that elevated auxin concentrations in the root tip lead to the consumption of the RSCN and WOX5 expression inhibition. It is likely that some of these apparent contradictions can be explained by invoking the different

responses and roles of the members of the ARF, Aux/IAA and TIR1/AFB gene families. However, another complementary hypothesis that may help reconcile such apparently contradictory results is that different responses to auxin signaling are explained by the self-organizing and self-regulating properties of the pathway. For example, self-organizing mechanisms generally involve, as has been uncovered for biological networks, many regulatory motifs such as feedback loops, which provide several properties to self-organizing processes. Positive feedback loops amplify a received signal or stimulus, allowing switch-like behavior, bistability, and hysteresis (Kitano 2004; Mitrophanov and Groisman 2008). On the other hand, negative feedback loops play an important role by dampening fluctuations, providing stability and limiting the fluctuating range of the components (Kitano 2004; Becskei and Serrano 2000). As mentioned above, positive and negative feedback loops are present in the auxin signaling pathway self-organizing process. The expression of ARF16, which is a putative ARFr, and ARF19, which is an ARFa, is promoted by auxin, thus creating a negative and a positive feedback loop, respectively (Wang et al. 2005; Paponov et al. 2008). The presence of these feedback loops could generate different auxin responses under different conditions, which could help explain why, under some circumstances, auxin inhibits *WOX5* expression, while in other conditions auxin promotes *WOX5* expression. For example, ARFa and ARFr compete for the same target genes (Ulmasov et al. 1999), and the expression patterns of ARF16 and ARF19 in the root tip are similar (Rademacher et al. 2011). Thus, if ARF16 expression is promoted to a greater extent by auxin than ARF19 expression, we expect that auxin addition would repress *WOX5* expression as observed by Ding and Friml (2010). However, if ARF19 is induced by auxin to a greater extent than ARF16, we could expect an induction of *WOX5* under auxin addition conditions as observed by the research of Gonzali et al. (2005) and Sugimoto et al. (2010). Hence, we may observe auxin inductive and repressive responses over *WOX5* under different conditions, and this would not imply contradictory experimental observations.

Missing links in the RSCN network

The analyses of structural and dynamic MRM properties also allow for the detection of missing links and non–intuitive behaviors in the MRM that may guide future experimental studies that may otherwise be obviated. For example, Miyashima et al. (2011) suggested that miR165/6 acts as a morphogen. Theoretical research has demonstrated that the morphogen graded distribution alone is not capable of generating such highly precise patterns as the ones observed in the root vasculature. Theoretical analyses of complex systems have demonstrated that feedback loops have a critical role in the generation of robust and precise patterns (e.g., Jaeger et al. 2008). HD-ZIP III genes form a negative feedback loop with ZPR proteins in the shoot (Kim et al. 2008). It will be interesting to investigate if HD-ZIP III genes also create this or similar feedback loops in the root as suggested by theoretical studies and the observed patterns (Jaeger et al. 2008).

CLE40/WOX5 MRM is fundamental for RSCN maintenance (Sarkar et al. 2007; Stahl et al. 2009). However, until now, little information has been gathered regarding this MRM in the RSCN. Stahl et al. (2009) reported that CLE40 reduces *WOX5* expression. A similar MRM acts in the shoot stem cell niche, where the expression of WUS, a WOX5 homolog, is repressed by CLV3 (Sablowski 2011). The WOX5/CLE40 and WUS/CLV3 MRMs are likely similar in structure and dynamic behavior. This is supported by the fact that WOX5 can be substituted by WUS, that CLV3 can be partially substituted by CLE40 in the shoot, and that *CLV3* and *CLE40* over expression and peptide addition produce similar root phenotypes (Hobe et al. 2003; Fiers et al. 2005; Sarkar et al. 2007). Moreover, the protein phosphatases POLTERGEITS (POL) and PLL1 act downstream of the WOX5/CLE40 and WUS/CLV3 MRMs. In both cases, the CLV pathway inhibits POL and PLL1 activity, which is necessary for *WOX5* and *WUS* expression in the root and shoot, respectively (Song et al. 2008; Gagne et al. 2010). However, unlike the WOX5/CLE40 MRM, the WUS/CLV3 MRM has been thoroughly studied, revealing the presence of many feedback loops (Gordon et al. 2009; Chickarmane et al. 2012). The similarity between the WOX5/CLE40 and the WUS/CLV3 MRMs and the key importance of feedback loops in network behavior and emerging pattern robustness may guide researchers to search for feedback motifs that are similar to the ones that have been uncovered in the shoot in the WOX5/CLE40 MRM. Our own studies suggest a few yet uncovered feedback loops in the root MRMs that should be experimentally documented: a negative feedback loop between CLE40 and WOX5 and a positive self-regulation of WOX5, which likely occurs via the auxin signaling pathway (Azpeitia et al. 2010, and unpublished data).

Conclusions

Complex systems approaches are becoming fundamental to the understanding of regulatory systems that result from non-linear interactions among multiple components that act in concert during a particular cell differentiation or morphogenetic process, rather than by being directed by single and isolated genes or any type of central controller. In this review, we have used structural and dynamic properties of

complex networks, like modularity and self-organization, to integrate and provide novel explanations for the plethora of molecular genetic involved in the RSCN of *A. thaliana*. Due to space limitations, we only focused on a few structural and dynamic properties of complex networks. However, there are other properties, such as robustness, which are pervasive among complex systems. Robustness refers to the ability of systems to retain their functionality despite perturbations. For the interested reader, excellent reviews have focused on this aspect (Kitano 2007; Whitacre 2012) and other important properties of complex systems (Mitchell 2009).

These properties constitute useful conceptual frameworks for analysis at the systemic level, and importantly, they yield complementary information to achieve a better and more profound mechanistic understanding of complex systems such as the regulatory networks involved in the patterning of SC niches and other biological structures. For example, structural analyses allowed for a global picture of the involved network topology, which may be useful for uncovering missing components or interactions and identifying novel behaviors or roles for particular nodes. Modularity at the structural level also helps us understand why relying on only the simplest structural traits, such as degree and degree distribution, may be misleading with regards to the role of particular nodes in overall network dynamics. However, importantly, structural modularity does not necessarily coincide with functional modularity; hence, when trying to uncover the structure–function relationship, additional dynamic approaches are required to verify the necessity and sufficiency of the components that are being considered in the overall system behavior or dynamics. Hence, structural and dynamic analyses complement each other, which also allows for the prediction of novel components and interactions and the evaluation of the functional role of characterized components or the proposal of innovative systemic explanations. As we observed, all of these properties are interconnected and together provide a powerful vision for the study of complex systems.

In this review, we have shown that enough molecular genetic information has been uncovered for the MRMs involved in RSCN patterning to allow for an integrative approach that explores the structural and dynamic properties characteristic of complex systems. This approach has allowed us to postulate a novel, non-intuitive hypothesis, which may guide future experimental studies, and provide explanations for apparently contradictory experimental evidence. Therefore, this type of analysis may guide research and then feedback to further the understanding of RSCN patterning. A dynamic interplay among theoretical, experimental and comparative analyses will greatly contribute to the further understanding of the complex nature of the regulatory systems involved in cell differentiation and morphogenesis during plant and animal development.

Acknowledgments This paper constitutes a partial fulfillment of the Graduate Program in Biological Sciences of the National Autonomous University of México (UNAM). E.A. acknowledges the scholarship and financial support provided by the National Council of Science and Technology (CONACyT), and UNAM. E.A.B. thanks financial support from Conacyt (81433, 81542, 1667705,180098,180380) and PAPIIT (IN229003-3, IN226510-3, IN204011-3, IB201212-2). E.A.B. is currently sponsored by the Miller Institute for Basic Research in Science, University of California, Berkeley, USA. We thank Rigoberto V. Perez-Ruız and Diana Romo for technical and logistical assistance. We thank Lynna Kiere for the detailed revision of the manuscript. Finally, we also thank Dr. Joseph Dubrovsky, Dr. Carlos Villarreal, Dr. Mariana Benítez and M.S. Úrsula Abad for their thoughtful comments.

References

Aida M, Beis D, Heidstra R, Willemsen V, Blilou I, Galinha C, Nussaume L, Noh YS, Amasino R, Scheres B (2004) The PLETHORA genes mediate patterning of the Arabidopsis root stem cell niche. Cell 119:109–120

Albert R (2007) Network inference, analysis, and modeling in systems biology. Plant Cell 19:3327–3338

Alvarez-Buylla ER, Benítez M, Dávila EB, Chaos A, Espinosa-Soto C, Padilla-Longoria P (2007) Gene regulatory network models for plant development. Curr Opin Plant Biol 10:83–91

Ay A, Arnosti DN (2011) Mathematical modeling of gene expression: a guide for the perplexed biologist. Crit Rev Biochem Mol Biol 46:137–151

Azpeitia E, Benítez M, Vega I, Villarreal C, Alvarez-Buylla ER (2010) Single-cell and coupled GRN models of cell patterning in the *Arabidopsis thaliana* root stem cell niche. BMC Syst Biol 4:134

Babu MM, Luscombe NM, Aravind L, Gerstein M, Teichmann SA (2004) Structure and evolution of transcriptional regulatory networks. Curr Opin Struct Biol 14:283–291

Barabási AL, Oltvai ZN (2004) Network biology: understanding the cell's functional organization. Nat Rev Genet 5:101–113

Becskei A, Serrano L (2000) Engineering stability in gene networks by autoregulation. Nature 405:590–593

Benková E, Hejátko J (2009) Hormone interactions at the root apical meristem. Plant Mol Biol 69:383–396

Blilou I, Xu J, Wildwater M, Willemsen V, Paponov I, Friml J, Heidstra R, Aida M, Palme K, Scheres B (2005) The PIN auxin efflux facilitator network controls growth and patterning in Arabidopsis roots. Nature 433:39–44

Brunoud G, Wells DM, Oliva M, Larrieu A, Mirabet V, Burrow AH, Beeckman T, Kepinski S, Traas J, Bennett MJ, Vernoux T (2012) A novel sensor to map auxin response and distribution at high spatio-temporal resolution. Nature 482:103–106

Calderón Villalobos LI, Lee S, De Oliveira C, Ivetac A, Brandt W, Armitage L, Sheard LB, Tan X, Parry G, Mao H, Zheng N, Napier R, Kepinski S, Estelle M (2012) A combinatorial TIR1/AFB-Aux/IAA co-receptor system for differential sensing of auxin. Nat Chem Biol 8:477–485

Carlsbecker A, Lee JY, Roberts CJ, Dettmer J, Lehesranta S, Zhou J, Lindgren O, Moreno-Risueno MA, Vatén A, Thitamadee S, Campilho A, Sebastian J, Bowman JL, Helariutta Y, Benfey PN (2010) Cell signalling by microRNA165/6 directs gene dose-dependent root cell fate. Nature 465:316–321

Chen Q, Sun J, Zhai Q, Zhou W, Qi L, Xu L, Wang B, Chen R, Jiang H, Qi J, Li X, Palme K, Li C (2011a) The basic helix-loop-helix transcription factor MYC2 directly represses PLETHORA expression during jasmonate-mediated modulation of the root stem cell niche in Arabidopsis. Plant Cell 23:3335–3352

Chen M, Liu H, Kong J, Yang Y, Zhang N, Li R, Yue J, Huang J, Li C, Cheung AY, Tao LZ (2011b) RopGEF7 regulates PLETHORA-dependent maintenance of the root stem cell niche in Arabidopsis. Plant Cell 23:2880–2894

Chen ZH, Bao ML, Sun YZ, Yang YJ, Xu XH, Wang JH, Han N, Bian HW, Zhu MY (2011c) Regulation of auxin response by miR393-targeted transport inhibitor response protein 1 is involved in normal development in Arabidopsis. Plant Mol Biol 77:619–629

Chickarmane VS, Gordon SP, Tarr PT, Heisler MG, Meyerowitz EM (2012) Cytokinin signaling as a positional cue for patterning the apical-basal axis of the growing Arabidopsis shoot meristem. Proc Natl Acad Sci USA 109:4002–4007

Cui H, Benfey PN (2009) Interplay between SCARECROW, GA and LIKE HETEROCHROMATIN PROTEIN 1 in ground tissue patterning in the Arabidopsis root. Plant J 58:1016–1027

Cui H, Hao Y, Kovtun M, Stolc V, Deng XW, Sakakibara H, Kojima M (2011) Genome-wide direct target analysis reveals a role for SHORT-ROOT in root vascular patterning through cytokinin homeostasis. Plant Physiol 157:1221–1231

Cui H, Hao Y, Kong D (2012) SCARECROW has a SHORT-ROOT independent role in modulating sugar response. Plant Physiol 158:1769–1778

Dello Ioio R, Nakamura K, Moubayidin L, Perilli S, Taniguchi M, Morita MT, Aoyama T, Costantino P, Sabatini S (2008) A genetic framework for the control of cell division and differentiation in the root meristem. Science 322:1380–1384

Ding Z, Friml J (2010) Auxin regulates distal stem cell differentiation in Arabidopsis roots. Proc Natl Acad Sci USA 107:12046–12051

Dolan L, Janmaat K, Willemsen V, Linstead P, Poethig S, Roberts K, Scheres B (1993) Cellular organisation of the *Arabidopsis thaliana* root. Development 119:71–84

Dreher K, Callis J (2007) Ubiquitin, hormones and biotic stress in plants. Ann Bot 99:787–822

Espinosa-Soto C, Wagner A (2010) Specialization can drive the evolution of modularity. PLoS Comput Biol 6:e1000719

Espinosa-Soto C, Padilla-Longoria P, Alvarez-Buylla ER (2004) A gene regulatory network model for cell-fate determination during *Arabidopsis thaliana* flower development that is robust and recovers experimental gene expression profiles. Plant Cell 16:2923–2939

Exner V, Aichinger E, Shu H, Wildhaber T, Alfarano P, Caflisch A, Gruissem W, Köhler C, Hennig L (2009) The chromodomain of LIKE HETEROCHROMATIN PROTEIN 1 is essential for H3K27me3 binding and function during Arabidopsis development. PLoS ONE 4:e5335

Fiers M, Golemiec E, Xu J, van der Geest L, Heidstra R, Stiekema W, Liu CM (2005) The 14-amino acid CLV3, CLE19, and CLE40 peptides trigger consumption of the root meristem in Arabidopsis through a CLAVATA2-dependent pathway. Plant Cell 17:2542–2553

Gagne JM, Gish LA, Clark SE (2010) The role of the acyl modification, palmitoylation, in Arabidopsis stem cell regulation. Plant Signal Behav 5:1048–1051

Galinha C, Hofhuis H, Luijten M, Willemsen V, Blilou I, Heidstra R, Scheres B (2007) PLETHORA proteins as dose-dependent master regulators of Arabidopsis root development. Nature 449:1053–1057

Goh KI, Oh E, Jeong H, Kahng B, Kim D (2002) Classification of scale-free networks. Proc Natl Acad Sci USA 99:12583–12588

González-García MP, Vilarrasa-Blasi J, Zhiponova M, Divol F, Mora-García S, Russinova E, Caño-Delgado AI (2011) Brassinosteroids control meristem size by promoting cell cycle progression in Arabidopsis roots. Development 138:849–859

Gonzali S, Novi G, Loreti E, Paolicchi F, Poggi A, Alpi A, Perata P (2005) A turanose-insensitive mutant suggests a role for WOX5 in auxin homeostasis in *Arabidopsis thaliana*. Plant J. 44: 633–645

Gordon SP, Chickarmane VS, Ohno C, Meyerowitz EM (2009) Multiple feedback loops through cytokinin signaling control stem cell number within the Arabidopsis shoot meristem. Proc Natl Acad Sci USA 106:16529–16534

Grieneisen VA, Xu J, Marée AF, Hogeweg P, Scheres B (2007) Auxin transport is sufficient to generate a maximum and gradient guiding root growth. Nature 449:1008–1013

Grigg SP, Galinha C, Kornet N, Canales C, Scheres B, Tsiantis M (2009) Repression of apical homeobox genes is required for embryonic root development in Arabidopsis. Curr Biol 19:1485–1490

Guilfoyle TJ, Hagen G (2007) Auxin response factors. Curr Opin Plant Biol 10:453–460

Hardtke CS, Ckurshumova W, Vidaurre DP, Singh SA, Stamatiou G, Tiwari SB, Hagen G, Guilfoyle TJ, Berleth T (2004) Overlapping and non-redundant functions of the Arabidopsis auxin response factors MONOPTEROS and NONPHOTOTROPIC HYPOCOTYL 4. Development 131:1089–1100

Helariutta Y, Fukaki H, Wysocka-Diller J, Nakajima K, Jung J, Sena G, Hauser MT, Benfey PN (2000) The SHORT-ROOT gene controls radial patterning of the Arabidopsis root through radial signaling. Cell 101:555–567

Heylighen F (2001) The science of self-organization and adaptivity. In: Kiel LD (ed) Knowledge management, organizational intelligence and learning, and complexity. The encyclopedia of life support systems. Eolss Publishers, Oxford

Hobe M, Müller R, Grünewald M, Brand U, Simon R (2003) Loss of CLE40, a protein functionally equivalent to the stem cell restricting signal CLV3, enhances root waving in Arabidopsis. Dev Genes Evol 213:371–381

Izhaki A, Bowman JL (2007) KANADI and class III HD-Zip gene families regulate embryo patterning and modulate auxin flow during embryogenesis in Arabidopsis. Plant Cell 19:495–508

Jaeger J, Irons D, Monk N (2008) Regulative feedback in pattern formation: towards a general relativistic theory of positional information. Development 135:3175–3183

Jones B, Gunnerås SA, Petersson SV, Tarkowski P, Graham N, May S, Dolezal K, Sandberg G, Ljung K (2010) Cytokinin regulation of auxin synthesis in Arabidopsis involves a homeostatic feedback loop regulated via auxin and cytokinin signal transduction. Plant Cell 22:2956–2969

Kepinski S, Leyser O (2005) The Arabidopsis F-box protein TIR1 is an auxin receptor. Nature 435:446–451

Kim YS, Kim SG, Lee M, Lee I, Park HY, Seo PJ, Jung JH, Kwon EJ, Suh SW, Paek KH, Park CM (2008) HD-ZIP III activity is modulated by competitive inhibitors via a feedback loop in Arabidopsis shoot apical meristem development. Plant Cell 20:920–933

Kitano H (2002) Computational systems biology. Nature 420: 206–210

Kitano H (2004) Biological robustness. Nat Rev Genet 5:826–837

Kitano H (2007) Towards a theory of biological robustness. Mol Syst Biol 3:137

Kondo Y, Hirakawa Y, Kieber JJ, Fukuda H (2011) CLE peptides can negatively regulate protoxylem vessel formation via cytokinin signaling. Plant Cell Physiol 52:37–48

Levesque MP, Vernoux T, Busch W, Cui H, Wang JY, Blilou I, Hassan H, Nakajima K, Matsumoto N, Lohmann JU, Scheres B, Benfey PN (2006) Whole-genome analysis of the SHORT-ROOT developmental pathway in Arabidopsis. PLoS Biol 4:e143

Leyser O (2011) Auxin, self-organisation, and the colonial nature of plants. Curr Biol 21:R331–R337

Lucas M, Swarup R, Paponov IA, Swarup K, Casimiro I, Lake D, Peret B, Zappala S, Mairhofer S, Whitworth M, Wang J, Ljung K,

Marchant A, Sandberg G, Holdsworth MJ, Palme K, Pridmore T, Mooney S, Bennett MJ (2011) Short-Root regulates primary, lateral, and adventitious root development in Arabidopsis. Plant Physiol 155:384–398

Matsuzaki Y, Ogawa-Ohnishi M, Mori A, Matsubayashi Y (2010) Secreted peptide signals required for maintenance of root stem cell niche in Arabidopsis. Science 329:1065–1067

Mironova VV, Omelyanchuk NA, Yosiphon G, Fadeev SI, Kolchanov NA, Mjolsness E, Likhoshvai VA (2010) A plausible mechanism for auxin patterning along the developing root. BMC Syst Biol 4:98

Mitchell M (2009) Complexity: a guided tour. Oxford University Press, Oxford

Mitrophanov AY, Groisman EA (2008) Positive feedback in cellular control systems. BioEssays 30:542–555

Miyashima S, Koi S, Hashimoto T, Nakajima K (2011) Non-cell-autonomous microRNA165 acts in a dose-dependent manner to regulate multiple differentiation status in the Arabidopsis root. Development 138:2303–2313

Mockaitis K, Estelle M (2008) Auxin receptors and plant development: a new signaling paradigm. Annu Rev Cell Dev Biol 24:55–80

Müller B, Sheen J (2008) Cytokinin and auxin interaction in root stem-cell specification during early embryogenesis. Nature 453:1094–1097

Nordström A, Tarkowski P, Tarkowska D, Norbaek R, Astot C, Dolezal K, Sandberg G (2004) Auxin regulation of cytokinin biosynthesis in *Arabidopsis thaliana*: a factor of potential importance for auxin-cytokinin-regulated development. Proc Natl Acad Sci USA 101:8039–8044

Ogasawara H, Kaimi R, Colasanti J, Kozaki A (2011) Activity of transcription factor JACKDAW is essential for SHR/SCR-dependent activation of SCARECROW and MAGPIE and is modulated by reciprocal interactions with MAGPIE, SCARECROW and SHORT ROOT. Plant Mol Biol 77:489–499

Ortega-Martínez O, Pernas M, Carol RJ, Dolan L (2007) Ethylene modulates stem cell division in the *Arabidopsis thaliana* root. Science 317:507–510

Paponov IA, Paponov M, Menges M, Teale W, Chakrabortee S, Murray JA, Palme K (2008) Comprehensive transcriptome analysis of auxin responses in Arabidopsis. Mol Plant 1:321–337

Parry G, Calderon-Villalobos LI, Prigge M, Peret B, Dharmasiri S, Itoh H, Lechner E, Gray WM, Bennett M, Estelle M (2009) Complex regulation of the TIR1/AFB family of auxin receptors. Proc Natl Acad Sci USA 106:22540–22545

Petersson SV, Johansson AI, Kowalczyk M, Makoveychuk A, Wang JY, Moritz T, Grebe M, Benfey PN, Sandberg G, Ljung K (2009) An auxin gradient and maximum in the Arabidopsis root apex shown by high-resolution cell-specific analysis of IAA distribution and synthesis. Plant Cell 21:1659–1668

Prigogine I (1978) Time, structure, and fluctuations. Science 201: 777–785

Rademacher EH, Möller B, Lokerse AS, Llavata-Peris CI, van den Berg W, Weijers D (2011) A cellular expression map of the Arabidopsis AUXIN RESPONSE FACTOR gene family. Plant J 68:597–606

Rademacher EH, Lokerse AS, Schlereth A, Llavata-Peris CI, Bayer M, Kientz M, Freire Rios A, Borst JW, Lukowitz W, Jürgens G, Weijers D (2012) Different auxin response machineries control distinct cell fates in the early plant embryo. Dev Cell 22:211–222

Rahman A, Amakawa T, Goto N, Tsurumi S (2001) Auxin is a positive regulator for ethylene-mediated response in the growth of Arabidopsis roots. Plant Cell Physiol 42:301–307

Ruzicka K, Ljung K, Vanneste S, Podhorská R, Beeckman T, Friml J, Benková E (2007) Ethylene regulates root growth through effects on auxin biosynthesis and transport-dependent auxin distribution. Plant Cell 19:2197–2212

Ruzicka K, Simásková M, Duclercq J, Petrásek J, Zazímalová E, Simon S, Friml J, Van Montagu MC, Benková E (2009) Cytokinin regulates root meristem activity via modulation of the polar auxin transport. Proc Natl Acad Sci USA 106:4284–4289

Sablowski R (2011) Plant stem cell niches: from signalling to execution. Curr Opin Plant Biol 14:4–9

Sarkar AK, Luijten M, Miyashima S, Lenhard M, Hashimoto T, Nakajima K, Scheres B, Heidstra R, Laux T (2007) Conserved factors regulate signalling in *Arabidopsis thaliana* shoot and root stem cell organizers. Nature 446:811–814

Sauer M, Balla J, Luschnig C, Wisniewska J, Reinöhl V, Friml J, Benková E (2006) Canalization of auxin flow by Aux/IAA-ARF-dependent feedback regulation of PIN polarity. Genes Dev 20:2902–2911

Scheres B (2007) Stem-cell niches: nursery rhymes across kingdoms. Nat Rev Mol Cell Biol 8:345–354

Seeley TD (2002) When is self-organization used in biological systems? Biol Bull 202:314–318

Sena G, Wang X, Liu HY, Hofhuis H, Birnbaum KD (2009) Organ regeneration does not require a functional stem cell niche in plants. Nature 457:1150–1153

Shen WH, Xu L (2009) Chromatin remodeling in stem cell maintenance in *Arabidopsis thaliana*. Mol Plant 2:600–609

Smith ZR, Long JA (2010) Control of Arabidopsis apical-basal embryo polarity by antagonistic transcription factors. Nature 464:423–426

Song SK, Hofhuis H, Lee MM, Clark SE (2008) Key divisions in the early *Arabidopsis embryo* require POL and PLL1 phosphatases to establish the root stem cell organizer and vascular axis. Dev Cell 15:98–109

Sozzani R, Cui H, Moreno-Risueno MA, Busch W, Van Norman JM, Vernoux T, Brady SM, Dewitte W, Murray JA, Benfey PN (2010) Spatiotemporal regulation of cell-cycle genes by SHORTROOT links patterning and growth. Nature 466:128–132

Stahl Y, Wink RH, Ingram GC, Simon R (2009) A signaling module controlling the stem cell niche in Arabidopsis root meristems. Curr Biol 19:909–914

Stepanova AN, Hoyt JM, Hamilton AA, Alonso JM (2005) A Link between ethylene and auxin uncovered by the characterization of two root-specific ethylene-insensitive mutants in Arabidopsis. Plant Cell 17:2230–2242

Stepanova AN, Yun J, Likhacheva AV, Alonso JM (2007) Multilevel interactions between ethylene and auxin in Arabidopsis roots. Plant Cell 19:2169–2185

Stepanova AN, Robertson-Hoyt J, Yun J, Benavente LM, Xie DY, Dolezal K, Schlereth A, Jürgens G, Alonso JM (2008) TAA1-mediated auxin biosynthesis is essential for hormone crosstalk and plant development. Cell 133:177–191

Strogatz SH (2001) Exploring complex networks. Nature 410: 268–276

Sugimoto K, Jiao Y, Meyerowitz EM (2010) Arabidopsis regeneration from multiple tissues occurs via a root development pathway. Dev Cell 18:463–471

Swarup R, Perry P, Hagenbeek D, Van Der Straeten D, Beemster GT, Sandberg G, Bhalerao R, Ljung K, Bennett MJ (2007) Ethylene upregulates auxin biosynthesis in Arabidopsis seedlings to enhance inhibition of root cell elongation. Plant Cell 19: 2186–2196

Ten Tusscher KH, Hogeweg P (2011) Evolution of networks for body plan patterning; interplay of modularity, robustness and evolvability. PLoS Comput Biol 7:e1002208

Tiwari SB, Wang XJ, Hagen G, Guilfoyle TJ (2001) AUX/IAA proteins are active repressors, and their stability and activity are modulated by auxin. Plant Cell 13:2809–2822

Tsuchisaka A, Theologis A (2004) Unique and overlapping expression patterns among the Arabidopsis 1-amino-cyclopropane-1-carboxylate synthase gene family members. Plant Physiol 136: 2982–3000

Ulmasov T, Hagen G, Guilfoyle TJ (1999) Dimerization and DNA binding of auxin response factors. Plant J 19:309–319

van den Berg C, Willemsen V, Hage W, Weisbeek P, Scheres B (1995) Cell fate in the Arabidopsis root meristem determined by directional signalling. Nature 378:62–65

van den Berg C, Willemsen V, Hendriks G, Weisbeek P, Scheres B (1997) Short-range control of cell differentiation in the Arabidopsis root meristem. Nature 390:287–289

Vernoux T, Brunoud G, Farcot E, Morin V, Van den Daele H, Legrand J, Oliva M, Das P, Larrieu A, Wells D, Guédon Y, Armitage L, Picard F, Guyomarc'h S, Cellier C, Parry G, Koumproglou R, Doonan JH, Estelle M, Godin C, Kepinski S, Bennett M, De Veylder L, Traas J (2011) The auxin signalling network translates dynamic input into robust patterning at the shoot apex. Mol Syst Biol 7:508

Vieten A, Vanneste S, Wisniewska J, Benková E, Benjamins R, Beeckman T, Luschnig C, Friml J (2005) Functional redundancy of PIN proteins is accompanied by auxin-dependent cross-regulation of PIN expression. Development 132:4521–4531

von Dassow G, Munro E (1999) Modularity in animal development and evolution: elements of a conceptual framework for Evo-Devo. J Exp Zool 285:307–325

Wagner A, Fell DA (2001) The small world inside large metabolic networks. Proc Biol Sci 268:1803–1810

Wagner GP, Pavlicev M, Cheverud JM (2007) The road to modularity. Nat Rev Genet 8:921–931

Wang JW, Wang LJ, Mao YB, Cai WJ, Xue HW, Chen XY (2005) Control of root cap formation by MicroRNA-targeted auxin response factors in Arabidopsis. Plant Cell 17:2204–2216

Watts DJ, Strogatz SH (1998) Collective dynamics of 'small-world' networks. Nature 393:440–442

Welch D, Hassan H, Blilou I, Immink R, Heidstra R, Scheres B (2007) Arabidopsis JACKDAW and MAGPIE zinc finger proteins delimit asymmetric cell division and stabilize tissue boundaries by restricting SHORT-ROOT action. Genes Dev 21:2196–2204

Whitacre JM (2012) Biological robustness: paradigms, mechanisms, and systems principles. Front Genet 3:67

Xu J, Hofhuis H, Heidstra R, Sauer M, Friml J, Scheres B (2006) A molecular framework for plant regeneration. Science 311:385–388

Zhang H, Han W, De Smet I, Talboys P, Loya R, Hassan A, Rong H, Jürgens G, Paul Knox J, Wang MH (2010) ABA promotes quiescence of the quiescent centre and suppresses stem cell differentiation in the Arabidopsis primary root meristem. Plant J 64:764–774

Zhang W, To JP, Cheng CY, Eric Schaller G, Kieber JJ (2011) Type-A response regulators are required for proper root apical meristem function through post-transcriptional regulation of PIN auxin efflux carriers. Plant J 68:1–10

Zhou GK, Kubo M, Zhong R, Demura T, Ye ZH (2007) Overexpression of miR165 affects apical meristem formation, organ polarity establishment and vascular development in Arabidopsis. Plant Cell Physiol 48:391–404

Zhou W, Wei L, Xu J, Zhai Q, Jiang H, Chen R, Chen Q, Sun J, Chu J, Zhu L, Liu CM, Li C (2010) Arabidopsis Tyrosylprotein sulfotransferase acts in the auxin/PLETHORA pathway in regulating postembryonic maintenance of the root stem cell niche. Plant Cell 22:3692–3709

Zhou ZY, Zhang CG, Wu L, Zhang CG, Chai J, Wang M, Jha A, Jia PF, Cui SJ, Yang M, Chen R, Guo GQ (2011) Functional characterization of the CKRC1/TAA1 gene and dissection of hormonal actions in the Arabidopsis root. Plant J 66:516–527

2.3.- Modelos matemático-computacionales y redes de regulación genética

La complejidad de los sistemas biológicos y en este caso específico, la complejidad de los procesos moleculares involucrados en el desarrollo y mantenimiento del nicho de células troncales de la raíz, ha motivado el comienzo de nuevos proyectos interdisciplinarios (ver Azpeitia y Alvarez-Buylla 2012) para comprender mejor el desarrollo y la evolución (e.g., Salazar-Ciudad 2006; Lander et al., 2011; Jaeger et al., 2012). Además, debido a que ésta complejidad muchas veces excede la capacidad humana para entenderlos en su globalidad, las herramientas matemático-computacionales se han ido convirtiendo en un herramienta imprescindible para el análisis de estos procesos (Weiss et al., 2003; ten Tusscher y Scheres 2011; Liberman et al., 2012).

Una de las herramientas matemático-computacionales más utilizadas para estudiar estos procesos son las redes de regulación genética. Las redes (en general) se pueden estudiar tanto desde un punto de vista estructural, como desde uno dinámico (Barabasi y Oltvai 2004). Aunque los análisis estructurales y dinámicos son complementarios, se suelen llevar a cabo de forma independiente. Los análisis estructurales normalmente se llevan a cabo en redes muy grandes y sirven sobre todo para conocer las propiedades generales de la topología de la red. Esta incluye estudiar si son de mundo pequeño, caracterizar su modularidad, o recabar datos de centralidad, entre otros (Barabasi y Oltvai 2004; Alvarez-Buylla et al., 2007). Por otra parte, los análisis dinámicos generalmente se hacen en redes más pequeñas y sirven para analizar el comportamiento del sistema a lo largo del tiempo. Por ejemplo, se pueden estudiar los estados estables de la red, los cuales deben coincidir con estados biológicamente significativos, como los son las configuraciones genéticas observadas en los distintos tipos celulares (Alvarez-Buylla 2007).

Las redes dinámicas han sido utilizadas con éxito para estudiar una gran gama de procesos en diferentes organismos, así como para analizar propiedades genéricas de las redes o cuestiones teóricas. Por ejemplo, se han usado para estudiar el desarrollo de los órganos florales (Espinosa-Soto et al., 2004; Alvarez-Buylla et al., 2010), el patrón de la epidermis de *A. thaliana* (Benítez y Alvarez-Buylla 2010; Benítez et al., 2013), el patrón de los genes de segmentación de *Drosophila* (Albert

y Othmer 2003), el ciclo celular en animales (Faure et al., 2006), levadura (Davidich y Bornholdt 2008; Faure et al., 2009) y plantas (Ortiz y colaboradores, comunicación personal), enfermedades como la anemia de falconi (Rodríguez et al., 2012), la apoptosis (Schaltter et al., 2009), la evolución de los patrones corporales (ten Tusscher y Hogeweg 2011), por mencionar algunos.

Es importante notar que se han comenzado a utilizar aproximaciones computacionales y redes de regulación genética, tanto a nivel estructural como dinámico para el estudio de las plantas. Por ejemplo, se han utilizado para estudiar el transporte de auxinas en diferentes órganos (Grieneissen et al., 2007; Stoma et al., 2008; Mironova et al., 2012; Barrio et al., 2013), el patrón de filotaxis (Reinhardt et al., 2003; Jönsson et al., 2006; Smith et al., 2006; Mirabet et al., 2012), la dominancia apical (Prusinkiewicz et al., 2007; Shinohara et al., 2013), el mantenimiento del nicho de tallo (Gordon et al., 2009; Chickarmane et al., 2012), las vías de señalización (Díaz y Alvarez-Buylla 2006; Bugs et al., 2011; Sankar et al., 2011), entre muchos más. Durante mi doctorado, me enfoqué en abordar el estudio de la formación de patrones celulares en el nicho de células troncales con este enfoque, y también colaboré en otros estudios relacionados, logrando concretar varias publicaciones (Alvarez-Buylla et al., 2010; Benítez et al., 2013; Barrio et al., 2013). Copia de dichas publicaciones se encuentra en el apéndice.

Por último, es importante resaltar que debido al fuerte incremento en el uso de redes para el estudio de los procesos moleculares, en los últimos años estos han avanzado mucho, permitiendo ahora hacer una gran cantidad de análisis (e.g., Wang et al., 2012). Muchos de estos análisis ya se encuentran automatizados gracias a la generación de software especializado para el análisis de redes o de simulaciones de sistemas biológicos (e.g., Müssel et al., 2010; Arellano et al., 2011; Boudon et al., 2012; Swat et al., 2012). El software de Arellano y colaboradores (2011), se desarrolló en colaboración con el laboratorio, al igual que otros trabajos donde pude colaborar, esta publicación se encuentran en el apéndice de la tesis.

En mi proyecto use herramientas matemático-computacionales para estudiar los procesos moleculares, especialmente la red de regulación genética, involucrada en el mantenimiento y desarrollo del nicho de células troncales. Los objetivos principales fueron comprender como se establecen los diferentes tipos celulares

que conforman el nicho, tanto de forma temporal como de forma espacio-temporal. En este proyecto usamos principalmente el formalismo de redes dinámicas, para analizar los procesos moleculares involucrados en el mantenimiento, desarrollo y localización del nicho de raíz. Sin embargo también analizamos algunas propiedades genéricas de las redes dinámicas y proponemos un conjunto de procedimientos para detectar información faltante o errónea en redes biológicas, así como para verificar si es posible explicar resultados experimentales a partir de la topología de una red dada. Finalmente, en colaboración con la estudiante de maestría Mónica García, modelamos la red en un espacio bidimensional, lo que nos permitió comenzar a estudiar cómo interactúa la red con procesos como el transporte hormonal.

3.- Hipótesis y objetivo general

A lo largo de mi proyecto doctoral se trabajó bajo una hipótesis general que explico en este capítulo. En cada uno de los capítulos y artículos de mi proyecto, además se plantearon y probaron varias hipótesis y objetivos particulares que se plantean y explican en las secciones correspondientes.

El objetivo general fue estudiar los mecanismos moleculares que sustentan el establecimiento y mantenimiento de los patrones celulares del nicho de células madre de raíz, a través de modelos temporales y espacio-temporales de la red de regulación genética del nicho de células troncales de raíz, anclados en datos experimentales. Los modelos se validaron comparando los resultados de simular la red sin alteraciones y mutada, con los perfiles de activación genética observados de forma experimental en el nicho de la raíz, en las plantas silvestres y en las alteradas, respectivamente. Dichos modelos fueron utilizados para comprender la dinámica acoplada de los mecanismos involucrados en el establecimiento y mantenimiento de la estructura celular del nicho, así como para saber si la información experimental es suficiente para explicar los comportamientos observados experimentalmente para los genes hasta ahora estudiados. Cuando la información no fue suficiente, los modelos se utilizados para detectar y predecir información faltante, así como información errónea.

Por lo tanto, la hipótesis general que guió el trabajo es que los atractores de los modelos de red postulados corresponderán, tanto de forma temporal como espacial, a los perfiles de expresión genética encontrados experimentalmente en los distintos tipos celulares en el nicho de células troncales de la raíz de la planta silvestre, como de la planta con diferentes genes mutados.

4.- Métodos

4.1. Introducción al modelaje de las redes dinámicas de regulación genética

Los detalles generales de cómo se construye una red y cómo se hacen los análisis más generales fueron revisados en Azpeitia y colaboradores (2014). El capítulo de Springer se presenta más adelante en la subsección 4.2. de los Métodos. Dado que el capítulo de Springer revisa los análisis más tradicionales de una red, algunos de los análisis hechos durante nuestro trabajo no se describen allí. El detalle de estos análisis se encuentra dentro de cada uno de sus capítulos específicos. Aquí presentamos una introducción al formalismo de redes, el cual fue la base del desarrollo de este proyecto.

En las redes biomoleculares los nodos representan las diferentes moléculas (e.g., genes, RNA, proteínas, miRNAs). Los nodos son las variables, entradas y salidas de la red y pueden tomar valores discretos o continuos. El valor de un nodo también puede representar diferentes cosas, como la presencia o la concentración de una proteína, de RNA o de complejos proteínicos y las ligas representan cómo es que interactúan los nodos. Las interacciones puedes ser adireccionales o direccionales, las cuales se usan para representar diferentes tipos de interacciones. Por ejemplo, las interacciones físicas, como cuando se forma un dímero, se representa con las ligas adireccionales, mientras que las regulaciones transcripcionales se representan con ligas direccionales. En las ligas direccionales, las flechas generalmente representan activaciones y las uniones "chatas" inhibiciones (e.g., Azpeitia et al., 2010).

Hay varios formalismos para modelar y analizar redes de forma dinámica (de Jong 2002). En las redes dinámicas, el estado de expresión de cada uno de los genes de la red cambia con el tiempo de acuerdo a:

$$x_i(t+\tau) = F_i(x_{i_1}(t), x_{i_2}(t), \ldots, x_{i_k}(t)). \qquad (1)$$

En esta ecuación, $x_i(t+\tau)$ es el estado del gen i en el tiempo $(t+\tau)$, donde τ puede ser un número real positivo o un entero positivo. $\{x_{i_1}(t), x_{i_2}(t), \ldots, x_{i_k}(t)\}$ son los reguladores del gen x_i, y F_i es una función que se describe la acción combinatoria de los reguladores de x_i.

Los modelos Booleanos son la aproximación más simple de red dinámica y son el formalismo más usado a lo largo de esta tesis. Los modelos Booleanos de redes de regulación genética han demostrado ser útiles para dilucidar la lógica de regulación genética e integrar la acción concertada de muchos genes (Alvarez-Buylla et al., 2007; Wang et al., 2012). Por este motivo, han sido empleados para estudiar una gran cantidad de procesos exitosamente (e.g., Espinosa-Soto et al., 2004; Benítez y Alvarez-Buylla 2010; Rodríguez et al., 2012).

En las redes Booleanas, sólo existen dos estados posibles de un nodo: activo y desactivado. Formalmente, decimos que cada gen se representa por una variable Booleana, x que toma el valor de $x = 1$, si está activo o expresado, y toma el valor $x = 0$, si no lo está. El estado de todos los genes de la red queda definido por un vector: $\{x_1, x_2, \ldots, x_n\}$, donde x_n es el estado de expresión del n^{th} gen de la red, y n es igual al número total de genes en la red.

En las redes Booleanas τ tiene el valor de un entero positivo y la ecuación (1) está definida por reglas lógicas, también conocidas como tablas de verdad o expresiones Booleanas. Éstas definen las reglas de evolución dinámica de la transición de activación de cada uno de los genes de la red en función de sus entradas, de una iteración a la siguiente y se derivan de los datos experimentales, por lo tanto, cada gen tendrá su propia función Booleana. El número total de estados del sistema es finito ($\Omega = 2^n$), y entonces, bajo la dinámica regida por la ecuación (1), la red eventualmente regresará a un estado previamente visitado. La red puede entonces entrar en un patrón cíclico, o quedar fijo en un estado puntual; estos estados corresponden a los atractores cíclicos o de punto fijo, respectivamente. Todas las condiciones iniciales que llevan a un atractor, constituyen su cuenca de atracción y una vez que se llega a un atractor en una dinámica definida por la ecuación (1), el sistema queda ahí indefinidamente.

De acuerdo a S. Kauffman, los atractores corresponderán a los patrones de expresión genética observados experimentalmente (Kauffman 1969). Esta hipótesis ha sido validada en innumerables ocasiones. Una vez obtenidos los atractores, una forma de continuar validando los modelos de redes genéticas, es con un análisis de robustez observando el efecto de pequeños cambios sobre los

atractores del sistema (Espinosa-Soto et al., 2004; Alvarez-Buylla et al., 2007). Si a pesar de las modificaciones se recuperan los mismos atractores, se considera que el modelo es robusto. También se pueden simular mutaciones en el modelo y observar si se recuperan los atractores que corresponden a los perfiles genéticos observados en las plantas con la mutación simulada (Alvarez-Buylla et al., 2007).

Aunque las redes Booleanas son excelentes herramientas para analizar la dinámica de los procesos moleculares, pero su uso está restringido a análisis discretos y cualitativos. Una aproximación muy común que soluciona dichas limitaciones, aunque complica la modelación, son las redes continuas, que generalmente se modelan utilizando sistemas de ecuaciones diferenciales. En estos sistemas el valor de un nodo esta dado por:

$$\frac{dx_i(t+\tau)}{dt} = F_i(x_{i_1}(t), x_{i_2}(t), \ldots, x_{i_k}(t)). \qquad (2)$$

donde $\frac{dx_i}{dt}$ representa el cambio en la expresión/concentración de un nodo, el cual esta dado por F_i. En estos sistemas tanto el tiempo como el valor de los nodos toman valores reales positivos, lo que permite elaborar modelos que den valores realistas de la expresión/concentración de los nodos a lo largo del tiempo; resolviendo así, algunas de las limitaciones de las redes Booleanas.

Ahora presentamos el capítulo de Springer, donde se describe con mayor detalle como se construyen y como se analiza la dinámica de una red (Azpeitia et al., 2014).

Chapter 26

Gene Regulatory Network Models for Floral Organ Determination

Eugenio Azpeitia, José Davila-Velderrain, Carlos Villarreal, and Elena R. Alvarez-Buylla

Abstract

Understanding how genotypes map unto phenotypes implies an integrative understanding of the processes regulating cell differentiation and morphogenesis, which comprise development. Such a task requires the use of theoretical and computational approaches to integrate and follow the concerted action of multiple genetic and nongenetic components that hold highly nonlinear interactions. Gene regulatory network (GRN) models have been proposed to approach such task. GRN models have become very useful to understand how such types of interactions restrict the multi-gene expression patterns that characterize different cell-fates. More recently, such temporal single-cell models have been extended to recover the temporal and spatial components of morphogenesis. Since the complete genomic GRN is still unknown and intractable for any organism, and some clear developmental modules have been identified, we focus here on the analysis of well-curated and experimentally grounded small GRN modules. One of the first experimentally grounded GRN that was proposed and validated corresponds to the regulatory module involved in floral organ determination. In this chapter we use this GRN as an example of the methodologies involved in: (1) formalizing and integrating molecular genetic data into the logical functions (Boolean functions) that rule gene interactions and dynamics in a Boolean GRN; (2) the algorithms and computational approaches used to recover the steady-states that correspond to each cell type, as well as the set of initial GRN configurations that lead to each one of such states (i.e., basins of attraction); (3) the approaches used to validate a GRN model using wild type and mutant or overexpression data, or to test the robustness of the GRN being proposed; (4) some of the methods that have been used to incorporate random fluctuations in the GRN Boolean functions and enable stochastic GRN models to address the temporal sequence with which gene configurations and cell fates are attained; (5) the methodologies used to approximate discrete Boolean GRN to continuous systems and their use in further dynamic analyses. The methodologies explained for the GRN of floral organ determination developed here in detail can be applied to any other functional developmental module.

Key words Gene regulatory networks, Functional module, Flower development, Cell differentiation, Attractors, Morphogenesis, Dynamics, Floral organ determination, Attractors, Basins of attraction, Stochastic networks, Mathematical models, Computational simulations, Robustness

---

Eugenio Azpeitia, José Davila-Velderrain, and Carlos Villarreal contributed equally to this work.

José Luis Riechmann and Frank Wellmer (eds.), *Flower Development: Methods and Protocols*, Methods in Molecular Biology, vol. 1110, DOI 10.1007/978-1-4614-9408-9_26,

1 Introduction

The mapping of the genotype unto the phenotypes implies the concerted action of multiple components during cell differentiation and morphogenesis that comprise development [1]. These components are part of regulatory motifs, which hold nonlinear interactions that produce complex behaviors [2, 3]. Such complexity cannot be understood in terms of individual components, and rather emerges as a result of the interactions among the components of the whole system. In order to integrate the action of multiple molecular components and follow their dynamics, it is indispensable to postulate mathematical and computational models. Gene regulatory network (GRN) models have appeared as one of the most powerful tools for the study of complex molecular systems. Small GRNs can sometimes be studied with analytical mathematical formulations, while medium or large size GRNs are amenable for dynamical analyses only with computer simulations [4]. As following the dynamics of the genomic interactomes is still intractable even with the most powerful computers, and given the fact that genomic networks are composed of multiple structural and functional modules, others and we have proposed to search for such modules for the study of biomolecular systems dynamics using GRN models (e.g., [5–7]).

Boolean models are probably the simplest type of formalism employed for the study of GRNs. Nonetheless, Boolean models provide meaningful information about the system. Importantly, Boolean GRNs can be approximated to continuous models that enable the use of additional mathematical tools [4, 8]. Given that: (a) the logic of GRNs is adequately formalized with Boolean models; (b) obtaining real biological parameters from biological molecular systems is still a complicated task; and (c) the use of realistic models can be computationally expensive, we believe that Boolean models and their continuous approximations are becoming a fundamental and practical tool to study GRN dynamics and to understand the complex behaviors observed in developmental processes (*see* refs. 9–11).

Based on the above rationale, the first step in building a GRN model is the identification of a developmental module and the integration of all the experimental data on the molecular components participating in it. The ABC genetic model of floral organ determination (*see* refs. 3, 12) (*see* Chapter 1) is part of a clearly circumscribed developmental module that underlies the subdifferentiation of the floral meristem in four concentric rings early on during flower development. From the outermost part of the floral meristem to its center, each ring comprises the primordial cells of sepals, petals, stamens, and carpels. Based on experimental

evidence [13], it became obvious that although necessary, the ABC genes are not sufficient to specify floral organs. The ABC model has been instrumental to understanding flower development and evolution. However, it does not constitute a dynamic model able to recover the ABC combinatory code, as well as explain how the expression profiles of the set of molecular components included in the flower organ determination GRN, which includes the ABC genes, is established to promote the sepal, petal, stamen and carpel cell fates. Importantly, such a dynamic GRN model is the basis to understand how such cell types are determined in time and space, and thus, how the morphogenetic pattern that characterizes young floral meristems will form adult flowers [12, 14].

In order to uncover the necessary and sufficient set of interacting components involved in floral organ specification, the first step implies recovering the experimental evidence of ABC gene interacting components that include both regulated and regulator genes. In the case of Boolean models, the experimental data is formalized in the form of Boolean functions, which determine the dynamics of the GRN. In Boolean or any other type of discrete network, it is possible to fully explore the whole set of configurations or states of the system, and find the steady state configurations (attractors; see below). Kauffman postulated that the attractors to which GRNs converge, could correspond to the states characterizing differentiated cells [15]. More recently, Boolean GRNs have been grounded on experimental data ([5]; *see* review in ref. 3) showing that the attractors of developmental networks indeed correspond to the stable gene configuration observed in different types of cells, as long as a sufficient set of components involved in a given developmental module are incorporated.

In this Chapter we focus on the regulatory module underlying floral organ determination in *Arabidopsis thaliana* during early stages of flower development. Some of the methodologies explained here have been used in previous publications on such GRN [5, 7, 16–19]. In this chapter we will use examples extracted mainly from our own studies to explain how to develop and extend experimentally supported Boolean GRN models. Then, we explain how to incorporate stochastic properties in the model, which can allow us to explore the temporal sequence with which attractors or cell gene configurations and cell-fates are attained (e.g., [4]). Finally, we explain how we can approximate the Boolean model to a continuous one that can then be used in other types of models, for example, to explore spatial aspects of morphogenesis [14]. It is important to keep in mind that the tools presented in this Chapter can be applied to any GRN. Consequently, we begin with general explanations and afterwards we use examples from the literature to illustrate each methodological step.

2 Methods

2.1 Definitions

GRN nodes and edges: In GRNs, nodes represent genes, proteins or other types of molecular components such as miRNAs and hormones, while edges represent regulatory interactions among the components. Usually the interactions are positive (activations) or negative (inhibitions), but other type of interactions can be included (e.g., protein-protein interactions).

Variables: Variables are the elements that describe the system under study (usually the nodes) and which can take different values at each time.

Variable/Gene state: The value that a node takes at a certain time represents its state. The state can be a discrete or continuous value. In the case of Boolean networks the states can only be "0" when "OFF" and "1" when "ON."

Network State/Configuration: The vector composed by a set of values, where each value corresponds to the state of a specific gene of the network. In a Boolean network such vectors or network configurations are arrays of "0's" and "1's."

Attractors: Stationary network configurations are known as attractors. Single-state, stationary configurations are known as fixed-point attractors (Fig. 1a) and these are generally the ones that correspond to the arrays of gene activation states that characterize

a

Time	GEN1	GEN2	GEN3
1	1	0	0
2	1	0	0
3	1	0	0
.			
.			
.			
n-1	1	0	0
n	1	0	0

Fixed-point attractor

b

Time	GEN1	GEN2	GEN3
1	0	1	1
2	1	0	1
3	0	1	1
.			
.			
.			
n-1	1	0	1
n	0	1	1

Cyclic attractor

c

Time	GEN1	GEN2	GEN3
1	1	1	1
2	1	1	0
3	0	0	1
.			
.			
.			
n-1	0	0	0
n	0	1	0

Transitory states

Fig. 1 Fixed-point attractors, cyclic attractors, and transitory states. (**a**) An example of a fixed-point attractor. As observed, fixed-point attractors have one unique state where they stay indefinitely unless something perturbs them. (**b**) An example of a cyclic attractor. Cyclic attractors are composed of two or more network states that orderly repeat. In this case we observe a two state cyclic attractor. (**c**) Transitory states. Transitory states are states that lead to an attractor, but are not attractors themselves

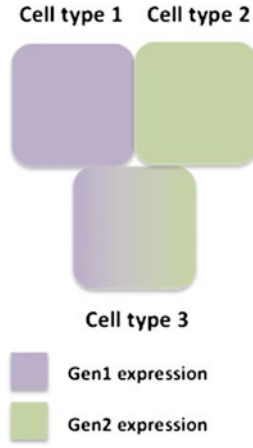

Expected attractors	GEN1	GEN2
Cell type 1	1	0
Cell type 2	0	1
Cell type 3	1	1

Fig. 2 The set of expected attractors. As explained in the main text, the set of expected attractors is obtained from the experimental information. In the case of cell types, the attractors correspond to the observed stable gene configuration of each cell type. Thus, if our system consists in three different cell types, one cell type with GEN1 expression, other with GEN2 expression, and a third one with both GEN1 and GEN2 expression, our set of expected attractors will be exactly this

different cell types. Whereas a set of network states that orderly repeat cyclically correspond to cyclic attractors (Fig. 1b).

Transitory states: All states that are not or do not form part of an attractor are transient or transitory states (Fig. 1c).

Basin of attraction: The set of all the initial configurations that eventually lead to a particular attractor constitute its basin of attraction.

Expected or observed attractors: Gene expression profiles or configurations that have been obtained from experimental assays and reported in the scientific literature for particular cell types are referred to here as the expected or observed attractors. Such attractors are expected to be recovered by the postulated GRN (Fig. 2).

Model Validation: The task of evaluating a model by means of contrasting its predictions with experimental results. For Boolean GRNs, model validation would imply, among others: recovering the observed gene configurations for the cells under study under *wt* and mutant or overexpression conditions, robustness analyses, etc. (see below).

Robustness: The ability of a system to maintain an output in the face of perturbations. For the case of a Boolean GRN model, it is evaluated, for example, by assessing if the system's attractors are still recovered under different transient and permanent mutations (alterations in the Boolean functions, nodes, or GRN topology).

2.2 General Protocol

A generic protocol to postulate a GRN model for a particular developmental module would be as follows:

(i) Identify a structural or functional developmental module (*see* **Note 1**).

(ii) Based on available experimental data, select the set of potential nodes or molecular components that will be incorporated in the GRN model with the aim of integrating the key necessary and sufficient components of the functional module under analysis. Then, explore the experimental data concerning the spatio-temporal expression patterns of the genes to be incorporated in the model and assemble a table with a Boolean format of the expected configurations that should be recovered with the GRN model (such configurations are the "expected attractors") (*see* **Note 2**).

(iii) Integrate and formalize the experimental data concerning the interactions among the selected nodes using Boolean logical functions that will rule the Boolean GRN dynamics.

(iv) The GRN is modeled as a dynamic system by exploring the states attained, given all possible initial configurations and the Boolean functions defined in (iii). The GRN is initialized in all possible configurations and followed until it reaches a fixed-point or cyclic attractor (*see* **Note 3**).

(v) Compare the simulated attractors to the ones observed experimentally (expected attractors; *see* **item** (**ii**) above). A perfect coincidence would suggest that a sufficient set of molecular components (nodes) and a fairly correct set of interactions have been considered in the postulated GRN model. If this is not the case, additional components and interactions can be incorporated or postulated, or the Boolean functions can be modified. This allows to refine interpretations of experimental data, or to postulate novel interactions to be tested experimentally in the future. In any case, the process can be repeated several times based on the dynamical behavior of the modified versions of the GRN under study until a regulatory module is postulated. Such module can include some novel hypothetical interactions or components, integrate available experimental data, and identify possible experimental contradictions or holes.

(vi) To validate the model, it is addressed if it recovers the *wt* and mutant (loss of function and gain of function) gene activation configurations that characterize the cells being considered. Perturbation analyses of the nodes and interactions, or the Boolean functions, can also be used for validating the model in order to test the robustness of the GRN under study. Eventually, novel predictions can be made and tested experimentally.

(vii) To recover the dynamics of the GRN and the temporal pattern of attractor attainment, the logical functions can be modeled as stochastic ones. Observed temporal patterns of cell-fate or gene configurations attainment can be used to validate the GRN model under consideration.

(viii) For further applications and also in cases that continuous functions are appropriate to describe the behavior of some of the components, the Boolean model can be approximated to a continuous one (*see* Subheading 2.5). Besides being useful for further modeling procedures, the continuous approximation is also a means of performing a robustness analysis of the GRN under study. Such a task hence implies as well a further validation of the model being postulated.

(ix) Equivalent approaches to the ones summarized in (vi) and (vii) for discrete systems can be used in continuous ones.

There are two types of materials needed when modeling dynamic GRNs. First, the expected results to be recovered by the model that are extracted from the literature and depend on the aims of the model and the nature of the developmental module being considered, but generally include stable gene configurations (attractors), mutant phenotypes, and developmental transitions, to name a few. The second set is the software required for the analyses of the GRN. Currently there are several available programs for GRN analyses (*see* **Note 8**). In the following sections, we explain with more detail and specific examples how this general protocol can be applied. We start by explaining the simplest Boolean approach for dynamical GRN modeling.

2.3 Deterministic Boolean GRN Model

In Boolean GRN models, nodes can only attain one of two possible values: "1" if the node is "ON," and "0" if the node is "OFF." A "0" node value usually represents that a gene is not being expressed, but can also represent the absence of a protein or hormone, while a "1" node value represents that a gene is expressed or another type of molecular component is present. As mentioned above, the first step in building a network is to extract the necessary experimental information to define the set of components to be considered in the GRN model, the set of expected attractors, and the Boolean functions that formally integrate the experimental data and define the dynamics of the GRN.

2.3.1 Expected Attractors

In Boolean GRNs, the network states (*see* Subheading 2.1) are defined by vectors of 0s and 1s. While a formal mathematical definition of attractors can be found on the chapter "Implicit Methods for Qualitative Modeling of Gene Regulatory Networks" of another Springer Protocols book [20], in Subheading 2.1 we give a more pragmatic definition of attractors, and we prefer to stick to it. In 1969, Kauffman proposed that the attractors of a GRN model

could correspond to stable gene configurations characteristic of particular cell types or physiological states (*see* Subheading 2.1; Fig. 2). Consequently, the expected attractors are defined from gene expression patterns obtained from the literature, as well as from other data sources that clearly define the spatio-temporal gene configuration of the system. For example, Espinosa-Soto and collaborators [7] defined the expected attractors from the gene expression patterns reported in scientific publications. In another study, La Rota and collaborators [19] integrated experimental data into a gene expression map for the sepal primordium. Based on its expression map they defined zones with different combinations of gene expression, and each zone corresponded to an expected attractor. Defining the expected set of attractors is an indispensable step when building the GRN model, because they are used to validate the GRN (see below). Although it should be clear that the postulation of the Boolean functions is an independent task, and hence, it does not imply circularity.

2.3.2 Boolean Functions

In a Boolean GRN model the state of expression of each gene changes along time according to the dynamic equation

$$x_i(t+\tau) = f_i\left(x_1(t), x_2(t), \ldots, x_k(t)\right), \tag{1}$$

in which the future state of gene i evolves temporally as a function of the current state of its k regulators. Boolean functions f_i can be formalized as logical statements or as truth tables. Logical statements use the logical operators "AND," "OR" and "NOT" to describe gene interactions, while in truth tables the state of the gene of interest is given for all possible state combinations of its k regulators (*see* **Note 4**). Logical operators can be combined in order to describe complex gene regulatory interactions, and can always be translated into an equivalent truth table. In Fig. 3, we provide examples of common gene regulatory interactions formalized as logical statements with their equivalent truth table. Consequently, in general, Boolean functions are generated from experimental evidence (but *see* **Note 5**). For example, if TGEN (a target gene) is ectopically expressed in a GEN1 loss-of-function background, it is inferred that GEN1 is a negative regulator of TGEN, and we use the "NOT" logical operator to describe GEN1 regulation over TGEN or its equivalent truth table (Fig. 4). In this Boolean function, the state of TGEN at time $t+\tau$ is 1 if GEN1 value is 0 at time t, and TGEN value at time $t+\tau$ is 0 if GEN1 value is 1 at time t (*see* **Note 6**).

The Boolean functions of the GRN developmental module being used here as an example, were grounded on available experimental information [5, 7, 17–19]. As with expected attractors, Boolean functions can be grounded on different types of experimental data, as long as they clearly state how genes interact (*see* **Note 7**). We now will provide an example of how the

GEN1(t)	GEN2(t)	TGEN(t+τ)
0	0	0
0	1	0
1	0	0
1	1	1

TGEN(t+τ) = GEN1(t) & GEN2(t)

GEN1(t)	GEN2(t)	TGEN(t+τ)
0	0	0
0	1	1
1	0	1
1	1	1

TGEN(t+τ) = GEN1(t) | GEN2(t)

GEN1(t)	GEN2(t)	TGEN(t+τ)
0	0	0
0	1	0
1	0	1
1	1	0

TGEN(t+τ) = GEN1(t) & ! GEN2(t)

GEN1(t)	GEN2(t)	TGEN(t+τ)
0	0	0
0	1	1
1	0	0
1	1	0

TGEN(t+τ) = ! GEN1(t) & GEN2(t)

Fig. 3 Examples of common Boolean functions. Here we present four examples of common Boolean functions for a target gene, in this case TGEN, with two regulators, namely, GEN1 and GEN2

experimental information was integrated and formalized as a Boolean function. During the transition from inflorescence to flower meristem, the expression of *TERMINAL FLOWER 1* (*TFL1*) needs to be repressed [21, 22], because *TFL1* is a promoter of inflorescence development [23]. *TFL1* is transcribed in the center of the meristem and from there it moves to peripheral cells [24]. *EMF1* is assumed to be a positive regulator of *TFL1* because the *emf1* mutant is epistatic to *tfl1* loss-of-function mutant, and both, *tfl1* and *emf1* mutants have similar phenotypes in terms of inflorescence meristem identity [25]. The over expression phenotype of *AP1* is similar to the loss-of-function of *TFL1*, and in the *ap1* mutant *TFL1* is ectopically expressed, suggesting that *AP1* is a negative regulator of *TFL1* [26]. Similarly, *TFL1* expression is not observed in *LFY* over expression and is ectopically expressed in *LFY* loss-of-function mutants [27]. According to these results, *EMF1* is a positive regulator of *TFL1*, while *AP1* and *LFY* are

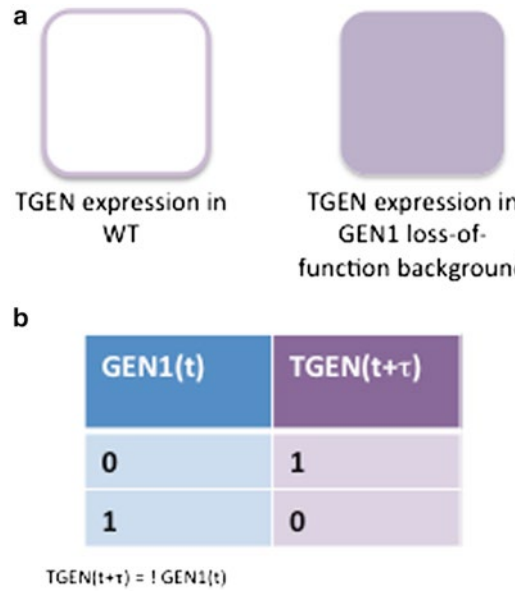

Fig. 4 Truth table and logical statement of the example explained in the main text. (**a**) TGEN expression is not observed in the GEN1 loss-of-function background. Hence, we can assume that GEN1 is a negative regulator of TGEN. This Boolean function can be represented with a (**b**) truth tab. or a (**c**) logical statement

negative regulators of *TFL1*. These results were formalized as a logical statement [18] as follows:

$$TFL1 = EMF1\ AND\ NOT\ AP1\ AND\ NOT\ LFY$$

A complete list of the Boolean functions and the experimental evidence for this model can be found in refs. 7, 18; *note some typographical errors corrected in* refs. 1, 12.

2.3.3 Validating the GRN: Simulated Attractors vs. Expected Attractors

Once the Boolean functions and the set of expected attractors of the GRN are obtained, we can proceed to make a first, necessary validation of the GRN. The first step is to use numerical simulations to recover the attractors that our set of Boolean functions generates (*see* **Note 8**). The attractors recovered in the simulations must coincide with the expected attractors, based on experimental data. In Espinosa-Soto and collaborators [7] ten attractors were recovered. Four out of the ten attractors corresponded to gene activation configurations that characterize meristematic cells of inflorescence meristems, while the rest corresponded to the gene configurations observed in sepal, petal, stamen and carpel primordial cells (Fig. 5). In the GRN for sepal development formulated by La Rota and collaborators [19], at least two attractors were recovered; one corresponding to the abaxial and the other one to the adaxial cells of the floral organ.

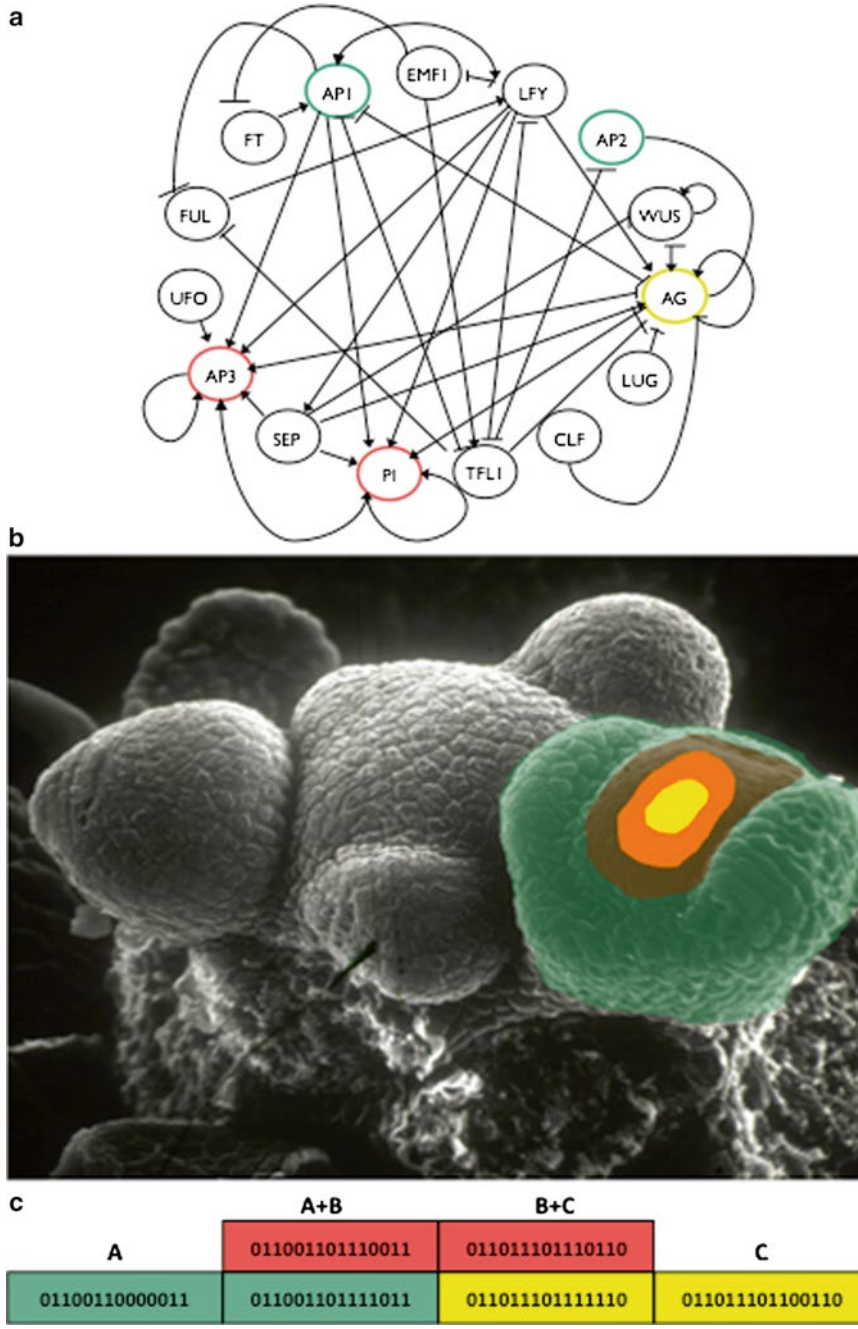

Fig. 5 Obtained attractors of the flower organ specification GRN. In (**a**) we present the graph of the flower organ specification GRN proposed by Espinosa-Soto and collaborators [7]. The GRN recovered 10 fixed-point attractors. Six of the attractors corresponded to the observed gene configuration in the primordial cell of sepals (one attractor), petals (two attractors), statements (two attractors), and carpels (one attractor). (**b**) A flower meristem in which the primordial sepal cells are colored in *green*, primordial petal cells in *brown grey*, primordial stamens in *orange*, and primordial carpel cells in *yellow*. In (**c**), the ABC model and the floral organ determination GRN attractors that correspond to A, A + B, B + C, and C gene combinations, which specify sepal, petal, stamen, and carpel primordial cells, respectively. The activation states correspond to each of the GRN nodes starting on the left with "EMF1" and consecutively progressing clockwise the rest of the genes in the GRN shown in (**a**)

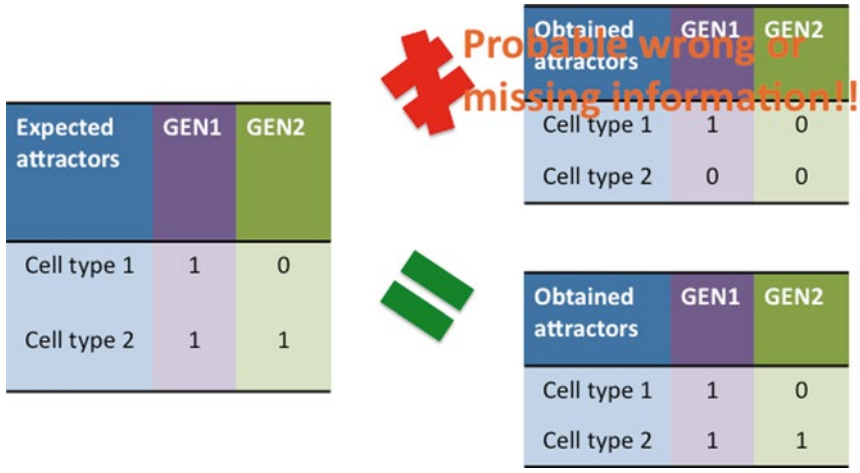

Fig. 6 The set of expected attractors vs. the set of obtained attractors. Both the set of expected and obtained attractors must coincide, when this do not happens it is usually assumed that there is some wrong or missing information

In cases in which the attractors recovered by the simulated GRN under study and those observed experimentally do not coincide, additional nodes or interactions can be considered, or the postulated Boolean functions can be modified (Fig. 6). Such novel hypotheses can be tested by running the GRN dynamics once more, and if the simulated and observed (expected) attractors now coincide, the model can be used to postulate novel interactions, missing data, or contradictions among those that had been proposed previously. For example, in Espinosa-Soto and collaborators [7] four missing interactions were predicted. Importantly, some of these predictions have been experimentally validated by independent and posterior research, demonstrating the predictive capacity and usefulness of this approach.

2.3.4 *Mutant Analysis*

An additional means to validate a GRN model is to simulate loss-of-function (fixing the mutated gene expression value to 0) and gain-of-function (fixing the overexpressed gene expression value to 1) mutants. The recovered attractors in the model with such altered fixed expression values must correspond to the effects experimentally observed in the corresponding mutants (*see* Fig. 7; **Note 9**). If a discrepancy is found in such a validation process, additional hypotheses concerning new nodes or interactions can be postulated. For the postulated GRN module underlying floral organ determination, most of the recovered attractors in the simulated mutants corresponded to the genetic configurations that have been observed experimentally [7, 17, 18]. In some cases, the simulated and observed (expected) attractors did not coincide and new interactions were postulated. For example, in Espinosa-Soto and collaborators [7] a positive feedback loop was predicted for the

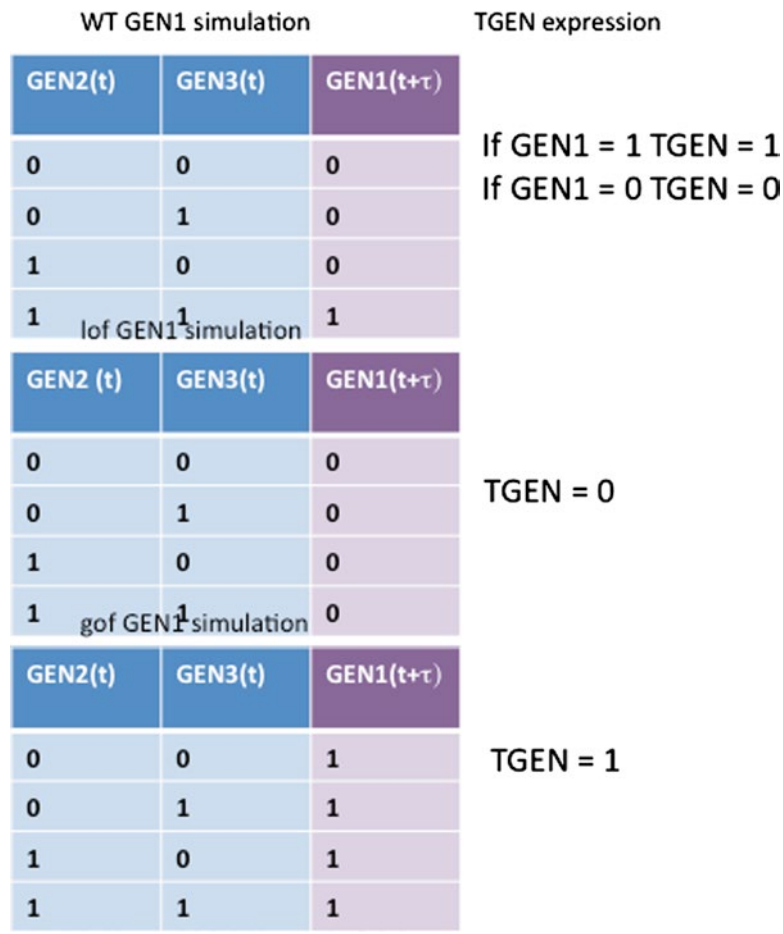

Fig. 7 Loss-of-function and gain of function mutant simulations. Loss-of-function and gain-of-function mutant simulations are done by fixing the state of the desired gene to 0 and 1, respectively. In (**a**) the Boolean function of a non-mutated GEN1. In (**b**) and (**c**) the Boolean function of the same gene in a loss-of-function and a gain-of-function simulation, respectively. The Boolean functions are presented as truth tables and as logical statements. lof = loss-of-function, gof = gain-of-function

gene *AGAMOUS* (*AG*), even though this seemed unlikely because in the *ag-1* loss-of-function mutant plants, the *AG* expression pattern is the same as in wild-type plants [28]. In a posterior study in an independent laboratory, the prediction was verified experimentally [29].

Simulations of mutants are also useful when trying to predict the effects of multiple mutants, which are complicated to generate in the laboratory. Moreover, even when the GRN involved in flower determination in *Arabidopsis* and *Petunia* seems to be conserved, the mutant phenotypes are not identical. Espinosa-Soto and collaborators [7] used mutant analyses to test the effect of a

duplication in B genes that has been reported in *Petunia*, and recovered the single mutant that had been described, and at the same time predicted the expected phenotype for the double mutant of the two duplicates.

2.3.5 Robustness Analyses

Experimental and theoretical work has demonstrated that living organisms are robust against perturbations. Moreover, at the molecular level the processes involved in different biological behaviors are also robust against internal and external variations. Such robustness implies that the overall functionality of the system remains when perturbed [30, 31]. In the case of GRNs, attractors should be robust when the Boolean functions are altered. In Espinosa-Soto and collaborators [7] the output value of every line of the truth tables was changed one by one. Interestingly, we found that the original attractors did not change for more than 95 % of the logical table alterations, indicating that the functionality of the postulated developmental module is robust to this type of perturbation. There are other types of perturbation analyses. For example, we could change with a certain probability the value of a line of the truth table, or the state of the network. Similarly, if we perturb the GRN with these other types of perturbations, the systems' attractors are expected to be maintained.

2.4 Stochastic Boolean GRN Model: Temporal Sequence of Cell-Fate Attainment

In deterministic GRN models, as the Boolean model exposed above, the system under study always converges to a single attractor if initialized from the same configuration, and once it attains such steady-state, it remains there indefinitely. However, during a developmental process, cells change from one stable cell configuration to another one in particular temporal and spatial or morphogenetic patterns. In order to explore questions such as how differentiating cells decide between one of the available attractors, or the order in which the system converges to the different attractors, given an initial condition, and to make statistical predictions of such possible behaviors, a stochastic formalism is needed.

In this section we develop a discrete stochastic model as an extension of the deterministic Boolean GRN. We then show how this approach can be used to explore the patterns of cell-fate attainment. Specifically, the model formalism explained here allows the investigation of the temporal sequence with which attractors are visited in the GRN when noise or random perturbations drive the system from one attractor to any other one.

2.4.1 From Deterministic to Stochastic Models

In a Boolean GRN model the dynamics given by Eq. 1 is deterministic: for a given set of Boolean functions f_i (*see* Subheading 2.3.2), the configuration of the network at time t completely determines the configuration of the network at the next time step $t+1$ (conventionally $\tau = 1$). If Eq. 1 is iterated starting from a given initial configuration (defined by an array of n entries with 0s and 1s

representing the activation states of the n genes), the network will eventually converge to an attractor. This deterministic version implies that once the system reaches an attractor, it remains there for all subsequent iterations. However, if noise is introduced into either the Boolean functions, or the gene states, there is a finite probability for the system to "jump" from one basin of attraction to another one (for definitions, *see* Subheading 2.1) and consequently, from one attractor to another one. Such a stochastic Boolean model of the GRN enables the study of transitions among attractors.

Noise can be implemented in a Boolean GRN model in several ways (*see* **Note 10**). Here we implement noise by introducing a constant probability of error ξ for the deterministic Boolean functions. In other words, at each time step, each gene "disobeys" its Boolean function with probability ξ, such that in the stochastic version, Eq. 1 is extended to

$$x_i(t+\tau) = \begin{cases} f_i(t), & \textit{with prob.} 1-\xi \\ 1-f_i(t) & \textit{with prob.} \xi \end{cases} \quad (2)$$

Note that the stochastic version (e.g., Eq. 2) reduces to a deterministic one (Eq. 1)) when $\xi = 0$. In the model, the stochastic perturbations are applied independently and individually to each gene at each iteration. This implementation of noise for stochastic Boolean modeling of GRNs has been referred to as the stochasticity in nodes (SIN) model with the assumption of a single fault at a time [20, 32].

2.4.2 The Transition Probability Matrix

When Eq. 2 is iterated, both the set of Boolean functions f_i and the error probability ξ determine the configuration of the network at the next time step. Under this stochastic dynamics, a given initial configuration will no longer converge to the same attractor each time. This situation allows us to estimate a probability of transition from one network state to another state as the frequency with which this transition occurs in a large number of repetitions of the same iteration (see below). The estimated transition probabilities can then be used to study the behavior of the system and to make statistical predictions.

As we want the model to be useful in the exploration of the patterns of temporal cell-fate attainment, the network states that we are interested in are the fixed-point attractor states that represent the cell types. Thus, we need to estimate the probability p_{ij} of transition from the attractor i to the attractor j. From the deterministic Boolean model, we already know to which attractors the network converges. In the following we use the term attractor to refer to both, the attractor and its basin. Thus, we can define a scalar (single-valued) variable X_t to describe the state of the network in terms of the specific attractor in which the network is in at

time t. Then, X_t will take at time t any value from the ordered set $(1,2,i,\ldots,K)$ where each i represents one specific attractor from the available k attractors. The configuration of the network at time t is then related to the configuration at time $t+1$ through what is known as the transition probabilities. If the network is in attractor i at time t, at the next time step $t+1$, it will either stay in attractor i or move to another attractor j.

Formally, p_{ij} denotes a one-step transition probability that is defined as the following conditional probability:

$$p_{ij} = Prob\{X_{t+1} = j / X_t = i\}, \tag{3}$$

the probability that the network at time $t+1$ is in the attractor j given that it was in the attractor i at the previous time t, where $i,j=1,2,\ldots,K$ for K attractors. The set of probabilities p_{ij} can be expressed in matrix form:

$$P = \begin{pmatrix} p_{11} & \cdots & p_{1k} \\ \vdots & \ddots & \vdots \\ p_{k1} & \cdots & p_{kk} \end{pmatrix}.$$

As the number of attractors K is finite, P is a $K \times K$ transition matrix. Operationally, under the current model, one can estimate the probabilities of the i-th row by first iterating Eq. 2 one time step starting from a given initial configuration corresponding to the basin of attraction of attractor i. If, after the iteration, the system remains in the same attractor, or the same basin of attraction, one count is added to the diagonal entry that corresponds to P_{ii}. If the configuration ends up in a different basin j, the count is added to the column j that corresponds to p_{ij}. This process is repeated a large number of times (e.g., 10,000) for each of the possible $\Omega = 2^n$ initial conditions. For each state (attractor), the one-step transition probabilities should satisfy $\sum_{j=i}^{K} p_{ij} = 1$ and $p_{ij} \geq 0$. This means that in the transition matrix P, the rows must sum to 1. This is achieved by dividing the number of counts in each matrix entry by the total number of configurations that started in the corresponding matrix row (e.g., basin i). As the dynamics in Eq. 2 are driven by both the Boolean functions f_i and the error probability ξ, given a fixed set of Boolean functions, different values of ξ will result in different values of the transition probabilities p_{ij} (*see* **Note 11**).

2.4.3 The Probabilistic Dynamics of Cell-Fate Attainment

Once the transition matrix P is calculated, it can be used in a dynamic model to describe how the probability of being in a particular attractor changes in time. In other words, we are now in position to derive a probabilistic dynamic model to simulate the dynamics of temporal cell-fate attainment.

In the previous subsection, the dynamics of transition between attractor states were defined in terms of transition probabilities.

When this is the case, the state of the network at any given time X_t can only be represented by its associated discrete probability distribution. We denote this distribution by the vector $p_X(t) = (p_1(t), p_2(t), \ldots, p_K(t))$, where $p_i(t)$ represents the probability of the network being in attractor i at time t, and $\sum_{i=i}^{K} p_i(t) = 1$.

Given $p_X(t)$, the probability distribution associated with X_{t+1} can be found by multiplying the transition matrix P by $p_X(t)$. We obtain the following dynamic equation

$$p_X(t+1) = p_X(t)P, \tag{4}$$

this latter equation projects the process forward in time, and it allows us to follow the dynamics of the probabilities of cell-fate attainment by means of straightforward iteration.

In order to do so, it is necessary to specify an initial vector $p_X(t=0)$ which represents the probability distribution of the network state at time $t=0$. In biological terms, this initial vector can be interpreted as the representation of how a large population of cells is distributed over the available attractors. In other words, how many cells of each type are in the population at the initial time $t=0$. As the probabilities p_i sum to one, an underlying assumption is that the number of cells in the population remains constant. In the next subsection we show how this initial distribution can be chosen based on a biological motivation in order to explore a specific question regarding the dynamics of cell-fate attainment during floral organ formation. When the matrix P and the initial vector $p_X(0)$ are specified, Eq. 4 can be iterated (*see* **Note 12**); this process will generate a trajectory for the temporal evolution of the probability of each of the attractors. Every attractor will have a maximum in the probability of being reached at particular times. This maximum corresponds to the moment at which the corresponding cell-fate is most likely. Thus, the order in which the maximal probability of the different attractors is reached may serve as an intrinsic explanation for the emerging temporal order during early stages of development. Note that, as the transition probabilities of the matrix P depend on the value of ξ used in Eq. 2, the trajectories for the probability of attractor attainment will vary for different values of the error probability ξ.

2.4.4 Temporal Cell-Fate Pattern During Early Stages of Flower Development

In this subsection we show how the modeling formalism presented above can be applied to propose mechanistic explanations of observed patterns of temporal cell-fate attainment. In the modeling framework presented here, stochasticity may seem just as a modeling artifact that allows the study of transitions among attractors. However, a multitude of studies have demonstrated both theoretically and experimentally that stochasticity and the so-called biological noise are ubiquitously present in biological systems given the chemical nature of biological processes (for example *see* refs. 33–36).

Table 1
Example of a transition matrix *P* estimated from the GRN model for the floral organ determination of *A. thaliana*. The matrix elements are the transition probabilities among pairs of the six attractors (S, P1, P2, S1, S2, and C). Probabilities where calculated in Alvarez-Buylla et al. [4] using ($\xi = 0.01$)

	sep	pe1	pe2	st1	st2	car
sep	0.939395	0.001943	0.009571	0.000083	0.000490	0.048517
pe1	0.036925	0.904162	0.009250	0.033900	0.000488	0.015275
pe2	0.009067	0.000464	0.941609	0.000024	0.048374	0.000461
st1	0.000084	0.001893	0.000020	0.936514	0.009960	0.051530
st2	0.000020	0.000001	0.002074	0.000356	0.987953	0.009597
car	0.002045	0.000034	0.000020	0.001951	0.010020	0.985930

Under the hypothesis that random fluctuations in a system may be important for cell behavior and pattern formation, Alvarez-Buylla and collaborators proposed a discrete stochastic model to address whether noisy perturbations of the GRN model for the floral organ determination of *A. thaliana* are sufficient to recover the stereotypical temporal pattern in gene expression during flower development [4]. As mentioned above, previous analysis of the deterministic Boolean GRN showed that the system converges only to ten fixed-point attractors, which correspond to the main cell types observed during early flower development [7]. Six of the attractors correspond to the four floral organ primordial cells within the flower meristem: sepals, petals, stamens, and carpels (S, P1, P2, S1, S2, and C).

Following Subheading 2.4.2, we can study the dynamics of cell-fate attainment of the floral organ primordial cells by defining a variable X_t which can take as a value any of the attractors (S, P1, P2, S1, S2, and C) at each time t. Then, given the six attractors of interest, we would like to estimate the transition matrix P, with the transition probabilities p_{ij} of transition from attractor i to attractor j as components. This matrix can be estimated by iterating Eq. 2 and following the algorithm described in Subheading 2.4.2. Alvarez-Buylla and collaborators [4] followed a similar approach, and estimated the matrix P shown in Table 1. This matrix was estimated using a value of 0.01 for the probability of error ξ in Eq. 2.

We follow the temporal evolution of the probability of reaching each attractor by iterating Eq. 4 using as P the matrix just estimated (*see* Table 1). However, as mentioned in Subheading 2.4.3, it is necessary to specify an initial distribution $p_X(0)$, which defines what fraction of the whole cell population corresponds to each of the cell-types (S, P1, P2, S1, S2, and C) at the initial time of the

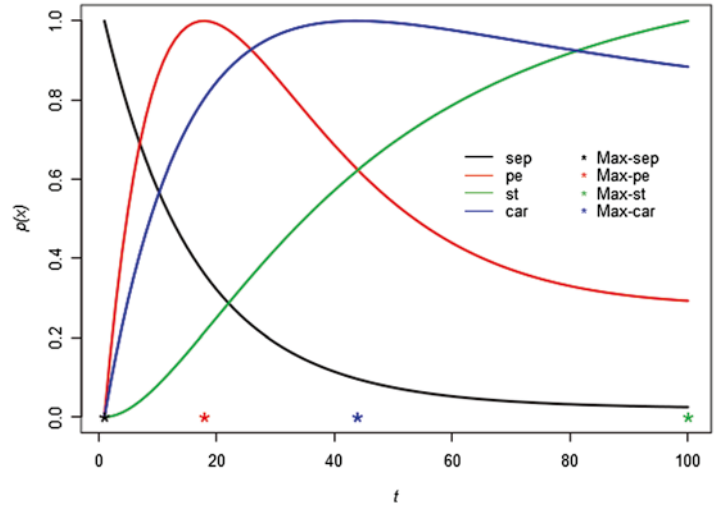

Fig. 8 Temporal sequence of cell-fate attainment pattern under the stochastic Boolean GRN model. Maximum relative probability p of attaining each attractor, as a function of time (in iteration steps). The value of the error probability used was $\xi = 0.01$. *Stars* mark the time when maximal probability of each attractor occurs. The most probable sequence of cell attainment: sepals, petals, carpels, and stamens

simulation. Since sepal primordial cells are the first to attain their fate in flower development, we use as an initial distribution a vector in which the value corresponding to the fraction of sepal cells is set to 1 and all the other values are set to zero; this is $p_X(0) = (1,0,0,0,0,0)$, where the order of the values is (S, P1, P2, S1, S2, and C). Thus, initially, all of the population of cells within a floral primordium is in the sepal attractor. Then, Eq. 4 can be iterated to follow the changes in the probability of reaching each one of the other attractors over time, given that the entire system started in the sepal configuration. The resulting normalized trajectories for the case in point are shown in Fig. 8 (*see* **Note 13**). The graph clearly shows how the trajectory for each of the attractor's probability reaches its maximum at a given time. One star for each of the attractors was drawn in the graph just above the x-axis at the time when its maximal probability occurs. In accordance with biological observations, the results show that the most probable sequence of cell attainment is: sepals, petals, and the stamens and carpels almost concomitantly.

The results presented here were calculated using just one value for the probability of error ($\xi = 0.001$). In the work of Alvarez-Buylla and collaborators [4], it was shown that the system exhibited a sequence of transitions among attractors that mimics the sequence of gene activation configurations observed in real flowers for a level of noise (value of ξ) of around 0.5–10 % (*see* **Note 11**).

The nonintuitive, constructive role of moderated noise perturbing the dynamics of nonlinear systems is a well-known phenomenon in physics [37]. Currently, there is a growing interest in understanding the interplay between noise and the nonlinearity of biological networks [38]. Using the model formalism presented here, Alvarez-Buylla and collaborators concluded that the stereotypical temporal pattern with which floral organs are determined may result from a stochastic dynamic system associated with a highly nonlinear GRN [4]. In the light of these findings, the modeling framework exposed in this section constitutes a simple approach to understanding morphogenesis, providing predictions on the population dynamics of cells with different genetic configurations during development.

2.5 Approximation to a Continuous GRN Model

2.5.1 Deterministic Approach

Boolean GRNs have been useful to study the complex logic of transcriptional regulation involved in cell differentiation because it seems that the qualitative topology of such networks, rather than the detailed form of the kinetic functions of gene interactions, rule the attractors reached. However, for some further mathematical developments and also for studies of the detailed behavior of GRN dynamics, the differences in genetic expression decay rates, threshold expression values, saturation rates, and other quantitative aspects of GRNs can become very relevant. These aspects of GRNs cannot be contemplated by a discrete approach. Hence, it becomes necessary to investigate also continuous representations of GRN dynamics. Several studies reviewed here show that such continuous approximations of the discrete GRNs lead to novel predictions, but at the same time recover consistent results with those arising in the Boolean framework.

Several approaches have been used to describe the Boolean GRN as a continuous system. A well-known scheme is the piecewise linear Glass dynamics of the network [39]. This model is based on a set of differential equations in which each continuous variable x_i, representing the level of expression of a given gene, has an associated discrete variable that represents the state of expression of that gene. This is accomplished by introducing the discrete variables $\hat{x}_i$ defined as $\hat{x}_i = H\left(x_i - \theta_i\right)$, where θ_i represents a threshold, and $H(x)$ is the Heaviside step function: $H(x) = 1$ if $x > 1$, and $H(x) = 0$ if $x < 1$. This definition implies that gene n displays a dichotomic expression driven by a more gradual continuous dynamics. The piece-wise continuous Glass dynamics of the GRN is described by

$$\frac{\mathrm{d}\, x_i(t)}{\mathrm{d}\, t} = \mu\left[f_i\left(\hat{x}_1(t), \ldots, \hat{x}_k(t) \right) - x_i(t) \right] \tag{5}$$

where f_i are the input functions of the discrete Boolean model, and $\mu = 1/\tau$ is the relaxation rate of the gene expression profile. Within this description, the microscopic configuration of the GRN

at a given time is described by the set of continuous values $\{x_1(t),\ldots,x_k(t)\}$; this set induces in turn the set of corresponding discrete values $\{\check{x}_1(t),\ldots,\check{x}_k(t)\}$ as the Boolean configuration of the network. The equilibrium states of the GRN that determine a given phenotype may be obtained from the condition $dx_i/dt=0$, which leads to

$$x_i^S = f_i\left(\check{x}_1^S(t),\ldots,\check{x}_k^S(t)\right) \tag{6}$$

independently of the value of the relaxation rate. Even when the Boolean input functions f_i are the same in the discrete and continuous approaches, there are infinitely many microscopic configurations compatible with the same Boolean configuration, and the discrete model of the GRN and the corresponding continuous piece-wise linear model are not necessarily equivalent, since the attractors of the two models can be different. However, numerical simulations to study the GRN for floral organ differentiation in *A. thaliana*, show that the Glass dynamics generate exactly the same ten fixed-point attractors obtained in the Boolean model, although the size of the corresponding attraction basins may display some variation [4].

An alternative approach consists in considering that the input functions display a saturation behavior characterized by a logistic or a Hill function, usually employed in biochemistry to describe ligand saturation as a function of its concentration. In the first case, the input associated to node i may be included in the form

$$\Theta\left[f_i(x_1,,\ldots,,x_k)\right] = \frac{1}{1+\exp\left[-b_i\left[f_i(x_1,,\ldots,,x_k)-\in_i\right]\right]} \tag{7}$$

where $\in_i$ is a threshold level (usually $\in_i=1/2$), and b_i the input saturation rate. It may

be easily seen that for $b_i>>1$, the input function becomes a Heaviside step function:

$$\Theta\left[f_i-\in_i\right]\to H\left[f_i-\in_i\right], \tag{8}$$

and thus displays a dichotomic behavior (in practice this may be achieved for, e.g., $b_i>10$). This approach has been employed, for example, in the modeling of the GRN for differentiation of Th cells of the immune response by Mendoza and Xenarios [40], or in the study of floral organ specification in *A. thaliana* [1].

On the other hand, Hill-type inputs of GRNs have been employed in a number of investigations on biological development and differentiation (*see* the review in ref. 41). They have the following structure:

$$\Xi^{(n)}\left[f_i\right] = \frac{A_i\left(f_i\right)^n}{\left(\in_i\right)^n+\left(f_i\right)^n}, \tag{9}$$

with the parameter n, an integer number, and A_i the maximum asymptotic value attained by the input. The latter approach was used by Zhou et al. [42], to model pancreatic cell fates; and by Wang and coworkers [43] to study myeloid and erythroid cell fates. The approximation to be used depends on the nature of the problem under study. In fact, the GRN inputs could be described also by any set of polynomial functions that reflect the biological interactions of the network.

Another approach that can be used to translate the logical into continuous functions involves the use of "fuzzy logics" proposed by L. A. Zadeh [44] to study systems that do not follow strictly 1 or 0 truth-values. This is achieved by using the following rules

$$\begin{aligned} & x_i(t)\ and\ x_j(t) \to \min\left[x_i(t), x_j(t)\right] \\ & x_i(t)\ or\ x_j(t) \to \max\left[x_i(t), x_j(t)\right] \\ & not\ x_i(t) \to 1 - x_i(t) \end{aligned} \quad . \tag{10}$$

Here, the operators, min and max mean to choose between the minimum and maximum values of the functions x_i and x_j at a given time t. It can be shown that these rules lead to a Boolean algebra [1]. One possible disadvantage of this proposition is that it involves only piece-wise differential functions. Another possibility is to consider the following algorithm:

$$\begin{aligned} & x_i(t)\ and\ x_j(t) \to x_i(t) \cdot x_j(t) \\ & x_i(t)\ or\ x_j(t) \to x_i(t) + x_j(t) - x_i(t) \cdot x_j(t). \\ & not\ x_i(t) \to 1 - x_i(t) \end{aligned} \tag{11}$$

The structure of the expressions associated to the logical connectors "and" and "not" is obvious, while the expression for "or" is derived by substituting such expressions into De Morgan's law: not(x_i or x_j) = (not x_i) and (not x_j). As before, it may be straightforwardly checked that these rules define a Boolean algebra. For example, a logic input like

$$f_1 = (x_1\ or\ x_2)\ and\ not\ (x_3)$$

would read:

$$f_1 = (x_1 + x_2 - x_1 \cdot x_2)(1 - x_3).$$

We now proceed to write the equation for the GRN continuous dynamics. By assuming that the source of gene activation can be characterized, for example, by a logistic-type behavior, we may introduce the following set of differential equations:

$$\frac{\mathrm{d}x_i}{\mathrm{d}t} = \Theta\left[f_i(x_1,,\ldots,,x_k)\right] - \mu_i x_i \tag{12}$$

where $\mu_i = 1/\tau_i$ represents the expression decay rate of node i of the GRN. Notice that within this approach we consider that, in gen-

eral, each gene may have its own characteristic decay rate. This assumption introduces further richness into the description, as a hierarchy of times of genetic expression may define alternative routes to cell fates. In particular, notice that the steady states of the GRN, given by the condition $dx_i/dt = 0$, lead to the expression

$$x_i^S = \frac{1}{\mu_i}\Theta\left[f_i\left(x_1^S,,\ldots,,x_k^S\right)\right]. \tag{13}$$

Taking into account that the node inputs are defined by logical sentences with a Boolean architecture, then the attractor set obtained in this case is equivalent by construction to the set derived in the discrete Boolean approach. Thus, if a given attractor arising in the discrete Boolean approach has an expression pattern like $\{1,0,0,1,1,\ldots\}$, the corresponding pattern in the continuous approach would have the structure $\{1/\mu_i, 0, 0, 1/\mu_4, 1/\mu_5, \ldots\}$, so that they become identical when $\mu_i = 1$ (with the possible exception of some isolated attractors). The consideration of the several relaxation rates for gene expression dynamics introduces an important difference with respect to Glass dynamics. For example, in the case that a gene has a large decay rate, corresponding to $\mu_i >> 1$, then $x_i^S \to 0$, and the expression pattern would differ with that arising when $\mu_i = 1$. Then, the dynamic behavior of a gene with a large decay rate (short expression time) would be equivalent to an effective mutation associated to lack of functionality. Similarly, the case $\mu_i << 1$ would correspond to an over-expression of that gene. We conclude that the gene expression dynamics is not only regulated by the GRN interactions topology, but also by the hierarchy of relative expression times of its components.

On the other hand, the system also may acquire very different behaviors depending on the value of the saturation rate. As mentioned before, for $b_i >> 1$, the input function becomes a Heaviside step function. In the case, $b_i = 1$, the input function would show a softer behavior. It turns out that in this latter case the attractor set may change drastically with respect to that obtained in the Boolean-like case. This plasticity could be employed to study regulatory systems with a hybrid functionality consisting of transcriptional regulatory logics that are well described with Boolean GRN, and external or coupled signaling transduction pathways that have continuous behaviors and which can impact the dynamics of some of the GRN components.

3 Notes

1. A developmental module incorporates a set of necessary and sufficient molecular components for a particular cell differentiation or morphogenetic process. It is considered a module because it is largely robust to initial conditions and it attains

GEN1(t)	GEN2(t)	GEN3(t)	TGEN(t+τ)
0	0	0	0
0	0	1	0
0	1	0	0
0	1	1	0
1	0	0	0
1	0	1	1
1	1	0	1
1	1	1	1

$$
\begin{aligned}
&\mathrm{TGEN}(t+\tau) = \mathrm{GEN1}(t)\ \&\ (\mathrm{GEN2}(t)\ |\ \mathrm{GEN3}(t))\\
&\mathrm{TGEN}(t+\tau) = (\mathrm{GEN1}(t)\ \&\ \mathrm{GEN3}(t))\ |\\
&\qquad\qquad (\mathrm{GEN1}(t)\ \&\ \mathrm{GEN2}(t))\\
=\ &\mathrm{TGEN}(t+\tau) = (\mathrm{GEN1}(t)\ \&\ !\,\mathrm{GEN2}(t)\ \&\ \mathrm{GEN3}(t))\ |\\
&\qquad\qquad (\mathrm{GEN1}(t)\ \&\ \mathrm{GEN2}(t)\ \&\ !\,\mathrm{GEN3}(t))\ |\\
&\qquad\qquad (\mathrm{GEN1}(t)\ \&\ \mathrm{GEN2}(t)\ \&\ \mathrm{GEN3}(t))\\
&\mathrm{TGEN}(t+\tau) = !\,(\,!\,\mathrm{GEN1}(t)\ \&\ (\,!\,\mathrm{GEN2}(t)\ |\ !\,\mathrm{GEN3}(t)))
\end{aligned}
$$

Fig. 9 Equivalence between truth tables and logical statements. As observed each truth table have many equivalent logical statements while each logical statement is represented by a unique truth table

certain attractors robustly. The uncovered GRN underlying the ABC patterns of gene activation and the early subdifferentiation of the flower meristem into four concentric regions or primordial floral organ cells, thus constitutes a developmental model. Other developmental modules involved in flower development could be those involved in: the cellular subdifferentiation of each one of the floral organ primordia during organ maturation, determining floral organ number and spatial disposition, in the dorso-ventrality or shape of floral organs, ovule maturation, etc.

2. In the table that formalizes the experimental data, if the gene or protein is expressed register a "1," and if not a "0." If some components have expression patterns with cyclic behavior, they could be part of cyclic attractors. In some cases, a discrete network with more than two activation states can be postulated if deemed necessary. Quantitative variation in expression levels can be also incorporated later in a continuous model approximated from the discrete one.
3. Several other algorithms exist to numerically find the attractors of a Boolean Network in an efficient way. For examples, *see* ref. 20.
4. It is important to keep in mind that the "AND" and "OR" logical operators can be interconverted. For instance, the logical statement "GEN1 AND GEN2" is equivalent to the logical statement "NOT (NOT GEN1 OR NOT GEN2)." Because of this, most truth tables (except the simplest ones, like the constants) have many equivalent logical statements. Consequently, each Boolean function can be formalized as a unique truth table, but can be described with one or many equivalent logical statements (Fig. 9).
5. Sometimes, the experimental information is not enough to completely define the Boolean functions. For example, in La

Complete characterized Boolean function

GEN1(t)	GEN2(t)	TGEN(t+τ)
0	0	0
0	1	0
1	0	0
1	1	1

Incomplete characterized Boolean function

GEN1(t)	GEN2(t)	TGEN(t+τ)
0	0	*
0	1	0
1	0	0
1	1	1

Fig. 10 Complete and incomplete characterized Boolean functions. While in complete characterized Boolean functions the value of TGEN in all row of the truth tables is specified, in incomplete characterized Boolean functions in one or more rows of the truth table is not specified. Incomplete characterized Boolean function can be the result of missing information data, asynchrony or environmental perturbations and can be resolved with different approaches as explained in the main text

Rota and collaborators [19] Boolean functions were first generated considering only confirmed direct molecular interactions. However, gaps in the experimental information precluded the generation of a unique set of Boolean function determining the GRN. Consequently, they predicted possible interactions by looking for consensus binding sites in the promoters of the included nodes and introducing some speculative hypothesis of molecular interactions.

For example, imagine that TGEN expression disappears when you generate single loss-of-function alleles of GEN1 and GEN2, while TGEN expression is promoted if we over-express both GEN1 and GEN2. Consequently, we conclude that GEN1 and GEN2 are both positive and necessary regulators for TGEN expression. However, this experimental data do not say anything about what happens to TGEN expression in the simultaneous absence of GEN1 and GEN2. In such a case we would have an incompletely characterized Boolean Function (Fig. 10). Such incompletely characterized Boolean functions can also appear due to asynchrony and interactions with the environment [45]. The inclusion of asynchrony in the model provides a more realistic description of our system, while environmental inputs influence is pervasive in biological systems. Hence, the incorporation of incomplete Boolean functions in a model is an instrumental tool. There are many ways to approach this problem: we could test all possible Boolean functions (as in ref. 19), introduce asynchrony in our model, give a probability to each possible Boolean function, or even directly work with incomplete Boolean functions. Several free software programs are capable of considering asynchrony, probabilities for different logical functions or can work with incomplete Boolean functions, such as ANTELOPE [45] and BoolNet [46].

6. Sometimes we cannot represent the available experimental data with a Boolean formalism because we need more values to represent our nodes' activity. For example, imagine that GEN1 differentially affect TGEN in the loss-of function, when normally expressed and when over expressed. This can be resolved replacing the Boolean formalism with a multivalued or a continuous approach. In a multivalued approach, the nodes can take as many values as necessary. In the last example, we could allow GEN1 to have three values, namely, 0 when is OFF, 1 when is normally expressed and 2 when is over expressed. It is important to note that a Boolean formalism can be approximated to a continuous one as was explained in the last section of this paper. For example, Espinosa-Soto and collaborators [7] initially followed a multivalued modeling approach, which was later shown to yield the same qualitative results when transformed into a Boolean system [17]. Similar situations have been documented when transforming a continuous into a Boolean model (e.g., [6, 47]). Currently some software applications allow the analysis of discrete multivalued networks (e.g., GINSIM) [48].
7. As mentioned above, sometimes the experimental information is not enough to generate the Boolean function. We can also find contradictory information linked to particular gene interactions. For example, one author may report that GEN1 positively regulates TGEN, while another one may report that GEN1 is a negative regulator of TGEN. In cases like this, models are extremely helpful, even when they could be considered incomplete. With models we can test both suggestions in a fast and cheap way. The result that better reproduces the experimentally observed system's behavior should be considered the most likely hypothesis. For example, in La Rota and collaborators [19] GRN model of sepal primordium they generated multiple sets of Boolean functions describing their GRN and selected those that recovered the expected attractors and mutant phenotypes. At other times GRN models can be also used to explain apparent contradictions or disputes concerning the interpretation of experimental data.
8. There are several free software packages to recover the attractors and basins of attraction of Boolean GRN, including ANTELOPE [45], GINSIM [48], BoolNet [46], Atalia [12], GNbox [49], GNA [50], and BioCham [51].
9. It is important to note that recovering the expected attractors when the mutants are simulated does not guarantee that the model is correct, because networks with different topologies can sometimes reach the same attractors [52]. However, we can assure that a GRN model that is unable to reproduce all mutants is incorrect.

10. Although stochasticity in Boolean models of GRNs is commonly modeled using the SIN model (*see* Subheading 2.4.1), another method called the stochasticity in functions (SIF) has been introduced recently. The objective of this method is to model stochasticity at the level of biological functions (i.e., Boolean functions in the GRN), and not just by flipping the state of a gene as in the SIN model (for details *see* refs. 20, 32).
11. It could be the case that interesting, nontrivial behaviors may be uncovered just at certain levels of the error probability ξ (e.g., noise). Thus, as customary in numerical explorations, it is necessary to test different values of ξ. However, one expects generic, robust behavior to be observed under a relatively wide range of noise levels. Moreover, the stochastic modeling of GRN can thus be useful to make inferences concerning the range of noise levels that are experienced in particular developmental systems under study.
12. When trying to iterate Eq. 4, make sure that the order in which the position corresponding to each attractor state in the initial vector $p_X(0)$ is the same as the one for the columns in the transition the matrix P. In other words, if the fraction of cells in attractor A is specified in the position i of the initial vector, the row i of the transition matrix should correspond to the probabilities of transition from attractor A to the other attractors.
13. It can be the case that the heights of the trajectories, which correspond to the temporal evolution of the probability of being in each attractor, differ considerably. This is to be expected; given that the basins of the different attractors vary in size, and so do their absolute probabilities. One way to transform the data in order to obtain a graph where the heights of the trajectories are of comparable size is to normalize each probability value with respect to the maximum of each attractor's curve (e.g., dividing the probability value by the maximum value). We followed this approach to obtain the graph in Fig. 8, where also the trajectories corresponding to attractors *se1* and *se2*; and *st1* and *st2* where respectively added to obtain only one trajectory for the attractor *se* and one for *st*. However, it is important to note that, as we are interested in the temporal order in which the attractors reach its maximum probability, this normalization process is not necessary. The order of appearance of the maximum value of the probability of each attractor in the original simulated trajectories would be the same as the one observed in the normalized trajectories. The normalization step just allows us to obtain a clearer graph. In the graph in Fig. 7, we draw one star for each of the attractors just above the x-axis at the time when its maximal probability occurs. The observed pattern is exactly the same in the simulated trajectories before the normalization.

References

1. Villarreal C, Padilla-Longoria P, Alvarez-Buylla ER (2012) General theory of genotype to phenotype mapping: derivation of epigenetic landscapes from N-node complex gene regulatory networks. Phys Rev Lett 109(118102):1–5
2. Alvarez-Buylla ER, Balleza E, Benítez M, Espinosa-Soto C, Padilla-Longoria P (2008) Gene regulatory network models: a dynamic and integrative approach to development. SEB Exp Biol Ser 61:113–139
3. Alvarez-Buylla ER, Azpeitia E, Barrio R, Benítez M, Padilla-Longoria P (2010) From ABC genes to regulatory networks, epigenetic landscapes and flower morphogenesis: making biological sense of theoretical approaches. Semin Cell Dev Biol 21(1):108–117
4. Alvarez-Buylla ER, Chaos A, Aldana M, Benítez M, Cortes-Poza Y, Espinosa-Soto C, Hartasánchez DA, Lotto RB, Malkin D, Escalera Santos GJ, Padilla-Longoria P (2008) Floral morphogenesis: stochastic explorations of a gene network epigenetic landscape. PLoS One 3(11):e3626
5. Mendoza L, Alvarez-Buylla ER (1998) Dynamics of the genetic regulatory network for *Arabidopsis thaliana* flower morphogenesis. J Theor Biol 193(2):307–319
6. Albert R, Othmer HG (2003) The topology of the regulatory interactions predicts the expression pattern of the segment polarity genes in *Drosophila melanogaster*. J Theor Biol 223(1): 1–18
7. Espinosa-Soto C, Padilla-Longoria P, Alvarez-Buylla ER (2004) A gene regulatory network model for cell-fate determination during *Arabidopsis thaliana* flower development that is robust and recovers experimental gene expression profiles. Plant Cell 16:2923–2939
8. Azpeitia E, Benítez M, Vega I, Villarreal C, Alvarez-Buylla ER (2010) Single-cell and coupled GRN models of cell patterning in the *Arabidopsis thaliana* root stem cell niche. BMC Syst Biol 4:134
9. Albert I, Thakar J, Li S, Zhang R, Albert R (2008) Boolean network simulations for life scientists. Source Code Biol Med 3:16
10. Albert R, Wang RS (2009) Discrete dynamic modeling of cellular signaling networks. Methods Enzymol 467:281–306
11. Assmann SM, Albert R (2009) Discrete dynamic modeling with asynchronous update, or how to model complex systems in the absence of quantitative information. Methods Mol Biol 553:207–225
12. Alvarez-Buylla ER, Benítez M, Corvera-Poiré A, Chaos CA, de Folter S, Gamboa de Buen A, Garay-Arroyo A, García-Ponce B, Jaimes- MF, Pérez-Ruiz RV, Piñeyro-Nelson A, Sánchez-Corrales YE (2010) Flower development. Arabidopsis Book 8:e0127
13. Pelaz S, Tapia-López R, Alvarez-Buylla ER, Yanofsky MF (2001) Conversion of leaves into petals in Arabidopsis. Curr Biol 11(3): 182–184
14. Barrio RÁ, Hernández-Machado A, Varea C, Romero-Arias JR, Alvarez-Buylla E (2010) Flower development as an interplay between dynamical physical fields and genetic networks. PLoS One 5(10):e13523
15. Kauffman S (1969) Homeostasis and differentiation in random genetic control networks. Nature 224:177–178
16. Mendoza L, Thieffry D, Alvarez-Buylla ER (1999) Genetic control of flower morphogenesis in *Arabidopsis thaliana*: a logical analysis. Bioinformatics 15(7–8):593–606
17. Chaos Á, Aldana M, Espinosa-Soto C et al (2006) From genes to flower patterns and evolution: dynamic models of gene regulatory networks. J Plant Growth Regul 25(4):278–289
18. Sanchez-Corrales YE, Alvarez-Buylla ER, Mendoza L (2010) The *Arabidopsis thaliana* flower organ specification gene regulatory network determines a robust differentiation process. J Theor Biol 264:971–983
19. La Rota C, Chopard J, Das P, Paindavoine S, Rozier F, Farcot E, Godin C, Traas J, Monéger F (2011) A data-driven integrative model of sepal primordium polarity in Arabidopsis. Plant Cell 23(12):4318–4333
20. Garg A, Mohanram K, De Micheli G, Xenarios I (2012) Implicit methods for qualitative modeling of gene regulatory networks. Methods Mol Biol 786:397–443
21. Alvarez J, Guli CL, Yu XH, Smyth DR (1992) terminal flower: a gene affecting inflorescence development in *Arabidopsis thaliana*. Plant J 2(1):103–116
22. Shannon S, Meeks-Wagner DR (1991) A mutation in the Arabidopsis TFL1 gene affects inflorescence meristem development. Plant Cell 3(9):877–892
23. Parcy F, Bomblies K, Weigel D (2002) Interaction of LEAFY, AGAMOUS and TERMINAL FLOWER1 in maintaining floral meristem identity in Arabidopsis. Development 129(10):2519–2527

24. Conti L, Bradley D (2007) TERMINAL FLOWER1 is a mobile signal controlling Arabidopsis architecture. Plant Cell 19(3): 767–778
25. Chen L, Cheng JC, Castle L, Sung ZR (1997) EMF genes regulate Arabidopsis inflorescence development. Plant Cell 9(11):2011–2024
26. Liljegren SJ, Gustafson-Brown C, Pinyopich A (1999) Interactions among APETALA1, LEAFY, and TERMINAL FLOWER1 specify meristem fate. Plant Cell 11(6):1007–1018
27. Ratcliffe OJ, Bradley DJ, Coen ES (1999) Separation of shoot and floral identity in Arabidopsis. Development 126(6):1109–1120
28. Gustafson-Brown C, Savidge B, Yanofsky MF (1994) Regulation of the Arabidopsis floral homeotic gene APETALA1. Cell 76(1): 131–143
29. Gómez-Mena C, de Folter S, Costa MMR, Angenent GC, Sablowski R (2005) Transcriptional program controlled by the floral homeotic gene agamous during early organogenesis. Development 132(3):429–438
30. Kitano H (2007) Towards a theory of biological robustness. Mol Syst Biol 3:137
31. Whitacre JM (2012) Biological robustness: paradigms, mechanisms, and systems principles. Front Genet 3:67
32. Garg A, Mohanram K, Di Cara A, De Micheli G, Xenarios I (2009) Modeling stochasticity and robustness in gene regulatory networks. Bioinformatics 25:i101–i109
33. Samoilov MS, Price G, Arkin AP (2006) From fluctuations to phenotypes: the physiology of noise. Sci STKE 2006:re17
34. Hoffmann M, Chang HH, Huang S, Ingber DE, Loeffler M, Galle J (2008) Noise-driven stem cell and progenitor population dynamics. PLoS One 3(8):e2922
35. Eldar A, Elowitz MB (2010) Functional roles for noise in genetic circuits. Nature 467(7312):167–173
36. Balázsi G, van Oudenaarden A, Collins JJ (2011) Cellular decision making and biological noise: from microbes to mammals. Cell 144(6):910–925
37. Horsthemke W, Lefever R (1984) Noise-induced transitions: theory and applications in physics, chemistry, and biology. Springer, Berlin
38. Chalancon G, Ravarani CNJ, Balaji S, Martinez-Arias A, Aravind L, Jothi R, Babu MM (2012) Interplay between gene expression noise and regulatory network architecture. Trends Genet 28(5):221–232
39. Glass L (1975) Classification of biological networks by their qualitative dynamics. J Theor Biol 54:85–107
40. Mendoza L, Xenarios I (2006) A method for the generation of standardized qualitative dynamical systems of regulatory networks. Theor Biol Med Model 3:13
41. Ferrell JE Jr (2012) Bistability, bifurcations, and Waddington's epigenetic landscape. Curr Biol 22:R458–R466
42. Zhou JX, Brusch L, Huang S (2011) Predicting pancreas cell fate decisions and reprogramming with a hierarchical multi-attractor model. PLoS One 6(3):e14752
43. Wang J, Zhang K, Xua L, Wang E (2011) Quantifying the Waddington landscape and biological paths for development and differentiation. Proc Natl Acad Sci 108:8257–8262
44. Zadeh LA (1965) Fuzzy sets. Inf Control 8:338–353
45. Arellano G, Argil J, Azpeitia E, Benítez M, Carrillo M, Góngora P, Rosenblueth DA, Alvarez-Buylla ER (2011) "Antelope": a hybrid-logic model checker for branching-time Boolean GRN analysis. BMC Bioinformatics 12:490
46. Müssel C, Hopfensitz M, Kestler HA (2010) BoolNet—an R package for generation, reconstruction and analysis of Boolean networks. Bioinformatics 26(10):1378–1380
47. von Dassow G, Meir E, Munro EM, Odell GM (2000) The segment polarity network is a robust developmental module. Nature 406(6792):188–192. doi:10.1038/35018085
48. Naldi A, Berenguier D, Fauré A, Lopez F, Chaouiya C (2009) Logical modelling of regulatory networks with GINsim 2.3. Biosystems 97(2):134–139
49. Corblin F, Fanchon E, Trilling L (2010) Applications of a formal approach to decipher discrete genetic networks. BMC Bioinformatics 11(1):385
50. de Jong H, Geiselmann J, Hernandez C, Page M (2003) Genetic network analyzer: qualitative simulation of genetic regulatory networks. Bioinformatics 19(3):336–344
51. Calzone L, Fages F, Soliman S (2006) Biocham: an environment for modeling biological systems and formalizing experimental knowledge. Bioinformatics 22(14):1805–1807
52. Azpeitia E, Benítez M, Padilla-Longoria P, Espinosa-Soto C, Alvarez-Buylla ER (2011) Dynamic network-based epistasis analysis: boolean examples. Front Plant Sci 2:92

5.- RESULTADOS

5.1.- Parte I: "Single-cell and coupled GRN models of cell patterning in the *Arabidopsis thaliana* root stem cell niche"

El primer objetivo del proyecto fue ver si la información experimental era suficiente para explicar cómo se determinan los distintos tipos celulares presentes en el nicho de células troncales de la raíz de *Arabidopsis thaliana*, tanto de forma temporal, como espacio-temporal. Por lo tanto el primer paso fue hacer una revisión exhaustiva de la información experimental disponible sobre el tema. La revisión consistió en la lectura detallada de más de 300 artículos a partir de la cual se encontró que son al menos tres las vías principales para el desarrollo y mantenimiento del nicho de células troncales de raíz. La primer vía contiene a los factores de transcripción de la familia GRAS, *SHR y SCR*, así como algunos de sus genes blanco y algunas proteínas que interactúan con ellos (Sabatini et al., 2003; Levesque et al., 2006). La segunda a la vía de las auxinas y los factores de transcripción PLT de la familia AP2/EREBP (Aida et al., 2004). Por último, al gen *WOX5* y a sus represores (Stahl et al., 2009).

Estos datos se integraron tanto en una red Booleana, como en una red continua cualitativa, como se explica en la subsección 4.2. del capítulo de Métodos. En el análisis de esta red encontramos que los datos disponibles en la literatura eran insuficientes para reproducir los comportamientos observados en el nicho. Esto permitió generar algunas predicciones sobre posibles nodos o interacciones faltantes en la red, algunas de las cuales han sido posteriormente verificadas experimentalmente por otros grupos demostrando la capacidad predictiva del enfoque usado en nuestro trabajo (Stahl et al., 2009; Ding et al., 2010). En nuestro trabajo computacional también analizamos características globales de la red mediante pruebas de robustez, derivación de la curva de Derrida y la red fue validada explorando simulaciones de mutantes, y comparando con configuraciones reportadas para plantas con los genes alterados para cada simulación.

Finalmente, se exploró si el patrón espacial de distintos tipos celulares en el nicho se podía recuperar acoplando las dinámicas de las redes Booleanas intracelulares con el movimiento de algunos de los componentes de la red de acuerdo con datos

experimentales. Con estas simulaciones de redes acopladas, pudimos confirmar que, una vez añadidas ciertas predicciones, el modelo no sólo era capaz de reproducir las configuraciones genéticas observadas en el nicho para cada tipo celular, sino que también era capaz de reproducir su arreglo espacial a partir de configuraciones espaciales aleatorias o uniformes.

Todo esto fue reportado en un artículo publicado por la revista BMC Systems Biology (Azpeitia et al., 2010) del cual presentamos copia a continuación.

Azpeitia et al. BMC Systems Biology 2010, 4:134
http://www.biomedcentral.com/1752-0509/4/134

BMC Systems Biology

RESEARCH ARTICLE Open Access

Single-cell and coupled GRN models of cell patterning in the *Arabidopsis thaliana* root stem cell niche

Eugenio Azpeitia[1], Mariana Benítez[1], Iliusi Vega[2], Carlos Villarreal[2], Elena R Alvarez-Buylla[1*]

Abstract

Background: Recent experimental work has uncovered some of the genetic components required to maintain the *Arabidopsis thaliana* root stem cell niche (SCN) and its structure. Two main pathways are involved. One pathway depends on the genes *SHORTROOT* and *SCARECROW* and the other depends on the *PLETHORA* genes, which have been proposed to constitute the auxin readouts. Recent evidence suggests that a regulatory circuit, composed of *WOX5* and *CLE40*, also contributes to the SCN maintenance. Yet, we still do not understand how the niche is dynamically maintained and patterned or if the uncovered molecular components are sufficient to recover the observed gene expression configurations that characterize the cell types within the root SCN. Mathematical and computational tools have proven useful in understanding the dynamics of cell differentiation. Hence, to further explore root SCN patterning, we integrated available experimental data into dynamic Gene Regulatory Network (GRN) models and addressed if these are sufficient to attain observed gene expression configurations in the root SCN in a robust and autonomous manner.

Results: We found that an SCN GRN model based only on experimental data did not reproduce the configurations observed within the root SCN. We developed several alternative GRN models that recover these expected stable gene configurations. Such models incorporate a few additional components and interactions in addition to those that have been uncovered. The recovered configurations are stable to perturbations, and the models are able to recover the observed gene expression profiles of almost all the mutants described so far. However, the robustness of the postulated GRNs is not as high as that of other previously studied networks.

Conclusions: These models are the first published approximations for a dynamic mechanism of the *A. thaliana* root SCN cellular pattering. Our model is useful to formally show that the data now available are not sufficient to fully reproduce root SCN organization and genetic profiles. We then highlight some experimental holes that remain to be studied and postulate some novel gene interactions. Finally, we suggest the existence of a generic dynamical motif that can be involved in both plant and animal SCN maintenance.

Background

Stem cell (SC) research has received much attention during the last decade [1], as these cells are the source of new pluripotent cells in plants and animals and are fundamental for the maintenance of tissues during adulthood. Hence, understanding the dynamics and molecular genetics of SC niches (SCNs) has become a central question in biological and medical research [2,3]. Interestingly, SCNs share important structural and dynamic characteristics across distantly related multicellular organisms [3-6], which suggests the existence of underlying generic mechanisms. Thus, the study of plant SCNs, which are often more amenable to experimental and modeling studies than those of animals, may help researchers understand some such generic traits and may shed light on issues related to human health [7].

* Correspondence: eabuylla@gmail.com
[1]Laboratorio de Genética Molecular, Desarrollo y Evolución de Plantas, Instituto de Ecología & Centro de Ciencias de la Complejidad (C3), Universidad Nacional Autónoma de México, Ciudad Universitaria, Coyoacán, México D.F. 04510. México
Full list of author information is available at the end of the article

In contrast to animals, structures arise throughout the whole life cycle of plants from active SCNs, which are exposed in the so-called meristems. *Arabidopsis thaliana* has two main SCNs. One of these is in the Shoot Apical Meristem (SAM), located at the tip of the aerial part of the plant, and another is located in the Root Apical Meristem (RAM), at the acropetal end of the primary root. The *A. thaliana* root and root SC niche (SCN) are well described at the anatomical level. The root SCN includes four cells that rarely divide and constitute the quiescent center (QC), surrounded by four sets of initial cells that give rise to the different types of differentiated cells in the root (i.e., stele, cortex, endodermis, epidermis, lateral root-cap and columella cells) [8].

Besides the thorough anatomical characterization of this system, some of the molecular components that are necessary to establish and maintain the *A. thaliana* RAM and its SCN cellular patterning have been uncovered and characterized only recently (Table 1). One of these components implicates the module of *SHORTROOT* (*SHR*), its target gene *SCARECROW* (*SCR*), the immediately downstream genes of the dimer SHR/SCR and other genes that interact with them. Another regulatory circuit includes the *PLETHORA* (*PLT*) genes, which have been proposed to be key components of the molecular readout of the plant hormone auxin [9-12].

SHR is a gene that is expressed in the stele at the transcriptional level; its protein then moves to the adjacent cellular layer (i.e., cells in the QC, endodermis-cortex initials (CEI) and endodermis), where it activates *SCR* [13]. SCR is necessary for its own activation in the QC and CEI [10,14]. Both genes have been implicated in the maintenance of the RAM and SCN and the radial organization of the root [9,10,15]. SHR and SCR interact through their central domains; together, they control the transcription of several genes [14,16]. *MAGPIE* (*MGP*) is a target gene of SHR/SCR and has been implicated in the regulation of the root radial pattern, although its function is not yet fully understood. *JACKDAW (JKD)* is expressed in the QC and CEI. Mutations in *JKD* lack *SCR* expression in the QC and CEI, causing a misspecification of the QC, which is perhaps due to its effect on *SCR* expression. Yeast two-hybrid assays

Table 1 Summary of the experimental evidence

INTERACTIONS	EXPERIMENTAL EVIDENCE	REFERENCE
SHR →SCR	The expression of *SCR* is reduced in *shr* mutants. ChIP-QRTPCR experiments show that *SHR* directly binds *in vivo* to the regulatory sequences of *SCR* and positively regulates its transcription.	[9,16]
SCR →SCR	In the *scr* mutant background promoter activity of *SCR* is absent in the QC and CEI. A ChIP-PCR assay confirmed that *SCR* directly binds to its own promoter and directs its own expression.	[10,14]
JKD →SCR	*SCR* mRNA expression as probed with a reporter lines is lost in the QC and CEI cells in *jkd* mutants from the early heart stage onward.	[17]
MGP–|SCR	The double mutant *jkd mgp* rescues the expression of SCR in the QC and CEI, which is lost in the *jkd* single mutant.	[17]
SHR →MGP	The expression of *MGP* is severely reduced in the *shr* background. Experimental data using various approaches have suggested that *MGP* is a direct target of *SHR*. This result was later confirmed by ChIP-PCR.	[14,16,17]
SCR →MGP	*SCR* directly binds to the *MGP* promoter, and *MGP* expression is reduced in the *scr* mutant background.	[14,17]
SHR →JKD	The post-embryonic expression of *JKD* is reduced in *shr* mutant roots.	[17]
SCR →JKD	The post-embryonic expression of *JKD* is reduced in *scr* mutant roots.	[17]
SCR →WOX5	*WOX5* is not expressed in *scr* mutants.	[24]
SHR →WOX5	*WOX5* expression is reduced in *shr* mutants.	[24]
ARF(MP) →WOX5	*WOX5* expression is rarely detected in *mp* or *bdl* mutants.	[24]
ARF→PLT	*PLT1* mRNA region of expression is reduced in multiple mutants of *PIN* genes, and it is overexpressed under ectopic auxin addition. *PLT1 &2* mRNAs are absent in the majority of *mp* embryos and even more so in *mp nph4* double mutant embryos.	[11,12]
Aux/IAA–|ARF	Overexpression of Aux/IAA genes represses the expression of DR5 both in the presence and absence of auxin. Domains III & IV of Aux/IAA genes interact with domains III & IV of ARF stabilizing the dimerization that represses ARF transcriptional activity.	[22,23]
Auxin–| Aux/IAA	Auxin application destabilizes Aux/IAA proteins. Aux/IAA proteins are targets of ubiquitin-mediated auxin-dependent degradation.	[reviewed in [18]]
CLE40 –| WOX5	Wild type root treated with CLE40p show a reduction of *WOX5* expression, whereas in *cle40* loss of function plants *WOX5* is overexpressed.	[25]

Experimental evidence used to generate the four single cell GRNs. These previously reported results were the basis for the interactions postulated in the SCN GRN models graphs of figure 1.

have shown that SHR, SCR, JKD and MGP can physically interact, which suggests that protein-protein complexes among them are involved in SC regulation [17].

In addition to the SHR/SCR SCN regulation, *PLT* genes are also necessary for the maintenance of the root SCN. The double mutant *plt1 plt2* fail to maintain the SCN, and in this mutant, eventually all cells in the RAM differentiate [11]. *PLT* genes act redundantly, and *plt1 plt2 pl3* triple mutants are rootless and resemble the Auxin Response Factor (ARF) *monopteros* (*mp*) single mutant. Indeed, *mp* single and *mp arf7/nhp4 (nonphototropic hypocotyl4)* double mutants show reduced or no expression of *PLT1* and *PLT2* transcripts from heart stage onward, which suggests that the activation of *PLT* transcription occurs downstream of the ARFs [11,12]. Moreover, application of exogenous auxin increases *PLT* transcription.

The transcriptional activity of the ARFs has been widely studied, and the Aux/IAA proteins have been proposed as their key negative regulators [18-21]. The Aux/IAA proteins repress the transcriptional activity of the ARF forming hetero-dimers. The SCF^{TIR1} ubiquitin ligase complex promotes Aux/IAA degradation in the presence of auxin [22,23].

Finally, *WUSCHEL RELATED HOMEOBOX 5* (*WOX5*) is a gene expressed exclusively in the QC. In *wox5* mutants, the QC fails to maintain correct gene expression and to keep the distal SC undifferentiated. *WOX5* is hardly detected in *shr*, *scr*, or *mp* [24]. The *WOX5* distribution is expanded in the *wox5* background, suggesting that this gene has a negative feedback loop [24]. Recently, *CLAVATA-like 40* (*CLE40*), a secreted peptide, was found to negatively regulate *WOX5* expression through *ARABIDOPSIS CRINKLY4* (*ACR4*) in the more distal part of the meristem [25]. Other studies suggest that additional *CLE-like* genes could be involved in RAM maintenance [26-29].

Despite the thorough description of mutants and paired gene interactions, it still remains unclear how the concerted action of all the studied genes and their regulatory interactions collectively yield the gene profiles (configurations) characteristic of the cell types within the root SCN. Indeed, soon after cells depart from the QC, they attain distinct gene expression configurations, each characterizing a set of SC or initial cell types that eventually give rise to the distinct cell lineages conforming the mature root. How such cellular heterogeneity in SCs is dynamically established while the QC cells are kept undifferentiated, considering that all cells within the SCN have the same genetic information, is still not well understood. Dynamic gene regulatory models are of great value for addressing these issues.

Gene Regulatory Network (GRN) models have proven to be useful tools for studying the concerted action of molecular entities acting during cell differentiation and pattern formation [30-36]. These models are made up of nodes representing genes, proteins or other molecules and edges that stand for the regulatory interactions among these elements [37]. The dynamics of these networks may be described using systems of coupled equations, either continuous or discrete [37,38]. For Gene Regulatory Networks (GRNs) involved in cell fate determination, it has been proposed that their steady-state gene configurations (also referred to as attractors) correspond to gene activation profiles typical of different cell types [39]. Therefore, investigating the dynamics of such GRNs may be key for understanding cell differentiation, cell patterning and morphogenesis during developmental processes.

Some theoretical approaches have addressed lineage specification, regeneration and other aspects of SCNs in animals [40-42] and plants [43,44]. However, to our knowledge, dynamic models that aim at understanding cell-fate determination and patterning in SCNs are still scarce. Specifically, such a model is lacking for the *A. thaliana* root meristem. Hence, although some of the genes necessary for the root SCN specification and maintenance have been identified and functionally characterized [45], there is no dynamic characterization of the whole regulatory module. Additionally, it is still unclear if the molecular components and interactions reported previously are sufficient to dynamically and robustly recover the cell types and patterns of the *A. thaliana* root SCN.

In this paper, we have integrated the available experimental data on root SCN maintenance into discrete GRN dynamic models. We postulate several alternative regulatory modules to investigate if alternative topologies of regulatory interactions, which include those uncovered so far in addition to a few additional predictions, are sufficient to recover genetic profiles characteristic of the main cell types within the SCN.

Given that roots, when exposed to diverse environmental conditions or even to multiple genetic mutations [e.g., [11,17,46-48]], still harbor a normal or almost normal SCN, we hypothesized that the niche cellular patterning should be regulated by a robust GRN. The formal models proposed here enabled tests of such a hypothesis by addressing if the proposed GRN models attained the same gene configurations in the face of transient (e.g., initial conditions or inputs from other modules connected to the one under study) or permanent perturbations. We also investigated the robustness of the models by translating the discrete GRN models to continuous ones and by verifying if the SCN GRN attractors were maintained. Additionally, we validated the proposed GRN models by testing if they also recovered gene configurations of experimentally characterized

loss and gain of function mutants. Comparisons of the alternative GRN models tested helped us detect experimental gaps and postulate novel predictions that could guide future experiments.

We also designed a discrete spatial version of coupled GRNs to address if the intracellular GRN coupled by the reported cell-to-cell communication via movement of four of the GRN components could also yield the gene configurations observed in different cell types and positions within the *A. thaliana* root SCN. A local activator and lateral inhibitor motif were included as part of the coupled network model as a prediction, in part given that such a motif has been postulated for the SAM, which has important similarities with the RAM maintenance [49,50].

The results obtained in this work show that the genes that have been characterized in SCN patterning are largely sufficient to recover both the gene configurations observed in the main cell types within the root SCN and the overall spatial pattern of such cells. However, our work strongly suggests that additional components and circuits are still to be discovered, and these may render the root SCN robust in the face of transient perturbations as well as some genetic mutations.

Results

Four alternative GRN models sufficient to recover observed gene expression profiles in cells within the root stem cell niche

Based on the experimental data summarized above and in Table 1, we generated a discrete root SCN GRN model (see Methods for details). The regulatory interactions are indicated by arrows (activation) or flat-end edges (repression) in the GRN (Figure 1). It is important to note that even though in figure 1 all the interactions between nodes appear to be direct, the arrows can represent a direct interaction or an interaction mediated by one or more intermediate molecular components (i.e., indirect interaction). We still lack experimental data to discern between these two possibilities in many instances. In figure 1, we indicate which interactions are experimentally confirmed as direct interactions, whereas the rest are indirect. In the logical functions (Additional file 1), *0* represents a non-functional protein or non-expressed gene, except for *PLT* and auxin, which have a graded expression and for which *0* represents a level of expression insufficient to exert their function in the SCN.

A few articles have demonstrated that *SHR* movement depends on both cytoplasmic and nuclear localization [51,52] and its activity depends on its nuclear localization. Our GRN models do not consider how *SHR* or any other node intracellular localization affects in mobility and function. Nonetheless, the logical rules postulated for this gene qualitatively recover and agree with the available data related to both aspects of this gene function. Because each of the *ARF, PLT* and *Aux/IAA* genes have redundant functions and overlapping expression patterns and the particular function of single genes in the SCN is not clear, we collapsed each of these groups of genes into a single node for each gene family (Figure 1). The postulated GRN does not distinguish between columella and epidermis-lateral root cap initials due to lack of experimental evidence, and we thus refer to them as CEpI (for columella epidermis initials) (Figure 2). Hence, we expected only four GRN attractors; namely, those corresponding to the QC, vascular initials, Cortex-Endodermis initials (CEI) and CEpI.

While we were integrating available published data into a preliminary GRN model, we detected experimental gaps or ambiguities in five of the genes considered in the network. All of the gaps and ambiguities concern gene transcriptional regulation and were found in *SHR*, *SCR*, *JKD*, *MGP* and *WOX5* genes. As far as we know, some of the regulators of these genes have not been discovered or published yet.

Much research has been conducted regarding the function of *SHR*, but we did not find any reported gene directly regulating its transcription. In our model, this result implies that because *SHR* activity does not have any positive or negative input regulator, its final state will depend only on its initial state.

It has also been reported that *scr* and *shr* single mutants severely reduce postembryonic *JKD* expression [17] and that the dimer SHR/SCR positively regulates *MGP* expression [14]. This result means that SCR and SHR are both necessary for a postembryonic wild type expression of *JKD* and *MGP*. Nevertheless, *MGP* expression is absent in the QC, where both *SCR* and *SHR* genes are expressed. Similarly, *JKD* express in a different region than the SHR and SCR region. So, SHR and SCR are not sufficient to explain the *JKD* and *MGP* expression because the region of expression of the latter genes is different than that of *SCR* and *SHR*. Hence, it is likely that *JKD* and *MGP* have additional regulators. However, in the model, we assumed that the latter two genes are only under *SCR* and *SHR* regulation. As mentioned above, also the positive regulators described for *WOX5* (i.e., *SHR*, *SCR* and *ARF*) are present in the CEI, where *WOX5* is not expressed, which suggests that there are also uncovered *WOX5* regulators.

Sabatini and collaborators [10] reported that *SCR* SCN expression depends on itself, but other reports [e.g., [53]] showed that ectopic *SHR* expression alone (i.e., without *SCR* ectopic expression) is able to induce *SCR* expression outside the QC, CEI or endodermis cells. So, it is not well understood why even when SHR protein is present in the vascular initials, *SCR* is not, but when

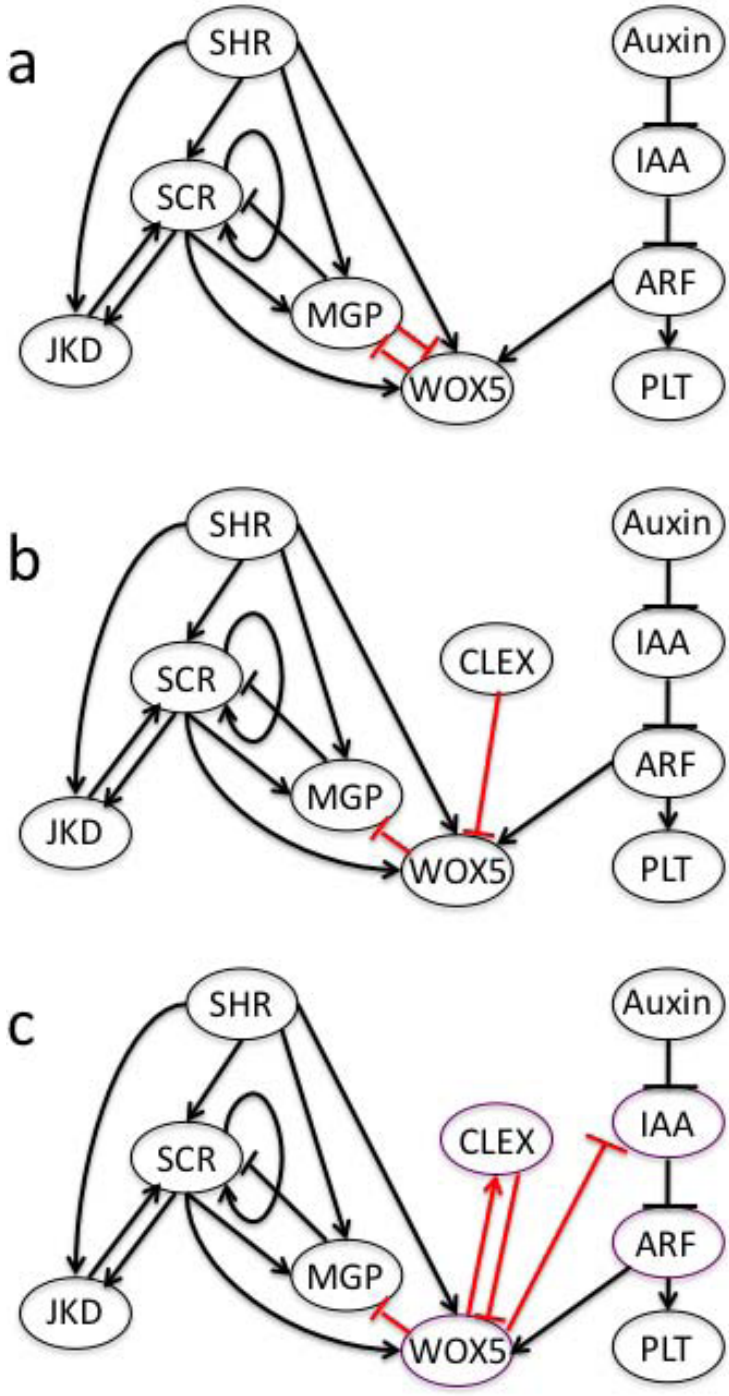

Figure 1 Root stem cell niche GRN models. Nodes represent the genes or hormones in the case of auxin. Arrows correspond to activations, and flat arrows correspond to repressions. Four models were tested. Model A and A' (a) differ from B and B' (b) in the *WOX5* negative regulation. In models A and A', *WOX5* is downregulated by MGP, whereas in models B and B' *WOX5* is downregulated by the hypothetical gene *CLEX*. Models A' and B' differ from models A and B in the SCR value in line 14 of their logical rule as shown in Additional file 1. In (c), the GRN used for the coupled GRN model is depicted. Even when *CLE40* is an experimentally reported data, in our model, we assume negative regulation of *WOX5* in all SCs, so *CLEX* is treated as a novel prediction. In all GRNs, red arrows indicate the novel postulated interactions, and black arrows indicate interactions based on experimental data. Purple nodes in (c) are the nodes involved in the activator-inhibitor motif. The *IAA* node in the GRN graph represents the *Aux/IAA* gene family, not auxin. Of all the interaction considered here, the dimer SHR/SCR activating *SCR* and *MGP*, auxin repressing Aux/IAA and Aux/IAA repressing ARF had been experimentally confirmed as direct interactions.

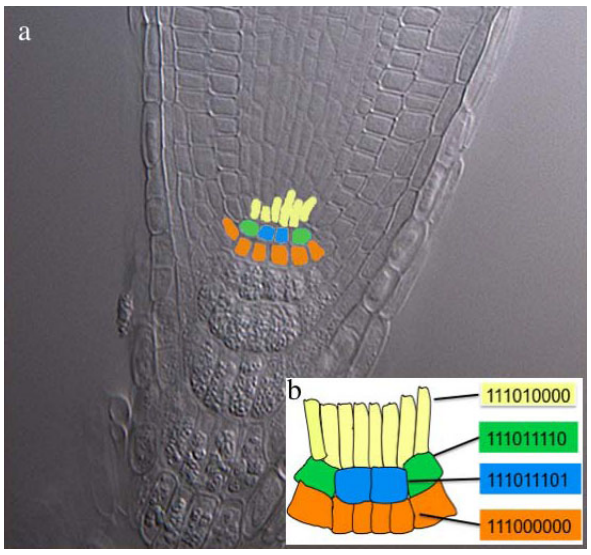

Figure 2 Simplified cellular pattern of the root stem cell niche compared to a real root. The four cell types within the SCN, each of which corresponds to one of four stable attractors recovered by the models in figure 1. The vascular initials (yellow), cortex-endodermis initials (green), quiescent center (blue) and columella-epidermis-lateral root cap initials (orange) (b) in the cleared root tip of *Arabidopsis thaliana* colorized to show the corresponding cell types represented by the attractors recovered by the single-cell GRN models in figure 1 and schematized in (a). The activation states of the nodes are represented by *0* and *1* in the following order: *PLT*, auxin, *ARF*, *Aux/IAA*, *SHR*, *SCR*, *JKD*, *MGP* and *WOX5*.

SHR is ectopically expressed in epidermis and lateral root cap initials, *SCR* turns on. One possibility is that *SHR* alone is capable of activating *SCR*, but our analysis shows that even if this is the case additional *SCR* regulators are still waiting to be discovered (see details below). This and further analysis demonstrate that even though a great amount of research has been carried out on *SCR* regulation, it is not yet fully clear how this gene expression pattern is maintained in the root SCN. With this in mind, we propose a *SCR* logical rule (see Additional file 1) that together with the logical rules of the genes included in the GRN seems to be sufficient for recovering observed gene expression profiles.

We also noted that given the conditions considered in the GRN, *PLT*, *ARF*, *Aux/IAA* and auxin form a linear pathway with no inputs from other nodes included in the GRN. These nodes always have the same state in the models and contribute little to our understanding of the SCN GRN as far as it has been uncovered, but we decided to keep these nodes for two reasons: i) this pathway has been shown to be important in SCN patterning experimentally, and ii) by including them, we provide a more comprehensive formal framework that may later enable connections to other regulatory modules, such as those controlling the cell cycle or a more realistic auxin transport model, in both of which *PLT* and auxin are known to play essential roles.

The SCN GRN that only incorporated published data was not sufficient to recover the observed gene configurations in the SCN. This first GRN model lead to stable gene configurations that did not include the attractors corresponding to that observed in the QC and the CEI cells, and it also yields an attractor, which combined QC/CEI gene activities. The latter combination has not been observed in any of the wild type *A. thaliana* root SCN cell types. Therefore, we decided to postulate two predictions concerning additional regulatory interactions that, in the context of the root SCN GRN uncovered up to now, are sufficient to recover the expected attractors or stable gene expression configurations that have been described for the different cell-types in the root SCN (Figure 2 and table 2 and 3). Our simulations showed that by assuming a down-regulation of *WOX5* in the CEI and of *MGP* in the QC, the modeled GRN models were sufficient to recover the observed gene expression configurations.

The assumed down-regulations discussed above lack experimental support and hence constitute novel predictions. However, there is, in principle, more than one minimal way to model *WOX5* inhibition in a manner that is consistent with the rest of the available data and the observed gene configurations within the SCN. In a first model (A), we assumed that *MGP* represses *WOX5* and *vice versa*. We made this assumption for several reasons: i) the reported conditions for *WOX5* transcription (i.e., *ARF*, *SHR* and *SCR* expression that positively regulate *WOX5* expression) are also present in the CEI, and ii) the reported conditions for *MGP* transcription are observed in the QC (i.e., *SHR* and *SCR* expression

Table 2 Simulated configurations of models A and A' compared to those observed in real roots of *Arabidopsis thaliana*

Cell type	PLT	Auxin	ARF	Aux/IAA	SHR	SCR	JKD	MGP	WOX5
QC	1(1)	1(1)	1(1)	0(0)	1(1)	1(1)	1(1)	0(0)	1(1)
Vascular Initials	1(1)	1(1)	1(1)	0(0)	1(1)	0(0)	0(0)	0(0)	0(0)
CEI	1(1)	1(1)	1(1)	0(0)	1(1)	1(1)	1(1)	1(1)	0(0)
Cepl	1(1)	1(1)	1(1)	0(0)	0(0)	0(0)	0(0)	0(0)	0(0)

A value of *1* means that the gene is "ON", whereas a value of *0* means that it is "OFF". Simulated gene states for each cell type are shown first and observed gene states are in parenthesis.

Table 3 Simulated configurations of models B and B' compared to those observed in real roots of *Arabidopsis thaliana*

Cell type	PLT	Auxin	ARF	Aux/IAA	SHR	SCR	JKD	MGP	WOX5	CLEX
QC	1(1)	1(1)	1(1)	0(0)	1(1)	1(1)	1(1)	0(0)	1(1)	0(0)
Vascular Initials	1(1)	1(1)	1(1)	0(0)	1(1)	0(0)	0(0)	0(0)	0(0)	1(1 or 0)
CEI	1(1)	1(1)	1(1)	0(0)	1(1)	1(1)	1(1)	1(1)	0(0)	1(1)
CepI	1(1)	1(1)	1(1)	0(0)	0(0)	0(0)	0(0)	0(0)	0(0)	0(0)

A value of *1* means that the gene is "ON", whereas a value of *0* means that it is "OFF". Simulated gene states for each cell type are shown first and observed gene states are in parenthesis. It is important to note that the extra attractors of the simulated configurations in these models are the same as the one corresponding to the vascular initials but with *CLEX* OFF.

that positively regulate *MGP* expression). *WOX5* and *MGP* expression patterns are complementary, so even when we are aware that *MGP* and *WOX5* possibly do not regulate each other directly, our assumption considers a potential indirect regulation.

In another model (B), we assumed that the proximal expression of *WOX5* is negatively regulated by an unknown gene that could be a *CLE-like* gene. We decided to use the *CLEX* name for this hypothetical regulator of *WOX5* because recent evidence demonstrated that *CLE40* inhibits *WOX5* expression [25]. We did not use *CLE40* directly because the hypothetical regulator (*CLEX*) should have a region of expression or activity wider to that reported for *CLE40*. Also, *CLEX* could represent more than one gene, including *CLE40*. Moreover, it is important to also acknowledge that the role of the node marked in our GRN model by *CLEX* could, in fact, involve other genes as well. For example, Williams and collaborators [54] proposed that HD-ZIPIII genes regulate *WUS* expression in the SAM. Several similarities between the SAM and RAM SCNs have been described [e.g., [24]]. In the SAM, HD-ZIPIII genes are negatively regulated by miRNA165/6, which, in turn, are direct targets of the dimer SHR/SCR [55]. HD-ZIPIII genes function is not clear in the root, so including them would not be justified based on the available experimental information. Nonetheless, the *CLEX* could represent the latter or other yet to be uncovered genes. So in model B, the negative regulation of *WOX5* over *MGP* was kept, but we removed the regulation of *MGP* over *WOX5*. Both A and B models have two distinct versions that differ only in line 14 of the *SCR* logical rule. The A' and B' models have a different assumption in this logical rule than the A and B models (Additional file1). We performed analyses on all four of these models.

To identify the attractors of each model, we used the program *Atalia* [[56]; freely available] by following the dynamics of all possible initial configurations of gene expression. Both versions of model A converge to only four attractors that coincide with experimentally reported gene profiles for the cells within the root SCN (Table 2); namely, QC, CEpI, CEI, and the vascular initials (Figure 2). Both versions of model B converge to five attractors. These attractors correspond to the same four attractors as those recovered with models A and A', but the vascular initials are duplicated with the hypothetical gene *CLEX* being either "ON" or "OFF" in each case (Table 3). This first result already suggests that the proposed GRN models assuming *WOX5* down-regulation suffices for recovering the expected attractors and, therefore, constitutes a useful tool for exploring the qualitative dynamic traits of the system under study.

We found that in spite of the intricacy and complexity of the regulatory system, the root SCN GRN implies relatively straightforward dynamics, where the activation states of *SHR* and *SCR* determine the final attractor. The lack of *SHR* activity in the GRN unequivocally leads to the CEpI attractor, whereas the presence of *SHR* activity leads to the vascular initials if *SCR* is "OFF" and to the CEI or QC attractor if *SCR* is "ON". This result is confirmed by checking the basins of attraction, where half of the configurations lead to the CEpI attractor, as expected from the dynamics, and the other half lead to vascular initials, QC or CEI depending on the initial *SCR* state. As proposed before [11,12], *PLT* does not seem to be important for cell-fate determination within the SCN but rather for the apical-basal patterning of cell behavior as a read-out of auxin gradients along the longitudinal root axis (Additional file 2). Our models are useful for showing that the two modules important for the SCN patterning (the SHR/SCR and the auxin-PLT) are only connected by *WOX5* and together render stable gene expression configurations similar to those observed in the main cell types of the root SCN.

Validation of the single-cell GRN models with simulations for loss and gain of function mutants

To challenge and thus validate the proposed models, we simulated experimentally described mutations and addressed if the recovered gene expression configurations in the simulated mutants corresponded to those observed in the actual root SCN of such lines or could help to pose novel predictions. Gain-of-function mutations were simulated by fixing the over-expressed gene's value to *1* while fixing the mutated gene's value to *0* simulated loss-of-function mutants. Most simulated mutants of all models reproduced the gene

configurations that have been reported experimentally (Table 4 and 5), but some discrepancies were encountered.

Welch and collaborators [17] reported that in *jkd* loss-of-function mutants, *SCR* transcription in the SCN diminished or disappeared and also showed miss-specified QC cells, but the CEI were not lost. In concordance with this, the *SCR* logical rules of our A and B models determine that *SCR* expression is lost if *JKD* is not present. When we simulate *jkd* loss of function, *WOX5*, which marks our QC attractor, is still expressed, and *SCR* does not disappear in the QC, but it does cause the loss of the CEI attractor. These results contradict the observed gene profile pattern of *jkd*. We reasoned that because experimental *jkd* mutants still have CEI and keep *QC25* expression until 8-9dpg [17], which is SCR-dependent, JKD function could be enhancing *SCR* transcription to a wild-type level; however, in a *jkd* background, SCR could remain expressed and functional at a low level. This hypothesis implies that JKD is dispensable for *SCR* expression or SCR function. We simulated the latter possibility by altering line 14 of the *SCR* truth table (this change produced our A' and B' versions of models A and B, respectively), which allowed *SCR* transcription in *jkd*. In fact, by making this change, we could recover the *jkd* loss of function phenotype (i.e., we did not lose CEI as observed in this mutant), and we predicted that even when the QC is miss-specified, *WOX5* may remain active, at least for as long as *QC25* remains active. In this case, *SCR* must also remain expressed, but at a lower level than in wild type. These simulated alterations of the truth tables suggest a need for further experiments (see discussion).

mgp loss-of-function single mutant does not have a visible experimental phenotype, but in model A and A' the CEI attractor disappears, and the initial conditions that originally lead to this attractor now lead to the QC attractor. Models B and B' do not show any altered profiles when a loss-of-function *mgp* is simulated. This result coincides with what is observed experimentally, and such a result depends upon the introduction of the hypothetical gene *CLEX* into the models. Our simulations predict that *CLEX* over-expression suffices for the consumption of the QC.

Table 4 Simulations of loss of function mutants

Gene	Model A	Model A'	Model B	Model B'	Model A-I
SHR	YES	YES	YES	YES	YES
SCR	YES	YES	YES	YES	YES
MGP	NR	NR	YES	YES	YES
JKD	NR	YES	NR	YES	YES
WOX5	NC	NC	YES	YES	YES
PLT	YES	YES	YES	YES	YES
ARF	YES	YES	YES	YES	YES
Aux/IAA	YES	YES	YES	YES	YES
Auxin	YES	YES	YES	YES	YES

As observed, in most cases simulations recovered the experimentally observed configurations. When we did not recover the expected genetic configurations, we distinguish two situations: not recovered (NR), which indicates that even though experimental data was available it was not recapitulated and not enough data for comparison (NC), which indicates that experimental data was lacking, so in these cases a comparison could not be done. The coupled GRN results are reported in (A-I).

Table 5 Simulations of gain of function mutants

Gene	Model A	Model A'	Model B	Model B'	Model A-I
SHR	NR	NR	NR	NR	YES
SCR	NC	NC	NC	NC	NC
MGP	NC	NC	NC	NC	NC
JKD	NC	NC	NC	NC	NC
WOX5	YES	YES	YES	YES	YES
PLT	YES	YES	YES	YES	YES
ARF	NC	NC	NC	NC	NC
Aux/IAA	YES	YES	YES	YES	YES
Auxin	NC	NC	NC	NC	NC

When we did not recover the expected genetic configurations, we distinguish two situations: not recovered (NR), which indicates that even though experimental data was available it was not recapitulated and not enough data for comparison (NC), which indicates that experimental data was lacking, so in these cases a comparison could not be done. The coupled GRN results are reported in (A-I).

It is well documented that *PLT* genes are key regulators of SC identity and maintenance [11,12], but their direct target genes have not been found. When we mutated the *PLT* node, in the four models, the only effect observed was a lack of expression or constitutive expression of this component, which depended on whether or not we were simulating a loss or gain-of-function mutation, respectively. To further verify the validity of our model and gain insights about the role of *PLT* activity in the root SCN GRN, we added a *PIN-FORMED* gene (namely *PINX*) and *QC46,* a QC marker to our GRN models, both of which have been experimentally found to be under the control of *PLT* and other genes already considered in our GRN models [11,46]. We decided to use the generic name *PINX* and not a specific *PIN* because it has been reported that *PLT* genes regulate the expression of more than one *PIN* gene, and several *PIN* genes are expressed in the root SCN. By including these genes, we recovered the genetic configuration observed in *PLT* loss-of-function mutant, which also lacks *PINX* and *QC46*, thereby verifying that an adequate activity of *PLT* was being simulated in our models. *PINX* and *QC46* were introduced in the GRN models only for this analysis.

We were unable to fully validate other gain of function simulations because data on the additional markers for columella and epidermis markers, as well as crosses

of over-expression lines with cell-marker lines, are lacking (Table 5). The only two discrepancies found between our simulations and observed configurations concerns *jkd* in models A and B and *mgp* in models A and A'. These discrepancies lead to novel predictions (see discussion section and Table 4).

In conclusion, all of our analyses suggest that the regulatory module proposed here in various versions is indeed largely sufficient for explaining most of the cell-fate determination gene expression profiles in the SCN. The latter is true for the wild type and most mutant cases reported up to now. Our simulations suggest that model B', which assumes that *CLEX* is a negative regulator of *WOX5* and that *SCR* expression is independent of JKD activity, renders gene expression configurations reproducing the available experimental data. However, it is intriguing that model B' is not as robust to perturbations as models A and A' (see below). This lack of robustness could be due to the introduction of the *CLEX* node, which is necessary to repress *WOX5* activity without a *MGP* loss of function phenotype but may interact with *WOX5* in a way that is different to that assumed here. Nonetheless, these analyses illustrate that dynamic GRN models, like the ones used here, are useful tools to test how single gene mutations may yield contrasting stable gene configurations depending on the overall network topologies. It is interesting to note that configurations and cellular patterns may be drastically affected by some relatively small changes in the logical rules of certain genes but are not affected by a great majority of alterations.

The recovered cell-type gene configurations are robust to genetic perturbations

The above analyses already show that the recovered gene configurations are robust to transient gene modifications because all possible initial configurations lead to a few attractors, which overall correspond to configurations observed in the different types of cells within the root SCN. However, to test the robustness of the uncovered SCN GRN module to genetic alterations, we performed simulations to explore alterations in which node's logical rules yield the greatest modifications in the attractors. To this end, we altered, one by one, the output of every logical rule and ran the system to recover all the attractors from all the possible initial configurations of each altered network. We found that for B and B' and for A and A', 55.4% and 62.85%, respectively, of the tested alterations do not yield novel attractors or cause any of the originally encountered ones to disappear. The remaining 44.6% and 37.15% of the alterations rendered fewer or additional attractors for models A and A' and for B and B', respectively. These results suggest that the postulated SCN GRN models are relatively robust. Nonetheless, other previously characterized GRN for *A. thaliana* cell differentiation have been shown to be more robust than the models proposed here [e.g., [32,33]]. Hence, as an additional robustness test, we decided to perform two additional analyses: i) a Derrida analysis [57-59] to test if the GRN models postulated here are under chaotic, ordered or critical dynamics and ii) a continuous approximation of the Boolean model to address if the same attractors are recovered when the kinetic functions are continuous.

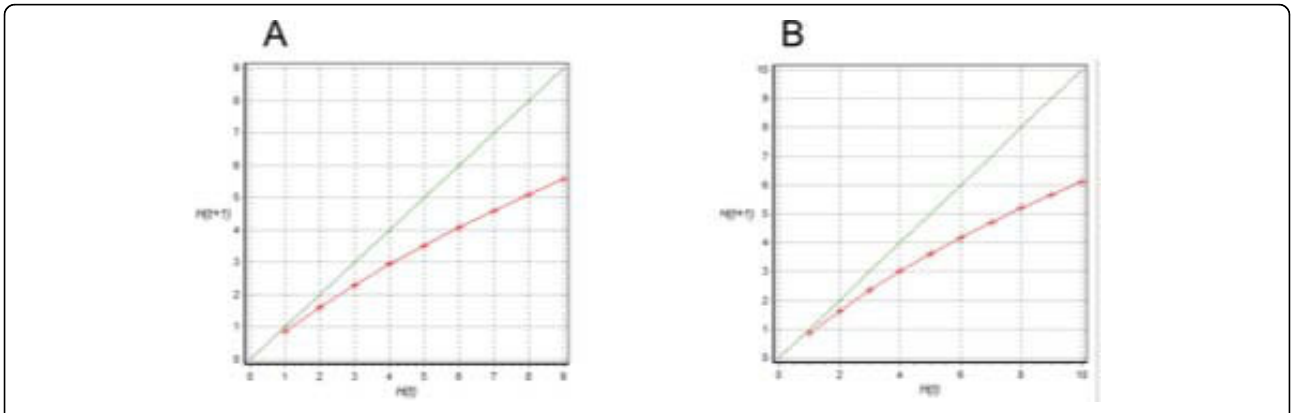

Figure 3 The Derrida curve of models A and B. The Derrida test allows for assessment of whether or not the GRN in question is in a chaotic, ordered or intermediate (critical) state. It has been suggested that living systems are located in a critical state, in which they exhibit both a degree of organization and also of flexibility [59]. This analysis is based on a comparison of the trajectories of similar initial conditions. If they diverge rapidly, then the system is said to be chaotic, whereas if they do not diverge or diverge very slowly, the system is said to be ordered. In this graph, it is shown that the curve describing the dynamic of the GRN is very similar to the identity line at the beginning (i.e., for small *t* values) and then diverges, which seems to characterize systems that are in a critical regime [[59] and references there in]. The (A) Derrida curve of model A and (B) Derrida curve of model B. Similar curves were found for model A' and model B'.

The Derrida analysis for the four GRN models in this study was performed using *Atalia*, and we found that the SCN GRN models also exhibit a critical dynamics in the face of perturbations (Figure 3).

Finally, we put forward a continuous version of the discrete GRN model to address if a system of differential equations was able to recover the same attractors. This approach enables us to test if the postulated logical discrete rules imposed artifacts in recovering some of the stable gene configurations, and if using continuous kinetic functions different or additional attractors are recovered. To obtain the system of differential equations, we transformed each discrete function into a differential equation (see methods and Additional file 3 for details). Interestingly, for all of the models postulated and tested in the discrete case, the corresponding continuous models recovered the same attractors, plus an additional unstable attractor in the cases of models A and A'. This extra attractor seems to stem from the assumption that *MGP* acts as a negative regulator of *WOX5*. This extra steady state is between those corresponding to the CEI and QC attractors, with an activation level of 0.5 for both *MGP* and *WOX5*. To calculate the stability of the extra attractor, we ran the dynamics of the continuous system 1000 times, but considering perturbed steady states with alterations of up to 30% of recovered values as the initial conditions. As a result, we found that the extra attractor is rather unstable because it converges to either CEI or QC stable configurations in the face of very small perturbations (see methods for details).

Taken together, the fact that all possible initial configurations only converge to the expected attractors, the analyses done by directly perturbing the logical functions, the continuous approximation, and the Derrida graph analyses confirm that the GRN models studied here are relatively robust. In any case, the fact that these GRN models are not as robust as other GRN models previously studied [e.g., [32,33]] and that the actual root SCN has been shown to be robust to several perturbations [e.g., [11,12,46,48]] suggests that additional redundant circuits, as found in other systems [60], underlie SCN patterning. Additionally, further components of the SCN GRN may still remain undiscovered.

A model of coupled GRN recovers observed spatial configurations in the root stem cell niche

Recent experimental evidence suggests that *CLE40* and *WOX5* behave in a similar way to *WUS* and *CLV3* in the SAM [24,25], where the latter exerts a lateral inhibition of the former. To simulate such negative regulation in a non-cell autonomous way and to create a model that recovers the spatial cellular configuration observed in the root SCN, we developed a spatial model of coupled single-cell GRNs [e.g., [61]]. We use model B', which, as mentioned before, we believe is the model that best fits the available experimental data.

We simplified the cellular structure of the root SCN by considering four types of cells, one for each attractor found in the previous single cell GRN models, arranged symmetrically based on their observed spatial location (Figure 4). Such an arrangement recovers the main qualitative aspects of the SCN cellular pattern. The spatial information in this coupled GRN model was incorporated by considering cell-to-cell movement or the non-cell autonomous action of four of the intracellular components, namely *SHR*, *WOX5*, *CLEX* and auxin, according to experimental data. Based on each cell's spatial position, only certain directions of movement or communication between cells were allowed according to published data. The mobility patterns were fixed during the GRN dynamics.

CLEX and *WOX5* in one cell can affect the logical rules of all other cells (simulating *CLEX* diffusion and non-cell autonomous action of *WOX5*), whereas *SHR* and auxin were only able to affect the rules of certain SCN cells, according to experimental evidence (simulating acropetal active transport in the case of auxin and the role of SCR in constraining SHR movement). Hence, *CLEX* and *WOX5* activity in one cell affect all neighboring cells. SHR is assumed to move from any cell where it is expressed to any other cell, but its movement is only allowed if *SCR* is not expressed in the same cell, as previously reported [9,13,14].

In the model, auxin moves acropetally according to published data, which demonstrated that this hormone is transported by the *PIN* efflux facilitators to the SCN through vascular, endodermis and cortex cells [46]. It is known that, from the columella initials, auxin can move in many directions, but because we did not consider cells below the columella initials, these auxin movements were not included in the model.

The spatial information provided to the cells by the four mobile network components was incorporated into the logical rules of each network component, yielding a model of 40 different components. These 40 components correspond to ten nodes per intracellular network multiplied by four types of cells, which are distinguished by the mobile elements. The latter affect the logical rules of each one of the components, depending on the spatial position of each cell in which they are found with respect to other cells (positional information) within the niche, as explained above. Hence, in the new meta-GRN model, each component is identified by its node's identity (i.e., the gene or molecule that it represents) and the spatial location where it is found, which is distinguished by the initial letter of the attractor expected there (Figure 4; and see Methods for further detail).

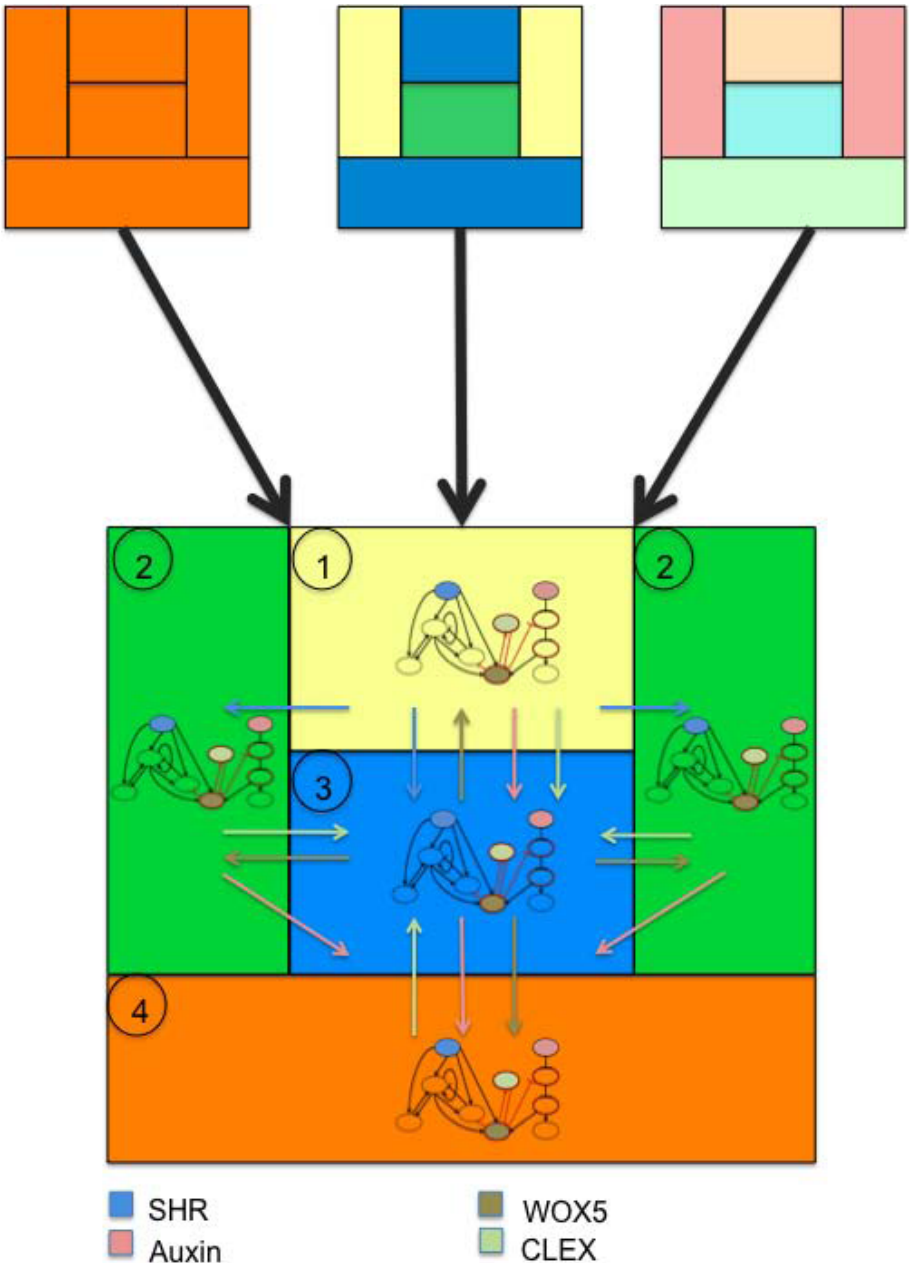

Figure 4 The coupled GRN. The four cell types considered in the coupled GRN are shown numbered in circles. They were represented by a GRN one for each attractor recovered in the single-cell models. Color filled nodes are the diffusible or mobile elements of the GRN. Note that these mobile elements can act non-cell autonomously or move among cells. For clarity we only show the main movement directions with arrows with the same color code as that used for the network nodes which movement is allowed. All the movements allowed in the model are listed in additional file 4. The figures show how, regardless of the initial configuration, the model always converges to the same attractor with the same spatial structure.

The updating dynamics of the intracellular GRN and of the intercellular movement of the mobile components were assumed to be synchronous and acted in a short-range. The latter is justified by experimental data [62]. The logical rules used for the meta-GRN are found in Additional file 4.

Some assumptions were made because of a lack of data or for simplicity. First, because auxin comes from the upper cells, which are not considered in our model, we fixed the auxin value to *1* in the vascular initials and CEI where it can move to the QC and then into CEpI as mentioned above. Also, given the recent evidence on

the similarities between the SAM and root SCN, we assumed an activator-inhibitor motif for the RAM SCN consisting of *WOX5* local auto-regulation enhancing the auxin signaling pathway. The latter could be due to a repression of *Aux/IAA* genes, which is suggested by the fact that *WUS* represses type *A-ARR* genes in the SAM thus enhancing ARF transcription activity. This could also be achieved if WOX5 up-regulates *ARF* transcription directly or through auxin synthesis, as has been suggested for auxin homeostasis before [63]. We tested all alternative coupling patterns, and all of them yielded the same result; therefore, we kept the negative regulation of *Aux/IAA* genes by *WOX5*. In [63], it was also reported that auxin addition up-regulates *WOX5* expression, so in such a circuit, the *ARF* node positively regulates *WOX5* [24,63], and *WOX5* positively regulates *CLEX*, which is assumed to inhibit *WOX5* [25]. Given that *WOX5* is exclusively expressed in the QC and that *CLE40* and other *CLE* genes are found outside the QC [64], we assumed that *WOX5* non-cell autonomously activates *CLEX* outside the QC, but not within the QC. All of these assumptions regarding *WOX5* and *CLEX* interactions and functions give rise to an activator-inhibitor motif in our root SCN GRN. It is important to note that the activator-inhibitor motif can explain many observed and suggested behaviors of the root SCN, such as the robustness (see discussion).

Finally, it is well known that *SHR* is exclusively expressed in the vascular cells [9], but no transcriptional regulators have been uncovered for this gene. In the vascular cells, SHR does not activate *SCR* [9], but is able to move into the QC, CEI and endodermis cells [13], where it activates *SCR* expression [9]. Based on these, *SHR* output was fixed to *1* in the vascular initials, and *SCR* transcription was not allowed there in the model. The impossibility to activate *SCR* in the vascular initials was the only topological change made in the meta-GRN model with respect to the single-cell GRN model B'.

We found that to recover the observed gene expression configurations in the right cell and spatial location, it was necessary to set *SCR* to *1* in the initial condition. Afterwards, from time t+2 and until the end of the simulation, *SCR* followed its original rule postulated for the single-cell model. This assumption implies that *SCR* basal expression, which cannot be explicitly considered in a Boolean model, is sufficient to activate *SCR* when SHR is present in the CEI and QC. Alternatively, it is possible that *SCR* expression depends on an unknown factor that could be expressed during early embryo development. Later on, *SCR* positive feedback may be required to maintain its own expression (see discussion). Another possibility is that the proposed single-cell GNR architecture, once coupled and solved in the spatial model, is not able to fully recover the observed spatial arrangement of gene configurations because of artifacts derived from the dynamics of the discrete model. To test this latter possibility, we ran the spatial network using our continuous approach (see Methods) and also set the expression state of *SCR* to "ON" in the initial conditions. Notably, with the continuous system we only recovered one attractor in which the observed gene expression configurations found in each cell location mimicked those observed in the root SCN; thus, we recovered the same results as with the discrete version (see below) if we set *SCR* "ON" at the beginning of the simulation. This result supports our prediction that an early acting factor or *SCR* basal expression is necessary for the up-regulation of *SCR* during embryo development.

In the discrete meta-GRN spatial model, we exhaustively explored all possible initial configurations (i.e., 2^{40} initials configurations) and recovered again the four gene expression configurations that characterize the cell types distinguished in the modeled SCN with only one cellular arrangement that resembles the arrangement found in real roots (Figure 4). This single attractor is attained regardless of the initial configuration used. In figure 4, we exemplify three of the 2^{40} different initial configurations that converged to the observed one.

We ran the discrete meta-model of four coupled GRNs using the model checker program *ANTELOPE* [Argil J, Azpeitia E, Benitez M, Carrillo M, Rosenblueth D and Alvarez-Buylla E, unpublished data, available upon request]. Model checkers have been widely used for hardware verification, which allow the verification of the different properties in discrete systems. These computational tools are based on a logical analysis and allow verification of different properties, such as the attractors of the system in question. Questions in *ANTELOPE* can be posed by using Hybrid Computational-Tree Logic language, which can be used to verify the properties of any discrete system. The *ANTELOPE* software and a better description of *ANTELOPE* are available upon request. Several accounts on model checking software and Hybrid Computational - Tree Logic are available [65-67].

To validate the spatial model, we simulated mutants that have been documented experimentally. In most cases we recovered the observed gene configurations for each cell type organized in the expected spatial positions (Table 4 and 5). For example, the simulated *SHR* gain of function simulation was able to not only recover the expected mutant configurations but also replaced the CEpI attractor with two different attractors, one corresponding to the CEI attractor and another in which the only difference from the CEpI attractor was the ectopic expression of *SHR*. Such configurations and spatial arrangements coincide with those observed

experimentally in this mutant's epidermis-lateral root cap and collumela initials, respectively.

Another example of the mutants analysis corresponds to the *scr* loss-of-function simulation in which the CEI and the QC configurations are lost and the SHR anomaly diffuses to the CEpI, as has been observed experimentally. Simulations of *mgp* do not yield any altered configuration, as has also been reported experimentally. All other simulated mutants recovered configurations that mimic those observed in their corresponding actual mutant plants. In a few cases, simulation results could not be compared to actual mutant configurations because such lines have not been reported yet (Table 5). Such simulations thus constitute novel predictions.

Discussion

GRN dynamic models that are sufficient to recover *A. thaliana* root SCN cell gene expression configurations

We have postulated novel, alternative GRN models that constitute the first dynamic regulatory system sufficient to explain how the *A. thaliana* root SCN is maintained. Such models are also able to reproduce cell-type determination and spatial patterning in the root SCN. This result suggests that some key components have been uncovered and that these components, given some additional newly predicted interactions, are sufficient to recover gene expression configurations that resemble those known for the main cell types within the root SCN. This study adds to previous ones that have shown the utility of using qualitative models to understand cell differentiation and spatial cellular patterning during development of other systems [30-33,35,36].

From the beginning of our analysis, we noted that the recovered GRN models describe a very simple dynamics, which are congruent with previous intuitive or schematic static models [e.g., [11]]. Still, several characteristics of the root SCN GRN could not have been predicted or analyzed without a dynamic framework like the one provided here.

For example, schematic models proposed from information available until now about root SCN maintenance have considered two critical modules for *A. thaliana* root SCN establishment and maintenance: i) the *SHR*/*SCR* and ii) the *PLT* pathways involved in the radial cell patterning and the apical-basal gradient of cell behavior. It has been suggested that the intersection or combination of the *PLT* and the *SHR*/*SCR* pathways is both necessary and sufficient for the localization, maintenance and patterning of the root SCN [11]. However, we found that the integration of these two modules into a single GRN dynamic did not explain how the symmetry is broken in the root SCN and how cell pattering is maintained.

As observed in the SCN GRN model based only on experimental evidence, the combination of these two modules did not allow us to reproduce the configurations matching those observed within different cell types in the SCN. Hence, our model shows that the connection of these two pathways via *WOX5* and the addition of the new element (*CLEX*) are necessary to explain the root SCN cellular pattern observed.

Therefore, we propose that the GRN underlying *A. thaliana* root SCN establishment and maintenance is more complex than previously suggested [11]. To break the symmetry of the apical root meristem, the combination of a radial and an apical-basal circuit are required. Nevertheless, the additional circuits proposed here, which have also been found in other SCN [e.g., [44,49]], are indeed necessary. The missing components could also add robustness to the GRN and are key for establishing and maintaining the cellular heterogeneity observed in the root SCN.

The fact that the results recovered for such a qualitative model are robust to alterations in the logical functions in over 60% of the cases suggests that knowledge regarding the detailed functioning of the genes is not relevant in determining the steady-state gene configurations. Rather, it is the overall topology of the GRN that determines its dynamics and recovered attractors. For example, several details of gene's functions that have been experimentally documented were not included explicitly. For example, this is the case with the movement and function of SHR, which depends on its intracellular localization [51,52]. Nonetheless, the expected role and behavior for this protein were recovered in the proposed models. Additionally, the robustness observed in the *A. thaliana* SCN is not as high as that documented for other small GRNs, which suggests the existence of additional components and/or redundant circuits as have been found in other systems [60,68].

As mentioned above, the analyses of the GRN models proposed here show that even though important components of the GRN underlying the *A. thaliana* root SCN patterning are already known, some are still missing. The existence of some of these gaps was already well known, such as those associated with *SHR* transcriptional regulation, but others were uncovered thanks to the dynamic approach presented here. This approach enabled us to compare simulated gene expression configurations when using GRNs that differed from those reported before.

The fact that all possible configurations attained with the GRNs proposed here converge to only those observed confirms that the SCN GRN is strongly canalized, and that regardless of the initial states used, the systems proposed lead to the expected stable configurations. This feature is also found in the spatial model of coupled GRNs. The strong canalization of these GRN models suggests that they must also be robust. This

robustness has been observed experimentally in several studies [e.g., [11,12,46,48]], and has been observed in other previously studied developmental GRNs [e.g., [32,33,69,70]].

Previously studied biological GRNs appear to be near criticality (Figure 3) [58,59] for other biological GRNs as well. Indeed, biological GRNs are expected to be robust in the face of perturbations, but these systems should be also able to respond and adapt to transient and permanent perturbations and thereby exhibit evolvability. Shmulevich and Kauffman [58] predicted that biological GRNs should be on the border between order and chaos, where robustness and evolvability coexist. Balleza and collaborators [59] show that experimentally grounded biological GRNs for bacteria, yeast, *Drosophila* and *A. thaliana* are in fact in the so-called critical state. Such analyses rely on the so-called Derrida analysis [57,59]. We performed this analysis, and strikingly, even when our GRN models show certain degree of robustness to perturbations and a critical dynamics, they are less robust than other GRNs [e.g. [32,33]]. The latter suggests that additional components or redundant circuits that render a higher robustness to alterations are likely to be discovered for the SCN GRN.

Additional robustness in the GRN can come from at least four sources. i) The fact that the *PLT*, *ARF* and *Aux/IAA* nodes actually represent several genes. If these were explicitly modeled, the GRN could become more robust. ii) A cross-talk with other developmental regulatory modules, as recently described [55,71-73], could also confer additional robustness to the SCN GRN. We could not include this cross-talk because important experimental information is still lacking. iii) Additional components that confer dynamic redundancy, and thus additional robustness, to the system could also be missing [60,68]. iv) Finally, additional undiscovered components that, even if they do not confer dynamic redundancy, may increase the GRN robustness.

The four possibilities have been documented in other experimental systems. For example, the root auxin gradient is a robust process, which is redundantly generated by the concerted action of several PIN genes and by the high self-regulating dynamics (composed of many feed forward and feedback loops), which regulates auxin transport, biosynthesis and signaling [18,46,48].

The conversion of the Boolean approach into a continuous one provides the possibility of exploring a richer dynamics of the GRN due to the continuous character of the variables and parameters of the system. It may lead, for example, to a different set of attraction basins. However, the sigmoidal structure of the activation functions involved in the continuous approach implies that the qualitative behavior of the solutions of the differential equation system have only a weak dependence on the specific values of the parameters [74]. In particular, in the limiting case where the activation functions acquire a step-like behavior, we recover the same set of (stable) attractors as those arising from the discrete model and an extra unstable one, as an analysis based on Lyapunov coefficients reveals. Thus, this kind of analysis constitutes an additional robustness test of the system. Furthermore, the continuous approach may become useful for future more sophisticated developments considering larger spatio-temporal implementations, which take into account cell cycle and signal transduction elements.

Experimental gaps and predictions

The models developed here are useful to postulate new predictions concerning the GRN underlying the root SCN cellular patterning and to uncover experimental gaps.

The *mgp* loss of function simulation suggested that additional components controlling *WOX5* expression in the proximal meristem have not yet been found. Specifically, we predict that *WOX5* is down-regulated by a gene that is able to move to the proximal SCN cells or a gene that is expressed in those cells. We think that this gene (or these genes) could be from the *CLE-like* gene family but are different from *CLE40*. This hypothesis is consistent with published data because several *CLE* genes are expressed throughout the root tissues, including the proximal meristem [29,64] and because even when recent evidence demonstrates that *CLE40* down-regulates *WOX5* in the initial cells, *CLE40* seems to be insufficient for the negative regulation of *WOX5* in the proximal meristem given that neither *CLE40* nor *ACR4*, the latter of which perceive CLE40, are expressed there [25].

Another important prediction was derived from comparisons of the A and B vs. A' and B' models, along with simulations to recover *jkd* loss of function and the spatial model analysis. Our analyses suggest that *JKD* could only enhance *SCR* expression rather than being an obligate activator; however, once *SCR* is activated, its activity depends upon its own positive feedback and SHR activity. To verify this hypothesis experimentally, one could assess if a reporter gene under the *SCR* promoter is enhanced when crossed to a 35S:SCR line and if the reporter level of expression is the same or lower in a *jkd* compared to a wild type background.

The latter prediction was complemented by another prediction detected from the spatial model analysis, which dealt with *SCR* transcriptional regulation. The positive feedback loops, like the one sustained by *SCR*, are well studied. They are commonly found as a motif that can provide an efficient switching mechanism, hysteresis, bi-stability and robustness in the presence of

noise and is also functional to change response time [75,76]. Hence, in the SCN GRN, the *SCR* positive feedback may give rise to a hysteretic, robust and efficient switching behavior in the face of transient and sometimes permanent perturbations but probably does not regulate the initial expression of *SCR*.

Simulations for *clex* loss-of-function as well as for *SHR*, *SCR*, *MGP*, *JKD* and *WOX5* gain-of-function lines showed that additional research is needed. For example, data for the lateral root cap-epidermis and collumela initials are scarce [e.g., [77-79]] and simulations concerning them are hard to validate.

Another way to validate the models presented here is to explore their behavior under contrasting environmental or hormonal conditions. To that end, we have also tested the GRN models under different auxin concentrations simulated in discrete steps. We found that the postulated GRN models are able to respond to changes in auxin concentrations in ways that resemble those observed experimentally [80] because the gene configurations recovered in the simulations are similar to those observed in real roots treated with different concentrations of auxin. Detailed results of these simulations are provided in Additional file 2.

Is there a generic motif for plant and animal SCN patterning?

To explore novel hypotheses concerning cellular patterns in the root SCN, we performed simulations of the coupled GRN. We achieved this by incorporating experimental evidence concerning the cell-to-cell movement of some of the GRN components into the logical rules that govern the dynamics of each cell GRN. Interestingly, such a simple spatial model converged to only one global attractor, which contained the cell-specific stable gene configurations that have been observed in each of the relative spatial locations within the real root SCN. Most importantly, this model was successfully validated, as it was able to recover altered configurations observed experimentally in the corresponding simulated mutants and yielded the same results in the continuous version. In the spatial model, we incorporated the lateral inhibition of *WOX5*, which is required to recover an activator-inhibitor motif in the root SCN GRN.

The activator-inhibitor system [81,82] is a variant of the reaction diffusion system [83]. The activator-inhibitor system consists of i) an activator that positively regulates itself and an inhibitor (in this case, *WOX5* and *CLEX*, respectively), and ii) an inhibitor that negatively regulates the activator and has a long-range effect. It is important to note that this kind of dynamic circuit has been used to explain robustness, reappearance of patterns and self-organization in biological systems [84-88]. Several studies have suggested that such traits also characterize the root SCN. Robustness of the niche cell pattern, as discussed in the context of this paper, has indeed been observed in several mutants. For example, all *PLT* and *PIN* single mutants [11,12,46,48] have subtle effects or wild type root SCN cell structures. SCN and QC ablation experiments [62,89], on the other hand, have shown the capacity of the SCN to regenerate and suggest a self-organization capacity. Furthermore, a recent study by Sugimoto and collaborators [90] demonstrated that the structures that appear from callus regeneration experiments have cellular structures reminiscent of root tip meristems, and this fact is true if they are derived from either root or aerial organs, which strongly suggests that root tip cell structure is self-organized. The self-organized GRN proposed here constitutes a first dynamic proposal explaining the robustness and regeneration capacity observed in the *A. thaliana* root SCN.

As other authors have already pointed out, the SAM and RAM SC specification mechanisms are similar in terms of the gene families involved and the regulatory interactions observed [2,3,6]. Indeed, in both meristems, genes promoting the QC identity (*WUS* in the SAM; and *WOX5* in the RAM) belong to the family of genes that encode for homeobox transcriptional regulators and both seem to locally self-activate and to positively regulate their inhibitors. Some lines of evidence suggest that the activator-inhibitor could account for SCN maintenance [24,25,53,91], but this experimental evidence is not sufficient to confirm this hypothesis. Interestingly, examining the experimental evidence of SC GRNs in other organisms suggests that this motif could be a generic regulatory motif for systems underlying SCN maintenance and patterning throughout multicellular eukaryotes [34,48,92,93].

Model limitations and perspectives

All models have limitations that stem from their assumptions. For instance, the coupled GRN model suggests that the GRN underlying root SCN patterning may involve an activator-inhibitor motif. However, as we have discussed here, the SCN specification systems in the RAM of *A. thaliana* are dynamically richer than this single motif and likely incorporate several regulatory motifs, some of which could also be dynamically redundant and provide robustness to SCN pattering [60,68]. Furthermore, the module controlling the root SCN must be interconnected with other modules, not considered here, which are indispensable for its establishment and maintenance, such as those controlling hormone signal transduction pathways, the cell cycle, the recently redescribed *SCHIZORIZA* gene [71,72], or other developmental modules [e.g., [55]]. Future models should prove useful for comparing the spatiotemporal dynamics of

the SAM and RAM, spot their commonalities and explore what changes in gene expression patterns, gene interactions, hormone signaling, cell size and geometry or other factors could account for the different sizes, cellular structures, dynamics and morphologies of these two meristems and SCNs.

Given the fact that our models where completely discrete or were continuous approximations of the discrete version, we could not test several observed behaviors of the root and the root SCN. For example, auxin forms a gradient trough the root with the maximum concentration in the SCN, especially in the QC and columella initials, but the importance and implication of this subtle gradient was impossible to test with this model. Also, a more realistic model than this one, in which non-cell-autonomous regulation dynamically emerges rather than being pre-specified, will be helpful. Hence, future models should allow the GRN nodes' movement or other types of intercellular communication to be established and maintained dynamically rather than fixed.

Our GRN recovers the main traits of the *A. thaliana* root SCN given the available gene interaction data and some additional assumptions, thus providing the first GRN framework along with novel predictions. However, given the multiple ways in which novel interactions or nodes can be connected to the uncovered network, genomic approaches will complement the modeling approach and results put forward here and help obtain a more complete GRN underlying SCN cellular pattering in the *A. thaliana* root. It is likely that additional and redundant circuits connected to those discovered up to now and integrated in the models proposed here will yield more robust GRN models as those described for other systems [60,68].

The integration and modeling of a GRN like the one studied here will also foster work on comparative and evolutionary developmental biology. For instance, the main components of the transcriptional regulatory networks involved in SC specification in *A. thaliana* belongs to plant-specific families, but it has been found that some animal and plant developmental systems share analogous regulatory circuits [e.g., [92,93]]. Given that the SCN of all multicellular organisms share common features and that animal and plant niches share structural and dynamic traits, it will be important to uncover and dynamically characterize the GRNs involved in their maintenance in other multicellular species and examine if there are conserved or analogous regulatory motives, modules or mechanisms. These kinds of analyses would be of great value for understanding the evolution of such a system, which is key for eukaryote development, and to address questions concerning structural constraints during GRN assemblage along plant and animal evolution.

Conclusions

We report the first GRN models capable of recovering the main traits of the *A. thaliana* root SCN cellular structure. The proposed dynamic approximation to the *A. thaliana* root SCN GRN has enabled us to detect several important gaps in the published data, some concerning the transcriptional regulators of genes considered in our GRN. These gaps involve *SCR*, *SHR*, *JKD*, *MGP* and *WOX5*, which still lack important regulators. We also detected one contradiction about *JKD* function, which we predict is not indispensable for *SCR* expression or function. Finally, we predict the existence of *WOX5* negative regulators in the vascular initials and probably in the CEI.

Some of these predictions are amenable to experimental tests. A more robust GRN will probably imply additional components and redundant circuits. However, our models suggest that some of the key genes involved in root SCN maintenance have been discovered, but other important components remain to be found. Additional efforts on GRN simulations and genomic approaches will be fundamental for postulating more complete models for explaining the root SCN cellular patterning.

Methods

Boolean single cell and coupled GRNs

In the autonomous single cell and coupled GRN models, N nodes are defined and these represent the genes and molecules involved in cell patterning and maintenance of the root SCN. The state of every node can only take two possible values, *0* (gene off) or *1* (gene on), depending on the function:

$$x_n(t+\tau) = F_n(x_{n_1}(t), x_{n_2}(t), \ldots, x_{n_k}(t))$$

For the single cell model, x_n represents the state of a gene at the time $(t+\tau)$ and $\{x_{n_1}(t), x_{n_2}(t), \ldots, x_{n_k}(t)\}$ represents all of the regulators of gene x_n at time t. For the coupled GRN the function:

$$x_n^m(t+\tau) = F_n(x_{n_1}^1(t), x_{n_2}^1(t), \ldots, x_{n_k}^1(t), x_{n_1}^2(t), \ldots, x_{n_k}^p(t))$$

defines the state of every node, where x_n^m resspresents the state of a gene in a specific cell type m at the time $(t+\tau)$ and $\{x_{n_1}^1(t), x_{n_2}^1(t), \ldots, x_{n_k}^1(t), x_{n_1}^2(t), \ldots, x_{n_k}^p(t)\}$ represents all the regulators of gene x_n^m at time t including those from other cell types capable of moving and acting non-cell autonomously. For both kinds of models, F_n is a Boolean logical function based on experimental evidence. The models are deterministic and have a finite

number of possible initial conditions represented by Ω (Ω = 2_N). Therefore, the future states of all possible initial conditions can be determined. The models were iterated synchronously until they reached a steady state starting from all possible initial conditions.

PLT, *ARF* and *Aux/IAA* represent families of genes that, given their redundancy, are modeled as one node. The value of *1* for the auxin node does not represent any concentration; rather, it represents a wild type concentration sufficient for the specific function under consideration in the model. All other nodes represent a single gene. Loss-of-function simulations were done by fixing the state of the node to *0*; for gain-of-function simulations it was set to *1*.

For the meta-GRN of the coupled GRN, we defined four domains; each one represented a SC type (Figure 4) and there was one for every attractor in the one-cell models. The logical rules enabled communication between each GRN based on experimental evidence and our activator-inhibitor prediction. In this case, we have now four coupled GRNs. Thus, when we ran the model, we expected only one global attractor.

Continuous model

We considered a GRN with N nodes. We represented the activation level at node k by X_k. Within a continuous scheme, the rate of change of the activation level was represented by the set of differential equations:

$$\frac{dx_K}{dt} = f[w_K(x)] - \gamma_K x_K$$

where γ_k is the activation decay rate, and $f[w_k(X_1,..., X_N)]$ is a logistic functional determined by the node input function $w_k(X_1,...,X_N)$:

$$f_K[w_K(x_1,...,x_N)] = \frac{1}{1+\exp[-h(w_K - w_K^{thr})]}$$

where w_K^{thr} is the threshold activation level and h is a measure of the activation speed. Notice that in the limit $hw_K^{thr} \gg 1, f_K[w_K < w_K^{thr}] \to 0, f_K[w_K = w_K^{thr}] \to 1/2$, and $f_K[w_K > w_K^{thr}] \to 1$, so that f_k behaves as a (differentiable) step-like function $f[w_K] \simeq \Theta(w_K - w_K^{thr})$. To obtain explicit solutions of the differential equation set, we assume that y_k = 1, and w_K^{thr} = 1/2. Notice, however, that the solution method applies also for arbitrary values of these parameters. The attractors of the system may be analytically derived from the condition dx_K/dt = 0, which leads to a set of non-linear algebraic equations with the general form

$$x_K = \Theta[w_K(x_1,...x_N)]$$

which implies in turn obtaining the solutions for the cases w_K > 1/2, w_K = 1/2, and w_K < 1/2. The expression for the total input at a given node, w_i, representing the logical rules are given in Additional files 3 and 4. The program used for this model is freely available upon request.

Additional material

Additional file 1: This file contains the detailed topology and updating single cell GRN discrete functions.

Additional file 2: This file contains additional GRN analysis under different auxin concentrations.

Additional file 3: This file contains the detailed topology and updating single cell GRN continuous functions.

Additional file 4: This file contains the detailed topology and updating coupled GRN discrete and continuous functions.

Acknowledgements

Financial support was received from the Programa de Apoyo a Proyectos de Investigación e Innovación Tecnológica Universidad Nacional Autónoma de México IN229009-3; Consejo Nacional de Ciencia y Tecnología grant to E.A.B, 81542; and PhD scholarship from Consejo Nacional de Ciencia y Tecnología to M.B. I.V. and E.A. E.A's PhD research is done at the Posgrado en Ciencias Biomédicas, Universidad Nacional Autónoma de México (Instituto de Ecología). I.V.'s research is done at the Posgrado en Ciencias Físicas, Universidad Autónoma de México (Instituto de Física). We thank R. V. Pérez Ruiz and D. Romo for technical and logistical assistance. We thank M. A. Pacheco for the root tip photography. We also thank our anonymous reviewers' comments that helped us improve the manuscript.

Author details

[1]Laboratorio de Genética Molecular, Desarrollo y Evolución de Plantas, Instituto de Ecología & Centro de Ciencias de la Complejidad (C3), Universidad Nacional Autónoma de México, Ciudad Universitaria, Coyoacán, México D.F. 04510. México. [2]Instituto de Física, Universidad Nacional Autónoma de México, Ciudad Universitaria, Coyoacán, México D.F. 04510. México Apdo. Postal 20-364. México D.F., 04510, Mexico & Centro de Ciencias de la Complejidad (C3), Universidad Nacional Autónoma de México, Ciudad Universitaria, Coyoacán, México D.F. 04510. México.

Authors' contributions

EAB conceived and coordinated the study. EAB, EA and MB designed the study. EA gathered, integrated and analyzed the experimental data and postulated the models with help from EAB and MB. EA ran the simulations for the discrete case. IV and CV established the continuous system, and IV ran its simulations. EAB, EA and MB wrote the paper. All of the authors helped interpret the results and read and validated the final version of the paper.

Received: 22 February 2010 Accepted: 5 October 2010
Published: 5 October 2010

References

1. Walker MR, Patel KK, Stappenbeck TS: **The stem cell niche.** *J Pathol* 2009, **217**:169-80.
2. Sablowski R: **Plant and animal stem cells: conceptually similar, molecularly distinct?** *Trends Cell Biol* 2004, **14**:605-11.
3. Scheres B: **Stem-cell niches: nursery rhymes across kingdoms.** *Nat Rev Mol Cell Biol* 2007, **8**:345-54.
4. Benfey PN: **Stem cells:A tale of two kingdoms.** *Current Biology* 1999, **9**: R171-R172.

5. Birnbaum KD, Sánchez Alvarado A: **Slicing across kingdoms: regeneration in plants and animals.** *Cell* 2008, **132**:697-710.
6. Dinneny JR, Benfey PN: **Plant Stem Cell Niches: Standing the Test of Time.** *Cell* 2008, **132**:553-7.
7. Jones AM, Chory J, Dangl JL, Estelle M, Jacobsen SE, Meyerowitz EM, Nordborg M, Weigel D: **The impact of Arabidopsis on human health: diversifying our portfolio.** *Cell* 2008, **133**:939-43.
8. Dolan L, Janmaat K, Willemsen V, Linstead P, Poethig S, Roberts K, Scheres B: **Cellular organisation of the Arabidopsis thaliana root.** *Development* 1993, **119**:71-84.
9. Helariutta Y, Fukaki H, Wysocka-Diller J, Nakajima K, Jung J, Sena G, Hauser MT, Benfey PN: **The SHORT-ROOT gene controls radial patterning of the Arabidopsis root through radial signaling.** *Cell* 2000, **101**:555-67.
10. Sabatini S, Heidstra R, Wildwater M, Scheres B: **SCARECROW is involved in positioning the stem cell niche in the Arabidopsis root meristem.** *Genes Dev* 2003, **17**:354-8.
11. Aida M, Beis D, Heidstra R, Willemsen V, Blilou I, Galinha C, Nussaume L, Noh YS, Amasino R, Scheres B: **The PLETHORA genes mediate patterning of the Arabidopsis root stem cell niche.** *Cell* 2004, **119**:109-20.
12. Galinha C, Hofhuis H, Luijten M, Willemsen V, Blilou I, Heidstra R, Scheres B: **PLETHORA proteins as dose-dependent master regulators of Arabidopsis root development.** *Nature* 2007, **449**:1053-7.
13. Nakajima K, Sena G, Nawy T, Benfey PN: **Intercellular movement of the putative transcription factor SHR in root patterning.** *Nature* 2001, **413**:307-11.
14. Cui H, Levesque MP, Vernoux T, Jung JW, Paquette AJ, Gallagher KL, Wang JY, Blilou I, Scheres B, Benfey PN: **An evolutionarily conserved mechanism delimiting SHR movement defines a single layer of endodermis in plants.** *Science* 2007, **316**:421-5.
15. Di Laurenzio L, Wysocka-Diller J, Malamy JE, Pysh L, Helariutta Y, Freshour G, Hahn MG, Feldmann KA, Benfey PN: **The SCARECROW gene regulates an asymmetric cell division that is essential for generating the radial organization of the Arabidopsis root.** *Cell* 1996, **86**:423-33.
16. Levesque MP, Vernoux T, Busch W, Cui H, Wang JY, Blilou I, Hassan H, Nakajima K, Matsumoto N, Lohmann JU, Scheres B, Benfey PN: **Whole-genome analysis of the SHORT-ROOT developmental pathway in Arabidops.** *PLoS Biol* 2006, **4**:e143.
17. Welch D, Hassan H, Blilou I, Immink R, Heidstra R, Scheres B: **Arabidopsis JACKDAW and MAGPIE zinc finger proteins delimit asymmetric cell division and stabilize tissue boundaries by restricting SHORT-ROOT action.** *Genes Dev* 2007, **21**:2196-204.
18. Woodward AW, Bartel B: **Auxin: regulation, action, and interaction.** *Ann Bot (Lond)* 2005, **95**:707-35.
19. Guilfoyle TJ, Hagen G: **Auxin response factors.** *Curr Opin Plant Biol* 2007, **10**:453-60.
20. Mockaitis K, Estelle M: **Auxin receptors and plant development: a new signaling paradigm.** *Annu Rev Cell Dev Biol* 2008, **24**:55-80.
21. Lau S, Jürgens G, De Smet I: **The evolving complexity of the auxin pathway.** *Plant Cell* 2008, **20**:1738-46.
22. Tiwari SB, Wang XJ, Hagen G, Guilfoyle TJ: **AUX/IAA proteins are active repressors, and their stability and activity are modulated by auxin.** *Plant Cell* 2001, **13**:2809-22.
23. Tiwari SB, Hagen G, Guilfoyle TJ: **Aux/IAA proteins contain a potent transcriptional repression domain.** *Plant Cell* 2004, **16**:533-43.
24. Sarkar AK, Luijten M, Miyashima S, Lenhard M, Hashimoto T, Nakajima K, Scheres B, Heidstra R, Laux T: **Conserved factors regulate signalling in Arabidopsis thaliana shoot and root stem cell organizers.** *Nature* 2007, **446**:811-4.
25. Stahl Y, Wink RH, Ingram GC, Simon R: **A Signaling Module Controlling the Stem Cell Niche in Arabidopsis Root Meristems.** *Curr Biol* 2009, **19**:909-14.
26. Hobe M, Müller R, Grünewald M, Brand U, Simon R: **Loss of CLE40, a protein functionally equivalent to the stem cell restricting signal CLV3, enhances root waving in Arabidopsis.** *Dev Genes Evol* 2003, **213**:371-81.
27. Fiers M, Golemiec E, Xu J, van der Geest L, Heidstra R, Stiekema W, Liu CM: **The 14-amino acid CLV3, CLE19, and CLE40 peptides trigger consumption of the root meristem in Arabidopsis through a CLAVATA2-dependent pathway.** *Plant Cell* 2005, **17**:2542-53.
28. Hirakawa Y, Shinohara H, Kondo Y, Inoue A, Nakanomyo I, Ogawa M, Sawa S, Ohashi-Ito K, Matsubayashi Y, Fukuda H: **Non-cell-autonomous control of vascular stem cell fate by a CLE peptide/receptor system.** *Proc Natl Acad Sci USA* 2008, **105**:15208-13.
29. Sharma VK, Ramirez J, Fletcher JC: **The Arabidopsis CLV3-like (CLE) genes are expressed in diverse tissues and encode secreted proteins.** *Plant Mol Biol* 2003, **51**:415-25.
30. Mendoza L, Alvarez-Buylla ER: **Dynamics of the genetic regulatory network for Arabidopsis thaliana flower morphogenesis.** *J Theor Biol* 1998, **193**:307-19.
31. Albert R, Othmer HG: **The topology of the regulatory interactions predicts the expression pattern of the segment polarity genes in Drosophila melanogaster.** *J Theor Biol* 2003, **223**:1-18.
32. Espinosa-Soto C, Padilla-Longoria P, Alvarez-Buylla ER: **A gene regulatory network model for cell-fate determination during Arabidopsis thaliana flower development that is robust and recovers experimental gene expression profiles.** *Plant Cell* 2004, **16**:2923-39.
33. Benítez M, Espinosa-Soto C, Padilla-Longoria P, Alvarez-Buylla ER: **Interlinked nonlinear subnetworks underlie the formation of robust cellular patterns in Arabidopsis epidermis: a dynamic spatial model.** *BMC Syst Biol* 2008, **2**:98.
34. Chickarmane V, Peterson C: **A computational model for understanding stem cell, trophectoderm and endoderm lineage determination.** *PLoS ONE* 2008, **3**:e3478.
35. Li S, Assmann SM, Albert R: **Predicting essential components of signal transduction networks: a dynamic model of guard cell abscisic acid signaling.** *PLoS Biol* 2006, **4**:e312.
36. Albert R, Wang RS: **Discrete dynamic modeling of cellular signaling networks.** *Methods Enzymol* 2009, **467**:281-306.
37. Alvarez-Buylla ER, Benítez M, Dávila EB, Chaos A, Espinosa-Soto C, Padilla-Longoria P: **Gene regulatory network models for plant development.** *Curr Opin Plant Biol* 2007, **10**:83-91.
38. de Jong H: **Modeling and simulation of genetic regulatory systems: a literature review.** *J Comput Biol* 2002, **9**:67-103.
39. Kauffman SA: **Metabolic stability and epigenesis in randomly constructed genetic nets.** *J Theor Biol* 1969, **22**:437-67.
40. Roeder I, Loeffler M: **A novel dynamic model of hematopoietic stem cell organization based on the concept of within-tissue plasticity.** *Exp Hematol* 2002, **30**:853-861.
41. Glauche I, Cross M, Loeffler M, Roeder I: **Lineage specification of hematopoietic stem cells: mathematical modeling and biological implications.** *Stem Cells* 2007, **25**:1791-9.
42. Roeder I, Kamminga LM, Braesel K, Dontje B, de Haan G, Loeffler M: **Competitive clonal hematopoiesis in mouse chimeras explained by a stochastic model of stem cell organization.** *Blood* 2005, **105**:609-16.
43. Geier F, Lohmann JU, Gerstung M, Maier AT, Timmer J: **A Quantitative and Dynamic Model for Plant Stem Cell Regulation.** *PLoS ONE* 2008, **3**:e3553.
44. Hohm T, Zitzler E, Simon R: **A dynamic model for stem cell homeostasis and patterning in Arabidopsis meristems.** *PLoS ONE* 2010, **5**:e9189.
45. Iyer-Pascuzzi AS, Benfey PN: **Transcriptional networks in root cell fate specification.** *Biochim Biophys Acta* 2009, **1789**:315-25.
46. Blilou I, Xu J, Wildwater M, Willemsen V, Paponov I, Friml J, Heidstra R, Aida M, Palme K, Scheres B: **The PIN auxin efflux facilitator network controls growth and patterning in Arabidopsis roots.** *Nature* 2005, **433**:39-44.
47. Nawy T, Lee JY, Colinas J, Wang JY, Thongrod SC, Malamy JE, Birnbaum K, Benfey PN: **Transcriptional profile of the Arabidopsis root quiescent center.** *Plant Cell* 2005, **17**:1908-25.
48. Vieten A, Vanneste S, Wisniewska J, Benková E, Benjamins R, Beeckman T, Luschnig C, Friml J: **Functional redundancy of PIN proteins is accompanied by auxin-dependent cross-regulation of PIN expression.** *Development* 2005, **132**:4521-31.
49. Gordon SP, Chickarmane VS, Ohno C, Meyerowitz EM: **Multiple feedback loops through cytokinin signaling control stem cell number within the Arabidopsis shoot meristem.** *Proc Natl Acad Sci USA* 2009, **106**:16529-34.
50. Veit B: **Stem cell signalling networks in plants.** *Plant Mol Biol* 2006, **60**:793-810.
51. Gallagher KL, Paquette AJ, Nakajima K, Benfey PN: **Mechanisms regulating SHORT-ROOT intercellular movement.** *Curr Biol* 2004, **14**:1847-51.
52. Gallagher KL, Benfey PN: **Both the conserved GRAS domain and nuclear localization are required for SHORT-ROOT movement.** *Plant J* 2009, **57**:785-97.
53. Sena G, Jung JW, Benfey PN: **A broad competence to respond to SHORT ROOT revealed by tissue-specific ectopic expression.** *Development* 2004, **131**:2817-26.

54. Williams L, Grigg SP, Xie M, Christensen S, Fletcher JC: **Regulation of Arabidopsis shoot apical meristem and lateral organ formation by microRNA miR166g and its AtHD-ZIP target genes.** *Development* 2005, **132**:3657-68.
55. Carlsbecker A, Lee JY, Roberts CJ, Dettmer J, Lehesranta S, Zhou J, Lindgren O, Moreno-Risueno MA, Vatén A, Thitamadee S, Campilho A, Sebastian J, Bowman JL, Helariutta Y, Benfey PN: **Cell signalling by microRNA165/6 directs gene dose-dependent root cell fate.** *Nature* 2010, **465**:316-21.
56. Chaos Á: **Atalia version 1.** Published by the author 2009, Mexico[http://www.ecologia.unam.mx/~achaos/Atalia/ataliaen.htm].
57. Aldana M, Balleza E, Kauffman S, Resendiz O: **Robustness and evolvability in genetic regulatory networks.** *J Theor Biol* 2007, **245**:433-48.
58. Shmulevich I, Kauffman SA: **Activities and sensitivities in boolean network models.** *Phys Rev Lett* 2004, **93**:048701.
59. Balleza E, Alvarez-Buylla ER, Chaos A, Kauffman S, Shmulevich I, Aldana M: **Critical dynamics in genetic regulatory networks: examples from four kingdoms.** *PLoS ONE* 2008, **3**:e2456.
60. Benítez M, Alvarez-Buylla ER: **Dynamic-module redundancy confers robustness to the gene regulatory network involved in hair patterning of Arabidopsis epidermis.** *Biosystems* 2010.
61. González A, Chaouiya C, Thieffry D: **Logical modelling of the role of the Hh pathway in the patterning of the Drosophila wing disc.** *Bioinformatics* 2008, **24**:i234-40.
62. van den Berg C, Willemsen V, Hendriks G, Weisbeek P, Scheres B: **Short-range control of cell differentiation in the Arabidopsis root meristem.** *Nature* 1997, **390**:287-9.
63. Gonzali S, Novi G, Loreti E, Paolicchi F, Poggi A, Alpi A, Perata P: **A turanose-insensitive mutant suggests a role for WOX5 in auxin homeostasis in Arabidopsis thaliana.** *Plant J* 2005, **44**:633-45.
64. Birnbaum K, Shasha DE, Wang JY, Jung JW, Lambert GM, Galbraith DW, Benfey PN: **A gene expression map of the Arabidopsis root.** *Science* 2003, **302**:1956-60.
65. Emerson EA: **The Beginning of Model Checking: A Personal Perspective.** *25 Years of Model Checking* 2008, **5000**:27-45.
66. Franceschet M, de Rijke M: **Model checking hybrid logic (with an application to semistructured data).** *Journal of Applied Logic* 2006, **4(2)**:168-191.
67. Areces C, ten Cate B: **Hybrid Logics.** In *Handbook of Modal Logics.* Edited by: Blackburn P, Wolter F, van Benthem J. Elsevier; 2006:821-868.
68. Irons DJ, Wojcinski A, Glise B, Monk NA: **Robustness of positional specification by the Hedgehog morphogen gradient.** *Dev Biol* 2010, **342**:180-93.
69. Savage NS, Walker T, Wieckowski Y, Schiefelbein J, Dolan L, Monk NA: **A mutual support mechanism through intercellular movement of CAPRICE and GLABRA3 can pattern the Arabidopsis root epidermis.** *PLoS Biol* 2008, **6**:e235.
70. von Dassow G, Meir E, Munro EM, Odell GM: **The segment polarity network is a robust developmental module.** *Nature* 2000, **406**:188-92.
71. Pernas M, Ryan E, Dolan L: **SCHIZORIZA controls tissue system complexity in plants.** *Curr Biol* 2010, **20**:818-23.
72. ten Hove CA, Willemsen V, de Vries WJ, van Dijken A, Scheres B, Heidstra R: **SCHIZORIZA encodes a nuclear factor regulating asymmetry of stem cell divisions in the Arabidopsis root.** *Curr Biol* 2010, **20**:452-7.
73. Hassan H, Scheres B, Blilou I: **JACKDAW controls epidermal patterning in the Arabidopsis root meristem through a non-cell-autonomous mechanism.** *Development* 2010, **137**:1523-9.
74. Mendoza L, Xenarios I: **A method for the generation of standardized qualitative dynamical systems of regulatory networks.** *Theor Biol Med Model* 2006, **3**:13.
75. Brandman O, Meyer T: **Feedback loops shape cellular signals in space and time.** *Science* 2008, **322**:390-5.
76. Mitrophanov AY, Groisman EA: **Positive feedback in cellular control systems.** *Bioessays* 2008, **30**:542-55.
77. Cnops G, Wang X, Linstead P, Van Montagu M, Van Lijsebettens M, Dolan L: **Tornado1 and tornado2 are required for the specification of radial and circumferential pattern in the Arabidopsis root.** *Development* 2000, **127**:3385-94.
78. Mylona P, Linstead P, Martienssen R, Dolan L: **SCHIZORIZA controls an asymmetric cell division and restricts epidermal identity in the Arabidopsis root.** *Development* 2002, **129**:4327-34.
79. Willemsen V, Bauch M, Bennett T, Campilho A, Wolkenfelt H, Xu J, Haseloff J, Scheres B: **The NAC domain transcription factors FEZ and SOMBRERO control the orientation of cell division plane in Arabidopsis root stem cells.** *Dev Cell* 2008, **15**:913-22.
80. Sabatini S, Beis D, Wolkenfelt H, Murfett J, Guilfoyle T, Malamy J, Benfey P, Leyser O, Bechtold N, Weisbeek P, Scheres B: **An auxin-dependent distal organizer of pattern and polarity in the Arabidopsis root.** *Cell* 1999, **99**:463-72.
81. Meinhardt H: **Models of biological pattern formation.** London: Academic Press 1982.
82. Gierer A, Meinhardt H: **A theory of biological pattern formation.** *Kybernetik* 1972, **12**:30-9.
83. Turing AM: **The chemical basis of morphogenesis.** *Phil Trans R Soc Lond B* 1952, **237**:5-72.
84. Meinhardt H: **Organizer and axes formation as a self-organizing process.** *Int J Dev Biol* 2001, **45**:177-88.
85. Yamaguchi M, Yoshimoto E, Kondo S: **Pattern regulation in the stripe of zebrafish suggests an underlying dynamic and autonomous mechanism.** *Proc Natl Acad Sci USA* 2007, **104**:4790-3.
86. Goodwin B: **How the Leopard Changed its Spots.** London: Weidenfeld and Nicolson 1994.
87. Salazar-Ciudad I, Jernvall J: **A computational model of teeth and the developmental origins of morphological variation.** *Nature* 2010, **464**:583-6.
88. Meinhardt H: **Computational modelling of epithelial patterning.** *Curr Opin Genet Dev* 2007, **17**:272-80.
89. Xu J, Hofhuis H, Heidstra R, Sauer M, Friml J, Scheres B: **A molecular framework for plant regeneration.** *Science* 2006, **311**:385-8.
90. Sugimoto K, Jiao Y, Meyerowitz EM: **Arabidopsis regeneration from multiple tissues occurs via a root development pathway.** *Dev Cell* 2010, **18**:463-71.
91. Dolan L: **Meristems: the root of stem cell regulation.** *Curr Biol* 2009, **19**: R459-60.
92. Pesch M, Hülskamp M: **Creating a two-dimensional pattern de novo during Arabidopsis trichome and root hair initiation.** *Curr Opin Genet Dev* 2004, **14**:422-7.
93. Sick S, Reinker S, Timmer J, Schlake T: **WNT and DKK determine hair follicle spacing through a reaction-diffusion mechanism.** *Science* 2006, **314**:1447-50.

doi:10.1186/1752-0509-4-134
Cite this article as: Azpeitia *et al.*: Single-cell and coupled GRN models of cell patterning in the *Arabidopsis thaliana* root stem cell niche. *BMC Systems Biology* 2010 **4**:134.

5.2.- Parte II: "Dynamic network-based epistasis analysis: boolean examples"

Una vez terminada la primera parte del trabajo quedaron en evidencia al menos un par de cosas. Que la información experimental más un par de predicciones en aquel momento, eran suficientes para explicar la emergencia de las configuraciones genéticas observadas experimentalmente en los distintos tipos de células en el nicho de células troncales del ápice de la raíz de *A. thaliana*, tanto de la red de la planta tipo silvestre y de las mutantes, así como la organización espacial de los distintos tipos de células. Sin embargo, la información era aún muy limitada para hacer análisis más profundos, ya fuera de la dinámica o de alguno de los procesos moleculares más específicos. Por este motivo se comenzó a discutir cómo sería posible ahondar más en el estudio de la red, ya fuera estudiando a mayor detalle sus componentes o encontrando cómo incluir más información aún faltante o desarticulada del resto.

Por este motivo, en un segundo momento del proyecto, analizamos cómo podríamos utilizar redes Booleanas de forma sistemática para encontrar información experimental faltante dentro de motivos de regulación, como los analizados por medio de los análisis de epistasis tradicionales. Esto fue analizado a mayor profundidad en un siguiente artículo, el cual también dió pie a generar una hipótesis sobre como continuar estudiando la red del nicho de células troncales de raíz.

En esta parte del trabajo se estudiaron los alcances del formalismo Booleano al ser empleado para analizar la información experimental disponible. Este trabajo mostró como a partir del formalismo Booleano era posible conocer de forma más integral y completa las posibles interpretaciones de los resultados, dejando al descubierto bajo que circunstancias es posible mal interpretar los datos experimentales, lo que podría generar datos o conclusiones falsas. A su vez, mostró cómo los análisis con redes Booleanas podrían ayudar a identificar posible información faltante.

Ahora hemos de presentar el trabajo publicado sobre el uso de redes Booleanas para el análisis de epistasis, el cual fue publicado en Frontiers in Plant Science en 2011.

frontiers in
PLANT SCIENCE

HYPOTHESIS AND THEORY ARTICLE
published: 15 December 2011
doi: 10.3389/fpls.2011.00092

Dynamic network-based epistasis analysis: Boolean examples

Eugenio Azpeitia[1,2], Mariana Benítez[2,3,4], Pablo Padilla-Longoria[2,5], Carlos Espinosa-Soto[2,6] and Elena R. Alvarez-Buylla[1,2]*

[1] *Instituto de Ecología, Universidad Nacional Autónoma de Mexico, Mexico D.F., Mexico*
[2] *Centro de Ciencias de la Complejidad, Universidad Nacional Autónoma de Mexico, Mexico D.F., Mexico*
[3] *Department of Functional Genomics and Proteomics, Masaryk University, Brno, Czech Republic*
[4] *Central European Institute of Technology, Masaryk University, Brno, Czech Republic*
[5] *Instituto de Investigaciones en Matemáticas Aplicadas y en Sistemas, Mexico D.F., Mexico*
[6] *Cinvestav-IPN, Irapuato, Mexico*

Edited by:
Holger Puchta, Karlsruhe Institute of Technology, Germany

Reviewed by:
Stewart Gillmor, Cinvestav-IPN, Mexico
Asa Ben-Hur, Colorado State University, USA

Correspondence:
Elena R. Alvarez-Buylla, Laboratorio de Genética Molecular, Desarrollo y Evolución de Plantas, Dpto de Ecología Funcional, Instituto de Ecología, 3er Circuito Exterior, Junto a Jardín Botánico, CU, Coyoacán, Mexico D.F. 04510, Mexico.
e-mail: eabuylla@gmail.com

In this article we focus on how the hierarchical and single-path assumptions of epistasis analysis can bias the inference of gene regulatory networks. Here we emphasize the critical importance of dynamic analyses, and specifically illustrate the use of Boolean network models. Epistasis in a broad sense refers to gene interactions, however, as originally proposed by Bateson, epistasis is defined as the blocking of a particular allelic effect due to the effect of another allele at a different locus (herein, classical epistasis). Classical epistasis analysis has proven powerful and useful, allowing researchers to infer and assign directionality to gene interactions. As larger data sets are becoming available, the analysis of classical epistasis is being complemented with computer science tools and system biology approaches. We show that when the hierarchical and single-path assumptions are not met in classical epistasis analysis, the access to relevant information and the correct inference of gene interaction topologies is hindered, and it becomes necessary to consider the temporal dynamics of gene interactions. The use of dynamical networks can overcome these limitations. We particularly focus on the use of Boolean networks that, like classical epistasis analysis, relies on logical formalisms, and hence can complement classical epistasis analysis and relax its assumptions. We develop a couple of theoretical examples and analyze them from a dynamic Boolean network model perspective. Boolean networks could help to guide additional experiments and discern among alternative regulatory schemes that would be impossible or difficult to infer without the elimination of these assumption from the classical epistasis analysis. We also use examples from the literature to show how a Boolean network-based approach has resolved ambiguities and guided epistasis analysis. Our article complements previous accounts, not only by focusing on the implications of the hierarchical and single-path assumption, but also by demonstrating the importance of considering temporal dynamics, and specifically introducing the usefulness of Boolean network models and also reviewing some key properties of network approaches.

Keywords: epistasis, gene regulatory networks, Boolean networks, feedback loops, feed-forward loops, temporal dynamics, modeling, gene interactions

INTRODUCTION

Most of the commonly used approaches to analyze gene regulatory interactions, such as epistasis analysis, rely on some implicit assumptions. As we will show, one common of such implicit assumptions is that genes are arranged in a hierarchical pattern of interactions in which each gene can either be upstream or downstream, but not both, as it occurs in feedback loops (**Figures 1A,B**). Another commonly implicit assumption is that gene interactions are part of a single-path, in contrast to cases in which a given gene can regulate another gene via two different pathways at the same time, as it occurs in feed-forward loops (**Figures 1C,D**). The notion of hierarchical and single-path gene regulation is consistent with the search of pathways or cascades rather than networks (Greenspan, 2001; Aylor and Zeng, 2008). However, experimental and theoretical work has demonstrated that biological molecular mechanisms contain regulatory feedback and feed-forward loops that do not fulfill the hierarchical and single-path assumptions, but are rather consistent with a network-based perspective. Such traits of gene regulation are key for understanding gene regulatory dynamics of almost any biological process (Mangan and Alon, 2003; Brandman and Meyer, 2008; Jaeger et al., 2008; Kaplan et al., 2008; Mitrophanov and Groisman, 2008). Hence, methods that consider regulatory feedback loops, feed-forward loops, and temporal dynamics at the same time will likely improve previous approaches. In this article we use epistasis analysis as an example, to explore the effect of these three aspects of gene

regulation on the results and interpretation of gene interaction analyses.

Epistasis is ubiquitous within gene regulatory networks in living organisms (Tyler et al., 2009). As acknowledged by many authors, epistasis has important implications in a broad range of biological issues, from biomedicine to evolutionary studies (see Phillips, 2008 and references therein). Is important to note that there are different notions of the term epistasis: the original one proposed by Bateson in 1907 (herein called classical epistasis) that refers to the masking of the effect of one allele by another allele in a different locus, and a broader definition referring to gene interactions in general.

We focus here on classical epistasis, but it is important to note that the different notions of epistasis are related. Hence, some works have aimed to bring together these different notions of the term epistasis (e.g., Moore and Williams, 2005), allowing elegant and improved analyses of classical epistasis for quantitative traits as well as qualitative discrete ones (e.g., Aylor and Zeng, 2008; Phenix et al., 2011). In any case, the original analysis proposed for classical epistasis (herein called classical epistasis analysis) as described by Avery and Wasserman (1992) is still one of the most powerful and widely used tools in molecular biology to infer biological pathways and regulatory interactions among genes and to validate predictions derived from high-throughput experimental analysis. It is simple, very powerful, and relies on some explicit and implicit assumptions that, when met, allow this analysis to be taken almost as a recipe to order genes along control pathways (Avery and Wasserman, 1992; Huang and Sternberg, 2006; Roth et al., 2009; **Figure 2**).

The explicit assumptions of the classical epistasis analysis are: (1) there is a signal or input that determines the state of the phenotype under analysis, (2) the signal also determines the state of the upstream gene, (3) the signal and the two genes are the only determinants of the phenotype, at least in the context of an experimental model, and finally, (4) the mutants analyzed are null or complete loss-of-function mutants (based on Avery and Wasserman, 1992; Huang and Sternberg, 2006). However, classical epistasis analysis also relies on the implicit assumptions of hierarchical and single-path gene regulation. As we will show, the accomplishment of the implicit assumptions is fundamental for the validity of the classical epistasis analysis.

Many authors have focused on diverse assumptions of classical epistasis analysis and discussed the implications of violating some of them (e.g., Avery and Wasserman, 1992; Huang and Sternberg, 2006; Phenix et al., 2011). This has motivated efforts to attain better interpretations, relax the assumption of epistasis analyses and expand its applicability (see an excellent review in Phillips, 2008). Anyhow, to our knowledge, no previous work has explored the joint effect of the hierarchical and single-path aspects of gene regulatory interactions on classical epistasis analysis.

Network-based approaches can almost naturally overcome many of the limitations of classical epistasis analysis and gene interaction analyses in general. Partly because of this, most of the improvements of the epistasis analyses have relied on the use of networks. For example, systems biology is creating epistatic networks that take into account many gene interactions (e.g., Tong et al., 2004; St Onge et al., 2007; Battle et al., 2010). These studies

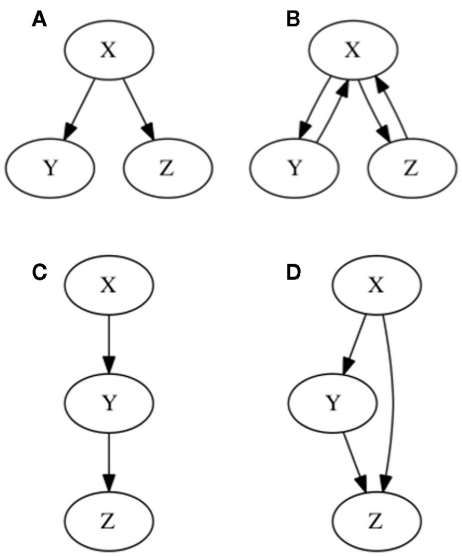

FIGURE 1 | Graphical representation of hierarchical and single-path notions of gene regulation. In **(A)** hierarchical gene regulation is represented. As observed all nodes are either "upstream," "downstream," or at the same level. Consequently *X* regulates *Y* and *Z*, but *X* is not regulated by either *Y* or *Z*. No gene can by upstream and downstream at the same time. In **(B)** two feedback loops are included, by assuming that *Y* and *Z* regulate *X*. Hence, it is not possible to establish a hierarchy on gene regulation, since all genes can by upstream and downstream at the same time. In **(C)** a single-path gene regulation pattern is represented. In **(D)** a feed-forward loop is incorporated yielding two alternative pathways starting at *X*: one is a direct regulation of *Z*, and the other one implies an indirect regulation of *Z*, via *Y*.

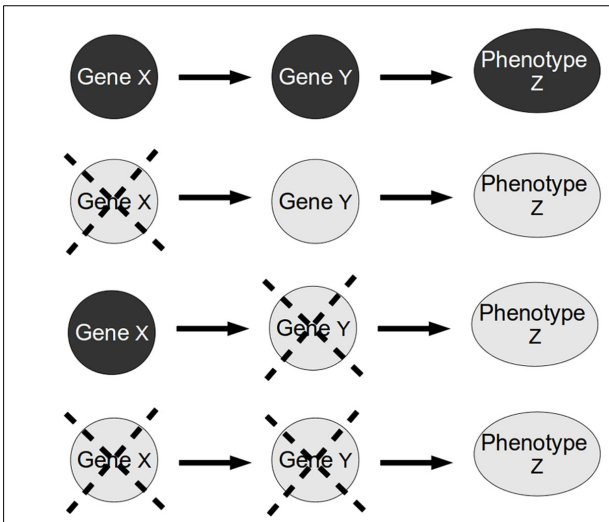

FIGURE 2 | Standard epistasis analysis. In epistasis analysis one compares the effect of each single mutant (*X* and *Y* single gene mutants) against the double mutant (*XY* double mutant) of the genes under study on the phenotype of a trait (in this paper, the trait represents a gene). The masking of the effect of one gene mutation in the double mutant is called epistasis. The gene whose phenotype persists is called epistatic gene.

propose the use of network-based approaches applying modifications to the standard methods, with the incorporation of graph theory, Bayesian networks, as well as statistical or probabilistic properties, among others, for the study of epistasis (Phillips, 2008; Tyler et al., 2009; Battle et al., 2010; Jiang et al., 2011; Phenix et al., 2011). Such approaches have allowed inferences of gene interactions with high statistical confidence levels, but the validation of the predicted gene interactions with such methods usually requires further confirmations with more detailed experiments because false interactions or wrong gene order can sometimes be inferred (e.g., Battle et al., 2010). Only a few of these reports have addressed the improvement of classical epistasis analysis in particular. However, improved classical epistasis analysis approaches are also available (Aylor and Zeng, 2008; Phenix et al., 2011). Aylor and Zeng (2008) present a method for experimentally estimating and interpreting classical epistasis that combines the approaches of classical and quantitative genetics, while Phenix et al. (2011) present a quantitative method for interpreting classical epistasis and inferring pathways from vast sets of data. These previous publications have mainly explored how to overcome the single-path assumption or assumptions 2, 3, and the problem of how to use huge amounts of data to infer precise gene interactions.

We specially focus on the use of Boolean network formalism as an improvement of classical epistasis analysis. Boolean networks have been shown to be useful tools to analyze discrete dynamic systems that rely on a pure logical formalism (Bornholdt, 2008). They can incorporate feedback loops, feed-forward loops, and are dynamic. Interestingly, integration of experimental gene interaction data into Boolean networks may be particularly useful for classical epistasis analysis because the latter also relies on a pure logical, discrete formalism. However, the Boolean network approach does not imply the limiting assumptions that the classical epistasis analysis does; indeed, a Boolean approach is useful for analyzing and integrating much more information than classical epistasis analysis alone.

Importantly, Boolean networks can be modified for more detailed analysis when noise (Bornholdt, 2008) or multivalued genes (genes that can perform different activities depending on their level of expression; Didier et al., 2011) are considered. Furthermore, once a Boolean network is validated it can be transformed into an equivalent continuous system (Wittmann et al., 2009), which can be amenable to further formal analyses. Given that the Boolean network formalism is very intuitive and there are a handful of freely available tools for its analysis (e.g., *SQUAD*, Di Cara et al., 2007; *Atalia*, Alvarez-Buylla et al., 2010; *BoolNet*, Müssel et al., 2010; *SimBoolNet*, Zheng et al., 2010), this formalism can be easily integrated into classical epistasis analysis. We therefore propose here the use of Boolean networks for an easy, but more powerful analysis of classical epistasis experiments.

After providing a historical perspective of hierarchical and single-path gene regulation, we will provide a detailed explanation of how classical epistasis analysis works, explore some of the implications of violating the hierarchical and single-path assumptions and discuss the importance of considering the temporal dynamics of gene interactions. We will show that classical epistasis analysis can be useful and precise, but that it can also conceal relevant information concerning the nature of gene interactions underlying biological processes. Next, we will argue that complementary experiments can uncover the information that is "hidden" to epistasis analysis, namely, unknown non-hierarchical and non-single-path genetic interactions. Then we will show that the use of a dynamical network-based approach can facilitate the access to this information. Finally, we will review how Boolean networks work and use experimental and theoretical examples to illustrate ways in which Boolean networks can be used to complement and improve classical epistasis analysis.

THE HIERARCHICAL NOTION OF GENE REGULATION

The single-path and hierarchical notions of gene regulation are not assumptions that were incorporated in classical epistasis analysis just for simplicity. These views are historically rooted and hence, they are not exclusive of classical epistasis analysis, but have permeated almost all of biological research. In fact, these assumptions affect the way biologists still design, analyze, and interpret experimental data in many areas of research. Hence, we briefly review some of the historical roots of the single-path and hierarchical notions of gene regulation.

At the beginning of the twentieth century, during the so-called "eclipse of Darwinism" (Bowler, 1983), genes were conceptualized as functional units of recombination (here referred to as the functional gene, similar to Longo and Tendero, 2007), and their phenotypic effects were inferred from hybridization experiments. DNA structure was discovered many decades afterward (Watson and Crick, 1953) revealing that genes were encoded in the double helix DNA sequence (here we refer to the coding DNA as the structural gene), and thus provided an apparently clear material basis for the action of functional genes. Before this, in the framework of the modern synthesis of evolutionary biology, it was suggested that inheritable phenotypic traits with modifications guided evolution and that all or most inheritable variable traits were encoded almost exclusively in the genes, without making a distinction between the functional and the structural gene (Mayr and Provine, 1980). Based on this and other and historical issues (for instance, experiments regarding the role of the homeotic genes showing a key control of genes over phenotypes; Morata and Lawrence, 1977), an apparently logical and immediate direct link between the functional and the structural conception of genes was made (Longo and Tendero, 2007). All such events led the way to a "genocentric" approach that assumed that phenotypic traits are almost completely determined by the information, or *blueprint*, contained in genes (Lorenz, 1965; Nijouth, 1990). Consequently, during the decades that followed the modern synthesis, the research of many biological fields has focused almost exclusively on genetics and molecular research. However, all of this was done without a distinction between the functional and structural notions of genes, although in reality these could represent different units.

Little was known at that time about gene interactions or epigenetic mechanisms, and according to an extreme genocentric view, development and organismal organization could be explained through pivotal genes that regulate the activity of other

downstream genes, which in turn regulate other further downstream genes, and so on (i.e., a single-path and hierarchical view; e.g., Davidson and Erwin, 2006). Under such a perspective, one could understand the order of gene action using straightforward genetic analyses, such as the classical epistasis analysis. However, as pervasive and useful as it has been, the extreme genocentric approach has been severely criticized (e.g., Oyama, 1985; Alberch, 1989; Nijouth, 1990; Griffiths and Gray, 1994; Goodwin, 2001; Greenspan, 2001; Gould, 2002; Jablonka and Lamb, 2005; Salazar-Ciudad, 2006; Pigliucci and Müller, 2010). It has become evident that most phenotypes depend on highly non-linear regulatory interactions among multiple elements and therefore that single and direct causes are rare (Wagner, 1999; Lewontin, 2000; Robert, 2004; Longo and Tendero, 2007). Studies on the gene interactions underlying transcriptional regulatory networks (e.g., Albert and Othmer, 2003; Espinosa-Soto et al., 2004; Davidich and Bornholdt, 2008) support this idea and show that many phenotypic traits depend on the distributed (non-hierarchical) action of many interacting genes and also on environmental and developmental factors (e.g., Lewontin, 2000; Greenspan, 2001; Salazar-Ciudad, 2006; Gordon et al., 2009). Hence, the assumption of single-path and hierarchical gene interactions often leads to oversimplified models, which are instrumental starting points for exploratory purposes, but that need to be improved later on.

Confronted with these kinds of criticism and the growing set of experimental evidence that challenges the genocentric view, the modern synthesis seems to be ready for at least an extension (Griffiths and Gray, 1994; Jablonka and Lamb, 2005; Pigliucci, 2007, 2009; Pigliucci and Müller, 2010). Indeed, it is becoming generally accepted that we need to embrace an "interactionist" view and accept that development unfolds and emerges as a consequence of complex interactions among several genetic, organismal, and environmental factors (Oyama, 1985; Robert, 2004). Yet, a closer inspection of the literature and some recent data show that, in practice, many experimental setups and analyses assume a single-pathway and hierarchical idea of gene regulation. This could be due to the persistence of the genocentric view, the assumption that the hierarchical action of genes is a necessary first step in tackling complex biological systems, and that the methods, techniques, and conceptual frameworks that enable going beyond a hierarchical view of development and evolution are still under construction.

Before we try to explore the effect of ubiquitous complex, non-hierarchical gene interactions, let us briefly explain how classical epistasis analysis is traditionally done (see more detail in Avery and Wasserman, 1992; Huang and Sternberg, 2006; Roth et al., 2009 and references therein) to use it as an example to illustrate the type of problems we can encounter if hierarchical and single-path interactions are assumed.

CLASSICAL EPISTASIS ANALYSIS

Classical epistasis analysis states that in a double mutant experiment, the two genes act in the same pathway if the phenotype of the double mutant is the same as that of organisms carrying a single mutation for one of the genes. The gene with the allele whose phenotype persists in the double mutant is called epistatic gene, while the other is the hypostatic gene. As mentioned above, if some assumptions regarding the nature of gene regulation are met, few simple rules allow the use of this information to order genes in a hierarchical way (Avery and Wasserman, 1992; Roth et al., 2009). The rules are as follows:

1. In the double mutant, the epistatic gene is upstream and positively regulates the downstream gene when the two genes used in the double mutant display a characteristic single mutant phenotype under the same condition (e.g., both genes have certain mutant phenotype only when a signaling pathway is active or only when the pathway is inactive).
2. In the double mutant, the epistatic gene is downstream and is negatively regulated by the upstream gene when the two genes display a characteristic single mutant phenotype under different conditions (e.g., one gene has a mutant phenotype when a signaling pathway is active and the other when the pathway is inactive).

These simple rules are useful and applicable for many cases (Avery and Wasserman, 1992; Huang and Sternberg, 2006; Roth et al., 2009). But, what happens when the single-path and hierarchical assumptions are not met or if temporal dynamics are considered? We use some examples to illustrate these cases.

Consider generic nodes *X*, *Y*, and *Z* to represent genes (although they can represent other entities, see Huang and Sternberg, 2006). If *X* positively controls the expression of *Y* and *Y* positively controls the expression of *Z* (**Figure 3A**), then the single and double loss-of-function mutants yield the results shown in **Table 1**. Applying the rules of the classical epistasis analysis to these results we correctly conclude that *X* is upstream in relation to *Y*.

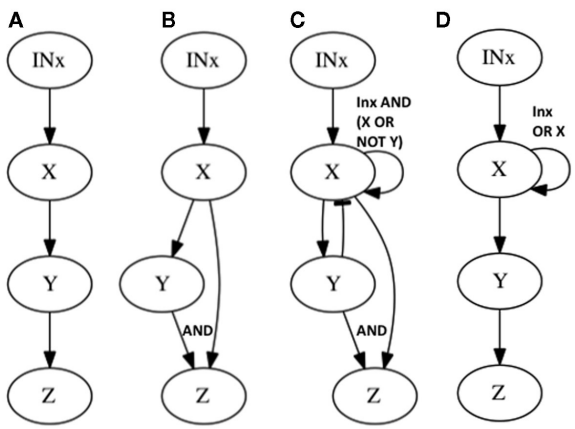

FIGURE 3 | Subgraphs to be inferred with epistasis analysis. The graphs of the examples explained in the main text are shown. All these subgraphs yield the same results with a classical epistasis analysis. IN_x (Input of *X*) is included to meet assumptions 1, 2, and 3 of epistasis analysis, but it could be obviated, as it is commonly done. According to Huang and Sternberg (2006) we can call such cases to be "substrate dependent pathways," and we can only order genes in this kind of pathways through epistasis when they do not display the same mutant phenotype. The logical rules for each motif are: **(A)** $x = IN$, $y = x$, $z = y$, **(B)** $x = IN_x$, $y = x$, $z = x \wedge y$, $z = y$, **(C)** $x = IN_x \wedge (x \vee \neg y)$, $y = x$, $z = x \wedge y$, and **(D)** $x = IN_x \vee x$, $y = x$, $z = y$.

Now let us see what happens in the same example if we add one more interaction. Let us assume that *X* positively and directly regulates *Z* as well (feed-forward case, **Figure 3B**). If we proceed to generate all loss-of-function mutant combinations we recover exactly the same results as in the previous case (without $X \rightarrow Z$). This simple example shows that there are categories of gene regulatory networks that render the same set of results in the single and double loss-of-function mutant analyses but that, nevertheless, have different regulatory interactions or architectures.

It is important to note that the graph just described is well known and widely distributed in real gene networks (Milo et al., 2002; Shen-Orr et al., 2002). This subgraph is usually referred to as a coherent feed-forward loop (Mangan and Alon, 2003; Mangan et al., 2003). This subgraph has also been reported in experimental research. For instance, in the gene regulatory network of the radial root pattern of *Arabidopsis thaliana* the transcription factor *SHORTROOT* (*SHR*) has been shown to positively regulate *SCARECROW* (*SCR*) gene transcription in the endodermis, and both *SHR* and *SCR* together regulate the expression of many other genes, including *SCR* itself (Levesque et al., 2006).

The feed-forward loop is not the only subgraph that can mimic the results of the subgraph in **Figure 3A**, there are many others, and as larger gene networks are considered, more cases would render the same inference. Let us consider one more example. If *X* positively regulates *Y*, and both *X* and *Y* positively regulate *Z*, but at the same time *Y* negatively regulates *X* (creating a feedback loop between *X* and *Y*) and finally *X* positively self-regulates (a second feedback loop; **Figure 3C**), the same inference as in the two previous examples is reached from the single and double loss-of-function mutants. In all of these cases, classical epistasis analysis would not be completely misleading, as it would suggest that *X* positively regulates *Y* and *Y* positively regulates *Z*, which is true for all three examples, but it would not be able to yield information concerning the additional regulatory interactions included in **Figures 3B,C**. Indeed, such interactions can rarely be detected if we are not looking for them or if we assume that genes act in a hierarchical and single-path way.

In fact, in the last example, the notion of upstream and downstream gene does not make any sense. In most real systems the genes feed back to each other creating not a pathway, but a complex circuit or a subgraph that, in **Figure 3C** corresponds to a very well studied – and seemingly ubiquitous – system known as activator–inhibitor system (Gierer and Meinhardt, 1972; Meinhardt and Gierer, 2000; Kondo and Miura, 2010). Actually, this system has been found to underlie developmental processes of several structures in many organisms (Meinhardt and Gierer, 2000). For instance, it is found in the regulation of stem cell pools in *A. thaliana* shoot apical meristem by *CLAVATA3* (*CLV3*) and *WUSCHEL* (*WUS*) genes where CLV3 represses *WUS* transcription while WUS self-activates and activates *CLV3* (Schoof et al., 2000; Fujita et al., 2011). The activator–inhibitor system has also been used as an example to challenge the linear causality often attributed to gene action (Goodwin, 2001).

In conclusion, classical epistasis analysis could not discern the topologies shown in **Figures 3A–C**. However if additional combinations of loss and gain-of-function lines, as well as all the gene expression patterns were available, these three topologies could be distinguished. This requires a considerable experimental effort that, as we will show, could be optimized by adopting a network approach. Moreover, there are some topologies that even if the whole set of individual and combined loss-of-function and gain-of-function mutants were available, would still be indiscernible under a classical epistasis analysis. Such an example is provided in **Figure 3D**, which depicts a topology that cannot be discerned from **Figure 3A** even with an exhaustive set of mutants of the genes conforming the graph under analysis. However, if one could manipulate the input (or inputs), one could, in principle, perform nested classical epistasis analysis based on complete sets of single and combined loss and gain-of-function mutants, in order to infer the correct topology. The fact that one cannot distinguish the topologies in **Figures 3A,D** with classical epistasis analysis is due

Table 1 | Results obtained from epistasis analysis of examples in Figure 3.

Gene state/mutation	*X*	*Y*	*Z*
x	0	0	0
y	1	0	0
xy	0	0	0
WT	1	1	1

*The results for all the examples are the same shown in the table. The examples of **Figures 3B,C,D** have some extra interactions than the one shown in **Figure 3A**, but we could not detect these extra interactions with the epistasis analysis alone. Is important to note, that even when Huang and Sternberg (2006) advise us that we cannot order genes with the same phenotype in this kind of pathways, we can do it here with the table. This is because we observe that when X is mutated we obtain the same values for X, Y, and Z as in the double mutant of X and Y. Moreover, the presence of X in Y mutant could indicate the presence of a substrate product of X activity (as could be assumed in Huang and Sternberg, 2006) indicating that X is epistatic to Y and hence is upstream of Y.*

Table 2 | Results of epistasis analysis for regulatory motifs in Figures 4A,B, respectively.

Gene state/mutation	*X*	*Y*	*Z*
A			
x	0	1	0
y	1	0	1
xy	0	0	1
WT	1	0	1
B			
x	0	1	0
y	0	0	1
Xy	0	0	1
WT	1	1	1

Given that these are switch regulatory pathways, the presence of a substrate, as explained by Huang and Sternberg (2006), is neglected and epistasis analysis may discern between them only with additional experiments.

to the presence of an input and a positive feedback loop acting on *X*. Importantly, this appears to be a relatively common situation in real data sets (see Examples From the Literature for examples below).

We now consider a few additional graphs in which a classical epistasis analysis may be insufficient and could be somewhat misleading. Let us assume that *X* negatively regulates *Y*, and *Y* negatively regulates *Z* (**Figure 4A**). Now assume another subgraph where *X* positively regulates *Y* and negatively regulates *Z* (generating a feed-forward loop from *X* to *Z*), while *Y* positively regulates *X* and *Z* (generating a feedback loop between *X* and *Y*), and both *X* and *Y* nodes, have an input (**Figure 4B**; since no gene is upstream or downstream, and since the input should be over the upstream gene, in this case both *X* and *Y* have inputs). The results from the classical epistasis analysis of these two subgraphs are shown in **Table 2**. Following the classical epistasis analysis rules to order gene interactions, we can conclude that gene *Y* negatively regulates gene *Z*, which is not true for both subgraphs. It can be argued that our assumption that *Y* and *X* regulate *Z* in the subgraph of **Figure 4B** (through an exclusive OR (XOR) rule, see below) is a rare situation (Davidson, 2001). However, this kind of examples, where we can be misguided without the XOR rule, become frequent as the regulation of *Z* becomes more complex, for instance, having several inputs.

In addition to feedback and feed-forward loops, it is important to acknowledge the time it takes for genes to interact with other genes in the analysis (i.e., temporal dynamics). In classical epistasis analysis it is implicitly assumed that gene interactions are synchronous. This is an unrealistic assumption (Fauré et al., 2006). In cases where the single-path and hierarchical assumptions are not met, if temporal dynamics are not considered, classical epistasis analysis can also reach wrong inferences (e.g., Fauré et al., 2006). Consider, for example, that *X* activates itself (feedback loop) and at the same time inhibits *Y* and *Z* (feed-forward loop). Correspondingly, *Y* also activates itself (second feedback loop) and *Z*, and it inhibits *X* (third feedback loop; **Figure 5A**). Additionally, all inhibitions are stronger than any activation. We analyze two cases. In the first one, the network is updated synchronously. That is, the states of all genes in the subgraph at time $t+1$ are updated

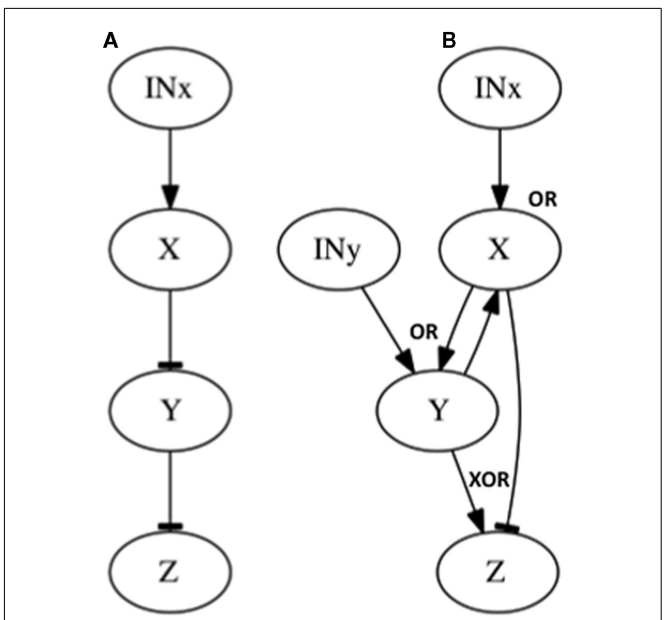

FIGURE 4 | Subgraphs to be inferred with epistasis analysis. The graphs of the examples explained in the main text are shown. All these subgraphs yield the same results with a classical epistasis analysis. INx (Input of *X*) is included to meet assumptions 1, 2 and 3 of epistasis analysis, but it could be obviated, as it is commonly done (see **Figure 2**). The logical rules for each motif are: **(A)** $x = \mathrm{IN}_x$, $y = x$, $z = y$, **(B)** $x = \mathrm{IN}_x \wedge y$, $y = \mathrm{IN}_y \wedge x$, $z = x\mathrm{XOR} \neg y$.

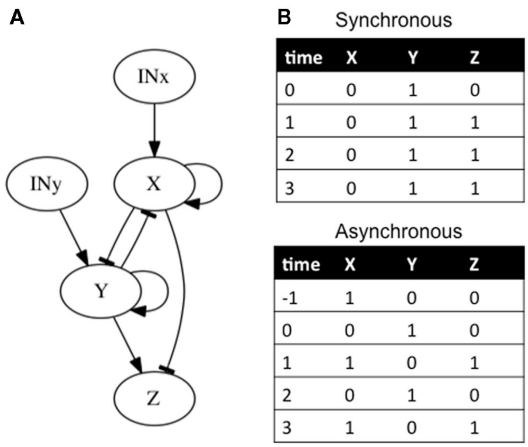

FIGURE 5 | Subgraphs to be inferred with epistasis analysis. As explained in the main text, these networks yield different results if we add a temporal dynamic analysis. **(B)** The possible attractors reached from the same condition are shown. If a synchronous updating of the gene states is assumed, the system reaches a fix-point attractor, while with an asynchronous updating the system reaches a periodic attractor. The logical rules of the motif are: **(A)** $x = (\mathrm{IN}_x \vee x) \wedge \neg y$, $y = (\mathrm{IN}_y \vee y) \wedge \neg x$, and $z = \neg x \wedge y$.

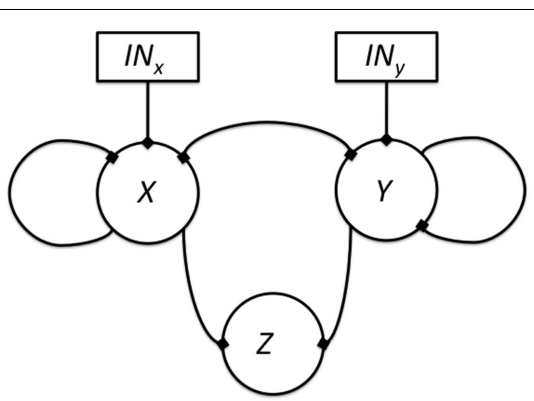

FIGURE 6 | All possible topologies in a motif where gene *X* and gene *Y* regulate the state of a gene *Z*. The edges represent possible regulatory interactions. These interactions can be positive, negative or null (i.e., inexistent). The inclusion of an input over genes *X* and *Y* is assumed because it is not clear which gene is upstream and which one is downstream.

at the same time and are determined by the gene states at time *t*. It is straightforward to check that if the network is initialized with *X* off and *Y* on, the system will remain there, with *X* off, and *Y* and *Z* on (**Figure 5B**). On the other hand, if the updating is not synchronous, and for example, the state of *X* and *Y* at time *t* are determined by the gene states at time $t-1$ and the state of *Z* is determined by the gene states at time *t* (i.e., *Z* regulation is faster than the expression of *X* and *Y*), the same condition can lead to a periodic expression of genes (**Figure 5B**). Here, a classical epistasis analysis would correctly infer that *X* inhibits *Y* and *Y* activates *Z*, but would not render any useful information about the other subgraph interactions nor its behavior.

The above examples illustrate how if we do not consider the possible presence of feedback loops, feed-forward loops, and temporal dynamics, analysis like classical epistasis may help to infer some gene interactions and the order in which they occur, but can "hide" or even be misleading in other aspects of the regulatory system under consideration. Network-based approaches can improve gene interaction inferences.

EPISTASIS AND (BOOLEAN) NETWORKS

Network theory has been fruitfully applied to ask and address novel questions in the fields of evolution, development, and behavior (see for examples von Dassow et al., 2000; Newman et al., 2006; Aldana et al., 2007; Balleza et al., 2008; Wagner, 2009). Importantly, network-based approaches have been already applied for the study of epistasis (e.g., Tyler et al., 2009; Battle et al., 2010; Jiang et al., 2011; Phenix et al., 2011). Network models provide a formal framework for integrating detailed and high-quality experiments that, although extremely valuable, often remain isolated. The integration of such experimental data into dynamic network models can help discern among possible topologies among which classical epistasis analysis is unable to distinguish. Furthermore, dynamic network models may be used to make novel predictions and provide integrative system-level explanations for the behavior of large data sets.

In the last section we provided several examples in which certain sets of gene interactions involving the same elements (genes) may render the same phenotypes for single and double mutations, but that nevertheless may have different gene interaction topologies. Dynamical network models provide a formal framework for integrating experiments that can help discriminate among alternative topologies yielding the same results when subject to a classical epistasis analysis. Furthermore, this integration enables the specification of larger dynamic models that may feedback independent experiments and are helpful to validate a whole set of data.

There are many ways in which we could use dynamical network models to improve classical epistasis analysis. For instance, we could keep a catalog of possible regulatory graphs that render the same results, as for the cases shown above. This would help us to bear in mind some of the possible topologies that are consistent with a set of genetic data, as well as to design experiments and crosses in order to discern among them. It is also possible to perform exhaustive (if our network is finite, discrete, and deterministic) computational simulations of the dynamic consequences of alternative regulatory graphs, enabling to test and compare their dynamics with available evidence. This has already been done for other purposes and in different ways (e.g., Nochomovitz and Li, 2006; Giacomantonio and Goodhill, 2010), and its applicability is being studied now in the specific context of classical epistasis (E. Azpeitia and E. R. Alvarez-Buylla, unpublished data). Also, using networks to predict experimental results or to systematically explore the perturbations that may affect a system can be very helpful (e.g., Espinosa-Soto et al., 2004; Azpeitia et al., 2010).

Gathering data from additional related loss and gain-of-function lines, as well as from other types of molecular genetic experiments, and building larger network models can also help to discern among possible network topologies. Stable networks states or configurations (attractors) can be obtained for a network grounded on several classical epistasis analyses and systematically test the different topological possibilities. In order to avoid circular explanations, the networks under study should reproduce the data with which they were built, as well as expression patterns or other results that were not fed into the model. Ideally, the network being challenged should also lead to novel and testable predictions. However, such approach is limited because the number of possible network topologies and configurations greatly increase as a function of the number of nodes considered. Nonetheless, it is possible to focus on relatively small subnetworks or modules that are relatively isolated from the rest of the network.

All the above suggestions can be achieved with any kind of dynamic network approach, but we contend that Boolean networks are particularly useful and easily applicable in the context of classical epistasis analysis because they use exactly the same logical formalism. Several programs are available for Boolean network analysis (e.g., Atalia, Alvarez-Buylla et al., 2010; SQUAD, Di Cara et al., 2007; GNA, de Jong et al., 2003; BoolNet, Müssel et al., 2010; BIOCHAM, Calzone et al., 2006; Antelope, Arellano et al., accepted; among many others), and Boolean networks have been successfully applied and validated in many systems, such as cell type determination in *A. thaliana* (Espinosa-Soto et al., 2004; Benítez et al., 2008; Savage et al., 2008), body segmentation in *Drosophila melanogaster* (von Dassow et al., 2000; Albert and Othmer, 2003), and yeast cell-cycle (Li et al., 2004), among others. Now, let us explain how the logical analysis approach using Boolean networks works.

Kauffman first proposed gene regulatory Boolean network models in 1969. These are discrete networks where nodes (commonly representing genes) can only attain two values, 1 when the gene is active and 0 when it is non-active. The dynamics of node activity depends on the interactions among nodes in the network. Thus, a node's activation state changes according to the function:

$$x_n(t+\tau) = F_n(x_{n_1}(t), x_{n_2}(t), K, x_{n_k}(t)).$$

where x_n represents the state of node *n* at the time $(t+\tau)$ (τ representing a positive integer) and $\{x_{n_1}(t), x_{n_2}(t), K, x_{n_k}(t)\}$ represents all of the *k* regulators of node x_n at time *t*, and the set of states of all the nodes included in the network at a given time is referred to as the system configuration. Since these are discrete and deterministic systems, the number of possible configurations is finite and configurations at posterior time steps can be assessed from previous ones. Some network configurations (represented as a vector of

zeros and ones) do not change once they are reached. These configurations are known as fixed-point attractors. Other network configurations oscillate among them and are known as cyclic or periodic attractors. Kauffman (1969) proposed that attractors represent the experimentally observed stable configurations of gene activity that occur, for example, in an already determined cell type or that characterize a cell-fate.

Defining the logical function of each of the possible interaction sets according to available experimental evidence and following the dynamics of such sets can be very useful when analyzing experimental data. For example, consider one of the networks depicted in the previous section (**Figure 3C**). It is possible to derive transition tables for all genes, as shown in **Table 3** for *X*, *Y*, and *Z*, with the use of Boolean equations. The Boolean equations use the logical operators AND, OR, and NOT to formalize biological data regarding gene interactions. For instance, if a logical operator AND is placed in a Boolean equation it could represent that *X* and *Y* form a dimer. This can be represented as the Boolean function: $Z = X$ AND *Y*. In a similar way, the OR and NOT operators can represent different kinds of gene interactions. Once we have the complete set of Boolean equations, a transition table that integrates all the Boolean equations of the system, gives the system state that will follow at time $(t + t)$, given a system state at time *t*. Then, it is possible to obtain attractors for each tested network and compare them with the expected equilibrium states for the system under study (see methodological details in Kauffman, 1969; de Jong, 2002; Alvarez-Buylla et al., 2007, 2008; Bornholdt, 2008).

This approach may seem insufficient for some instances, but almost all limitations can be resolved by introducing certain modifications. If, for example, experimental evidence suggests the existence of more than two gene activity states, nodes taking additional activity states could be used (e.g., Espinosa-Soto et al., 2004; Benítez et al., 2008; Didier et al., 2011). If non-determinism is not important for the system under study, probabilistic networks can be used (e.g., Shmulevich and Kauffman, 2004; Bornholdt, 2008). On the other hand, if quantitative data is available, continuous networks described by ordinary differential equations could be approximated, and so on (Wittmann et al., 2009). For the purposes of classical epistasis analysis discussed here, Boolean networks are generally sufficient.

Table 3 | Transition table for all the possible configurations of the subgraph shown in Figure 3C.

t			*t* + 1		
X	***Y***	***Z***	***X***	***Y***	***Z***
0	0	0	1	0	0
0	0	1	1	0	0
0	1	0	0	0	0
0	1	1	0	0	0
1	0	0	1	1	0
1	0	1	1	1	0
1	1	0	**1**	**1**	**1**
1	1	1	**1**	**1**	**1**

The fixed-point attractor is marked in bold.

Conveniently, one only requires basic notions of logic to improve classical epistasis analysis with the use of Boolean networks. Suppose we want to explore the interactions between two genes for which we do not have any previous information. In order to find how they interact, we perform a classical epistasis analysis. Yet, as an extension of the classical epistasis analysis we assume a non-hierarchical and multi-path organization of gene interactions.

If we think that the genes under study may not be hierarchically organized, but all other epistasis assumptions are met, five new interactions are possible: (1) there can be an input for both genes, (2) feedback circuits where both genes regulate each other's expression, (3 and 4) either or both genes can self-regulate, and finally, (5) both genes can control the output (**Figure 6**). All these interactions can be positive or negative. All the possible ways in which *X* and *Y* can control the output value based on a Boolean approach are shown in **Table 4**, including the case in which neither *X* nor *Y* are regulators of *Z*. Some topologies can be represented with different logical rules, and different logical rules can display the same behavior, which are then dynamically equivalent topologies.

Suppose that classical epistasis analysis yields the results observed in **Table 5**. There are several observations we can draw from **Tables 4** and **5**. First, if we use the rules of classical epistasis analysis we can conclude that *X* is upstream of *Y*, and that *X* negatively regulates *Y*, which negatively regulates *Z*. Nevertheless, based on **Table 4** we can observe that not only *Y* negatively regulating *Z* can explain the results obtained from the epistasis analysis. Using a discrete Boolean formalism there are three different networks that could explain these results assuming that only *X* and *Y* regulate *Z*. The question that arises then, is how can we distinguish which of the possible explanations is the correct one and, equally important, how do *X* and *Y* interact? Are they hierarchically organized? How can we use networks to infer the correct regulatory graph of *Z*?

A further step would involve identifying the attractors needed in order to explain the results obtained in the classical epistasis analysis. If we do this we observe that depending on how *Z* is regulated, different attractors are expected. Hence, if the expression patterns of *X* and *Y* are obtained, the possibilities are constrained. Suppose that when the input is active, *X* is expressed and *Y* is not expressed, and vice versa when the input is inactive. This will leave only two possibilities (**Table 4**) from which we can easily distinguish the correct one with one additional experiment.

Finally we want to know how *X* and *Y* interact with each other. First we want to know how *Y* can be regulated. Then again, we only need to know if the expression of *Y* is stable or not under the possible regulatory graphs, both in a wild-type and mutant cases. Then, we can compare the stability of *Y* expression in each graph with that expected from available evidence (e.g., *Y* activity is expected to be stable if its expression is observed in wild-type lines). If we do this we will find that there are nine possible ways to explain the observed gene *Y* behavior. Two of these possibilities are negligible since no regulation of gene *X* over *Y* is inferred and the observed results in the classical epistasis analysis cannot be explained this way. Now, two experiments (one to see if gene

Table 4 | Logical rules for *Z*.

***X* value**	***Y* value**	***X*+**	***X*−**	***Y*+**	***Y*−*^**	***X*+ or *Y*+**	***X*+ and *Y*+**	***X*+ or *Y*−*^**	***X*+ and *Y*−**
0	0	0	1	0	1	0	0	1	0
0	1	0	1	1	0	1	0	0	0
1	0	1	0	0	1	1	0	1	1
1	1	1	0	1	0	1	1	1	0
***X* value**	***Y* value**	***X*− or *Y*+**	***X*− and *Y*+**	***X*− or *Y*−**	***X*− and *Y*−**	***X*+ XOR *Y*+**	***X*+ XOR *Y*−***	**Constant "0"**	**Constant "1"**
0	0	1	0	1	1	0	1	0	1
0	1	1	1	1	0	1	0	0	1
1	0	0	0	1	0	1	0	0	1
1	1	1	0	0	0	0	1	0	1

It is assumed that X, Y, or X and Y together can regulate Z. An X or a Y followed by a "+," stands for a positive regulation over Z and followed by a "−" for a negative one. Based on the results of the epistasis analysis mentioned in the main text and shown in ***Table 5*** *we can discard all logical rules in which Z activity is observed when X is mutated (i.e., we discard all logical functions in which Z is 1 in both lines when X is 0), and all logical rules where no Z activity is observed when Y is mutated or in the double mutant of X Y nodes. These leave us only with the three possibilities marked with an "*." "^" is used to denote the final two options that we obtain when we know the attractors of the motif.*

Table 5 | Results obtained through epistasis analysis of the theoretical example described in the main text.

Gene state/mutation	***X***	***Y***	***Z***
x	0	*	0
y	*	0	1
xy	0	0	1
WT	*	*	1

"" Indicates an unknown value, this is because we are assuming non-hierarchical regulation and hence, self-regulation and feedback are allowed, which can result in different values for X and Y in the Y and X mutants, respectively.*

X positively or negatively regulates *Y*, and another one to verify if gene *Y* can self-regulate) will be enough to distinguish the correct graph.

The kind of dynamic analysis proposed here is doable even without a computer and it will only render non-trivial information if there are multiple-path or non-hierarchical interactions in the network architectures under analysis. However, as mentioned above, there are now several computational tools that are available to analyze the dynamics of larger networks.

It would seem like networks could grow indefinitely before they can tell us something about a process. Is it possible to learn something about a particular biological process, for instance, cell type determination during flower organ specification, or body segmentation, without considering every genetic and epigenetic regulatory interaction in the organism? To answer this question one must turn to one of the central concepts in current biology and network studies, that of modularity.

Modules are characterized by their greater internal than external integration (Müller, 2007). In the context of networks, modules are often defined as highly connected subsets (Wagner et al., 2007) or as sets of nodes with more interactions among them than with the rest of the elements of the network. Modular organization seems to permeate biological systems at all levels: molecular, metabolical, structural, functional, developmental, etc. (Wagner et al., 2007; Callebaut and Rasskin-Gutman, 2009).

Modularity is central to our discussion because the modular organization of networks and biological processes allows us to focus on a limited set of interacting elements that are relatively isolated from the rest. Thus, modules have a relatively autonomous behavior with respect to the rest of the network. Of course, the definition of modules does not precede the inference of networks, but one can aim to uncover networks that are necessary and sufficient for processes to take place and that, therefore, constitute a functional module.

EXAMPLES FROM THE LITERATURE

We have already discussed what kind of information could be hidden or even misinterpreted with classical epistasis analysis in several cases of non-hierarchical and non-single-path gene regulatory theoretical subgraphs. Now we will describe some of the results, and the kinds of interactions found when complex discrete networks have been used to integrate available molecular information in particular experimental systems. First, we will briefly discuss a case in which one of the gene interactions was predicted by a network model, and it was later corroborated experimentally. Importantly, this case involves a feedback loop or gene regulatory circuit, such as those likely overlooked in classical epistasis analyses.

In the flower organ specification network proposed for *A. thaliana* (Espinosa-Soto et al., 2004) a positive feedback loop was predicted for the gene *AGAMOUS* (*AG*; Espinosa-Soto et al., 2004). This seemed unlikely to occur given that in the *ag-1* mutant plants, which produce a non-functional *AG* mRNA, the pattern of *AG* mRNA expression is as in wild-type *Arabidopsis* lines (Gustafson-Brown et al., 1994). However, these data could still be compatible with an *AG* positive feedback loop because in the *ag-1* background the non-active mutant *AG* protein is unable to down-regulate *AG*'s activator *WUSCHEL* (*WUS*). Thus *WUS*, in the *ag-1* background, would permanently upregulate transcription of the non-functional *AG* mRNA.

To test the dynamic consequences of the *AG* positive feedback loop, a gene regulatory network model was used to simulate a network lacking the loop for *AG*. The results showed that in this case, some of the expected network features were lost. Here, the whole set of data (including many classical epistasis analyses) helped to build a dynamic network and to predict a gene regulatory subgraph that had been overlooked and that was later verified by independent experiments in another laboratory (Gómez-Mena et al., 2005). Other experiments to test this were also suggested from the network analyses and included ectopic GUS staining in an AG:GUS × 35S::AG cross.

A similar case was found in the network underlying *Arabidopsis* root epidermis cellular sub-differentiation. This system has been relatively well studied from experimental and theoretical perspectives and there are two non-exclusive models that aim to provide a dynamic account of said patterning process. One of these models is the "Mutual Support" model put forward by Savage et al. (2008) and the other one is the so-called "WER self-activation" model put forward by Benítez et al. (2008). As its name suggests, the latter relies on the self-activation of the gene *WER* (see recent review in Benítez et al., 2011).

In order to help discern between these two models, Savage and coworkers assessed the activity of the *WER* promoter in a *wer* loss-of-function line. In this line, *WER* is still present. If this gene were located on a linear regulatory pathway, this experiment would have sufficed to rule out the "WER self-activation" model, as some authors have suggested (Savage et al., 2008; Roeder et al., 2011a), but since this gene is immersed in a complex network, this experiment is not conclusive. It is possible to picture a scenario in which *WER* has more than one possible input and therefore sustains its expression even when one of these inputs is lacking. A network-based study of this patterning system suggests that these two models act in a partially redundant manner during root development, conferring robustness to the overall system when both are considered (see a more detailed discussion in Alvarez-Buylla et al., 2011; Roeder et al., 2011b; Benítez et al., 2011). Further theoretical and empirical work will be required in order to establish how common the reinforcing action of partially redundant subgraphs is, in which types of regulatory networks they arise, and which experimental setups can help uncover them.

There are other examples like the two reviewed here among the gene regulatory network literature (Li et al., 2006; Chickarmane and Peterson, 2008; Azpeitia et al., 2010; Faculty of 1000, 2010[1]). They show that Boolean network models are useful tools in integrating the reported experimental molecular data, as well as to detect missing interactions, postulate novel ones and design new crosses and experiments.

CONCLUDING REMARKS

In this article we have focused on the assumptions of hierarchical and single-path notions of gene regulation, as well as on the importance of considering temporal dynamics of gene regulation when performing a classical epistasis analysis. With the use of simple examples, we have shown how if we assume non-synchronous dynamics and complex non-hierarchical, multi-path gene interactions, more precise inferences of gene interactions can be reached. A network-based perspective not only complements classical epistasis analysis, but it also challenges the notion of a *blueprint* contained in genes, a linear relationship between genotype and phenotype, and the atomization of an organism's traits and cell types based on the premise that genes are particulate, stable, and separable and hence can be studied in isolation of other regulatory elements (Greenspan, 2001; Newman et al., 2006; Alvarez-Buylla et al., 2008).

Besides the use of network modeling to address how genes map onto phenotypical traits and such developmental processes evolve (Albert and Othmer, 2003; Espinosa-Soto et al., 2004; Batten et al., 2008; Kwon and Cho, 2008; Wagner, 2009), some authors have addressed the use of such models specifically for epistasis analyses (e.g., Phillips, 2008; Tyler et al., 2009; Battle et al., 2010; Jiang et al., 2011; Phenix et al., 2011) in order to relax some of its assumptions, expand its applicability, and improve its inference capacity. We specifically argued that Boolean network approaches, which like classical epistasis analysis use a logical approach, naturally complement it and provide more accurate inferences of gene interactions. We provided several theoretical and real examples. Boolean network modeling is intuitive and practical and has been validated for several biological systems.

Network approaches are contributing to the integration of complex interactions at the genetic and other levels of organization, creating a formal language to build up rigorous databases, and the creation of a novel set of terms and concepts for understanding biological research. We think that the use of network-based approaches is a promising field and its application in order to understand a wide range of biological systems is underway.

ACKNOWLEDGMENTS

Financial support for Eugenio Azpeitia was provided by the Ph.D. grant program of CONACyT; financial support for Mariana Benítez was provided by C3, Centro de Ciencias de la Complejidad (Torre de Ingeniería, UNAM) and by the Czech Ministry of Education, youth and sports (grant LC06034). Elena R. Alvarez-Buylla thanks financial support from Conacyt (81433, 81542, 90565) and PAPIIT (IN210408, IN229009-3, IN223607-3). Carlos Espinosa-Soto is supported by a CONACyT postdoctoral fellowship. We thank Rigoberto V. Perez-Ruiz and Diana Romo for technical and logistical assistance. We thank Lynna Kiere for a thoughtful revision of the manuscript. We also thank two anonymous reviewers for their thoughtful comments.

[1]Faculty of 1000 evaluations, dissents, and comments for [Hassan, H. et al. (2010). JACKDAW controls epidermal patterning in the Arabidopsis root meristem through a non-cell-autonomous mechanism. *Development* 137, 1523–1529]. Faculty of 1000, 03 Jun 2010. F1000.com/3432957.

REFERENCES

Alberch, P. (1989). The logic of monsters: evidence for internal constraint in development and evolution. *Geobios Mem. Spec.* 12, 21–57.

Albert, R., and Othmer, H. G. (2003). The topology of the regulatory interactions predicts the expression pattern of the segment polarity genes in *Drosophila melanogaster*. *J. Theor. Biol.* 223, 1–18.

Aldana, M., Balleza, E., Kauffman, S., and Resendiz, O. (2007). Robustness and evolvability in genetic regulatory networks. *J. Theor. Biol.* 245, 433–448.

Alvarez-Buylla, E. R., Balleza, E., Benítez, M., Espinosa-Soto, C., and Padilla-Longoria, P. (2008).

"Gene regulatory network models: a dynamic and integrative approach to development," in *Practical Systems Biology*, eds A. Hetherington and C. Grierson (New York, NY: Taylor and Francis).

Alvarez-Buylla, E. R., Benítez, M., Corvera-Poiré, A., Candor, A. C., de Folter, S., de Buen, A. G., Garay-Arroyo, A., García-Ponce, B., Jaimes-Miranda, F., Pérez-Ruiz, R. V., neiro Nelson, A. P., and Sánchez-Corrales, Y. E. (2010). Flower development. *Arabidopsis Book* 8, e0999.

Alvarez-Buylla, E. R., Benítez, M., Dávila, E. B., Chaos, A., Espinosa-Soto, C., and Padilla-Longoria, P. (2007). Gene regulatory network models for plant development. *Curr. Opin. Plant Biol.* 10, 83–91.

Alvarez-Buylla, E. R., Benítez, M., and Espinosa-Soto, C. (2011). Mutually reinforcing patterning mechanisms. *Nat. Rev. Mol. Cell. Biol.* 12, 533.

Avery, L., and Wasserman, S. (1992). Ordering gene function: the interpretation of epistasis in regulatory hierarchies. *Trends Genet.* 8, 312–316.

Aylor, D. L., and Zeng, Z. B. (2008). From classical genetics to quantitative genetics to systems biology: modeling epistasis. *PLoS Genet.* 4, e1000029. doi:10.1371/journal.pgen.1000029

Azpeitia, E., Benítez, M., Vega, I., Villarreal, C., and Alvarez-Buylla, E. R. (2010). Single-cell and coupled GRN models of cell patterning in the *Arabidopsis thaliana* root stem cell niche. *BMC Syst. Biol.* 4, 134. doi:10.1186/1752-0509-4-134

Balleza, E., Alvarez-Buylla, E. R., Chaos, A., Kauffman, S., Shmulevich, I., and Aldana, M. (2008). Critical dynamics in genetic regulatory networks: examples from four kingdoms. *PLoS ONE* 3, e2456. doi:10.1371/journal.pone.0002456

Batten, D., Salthe, S., and Boschetti, F. (2008). Visions of evolution: self-organization proposes what natural selection disposes. *Biol. Theory* 3, 17–29.

Battle, A. l., Jonikas, M. C., Walter, P., Weissman, J. S., and Koller, D. (2010). Automated identification of pathways from quantitative genetic interaction data. *Mol. Syst. Biol.* 8, 379.

Benítez, M., Espinosa-Soto, C., Padilla-Longoria, P., and Alvarez-Buylla, E. R. (2008). Interlinked nonlinear subnetworks underlie the formation of robust cellular patterns in Arabidopsis epidermis: a dynamic spatial model. *BMC Syst. Biol.* 2, 98. doi:10.1186/1752-0509-2-98

Benítez, M., Monk, N. A., and Alvarez-Buylla, E. R. (2011). Epidermal patterning in Arabidopsis: models make a difference. *J. Exp. Zool. B Mol. Dev. Evol.* 316, 241–253.

Bornholdt, S. (2008). Boolean network models of cellular regulation: prospects and limitations. *J. R. Soc. Interface* 5(Suppl. 1), S85–S94.

Bowler, P. J. (1983). *The Eclipse of Darwinism: Anti-Darwinian Evolution Theories in the Decades Around 1900.* Baltimore: Johns Hopkins University Press.

Brandman, O., and Meyer, T. (2008). Feedback loops shape cellular signals in space and time. *Science* 322, 390–395.

Callebaut, W., and Rasskin-Gutman, D. (2009). *Modularity: Understanding the Development and Evolution of Natural Complex Systems.* Cambridge: MIT Press.

Calzone, L., Fages, F., and Soliman, S. (2006). BIOCHAM: an environment for modeling biological systems and formalizing experimental knowledge. *Bioinformatics* 22, 1805–1807.

Chickarmane, V., and Peterson, C. (2008). A computational model for understanding stem cell, trophectoderm and endoderm lineage determination. *PLoS ONE* 3, e3478. doi:10.1371/journal.pone.0003478

Davidich, M. I., and Bornholdt, S. (2008). Boolean network model predicts cell cycle sequence of fission yeast. *PLoS ONE* 3, e1672. doi:10.1371/journal.pone.0001672

Davidson, E. (2001). *Genomic Regulatory Systems. Development and Evolution.* New York: Academic Press.

Davidson, E. H., and Erwin, D. H. (2006). Gene regulatory networks and the evolution of animal body plans. *Science* 311, 796–800.

de Jong, H. (2002). Modeling and simulation of genetic regulatory systems: a literature review. *J. Comput. Biol.* 9, 67–103.

de Jong, H., Geiselmann, J., Hernández, C., and Page, M. (2003). Genetic network analyzer: qualitative simulation of genetic regulatory networks. *Bioinformatics* 19, 336–344.

Di Cara, A., Garg, A., De Micheli, G., Xenarios, I., and Mendoza, L. (2007). Dynamic simulation of regulatory networks using SQUAD. *BMC Bioinformatics* 8, 462. doi:10.1186/1471-2105-8-462

Didier, G., Remy, E., and Chaouiya, C. (2011). Mapping multivalued onto Boolean dynamics. *J. Theor. Biol.* 270, 177–184.

Espinosa-Soto, C., Padilla-Longoria, P., and Alvarez-Buylla, E. R. (2004). A gene regulatory network model for cell-fate determination during *Arabidopsis thaliana* flower development that is robust and recovers experimental gene expression profiles. *Plant Cell* 16, 2923–2939.

Fauré, A., Naldi, A., Chaouiya, C., and Thieffry, D. (2006). Dynamical analysis of a genetic Boolean model for the control of the mammalian cell cycle. *Bioinformatics* 22, e124–e131.

Fujita, H., Toyokura, K., Okada, K., and Kawaguchi, M. (2011). Reaction-diffusion pattern in shoot apical meristem of plants. *PLoS ONE* 6, e18243. doi:10.1371/journal.pone.0018243

Giacomantonio, C. E., and Goodhill, G. J. (2010). A Boolean model of the gene regulatory network underlying Mammalian cortical area development. *PLoS Comput. Biol.* 6, e1000936. doi:10.1371/journal.pcbi.1000936

Gierer, A., and Meinhardt, H. (1972). A theory of biological pattern formation. *Kybernetik* 12, 30–39.

Gómez-Mena, C., de Folter, S., Costa, M. M., Angenent, G. C., and Sablowski, R. (2005). Transcriptional program controlled by the floral homeotic gene AGAMOUS during early organogenesis. *Development* 132, 429–438.

Goodwin, B. (2001). *How the Leopard Changed Its Spots: The Evolution of Complexity.* New Jersey: Princeton University Press.

Gordon, S. P., Chickarmane, V. S., Ohno, C., and Meyerowitz, E. M. (2009). Multiple feedback loops through cytokinin signaling control stem cell number within the Arabidopsis shoot meristem. *Proc. Natl. Acad. Sci. U.S.A.* 106, 16529–16534.

Gould, S. J. (2002). *The Structure of Evolutionary Theory.* Cambridge: Belknap Press of Harvard University Press.

Greenspan, R. J. (2001). The flexible genome. *Nat. Rev. Genet.* 2, 383–387.

Griffiths, P. E., and Gray, R. D. (1994). Developmental systems and evolutionary explanation. *J. Philos.* XCI, 277–304.

Gustafson-Brown, C., Savidge, B., and Yanofsky, M. F. (1994). Regulation of the Arabidopsis floral homeotic gene AP1. *Cell* 76, 131–143.

Huang, L. S., and Sternberg, P. W. (2006). Genetic dissection of developmental pathways. *WormBook* 14, 1–19.

Jablonka, E., and Lamb, M. J. (2005). *Evolution in Four Dimensions. Genetic, Epigenetic, Behavioral, and Symbolic Variation in the History of Life.* Cambridge: MIT Press.

Jaeger, J., Irons, D., and Monk, N. (2008). Regulative feedback in pattern formation: towards a general relativistic theory of positional information. *Development* 135, 3175–3183.

Jiang, X., Neapolitan, R. E., Barmada, M. M., and Visweswaran, S. (2011). Learning genetic epistasis using Bayesian network scoring criteria. *BMC Bioinformatics* 12, 89. doi:10.1186/1471-2105-12-89

Kaplan, S., Bren, A., Dekel, E., and Alon, U. (2008). The incoherent feed-forward loop can generate non-monotonic input functions for genes. *Mol. Syst. Biol.* 4, 203.

Kauffman, S. (1969). Homeostasis and differentiation in random genetic control networks. *Nature* 224, 177–178.

Kondo, S., and Miura, T. (2010). Reaction-diffusion model as a framework for understanding biological pattern formation. *Science* 329, 1616–1620.

Kwon, Y. K., and Cho, K. H. (2008). Coherent coupling of feedback loops: a design principle of cell signaling networks. *Bioinformatics* 24, 1926–1932.

Levesque, M. P., Vernoux, T., Busch, W., Cui, H., Wang, J. Y., Blilou, I., Hassan, H., Nakajima, K., Matsumoto, N., Lohmann, J. U., Scheres, B., and Benfey, P. N. (2006). Whole-genome analysis of the SHORT-ROOT developmental pathway in Arabidopsis. *PLoS Biol.* 4, e143. doi:10.1371/journal.pbio.0040143

Lewontin, R. (2000). "Foreword," in *The Ontogeny of Information: Developmental Systems and Evolution*, ed. S. Oyama (Durham: Duke University Press), vii–xv.

Li, F., Long, T., Lu, Y., Ouyang, Q., and Tang, C. (2004). The yeast cell-cycle network is robustly designed. *Proc. Natl. Acad. Sci. U.S.A.* 101, 4781–4786.

Li, S., Assmann, S. M., and Albert, R. (2006). Predicting essential components of signal transduction networks: a dynamic model of guard cell abscisic acid signaling. *PLoS Biol.* 4, e312. doi:10.1371/journal.pbio.0040312

Longo, G., and Tendero, P.-E. (2007). The differential method and the causal incompleteness of Programming Theory in Molecular Biology. *Found. Sci.* 12, 337–366.

Lorenz, K. (1965). *Evolution and Modification of Behaviour.* Chicago: The University of Chicago Press.

Mangan, S., and Alon, U. (2003). Structure and function of the feed-forward loop network motif. *Proc. Natl. Acad. Sci. U.S.A.* 100, 11980–11985.

Mangan, S., Zaslaver, A., and Alon, U. (2003). The coherent feedforward loop serves as a sign-sensitive delay element in transcription networks. *J. Mol. Biol.* 334, 197–204.

Mayr, E., and Provine, W. B. (1980). *The Evolutionary Synthesis: Perspectives on the Unification of Biology*. Cambridge: Harvard University Press.

Meinhardt, H., and Gierer, A. (2000). Pattern formation by local self-activation and lateral inhibition. *Bioessays* 22, 753–760.

Milo, R., Shen-Orr, S., Itzkovitz, S., Kashtan, N., Chklovskii, D., and Alon, U. (2002). Network motifs: simple building blocks of complex networks. *Science* 298, 824–827.

Mitrophanov, A. Y., and Groisman, E. A. (2008). Positive feedback in cellular control systems. *Bioessays* 30, 542–555.

Moore, J. H., and Williams, S. M. (2005). Traversing the conceptual divide between biological and statistical epistasis: systems biology and a more modern synthesis. *Bioessays* 27, 637–646.

Morata, G., and Lawrence, P. A. (1977). Homoeotic genes, compartments and cell determination in Drosophila. *Nature* 265, 211–216.

Müller, G. B. (2007). Evo-devo: extending the evolutionary synthesis. *Nat. Rev. Genet.* 8, 943–949.

Müssel, C., Hopfensitz, M., and Kestler, H. A. (2010). BoolNet – an R package for generation, reconstruction and analysis of Boolean networks. *Bioinformatics* 26, 1378–1380.

Newman, M., Barabasi, A.-L., and Watts, D. (2006). *The Structure and Dynamics of Networks.* New Jersey: Princeton Studies in complexity.

Nijouth, H. F. (1990). Metaphors and the role of genes in development. *Bioessays* 12, 441–446.

Nochomovitz, Y. D., and Li, H. (2006). Highly designable phenotypes and mutational buffers emerge from a systematic mapping between network topology and dynamic output. *Proc. Natl. Acad. Sci. U.S.A.* 103, 4180–4185.

Oyama, S. (1985). *The Ontogeny of Information: Developmental Systems and Evolution*. Cambridge: Cambridge University Press.

Phenix, H., Morin, K., Batenchuk, C., Parker, J., Abedi, V., Yang, L., Tepliakova, L., Perkins, T. J., and Kærn, M. (2011). Quantitative epistasis analysis and pathway inference from genetic interaction data. *PLoS Comput. Biol.* 7, e1002048. doi:10.1371/journal.pcbi.1002048

Phillips, P. C. (2008). Epistasis – the essential role of gene interactions in the structure and evolution of genetic systems. *Nat. Rev. Genet.* 9, 855–867.

Pigliucci, M. (2007). Do we need an extended evolutionary synthesis? *Evolution* 61, 2743–2749.

Pigliucci, M. (2009). An extended synthesis for evolutionary biology. *Ann. N. Y. Acad. Sci.* 1168, 218–228.

Pigliucci, M., and Müller, G. B. (2010). *Evolution – the Extended Synthesis.* Cambridge: The MIT Press.

Robert, J. S. (2004). *Embryology, Epigenesis and Evolution: Taking Development Seriously*. Cambridge: Cambridge University Press.

Roeder, A. H., Tarr, P. T., Tobin, C., Zhang, X., Chickarmane, V., Cunha, A., and Meyerowitz, E. M. (2011a). Computational morphodynamics of plants: integrating development over space and time. *Nat. Rev. Mol. Cell Biol.* 12, 265–273.

Roeder, A. H., Tarr, P. T., Tobin, C., Zhang, X., Chickarmane, V., Cunha, A., and Meyerowitz, E. M. (2011b). Mutually reinforcing patterning mechanisms: authors' reply. *Nat. Rev. Mol. Cell Biol.* 12, 533.

Roth, F. P., Lipshitz, H. D., and Andrews, B. J. (2009). Q&A: epistasis. *J. Biol.* 8, 35.

Salazar-Ciudad, I. (2006). Developmental constraints vs. variational properties: how pattern formation can help to understand evolution and development. *J. Exp. Zool. B Mol. Dev. Evol.* 306, 107–125.

Savage, N. S., Walker, T., Wieckowski, Y., Schiefelbein, J., Dolan, L., and Monk, N. A. (2008). A mutual support mechanism through intercellular movement of CAPRICE and GLABRA3 can pattern the Arabidopsis root epidermis. *PLoS Biol.* 6, e235. doi:10.1371/journal.pbio.0060235

Schoof, H., Lenhard, M., Haecker, A., Mayer, K. F., Jürgens, G., and Laux, T. (2000). The stem cell population of Arabidopsis shoot meristems is maintained by a regulatory loop between CLAVATA and WUSCHEL genes. *Cell* 100, 635–644.

Shen-Orr, S. S., Milo, R., Mangan, S., and Alon, U. (2002). Network motifs in the transcriptional regulation network of *Escherichia coli*. *Nat. Genet.* 31, 64–68.

Shmulevich, I., and Kauffman, S. A. (2004). Activities and sensitivities in boolean network models. *Phys. Rev. Lett.* 93, 048701.

St Onge, R. P., Mani, R., Oh, J., Proctor, M., Fung, E., Davis, R. W., Nislow, C., Roth, F. P., and Giaever, G. (2007). Systematic pathway analysis using high-resolution fitness profiling of combinatorial gene deletions. *Nat. Genet.* 39, 199–206.

Tong, A. H., Lesage, G., Bader, G. D., Ding, H., Xu, H., Xin, X., Young, J., Berriz, G. F., Brost, R. L., Chang, M., Chen, Y., Cheng, X., Chua, G., Friesen, H., Goldberg, D. S., Haynes, J., Humphries, C., He, G., Hussein, S., Ke, L., Krogan, N., Li, Z., Levinson, J. N., Lu, H., Ménard, P., Munyana, C., Parsons, A. B., Ryan, O., Tonikian, R., Roberts, T., Sdicu, A. M., Shapiro, J., Sheikh, B., Suter, B., Wong, S. L., Zhang, L. V., Zhu, H., Burd, C. G., Munro, S., Sander, C., Rine, J., Greenblatt, J., Peter, M., Bretscher, A., Bell, G., Roth, F. P., Brown, G. W., Andrews, B., Bussey, H., and Boone, C. (2004). Global mapping of the yeast genetic interaction network. *Science* 303, 808–813.

Tyler, A. L., Asselbergs, F. W., Williams, S. M., and Moore, J. H. (2009). Shadows of complexity: what biological networks reveal about epistasis and pleiotropy. *Bioessays* 31, 220–227.

von Dassow, G., Meir, E., Munro, E. M., and Odell, G. M. (2000). The segment polarity network is a robust developmental module. *Nature* 406, 188–192.

Wagner, A. (1999). Causality in complex systems. *Biol. Philos.* 14, 83–101.

Wagner, A. (2009). Evolutionary constraints permeate large metabolic networks. *BMC Evol. Biol.* 9, 231. doi:10.1186/1471-2148-9-231

Wagner, G. P., Pavlicev, M., and Cheverud, J. M. (2007). The road to modularity. *Nat. Rev. Genet.* 8, 921–931.

Watson, J. D., and Crick, F. H. (1953). Molecular structure of nucleic acids; a structure for deoxyribose nucleic acid. *Nature* 171, 737–738.

Wittmann, D. M., Krumsiek, J., Saez-Rodriguez, J., Lauffenburger, D. A., Klamt, S., and Theis, F. J. (2009). Transforming Boolean models to continuous models: methodology and application to T-cell receptor signaling. *BMC Syst. Biol.* 3, 98. doi:10.1186/1752-0509-3-98

Zheng, J., Zhang, D., Przytycki, P. F., Zielinski, R., Capala, J., and Przytycka, T. M. (2010). SimBoolNet – a Cytoscape plugin for dynamic simulation of signaling networks. *Bioinformatics* 26, 141–142.

Conflict of Interest Statement: The authors declare that the research was conducted in the absence of any commercial or financial relationships that could be construed as a potential conflict of interest.

Received: 03 May 2011; accepted: 17 November 2011; published online: 15 December 2011.

Citation: Azpeitia E, Benítez M, Padilla-Longoria P, Espinosa-Soto C and Alvarez-Buylla ER (2011) Dynamic network-based epistasis analysis: Boolean examples. Front. Plant Sci. ***2****:92. doi: 10.3389/fpls.2011.00092*

This article was submitted to Frontiers in Plant Genetics and Genomics, a specialty of Frontiers in Plant Science.

5.3.- Parte III: "Finding Missing Interactions of the *Arabidopsis thaliana* Root Stem Cell Niche Gene Regulatory Network" y "Finding Missing Interactions in Gene Regulatory Networks Using Boolean Models"

El estudio de los procesos moleculares involucrados en el desarrollo y mantenimiento del nicho de células troncales en los años posteriores a nuestra publicación del 2010, reveló información importante sobre los mismos. Al incorporar la nueva información experimental disponible y quitar las predicciones hechas en el 2010, la red no sólo seguía sin recuperar las configuraciones genéticas observadas en los distintos tipos celulares del nicho, sino que además el comportamiento dinámico de la red empeoró con respecto a la red publicada en 2010. Esto se debió a que aumentó la cantidad de comportamientos experimentalmente no observados predichos, y a que se encontró un mayor número de atractores cíclicos no observados.

El trabajo publicado en el 2011, mostró parte del alcance de la aproximación Booleana para el análisis de motivos moleculares. Gracias a que la aproximación Booleana simplifica y facilita la formalización de resultados experimentales, sin dejar de producir resultados relevantes, se puede usar como una herramienta para buscar información faltante o errónea en un red con gran eficiencia y bajos costos computacionales. Tal vez, la mayor limitante de las redes Booleanas es que la combinatoria de posibles redes explota rápidamente conforme la red crece. Por este motivo es importante restringir su uso a redes que tengan significado biológico. De esta forma, un siguiente objetivo fue, una vez incorporada la nueva información experimental a la red, generar un conjunto de procedimientos a partir de los cuales fuera posible encontrar posible información faltante o errónea, discriminar entre redes con significado biológico de redes que no lo tienen y que fueran capaces de mantener la información experimental contenida en las funciones dinámicas de la red. Una vez propuestos los procedimientos, serían utilizados para buscar conjuntos de funciones lógicas cuyo comportamiento reprodujera lo observado experimentalmente, con la finalidad de encontrar posible información faltante o errónea en la red.

Como resultado de este análisis detectamos tres interacciones fundamentales para recuperar el comportamiento esperado de la red. Fue interesante notar, que para

todas estas interacciones había algún gen candidato no incluido en la red que la podría estar llevando a cabo, pero que su presencia en la raíz no había sido confirmada.

Tanto los datos como los procedimientos fueron reportados a detalle en un artículo publicado en Frontiers In Plant Sciences, el cuál reproducimos a continuación. Es importante mencionar que este trabajo se presentó de forma oral en la European Conference on Complex System en 2012, la cual quedó registrada dentro de un capítulo de sus proceedings, y se presentará también a continuación.

frontiers in
PLANT SCIENCE

HYPOTHESIS AND THEORY ARTICLE
published: 30 April 2013
doi: 10.3389/fpls.2013.00110

Finding missing interactions of the *Arabidopsis thaliana* root stem cell niche gene regulatory network

Eugenio Azpeitia[1,2], Nathan Weinstein[3], Mariana Benítez[2,4], Luis Mendoza[3]* and Elena R. Alvarez-Buylla[1,2]*†

[1] Laboratorio de Genética Molecular, Desarrollo y Evolución de Plantas, Instituto de Ecología, Universidad Nacional Autónoma de México, Ciudad Universitaria, México DF, México
[2] C3, Centro de Ciencias de la Complejidad, Universidad Nacional Autónoma de México, México DF, México
[3] Instituto de Investigaciones Biomédicas, Universidad Nacional Autónoma de México, Cd. Universitaria, México DF, México
[4] Departamento de Ecología de la Biodiversidad, Instituto de Ecología, Universidad Nacional Autónoma de México, Ciudad Universitaria, México DF, México

Edited by:
Wolfgang Schmidt, Academia Sinica, Taiwan

Reviewed by:
Reka Albert, Pennsylvania State University, USA
Sebastian Klie, Max-Planck Intitute dor Molecular Plant Physiology, Germany

***Correspondence:**
Luis Mendoza, Instituto de Investigaciones Biomédicas, Universidad Nacional Autónoma de México, Apartado Postal 70228, Ciudad Universitaria, México DF 04510, México.
e-mail: lmendoza@biomedicas.unam.mx;
Elena R. Alvarez-Buylla, Laboratorio Genética Molecular, Desarrollo y Evolución de Plantas, Instituto de Ecología, Universidad Nacional Autónoma de México, Circ. Exterior anexo al Jardín Botánico, Ciudad Universitaria, Del. Coyoacán, 04510 México DF, México.
e-mail: eabuylla@gmail.com

†Present address:
Elena R. Alvarez-Buylla, Department of Plant and Microbial Biology, College of Natural Resources, University of California, Berkeley, 431 Koshland Hall, Berkeley, CA 94720, USA.

Over the last few decades, the *Arabidopsis thaliana* root stem cell niche (RSCN) has become a model system for the study of plant development and stem cell niche dynamics. Currently, many of the molecular mechanisms involved in RSCN maintenance and development have been described. A few years ago, we published a gene regulatory network (GRN) model integrating this information. This model suggested that there were missing components or interactions. Upon updating the model, the observed stable gene configurations of the RSCN could not be recovered, indicating that there are additional missing components or interactions in the model. In fact, due to the lack of experimental data, GRNs inferred from published data are usually incomplete. However, predicting the location and nature of the missing data is a not trivial task. Here, we propose a set of procedures for detecting and predicting missing interactions in Boolean networks. We used these procedures to predict putative missing interactions in the *A. thaliana* RSCN network model. Using our approach, we identified three necessary interactions to recover the reported gene activation configurations that have been experimentally uncovered for the different cell types within the RSCN: (1) a regulation of *PHABULOSA* to restrict its expression domain to the vascular cells, (2) a self-regulation of *WOX5*, possibly by an indirect mechanism through the auxin signaling pathway, and (3) a positive regulation of *JACKDAW* by MAGPIE. The procedures proposed here greatly reduce the number of possible Boolean functions that are biologically meaningful and experimentally testable and that do not contradict previous data. We believe that these procedures can be used on any Boolean network. However, because the procedures were designed for the specific case of the RSCN, formal demonstrations of the procedures should be shown in future efforts.

Keywords: gene regulatory networks, Boolean models and functions, root stem cell niche, incomplete networks, predictive modeling, *Arabidopsis thaliana*

INTRODUCTION

The *Arabidopsis thaliana* root stem cell niche (RSCN) consists of a group of cells that rarely divide, known as the quiescent center, surrounded by four different types of stem cells (**Figure 1**; Dolan et al., 1993). The root stem cells produce all cell types necessary for the development of the primary root. Due to its architectural simplicity and its accessibility for experimental research at the genetic and molecular levels, the *A. thaliana* RSCN has become an important experimental model for molecular genetic studies in the last few decades. During this time, many important molecular mechanisms involved in the maintenance and development of the RSCN have been described (Sablowski, 2011; Azpeitia and Alvarez-Buylla, 2012). At least three molecular mechanisms have been uncovered as being fundamental for RSCN maintenance and development. The first mechanism involves auxin signaling and the PLETHORA (PLT) transcription factors that regulate auxin signaling (Galinha et al., 2007; Ding and Friml, 2010). The second mechanism involves the transcription factors SHORTROOT (SHR), SCARECROW (SCR), and some of their target genes (TGEN), as well as proteins that interact with them (Sabatini et al., 2003; Welch et al., 2007). The third mechanism includes CLAVATA-like 40 (CLE40) and WUSCHEL-RELATED HOMEOBOX 5 (WOX5; Stahl et al., 2009). Importantly, these three mechanisms are interconnected and present complex non-linear behaviors (reviewed in Azpeitia and Alvarez-Buylla, 2012).

Network models are an excellent tool for the integration and analysis of complex biomolecular systems, such as RSCN molecular mechanisms, at the structural and dynamic levels (de Jong, 2002; Alvarez-Buylla et al., 2007). In such models, the network nodes represent genes, proteins, RNA, or other molecular factors, while the edges correspond to positive or negative regulatory interactions among the nodes. Each node attains different values that

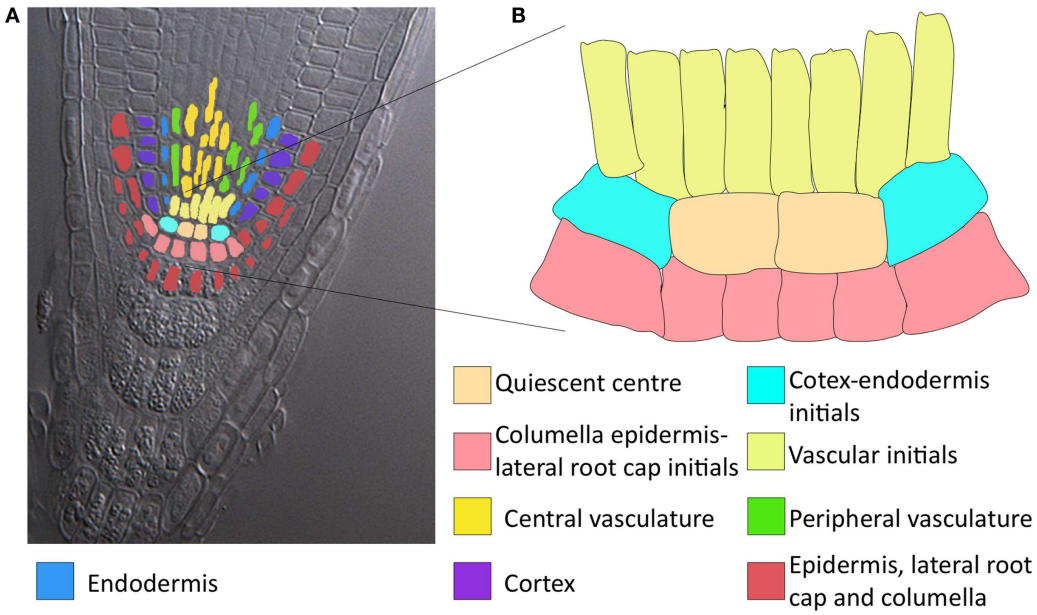

FIGURE 1 | Colour tracing of a confocal longitudinal section of an Arabidopsis root tip and a magnification of the RSCN. **(A)** Cleared root tip of Arabidopsis thaliana. The expected stable gene configurations that characterise each cell type are distinguished with different colours. As observed, some of the expected attractors represent more than one cellular type. QC, quiescent centre; END, endodermis; VI, vascular initials; CEI, cortex-endodermis initials; COR, cortex; PVC, peripheral vascular cells; CLEI, collumela-epidermis-lateral-root-cap initials; LCC, collumela and lateral root cap; and CVC, central vascular cells. **(B)** Amplification of the RSCN.

correspond to its expression or activity level, and the node's state changes in time depending on the state of the regulating nodes. The regulatory functions can be specified by different mathematical formalisms, but in all cases, these rules allow to follow the system's collective dynamics over time and find relevant dynamic properties of the entire regulatory system. Among these properties, self-sustained network states, referred to as attractors, have been found to be particularly relevant. Attractors may be either cyclic or fixed-point.

Dynamic network models allow analyses of the sufficiency of reported data to explain the observed behaviors and properties of a particular system (de Jong, 2002). For example, Kauffman (1969) proposed that the attractors of a given gene regulatory network (GRN) could represent the experimentally observed gene expression profiles or configurations that characterize different cell types in biological systems. If the experimental data are sufficient, the GRN model attractors should coincide with the gene configurations experimentally documented for the different cell types. This hypothesis has been explored and validated with networks based on biological data (e.g., Mendoza and Alvarez-Buylla, 1998; Albert and Othmer, 2003; Espinosa-Soto et al., 2004). In fact, we published a GRN model of the RSCN a few years ago (Azpeitia et al., 2010).

Over the past few years, experimental reports have improved our knowledge about the RSCN GRN (reviewed in Azpeitia and Alvarez-Buylla, 2012). Interestingly, when we incorporated new experimental data, the set of attractors recovered by the model drastically changed. The new GRN model was not able to recover the observed attractors and generated many attractors that had not been observed experimentally. In this case, some key components or interactions are presumed to be missing. In principle, with the inclusion of putative missing components or interactions it should be possible to recover the expected attractors. However, the identification of the missing data in general is a non-trivial task.

In continuous systems, the inference of missing data is complicated partly because once the new information is introduced, new parameters must be estimated or incorporated into the postulated kinetic functions, and this procedure can cause the reformulation of such functions. In contrast, discrete networks usually do not need to deal with complicated parameter estimation or adjustment, and the redesign of the interaction functions is usually simpler. Boolean networks (BNs) are arguably the simplest discrete modeling approach for dynamic networks. In BNs, nodes may attain only one of two values or states: *0* if the node is OFF, and *1* if the node is ON. The level of expression for a given node may be represented by a discrete variable x, and its value at a particular time $(t+\tau)$ depends on the state of other components in the network $(x_1, x_2, \ldots, x_n)$ at a previous time. The state of every node x therefore changes according to the following equation:

$$x_n\ (t+\tau) = F_n\left(x_{n_1}(t),\ x_{n_2}(t),\ \ldots,\ x_{n_k}\right) \qquad (1)$$

In this equation, $(x_{n_1}(t), x_{n_2}(t), \ldots, x_{n_k}(t))$ are the regulators of gene x_n, and F_n is a discrete function known as a Boolean function (BF). Such functions can be highly non-linear. Despite their simplicity, BN models have rich behaviors that yield meaningful information about the properties of the network under study. Because of this characteristic, BNs have been successfully used for the analysis of diverse GRNs (e.g., Albert and Othmer, 2003;

Espinosa-Soto et al., 2004). The main constraint for the detection of putative missing interactions in BNs is that the number of possible BFs for a node increases as a double exponential function, namely 2^{2^i}, where i represents the number of inputs regulating a target node. For example, a node with five regulatory inputs has 2^{32} ($\approx 4 \times 10^9$) possible BFs determining its dynamic response (**Figure 2A**). Similarly, the number of possible network topologies in a network is 2^{n^2}, where n represents the number of nodes. Hence, in a BN with five nodes, a total of 2^{25} ($\approx 3.35 \times 10^7$) possible topologies determine the GRN connectivity (**Figure 2B**). Most GRN topologies can be described by different sets of BFs. Thus, if we consider a BN with five nodes where all nodes interact with each other in every possible manner, $(2^{2^i})^5$ ($\approx 1.46 \times 10^{48}$) sets of BFs describe this topology. As observed, modeling the number of possibilities caused by additional components or links quickly becomes computationally intractable, even for such small networks using a simple Boolean formalism. Nevertheless, the dynamics of BNs with tens of nodes can be exhaustively analyzed in a relatively short amount of time, compared with other types of networks (e.g., Arellano et al., 2011). Thus, a methodology that allows for systematic integration and prediction of missing interactions in BNs would provide an instrumental tool in the proposal of a more complete RSCN GRN model and likely any other GRN.

Pal et al. (2005) studied how to produce a BN with a predefined set of expected attractors. Later, Zou (2010) studied how to obtain a set of expected attractors if the network topology exists and the BFs are partially known. Other researchers have investigated how to construct a BN from knowledge of the state-transition dynamics (e.g., Jarrah et al., 2007). Finally, Raeymaekers (2002) proposed that not all BFs are biologically meaningful and postulated a set of meaningful functions. The work of Raeymaekers is tightly linked to the so-called "canalizing BFs," which produce stable and more biologically realistic BNs (Kauffman et al., 2004). Because the RSCN GRN model already relies on published experimental data, the methodology should be able to not only produce meaningful BFs, maintain the topology and recover the set of expected attractors but also agree with previous data regarding the reported molecular interactions. Moreover, taking into account reported molecular experimental data may greatly reduce the number of possible BFs to test. For example, SHR and SCR are known to directly and positively regulate *MAGPIE* (*MGP*) expression (Levesque et al., 2006; Cui et al., 2007); therefore, the BFs where SHR or SCR do not promote *MGP* expression directly do not need to be tested.

In this paper, we updated the RSCN GRN model using experimental data that were reported after we published our last model. Interestingly, when we incorporated the new experimental data, the set of recovered attractors did not correspond with the experimentally observed gene configuration states in the RSCN. Thus, we designed a set of procedures to add all possible missing interactions one-by-one to the model without contradicting experimental data and to greatly reduce the number of possible BFs when trying to predict missing interactions for a particular node. Using these procedures, we explored the effect of adding putative missing interactions in the set of attractors. We considered that the addition of a putative missing interaction improved our model if the interaction reduced the number of non-expected attractors or increased the number of expected attractors recovered by the model. The interaction that most improved the model, by removing non-expected attractors or adding expected attractors, was incorporated into the model. If more than one interaction equally improved the model, one interaction was randomly selected and added to the BN model. After the inclusion of an interaction, we repeated the process until the inclusion of three consecutive interactions did not improve the model, or we exclusively obtained the set of expected attractors. Based on our results, we proposed three putative missing interactions that were biologically meaningful, could be tested experimentally and in conjunction were sufficient to recover the set of observed attractors of the RSCN GRN; however, these interactions were not sufficient to eliminate the non-meaningful attractors in the model. Interestingly, these three interactions were always the first to appear as putative missing interactions. After adding the three interactions, the procedures produced more putative missing interactions that reduced the number of meaningless attractors. However, this second set of putative missing interactions was more variable, and we were never able to exclusively recover the set of expected attractors, strongly suggesting that additional components are yet to be discovered. Nevertheless, we provide three concise and testable predictions that are in agreement with the data that have been reported on RSCN patterning.

We believe that these procedures are useful for detecting missing interactions and possible incorrect gene regulatory or topological inferences due to incomplete data in any other GRN. However, because the procedures were generated *ad hoc* for the RSCN molecular interactions, generalization, and mathematical demonstrations of the procedures should be performed in the future to formally analyze the implications of using these procedures for any other GRN. Nevertheless, in the context of this study, we believe that these procedures may lead to novel research questions concerning general issues, such as the constraints that a given network topology imposes on the set of attractors.

METHODS

In this section, we describe the update to the RSCN GRN and the procedures used to reduce the number of possible BFs generated when trying to predict missing interactions and maintain previous experimental data. Then, we describe an evolutionary algorithm used to test the procedures in the GRN of the RSCN.

RSCN GRN UPDATE

Three main regulatory mechanisms have been involved in the development and maintenance of the RSCN. The first mechanism involves the transcription factor SHR of the GRAS gene family (Sena et al., 2004). SHR is transcribed in the stele, but its protein moves to the adjacent cell layer (i.e., QC, cortex/endodermis initials, and endodermis) (Nakajima et al., 2001). In the QC, cortex/endodermis initials and endodermis, SHR promotes the expression of SCR, another GRAS transcription factor (Cui et al., 2007). SHR and SCR form a complex and together they regulate the expression of many genes, including other transcription factors and miRNAs. Their targets include the transcription factors

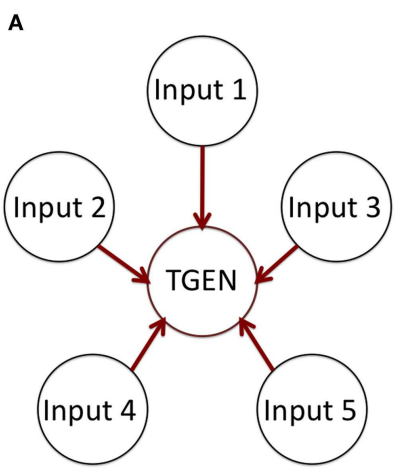

In 1	In 2	In 3	In 4	In 5	TGEN
0	0	0	0	0	*
0	0	0	0	1	*
.	.	.	.	.	.
.	.	.	.	.	.
.	.	.	.	.	.
1	1	1	1	0	*
1	1	1	1	1	*

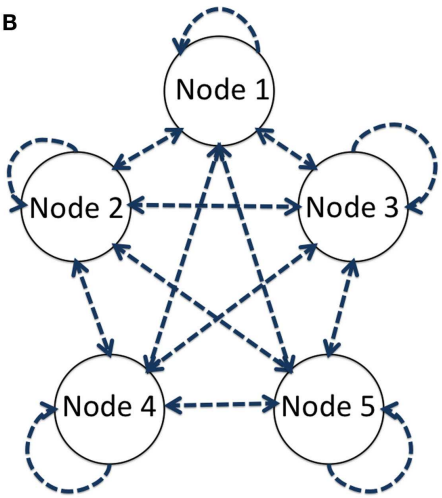

	N1	N2	N3	N4	N5
N1	*	*	*	*	*
N2	*	*	*	*	*
N3	*	*	*	*	*
N4	*	*	*	*	*
N5	*	*	*	*	*

FIGURE 2 | Number of possible BFs in a node and the topologies of a network. **(A)** The number of possible BFs for a particular node depends on the number of inputs or regulators of the node. In each possible state of its inputs, the node can assume a 0 or 1 expression value. Thus, 2^{2^i} possible BFs are available to describe the regulation of a node with i inputs. **(B)** The number of possible topologies of a network depends on the number of nodes. In a network, each node can interact with itself and any other node. Thus, n^2 possible interactions exist. Because each interaction can either exist or not exist, 2^{n^2} possible topologies describe a network with N nodes. E, Exist, and D, Do not exist.

JKD and *MGP*, as well as miRNA165/6 (Sozzani et al., 2010). JKD and MGP physically interact with SHR and SCR and are important for the regulation of *SCR* expression (Welch et al., 2007). The miRNA165/6 moves from its transcription domain and negatively regulates the expression of HD-ZIP III genes in the stele (Carlsbecker et al., 2010). The second mechanism is comprised of the auxin signaling pathway and their TGENs, such as the PLT transcription factors (Galinha et al., 2007). In the auxin signaling pathway, the transcription factors AUXIN RESPONSE FACTORS (ARF) form dimers with proteins of the Aux/IAA family (Guilfoyle and Hagen, 2007). In an Aux/IAA-ARF dimer, the ARFs cannot promote the expression of their TGENs. However, auxin promotes Aux/IAA degradation (Calderón Villalobos et al., 2012). Thus, as auxin concentration increases, the ARFs are released from the Aux/IAA negative regulation and promote the expression of their TGENs. The third mechanism involves the transcription factor WOX5, the mobile protein CLE40 (a negative regulator of WOX5) and their receptor ACR4 (Stahl et al., 2009, 2013). Importantly, these mechanisms interact with each other (Azpeitia et al., 2010).

To update our previous GRN, we first omitted the interactions predicted by our previous work that had not yet been confirmed experimentally and that were rather hypothetical (Azpeitia et al., 2010). The reason for this omission is that the objective of this work was to detect and predict missing interactions using a systematic approach that could be applied to any system. The only prediction in our previous model that we conserved is the negative regulation of WOX5 by CLE40 because this result was experimentally documented while the model was under review (Stahl et al., 2009). Then, we removed *PLT* genes from the model because even though these genes are essential for RSCN maintenance (Galinha et al., 2007), the *PLT* genes do not regulate any other node in the model under analysis and can therefore be collapsed (**Figures 3A,B**). We also corrected or completed data about the interactions among SCR, MGP, and JKD according to the results of Ogasawara et al. (2011). Thus, in this model, MGP does not act as a negative regulator of *SCR*; JKD is a positive regulator of *MGP* and itself; and MGP negatively self regulates (Ogasawara et al., 2011). Stahl et al. (2009) reported that the receptor ACR4 is necessary for CLE40 negative regulation of *WOX5* and is positively regulated by CLE40. Apparently, SHR and SCR regulation of *WOX5* is not direct (Sozzani et al., 2010). Moreover, SHR and SCR promote *miRNA165/6* expression, while miRNA165/6 represses PHB mRNA translation (Carlsbecker et al., 2010). According to Grigg et al. (2009), PHB overexpression prevents *WOX5* expression. Hence, we decided to delete the positive, direct regulation of *WOX5* by SHR and SCR because the regulation is not direct, and incorporate this positive regulation indirectly by the repression of PHB. Recently, PHB was reported to be a negative regulator of *JKD* (Miyashima et al., 2011). Because our model does not incorporate

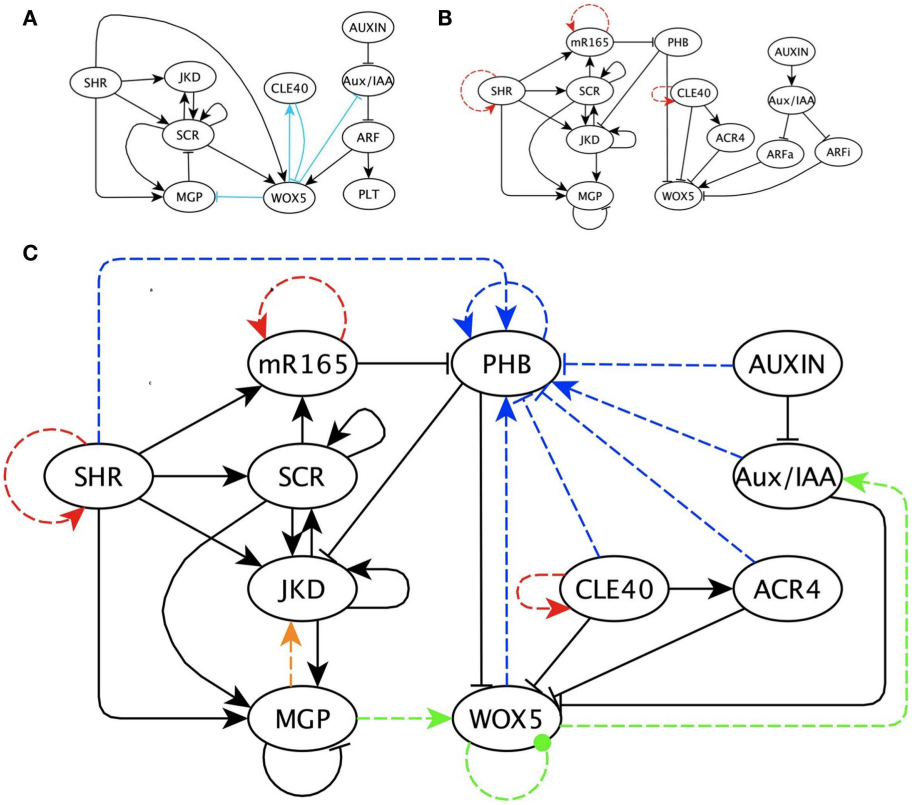

FIGURE 3 | The previous and updated RSCN GRN with predicted missing interactions. **(A)** Previously published RSCN GRN (Azpeitia et al., 2010). The light blue edges indicate previous predicted missing interactions. **(B)** Updated RSCN GRN as explained in the main text. The red edges are the self-regulations introduced to represent protein movement. **(C)** RSCN GRN with predicted missing interactions. For simplicity and clarity, intermediary nodes were not included in this GRN; however, these nodes are available in Supplementary Material. Yellow, green and blue edges are the three predicted interactions required to recover the expected attractors and are grouped according to the node's functions. The blue edges always indicate regulation of PHB. The yellow edge is a positive regulation of JKD by MGP. The green edges correspond to regulation of WOX5. The dotted green edge indicates a negative or positive regulation of WOX5 by itself.

space explicitly, we replaced molecular diffusion and movement by including a positive self-regulatory edge in nodes that move among cells (i.e., SHR, CLE, and miRNA165/6) to allow expression of these nodes where they move and no node positively regulates them. Finally, we reduced the auxin signaling pathway to the auxin and Aux/IAA nodes because the pathway is composed of linear path-like interactions that can be collapsed. In this way, we reduced the number of nodes in our network, and this change reduced the number of possible topologies and BFs describing the network once we incorporated putative missing interactions. In Section "Appendix 1 in the Appendix" we present the data and results of the analysis performed to reduce the auxin signaling pathway. We incorporated this information in the updated regulatory network model proposed here (**Figure 3B**). The main experimental data about gene interactions are presented in **Table 1**.

Importantly, the inclusion of a putative missing interaction in a node with four inputs was excessively demanding. To allow the addition of putative missing interactions in nodes with four inputs, we created intermediary nodes that integrate the influence of two regulators over any gene with four regulators (see Supplementary Material).

INTEGRATING AND FORMALIZING EXPERIMENTAL DATA INTO BN MODELS

As mentioned above, experimental data are formalized as BFs in BNs. BFs follow the equation:

$$x_n(t+\tau) = F_n(x_{n_1}(t), x_{n_2}(t), \ldots, x_{n_k}(t))$$

where $x_n(t+\tau)$ represents the state of node n at time $t+\tau$ (τ representing a positive integer), and $(x_{n_1}(t), x_{n_2}(t), ..., x_{n_k}(t))$ represents the state of the regulators of node x_n at time t. BFs can be described either as logical statements or as truth tables. Logical statements use the logical operators AND, OR, and NOT, while the state of node n at time $t+\tau$ is given for all possible combinations of its k regulator states of activation at time t in truth tables. Using the BFs of all nodes, we can follow the dynamics of the GRN until it reaches a stationary network configuration or state (attractor). A network configuration is the vector comprised of a set of values, where each value corresponds to the state of a specific node of the network. Single-state, stationary configurations are known as fixed-point attractors, while a set of network states that orderly repeat among each other cyclically correspond

Table 1 | Main experimental information used in the RSCN GRN.

INTERACTIONS	EXPERIMENTAL EVIDENCE	REFERENCE
SHR → *SCR*	The expression of *SCR* is reduced in *shr* mutants background. ChIP-QRTPCR experiments show that *SHR* interacts *in vivo* with the predicted regulatory sequences of *SCR* and positively regulate it	Helariutta et al. (2000), Levesque et al. (2006), Cui et al. (2007)
SCR → *SCR*	In *scr* mutant background promoter activity of *SCR* is absent in the QC and CEI. A ChIP-PCR assay confirmed that *SCR* binds to its own promoter and promotes its own expression	Sabatini et al. (2003), Cui et al. (2007)
JKD → SCR	The SCR promoter expression in QC and CEI is not detected in JKD mutants from early heart stage onward. JKD was able to activate luciferase gene expression driven by a 1.5 kb SCR promoter region	Welch et al. (2007), Ogasawara et al. (2011)
JKD → JKD	JKD was able to activate luciferase gene expression driven by a 3.5 kb JKD promoter region	Ogasawara et al. (2011)
JKD → MGP	JKD was able to activate luciferase gene expression driven by a 3.5 kb MGP promoter region	Ogasawara et al. (2011)
MGP −| MGP	MGP addition was able to inhibit the SHR, SCR, and JKD induced luciferase gene expression driven by a 3.5 kb MGP promoter region	Ogasawara et al. (2011)
SHR → KD	The post-embryonic expression of JKD is reduced in shr roots. A CHIP-chip analysis detected JKD as a direct target gene of SHR	Welch et al. (2007), Cui et al. (2011)
SCR → JKD	The post-embryionic expression of JKD is reduced in scr roots	Welch et al. (2007)
SCR → *WOX5*	WOX5 expression is reduced in shr mutants	Sarkar et al. (2007)
SHR → *WOX5*	WOX5 expression is undetectable in scr mutants	Sarkar et al. (2007)
Auxin signalin pathway → WOX5	In mp or bdl mutants background WOX5 expression is rarely detected	Sarkar et al. (2007)
Auxin signalin pathway −| *WOX5*	In *iaa17* mutants background *WOX5* expression is decreased	Ding and Friml (2010)
SCR → *miRNA165/6*	In *scr* single mutants, miRNA165/6 expression is greatly reduced. A ChIP-PCR assay confirmed that *SCR* binds to miRNA165/6 promoter	Carlsbecker et al. (2010), Miyashima et al. (2011)
SHR → *miRNA165/6*	In *shr* single mutants, miRNA165/6 expression is greatly reduced. A ChIP-PCR assay confirmed that *SHR* binds to miRNA165/6 promoter	Carlsbecker et al. (2010), Miyashima et al. (2011)
miRNA165/6 −| *PHB*	Over expression of *miRNA165/6* causes a decrease in the transcript levels of *PHB*. The allele *phb-1d* that expresses miRNA165/6-resistant PHB transcripts has ectopic *PHB* transcripts expression	Zhou et al. (2007), Miyashima et al. (2011)
PHB −| WOX5	In se mutants, which fail to repress PHB expression, embryonic WOX5 expression is absent	Grigg et al. (2009)
PHB → JKD	jkd transcripts levels are reduced in the phb-1d miRNA-resistant PHB allele	Miyashima et al. (2011)
CLE40 → *ACR*	CLE40p treatment strongly increased *ACR* expression	Stahl et al. (2009)
CLE40 −| *WOX5*	In *cle40* mutants the WOX5 expression domain is expanded, and CLE40p treatment reduced WOX5 expression in the QC	Stahl et al. (2009)
SHR → MGP	The expression of MGP is severely reduced in the shr background. Experimental data using various approaches have suggested that MGP is a direct target of SHR. This result was later confirmed by ChIP-PCR	Levesque et al. (2006), Cui et al. (2007, 2011), Welch et al. (2007)
SCR → *MGP*	SCR directly binds to the MGP promoter, and MGP expression is reduced in the scr mutant background	Levesque et al. (2006), Welch et al. (2007)

to cyclic attractors. Importantly, fixed-point attractors usually correspond to the arrays of gene activation states that characterize different cell types. Once we recover the set of attractors in the GRN, we can compare the attractors with the expected attractors, which are the experimentally observed stable gene expression configurations. The expected set of attractors are defined from gene expression patterns obtained from the literature that clearly define the spatio-temporal gene configuration of the system. Different data types, such as that obtained from transcriptional and translational reporter assays and microarrays, can be used to define the expected attractors. If the experimental information is correct, but the recovered and the expected attractors are not the same, then the GRN is likely missing information. One possibility is that there are missing interactions within the network.

To add putative missing interactions, two important issues must be considered.

(1) One needs to understand how the experimental data are contained in the BFs. In general, more than one logical statement exists for most BFs. Importantly, such equivalent logical statements can use different logical operators. For example, the logical statement "RGEN1 AND RGEN2" that uses the AND operator is equivalent to the logical statement "NOT (NOT RGEN1 OR NOT RGEN2)" which uses the OR and NOT logical operators. In contrast, a unique truth table represents each BF, indicating that the truth table is not arbitrarily selected. Indeed, each logical statement has an equivalent representation in a truth table, while each truth table can have many equivalent logical statements. Thus, in this paper, we use truth tables to analyze how the experimental information is formalized and contained in the BFs.
(2) One needs to realize that the same BF can formalize regulatory interactions documented with various types of experimental data. For example, we can infer that TGEN is regulated by Regulatory Gene 1 (RGEN1) through a loss-of-function mutant analysis or with a chromatin immunoprecipitation assay. Consequently, we may need to preserve the information gathered from different experiments and then formalize the same BF. Thus, the procedure through which we add putative missing interactions while maintaining congruence with the available experimental data depends on the specific set of experimental data available. In this work, we generated four different procedures by analyzing how the experimental information of the RSCN GRN is contained in the truth tables. The procedures were designed as follows.

Procedure 1

Add a putative missing interaction generated by gain and loss-of-function mutants (**Table 2**). When this procedure is used, each row of the truth table represents an experiment, and we can only state that under certain conditions the TGEN responds differentially to changes in the expression levels of other genes.

Procedure 2

Add a putative missing interaction to a truth table while maintaining the sign of the regulation of previously reported regulators (**Table 2**). Some experimental data clearly determine whether a gene is a positive or a negative regulator. When this case is true, we want to maintain that regulation with the same sign. Using this procedure, when we add a putative missing interaction, we exclusively generate BFs without changing the sign of the regulation of the RGENs that we want to maintain as positive or negative regulators.

Procedure 3

Add a putative missing interaction to a truth table while maintaining documented protein–protein interactions (**Table 2**). The experimental data can indicate that a pair or a group of genes act as complexes. However, this fact does not mean that all the proteins in a complex only function in the context of the complex. The proteins could act as individual units or form complexes with different proteins. This procedure allows putative missing interactions to be added while maintaining the functionality of the documented complexes. However, in the new BFs, the proteins in the complex can have new functionalities by themselves or with the putative missing regulator; the proteins can be substituted in or deleted from the complex under certain conditions; and new regulators can become part of the complex. For example, imagine a complex formed by proteins A and B. Once protein C is added as a putative missing regulator, the original protein A-B complex will continue to be a protein A-B complex, but now proteins A and B could also function in a protein A-C, B-C, or A-B-C complex.

Procedure 4

Add a putative missing interaction to a truth table where one or more of the nodes can act exclusively as part of a protein complex (**Table 2**). Contrary to the last procedure, the experimental data can indicate that a pair or a group of proteins are only functional when they work together. Using this procedure, we can maintain proteins as functional only when they form a complex, once a putative missing interaction is added. Importantly, proteins cannot be substituted or deleted from the complex under any condition. In contrast to procedure 3, the A-B complex cannot become an A-C or B-C complex. However, protein C could be included in the complex and function in an A-B-C complex.

We also designed two procedures that stem from the limits of the Boolean formalism, and we propose these procedures to simplify the interpretation of the predicted missing interactions. These procedures were designed as follows.

Procedure 5

Add a putative missing interaction while avoiding the generation of BFs where one or more nodes do not influence the activity of the target node (Raeymaekers, 2002) (**Table 2**). Notably, certain types of regulatory interactions cannot be expressed with a Boolean formalism (e.g., the modulation of protein activity by another protein). Thus, a TGEN may be regulated by a given RGEN even if this regulation is not explicitly reflected in the BFs. Given this uncertainty, we avoided generating these BFs.

Procedure 6

Add a putative missing interaction while avoiding the generation of BFs where one or more nodes act as positive and negative regulators in the same truth table (Raeymaekers, 2002) (**Table 2**). This

Table 2 | Summary of the procedures proposed to infer putative missing interactions in data-based network models.

Procedure	Application to inferring putative interactions
PROCEDURE 1	
Adding missing links in congruence with available experimental data that can be represented in single rows of truth tables	This is probably the most simple procedure. It allows modifying the network adding missing putative interactions, and at the same time the regulatory effects of the nodes whose role is based on experimental that is represented by single rows of the true tables is preserved. Examples of experiments represented by single rows are loss and gain-of-function mutants
PROCEDURE 2	
Adding missing links while maintaining the sign of the regulation	Prevents changes in the regulatory sign of genes when we introduce putative missing interactions
PROCEDURE 3	
Adding missing links while maintaining documented protein–protein interactions	This procedure guarantee that the joint action of proteins acting as complexes is respected in the new rows that result from the addition of new interactions. However, it allows new complexes to be formed, replacing, deleting or including one or more components in the complex
PROCEDURE 4	
Adding missing links while maintaining necessary protein–protein interactions	Procedure 4 is similar to procedure 3, since it also guarantee the joint action of proteins acting as complexes. However, this procedure do not allows the substitution or deletion of any of the components of the complexes. Importantly, it does allow the incorporation of other components in the complex
PROCEDURE 5	
Adding missing links without independent TGEN activity	Procedure 5 prevents the generation of BFs where one or more regulator has no effect on its target gene
PROCEDURE 6	
Adding missing links without ambiguous regulators	Procedure 6 prevents the emergence of nodes that act as global positive and negative (ambiguous) regulators at the same time

assumption is a simplification because these types of regulatory interactions have been reported experimentally. However, these interactions appear to be infrequent, and exclusion of these interactions allowed us to greatly reduce the number of BFs when we added a putative missing interaction.

A more detailed description of the procedures and their design is available in Section "Appendix 2 in the Appendix."

APPLICATION OF THE PROCEDURES TO POSTULATE A SET OF POSSIBLE NEW BFS GIVEN PUTATIVE MISSING INTERACTIONS IN THE *A. THALIANA* RSCN GRN

To detect and predict missing interactions, we applied an evolutionary algorithm using the following steps.

(1) Generate all putative single missing interactions. The putative missing interactions were those that were not already present in the model and were not contradicted by any available experimental evidence.
(2) Generate all possible BFs of the putative missing interactions maintaining consistency with available biological data using the above procedures.
(3) Test one-by-one all BFs generated and obtain the set of attractors generated with the added interaction.
(4) Select and incorporate into the model the BFs that most improved the model. The criteria to assess if the addition of a regulatory interaction conferred an improvement in the model were, in order of relevance: (a) if the BF increased the number of expected attractors recovered and (b) if the BF reduced the number of non-expected attractors. Here, we defined our expected attractors as the stable gene expression patterns observed experimentally in the RSCN of *A. thaliana* using transcriptional or translational reporter genes. Many genes have oscillatory expression behavior in the root (Moreno-Risueno et al., 2010). However, to our knowledge, none of the genes considered in the updated version of the RSCN GRN have this type of oscillatory expression behavior. Thus, for this particular case, reducing the number of non-expected attractors included eliminating the cyclic attractors.
(5) If more than one BF equally improved the fitness, one BF was randomly selected and added to the model.
(6) After the inclusion of a putative missing interaction, we returned to step 1 unless the model recovered only the expected attractors, or the inclusion of three consecutive BFs did not further improve the model fitness (**Figure 4**). In **Figure 5**, we present a pseudocode of the algorithm.

Using the above procedures, which greatly reduced the number of BFs to test (see below), the generation of all the predictions for each model implied testing approximately 100,000 different networks, which is a highly demanding computational process. Thus, we performed the algorithm 10 times, resulting in 10 different models that predicted different putative interactions. We were able to generate 10 different models because more than one BF equally improved the model each time, allowing us to randomly select different BFs. We applied our procedures using the algorithm to the Boolean GRN of the *A. thaliana* RSCN.

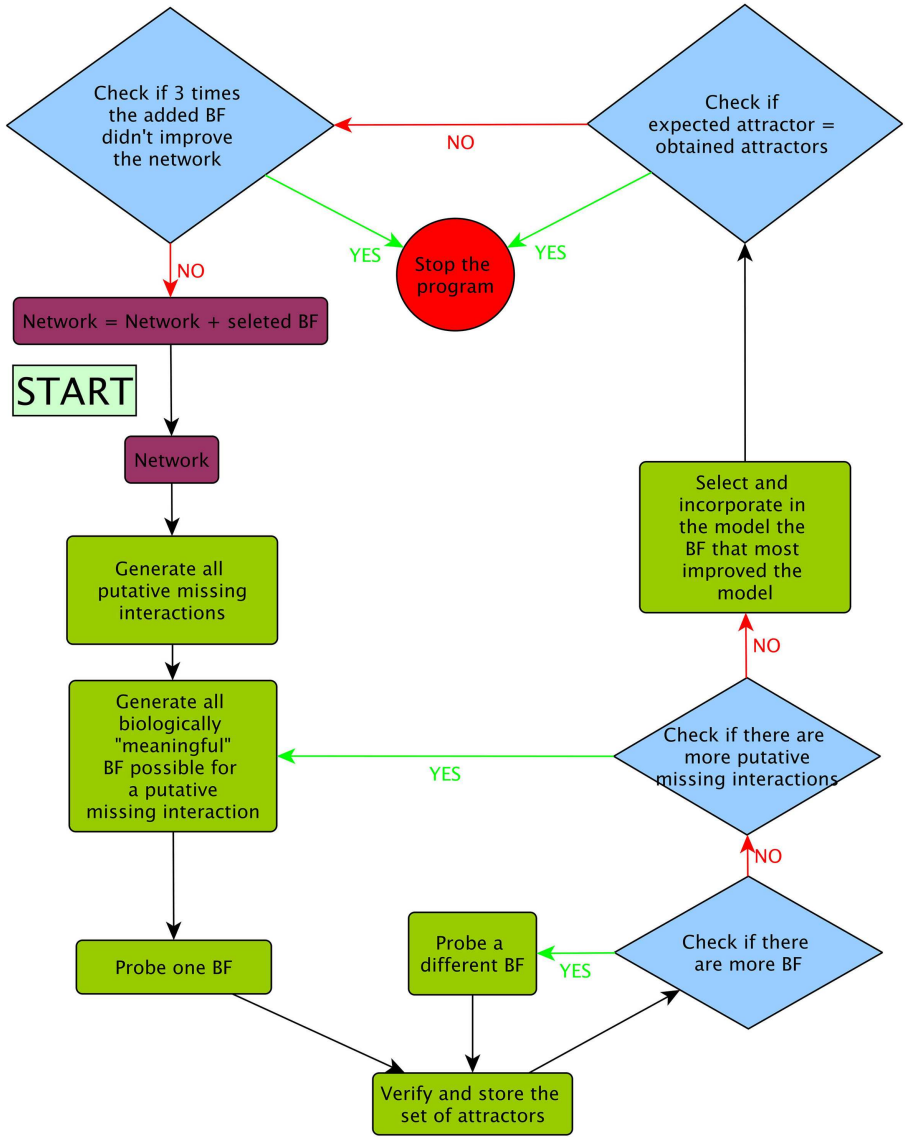

FIGURE 4 | Flux diagram of the evolutionary algorithm followed during the prediction of putative missing interactions using our procedures.

HYPOTHESIS

RSCN GRN updated model behavior

Based on available experimental data, we defined nine expected fixed-point attractors (**Table 3**) for each cell type in the RSCN and some root meristem cell types. Some attractors represented more than one cell type due to lack of experimental data in the model to distinguish among cell types (**Figure 1**). With the updated RSCN GRN model, we obtained 7 of the 9 expected attractors, 21 attractors without biological meaning in the RSCN context, and 4 cyclic attractors. This result suggests that missing data are yet to be incorporated into the RSCN GRN. Hence, we employed our set of procedures as described above to predict possible missing interactions in the network. The procedures used in each node depended on the type of available data for each gene. In **Table 4**, we present the procedures used to propose putative missing interactions for each gene, and the experimental information used in each case is provided in **Table 1**. The self-regulatory loops of nodes with movement must be positive, and hence, we applied procedure 2 in these nodes.

Predicted putative missing interactions in the RSCN GRN

The combined addition of three new regulatory interactions was sufficient to recover the expected attractors in the different cell types in the RSCN (**Figure 3C**). Interestingly, these three interactions were also the first ones to appear. No matter which order we included these three interactions, our methodology never proposed any other putative missing interactions until the three were included in the model. This result suggests that these three interactions are fundamental to recover the observed attractors in the RSCN. However, adding these three interactions was not sufficient

```
def improve_model(network_model, max_tries, expected_atractors):
  fitness = network_model.get_fitness(expected_atractors)
  possible_interactions = []
  new_networks = []
  if max_tries > 0:
    # Make a list of the other possible interactions
    possible_interactions = get_possible_interactions(network_model)
    # Try each additional interaction
    for interaction in possible_interactions:
      # Make a list of the rules for the additional interaction
      possible_rules = get_possible_rules(network_model, interaction)
      # Try each additional rule
      for rule in possible_rules:
        # Make a copy of the model
        new_network_model = NetworkModel(network_model.nodes,
                                         network_model.interactions,
                                         network_model.actualization_rules,
                                         network_model.atractors,
                                         network_model.fitness)
        # Add the new interaction
        new_network_model.add_interaction(interaction)
        # Add the new rule
        new_network_model.change_rule(interaction.target, rule)
        # Calculate the fitness of the new model
        new_fitness = new_network_model.get_fitness(expected_atractors)
        # Store_the_network at the correct place according to its fitness
        add_network_in_place(new_networks, new_network_model)
        if (new_fitness == 1):
          return new_networks
    # Find the fitness of the best new model
    new_fitness = new_networks[len(new_network) - 1].get_fitness(expected_atractors)
    # Find the index of one of the best models
    best_index = find_best(new_networks, expected_atractors)
  if new_fitnes > fitness:
        # If the best new model is better then the original one, continue improving it
    improve_model(new_networks[best_index], 3, expected_atractors)
  else:
        # If the best new model is not better then the original one, try to improve the result again
    improve_model(new_networks[len(new_network) - 1], max_tries - 1, expected_atractors)
```

FIGURE 5 | Pseudocode of the methodology used to incorporate putative missing interactions.

to eliminate cyclic attractors or several biologically meaningless attractors. In fact, the inclusion of these three interactions always increased the number of cyclic or unexpected attractors. We tried to avoid the increase of cyclic attractors by selecting only networks that simultaneously reduced the number of cyclic attractors and recovered biologically significant attractors. However, this procedure was unsuccessful (data not shown).

Interestingly, the three interactions mentioned above were functionally similar in the 10 replicas of the search process (**Figure 3C**). The first interaction is a regulation of PHB that restricts its expression domain to the vascular cells. The regulation of PHB was either positive regulation by those nodes with a similar expression domain (e.g., SHR and Aux/IAA) or negative regulation by those genes with a complementary expression pattern (e.g., CLE and ACR4). We postulate that the likely regulator of PHB is a member of the KANADI (KAN) gene family. *KAN* genes were not included in this GRN model because no connections with any node of the RSCN GRN in the root have been documented yet; however, KAN genes have antagonistic roles with PHB in the shoot and have a complementary expression pattern to *PHB* in the root (**Figure 3C**; Hawker and Bowman, 2004; Izhaki and Bowman, 2007).

The second interaction is a regulation over WOX5. Almost all the networks predicted that this regulation should be a feedback loop. The WOX5 loop could be direct or indirect, as well as positive or negative (**Figure 3C**). Interestingly, some experimental and theoretical evidence supports the existence of such a loop through the auxin signaling pathway (Gonzali et al., 2005; Azpeitia et al., 2010), and our results suggests that this feedback look could exist. However, contradictory experimental evidence has been reported on this issue. Positive regulation of *WOX5* by auxin has been reported (Gonzali et al., 2005), while other data suggest that auxin negatively regulates *WOX5* (Ding and Friml, 2010). Based on the interactome analysis, our model proposes that ARF activators are positive regulators, while ARF inhibitors are negative regulators of WOX5; therefore, this model includes both

Table 3 | Expected attractors.

CT/G	SHR	miR	JKD	MGP	PHB	SCR	IAA	A/I	WOX	CLE	ACR
CVC	1	0	0	0	1	0	0	1	0	0	0
PVC	1	1	0	0	0	0	0	1	0	0	0
End	1	1	1	1	0	1	0	1	0	0	0
Cor	0	1	1	0	0	0	0	1	0	0	0
LCC	0	0	0	0	0	0	1	0	0	1	1
VI	1	1	0	0	0	0	1	0	0	0	0
CEI	1	1	1	1	0	1	1	0	0	0	0
CLEI	0	1	0	0	0	0	1	0	0	1	1
QC	1	1	1	0	0	1	1	0	1	0	0

CT, Cell type; G, Gene; CVC, Central Vascular cells; PVC, Periferal vascular cells; End, Endodermis; Cor, Cortex; LCC, Lateral root-cap and columella cells; VI, Vascular initials; CEI, Cortex-endodermis initials; CLEI, Columella and lateral root-cap-epidermis initials; QC, Quiescent center; miR, miRNA165/6; IAA, Auxin; A/I, Aux/IAA; WOX, WOX5; CLE, CLE40; and ACR, ACR4.

Table 4 | Procedures used when adding putative missing interactions in each node.

	Procedure 1	Procedure 2	Procedure 3	Procedure 4	Procedure 5	Procedure 6
SHR	NO	YES	NO	NO	YES	YES
miR	YES	YES	YES	YES	YES	YES
JKD	YES	YES	YES	YES	YES	YES
MGP	YES	YES	YES	YES	YES	YES
PHB	YES	YES	NO	NO	YES	YES
SCR	YES	YES	YES	YES	YES	YES
Auxin	NO	YES	NO	NO	YES	YES
Aux/IAA	YES	YES	NO	NO	YES	YES
WOX5	YES	YES	YES	NO	YES	YES
CLE40	NO	YES	NO	NO	YES	YES
ACR	YES	YES	NO	NO	YES	YES

possibilities. With this model, we predict that *WOX5* should negatively regulate the auxin signaling pathway. Our model assumed that ARFa was always capable of promoting *WOX5* expression, as proposed by Vernoux et al. (2011). However, if the results that the negative regulation of *WOX5* by the auxin signaling pathway is stronger than the positive regulation, as Ding and Friml (2010) proposed, then the regulation of the auxin signaling pathway by WOX5 should be positive. The third interaction is a positive regulation of *JKD* by MGP (**Figure 3C**). The interplay between JKD, MGP, SCR, and SHR is complex (Welch et al., 2007; Ogasawara et al., 2011), and our simulations suggest that additional possible regulatory mechanisms should be considered, highlighting the ability of our procedures to detect probable missing data.

After the inclusion of 11–15 interactions, the performance of the resulting GRN models no longer improved. After this point, almost all models reduced both the number of cyclic and biologically meaningless attractors to three. Interestingly, some interactions were present in several of the 10 final models. Specifically, the most common interactions were: (1) inhibition of *SHR*, (2) activation of *SHR* by PHB, (3) negative regulation of auxin by PHB, and (4) negative regulation of *CLE40* by Aux/IAA or SHR. The BFs in the original model and the 10 models with putative missing interactions are available in Supplementary Material, and all putative missing interactions predicted by the whole set of simulations are available in Supplementary Material. Importantly, all putative missing interactions that were proposed using our procedures were biological meaningful, did not contradict previous experimental data, and are experimentally testable. Our results indicate key gaps in the data concerning the regulation of nodes in the RSCN GRN. Unraveling how these genes are regulated will be fundamental to our understanding of how the RSCN is maintained. However, our work already suggest possible nodes and missing interactions needed to obtain a sufficient model of RSCN patterning.

Efficiency of the procedures

The reduction of possible BFs obtained with our procedures is astonishing. For example, using procedures 4, 5, and 6 together on all regulatory genes, no matter the number of regulators, always resulted in 4 possible BFs. Using these procedures on all nodes is equivalent to reducing all nodes to 1, which represents a dimer or protein complex. This result was important for the RSCN GRN because SHR and SCR form a dimer that is only functional if both proteins are present (Cui et al., 2007). Thus, the TGENs of the dimer used procedure 4. Using this procedure, we only needed to test tens of BFs from the over four billion possible BFs of JKD

and MGP. Because of this reduction, we only tested ≈3,000 of $\approx 8 \times 10^9$ BFs to generate the first set of possible BFs in the model.

The efficiency of the use of procedures 1, 2, and 3 and combinations of the procedures needs to be formally analyzed in future studies. However, previous work demonstrated that using procedures 5 and 6 reduces the number of BFs from 16 to 8, 256 to 72, and 65,536 to 1882 for a node with 2, 3, and 4 RGENs (Raeymaekers, 2002), respectively. This previous study suggests that using combinations of our procedures should be able to reduce the number of BFs further, making the combinations useful in the prediction of putative missing interactions. The total reduction is completely dependent on the quantity and quality of the available experimental data, which will determine the procedures to use.

Usefulness of the procedures

In addition to the utility of the procedures for predicting putative missing interactions, we detected other important uses of the procedures. The first important use is evident when the experimental data are only sufficient to use procedure 1, or procedure 1 combined with procedures 5 or 6. In this case, positive regulators can be negative regulators, and *vice versa*. Thus, when we apply procedure 1 to predict a putative missing interaction, regulatory genes can change their sign of regulation. This result is important because it demonstrates that some experiments commonly used to infer gene regulatory interactions are not sufficient to assure the sign of regulation (see Appendix 2 in the Appendix). We can use procedure 1 to detect, and later test experimentally, if a positive regulator was identified as a negative regulator, and *vice versa*. We detected a second use when applying any single procedure or combination of procedures, except procedure 4. In this case, single proteins within protein complexes can act as independent units. The proteins are not necessarily required to act as independent units; however, this result helps us detect cases where proteins can, or need to, be substituted in a protein complex or when the proteins can regulate the activity of a TGEN as independent units or as units of different protein complexes. These predictions can be experimentally validated (see Appendix 2 in the Appendix).

DISCUSSION AND CONCLUSION

All, or most, GRN models are incomplete because they likely lack components or interactions due to incomplete experimental data and computational limitations. However, even for small BNs, the detection of such missing data is difficult because the number of possible BFs and topologies describing the interactions rapidly becomes overwhelming as the number of nodes and interactions being considered increases. We have proposed here a set of procedures that greatly reduce the number of possible interactions and enable the detection and prediction of biologically meaningful, putative missing interactions, while maintaining congruence with available and already incorporated experimental data. Our procedures were designed to maintain congruence with different types of experimental data and greatly reduce the number of possible BFs to be tested (≈3,000 out of over $\approx 8 \times 10^9$ in the example of the RSCN GRN). Importantly, we tested our procedures with smaller network motifs to assure that our procedures worked as expected before testing the procedures on the RSCN GRN.

The magnitude of the reduction in the putative BFs greatly depends on the quality of the available data and the nature of the interactions. Depending on the quality of the data, different BFs are generated. Importantly, our procedures demonstrate that some experiments that are usually used to determine the sign of a regulatory interaction are not reliable or are not adequate to uncover the actual interaction in diverse contexts (Lewontin, 2000). Similarly, some experiments that indicate the necessity of a protein complex for the expression of a TGEN are also not reliable. Furthermore, these situations are frequently not intuitive, and the procedures put forward here enable the detection of the circumstances under which such mistaken inferences can occur. Once the circumstance involved is known, we can easily design experiments to dismiss such situations. However, if we have enough experimental data to confirm the sign of the regulation or the presence of a complex, then we can use the proposed procedures to maintain these experimental data contained in the BF without change.

Using these procedures, we have designed an evolutionary algorithm to systematically predict possible missing interactions, and we have applied this approach to the *A. thaliana* RSCN GRN. Our work provides concise predictions concerning additional interactions and a novel RSCN GRN architecture that could be tested experimentally. Importantly, our work has identified three additional key interactions that could be studied: (i) regulation of *PHB* to maintain its expression pattern in the vascular cylinder, (ii) a feedback loop regulating *WOX5*, and (iii) positive regulation of *JKD* by MGP. However, we were not able to recover a network that attained only the experimentally observed gene configurations without the presence of unobserved attractors. Additional missing nodes, such as SCZ (ten Hove et al., 2010) or *root growth factors* (Matsuzaki et al., 2010), may be required to recover only the observed set of configurations. Because we were interested in finding missing interactions within already connected RSCN genes, we decided to dismiss genes that were unconnected from those included in this work, such as SCZ. Another possible explanation for why we never obtained only the expected attractors is that we only included putative missing interactions one-by-one. Including two or more putative missing interactions each time could change the results due to combinatorial effects. As explained previously, the computational demand for including one interaction can be very large. Hence, the computational demand of adding interactions simultaneously rapidly explodes. However, we believe that our approach provides a formal, systematic framework to postulate novel hypotheses concerning the way genes interact. For small networks, testing the effect of adding multiple interactions is possible.

There still are several improvements that could be done to the procedures. The inclusion of a genetic algorithm would allow a search for missing interactions not only one-by-one but also by sets of putative missing interactions at one time. Optimizing with Binary Decision Diagrams (BDDs) or more efficient algorithms could also allow for testing of more than one interaction. A way to simplify the use of our procedures is to incorporate them into an existing dynamic network analyzer (e.g., Arellano et al., 2011). Procedures that use information of the GRN topology or about the effect of how genes in the networks indirectly affect other genes should further reduce the number of BFs generated when we add

putative missing interactions. For example, we could already know that in the RGEN1 loss-of-function mutant, TGEN = 0, while RGEN3 = 1, but that RGEN3 is not a TGEN of RGEN1. In this case, if we add RGEN3 as a putative missing regulator of TGEN, we will know that in the new rows of the TGEN's truth table where RGEN1 = 0, TGEN expression value will be 0 when RGEN3 = 1 and TGEN's expression value will be unknown when RGEN3 = 0. The use of this type of data for the generation of more procedures was not explored in this work, but should be addressed in future research.

The fact that we used BNs in this work implies both strength and weakness. BNs allowed us to exhaustively test all the possible GRNs generated by adding putative missing interactions; however, BFs are unable to represent certain types of regulatory interactions, such as those implying fine-tuning modulations of regulatory activity. An improvement to our procedure would involve extending the procedures to consider multivalued discrete networks that can better evaluate more circumstances, although this method would also increase the computational demand.

Finally, given that the methodology used in this work can be applied to any BN, we believe that this type of exploration could help guide experimental research not only of biomolecular GRNs but also of any biological, physical, or theoretical system that can be formalized as a Boolean interaction network. For example, this methodology can be used to study the constraints that a given network topology imposes on attractor evolvability. However, formal mathematical demonstrations should be performed first.

ACKNOWLEDGMENTS

This paper constitutes a partial fulfillment of the Doctorado en Ciencias Biomédicas of the Universidad Nacional Autónoma de México (UNAM). Eugenio Azpeitia and Nathan Weinstein acknowledges the PhD scholarship and financial support provided by the Consejo Nacional de Ciencia y Teconología (CONACyT), and UNAM. This work is supported by CONACyT (180098; 180380; 167705; 152649; 105678) and DGAPA, UNAM (IN204011-3; IN203113-3; IN226510-3; IB201212-2) grants. Elena R. Alvarez-Buylla is currently sponsored by the Miller Institute for Basic Research in Science, University of California, Berkeley, USA. We thank Rigoberto V. Perez-Ruiz and Diana Romo for technical and logistical assistance. We thank M. S. Ursula Abad, Lynna Kiere, and Emilio Mora for their detailed revision of the manuscript as well as all of their comments. We also thank Dr. David Rosenblueth and Pedro Góngora for all the clarifying discussions about the project.

SUPPLEMENTARY MATERIAL

The Supplementary Material for this article can be found online at http://www.frontiersin.org/Plant_Systems_Biology/10.3389/fpls.2013.00110/abstract

REFERENCES

Albert, R., and Othmer, H. G. (2003). The topology of the regulatory interactions predicts the expression pattern of the segment polarity genes in *Drosophila melanogaster*. *J. Theor. Biol.* 223, 1–18.

Alvarez-Buylla, E. R., Benítez, M., Dávila, E. B., Chaos, A., Espinosa-Soto, C., and Padilla-Longoria, P. (2007). Gene regulatory network models for plant development. *Curr. Opin. Plant Biol.* 10, 83–91.

Arellano, G., Argil, J., Azpeitia, E., Benítez, M., Carrillo, M., Góngora, P., et al. (2011). "Antelope": a hybrid-logic model checker for branching-time Boolean GRN analysis. *BMC Bioinformatics* 12:490. doi:10.1186/1471-2105-12-490

Azpeitia, E., and Alvarez-Buylla, E. R. (2012). A complex systems approach to Arabidopsis root stem-cell niche developmental mechanisms: from molecules, to networks, to morphogenesis. *Plant Mol. Biol.* 80, 351–363.

Azpeitia, E., Benítez, M., Vega, I., Villarreal, C., and Alvarez-Buylla, E. R. (2010). Single-cell and coupled GRN models of cell patterning in the *Arabidopsis thaliana* root stem cell niche. *BMC Syst. Biol.* 4:134. doi:10.1186/1752-0509-4-134

Brady, S. M., Orlando, D. A., Lee, J. Y., Wang, J. Y., Koch, J., Dinneny, J. R., et al. (2007). A high-resolution root spatiotemporal map reveals dominant expression patterns. *Science* 318, 801–806.

Calderón Villalobos, L. I., Lee, S., De Oliveira, C., Ivetac, A., Brandt, W., Armitage, L., et al. (2012). A combinatorial TIR1/AFB-Aux/IAA co-receptor system for differential sensing of auxin. *Nat. Chem. Biol.* 8, 477–485.

Carlsbecker, A., Lee, J. Y., Roberts, C. J., Dettmer, J., Lehesranta, S., Zhou, J., et al. (2010). Cell signalling by microRNA165/6 directs gene dose-dependent root cell fate. *Nature* 465, 316–321.

Cui, H., Hao, Y., Kovtun, M., Stolc, V., Deng, X. W., Sakakibara, H., et al. (2011). Genome-wide direct target analysis reveals a role for SHORT-ROOT in root vascular patterning through cytokinin homeostasis. *Plant Physiol.* 157, 1221–1231.

Cui, H., Levesque, M. P., Vernoux, T., Jung, J. W., Paquette, A. J., Gallagher, K. L., et al. (2007). An evolutionarily conserved mechanism delimiting SHR movement defines a single layer of endodermis in plants. *Science* 316, 421–425.

Davidson, E. (2001). *Genomic Regulatory Systems. Development and Evolution.* New York: Academic Press.

de Jong, H. (2002). Modeling and simulation of genetic regulatory systems: a literature review. *J. Comput. Biol.* 9, 67–103.

Ding, Z., and Friml, J. (2010). Auxin regulates distal stem cell differentiation in Arabidopsis roots. *Proc. Natl. Acad. Sci. U.S.A.* 107, 12046–12051.

Dolan, L., Janmaat, K., Willemsen, V., Linstead, P., Poethig, S., Roberts, K., et al. (1993). Cellular organisation of the Arabidopsis thaliana root. *Development* 119, 71–84.

Espinosa-Soto, C., Padilla-Longoria, P., and Alvarez-Buylla, E. R. (2004). A gene regulatory network model for cell-fate determination during *Arabidopsis thaliana* flower development that is robust and recovers experimental gene expression profiles. *Plant Cell* 16, 2923–2939.

Galinha, C., Hofhuis, H., Luijten, M., Willemsen, V., Blilou, I., Heidstra, R., et al. (2007). PLETHORA proteins as dose-dependent master regulators of *Arabidopsis* root development. *Nature* 449, 1053–1057.

Gonzali, S., Novi, G., Loreti, E., Paolicchi, F., Poggi, A., Alpi, A., et al. (2005). A turanose-insensitive mutant suggests a role for WOX5 in auxin homeostasis in *Arabidopsis thaliana*. *Plant J.* 44, 633–645.

Grigg, S. P., Galinha, C., Kornet, N., Canales, C., Scheres, B., and Tsiantis, M. (2009). Repression of apical homeobox genes is required for embryonic root development in *Arabidopsis*. *Curr. Biol.* 19, 1485–1490.

Guilfoyle, T. J., and Hagen, G. (2007). Auxin response factors. *Curr. Opin. Plant Biol.* 10, 453–460.

Hawker, N. P., and Bowman, J. L. (2004). Roles for Class III HD-Zip and KANADI genes in *Arabidopsis* root development. *Plant Physiol.* 135, 2261–2270.

Helariutta, Y., Fukaki, H., Wysocka-Diller, J., Nakajima, K., Jung, J., Sena, G., et al. (2000). The SHORT-ROOT gene controls radial patterning of the *Arabidopsis* root through radial signaling. *Cell* 101, 555–567.

Izhaki, A., and Bowman, J. L. (2007). KANADI and class III HD-Zip gene families regulate embryo patterning and modulate auxin flow during embryogenesis in *Arabidopsis*. *Plant Cell* 19, 495–508.

Jarrah, A., Laubenbacher, R., Stigler, B., and Stillman, M. (2007). Reverse-engineering of polynomial dynamical systems. *Adv. Appl. Math.* 39, 477–489.

Kauffman, S., Peterson, C., Samuelsson, B., and Troein, C. (2004). Genetic networks with canalyzing Boolean rules are always stable. *Proc. Natl. Acad. Sci. U.S.A.* 101, 17102–17107.

Kauffman, S. A. (1969). Metabolic stability and epigenesis in randomly constructed genetic nets. *J. Theor. Biol.* 22, 437–467.

La Rota, C., Chopard, J., Das, P., Paindavoine, S., Rozier, F., Farcot, E., et al. (2011). A data-driven integrative model of sepal primordium polarity in *Arabidopsis*. *Plant Cell* 23, 4318–4333.

Levesque, M. P., Vernoux, T., Busch, W., Cui, H., Wang, Y., Blilou, I., et al. (2006). Whole-genome analysis of the SHORT-ROOT developmental pathway in *Arabidopsis*. *PLoS Biol.* 4:e143. doi:10.1371/journal.pbio.0040143

Lewontin, R. (2000). "*Prologue*" *in The ontogeny of Information: Developmental Systems and Evolution.* Cambridge: Cambridge University Press.

Matsuzaki, Y., Ogawa-Ohnishi, M., Mori, A., and Matsubayashi, Y. (2010). Secreted peptide signals required for maintenance of root stem cell niche in *Arabidopsis*. *Science* 329, 1065–1067.

Mendoza, L., and Alvarez-Buylla, E. R. (1998). Dynamics of the genetic regulatory network for *Arabidopsis thaliana* flower morphogenesis. *J. Theor. Biol.* 193, 307–319.

Miyashima, S., Koi, S., Hashimoto, T., and Nakajima, K. (2011). Non-cell-autonomous microRNA165 acts in a dose-dependent manner to regulate multiple differentiation status in the Arabidopsis root. *Development* 138, 2303–2313.

Moreno-Risueno, M. A., Van Norman, J. M., Moreno, A., Zhang, J., Ahnert, S. E., and Benfey, P. N. (2010). Oscillating gene expression determines competence for periodic *Arabidopsis* root branching. *Science* 329, 1306–1311.

Nakajima, K., Sena, G., Nawy, T., and Benfey, P. N. (2001). Intercellular movement of the putative transcription factor SHR in root patterning. *Nature* 413, 307–311.

Ogasawara, H., Kaimi, R., Colasanti, J., and Kozaki, A. (2011). Activity of transcription factor JACKDAW is essential for SHR/SCR-dependent activation of SCARECROW and MAGPIE and is modulated by reciprocal interactions with MAGPIE, SCARECROW and SHORT ROOT. *Plant Mol. Biol.* 77, 489–499.

Pal, R., Ivanov, I., Datta, A., Bittner, M. L., and Dougherty, E. R. (2005). Generating Boolean networks with a prescribed attractor structure. *Bioinformatics* 21, 4021–4025.

Picard, F., Miele, V., Daudin, J. J., Cottret, L., and Robin, S. (2009). Deciphering the connectivity structure of biological networks using MixNet. *BMC Bioinformatics* 10(Suppl. 6):S17. doi:10.1186/1471-2105-10-S6-S17

Rademacher, E. H., Möller, B., Lokerse, A. S., Llavata-Peris, C. I., van den Berg, W., and Weijers, D. (2011). A cellular expression map of the *Arabidopsis* AUXIN RESPONSE FACTOR gene family. *Plant J.* 68, 597–606.

Raeymaekers, L. (2002). Dynamics of Boolean networks controlled by biologically meaningful functions. *J. Theor. Biol.* 218, 331–341.

Sabatini, S., Heidstra, R., Wildwater, M., and Scheres, B. (2003). SCARECROW is involved in positioning the stem cell niche in the *Arabidopsis* root meristem. *Genes Dev.* 17, 354–358.

Sablowski, R. (2011). Plant stem cell niches: from signalling to execution. *Curr. Opin. Plant. Biol.* 14, 4–9.

Sarkar, A. K., Luijten, M., Miyashima, S., Lenhard, M., Hashimoto, T., Nakajima, K., et al. (2007). Conserved factors regulate signalling in *Arabidopsis thaliana* shoot and root stem cell organizers. *Nature* 446, 811–814.

Sena, G., Jung, J. W., and Benfey, P. N. (2004). A broad competence to respond to SHORT ROOT revealed by tissue-specific ectopic expression. *Development* 131, 2817–2826.

Sozzani, R., Cui, H., Moreno-Risueno, M. A., Busch, W., Van Norman, J. M., Vernoux, T., et al. (2010). Spatiotemporal regulation of cell-cycle genes by SHORTROOT links patterning and growth. *Nature* 466, 128–132.

Stahl, Y., Grabowski, S., Bleckmann, A., Kühnemuth, R., Weidtkamp-Peters, S., Pinto, K. G., et al. (2013). Moderation of *Arabidopsis* root stemness by CLAVATA1 and ARABIDOPSIS CRINKLY4 receptor kinase complexes. *Curr. Biol.* 23, 362–371.

Stahl, Y., Wink, R. H., Ingram, G. C., and Simon, R. (2009). A signaling module controlling the stem cell niche in *Arabidopsis* root meristems. *Curr. Biol.* 19, 909–914.

ten Hove, C. A., Willemsen, V., de Vries, W. J., van Dijken, A., Scheres, B., and Heidstra, R. (2010). SCHIZORIZA encodes a nuclear factor regulating asymmetry of stem cell divisions in the *Arabidopsis* root. *Curr. Biol.* 20, 452–457.

Ulmasov, T., Hagen, G., and Guilfoyle, T. J. (1999). Dimerization and DNA binding of auxin response factors. *Plant J.* 19, 309–319.

Vernoux, T., Brunoud, G., Farcot, E., Morin, V., Van den Daele, H., Legrand, J., et al. (2011). The auxin signalling network translates dynamic input into robust patterning at the shoot apex. *Mol. Syst. Biol.* 7, 508.

Welch, D., Hassan, H., Blilou, I., Immink, R., Heidstra, R., and Scheres, B. (2007). Arabidopsis JACKDAW and MAGPIE zinc finger proteins delimit asymmetric cell division and stabilize tissue boundaries by restricting SHORT-ROOT action. *Genes Dev.* 21, 2196–2204.

Zhou, G. K., Kubo, M., Zhong, R., Demura, T., and Ye, Z. H. (2007). Overexpression of miR165 affects apical meristem formation, organ polarity establishment and vascular development in *Arabidopsis*. *Plant Cell Physiol.* 48, 391–404.

Zou, Y. M. (2010). Modeling and analyzing complex biological networks incooperating experimental information on both network topology and stable states. *Bioinformatics* 26, 2037–2041.

Conflict of Interest Statement: The authors declare that the research was conducted in the absence of any commercial or financial relationships that could be construed as a potential conflict of interest.

Received: 23 February 2013; paper pending published: 12 March 2013; accepted: 10 April 2013; published online: 30 April 2013.

Citation: Azpeitia E, Weinstein N, Benítez M, Mendoza L and Alvarez-Buylla ER (2013) Finding missing interactions of the Arabidopsis thaliana root stem cell niche gene regulatory network. Front. Plant Sci. ***4****:110. doi: 10.3389/fpls.2013.00110*

This article was submitted to Frontiers in Plant Systems Biology, a specialty of Frontiers in Plant Science.

APPENDIX 1

AUXIN SIGNALING PATHWAY REDUCTION

In this section, we first briefly describe the auxin signaling pathway and then explain the analysis of the ARF-Aux/IAA interactome using MixNet, a publicly available software program designed for structural network analysis. For the interested reader a more detailed explanation of MixNet can be found in this reference (Picard et al., 2009).

In the auxin signaling pathway, the Aux/IAA genes repress the transcriptional activity of the ARFs by forming heterodimers. ARFs can be classified based on their transcriptional activity; ARFs 5, 6, 7, 8, and 19 are transcriptional activators (ARFa), while all other ARFs are putative transcriptional inhibitors (ARFi; Guilfoyle and Hagen, 2007). ARFa and ARFi compete for the same TGENs (Ulmasov et al., 1999). The SCF^{TIR1} ubiquitin ligase complex promotes Aux/IAA degradation in the presence of auxin, releasing ARFs from Aux/IAA inhibition. Once ARFs are released from Aux/IAA inhibition, ARFs are able to perform their transcriptional activity.

Recently, Vernoux et al. (2011) published an ARF and Aux/IAA interactome and analyzed how these proteins interact in the shoot and whole seedling using MixNet (Picard et al., 2009). MixNet uses a probabilistic clustering method that allows for the identification of structural connectivity patterns. Because MixNet relies on an algorithm that does not make any *a priori* assumptions about network structural properties, MixNet allows a blind search of highly or poorly interconnected groups of nodes. MixNet considers that nodes can be divided into Q connectivity classes, with Q being unknown. As a result, MixNet returns to the user a value α, which is the proportion of each group, and π, the connectivity of the groups. Finally, if $Z_{iq} = 1$, then node i belongs to class q. Hence, MixNet describes the network topology using connectivity probabilities among nodes, such that $\pi_q p$ represents the probability for a node from group q to be connected to a node from group p (Picard et al., 2009). Model selection in MixNet can be performed based on the ICL and incomplete data likelihood criteria.

Rademacher et al. (2011) reported the expression patterns of ARFs in the root, while Brady et al. (2007) created a high-resolution expression map of the root that included the Aux/IAA gene family. We defined the Aux/IAA and ARF genes that are expressed in the root based on these previous studies and analyzed their interactome reported previously (Vernoux et al., 2011). Based on these considerations, we considered the following ARF and Aux/IAA genes:

ARFs:
ARF1, ARF2, ARF5, ARF6, ARF7, ARF8, ARF9, ARF10, ARF16, and ARF19.

Aux/IAAs:
IAA1, IAA2, IAA3, IAA5, IAA6, IAA7, IAA8, IAA9, IAA10, IAA11, IAA12, IAA13, IAA14, IAA16, IAA17, IAA19, IAA20, IAA27, IAA28, IAA29, IAA30, IAA32, IAA21, and IAA33.

We applied the MixNet algorithm for $Q = 1$–15 clusters and used the ICL criterion for model selection. As Vernoux et al. (2011), reported, based on the ICL criterion, the MixNet analysis favors four clusters. However, this solution is only valid for a large N; therefore, we used the three cluster ($Q = 3$) solution as reported in Vernoux et al., 2011. This solution implies that the Aux/IAA and ARF proteins are divided into three different groups. The first group was comprised mostly of Aux/IAA proteins, which interact among themselves, and ARFa. The second group was mostly comprised of ARFa, which interacts only with Aux/IAA. The third group was mostly comprised of ARFi, which does not interact with any other group. This model of the auxin signaling pathway is very general; however, as more information becomes available, a more detailed auxin signaling pathway will be possible.

The probability matrix π, the nodes comprising each cluster and the interactions among the Aux/IAA and ARF proteins extracted from the work of Vernoux et al. (2011) are given below.

π Matrix:
0.110916, 0.0848193, 0.275044.
0.0848193, 0.745456, 0.856257.
0.275044, 0.856257, 0.240615.

Cluster 1:
ARF1, ARF2, ARF10, ARF16, ARF18, IAA6, IAA11, IAA29, IAA31, IAA32.

Cluster 2:
IAA1, IAA2, IAA3, IAA7, IAA8, IAA10, IAA12, IAA13, IAA14, IAA16, IAA17, IAA19, IAA20, IAA27, IAA28, IAA30, IAA33.

Cluster 3:
ARF5, ARF6, ARF7, ARF8, ARF9, ARF19, IAA5, IAA9.

The only nodes that do not behave as expected were IAA5, IAA11, IAA29, IAA31, and IAA32, which belong to cluster 1, and IAA5 and IAA9, which belong to cluster 3. We expected these nodes belonged to cluster 2.

The topology of the auxin signaling pathway according to this result eliminated the Aux/IAA-ARFi interaction. In this model, ARFi modulates the ARFa response once ARFa proteins are released from Aux/IAA inhibition. However, in the presence of high auxin concentration, ARFa always activates its TGENs (Vernoux et al., 2011). Boolean models cannot represent the degree of the response due to the ARFa/ARFi ratio. Consequently, we eliminated ARFi from the GRN, resulting in a linear pathway where ARFa activity is only regulated by Aux/IAA in the GRN. Moreover, ARFa proteins are constitutively expressed in all cells of the root meristem, including the RSCN. Hence, ARFa does not need to be included in the GRN because its activity is equally represented by the auxin response that is triggered when the auxin concentration promotes Aux/IAA degradation. Consequently, we reduced the auxin signaling pathway to the auxin and Aux/IAA nodes.

APPENDIX 2

DETAILED DESCRIPTION OF THE PROCEDURES

In this section, we describe how we designed the 6 procedures used to infer putative missing interactions in the RSCN GRN. As

explained in the main text, we used truth tables to analyze how the experimental data are contained in the BFs. However, we should be able to write a negative regulator with a NOT operator and a protein–protein interaction with an AND operator. For this reason, we will continue to use logical statements whenever useful in this section.

Procedure 1: adding missing links while maintaining congruence with available experimental data that can be represented by a single row in the truth table

Let us assume a TGEN is expressed when RGEN1 and RGEN2 are both expressed, which is represented by the last row of the truth table in **Figure A1A**. In addition, we will assume that TGEN is not expressed in the single loss-of-function RGEN1 and RGEN2 mutants, represented by the second and third rows of the truth table, respectively. Finally, we will suppose that TGEN is not expressed when both RGEN1 and RGEN2 are not present, and this scenario is represented in the first row of the truth table. In this example, each experiment is formalized as a single row of the truth table. Now, how can a third RGEN3 be added to the TGEN's BF without contradicting the previously incorporated experimental data? Knowing that each row of the truth table represents one experimental result can help us. As observed, in the first row of the truth table without the addition of RGEN3, the TGEN expression state is *0*. To maintain consistency with these data in the truth table once RGEN3 is added, the TGEN expression state must remain at *0* in at least one of the truth table's rows where RGEN1 and RGEN2 are not expressed. The possible rows that fit these criteria are shown in **Figure A1B**. To maintain consistency with the experimental data contained in the other rows, we perform the same analysis of all other rows in the truth table. Thus, in this example, we must maintain at least one *0* for the expression value of TGEN

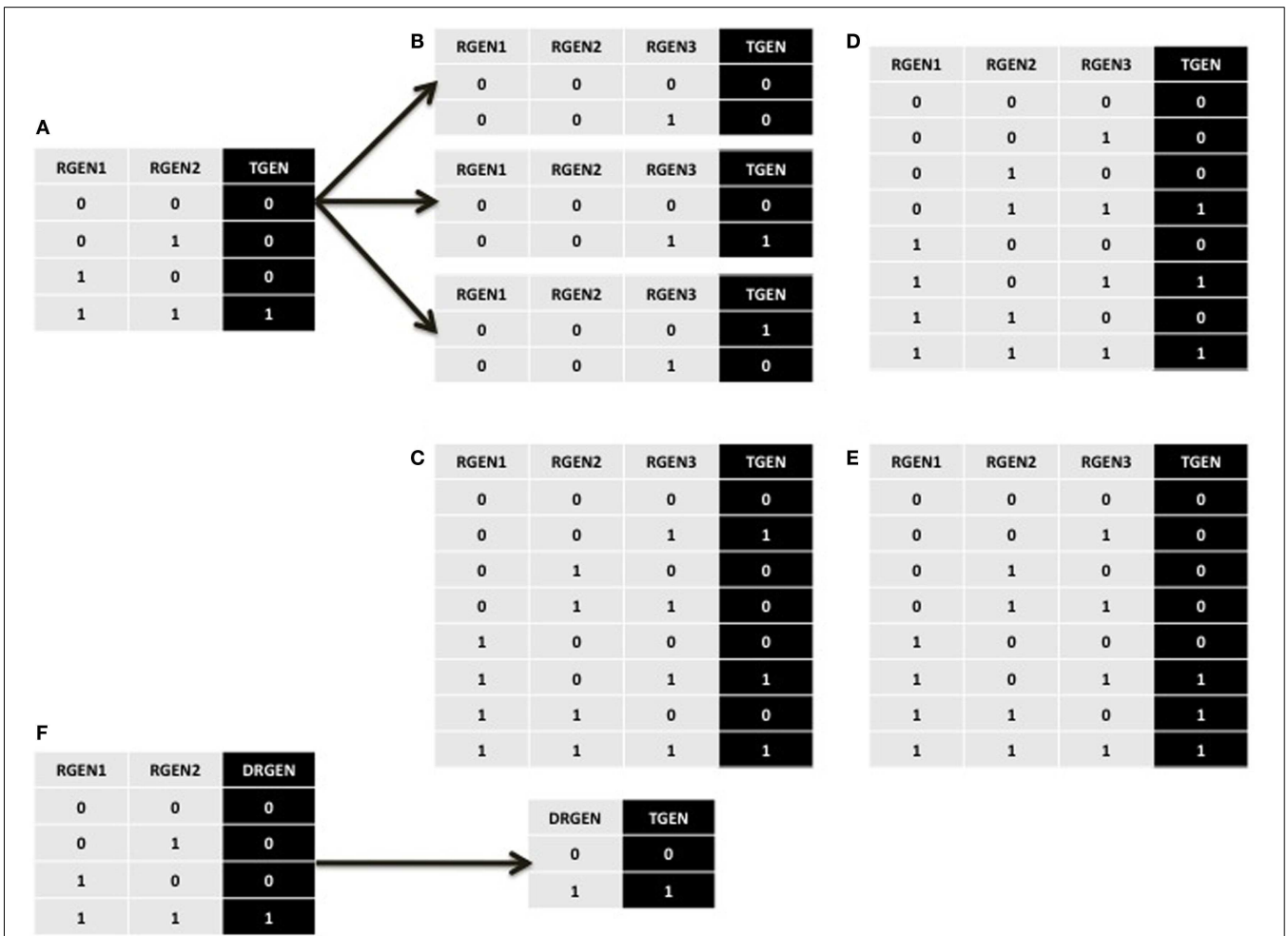

FIGURE A1 | Partial and complete truth tables describing the procedures explained in the main text. **(A)** Equivalent truth table for the logical statement "TGEN, RGEN1, AND RGEN2." **(B)** The three possibilities for the first line of the truth table if a putative missing interaction is added. Each line describes one experiment. **(C)** A truth table where the original positive regulation of TGEN by RGEN2 observed in **(A)** changes to a negative regulation. **(D)** A truth table where the original AND operator between RGEN1 and RGEN2 observed in **(A)** changes to an OR operator indicating that they do not need to form a dimmer. **(E)** A truth table where RGEN2 can be substituted by RGEN3 from the RGEN1-RGEN2 dimer. **(F)** When two RGENs can only act as a dimer, and none of them can be substituted in the dimer, we can create a node that represents the dimer. The truth table observed in **(A)** where RGEN1 and RGEN2 regulate TGEN activity is substituted by a new truth table where the activity of the RGEN1-RGEN2 dimer is incorporated into a single node.

whenever RGEN1 or RGEN2 are not expressed and a value of *1* whenever RGEN1 and RGEN2 are both expressed when RGEN3 is added. Hence, when each experiment is represented by a single row in a truth table, we need to maintain at least one *0* as the TGEN expression value under the conditions where no expression of TGEN was experimentally observed, and at least one *1* under the conditions where TGEN expression was experimentally observed; this process maintains consistency with the previously incorporated experimental data when putative missing interactions are added to the truth table. This procedure generates many possible BFs once we add a putative missing interaction. Nevertheless, the procedures is useful when an experiment is contained in a single row of a truth table. A common use of this procedure occurs when the only available experimental data are single and multiple gain- and loss-of-function mutants.

Procedure 2: adding missing links while maintaining the sign of the regulation

In **Figure A1C**, we present a truth table that we can be generated using procedure 1. One logical statement that can represent this function is "TGEN = RGEN3 AND (RGEN1 OR NOT RGEN2)." In this logical statement, RGEN2 changed from being a positive to a negative regulator of TGEN. However, we need to define positive and negative regulation in the BF context to assure that this change occurred.

If a RGEN positively regulates the TGEN, then we should observe in the truth table that when RGEN is ON, TGEN should also be ON, at least under one condition. Here, we defined a *condition* as the set of states where all RGENs of a TGEN have a fixed expression value, except the RGEN for which we are analyzing the sign of its regulation. Hence, we defined RGEN as a *local positive regulator* of TGEN, when TGEN and RGEN expression states are the same under identical conditions (**Figure A2A**). Conversely, we defined RGEN as a *local negative regulator* when TGEN and RGEN expression values are different under the same conditions (**Figure A2B**). Finally, we defined RGEN as a *local neutral regulator* of TGEN if the latter does not change its expression value irrespective of its regulator state (**Figure A2C**).

An absolute positive regulator of a TGEN should never be able to act as a local negative regulator of the target. However, this rule does not mean that a positive RGEN must activates the TGEN under all conditions. Thus, we defined a global positive regulator as a RGEN that acts as a local positive regulator or as a local positive and local neutral regulator. A global negative regulator acts as a local negative regulator or as a local negative and local neutral regulator. However, a global neutral regulator only acts as a local neutral regulator. Finally, we defined ambiguous global regulators as those RGENs that act as local positive and local negative regulators or as local positive, local negative, and local neutral regulators (**Figure A2D**).

A node labeled as a negative regulator according to our global regulator definitions can always be expressed with a NOT logical operator in the logical statement; however a negative regulator cannot be represented as a neutral regulator and may not be represented as a positive or ambiguous regulator as observed in **Figure A3A**. The same definitions apply to positive nodes. An ambiguous node according to our global regulator definitions can always be expressed as an ambiguous regulator, but not as

A

RGEN1	RGEN2	TGEN
0	0	0
0	1	1

C

RGEN1	RGEN2	TGEN
0	0	0
0	1	0

B

RGEN1	RGEN2	TGEN
0	0	1
0	1	0

RGEN1	RGEN2	TGEN
0	0	1
0	1	1

D

Type of global regulator	Positive local regulation	Negative local regulation	Neutral local regulation
Positive	Necessary	Forbidden	Allowed
Negative	Forbidden	Necessary	Allowed
Neutral	Forbidden	Forbidden	Necessary
Ambiguous	Necessary	Necessary	Allowed

FIGURE A2 | Partial truth tables representing local regulations and definitions of global regulators. A portion of the truth tables where RGEN2 acts as a local positive **(A)**, negative **(B)**, and neutral regulator **(C)**. **(D)** The definitions of global regulators based on local regulator definitions. The table shows which types of local regulations are necessary, allowed, or forbidden for each type of global regulation.

a positive, negative, or neutral regulator (**Figure A3B**). Finally, a truth table with a neutral global regulator can always be written as a logical statement without the inclusion of the regulator, even when the regulator can be included in another equivalent logical statement (**Figure A3C**). Thus, our global regulator definition assures that a regulator labeled as negative, positive, neutral, or ambiguous can be expressed in a logical statement with the correct logical operator.

Consequently, to verify the sign of the regulation, we use our global regulator definitions. Applying the global definitions, we can analyze the truth table in **Figure A1C** and observe that RGEN2 is a local negative and local neutral regulator of TGEN. Therefore, RGEN2 is a global negative regulator. In contrast, in the original truth table without RGEN3 added (**Figure A1A**), RGEN2 acted only as a local positive regulator; hence, RGEN2 was a global positive regulator. Thus, when we use procedure 1 to generate BFs, RGENs can change their sign of regulation. This result indicates that some experiments, such as the ones used in our example and which are commonly used to infer gene regulatory interactions, are not sufficient to assure that a RGEN is a positive or negative regulator. Importantly, the use of procedure 1 can identify the circumstances under which a positive regulator can be falsely identified as a negative regulator, and *vice versa*.

In some occasions, a RGEN is known to be either a positive or a negative regulator of its TGEN. For example, high quality experimental data, such as chromatin immunoprecipitation, might indicate that RGEN1 and RGEN2 are direct positive regulators of TGEN. These data will not change the truth table in **Figure A1A**. We can use our definitions to include putative missing interactions without changing the experimentally observed sign of the regulatory interaction. If RGEN is a known negative regulator, we use procedure 2 to exclusively generate all the BFs where RGEN acts as a negative local regulator or as a negative and neutral local regulator.

Using our global regulator definitions in procedure 2, the RGEN regulation sign can be expressed in the desired manner in a logical statement (e.g., with a NOT if we want a negative regulator). Thus, using our procedure, the RGEN regulatory sign can be expressed in a way that maintains consistency with the sign of regulation reported experimentally.

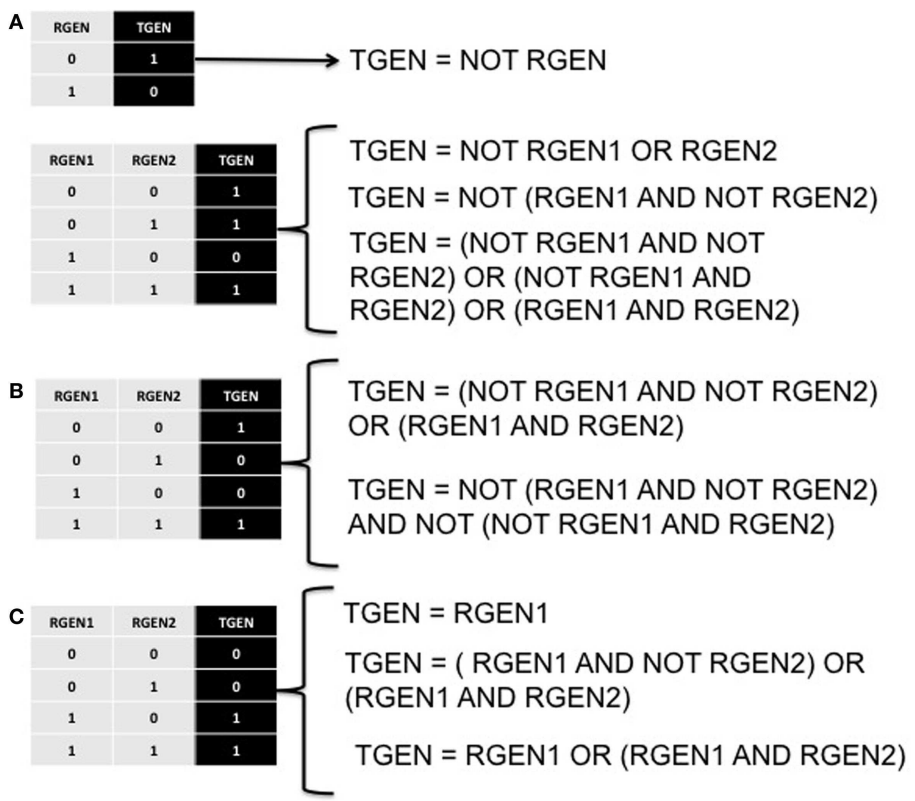

FIGURE A3 | Truth tables and equivalent logical statements for global negative, ambiguous, and neutral regulator definitions. **(A)** Two examples of a negative global regulator. As observed in the first example, the regulator can only be expressed with a NOT logical operator in the logical statement. In the example below, equivalent logical statements where RGEN1 acts as a negative and as an ambiguous regulator can be used. However, we can observe that if RGEN1 is labeled as a negative global regulator, we can always express RGEN1 in a logical statement with a NOT logical operator. **(B)** An example of ambiguous global regulators. In this example, the regulators can only be expressed as ambiguous regulators using a NOT logical operator in one part of the sentence and omitting the NOT operator in the other part of the sentence. **(C)** A neutral global regulator. The logical statement can be written without including the neutral global regulator (RGEN2). However, we can use an equivalent logical statement to include RGEN2 as a positive, negative, or neutral regulator. Neutral global regulators can always be removed from the logical statement.

Procedures 3 and 4: adding missing links while maintaining documented protein–protein interactions

In another scenario, a yeast two hybrid assay, or other method, confirmed that RGEN1 and RGEN 2 are not only positive regulators of TGEN, but RGEN1 and RGEN2 also interact at the protein level and form a dimer. In our example, when we add RGEN3, procedures 1 and 2 can generate the truth table observed in **Figure A1D**. One logical statement that can represent this function is "TGEN = RGEN3 AND (RGEN1 OR RGEN2)." Using this logical statement, RGEN1 and RGEN2 do not need to act as a dimer. However, we need to define the expression of a dimer in a BF before assuring the last statement.

Some transcriptional regulators act as dimers or more complex multimers. A TGEN activity is independent, locally, and globally, of a global neutral RGEN. However, if two RGENs function as a dimer, neither RGEN1 nor RGEN2 can act as local neutral regulators in the dimer. Anyhow, in the truth table in **Figure A1D**, RGEN1 and RGEN2 are local neutral regulators in both conditions where RGEN1 and RGEN2 could form a dimer, which is what we do not want that happens if we want to maintain the dimer functionality. Using the sign definitions defined previously, we can generate a procedure to generate BFs that maintain the dimer functionality, namely procedure 3. In this procedure, to maintain the dimer functionality, we need to verify that at least one local non-neutral regulation is specified for each RGEN in the same row, and in this row they must be capable to act as a dimmer (i.e., have a *1* expression value). Variations to this procedure can be used to maintain different types of interactions among regulators.

Finally, using procedure 3, we can generate the truth table observed in **Figure A1E**. One logical statement that can represent this function is "TGEN = RGEN1 AND (RGEN2 OR RGEN3)." This statement indicates that RGEN3 can substitute for RGEN2 in the dimer. However, the presence of a RGEN in a dimer can sometimes be necessary to regulate the expression of a TGEN. In this situation, the dimer RGEN1-RGEN2 is only functional when both proteins are together, and none of them can be substituted. The simplest way to maintain these data is by creating a new node, namely DRGEN (to indicate a dimer of RGENs) that represents the complex formed by RGEN1 and RGEN2. Subsequently, the TGEN truth table can be redefined in terms of DRGEN (**Figure A1F**). Using this method, none of the RGENs that form a complex can be substituted.

Is important to note that these first four procedures only use the available information about how RGENs regulate their TGENs. This implies that we do not include information about how RGENs affect each other or about the network topology nor any kind of partial information regarding possible indirect regulation of TGEN by RGENs. Thus, the procedures could be improved if we include data about the effect of RGENs on another RGENs of the GRN that are not their TGENs or if we use information about the network topology. The use of this data could reduce even more the number of BFs generated when we add a putative missing interaction, but will complicate the algorithm design and greatly increase the number of procedures. Because we did not include this kind of data to design the procedures, the number of possible BFs could be overestimated. However, the algorithms and procedures design is simpler.

Procedures 5 and 6: adding missing links without ambiguous regulators and incorporating independent TGEN activity

While the procedures described above were dependent on a set of experimental data that are available when reconstructing a truth

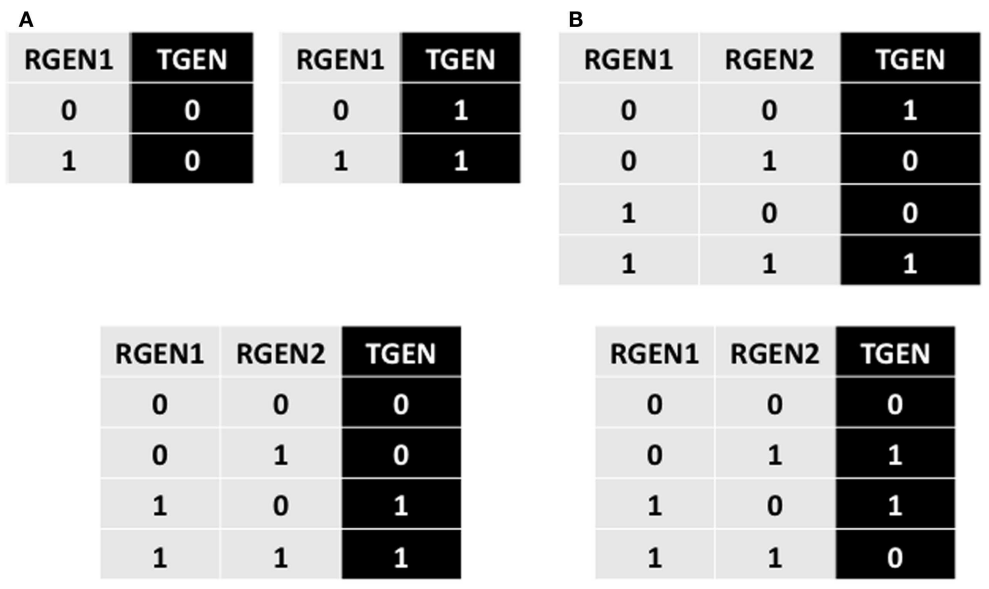

FIGURE A4 | Truth tables with global neutral and ambiguous regulations of TGEN. **(A)** Truth tables with global neutral regulations of TGEN by RGEN1 or RGEN2. In the top two truth tables, we observe that the expression of TGEN does not change independently of the expression value of RGEN1. In the truth table below, we observe that the change in TGEN's expression value depends only on the value of RGEN1 but not on the expression value of RGEN2. **(B)** Truth tables with global ambiguous regulation of TGEN by RGEN1 and RGEN2. In both truth tables, TGEN's expression value is positively and negatively regulated by RGEN1 and RGEN2 indicating that both factors are ambiguous regulators of TGEN.

table with added interactions and/or nodes, these two additional procedures stem from the limits of the Boolean formalism, and we propose these procedures to simplify the interpretation of the predicted missing interactions and reduce the number of BFs generated when we add a putative missing interaction.

The activity of a TGEN may be independent of the activity of one or more of its RGENs. For example, in the truth tables in **Figure A4A**, which are represented with the logical statements "TGEN = 0," "TGEN = 1" and "TGEN = RGEN1," TGEN activity is not affected by RGEN1 in the first two and is independent of RGEN2 in the third one. Some of these cases appear because certain gene regulations cannot be represented as BFs due to missing data or the nature of the interactions. For example, the role of some proteins whose function is to modulate the activity of other proteins cannot be represented as a BF. Consequently, BFs where one or more of the RGENs were global neutral regulators were not considered because these BFs indicate that the TGEN activation state is independent of one or more RGEN or the RGENs regulatory effect cannot be represented with a Boolean formalism. We refer to this procedure as procedure 5.

Finally, we decided not to consider BFs where one or more RGENs were ambiguous global regulators (**Figure A2D**; see example of an ambiguous regulator in **Figure A4B**). This is a simplifying assumption, because some genes are indeed ambiguous regulators. However, some authors propose that a dual regulatory role is not common (Davidson, 2001), and a biological interpretation is difficult to provide in cases where the number of ambiguous RGENs increases in the BF. Constraining the BF to only those with unambiguous global regulators greatly reduces the number of BFs (e.g., only 1882 of 65,536 for four regulators; La Rota et al., 2011). We refer to this procedure as procedure 6. Importantly, the use of these last two procedures has been discussed and analyzed previously, demonstrating its utility and biological importance (Raeymaekers, 2002).

Using our set of procedures, we can incorporate putative missing interactions that are congruent with the available experimental data and imply novel predictions without contradicting previously available experimental data. The methodology is explained above.

Chapter 67
Finding Missing Interactions in Gene Regulatory Networks Using Boolean Models

Eugenio Azpeitia, Nathan Weinstein, Mariana Benítez, Elena R. Alvarez-Buylla, and Luis Mendoza

Abstract Gene regulatory networks (GRNs) play a fundamental role in development and cellular behavior. However, due to a lack of experimental information, there are missing interactions in the GRNs inferred from published data. It is not a trivial task to predict the position and nature of such interactions. We propose a set of procedures for detecting and predicting missing interactions in Boolean networks that are biologically meaningful and maintain previous experimental information. We tested the utility of our procedures using the GRN of the *Arabidopsis thaliana* root stem-cell niche (RSCN). With our approach we were able to identify some missing interactions necessary to recover the reported gene stable state configurations experimentally uncovered for the different cell types within the RSCN.

67.1 Background

Dynamical modeling is one of the most commonly used approaches for studying gene regulatory networks (GRNs), which has provided key insights of system-level

E. Azpeitia · M. Benítez · E.R. Alvarez-Buylla (✉)
Instituto de Ecología, Universidad Nacional Autónoma de México, Cd. Universitaria, Mexico DF 04510, Mexico
e-mail: eabuylla@gmail.com

E. Azpeitia
e-mail: emazpeitia@gmail.com

M. Benítez
e-mail: marianabk@gmail.com

E. Azpeitia · E.R. Alvarez-Buylla
Centro de Ciencias de la Complejidad (C3), Universidad Nacional Autónoma de México, Cd. Universitaria, Mexico DF 04510, Mexico

N. Weinstein · L. Mendoza (✉)
Instituto de Investigaciones Biomédicas, Universidad Nacional Autónoma de México, Cd. Universitaria, Mexico DF 04510, Mexico
e-mail: lmendoza@biomedicas.unam.mx

N. Weinstein
e-mail: nathan.weinstein4@gmail.com

T. Gilbert et al. (eds.), *Proceedings of the European Conference on Complex Systems 2012*, Springer Proceedings in Complexity, DOI 10.1007/978-3-319-00395-5_67,

properties such as robustness and modularity [2, 6]. However, the construction of dynamic models is usually done with a limited amount of experimental data. This often results in incomplete models due to missing information. Nevertheless, the formalization that underlies dynamical modeling allows for the prediction of some missing interactions, though this is a non-trivial task.

Boolean networks (BNs) are one of the simplest dynamical modeling approaches. BNs consist in a set of nodes (usually representing genes), where each node can only have two values, 0 if the gene is OFF and 1 if the gene is ON. The state of each node at a given time is determined by a Boolean function (BF) of the activation states of its regulatory inputs. Despite their simplicity, BN models have a rich behavior that yields meaningful information about the network under study. Hence, BN models have been successfully used for the analysis of diverse GRNs, including *A. thaliana* flower organ determination [7], and *Drosophila melanogaster* segment polarity [1], among others.

In deterministic Boolean GRNs, the system eventually attains activation patterns that are stationary or that cycle through several configurations of gene activation. These patterns are known as fixed-point and cyclic attractors, respectively. Kauffman [13] proposed that the attractors of BNs could represent the experimentally observed gene expression patterns or configurations that characterize different cell types in biological systems. Usually, when the attractors do not coincide with the reported multigene activation configurations, it is assumed that there are some missing nodes or interactions.

In BNs the number of possible BFs of a node increase as a double exponential function (2^{2^i} where i represents the number of inputs). Thus, the number of possible BFs describing a BN quickly exploits, making impossible to test all the possibilities. However, not all BFs are biologically meaningful [17]. Moreover, the use experimental information could greatly reduce the number of BFs to tests. Hence, a set of procedures that allow us to generate only biologically meaningful BFs that at the same time do not contradict previous experimental information, could help us to generate a reduced number of BFs to test which should be experimentally testable. We developed here a set of procedures capable to do this.

Recently we developed a Boolean GRN of the root stem-cell niche (RSCN) [4]. Our study revealed that the inferred RSCN GRN still lacks some important information because the set of expected attractors did not coincide with the set of expected attractors. In order to test the utility of our procedures, we use them to generate the BFs of all possible missing interactions of the RSCN GRN. We analyze the effect in the set of attractors of including one by one each BF. Then, we examined in further detail the BFs whose inclusion allowed us to recover the attractors observed experimentally. Our procedures narrowed down the nature and number of missing interactions in the RSCN GRN, produce biologically meaningful BF that did not contradicted experimentally reported data and produced testable prediction. Importantly, the procedures are general enough to be used in any BN, thus making it suitable to explore more generic theoretical questions.

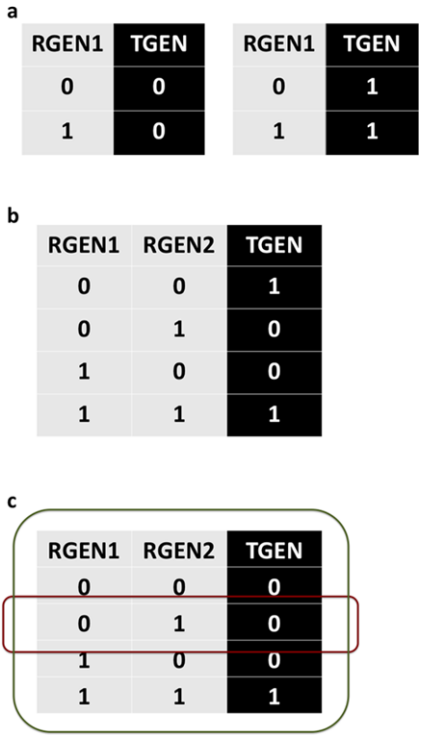

Fig. 67.1 Truth tables with examples of the procedures. In (**a**) two examples of a target gene (TGEN) whose expression is independent of its regulatory gene (RGEN1). As observed, TGEN value remains constant despite the expression value of its RGEN1. In (**b**) TGEN is negatively regulated by RGEN2 in the first pair of rows of the truth table, and positively in the second pair of rows of the truth tables. In (**c**) is highlighted how a loss-of-function mutant of RGEN1 may be represented in a single line of the truth table (enclosed in *purple*), while a yeast two hybrid analysis with a chromatin immunoprecipitation is represented by the whole truth table (enclosed in *grey*)

67.2 Methods

67.2.1 Procedures

We designed a set of procedures that omitted the generation of BFs in which: (1) one or more of the regulatory genes did not have any influence over the regulated gene, (2) the proposed Boolean function was not consistent with experimentally reported data, or (3) a gene could act as both a positive and negative regulator under different conditions. Is important to note that genes with positive and negative activity have been reported, however, they appear to be rare in biomolecular systems.

When a regulatory gene does not affect its target gene value, the expression value of the target gene must remain unchanged despite the expression value of the regulatory gene (Fig. 67.1(a)). When a regulatory gene acts as a positive and a negative regulator of its target gene, the expression value of the target gene must pass from 0 to 1 under some conditions when the regulatory gene changes from 0 to 1, and the expression value of the target gene must pass from 1 to 0 under other conditions when the regulatory gene changes from 0 to 1 (Fig. 67.1(b)). Finally, maintaining consistency with experimental data is more complicated and requires several procedures that depend on the quality and quantity of information available. For example, some experiments, like loss-of-function mutants, provide information that is represented in a single row of a BFs' truth table, while other, like a combination of

a yeast two hybrid analysis with a chromatin immunoprecipitation can provide information that is represented with the complete truth table of a BFs (Fig. 67.1(c)). Thus, we designed four different procedures that allow us to maintain consistency with experimental information when: (1) the information is represented by single row in the BFs' truth tables, (2) to maintain the sign of regulation (positive or negative) of a regulatory gene, (3) to maintain regulatory genes interactions (e.g., dimer formations) and (4) when the experimental information is represented by the whole BFs.

To test the utility of the procedure we designed an algorithm to use them in a real GRN. Our algorithm generated the BFs of all possible missing interaction in a GRN and then test the effect of including one by one each BF on the set of attractors. The interaction that most improved the model was incorporated into the model, and then this new model was tested in the same way. The criteria to asses if the addition of a regulatory interaction was an improvement are, in order of relevance: (1) the number of expected attractors obtained, (2) the number of non-expected attractors obtained, and (3) the number of total fixed-point attractors in the model. If more than one interaction equally improved the model, one of them was randomly selected and added to the BN model. After the inclusion of an interaction, we continued adding interactions with the same criteria until: (1) the model reached only the expected attractors, or (2) the inclusion of three consecutive interactions did not improve the model by increasing the number of expected attractors obtained, or reducing the number of non-expected attractors.

67.3 Results

To test our procedures we updated the RSCN GRN [4]. Because the objective of this research was to detect missing interactions, to update the GRN first we omitted the interactions predicted by our previous work. Then, even though it is well documented that PLT genes are essential for RSCN maintenance [8], we removed them, since *PLT* genes acted only as an output node in the model. Third, we included in the updated version of the model nodes for miRNA165/6, the transcription factor PHABULOSA (PHB), and the receptor kinase ACR4 [5, 18]. Fourth, because the auxin signaling pathway describe a unidirectional pathway we were able to reduced it to only two nodes. Fifth, we included novel regulatory interactions reported in the literature [15, 16]. Also, because our model does not incorporate space explicitly, to simulate molecular diffusion, we include a positive self-regulatory edge in nodes whose products diffuse (i.e. SHR, CLE, and miRNA165/6) (Fig. 67.2). Finally, some nodes in the network already have four inputs, and the addition of a 5th regulator over any node would be computationally very demanding, since the number of possible BFs increases from $\approx 6.5 \times 10^4$ to $\approx 4 \times 10^9$. For this reason, we created intermediary nodes that integrate the influence of two regulators over any gene with 4 regulators. For instance, *WOX5* expression is repressed when *CLE40* is perceived by the membrane receptor *ACR4*. Because *WOX5* had 4 regulators, we

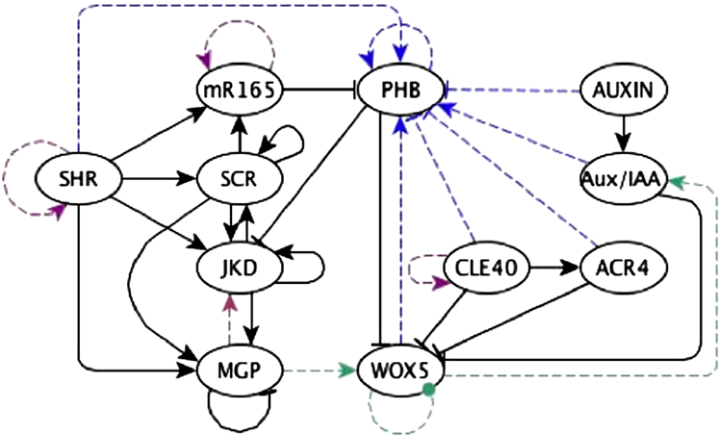

Fig. 67.2 The updated RSCN GRN with predicted missing interactions. RSCN GRN with predicted missing interactions. For clarity intermediary nodes were not included here. *Pink*, *green* and *blue edges* are the three predicted interactions required to recover the expected attractors, and are grouped according to the nodes functions. *Blue edges* are always a regulation over *PHB*. *The pink edge* is a positive regulation of MGP over *JKD*. *The green edges* are always a regulation over *WOX5*. *The doted green edge* can be a negative or a positive regulation of WOX5 over itself

Table 67.1 Expected attractors

CT/G	SHR	miR	JKD	MGP	PHB	SCR	IAA	A/I	WOX	CLE	ACR
CVC	1	0	0	0	1	0	0	1	0	0	0
PVC	1	1	0	0	0	0	0	1	0	0	0
End	1	1	1	1	0	1	0	1	0	0	0
Cor	0	1	1	0	0	0	0	1	0	0	0
LCC	0	0	0	0	0	0	1	0	0	1	1
VI	1	1	0	0	0	0	1	0	0	0	0
CEI	1	1	1	1	0	1	1	0	0	0	0
CLEI	0	1	0	0	0	0	1	0	0	1	1
QC	1	1	1	0	0	1	1	0	1	0	0

CT = Cell type, G = Gene, CVC = Central Vascular cells, PVC = Periferal vascular cells, End = Endodermis, Cor = Cortex, LCC = Lateral root-cap and columella cells, VI = Vascular initials, CEI = Cortex-endodermis initials, CLEI = Columella and lateral root-cap-epidermis initials, QC = Quiescent center, miR = miRNA165/6, IAA = Auxin, A/I = Aux/IAA, WOX = WOX5, CLE = CLE40 and ACR = ACR4

reduced *CLE40* and *ACR4* activity to a single node. This strategy allows for the exhaustive testing of BFs.

Based on available experimental data we expected 9 fixed-point attractors (Table 67.1). Some attractors represented more than one cell type due to lack of experimental information that is still required to distinguish among them (Fig. 67.3).

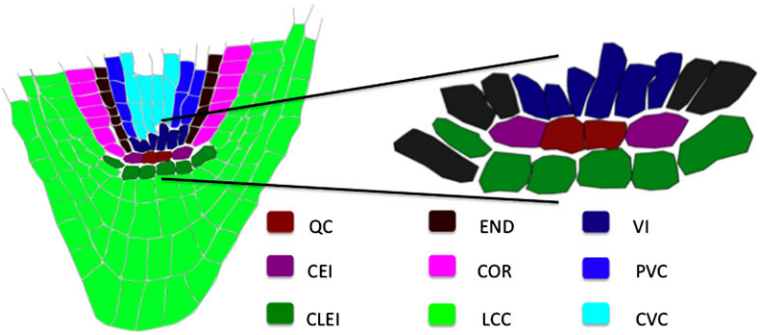

Fig. 67.3 The *A. thaliana* root tip and RSCN. Here, the expected attractors, which characterize each cell type stable gene configuration, are distinguished with different colors. As observed, some of the expected attractors represent more than one cellular type. QC = Quiescent center; END = Endodermis; VI = Vascular initials; CEI = Cortex-endodermis initials; COR = Cortex; PVC = Peripheral vascular cells; CLEI = Collumela-epidermis-lateral-root-cap initials; LCC = Collumela and lateral root cap; CVC = Central vascular cells

The BN model was not able to recover the expected attractors showed in Table 67.1. Thus, we algorithm to test our procedures utility with this GRN 10 times, ending with 10 different models that predicted different putative interactions. Finally, we analyzed the biological significance of the included interactions.

With the RSCN GRN model based exclusively on experimental information, we obtained 7 of the 9 expected attractors, 21 attractors without meaning in the RSCN context, and 4 cyclic attractors. Hence, as explained above, we included all possible interactions and their associated Boolean functions one by one, then we selected those changes that improved the consistency between the model and the experimental data. The inclusion of three types of interactions was sufficient to recover the expected attractors. However, the addition of these interactions did not eliminate cyclic attractors nor attractors without meaning in the RSCN context. In fact, the inclusion of these three interactions always increased the number of cyclic and/or unexpected attractors.

Interestingly, the three interactions mentioned above were functionally similar in the 10 replicas of the search process (Fig. 67.2). The first interaction is a regulation that *restricts PHB* expression domain to the vascular cells. This regulation was accomplished through positive regulation by those nodes with a similar expression domain (e.g. *SHR*) or through negative regulation by those genes with a complementary expression pattern (e.g. *CLE* and *ACR4*). Biologically, we believe that the likely regulator of *PHB* is a member of the *KANADI* (*KAN*) gene family. *KAN* genes were not included in this GRN model, because no connections with any node of the RSCN GRN in the root has been described yet, but *KAN* have antagonistic roles with *PHB* in the shoot and have a complementary expression pattern with *PHB* in the root [11, 12]. The second interaction is a *WOX5* self-regulatory loop. *WOX5* loop could be direct or indirect, and positive or negative (Figure 67.2). Interestingly, there is some experimental and theoretical evidence suggesting the existence of this

loop through the auxin signaling pathway [4, 9]. The third interaction is a positive regulation of MAGPIE (MGP) over *JACKDAW* (*JKD*). This is contrary to the proposed antagonistic relation between *JKD* and *MGP* through a negative regulation of MGP over *JKD* [19]. The interplay between *JKD*, *MGP*, *SCR* and *SHR* is complex [16, 19] and there is no consensus on its mechanism. Our simulations suggest that it is necessary to consider other possible regulatory mechanisms.

After the inclusion of 11 to 15 interactions, the performance of the resulting GRN models no longer improved. After this point, almost all models reduced both the number of cyclic and biologically meaningless attractors to 3. Interestingly, some interactions were present in several of the 10 final models. Specifically, the most common interactions were: (1) inhibition of *SHR*, (2) activation of *SHR* by PHB, (3) negative regulation of PHB over auxin, and (4) negative regulation of Aux/IAA or SHR over *CLE*. Our results emphasize the lack of data concerning the regulation of key nodes of the RSCN GRN. Unraveling how these genes are regulated will be fundamental to our understanding of how the RSCN is maintained.

As expected, the use of our procedures producer only experimentally testable predictions that did not contradicted previously reported experimental data. The procedures were capable to greatly reduce the number of BFs of putative missing interactions. For example, to predict the first putative missing interactions, sing our procedures we only tested ~ 3000 out of $\approx 8 \times 10^9$ possible BFs. Anyhow, to produce each of the RSCN GRN that recovered the expected attractors, we needed to test around 100000 BFs, which is a highly demanding computational process. Moreover, if we consider that the number of BFs increase as a double exponential function, there is still an important constrain that needs to be tackled in the future.

67.4 Conclusion

In GRNs it is possible to test the effect of adding or modifying all possible interactions. However, even for small BNs, the number of possible BFs is overwhelming. Nonetheless, we presented in this work a set of procedures to reduce the number of BFs of putative missing interactions. Our procedures produce only experimentally testable BFs that do not contradict experimental data. To systematically predict possible missing interactions, and we have applied our procedures to the *A. thaliana* RSCN GRN. Importantly, the procedures were capable to greatly reduce the number of BFs generated. However the total reduction is dependent on the quality of the experimental information and because the number BFs of a node increase as a double exponential function, its utility is constrained for network with low connectivity.

For the specific case of the RSCN GRN we could not recover a network topology that yielded the observed configurations alone, without additional unobserved attractors. However, our work provides important predictions concerning additional interactions and a novel RSCN GRN architecture that could be experimentally tested. One limitation of this approach is the fact that additional missing nodes may be required to recover the observed set of configurations without unobserved ones.

Interestingly, some of the genes involved in RSCN maintenance are also involved in other aspects of plant development such as epidermis differentiation [10] and vascular development [20]. This challenges the stem cell pedigree idea, and as proposed before, suggests that the stem cell state is not independent of the local cellular micro-environments characteristic of the stem cell niche [14].

We believe our method would be improved by its incorporation into an existent dynamical network analyzer (e.g. [3]). Another possible improvement for our methodology would be the inclusion of a genetic algorithm, which would allow us to search for additional missing interactions. Given that the methodology used in this study is very general, we believe that this kind of exploration could help guide experimental research of any system amenable to BN analyses, as well as theoretical questions. For instance, this methodology can be used to study the constraints that a given network topology imposes on attractor evolvability.

Acknowledgements This work constitutes a partial fulfillment of the doctorado en Ciencias Biomédicas of the Universidad Nacional Autónoma de México (UNAM). E. Azpeitia acknowledges the scholarship and financial support provided by the National Council of Science and Technology (CONACyT), and UNAM. E.R. Alvarez-Buylla thanks financial support from Conacyt (81433, 81542, 1667705,180098,180380) and PAPIIT (IN229003-3, IN226510-3, IN204011-3, IB201212-2). E.R. Alvarez-Buylla is currently sponsored by the Miller Institute for Basic Research in Science, University of California, Berkeley, USA. We thank Rigoberto V. Perez-Ruız and Diana Romo for technical and logistical assistance.

References

1. Albert R, Othmer HG (2003) The topology of the regulatory interactions predicts the expression pattern of the segment polarity genes in Drosophila melanogaster. J Theor Biol 223:1–18
2. Alvarez-Buylla ER, Benítez M, Dávila EB, Chaos A, Espinosa-Soto C, Padilla-Longoria P (2007) Gene regulatory network models for plant development. Curr Opin Plant Biol 10:83–91
3. Arellano G, Argil J, Azpeitia E, Benítez M, Carrillo M, Góngora P, Rosenblueth DA, Alvarez-Buylla ER (2011) "Antelope": a hybrid-logic model checker for branching-time Boolean GRN analysis. BMC Bioinform 12:490
4. Azpeitia E, Benítez M, Vega I, Villarreal C, Alvarez-Buylla ER (2010) Single-cell and coupled GRN models of cell patterning in the Arabidopsis thaliana root stem cell niche. BMC Syst Biol 4:134
5. Carlsbecker A, Lee JY, Roberts CJ, Dettmer J, Lehesranta S, Zhou J, Lindgren O, Moreno-Risueno MA, Vatén A, Thitamadee S, Campilho A, Sebastian J, Bowman JL, Helariutta Y, Benfey PN (2010) Cell signalling by microRNA165/6 directs gene dose-dependent root cell fate. Nature 465:316–321
6. de Jong H (2002) Modeling and simulation of genetic regulatory systems: a literature review. J Comput Biol 9:67–103
7. Espinosa-Soto C, Padilla-Longoria P, Alvarez-Buylla ER (2004) A gene regulatory network model for cell-fate determination during Arabidopsis thaliana flower development that is robust and recovers experimental gene expression profiles. Plant Cell 16:2923–2939
8. Galinha C, Hofhuis H, Luijten M, Willemsen V, Blilou I, Heidstra R, Scheres B (2007) PLETHORA proteins as dose-dependent master regulators of Arabidopsis root development. Nature 449:1053–1057

9. Gonzali S, Novi G, Loreti E, Paolicchi F, Poggi A, Alpi A, Perata P (2005) A turanose-insensitive mutant suggests a role for WOX5 in auxin homeostasis in Arabidopsis thaliana. Plant J 44:633–645
10. Hassan H, Scheres B, Blilou I (2010) JACKDAW controls epidermal patterning in the Arabidopsis root meristem through a non-cell-autonomous mechanism. Development 137:1523–1529
11. Hawker NP, Bowman JL (2004) Roles for class III HD-Zip and KANADI genes in Arabidopsis root development. Plant Physiol 135:2261–2270
12. Izhaki A, Bowman JL (2007) KANADI and class III HD-Zip gene families regulate embryo patterning and modulate auxin flow during embryogenesis in Arabidopsis. Plant Cell 19:495–508
13. Kauffman SA (1969) Metabolic stability and epigenesis in randomly constructed genetic nets. J Theor Biol 22:437–467
14. Loeffler M, Roeder I (2004) Conceptual models to understand tissue stem cell organization. Curr Opin Hematol 11:81–87
15. Miyashima S, Koi S, Hashimoto T, Nakajima K (2011) Non-cell-autonomous microRNA165 acts in a dose-dependent manner to regulate multiple differentiation status in the Arabidopsis root. Development 138:2303–2313
16. Ogasawara H, Kaimi R, Colasanti J, Kozaki A (2011) Activity of transcription factor JACKDAW is essential for SHR/SCR-dependent activation of SCARECROW and MAGPIE and is modulated by reciprocal interactions with MAGPIE, SCARECROW and SHORT ROOT. Plant Mol Biol 77:489–499
17. Raeymaekers L (2002) Dynamics of Boolean networks controlled by biologically meaningful functions. J Theor Biol 218:331–341
18. Stahl Y, Wink RH, Ingram GC, Simon R (2009) A signaling module controlling the stem cell niche in Arabidopsis root meristems. Curr Biol 19:909–914
19. Welch D, Hassan H, Blilou I, Immink R, Heidstra R, Scheres B (2007) Arabidopsis JACKDAW and MAGPIE zinc finger proteins delimit asymmetric cell division and stabilize tissue boundaries by restricting SHORT-ROOT action. Genes Dev 21:2196–2204
20. Zhou GK, Kubo M, Zhong R, Demura T, Ye ZH (2007) Overexpression of miR165 affects apical meristem formation, organ polarity establishment and vascular development in Arabidopsis. Plant Cell Physiol 48:391–404

5.4.- Parte IV: Modelo bidimensional del acoplamiento entre transporte de auxinas y el mantenimiento del nicho de células troncales de la raíz de *Arabidopsis thaliana*

Como ya hemos discutido en otros capítulos de esta tesis, las auxinas son fundamentales para el mantenimiento y desarrollo del nicho de células troncales de la raíz (Azpeitia y Alvarez-Buylla 2012). A lo largo del proyecto, nuestros resultados continuamente sugerían que las auxinas y *WOX5*, un factor de transcripción específico de centro quiescente y fundamental para el mantenimiento del nicho, debían formar un ciclo de retroalimentación entre ellos (Azpeitia et al., 2010 y 2013). Aun más, algunos trabajos experimentales comenzaban a sugerir que esta predicción podría ser correcta (e.g., Ding et al., 2010). Sin embargo, los resultados de los estudios experimentales presentaban comportamientos que en ocasiones parecían contradictorios. Por ejemplo, a pesar de que la máxima concentración de auxinas se encuentra justo en el centro quiescente, la adición de más auxinas ocasionaba la diferenciación de las células iniciales e inhibía la expresión de *WOX5* (Sabatini et al., 1999; Ding et al., 2010). Dado que nuestros resultados predecían la presencia del ciclo de retroalimentación entre las auxinas y WOX5, decidimos estudiar esta parte de la red con mayor detalle.

Esta parte del trabajo se desarrolló en colaboración con la MSc. Mónica García. El objetivo principal del trabajo fue generar un modelo del nicho en dos dimensiones, con transporte de auxinas y la parte de la red que considera la vía de señalización de las auxinas y sus interacciones con WOX5. El modelo de transporte de auxinas fue elaborado por la MSc. García y se encuentra detallado en su tesis de maestría (García 2013). La red de regulación genética fue elaborada por mi. Por último, el acople entre la red y el flujo de auxinas fue un trabajo conjunto. Por este motivo, en este capítulo se presenta como se modeló la red de regulación genética y como se integró con el transporte de auxinas, pero la modelación del transporte de auxinas no se presenta en detalle, y este se puede consultar en García (2013). Este trabajo aún se encuentra en desarrollo, por lo que sus resultados son preliminares y no han sido publicados.

A forma de introducción general es importante recordar que el nicho de células troncales se encuentra localizado en la punta de la raíz. Varios tipos celulares

conforman el nicho. En el centro de las células troncales o iniciales se encuentra el centro quiescente. Señales de corto alcance que se producen por las células del CQ son importantes para el mantenimiento del estado de indiferenciación de las células células troncales (*Figura 1*).

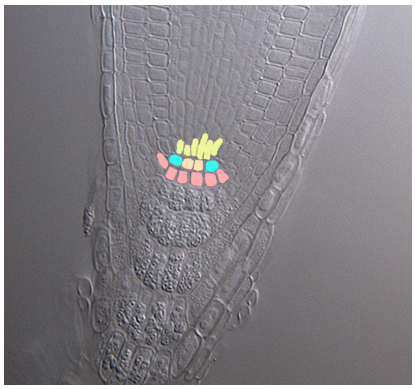

Figura 1. En esta figura se muestra el nicho de células troncales: en amarillo están las iniciales vasculares, en azul las iniciales de cortex y endodermis, en rosa las inciales de cofia lateral, epidermis y columnela y en naranja el centro quiescente. Como se puede observar, el centro quiescente se encuentra justo en el centro del nicho.

Las auxinas son transportadas entre células por medio de proteínas que las sacan y las meten a las células, entre ellas, destacan los transportadores de las familias *PINFORMED* (*PIN*) y *AUX1*. Las proteínas de los genes *PIN* son transportadores de salida y están localizados polarmente en la membrana plasmática. En la raíz, dicha localización cambia dependiendo del tipo celular (Blilou et al., 2005). Así, los transportadores PIN forman una red de transporte de auxina generando un flujo acropétalo por las células pro-vasculares acoplado a un flujo basipétalo por las células de la epidermis. Además en las células de la columnela, los PIN están localizados en todas las caras de la célula y en las células de endodermis hay PIN en la cara lateral alimentando el flujo de las células pro-vasculares. Estudios previos han mostrado como el flujo direccionado de auxina, debido a la localización polar de transportadores PIN, es capaz de generar un gradiente de concentración de auxina a lo largo de la raíz con un pico de concentración en la centro quiescente, como se observa experimentalmente (Sabatini et al., 1999; Blilou et al., 2005; Grieneisen et al., 2007).

Las auxinas disparan diferentes respuestas por medio de su vía de señalización. En la vía de señalización, la actividad de factores de transcripción llamados AUXIN RESPONSE FACTORS (ARF) es inhibida por las proteínas de los genes *Aux/IAA*

cuando se forma un dímero ARF-Aux/IAA. Sin embargo, bajo la presencia de auxinas, los Aux/IAA son degradados, liberando así a los ARF, quienes ahora son capaces de activar a sus genes blanco. Es importante notar que existen ARF que actúan como activadores transcripcionales, mientras que otros actúan como represores (Guilfoyle y Hagen 2007). Según un reporte reciente y nuestros propios análisis, únicamente los ARF activadores (ARFa) forman dímeros con los Aux/IAA, mientras que los ARF inhibidores (ARFi) se encuentran activos de forma constitutiva y en general no forman dímeros con los Aux/IAA (Vernoux et al., 2011; Azpeitia et al., 2013). Además los Aux/IAA son capaces de formar dímeros entre ellos mismos.

Se sabe que la expresión de *WOX5*, la cual es específica del centro quiescente, es indispensable para la identidad de nicho. Existe evidencia de que *WOX5* y las auxinas interactúan. Mientras que algunos reportes sugieren que *WOX5* es activado a nivel transcripcional por las auxinas (Gonzali et al., 2005; Sarkar et al., 2007; Azpeitia et al., 2010), otros sugieren que es inhibido por las auxinas (Ding y Friml 2010). De acuerdo a Ulmasov y colaboradores (1999), los ARFa y ARFi tienen la capacidad de unirse a los mismos promotores, entre los que cabe destacar que se encuentran los promotores de los *Aux/IAA*. Además, un análisis de la expresión de todos los *ARF* en la raíz (Rademacher et al., 2011) muestra que tanto los *ARFa* como los *ARFi* se expresan a lo largo de todo el meristemo de raíz en todos los tipos celulares. Por esto, en nuestro modelo, nosotros asumimos que la auxina activa y reprime a *WOX5* en la raíz. *WOX5* es activado por medio de los ARFa, como proponen artículos como el de Gonzali (2005), y a su vez es reprimido por medio de los ARFi.

Con base en estos datos generamos un modelo de transporte de auxinas y una primer versión de la red. Para nuestro modelo de transporte de auxinas, localizamos de forma fija a los PIN, en la cara basal de las células pro-vasculares y el centro quiescente, en la cara apical y lateral interna en la epidermis, en la cara basal y lateral interna en la endodermis y en todas las caras de las células de columnela (Figura 2). Esto corresponde con la polaridad de los PIN reportada experimentalmente (Blilou et al., 2005) y resumida arriba.

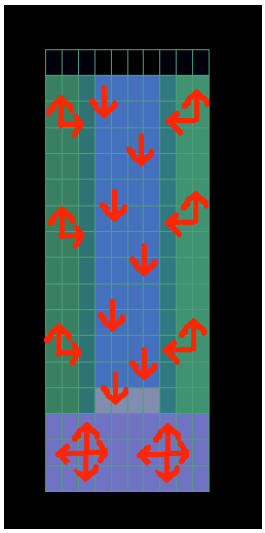

Figura 2. En esta figura se observa el flujo generado por el modelo de auxinas en el ápice de la raíz. Las células están representadas como rectángulos y la dirección del flujo de auxina en cada tipo celular se marca con las flechas. Los diferentes tipos celulares utilizados para localizar a los PIN se observan en distintos colores. Las células pro-vasculares están en azul, el centro quiescente en gris, las de epidermis en verde claro, las de endodermis en verde oscuro y en morado las de columnela.

En la simulación cada célula tiene una concentración inicial de auxina, la cual podía ser homogénea para todas las células o determinada de forma aleatoria. La auxina se puede distribuir a las células vecinas por medio de difusión y transporte activo. La dirección del transporte activo depende de la localización de los PIN y, por lo tanto, depende del tipo celular. Los detalles del modelo se pueden encontrar en García (2013). Los resultados del modelo de transporte de auxina establecen un gradiente de auxina que se mantiene constante (Figura 3) y concuerda con el gradiente observado de forma experimental (Sabatini et al., 1999).

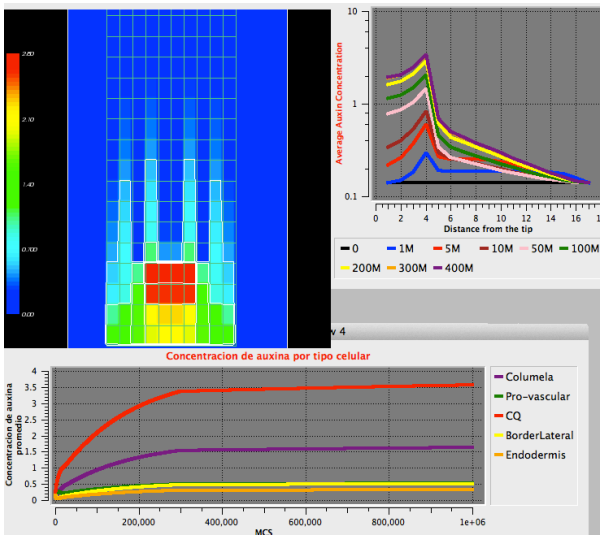

Figura 3. Gradiente de auxina con máximo en el centro quiescente. Arriba a la izquierda se ve el campo de concentración de auxina en la distribución celular y arriba a la derecha se ve la concentración de auxina en las células centrales en un corte longitudinal. A medida que el tiempo de la simulación corre, se alcanza un estado estacionario dinámico, como se ve cuando la línea de 300M se sobrelapa con la de 400M ("M" se refiere al número de pasos, que se median en Montecarlo steps (MCS), que ha dado el modelo, donde 1M=1,000 pasos). Abajo la gráfica muestra la concentración promedio de auxina por tipo celular y también se ve que después de 300,000 pasos no hay cambios.

Por otra parte, la gráfica de la red, basándonos exclusivamente en información experimental se observa en la *Figura 4*.

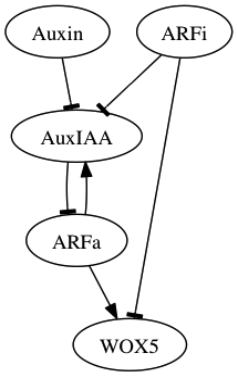

Figura 4. Gráfica de la red basada en información experimental. Auxin = Auxina, ARFi = ARF inhibidores, ARFa = ARF activadores, AuxIAA = Aux/IAA.

Esta red está descrita por el siguiente sistema de ecuaciones diferenciales:

$$\frac{dD_{ia}}{dt} = k_{ia}IA - k'_{ia}D_{ia} - \gamma_i\delta_i K_{aux}aux/(K_{aux}aux+1)D_{ia}$$

$$\frac{dD_{ii}}{dt} = k_{ii}II - k'_{ii}D_{ii} - \gamma_i\delta_i K_{aux}aux/(K_{aux}aux+1)D_{ii} - \delta_{ii}D_{ii}$$

$$\frac{dA}{dt} = \gamma_i\delta_i K_{aux}aux/(K_{aux}aux+1)D_{ia} - k_{ia}IA - k'_{ia}D_{ia}$$

$$\frac{dI}{dt} = \pi_i A^{n2}/(1+k_{am}^{n2}) - \gamma_i\delta_i K_{aux}aux/(K_{aux}aux+1)I$$

$$\frac{dW5}{dt} = \pi_{w5}A^{n}/(1+k_{am}^{n}) - \delta_{w5}W5$$

Donde $\frac{dD_{ia}}{dt}, \frac{dD_{ii}}{dt}, \frac{dA}{dt}, \frac{dI}{dt}$ y $\frac{dW5}{dt}$, representan los cambios en la concentración de IA, II, A, I y W5, que son la concentración del dímero Aux/IAA-ARFa, el dímero Aux/IAA-Aux/IAA, y las proteínas ARFa, Aux/IAA y WOX5, respectivamente. δ_x, π_x son las tasas de degradación y síntesis. k_{am} es la concentración de los ARFi y aux la concentración de auxinas. La k_{ix} y k'_{ix} son las tasas de asociación y disociación de los dímeros.

En este modelo el comportamiento de *WOX5* es proporcional a la concentración de auxinas. Es decir, a mayor concentración de auxina mayor expresión de *WOX5*, como se observa en la siguientes *Figuras 5, 6, 7 y 8*.

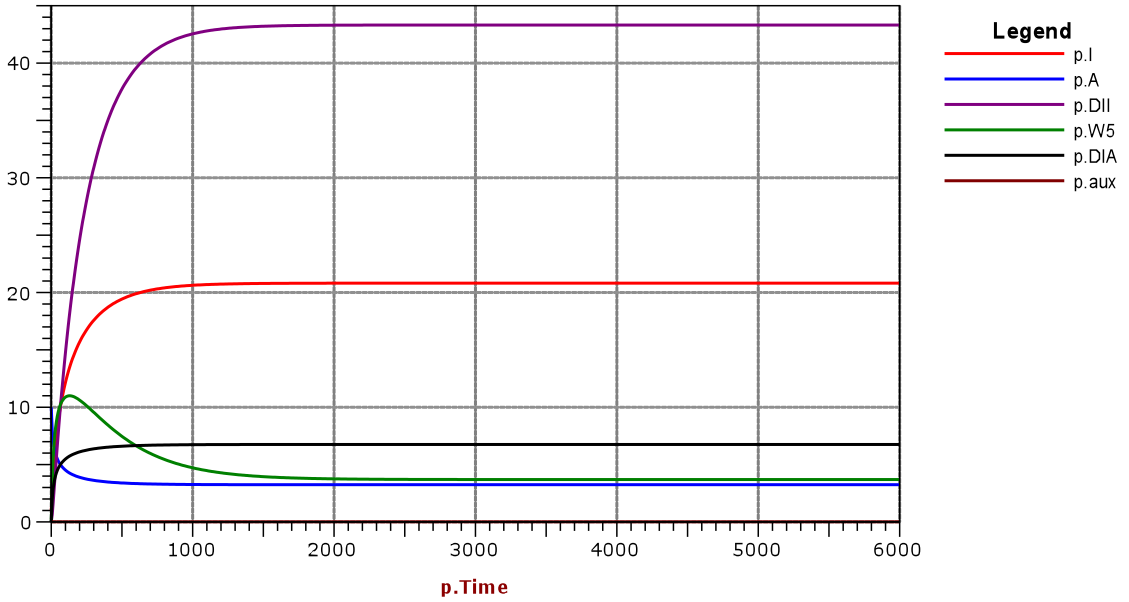

Figura 5. En esta figura se observa la expresión de los diferentes componentes de la red. Para esta gráfica la concentración inicial auxina fue fijada en 0.01u.a. (u.a. = unidades arbitrarias). Como se observa la expresión de *WOX5* se estabiliza en aproximadamente 4.5u.a. Se puede observar en la figuras de abajo como la expresión de *WOX5* aumenta conforme aumenta la concentración de auxina.

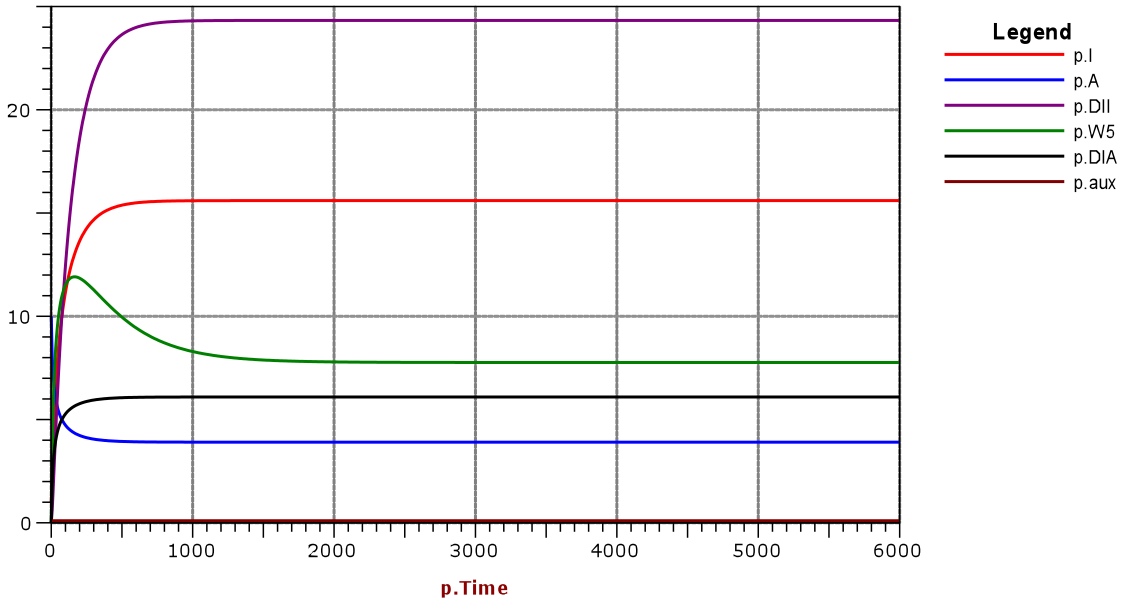

Figura 6. Para esta simulación la concentración de la auxina fue fijada en 0.1. Como se observa, la concentración de *WOX5* también aumenta.

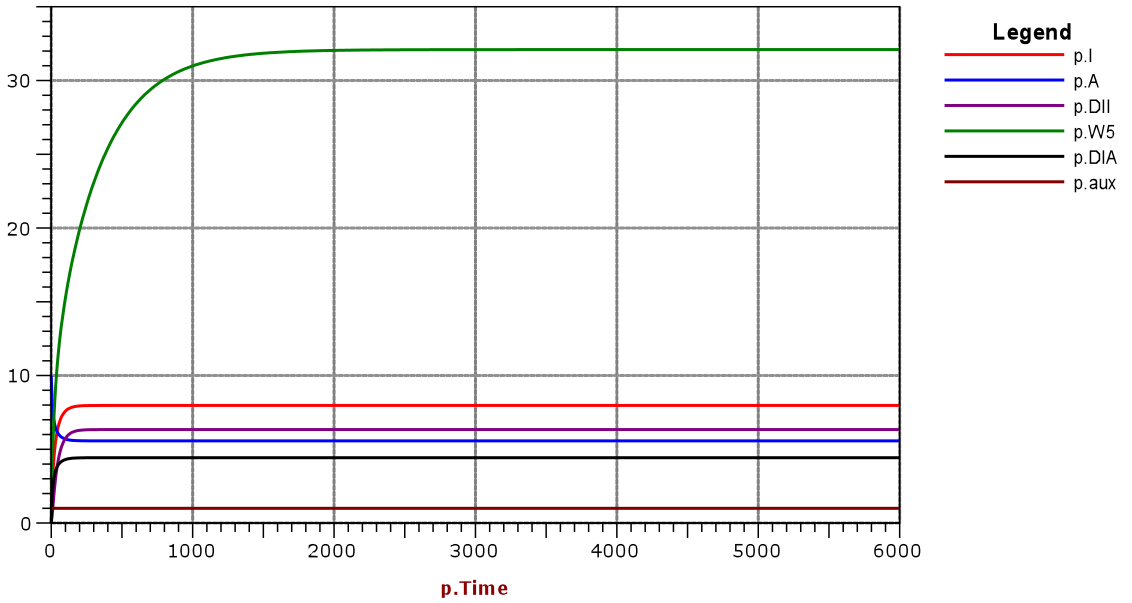

Figura 7. Para esta simulación la concentración de la auxina fue fijada en 1. Como se observa, la concentración de *WOX5* también aumenta.

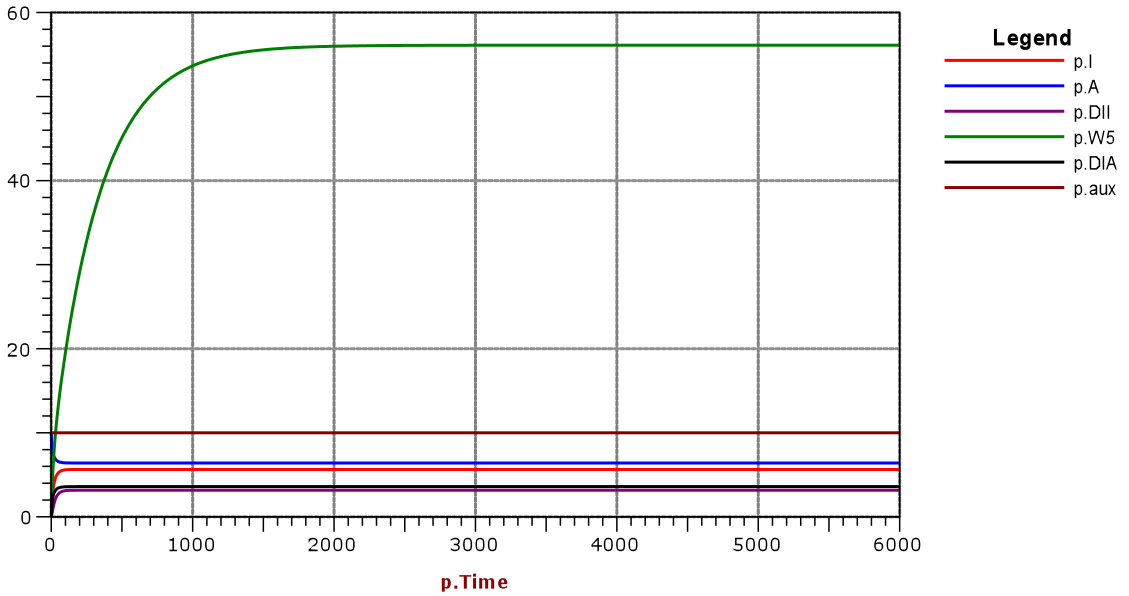

Figura 8. Para esta simulación la concentración de la auxina fue fijada en 10. Como se observa, la concentración de *WOX5* continua aumentando.

Experimentalmente se ha observado que la expresión de *WOX5* no sigue la concentración de auxina en la raíz, la cual forma un gradiente, sino que *WOX5* tiene una expresión discreta y especifica en el centro quiescente (Sarkar et al., 2007). Aunque no hay evidencia experimental concluyente, si existe evidencia, tanto teórica como experimental (e.g., Gonzali et al., 2005; Azpeitia et al., 2010), que indica que WOX5 podría promover de alguna forma la señalización de auxinas, ya sea por medio de inducir la síntesis de auxina o modificando la actividad de algún o algunos otros de los componentes de la vía (Gonzali et al., 2005). Además se sabe que las asas de retroalimentación positiva son necesarias para generar multiestabilidad en las redes. Nosotros buscamos una red biestable, donde bajo ciertas circunstancias (alta concentración de auxina) se exprese *WOX5* y bajo otras no lo haga (bajas e intermedias concentraciones de auxina). Por estos motivos incluimos un asa de retroalimentación de *WOX5* hacia la síntesis de auxina, dando origen a la red que se presenta en la siguiente *Figura 9*:

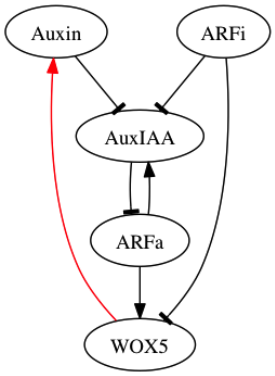

Figura 9. Gráfica de la red donde se incluye la hipótesis donde WOX5 promueve a las auxinas. La retroalimentación de *WOX5* hacia las auxinas se observa en rojo.

En esta nueva red, las auxinas ya no son un parámetro y se convierten en una variable, por lo que el sistema de ecuaciones que describe la red se convierte en este:

$$\frac{dD_{ia}}{dt} = k_{ia}IA - k'_{ia}D_{ia} - \gamma_i\delta_i K_{aux}aux/(K_{aux}aux+1)D_{ia}$$

$$\frac{dD_{ii}}{dt} = k_{ii}II - k'_{ii}D_{ii} - \gamma_i\delta_i K_{aux}aux/(K_{aux}aux+1)D_{ii} - \delta_{ii}D_{ii}$$

$$\frac{dA}{dt} = \gamma_i\delta_i K_{aux}aux/(K_{aux}aux+1)D_{ia} - k_{ia}IA - k'_{ia}D_{ia}$$

$$\frac{dI}{dt} = \pi_i A^{n2}/(1+k_{am}^{n2}) - \gamma_i\delta_i K_{aux}aux/(K_{aux}aux+1)I$$

$$\frac{dW5}{dt} = \pi_{w5}A^{n}/(1+k_{am}^{n}) - \delta_{w5}W5$$

$$\frac{daux}{dt} = \pi_{aux} + \pi'_{aux}W5 - \delta_{aux}aux$$

Donde δ_{aux} es la degradación de auxinas, π_{aux} es la síntesis basal de auxinas y π'_{aux} es la síntesis de auxinas debida a la presencia de *WOX5*.

Lamentablemente, este modelo no tiene biestabilidad en la expresión de *WOX5*. Sin embargo, en este modelo *WOX5* se expresa cuando hay mayor cantidad de ARFi que de ARFa, como se observan en las siguientes *Figuras 10 y 11*.

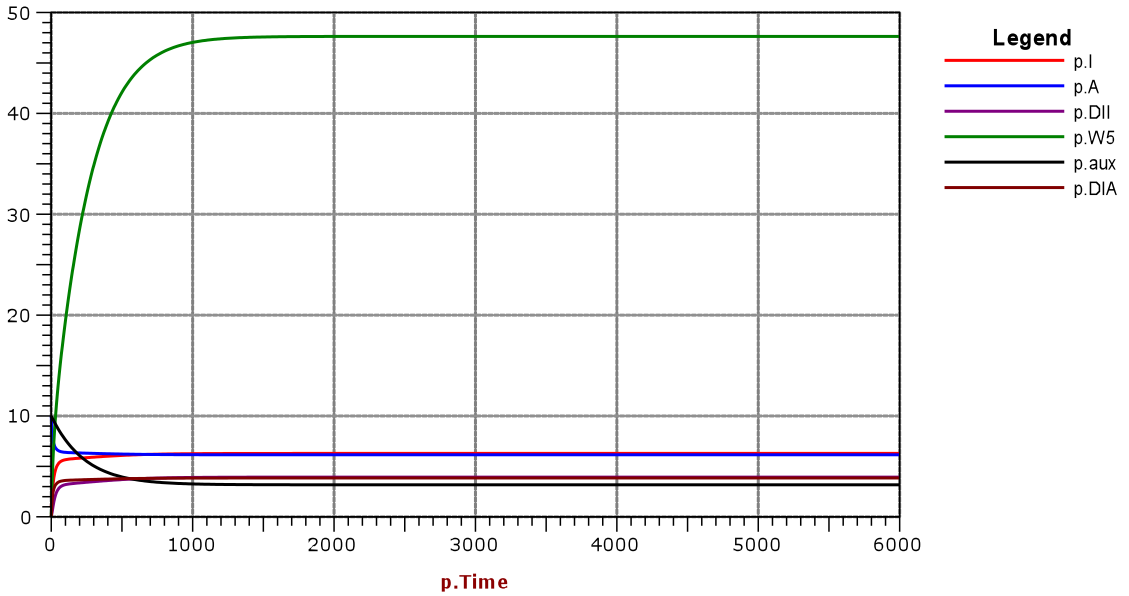

Figura 10. En esta gráfica se muestra como a un valor bajo de k_{am} (ARFi), *WOX5* se expresa. Valor $k_{am} = 1$.

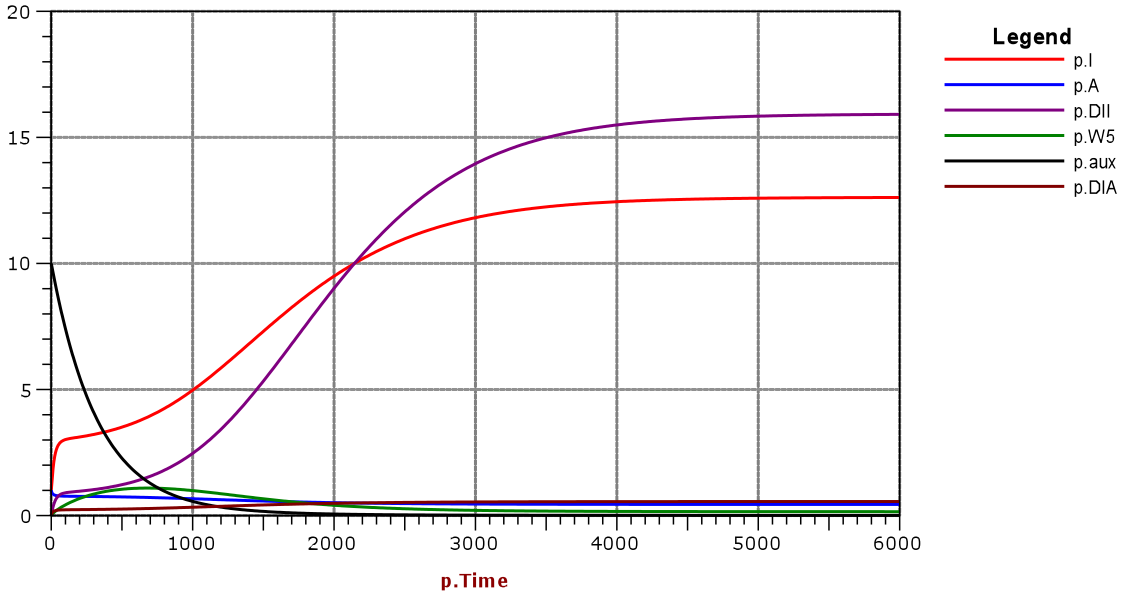

Figura 11. En esta gráfica se muestra como al elevar la concentración de los ARFi (el valor de la k_{am}), la expresión de *WOX5* se pierde. Valor $k_{am} = 3$.

Aunque este resultado es cercano al que buscamos, pues tenemos una condición en la que hay expresión de *WOX5* y otra en la que no, estos resultados no corresponden del todo a lo observado experimentalmente. Primero, la información experimental acerca de la expresión de *WOX5* parece estar definida por la concentración de auxina, mientras que en nuestro modelo depende de la relación

ARFa/ARFi, sin importar la cantidad de auxina. De esta forma, nosotros podíamos fijar manualmente la concentración de ARFi, de forma tal que obtuviéramos los resultados que nosotros queríamos, pero sin tener un modelo realmente explicativo. Por este motivo, decidimos incluir una segunda asa de retroalimentación y ver si así nos era posible obtener la biestabilidad. En un primer intento permitimos que *WOX5* reprimiera a los ARFi, pero de esta forma no conseguimos la biestabilidad. En un segundo intento permitimos que *WOX5* reprimiera a los Aux/IAA. La gráfica de las red se presenta en la *Figura 12*.

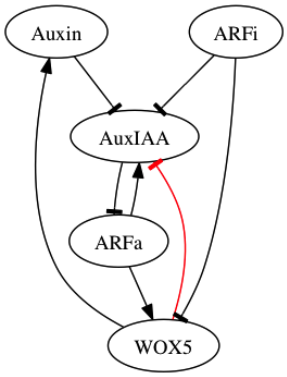

Figura 12. Gráfica de la red en la que se incluye la hipótesis donde *WOX5* inhibe a los Aux/IAA. La nueva interacción de *WOX5* sobre Aux/IAA se muestra en rojo.

La única diferencia de este modelo con respecto al otro se encuentra en la ecuación de Aux/IAA, que ahora queda así debido a la inhibición de *WOX5*:

$$\frac{dI}{dt} = \pi_i A^{n2}/(1 + k_{am}^{n2} + w5^{n3}) - \gamma_i \delta_i K_{aux} aux/(K_{aux} aux + 1) I$$

Esta red sí presenta un comportamiento biestable, como se muestra en las *Figuras 13 y 14*, donde se observa que dependiendo de la concentración inicial de auxinas la red llega a estados estables distintos, uno con y otro sin expresión de *WOX5*.

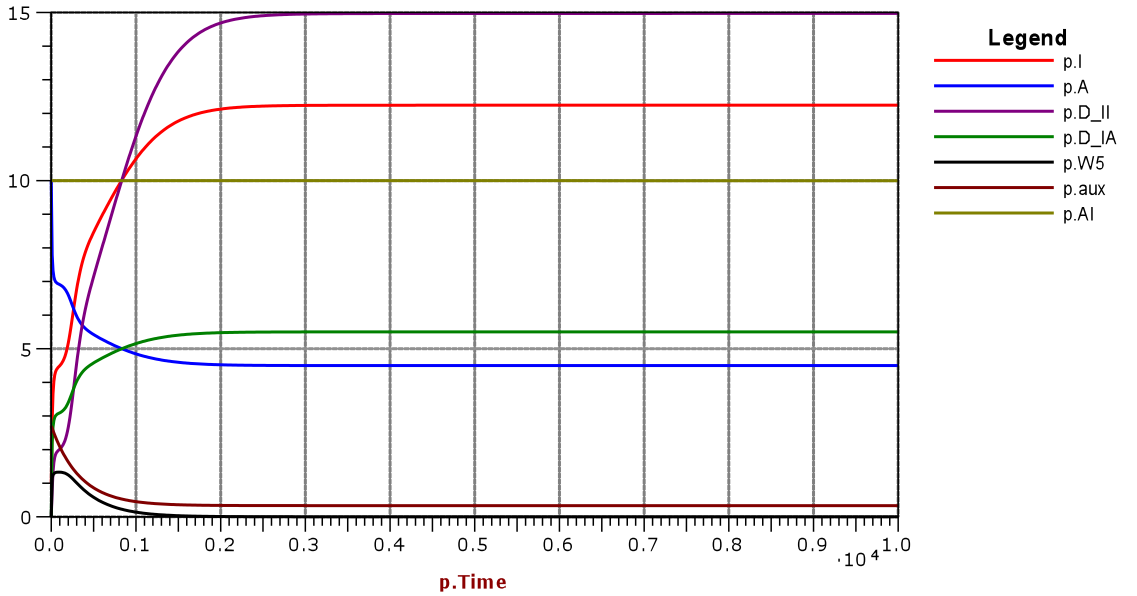

Figura 13. En esta gráfica se muestra como al iniciar el modelo con una concentración inicial auxina de 2.7, WOX5 no se expresa.

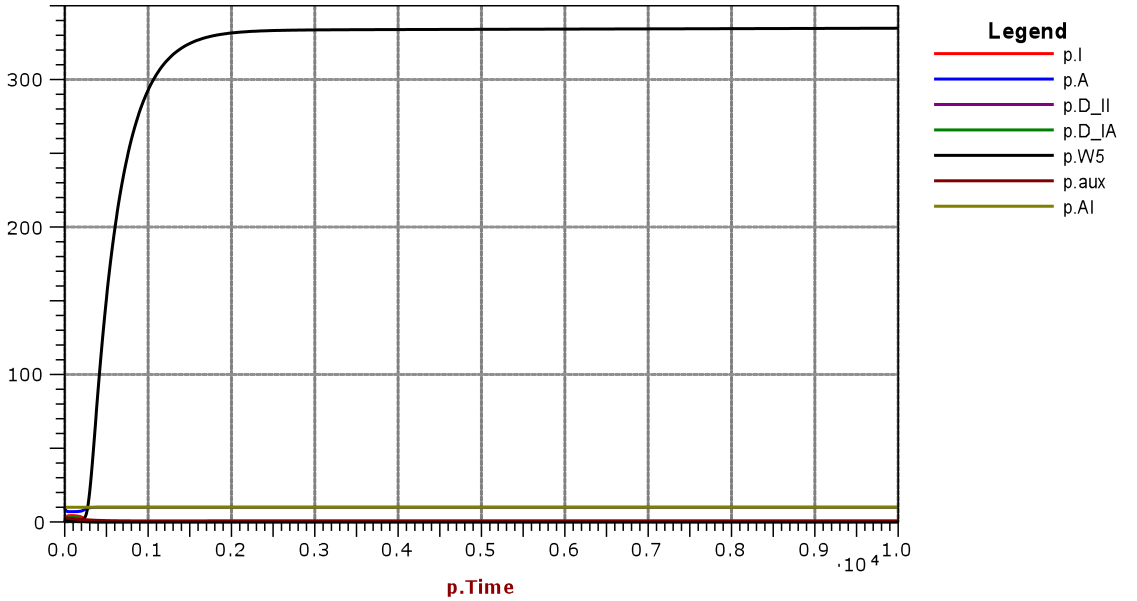

Figura 14. En esta gráfica se muestra como al iniciar el modelo con una concentración inicial auxina de 2.8, *WOX5* si se expresa.

Este modelo fue incorporado en el modelo de transporte de auxina. Los modelos anteriores de la red también se acoplaron con el transporte, sin embargo, los resultados obtenidos no concordaron con lo observado experimentalmente. Los resultados de integrar el modelo de transporte de auxina y la red biestable fueron los siguientes.

Debido a que el transporte de auxinas forma una gradiente a lo largo de la raíz, cuando acoplamos el transporte y la red, las células del centro quiescente son las únicas que tienen la concentración de auxina necesaria para detonar la expresión de *WOX5*. El gradiente no se ve afectado y se mantiene el máximo de concentración en el centro quiescente (*Figura 15*).

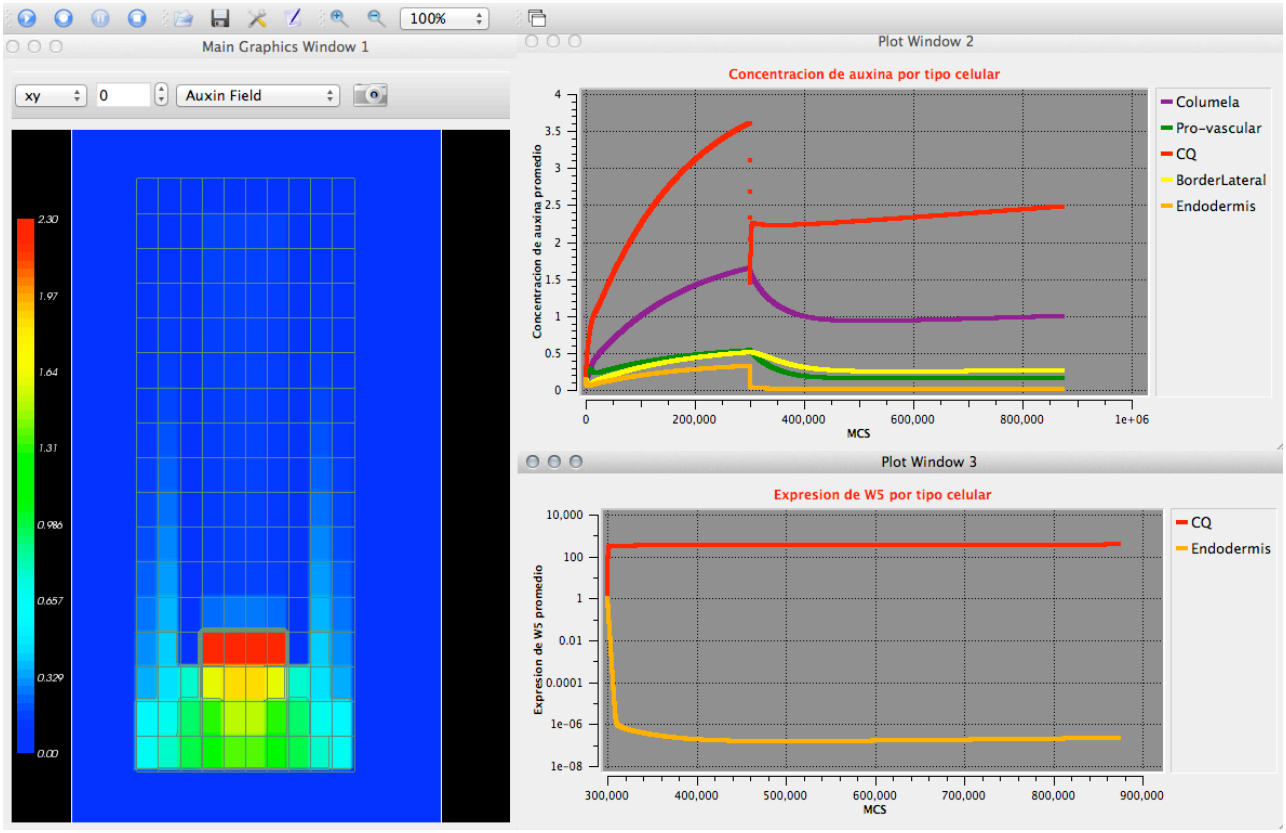

Figura 15. A la izquierda se ve el campo de concentración de auxina tras 890,000 pasos. Aunque disminuyen los valores de concentración de auxina en todas las células, el gradiente se mantiene. Arriba derecha se ve la concentración promedio de auxina por tipo celular. Abajo derecha se ve la concentración promedio de *WOX5* en centro quiescente y endodermis. Como se observa, *WOX5* solo se expresa en el centro quiescente.

Una vez obtenido este resultado, simulamos los mutantes para validar el modelo, aunque son pocos los mutantes reportados hasta el momento. Existen reportados mutantes de sobre expresión y perdida de función de *WOX5*. En el mutante de sobre expresión de *WOX5* se ha reportado que aumentan el número de células troncales, sin embargo no se sabe que pasa con el gradiente de auxinas ni con la expresión endógena del mismo *WOX5*, por lo tanto, al simular la sobre expresión de *WOX5* solamente estaríamos generando predicciones. Por otro lado la pérdida de función de *WOX5* parece aumentar el radio del dominio de expresión de *WOX5*

(Sarkar et al., 2007). Al simular este mutante, la expresión de *WOX5* se mantuvo en el mismo dominio, lo cual no corresponde con las observaciones experimentales. Los motivos por los que no logramos reproducir este mutante podrían depender de un motivo no incluido en el modelo, en el cual están involucrados péptidos móviles de la familia CLE-like (Stahl et al., 2009 y 2013). Sin embargo, se tendrán que hacer más pruebas para ver si esto es correcto.

También se sabe que la expresión de *WOX5* desaparece en los mutantes *mp* (Sarkar et al., 2007). *MP* es un *ARFa*, por lo tanto simulamos este mutante manteniendo la expresión de los *ARFa* en 0. En este mutante se pierde la expresión de *WOX5*, como se esperaba. No se sabe que ocurre cuando se aumentan o sobre expresan los *ARFa*, por lo que su simulación serían una predicción del modelo.

Se sabe que la sobre expresión de *ARFi*, disminuye la expresión de *WOX5* (Ding et al., 2010). En nuestro modelo la sobre expresión de *ARFi* (aumentado y fijando su concentración), ocasiona que desaparezca la expresión de *WOX5*, lo cual concuerda cualitativamente con lo observado experimentalmente. Finalmente, si se aumenta la concentración de auxinas se expande la expresión de *WOX5* en la capa de endodermis (Ding et al., 2010). Nosotros simulamos este mutante y nuestro primer resultado fue que *WOX5* expande su expresión a todas las células de la raíz.

Esto no concuerda con lo observado experimentalmente. Por este motivo pusimos una restricción en la expresión de *WOX5*, la cual esta basada en resultados tanto experimentales como teóricos. Se sabe que *WOX5* sólo se expresa en donde se encuentren los genes SHR y SCR, los cuales se expresan en centro quiescente y endodermis (Sabatini et al., 2003; Sarkar et al., 2007). También sabemos que somos capaces de reproducir este patrón de expresión, que es la red publicada por nosotros (Azpeitia et al., 2010). Al incluir esta restricción en la expresión de *WOX5* y volver a simular la adicción de WOX5 obtuvimos el resultado esperado. Es decir, si simulamos la adición de auxinas, *WOX5* expande su expresión a la capa de endodermis.

En un segundo momento, el aumentar la concentración de auxinas en la raíz ocasiona que la expresión de WOX5 desaparezca del centro quiescente y sólo se mantenga en endodermis en las capas más alejadas del centro quiescente (Zona de

transición o de elongación); el modelo no es capaz de reproducir esto. Con la finalidad de reproducir la desaparición de la expresión de *WOX5* al aumentar la concentración de auxinas hemos hecho dos modificaciones principales. En ambos casos lo que intentamos conseguir fue que los ARFi sean inducidos por la vía de las auxinas de la misma forma que lo es *WOX5*, pero con distintos umbrales, de tal forma que los *ARFi* sean inducidos a concentraciones más altas de los que es WOX5, permitiendo de esta manera que *WOX5* se reprima por los ARFi al aumentar la concentración de auxinas.

Sin embargo, hasta ahora ninguna de las variantes nos ha funcionado. Hemos conseguido mantener la biestabilidad, obtener oscilaciones y tener mono estabilidad, dependiendo del valor de los parámetros, pero nunca que se tenga expresión de *WOX5* en concentraciones intermedias de auxinas y que se pierda en concentraciones bajas y altas.

Como se puede observar, el trabajo de este modelo está aún en desarrollo, sin embargo comienza a producir los primeros resultados relevantes, y muestra como un motivo regulatorio relativamente pequeño y sencillo, pero con algunas asas de retroalimentación puede dar resultados complejos y difíciles de interpretar sin un modelo dinámico como el que se está usando para integrar e interpretar los datos experimentales que se han recabado en torno a la interacción de *WOX5* y las auxinas. Para la validación total del modelo será necesario poder recuperar los mutantes. Además, hasta el momento hemos usado los valores de parámetros reportados por Vernoux (2011), sin embargo hemos modificado las ecuaciones y han aparecido nuevos parámetros, por lo que se les tiene que hacer una validación al menos por una estimación de ellos. Por último, una vez validado el modelo, planeamos hacer algunas predicciones con él, como por ejemplo, que impacto tiene la sobre expresión de *WOX5* sobre las auxinas.

6. Conclusiones y discusión.

Como se mencionó antes, el objetivo principal del proyecto de doctorado fue generar y analizar los mecanismos moleculares involucrados en el desarrollo del nicho de células troncales de la raíz de *A. thaliana*, por medio del uso de herramientas matemático-computacionales, especialmente a través del uso de redes dinámicas de tipo Booleano (Azpeitia et al., 2010; Azpeitia y Alvarez-Buylla 2012; Azpeitia et al., 2013). Sin embargo, el proyecto me permitió explorar el uso de estos formalismos en otros sistemas (e.g., Alvarez-Buylla et al., 2010; Benítez et al., 2013), preguntas generales sobre los sistemas dinámicos (Azpeitia et al., 2011), así como abordar preguntas generales sobre las mismas herramientas (Azpeitia et al., 2013) y sobre la construcción de software para el uso de redes dinámicas (Arrellano et al., 2011).

En lo que respecta al objetivo principal de generar y analizar un modelo de la red de regulación genética del nicho de células troncales de raíz de *A. thaliana*, se obtuvo un primer modelo que mostró que la información experimental disponible hasta ese momento era insuficiente para explicar los resultados observados experimentalmente, pero que con la adición de posibles interacciones faltantes era posible recuperar de forma cualitativa, tanto la dinámica espacial como la dinámica temporal observada en el nicho. Es importante mencionar que las predicciones novedosas hechas por nosotros fueron confirmadas por grupos de investigación independientes al nuestro, ya fuera mientras nuestro manuscrito se encontraba en revisión (Stahl et al., 2009) o posterior a su publicación (Ding et al., 2010; Ogasawara et al., 2011).

La red mostró la falta de datos sobre algunos procesos que se sabe que son fundamentales para el mantenimiento del nicho, como lo es la información sobre los factores de transcripción *PLT*, de quienes no se sabe bien quien los regula y a quienes regulan, pero en cuyos mutantes múltiples el nicho se diferencia. La falta de datos, quedó evidenciada aún más cuando se actualizó la red, pues al incorporar nueva información experimental los resultados se alejaron más del comportamiento observado experimentalmente. Por este motivo generamos una metodología que nos permitiera identificar cuál podría ser la información faltante

en la red. Nuestra metodología consiste en seis procedimientos que permiten identificar posibles interacciones faltantes e información experimental errónea al mismo tiempo que se mantienen coherencia con los datos reportados experimentalmente (Azpeitia et al., 2013).

Tanto en el trabajo del 2010 como en el del 2013 apareció una predicción sobre las auxinas y su interacción con el factor de transcripción WOX5. Los datos experimentales mostraban que a pesar de que las auxinas que forman un máximo de concentración y de respuesta en el nicho, también inhiben la expresión de WOX5 (Sabatini et al., 1999; Ding et al., 2010). De acuerdo con nuestros modelo del 2010 y del 2013, un asa de retroalimentación de WOX5 a las auxinas era indispensable para mantener la expresión de WOX5 en el centro quiescente. Sin embargo, el asa de retroalimentación podía ser positiva o negativa dependiendo de la conectividad de otros genes de la red (Azpeitia et al., 2013). Por este motivo, en el trabajo en colaboración con la MSc. Mónica García, nos hemos enfocado en analizar el papel de las auxinas y su interacción con WOX5, con mucho mayor detalle. En este trabajo hemos logrado encontrar que sólo ciertas conectividades de la red, con comportamientos no lineales, son capaces de explicar los resultados observados experimentalmente. Aun así, esta parte del proyecto aún está en desarrollo y sus resultados son preliminares.

El proyecto de doctorado dejó varias preguntas abiertas. Quizá las que más nos interesan y hacia las que nos estamos dirigiendo son: ¿Cómo se regula el tamaño del nicho de células troncales? ¿Cómo se generan diferentes morfologías del nicho, cómo lo son la configuración abierta y la cerrada? ¿Cómo se integra la red del nicho con los procesos moleculares involucrados en otras partes de la raíz, como el desarrollo de la vasculatura, la transición a las distintas zonas de la raíz o del patrón radial de la raíz? ¿Cómo se integra la red del nicho con procesos a otras escalas y de otra naturaleza, como los son fuerzas físicas, celulares o de transporte de morfógenos, por mencionar algunos? ¿Hay similitudes entre la red de nicho de raíz, el de tallo y desarrollo vascular?¿Cuáles son las similitudes y las diferencias? Aun más, ¿hay similitudes a nivel dinámico, entre los mecanismos de mantenimientos de células troncales entre plantas y animales? Y si las hay, ¿cuáles son?

La respuesta a estas preguntas llevará tiempo. Sin embargo, creo que ha quedado un modelo suficiente para comenzar a investigar esta clase de preguntas. Aun más, el equipo del laboratorio se ha extendido y ha generado colaboraciones importantes para ir en esa dirección. Es importante destacar que respuesta a algunas de estas preguntas, probablemente se llevarán a cabo en colaboración con otros grupos de trabajo y proyectos en los que pude participar, como lo fue la generación de nuevos software (Arellano et al., 2011) o el rol de las fuerzas físicas en los procesos del desarrollo (Barrio et al., 2013).

El proyecto también se nutrió y nutrió de otros proyectos. Los análisis del comportamiento de la red fueron explorados a un nivel mesoscópico en colaboración con el grupo de Dr. Barrio. Los resultados de este trabajo mostraron que la dinámica de división celular observada en la raíz, se podía reproducir al integrar el flujo de auxinas, fuerzas mecánicas y a la división celular en un solo modelo. Es posible que este trabajo se integre en un futuro próximo con el trabajo de redes que se genera en el laboratorio. Esto permitiría comprender mejor como es que se da el proceso de desarrollo y morfogénesis de la raíz.

Por otra parte, se pudo llegar a una comprensión más profunda de las ventajas y limitaciones de las redes Booleanas en los trabajos desarrollados junto con el Dr. Rosenblueth y el Dr. Mendoza. Con el grupo del Dr. Rosenblueth se desarrollaron dos software para el análisis de redes Booleanas (Arellano et al., 2011; Muñoz Carrillo, Azpeitia y Rosenblueth *en preparación*). Quizás las mayores ventajas de el software desarrollado, es que son capaces de incorporar incertidumbres y restringir las posibles funciones Booleanas a funciones con significado biológico. Con el Dr. Mendoza se generaron los procedimientos utilizados en Azpeitia y colaboradores (2013) y luego se les uso para explorar su utilidad para llevar a cabo análisis de epistasis, idea planteada con anterioridad por nosotros (Azpeitia et al., 2011). Ambos trabajos dejan preguntan abiertas, pero quizá aun más importante es resaltar que se comienza un trabajo en conjunto, el cual pretende buscar características genéricas de las rede de regulación genética, haciendo uso del software y de los procedimientos.

Como conclusión general diría que en el proyecto de doctorado se ha generado una red del nicho, la cual es suficiente para comprender los mecanismos básicos

involucrados en su desarrollo y mantenimiento y que a la vez deja una gran gama de preguntas, desde preguntas especificas de los mecanismos, hasta preguntas genéricas de los procesos moleculares y preguntas evolutivas, ya sea de plantas o de plantas y animales. Pienso que estas preguntas ya pueden comenzar a ser trabajadas desde el punto en el que se encuentra actualmente la red. A su vez se propusieron y generaron procedimientos que formalizan y sistematizan la búsqueda de información faltante o errónea en una red genética.

7.- Referencias

Aida M, Beis D, Heidstra R, Willemsen V, Blilou I, Galinha C, Nussaume L, Noh YS, Amasino R, Scheres B. The PLETHORA genes mediate patterning of the Arabidopsis root stem cell niche. Cell. 2004 Oct 1;119(1):109-20.

Albert R, Othmer HG. The topology of the regulatory interactions predicts the expression pattern of the segment polarity genes in Drosophila melanogaster. J Theor Biol. 2003 Jul 7;223(1):1-18.

Alvarez-Buylla ER, Benítez M, Dávila EB, Chaos A, Espinosa-Soto C, Padilla-Longoria P. Gene regulatory network models for plant development. Curr Opin Plant Biol. 2007 Feb;10(1):83-91.

Alvarez-Buylla ER, Azpeitia E, Barrio R, Benítez M, Padilla-Longoria P. From ABC genes to regulatory networks, epigenetic landscapes and flower morphogenesis: making biological sense of theoretical approaches. Semin Cell Dev Biol. 2010 Feb;21(1):108-17.

Arellano G, Argil J, Azpeitia E, Benítez M, Carrillo M, Góngora P, Rosenblueth DA, Alvarez-Buylla ER. "Antelope": a hybrid-logic model checker for branching-time Boolean GRN analysis. BMC Bioinformatics. 2011 Dec 22;12:490.

Azpeitia E, Benítez M, Vega I, Villarreal C, Alvarez-Buylla ER. Single-cell and coupled GRN models of cell patterning in the Arabidopsis thaliana root stem cell niche. BMC Syst Biol. 2010 Oct 5;4:134. doi: 10.1186/1752-0509-4-134.

Azpeitia E, Benítez M, Padilla-Longoria P, Espinosa-Soto C, Alvarez-Buylla ER. Dynamic network-based epistasis analysis: boolean examples. Front Plant Sci. 2011 Dec 15;2:92.

Azpeitia E, Alvarez-Buylla ER. A complex systems approach to Arabidopsis root stem-cell niche developmental mechanisms: from molecules, to networks, to morphogenesis. Plant Mol Biol. 2012 Nov;80(4-5):351-63.

Azpeitia E, Weinstein N, Benítez M, Mendoza L, Alvarez-Buylla ER. Finding Missing Interactions of the Arabidopsis thaliana Root Stem Cell Niche Gene Regulatory Network. Front Plant Sci. 2013 Apr 30;4:110.

Azpeitia E, Davila-Velderrain J, Villarreal C, Alvarez-Buylla ER. Gene regulatory network models for floral organ determination. Methods Mol Biol. 2014;1110:441-69.

Barabási AL, Oltvai ZN. Network biology: understanding the cell's functional organization. Nat Rev Genet. 2004 Feb;5(2):101-13.

Barrio RA, Romero-Arias JR, Noguez MA, Azpeitia E, Ortiz-Gutiérrez E, Hernández-Hernández V, Cortes-Poza Y, Álvarez-Buylla ER. Cell patterns emerge from coupled chemical and physical fields with cell proliferation dynamics: the Arabidopsis thaliana root as a study system. PLoS Comput Biol. 2013 May;9(5):e1003026.

Benfey PN, Scheres B. Root development. Curr Biol. 2000 Nov 16;10(22):R813-5.

Benítez M, Alvarez-Buylla ER. Dynamic-module redundancy confers robustness to the gene regulatory network involved in hair patterning of Arabidopsis epidermis. Biosystems. 2010 Oct;102(1):11-5.

Benítez M, Azpeitia E, Alvarez-Buylla ER. Dynamic models of epidermal patterning as an approach to plant eco-evo-devo. Curr Opin Plant Biol. 2013 Feb;16(1):11-8.

Blilou I, Xu J, Wildwater M, Willemsen V, Paponov I, Friml J, Heidstra R, Alda M, Palme K, Scheres B. The PIN auxin efflux facilitator network controls growth and pattering in Arabidopsis roots. Nature, 2005 Jan 6; 433: 39-44.

Boudon F, Pradal C, Cokelaer T, Prusinkiewicz P, Godin C. L-py: an L-system simulation framework for modeling plant architecture development based on a dynamic language. Front Plant Sci. 2012;3:76.

Bugs CA, Librelotto GR, Mombach JC. A method to identify important dynamical states in Boolean models of regulatory networks: application to regulation of stomata closure by ABA in A. thaliana. BMC Genomics. 2011 Dec 22;12 Suppl 4:S10.

Chickarmane VS, Gordon SP, Tarr PT, Heisler MG, Meyerowitz EM. Cytokinin signaling as a positional cue for patterning the apical-basal axis of the growing Arabidopsis shoot meristem. Proc Natl Acad Sci U S A. 2012 Mar 6;109(10):4002-7.

Davidich M, Bornholdt S. The transition from differential equations to Boolean networks: a case study in simplifying a regulatory network model. J Theor Biol. 2008 Dec 7;255(3):269-77.

de Jong H. Modeling and simulation of genetic regulatory systems: a literature review. J Comput Biol. 2002;9(1):67-103.

Díaz J, Alvarez-Buylla ER. A model of the ethylene signaling pathway and its gene response in Arabidopsis thaliana: pathway cross-talk and noise-filtering properties. Chaos. 2006 Jun;16(2):023112.

Ding Z, Friml J. Auxin regulates distal stem cell differentiation in Arabidopsis roots. Proc Natl Acad Sci U S A. 2010 Jun 29;107(26):12046-51.

Espinosa-Soto C, Padilla-Longoria P, Alvarez-Buylla ER. A gene regulatory network model for cell-fate determination during Arabidopsis thaliana flower development that is robust and recovers experimental gene expression profiles. Plant Cell. 2004 Nov;16(11):2923-39.

Fauré A, Naldi A, Chaouiya C, Thieffry D. Dynamical analysis of a generic Boolean model for the control of the mammalian cell cycle. Bioinformatics. 2006 Jul 15;22(14):e124-31.

Fauré A, Naldi A, Lopez F, Chaouiya C, Ciliberto A, Thieffry D. Modular logical modelling of the budding yeast cell cycle. Mol Biosyst. 2009 Dec;5(12):1787-96.

García M. Modelos Celulares de Potts para la simulación espacio-temporal de la dinámica celular en el nicho de células troncales de la raíz de Arabidopsis thaliana. 2013. Tesis de Maestría en Química, Instituto de Ecología - Centro de Ciencias de la Complejidad , UNAM.

Galinha C, Hofhuis H, Luijten M, Willemsen V, Blilou I, Heidstra R, Scheres B. PLETHORA proteins as dose-dependent master regulators of Arabidopsis root development. Nature. 2007 Oct 25;449(7165):1053-7.

Gilbert SF. Developmental biology. Sixth edition. Sinauer Associates, Inc., Sunderland, MA, 2000, 749 p.

Gonzali S, Novi G, Loreti E, Paolicchi F, Poggi A, Alpi A, Perata P. A turanose-insensitive mutant suggests a role for WOX5 in auxin homeostasis in Arabidopsis thaliana. Plant J. 2005 Nov;44(4):633-45.

Gordon SP, Chickarmane VS, Ohno C, Meyerowitz EM. Multiple feedback loops through cytokinin signaling control stem cell number within the Arabidopsis shoot meristem. Proc Natl Acad Sci U S A. 2009 Sep 22;106(38):16529-34.

Grieneisen VA, Xu J, Marée AF, Hogeweg P, Scheres B. Auxin transport is sufficient to generate a maximum and gradient guiding root growth. Nature. 2007 Oct 25;449(7165):1008-13.

Guilfoyle TJ, Hagen G. Auxin response factors. Curr Opin Plant Biol. 2007 Oct;10(5):453-60.

Heisenberg CP, Bellaïche Y. Forces in tissue morphogenesis and patterning. Cell. 2013 May 23;153(5):948-62.

Jaeger J, Irons D, Monk N. The inheritance of process: a dynamical systems approach. J Exp Zool B Mol Dev Evol. 2012 Dec;318(8):591-612.

Jönsson H, Heisler MG, Shapiro BE, Meyerowitz EM, Mjolsness E. An auxin-driven polarized transport model for phyllotaxis. Proc Natl Acad Sci U S A. 2006 Jan 31;103(5):1633-8.

Lander AD. Pattern, growth, and control. Cell. 2011 Mar 18;144(6):955-69. doi: 10.1016/j.cell.2011.03.009.

Levesque MP, Vernoux T, Busch W, Cui H, Wang JY, Blilou I, Hassan H, Nakajima K, Matsumoto N, Lohmann JU, Scheres B, Benfey PN. Whole-genome analysis of the SHORT-ROOT developmental pathway in Arabidopsis. PLoS Biol. 2006 May;4(5):e143.

Liberman LM, Sozzani R, Benfey PN. Integrative systems biology: an attempt to describe a simple weed. Curr Opin Plant Biol. 2012 Apr;15(2):162-7.

Meyerowitz EM. Plants and the logic of development. Genetics. 1997 Jan;145(1):5-9.

Meyerowitz EM. Prehistory and History of Arabidopsis Research. Plant Physiology January 2001 vol. 125 no. 1 15-19

Mirabet V, Das P, Boudaoud A, Hamant O. The role of mechanical forces in plant morphogenesis. Annu Rev Plant Biol. 2011;62:365-85.

Mirabet V, Besnard F, Vernoux T, Boudaoud A. Noise and robustness in phyllotaxis. PLoS Comput Biol. 2012;8(2):e1002389.

Mironova VV, Omelyanchuk NA, Novoselova ES, Doroshkov AV, Kazantsev FV, Kochetov AV, Kolchanov NA, Mjolsness E, Likhoshvai VA. Combined in silico/in vivo analysis of mechanisms providing for root apical meristem self-organization and maintenance. Ann Bot. 2012 Jul;110(2):349-60.

Müller GB. Evo-devo: extending the evolutionary synthesis. Nat Rev Genet. 2007 Dec;8(12):943-9.

Müssel C, Hopfensitz M, Kestler HA. BoolNet--an R package for generation, reconstruction and analysis of Boolean networks. Bioinformatics. 2010 May 15;26(10):1378-80.

Newman SA, Bhat R. Dynamical patterning modules: a "pattern language" for development and evolution of multicellular form. Int J Dev Biol. 2009;53(5-6):693-705.

Ogasawara H, Kaimi R, Colasanti J, Kozaki A. Activity of transcription factor JACKDAW is essential for SHR/SCR-dependent activation of SCARECROW and MAGPIE and is modulated by reciprocal interactions with MAGPIE, SCARECROW and SHORT ROOT. Plant Mol Biol. 2011 Nov;77(4-5):489-99.

Perilli S, Di Mambro R, Sabatini S. Growth and development of the root apical meristem. Curr Opin Plant Biol. 2012 Feb;15(1):17-23.

Prusinkiewicz P, Crawford S, Smith RS, Ljung K, Bennett T, Ongaro V, Leyser O. Control of bud activation by an auxin transport switch. Proc Natl Acad Sci U S A. 2009 Oct 13;106(41):17431-6.

Purnell BA. Morphogenesis. Getting into shape. Introduction. Science. 2013 Jun 7;340(6137):1183.

Rademacher EH, Möller B, Lokerse AS, Llavata-Peris CI, van den Berg W, Weijers D. A cellular expression map of the Arabidopsis AUXIN RESPONSE FACTOR gene family. Plant J. 2011 Nov;68(4):597-606.

Reinhardt D, Pesce ER, Stieger P, Mandel T, Baltensperger K, Bennett M, Traas J, Friml J, Kuhlemeier C. Regulation of phyllotaxis by polar auxin transport. Nature. 2003 Nov 20;426(6964):255-60.

Rodríguez A, Sosa D, Torres L, Molina B, Frías S, Mendoza L. A Boolean network model of the FA/BRCA pathway. Bioinformatics. 2012 Mar 15;28(6):858-66.

Routier-Kierzkowska AL, Smith RS. Measuring the mechanics of morphogenesis. Curr Opin Plant Biol. 2013 Feb;16(1):25-32.

Sabatini S, Heidstra R, Wildwater M, Scheres B. SCARECROW is involved in positioning the stem cell niche in the Arabidopsis root meristem. Genes Dev. 2003 Feb 1;17(3):354-8.

Sablowski R. Plant stem cell niches: from signalling to execution. Curr Opin Plant Biol. 2011 Feb;14(1):4-9.

Salazar-Ciudad I. Developmental constraints vs. variational properties: How pattern formation can help to understand evolution and development. J Exp Zool B Mol Dev Evol. 2006 Mar 15;306(2):107-25.

Sankar M, Osmont KS, Rolcik J, Gujas B, Tarkowska D, Strnad M, Xenarios I, Hardtke CS. A qualitative continuous model of cellular auxin and brassinosteroid signaling and their crosstalk. Bioinformatics. 2011 May 15;27(10):1404-12.

Sarkar AK, Luijten M, Miyashima S, Lenhard M, Hashimoto T, Nakajima K, Scheres B, Heidstra R, Laux T. Conserved factors regulate signalling in Arabidopsis thaliana shoot and root stem cell organizers. Nature. 2007 Apr 12;446(7137):811-4.

Sabatini S, Beis D, Wolkenfelt H, Murfett J, Guilfoyle T, Malamy J, Benfey P, Leyser O, Bechtold N, Weisbeek P, Scheres B. An auxin-dependent distal organizer of pattern and polarity in the Arabidopsis root. Cell. 1999 Nov 24;99(5):463-72.

Schlatter R, Schmich K, Avalos Vizcarra I, Scheurich P, Sauter T, Borner C, Ederer M, Merfort I, Sawodny O. ON/OFF and beyond--a boolean model of apoptosis. PLoS Comput Biol. 2009 Dec;5(12):e1000595.

Shinohara N, Taylor C, Leyser O. Strigolactone can promote or inhibit shoot branching by triggering rapid depletion of the auxin efflux protein PIN1 from the plasma membrane. PLoS Biol. 2013;11(1):e1001474.

Smith RS, Guyomarc'h S, Mandel T, Reinhardt D, Kuhlemeier C, Prusinkiewicz P. A plausible model of phyllotaxis. Proc Natl Acad Sci U S A. 2006 Jan 31;103(5):1301-6.

Stahl Y, Wink RH, Ingram GC, Simon R. A signaling module controlling the stem cell niche in Arabidopsis root meristems. Curr Biol. 2009 Jun 9;19(11):909-14.

Stahl Y, Grabowski S, Bleckmann A, Kühnemuth R, Weidtkamp-Peters S, Pinto KG, Kirschner GK, Schmid JB, Wink RH, Hülsewede A, Felekyan S, Seidel CA, Simon R. Moderation of Arabidopsis root stemness by CLAVATA1 and ARABIDOPSIS CRINKLY4 receptor kinase complexes. Curr Biol. 2013 Mar 4;23(5):362-71.

Stoma S, Lucas M, Chopard J, Schaedel M, Traas J, Godin C. Flux-based transport enhancement as a plausible unifying mechanism for auxin transport in meristem development. PLoS Comput Biol. 2008 Oct;4(10):e1000207.

Swat MH, Thomas GL, Belmonte JM, Shirinifard A, Hmeljak D, Glazier JA. Multi-scale modeling of tissues using CompuCell3D. Methods Cell Biol. 2012;110:325-66.

ten Tusscher K, Scheres B. Joining forces: feedback and integration in plant development. Curr Opin Genet Dev. 2011 Dec;21(6):799-805.

Ten Tusscher KH, Hogeweg P. Evolution of networks for body plan patterning; interplay of modularity, robustness and evolvability. PLoS Comput Biol. 2011 Oct;7(10):e1002208.

Traas J, Hamant O. From genes to shape: understanding the control of morphogenesis at the shoot meristem in higher plants using systems biology. C R Biol. 2009 Nov;332(11):974-85.

Ulmasov T, Hagen G, Guilfoyle TJ. Dimerization and DNA binding of auxin response factors. Plant J. 1999 Aug;19(3):309-19.

van den Berg C, Willemsen V, Hage W, Weisbeek P, Scheres B. Cell fate and in the Arabidopsis root meristem determined by direccional signaling. Nature. 1995 Nov 2;378(6552):62-5.

van den Berg C, Willemsen V, Hendriks G, Weisbeek P, Scheres B. Short-range control of cell differentiation in the Arabidopsis root meristem. Nature. 1997 Nov 20;390(6657):287-9.

Van Norman JM, Benfey PN. Arabidopsis thaliana as a model organism in systems biology. Wiley Interdiscip Rev Syst Biol Med. 2009 Nov-Dec;1(3):372-9.

Van Speybroeck L, De Waele D, Van de Vijver G.Theories in early embryology: close connections between epigenesis, preformationism, and self-organization. Ann N Y Acad Sci. 2002 Dec;981:7-49.

Vernoux T, Brunoud G, Farcot E, Morin V, Van den Daele H, Legrand J, Oliva M, Das P, Larrieu A, Wells D, Guédon Y, Armitage L, Picard F, Guyomarc'h S, Cellier C, Parry G, Koumproglou R, Doonan JH, Estelle M, Godin C, Kepinski S, Bennett M, De Veylder L, Traas J. The auxin signalling network translates dynamic input into robust patterning at the shoot apex. Mol Syst Biol. 2011 Jul 5;7:508.

Wang RS, Saadatpour A, Albert R. Boolean modeling in systems biology: an overview of methodology and applications. Phys Biol. 2012 Oct;9(5):055001.

Weaver M, Hogan B. Powerful ideas driven by simple tools: lessons from experimental embryology. Nat Cell Biol. 2001 Jul;3(7):E165-7.

Weiss JN, Qu Z, Garfinkel A. Understanding biological complexity: lessons from the past. FASEB J. 2003 Jan;17(1):1-6.

8.- Apéndice

Utilizamos esta sección para presentar los trabajos de colaboración desarrollados a lo largo del doctorado que terminaron en la publicación del trabajo. De forma personal, los trabajos de colaboración fueron para mi unos de los trabajos más gratificantes y educativos. Las discusiones y posteriores reflexiones generados a partir de ellos fueron parte fundamental de mi desarrollo a lo largo del doctorado. Por este motivo, coloco copia de las publicaciones de estos trabajos, con la finalidad de no únicamente de hacerlos más accesibles a los lectores de esta tesis, sino también como forma de agradecimiento a todas las personas que estuvieron involucrados en ellos.

8.1. Parte I:

Artículo:

From ABC genes to regulatory networks, epigenetic landscapes and flower morphogenesis: making biological sense of theoretical approaches

Elena R. Alvarez-Buylla, Eugenio Azpeitia, Rafael Barrio, Mariana Benítez, Pablo Padilla-Longoria

Seminars in Cell & Developmental Biology

Seminars in Cell & Developmental Biology 21 (2010) 108–117

Contents lists available at ScienceDirect

Seminars in Cell & Developmental Biology

journal homepage: www.elsevier.com/locate/semcdb

Review

From ABC genes to regulatory networks, epigenetic landscapes and flower morphogenesis: Making biological sense of theoretical approaches

Elena R. Alvarez-Buylla[a,d,*], Eugenio Azpeitia[a,d], Rafael Barrio[b,d], Mariana Benítez[a,d], Pablo Padilla-Longoria[c,d]

[a] Instituto de Ecología, Universidad Nacional Autónoma de México, Cd. Universitaria, México, D.F. 04510, Mexico
[b] Instituto de Física, UNAM, Apdo, Postal 20-364, Mexico 01000, D.F. 04510, Mexico
[c] Instituto de Investigación en Matemáticas Aplicadas Sistemas, Universidad Nacional Autónoma de México, Cd. Universitaria, México, D.F. 04510, Mexico
[d] Centro de Ciencias de la Complejidad (C3), Universidad Nacional Autónoma de México, Cd. Universitaria, México, D.F. 04510, Mexico

ARTICLE INFO

Article history:
Available online 13 November 2009

Keywords:
Gene regulatory networks
Flower morphogenesis models
Simulations
Positional information
Epigenetic landscapes
Stochastic models

ABSTRACT

The ABC model postulates that expression combinations of three classes of genes (A, B and C) specify the four floral organs at early stages of flower development. This classic model provides a solid framework to study flower development and has been the foundation for multiple studies in different plant species, as well as for new evolutionary hypotheses. Nevertheless, it has been shown that in spite of being necessary, these three gene classes are not sufficient for flower organ specification. Rather, flower organ specification depends on complex interactions of several genes, and probably other non-genetic factors. Being useful to study systems of complex interactions, mathematical and computational models have enlightened the origin of the A, B and C stereotyped and robust expression patterns and the process of early flower morphogenesis. Here, we present a brief introduction to basic modeling concepts and techniques and review the results that these models have rendered for the particular case of the *Arabidopsis thaliana* flower organ specification. One of the main results is the uncovering of a robust functional module that is sufficient to recover the gene configurations characterizing flower organ primordia. Another key result is that the temporal sequence with which such gene configurations are attained may be recovered only by modeling the aforementioned functional module as a noisy or stochastic system. Finally, modeling approaches enable testable predictions regarding the role of non-genetic factors (noise, mechano-elastic forces, etc.) in development. These predictions, along with some perspectives for future work, are also reviewed and discussed.

Contents

* Corresponding author at: Instituto de Ecología, Universidad Nacional Autónoma de México, Cd. Universitaria, México, D.F. 04510, Mexico. Tel.: +52 55 56229013; fax: +52 55 56229013.
E-mail address: eabuylla@gmail.com (E.R. Alvarez-Buylla).

1084-9521/$ – see front matter © 2009 Elsevier Ltd. All rights reserved.
doi:10.1016/j.semcdb.2009.11.010

1. ABCs of flower development: from schemes to dynamic models

Although 20 years have passed since the publication of the ABC model of flower development [1–3], we still do not know why it works. We now have a thorough description of the spatiotemporal patterns of ABC gene expression patterns and mutant phenotypes (e.g., [4,5]) yet we do not know how the interactions among these and other genes dynamically render such patterns. Completely unraveling the dynamic mechanisms that underlie the ABC gene expression patterns and the stable ABC gene combinations necessary for floral organ specification and arrangement is still a challenge. These are, indeed, major issues since gene expression patterns, which are required for development to take place, are not a fixed or predetermined background field. Neither are they specified by single or simple combinations of genes, but are originated and dynamically maintained by several genetic and non-genetic factors that interact among themselves in non-linear manners [6,7]. Thus, in order to fully understand development, evolution and phenotypic transformation, it is essential to understand how gene expression patterns arise, and how such expression patterns coordinate with non-genetic factors during development.

We know that the ABC model works in *Arabidopsis thaliana, Antirrhinum majus* [3], as well as in other flowering species [8]. This suggests a robust underlying mechanism that resists environmental variations and that has been conserved throughout evolution. We have also learned from molecular genetics experiments that the genes involved in this model are necessary for the specification of the primordial cells that will eventually form sepals, petals, stamens and carpels from the floral primordium periphery to the center as flower development progresses [9]. However, we also know that these genes alone are not sufficient for this process [10,11]. Mathematical and computational models that integrate information systematically and help studying the dynamical aspects of flower development are useful for understanding how steady gene expression patterns, like those characterizing the ABC model, are generated. Actually, models that are able to follow the concerted and dynamic action of the ABCs with several other interactors have been used to postulate a regulatory module that is sufficient to recover ABC combinations in conjunction with other genes and proteins that have been shown to co-express with them (see review [12]). In contrast to schematic representations that depict gene regulatory interactions, dynamic models may consider the non-linear aspects of regulation and explore the way gene expression changes in time, both in wild type and perturbed simulated systems. Certainly, these models have helped to provide a dynamic account of the ABC model, as well as novel predictions and input for experimental studies. Nevertheless, important challenges, such as a complete understanding of the mechanisms and processes that lead to the observed morphogenetic patterns characteristic of flower development, are still open.

1.1. The gene regulatory module underlying cell-fate determination and morphogenesis during early flower development: the ABC genes are necessary, but not sufficient for flower organ specification

The ABC model integrates three classes of genes (A, B and C genes) and postulates that the combined expression of subsets of these classes specifies the different flower organs at early stages of flower development: A genes are necessary for sepal specification; A and B for petals; B and C for stamens; and C for carpels (reviewed in: [1,3–5], and elsewhere in this issue). A rather complete set of data concerning the interactors of the ABC genes has been gathered [5,12–15] for the model plant *A. thaliana* and, therefore, most modeling efforts concerning the ABCs have been done for this species.

Most plant species, including *A. thaliana* (Fig. 2), and especially eudicots, share an overall conserved flower body plan consisting of concentric whorls of organs: the two outermost rings are non-reproductive organs (sepals and petal) and the innermost are the reproductive organs (stamens and carpels) [9]. The temporal order with which ABC genes are expressed and the corresponding floral organ types specified are also quite conserved among higher eudicots. The A genes are turned on and the sepals determined first, then the B genes, and hence the AB combination and petals, and almost at the same time, the stamen and carpel cells are specified once the C genes are turned on and both BC and C genes alone are expressed ([16]; see Fig. 3).

Developmental processes, such as flower development, are often organized in a modular way, so different semi-autonomous processes or functions may be defined [17]. In this review, we focus on the regulatory module responsible for primordial cell-fate determination during early stages of flower development, in which the floral meristem is subdivided into the four concentric rings of cells that will form the floral organs [12,18,19]. We define a regulatory module as a set of molecules, signals or other kinds of interacting entities that constitute a functional unit and are sufficient for a process to occur. As units, modules can function fairly robustly and independently from other regulatory modules or entities (see, for e.g., [20,21]). Importantly, the gene regulatory module associated with cell-fate determination during the early stages of flower development seems to integrate environmental and internal signals (e.g., plant hormones) that also affect the flower meristem behavior, as well as to connect with other genetic modules involved in later stages of flower development (see review in [12]), for instance, in cell-type sub-differentiation and organogenesis processes.

Since the description of the ABC model, many other genes involved in flower organ determination have been described (reviewed in [14,15]). Several experiments have now demonstrated that flower organ determination depends on the expression and inter-regulation of the ABC genes (Fig. 2), but also of several non-ABC genes like *FLOWERING LOCUS T* (*FT*), *LEAFY* (*LFY*), *TERMINAL FLOWER1* (*TFL1*), *SEPALLATA genes* (*SEP1*, *SEP2*, *SEP3)* and *WUSCHEL* (*WUS*). The study of all of these genes has been instrumental for understanding flower development (e.g., [22–26]; and other reviews in this special issue) and has pointed at the genes and gene interactions that are fundamental to flower organ determination. Nevertheless, the characterization of isolated genes or of paired interactions is not enough to fully describe and understand the regulatory module that is necessary and sufficient for the spatial and temporal processes associated with flower organ determination. As we will review, studies of the collective action of many interacting genes are required and such studies have used mathematical models.

We now turn to the basic concepts and definitions of the models proposed by us and other groups in order to integrate molecular genetic experimental data on development. We then review the

achievements of such models, especially for understanding the ABC model.

2. GRN models for understanding development

Developmental processes involve complex interactions among multiple genetic and non-genetic elements, interactions that occur in a wide range of spatiotemporal scales. Consequently, different kinds of mathematical formalisms may be chosen depending on the scales relevant to the system under study and on the nature of the available data. Integrative approaches aiming at further understanding development may, however, encompass more than one type of model. Here, we summarize some of the basic mathematical methods and concepts related to gene regulatory network (GRN) modeling (see reviews by: [27,28]).

GRN models have been widely used to study gene collective dynamics as these and their regulatory interactions may be intuitively represented as dynamic networks. Moreover, these relatively simple models capture the non-linear character of the interactions associated with the logic of gene regulation and seem to be valid abstractions of such complex regulatory interactions, as they recover important features of their dynamics and observed stable multigenic configurations of cells at different stages of development. In these models, the nodes of the network correspond to genes, RNA, proteins or complexes that take part in gene regulation, while the edges stand for the positive or negative regulatory interactions among the network elements.

2.1. Discrete and continuous GRN models

There are two main approaches to modeling GRNs, namely, the *discrete* and *continuous* methods. These two approaches differ in scope; yet, they often yield equivalent qualitative results when applied to concrete biological systems (e.g., [21]). This equivalence suggests that the logic and overall dynamics of gene regulation depend mostly on the network architecture and signs of the interactions, rather than on the details of the mathematical specification of the GRN.

2.1.1. Discrete models

The simplest case of discrete GRNs is that of the so-called Boolean networks, first put forward by Kauffman ([29]; see Fig. 1). In such models, nodes can be in one of two activation states in time t, 0 (off) or 1 (on), depending on the state at time $t-1$ of the elements that regulate each of them. The regulatory interactions determining the changes in gene activation states are defined as logical rules in which logical connectors such as OR, AND or NOT are used. Equivalently, the logical rules might be represented as tables providing a corresponding output for a given input gene profile.

For GRNs based on empirical evidence, the information needed to define logical rules is obtained from diverse experimental results (gene expression patterns, loss and gain of function phenotypes, protein interaction assays, etc.). Then, the activation state of every gene is given by:

$$g_n(t+1) = F_n(g_{n_1}(t), g_{n_2}(t), \ldots, g_{n_{k_n}}(t)), \quad (1)$$

where $\{g_{n_1}, g_{n_2}, \ldots, g_{n_{k_n}}\}$ are the regulators of the gene g_n, and F_n is the discrete function or logical rule.

Given the set of logical rules defining the GRN dynamics, it is possible to update the gene states. In many cases of interest, they all eventually attain a steady or equilibrium state. Those GRN steady states at which all of the nodes (initial conditions) end up are usually referred to as *attractors*. Kauffman [29] suggested that GRN attractors corresponded to sustained gene activation profiles characteristic of particular cell types and this has been substantiated experimentally and validated in a handful of modeled systems (e.g., [21,30,31]; see Fig. 2). Additional experimental and theoretical studies suggest that regulation at the transcriptional level might be better represented by discrete, rather than continuous models (e.g. [32]).

2.1.2. Continuous models

Continuous GRNs are defined by coupled non-linear differential equations describing changes in the concentration (rather than the state of expression) of the molecules involved in the gene regulation processes. In continuous GRNs, nodes can take an infinite number of state values and the equilibrium points may be found by analytic means. Just like the attractors of discrete GRNs, these equilibrium points are thought to match gene activation configurations typical of particular cell types. This description stands on largely developed analytical tools and is especially useful when the system under consideration has few nodes, since large networks become intractable with this approach.

The continuous approach can incorporate effects such as active transport, diffusion, and elastic or mechanical phenomena, among others. Moreover, this kind of implementation can include more detail on the kinetics of gene regulation and yield quantitative predictions that have provided insights into signal transduction and oscillatory systems. The detailed experimental data to obtain parameter values for the differential equations representing such models are, however, extremely scarce.

As mentioned above, both discrete and continuous GRN models enable a characterization of the collective gene regulatory dynamics in terms of, among other features, the number and nature of attractors and equilibrium points.

2.2. Deterministic and stochastic GRN dynamics

Deterministic GRNs are those for which it is possible to know the state of every node at every moment, given an initial configuration. In contrast, stochastic GRNs consider the noise originated, for instance, by small numbers of molecules (example of a source of intrinsic stochastic fluctuation due to the small sample sizes), environmental fluctuations (example of a source of external stochastic fluctuations) or other sources of uncertainties. In stochastic models, the updating rules, discrete or continuous, depend partially on a stochastic variable, which, instead of attaining a fixed value, has a distribution of possible values or states. This is, in fact, a more realistic representation of a biological system (review in [33]). Introducing stochasticity into GRN models has provided interesting results suggesting, for example, that noise may play a constructive role in biological systems (details below and in [34]).

3. Morphogenetic models encompassing GRNs

Even though GRN models are indeed useful to study development and other biological processes, these generally constitute abstractions of the one-cell level gene regulatory processes and do not consider cell-to-cell communication, spatial components of development or cellular dynamics, among other important aspects of morphogenesis. In general, to understand cell-fate determination, one has to explain how identical cells become sufficiently different as to appear as a particular type of cell (Fig. 1). It is an undeniable fact that the expression of genes, through their organization in GRNs, is a central issue in the whole process of differentiation: undifferentiated cells share the same gene expressions and differentiated ones certainly express their genes differently. However, it is evident that the genes by themselves have no means of canalizing which attractors of their GRN to "choose", and it is mostly seen that this "decision" is driven by the situation (e.g., depending on its

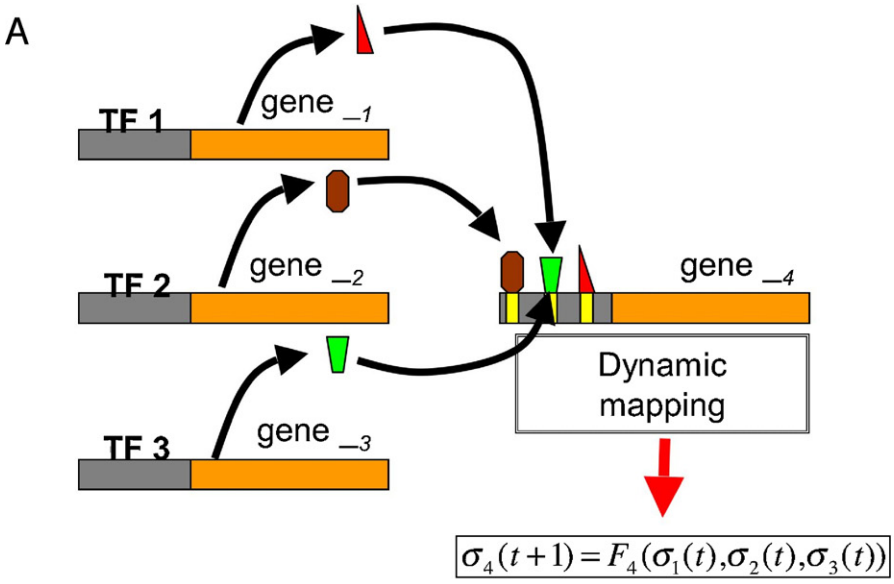

σ_1	σ_2	σ_3	$F(\sigma_1, \sigma_2, \sigma_3)$
1	1	1	1
1	1	0	1
1	0	1	1
1	0	0	1
0	1	1	0
0	1	0	0
0	0	1	1
0	0	0	0

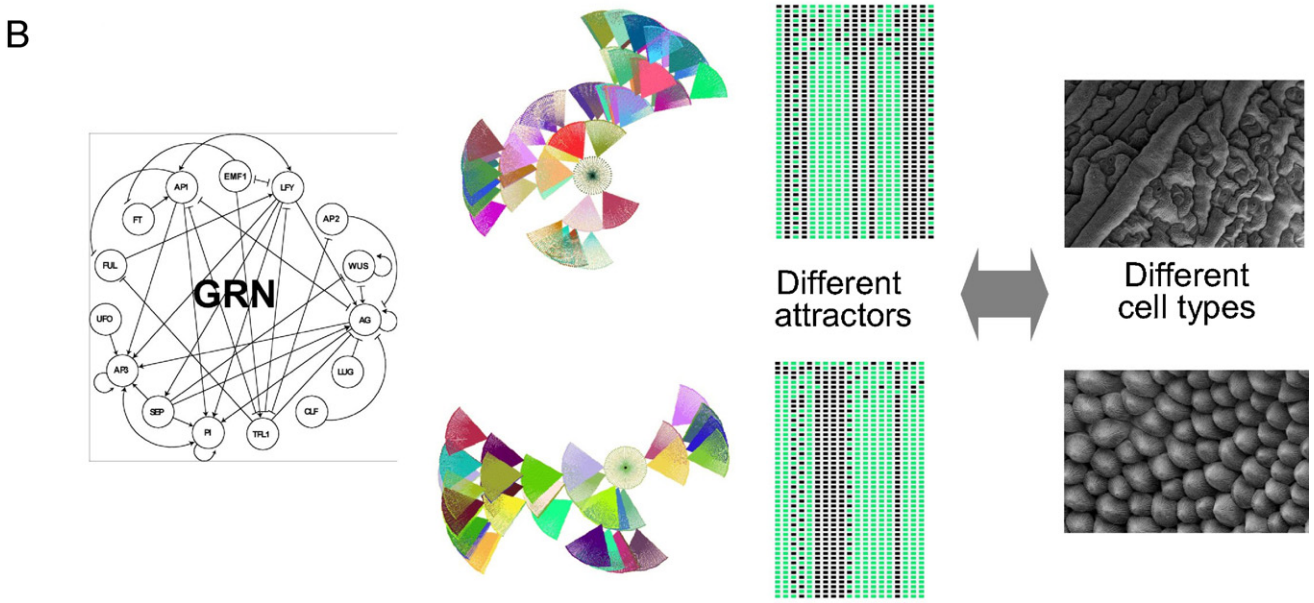

Fig. 1. The dynamic modeling of gene regulatory networks (GRNs). (A) GRNs are established by the non-linear cross-regulation of genes. Here, three transcription factors that regulate a target gene are exemplified. Each gene or node in a GRN is regulated by k transcription factors. If GRNs are modeled with discrete dynamic models, each gene has a truth table as the one shown here, in which the combinations of gene activation states (gene configurations of k entries, in this example, $k = 3$) leading to an "ON" or "OFF" activation state of the target gene are tabulated. Hence, the dynamics of the expression state of each gene is given by a Boolean logical function (Fn), which, in turn, depends on the expression states in previous time steps, of the genes that regulate it. Each gene configuration (conformed in the Boolean case of 0's and 1's or initial configuration of a GRN, will lead to a stable configuration, which is called an attractor state. Attractors can be of the fixed-point type (a single configuration), or cyclic (several configurations). Kauffman proposed that GRNs underlying cell differentiation may attain fixed-point attractors, in which configurations correspond to multigenic profiles characterizing each cell type. (B) In this figure, we show a diagram for the set of initial configurations that lead to the sepal and petal stable configurations or attractors. All of the configurations that lead to a given attractor are called basins of attraction. Hence the basins of attraction of sepal and petal primordial cells are shown in the form of colored fan diagrams with the attractors' configurations in the point in the central part or to which all other converge via connecting lines in these fan diagrams and all the possible configurations in the points around such central one. The colors, lengths or angles of the lines in the fan diagrams do not have any meaning and are drawn as such just for design reasons. However the number of points and lines do indicate the number of configurations that lead to each attractor (point to which all others converge). In tabular form, to the right of the basins of attraction, an example of how different initial configurations ("ON" in green and "OFF" states in black) lead to different attractors is shown. On the right, scanning electron micrographs of sepal (top) and petal (bottom) cell types are shown.

lineage) or position of the cell in the organism. Therefore, it is essential that each cell extracts temporal and positional information from its environment, and for this we need to postulate processes that generate this positional information at all times, and produce changes in the operation of the identical GRN accordingly (Fig. 4). That is, short-range (cell-to-cell) and long-range communication are needed to allow a complete relative positional information and the regulation of sizes and dimensions of tissues, as well as the relative position of organs.

This is why one of the challenges ahead consists of rendering spatio-temporal models that consider GRNs in cellularized domains and that encompass cellular dynamics, chemical gradients, cell-to-cell communication, etc. (Fig. 4). There have now been some efforts in this direction (e.g., [35,36]). For instance, GRN models have recently contributed to specify the metaphor of *epigenetic landscapes* [37,38] for particular systems. In such a metaphor, developmental processes are viewed as a ball rolling through pathways in a landscape, and the topology of the landscape is defined by the

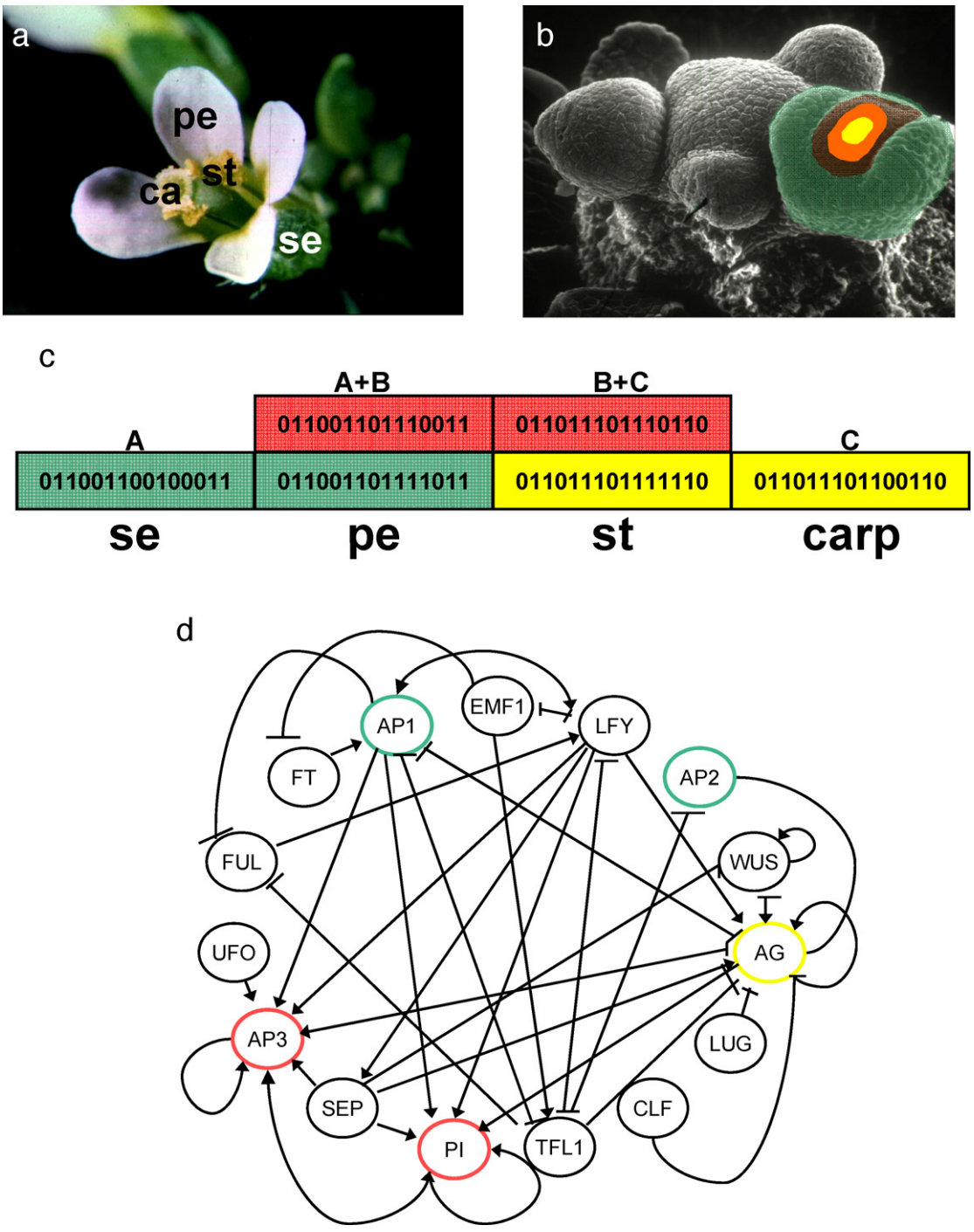

Fig. 2. The *Arabidopsis thaliana* flower has the stereotypical floral arrangement of eudicots, with sepals, petals, stamens and carpels from the periphery to the flower center. (a) Flower meristems form in the axils of rudimentary bracts that appear in the flanks of the inflorescence meristem of which a scanning electron micrograph is shown in (b). Here a flower meristem in which the sepal primordia are already visible is colored with the primordial cells of sepals in green (A function alone), those of petals in brown grey (green and red from A + B functions), the stamens in orange (yellow and red from B + C functions) and the carpels in yellow (C function alone). In (c), the ABC model and the floral organ determination GRN (FOS-GRN) stable configurations that correspond to A, A + B, B + C and C gene combinations necessary for sepal, petal, stamen and carpel development, respectively. The activation states correspond to each of the GRN nodes starting on the left with "EMF1" and consecutively progressing clockwise the rest of the genes in the GRN shown in (d). (d) The FOS-GRN that underlies the dynamic attainment of the ABC combinations, with the A, B and C genes colored as in (c). In the FOS-GRN, arrows correspond to activations and blunt ended edges to repressions.

interactions among genes and other elements (Fig. 3). Continuing with the metaphor, the bottoms of valleys correspond to steady states or final stages of development (e.g., the attractive states of GRNs as defined above). Yet further work needs to be done in order to generate integrative morphogenetic models. Some general ideas for advancing these kinds of models for the case of flower development will be discussed below.

4. The floral organ specification GRN (FOS-GRN): recovering the ABC gene configurations characteristic of primordial cell types during early flower development

We have modeled the experimentally grounded GRN model for flower organ specification (FOS-GRN) that integrates molecular genetic data for the ABC genes and their main interactors

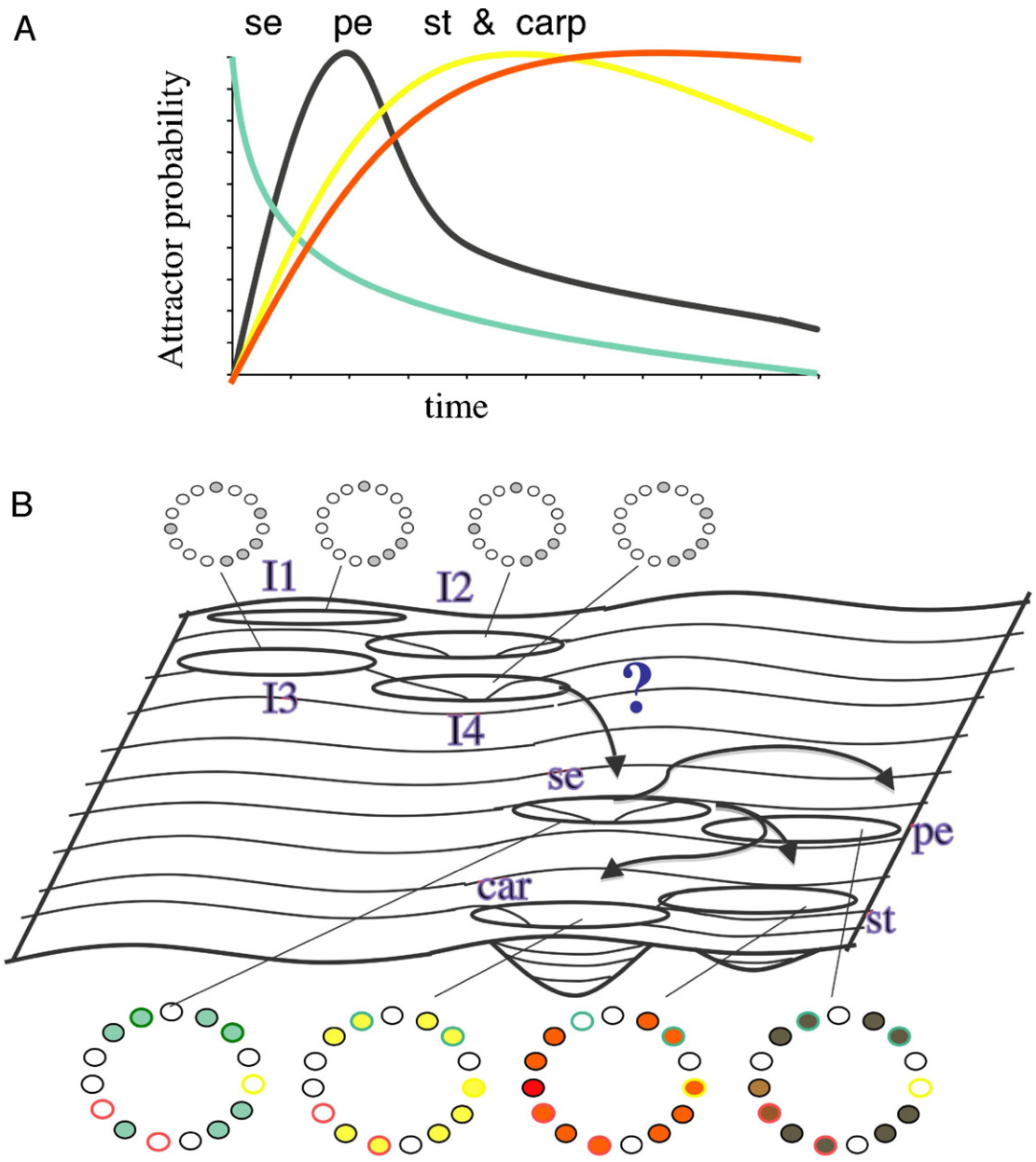

Fig. 3. The four floral organs appear in a well-defined temporal sequence that is recovered by a stochastic GRN model. Sepal primordial cells are the first to be specified (green), then petals (brown) and finally, almost at the same time, stamens (orange) and carpels (yellow). (A) Alvarez-Buylla et al. [34] demonstrated that stochastic perturbations in the FOS-GRN in Fig. 2 are sufficient to recover the observed temporal sequence of ABC gene expression and floral organ specification. (B) A schematic representation of the epigenetic landscape generated by a stochastic exploration of the FOS-GRN for flower development. This schematic landscape is equivalent to the epigenetic landscape proposed by Waddington [37]. Basins comprise the cell genetic configurations that lead to attractors (in this case, gene configurations characteristic of floral organ primordial cell-types: sepals, petals, stamens, and carpels. Se: Sepals (green), pe: petals (brown), st: stamens (orange), car: carpels (yellow).

([30,34,39,40]; Figs. 1 and 2). This GRN includes key regulators underlying the transition from shoot apical meristem once it produces the apical inflorescence (we call it the inflorescence meristem, IM) to flower meristem (FM) (*FT, TFL, EMF*, *LFY, AP1*, *FUL*), the ABCs and some of their interacting genes (*AP1*, *AP3*, *PI*, *AP2*, *AG*, *SEP*), as well as some genes that link floral organ specification to other modules regulating primordia formation and homeostasis (*AG*, *CLF* and *WUS)*, and some regulators of organ boundaries (*UFO* and *LUG)*.

Interestingly, the postulated discrete regulatory module has over 130,000 different 15-gene activation configurations, but it only converges to ten attractors: four corresponding to gene combinations characteristic of four sub-regions in the IM, and the rest to gene activation states configurations observed in sepal (one attractor), petal (two attractors; with and without *UFO* "ON"), stamen (two attractors; with and without *UFO* "ON") and carpel (one attractor) primordia (Figs. 1 and 2; see [30]). This first result is outstanding, as it is extremely rare that randomly generated complex networks of the size of this one attain so many fixed-point attractors (ten in this case). This result also suggests that the postulated regulatory module is robust to certain alterations (i.e., those stemming from its connections to other components not considered here and which modify the initial configurations of the FOS-GRN) and that this GRN is sufficient to specify gene configurations characteristic of primordial cells during the first stages of flower organ development, thus constituting a functional module.

Various robustness analyses were performed on the FOS-GRN and showed that the recovered attractors are also robust in the

face of permanent alterations of the logical functions of gene interactions and gene duplications [30,40,41]. These results suggest that the multigenic configurations that are sufficient for flower organ specification, dynamically and robustly emerge from complex networks of molecular components, rather than from a series of linear or hierarchical gene interactions, or from the action of particular genes or simple gene combinations. Moreover, the robustness analyses indeed support that such a GRN could account for the overall widespread conservation of the ABC patterns and floral bauplan (particularly that of eudicots; see [9,42,43]).

Since the first publications of the FOS-GRN [39,44], this GRN has been continuously updated. However, the basic structural characteristics of it have been stable and the additions, while providing important new insights, have not substantially altered the main conclusions originally put forward. Recent updates have been implemented with the new software, ATALIA (available at: http://www.ecologia.unam.mx/~achaos/Atalia/atalia.htm), developed in the Alvarez-Buylla laboratory by Alvaro Chaos. This software can run a GRN dynamics and obtain its attractors, basins of attraction, among other significant dynamic signatures (see examples in [12]).

In conclusion, the basic FOS-GRN proposed has provided a sufficient explanation for the observed ABC patterns and the stable gene expression configurations observed in IM and FM during early flower development in *A. thaliana*. Such dynamic account of the robustness and overall dynamic effects of particular genetic alterations would have been impossible to achieve without integrative approaches considering mathematical models and computer simulations.

5. Temporal and spatial patterns of cell-fate attainment during early flower development

The FOS-GRN reviewed above only considers a deterministic, single-cell GRN that is able to recover different gene configurations, which can be compared to observed gene profiles in different primordial cell types at early stages of flower development. However, in real developmental processes, groups or populations of cells attain distinct fates with certain spatial and temporal patterns. Thus, as mentioned above, we need morphogenetic models that are able to recover and enlighten such temporal and spatial morphogenetic patterns.

We have addressed the challenge of studying the temporal pattern of flower organ determination by exploring the sequence with which attractors for primordial flower organs are attained. We achieved this goal by introducing stochasticity into the GRN model described in the previous section. Since biological systems have evolved in inherently noisy environments, it is postulated that GRNs have been assembled in such a way that observed patterns are recoverable under noisy conditions. Indeed, recent studies show that stochasticity at the molecular scale may actually contribute to the formation of spatio-temporal patterns at higher levels of organization during development in other systems (see reviews in [33,45]).

Considering that noise could trigger transitions among attractors, we expected that in a stochastic model for a population of cells initialized in the sepal state (A genes expressed), the next most probable state would be AB (petals), then BC (stamens) and C (carpels) [9,46,47]. By introducing a certain degree of error in the updating of the dynamical rules of the FOS-GRN we actually recovered such a temporal sequence of cell-fate and ABC gene activation combinations ([34]; Fig. 3). In the latter study, this result was repeated with two GRN versions: the Boolean one described above and a continuous implementation that mimics the discrete case.

6. Recovering the epigenetic landscape of the FOS-GRN

Having shown that noisy fluctuations alone are able to drive transitions among attractors and that those transitions follow temporal patterns that reproduce the sequence with which ABC-genes are activated, it is reasonable to use the stochastic GRN model to postulate an epigenetic landscape (EL; [37,38]) associated with flower organ determination. Such an EL would be generated by the stochastic GRN dynamics and the GRN attractors would constitute the landscape's valleys (Fig. 3). It is interesting to note that, far from what could be intuitively expected, noise should not always be considered as a perturbation favoring disorder or instability. On the contrary, in view of these results, noise should be considered as a necessary factor in order for some developmental features to emerge in a robust way; in this case, the typical temporal sequence of activation of some genes, and probably also the spatial arrangement of gene configurations to some extent.

Studies with the stochastic version of the FOS-GRN also concluded that the relative position of the landscape's basins (GRN attractors) is important in determining the most probable temporal sequence of cell-fate attainment referred above [34]. This fascinating result certainly suggests that the stereotypical temporal pattern of cell-fate specification within the floral meristem at early stages of flower development may be an emergent and robust consequence of the complex GRN underlying cell-fate determination. In principle, such temporal sequence of cell differentiation could take place in the absence of inductive signals, emerging only as a result of the stochastic fluctuations that occur during transcriptional regulation [12].

Conceptually, this analysis was performed in a population of cells (or GRNs), updating each genetic configuration independently of each other. The next modeling step will be the integration of a collection of these networks, corresponding to the meristem, in a spatio-temporal framework (Fig. 4). This will allow a better understanding of the morphogenetic implications of the structure of the EL and is the object of current research. Moreover, this approach can also be used to test specific hypotheses. Questions of special interest are: (i) what is the mechanism by which the spatial disposition of the floral whorls is established, and (ii) what is the minimum number of necessary changes in the FOS-GRN and in the corresponding EL required for the whorls corresponding to stamens and carpels to be exchanged as in the atypical plant *Lacandonia schismatica* ([48,49]).

In another theoretical study, Lenser et al. [50] formulated a computational model that enabled the testing of the role of joint self-regulation of DEF-like and GLO-like floral homeotic genes in the robustness of petal and stamen development when stochastic noise is considered. In accordance with the results reviewed above, the authors found that the heterodimerization of these B floral homeotic proteins enhanced the robustness of cell-fate organ determination in the presence of stochasticity. Furthermore, their analysis suggests that mechanisms such as protein heterodimerization may play a central role in the canalization of flower development and evolution. This kind of prediction can hardly be formulated or tested without the aid of dynamical models.

7. Not in the genes: the role of geometrical and mechanical forces during development

A complete understanding of flower morphogenesis will continue to require multidisciplinary approaches and modeling tools that help at underpinning the coupling of such single-cell GRNs in explicit spatial and cellularized domains (e.g., [35,36,51]), with aspects like morphogen (e.g., auxin) metabolism, signaling pathways, gradients, cell growth and proliferation, mechanical forces,

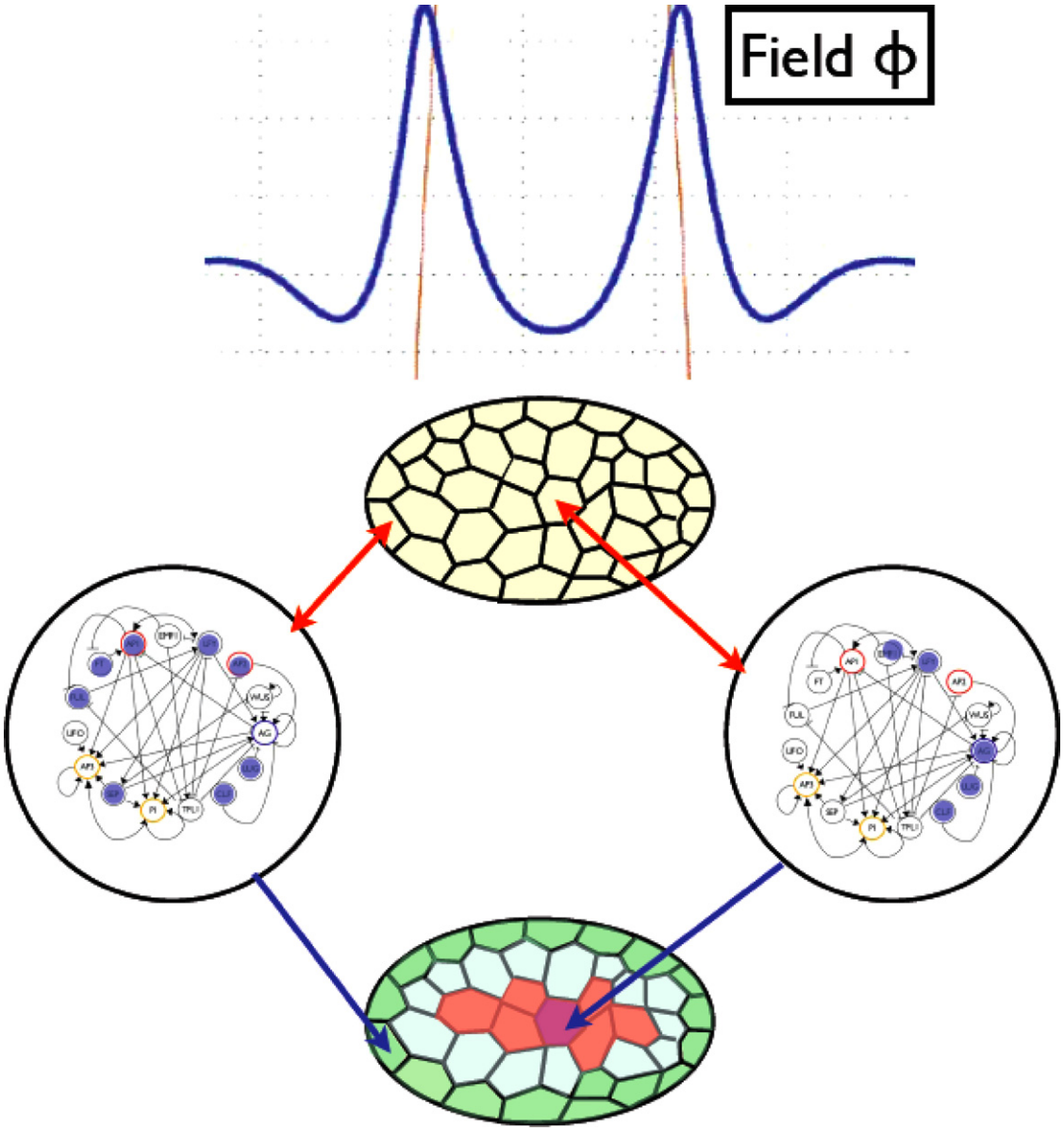

Fig. 4. Feedback between the FOS-GRN and physical fields could lead to the establishment of different regions within the meristem, each reaching the same stable multigene expression configurations or attractors. An idealized diagram illustrating the coevolution process of cell differentiation in a meristem is shown. A group of undifferentiated or stem cells (in yellow) secrete substances that produce a physical field of concentrations (ϕ) that forms a spatial pattern. According to the value of this field, the GRN of each cell (encircled) attains a different attractor, with a particular gene expression configuration that locally modifies the field, as well (double red arrows). Eventually, such a feedback process will allow cells to attain a different fate and become, for example, committed to form sepals or petals (cells with different colors at the bottom), depending on their relative position in the meristem.

and cell–cell communication mechanisms. All such aspects are likely to interact in non-linear ways both to and from the intracellular GRNs regulating cell differentiation and proliferation.

A central question in developmental biology is whether and how mechanical forces serve as cues for cellular behavior and thereby regulate morphogenesis [52]. Perhaps the most challenging aspect in understanding how mechanics, geometry and growth contribute to the formation of functional and robust structures is that these aspects not only influence each other, but are also coupled with at least two other fundamental interactions, genetic regulation and the cell cycle, at different time and spatial scales.

Several processes of cell communication may be relevant to understanding development, either by direct contact through their membranes, by the release of chemicals to the intercellular space, by electrical signals [53] or by the detection of pressure gradients and changes of curvature in tissue or organ surfaces [54]. Let us concentrate on the chemical signals, because meristematic cells are continuously exchanging and releasing all sorts of compounds (such as mRNAs, proteins, amino acids, hormones, etc.) to the extracellular matrix. These compounds must arrange themselves in space to form a macroscopic pattern of molecules, which, in turn, should be detected by GRNs in each cell altering their gene expression configurations accordingly. In other words, in order to accomplish this extraordinary choreography (without a choreographer!), the behavior of the chemicals and communication mechanisms should be coupled to the dynamics of the GRN in such a way that the chemical composition dictates the attractor of the GNR, and at the same time, the modified gene activity configuration of the GRN regulates the spatial pattern of chemical concentrations.

As mentioned before, the famous ABC model is able not only to predict the specification of the four whorl types in the flower, but also the different mutations found when one or several of the

ABC gene functions is lost. The problem is that this model does not explain why the spatial disposition of organs is ordered in concentric regions with the correct geometry or spatial arrangement and in the correct temporal sequence, that is, it does not address the central problem of self-organization in space–time during cell differentiation. In our opinion, this central issue remains unsolved.

The problem could be stated as follows: the GRN in each cell in the meristem is in a state of undifferentiated complacency, yet producing certain chemicals that act as transcription factors. These substances move in the intercellular space and respond to some physical field that dictates their concentrations in different regions of space, forming a geometrical pattern in space, which, in turn, provides each genetic network with a chemical environment that depends on this geometry (Fig. 4). The pertinent GRN for flower development in each cell senses this composition of chemicals and changes its configuration, expressing its genes in a different way, reaching a particular attractor (stable configuration of gene expression states), and consequently differentiating.

One could think of various physical fields that provide the size and form of the macroscopic domain where the microscopic processes (pertaining to the intracellular GRN dynamics) take place. A Turing mechanism is the most immediate and simple way of obtaining spatial stationary patterns through the diffusion of chemicals [51,55], but other mechanisms could be involved. In an ongoing work, we have proposed that a phase field with spontaneous curvature could be one of the mechanisms on which the accommodation of the ABC genes in space relies.

In other attempts to integrate physical fields and forces into models of development, meristem growth has been modeled using the principles of continuum mechanics (see review in [56–58]). Also, some quantitative mesoscopic models for flower development and growth in *A. thaliana* and other angiosperms have been put forward (e.g., [59–62]). More recently, it was shown that cells in the *A. thaliana* shoot apical meristem orient their microtubules along mechanical stress patterns generated during tissue formation, and this then affects the mechanical properties of the cell, thus establishing a feedback loop [52].

Even though, during the last years, genetics based approaches have been favored, it is recently being accepted that the richness and robustness of biological forms are not encoded only in the genes. Recent research is consistently showing that there are non-trivial interactions at all the levels mentioned above and, therefore, in order to achieve a global understanding of development, an integrated view has to be adopted [63,64].

If this program is to be carried out, the implementation of mathematical models becomes necessary. From the methodological perspective, modeling should be done in a multi-scale framework [65]. For the mechanical effects, the standard tool is continuum mechanics. There are several possibilities for GRN modeling, and assessing the performance of different models is still the subject of intensive research. However, we can safely say that no matter what formal mathematical description is used (a Boolean network, a system of ordinary differential equations, etc.), a non-linear dynamical system will account for the behavior of the genetic interactions.

However, this is only part of the required mathematical models, since, as it was pointed out before, all these three complexity levels interact non-trivially. We already mentioned that a central issue is how such levels of complexity are coupled. For example, what might have been considered as a parameter at some level becomes a variable dependent on variables at the other scales.

8. Conclusions

Understanding the emergence of spatiotemporal patterns that underlie organ formation during development remains a major challenge in biology. Moreover, understanding the origin and evolution of such patterns and developmental processes remains central to comprehending phenotypic transformations and is thus key to evolutionary biology in general [66–69]. Mathematical and computational modeling are playing a key role in the study of these central aspects of evolutionary developmental biology, as they (i) provide ways to uncover functional modules that are necessary and sufficient for developmental processes to occur, and (ii) can then be used to test how genetic or other kinds of variation in these modules that render new phenotypes. Pursuing this type of study could indeed shed light on the problem of the origin of morphological *themes* in plant and animals, this is, on the origin of structures that are observed in several lineages and that remain unchanged under a wide range of environmental conditions. Moreover, such research could help account for the origin of variations of these themes and morphogenetic novelties.

Modeling has proven particularly useful in the study of plant morphogenetic themes, specifically that of flower organ specification and arrangement. As reviewed above, theoretical efforts based on a vast set of experimental data resulted in the formulation of a functional module that includes the ABC genes and underlies cell-fate determination during early flower development. Furthermore, a morphogenetic model that could account for the spatiotemporal patterns that characterize flower organ arrangement is now being developed. We are starting to understand how the collective action of ABC genes, other genes and non-genetic factors give rise to the robust flower development theme. It is now possible to perform joint theoretical and experimental work aimed at exploring the variations that could underlie diversification and the generation of novelties throughout flower evolution.

Acknowledgements

We thank R.V. Pérez-Ruiz and D. Romo for technical and logistical assistance; and M. Aldana and A. Chaos for useful discussions and for contributions to build Fig. 1; and J. Bowman for the shoot apical meristem micrograph of Fig. 2. Financial support for this work was obtained from the Programa de Apoyo a Proyectos de Investigación e Innovación Tecnológica, Universidad Nacional Autónoma de México IN230002 and IX207104, University of California-MEXUS ECO IE 271 and Ciencia y Tecnología CO1.41848/A-1, CO1.0538/A-1 and CO1.0435.B-1 grants to E.A.B. RAB acknowledges support from Conacyt through Grant number 79641. MB and EA receive PhD scholarships from Conacyt.

References

[1] Bowman JL, Smyth DR, Meyerowitz EM. Genes directing flower development in Arabidopsis. Plant Cell 1989;1(1):37–52.
[2] Bowman JL, Smyth DR, Meyerowitz EM. Genetic interactions among floral homeotic genes of Arabidopsis. Development 1991;112:1–20.
[3] Coen HS, Meyerowitz EM. The war of the whorls: genetic interactions controlling flower development. Nature 1991;353:31–7.
[4] Schwarz-Sommer Z, Davies B, Hudson A. An everlasting pioneer: the story of Antirrhinum research. Nat Rev Genet 2003;4(8):657–66.
[5] Jack T. Molecular and genetic mechanisms of floral control. Plant Cell 2004;16(Suppl.):S1–17.
[6] Jaeger J, Reinitz J. On the dynamic nature of positional information. Bioessays 2006;28:1102–11.
[7] Newman SA, Müller GB. Epigenetic mechanisms of character origination. J Exp Zool 2000;288(4):304–17.
[8] Ferrario S, Immink RG, Angenent GC. Conservation and diversity in flower land. Curr Opin Plant Biol 2004;7(1):84–91.
[9] Rudall P. Anatomy of flowering plants. 3rd ed. Cambridge University Press; 2007.
[10] Honma T, Goto K. Complexes of MADS-box proteins are sufficient to convert leaves into floral organs. Nature 2001;409:525–9.
[11] Pelaz S, Tapia-López R, Alvarez-Buylla ER, Yanofsky MF. Conversion of leaves into petals in Arabidopsis. Curr Biol 2001;11:182–4.
[12] Alvarez-Buylla ER, Benítez M, Corvera-Poiré A, Chaos CA, de Folter S, Gamboa A, et al. Flower development. The Arabidopsis book. Rockville, MD: American Society of Plant Biologists; 2010, in press [http://www.aspb.org/publications/arabidopsis/].

[13] de Folter S, Busscher J, Colombo L, Losa A, Angenent GC. Transcript profiling of transcription factor genes during silique development in Arabidopsis. Plant Mol Biol 2004;56(3):351–66.
[14] Sablowski R. Flowering and determinacy in Arabidopsis. J Exp Bot 2007;58(5): 899–907.
[15] Sablowski R. Genes and functions controlled by floral organ identity genes. Semin Cell Dev Biol 2009;(September) [Epub ahead of print].
[16] Schmid M, Davison TS, Henz SR, Pape UJ, Demar M, Vingron M, et al. A gene expression map of Arabidopsis development. Nat Genet 2005;37:501–6.
[17] Wagner GP, Mezey J, Calabretta R. In: Callebaut W, Rasskin-Gutman D, editors. Modularity: understanding the development and evolution of complex systems. Cambridge, MA: MIT Press; 2004.
[18] Smyth DR, Bowman JL, Meyerowitz EM. Early flower development in Arabidopsis. Plant Cell 1990;2:755–67.
[19] Urbanus SL, de Folter S, Shchennikova AV, Kaufmann K, Immink RG, Angenent GC. In planta localization patterns of MADS domain proteins during floral development in *Arabidopsis thaliana*. BMC Plant Biol 2009;12(9):5.
[20] von Dassow G, Meir E, Munro EM, Odell GM. The segment polarity network is a robust developmental module. Nature 2000;406:188–93.
[21] Albert R, Othmer HG. The topology of the regulatory interactions predicts the expression pattern of the segment polarity genes in *Drosophila melanogaster*. J Theor Biol 2003;223:1–18.
[22] Ruiz-García L, Madueño F, Wilkinson M, Haughn G, Salinas J, Martínez-Zapater JM. Different roles of flowering-time genes in the activation of floral initiation genes in Arabidopsis. Plant Cell 1997;9(11):1921–34.
[23] Ratcliffe OJ, Bradley DJ, Coen ES. Separation of shoot and floral identity in Arabidopsis. Development 1999;126(6):1109–20.
[24] Pelaz S, Ditta GS, Baumann E, Wisman E, Yanofsky MF. B and C floral organ identity functions require SEPALLATA MADS-box genes. Nature 2000;405(6783):200–3.
[25] Komeda Y. Genetic regulation of time to flower in *Arabidopsis thaliana*. Annu Rev Plant Biol 2004;55:521–35.
[26] Kieffer M, Stern Y, Cook H, Clerici E, Maulbetsch C, Laux T, et al. Analysis of the transcription factor WUSCHEL and its functional homologue in Antirrhinum reveals a potential mechanism for their roles in meristem maintenance. Plant Cell 2006;18(3):560–73.
[27] Bower JM, Bolouri H. Computational modeling of genetic and biochemical networks. MIT Press; 2001.
[28] de Jong H. Modeling and simulation of genetic regulatory systems: a literature review. J Comput Biol 2002;9(1):67–103.
[29] Kauffman S. Metabolic stability and epigenesis in randomly constructed genetic nets. J Theor Biol 1969;22:437–67.
[30] Espinosa-Soto C, Padilla-Longoria P, Alvarez-Buylla ER. Gene regulatory network model for cell-fate determination during *Arabidopsis thaliana* flower development that is robust and recovers experimental gene expression profiles. Plant Cell 2004;6:2923–39.
[31] Huang S, Ingber DE. A non-genetic basis for cancer progression and metastasis: self-organizing attractors in cell regulatory networks. Breast Dis 2006;26:27–54.
[32] Paulsson J. Summing up the noise in gene networks. Nature 2004;427:415–8.
[33] Macarthur BD, Ma'ayan A, Lemischka IR. Systems biology of stem cell fate and cellular reprogramming. Nat Rev Mol Cell Biol 2009;10:672–81.
[34] Alvarez-Buylla ER, Chaos A, Aldana M, Benítez M, Cortes-Poza Y, Espinosa-Soto C, et al. Floral morphogenesis: stochastic explorations of a gene network epigenetic landscape. PLoS ONE 2008;3(11):e3626, doi:10.1371/journal.pone.0003626.
[35] Savage NS, Walker T, Wieckowski Y, Schiefelbein J, Dolan L, Monk NA. A mutual support mechanism through intercellular movement of CAPRICE and GLABRA3 can pattern the Arabidopsis root epidermis. PLoS Biol 2008;6(9):e235.
[36] Benítez M, Espinosa-Soto C, Padilla-Longoria P, Alvarez-Buylla ER. Interlinked nonlinear subnetworks underlie the formation of robust cellular patterns in Arabidopsis epidermis: a dynamic spatial model. BMC Syst Biol 2008;17(2):98.
[37] Waddington CH. The strategy of the genes. A discussion of some aspects of theoretical biology. New York, NY: MacMillan; 1957.
[38] Slack JM. Conrad Hal Waddington: the last Renaissance biologist? Nat Rev Genet 2002;3:889–95.
[39] Mendoza L, Alvarez-Buylla ER. Dynamics of the genetic regulatory network for *Arabidopsis thaliana* flower morphogenesis. J Theor Biol 1998;193:307–19.
[40] Chaos A, Aldana M, Espinosa-Soto C, García Ponce de León B, Garay-Arroyo A, Alvarez-Buylla ER. From genes to flower patterns and evolution: dynamic models of gene regulatory networks. J Plant Growth Regul 2006;25: 278–89.
[41] Vandenbussche M, Zethof J, Royaert S, Weterings K, Gerats T. The duplicated B-class heterodimer model: Whorlspecific effects and complex genetic interactions in Petunia hybrida flower development. Plant Cell 2004;16: 741–54.
[42] Whipple CJ, Ciceri P, Padilla CM, Ambrose BA, Bandong SL, Schmidt RJ. Conservation of B-class floral homeotic gene function between maize and Arabidopsis. Development 2004;131:6083–91.
[43] Adam H, Jouannic S, Morcillo F, Verdeil JL, Duval Y, Tregear JW. Determination of flower structure in Elaeis guineensis: do palms use the same homeotic genes as other species? Ann Bot 2007;100:1–12.
[44] Mendoza L, Thieffry D, Alvarez-Buylla ER. Genetic control of flower morphogenesis in *Arabidopsis thaliana* a logical analysis. Bioinformatics 1999;15:593–606.
[45] Raj A, van Oudenaarden A. Nature, nurture, or chance: stochastic gene expression and its consequences. Cell 2008;135:216–26.
[46] Yu H, Ito T, Zhao Y, Peng J, Kumar P, Meyerowitz EM. Floral homeotic genes are targets of gibberelin signaling in flower development. Proc Natl Acad Sci USA 2004;101:7827–32.
[47] Schmid M, Uhlenhaut NH, Godard F, Demar M, Bressan R, et al. Dissection of floral induction pathways using global expression analysis. Development 2003;130:6001–12.
[48] Vergara-Silva F, Espinosa S, Ambrose A, Vázquez-Santana S, Martínez-Mena A, Márquez-Guzmán J, et al. Inside-out flowers characteristic of *Lacandonia schismatica* evolved at least before its divergence from a closely related taxon, *Triuris brevistylis*. Int J Plant Sci 2003;164:345–57.
[49] Ambrose BA, Espinosa-Matías S, Vázquez-Santana S, Vergara-Silva F, Martínez E, Márquez-Guzmán J, et al. Comparative developmental series of the Mexican triurids support a euanthial interpretation for the unusual reproductive axes of *Lacandonia schismatica* (Triuridaceae). Am J Bot 2006;93:15–35.
[50] Lenser T, Theissen G, Dittrich P. Developmental robustness by obligate interaction of class B floral homeotic genes and proteins. PLoS Comput Biol 2009;5(1):e1000264.
[51] Jönsson H, Heisler M, Reddy GV, Agrawal V, Gor V, Shapiro BE, et al. Modeling the organization of the WUSCHEL expression domain in the shoot apical meristem. Bioinformatics 2005;21:i232–40.
[52] Hamant O, Heisler MG, Jönsson H, Krupinski P, Uyttewaal M, Bokov P, et al. Developmental patterning by mechanical signals in Arabidopsis. Science 2008;322:1650–5.
[53] Barlow PW. Reflections on 'plant neurobiology'. Biosystems 2008;92(2): 132–47.
[54] Kwiatkowska D. Flower primordium formation at the Arabidopsis shoot apex: quantitative analysis of surface geometry and growth. J Exp Bot 2006;57:571–80.
[55] Turing A. The chemical basis of morphogenesis. Philos Trans R Soc Lond B Biol Sci 1952;237:37–72.
[56] Kwiatkowska D. Flowering and apical meristem growth dynamics. J Exp Bot 2008;59(2):187–201.
[57] Baskin TJ. Anisotropic expansion of the plant cell wall. Annu Rev Cell Dev Biol 2005;21:203–22.
[58] Goodall CR, Green PB. Quantitative analysis of surface growth. Bot Gaz 1986;147:1–15.
[59] Rolland-Lagan J, Bangham A, Coen E. Growth dynamics underlying petal shape and asymmetry. Nature 2003;422:161–3.
[60] Lee HC, Chioub DW, Chenc WH, Markhartd AH, Chene YH, Lin TY. Dynamics of cell growth and endoreduplication during orchid flower development. Plant Sci 2004;166:659–67.
[61] Skryabin KG, Alekseev DV, Ezhova TA, Kozlov VN, Kudryavtsev VB, Nosov MV, et al. A mathematical model of genetic control of determination of floral organ identity in *Arabidopsis thaliana*. Biol Bull 2004;31:346–53.
[62] Mündermann L, Erasmus Y, Lane B, Coen E, Prusinkiewicz P. Quantitative modeling of Arabidopsis development. Plant Physiol 2005;139:960–8.
[63] Geitmann A, Ortega JK. Mechanics and modeling of plant cell growth. Trends Plant Sci 2009;14(9):467–78.
[64] Gordon SP, Chickarmane VS, Ohno C, Meyerowitz EM. Multiple feedback loops through cytokinin signaling control stem cell number within the Arabidopsis shoot meristem. Proc Natl Acad Sci USA 2009;106(38): 16529–34.
[65] Alarcón T, Byrne HM, Maini PK. Towards whole-organ modelling of tumour growth. Prog Biophys Mol Biol 2004;85(2–3):451–72.
[66] Hall BK. Evo-Devo: evolutionary developmental mechanisms. Int J Dev Biol 2003;47:491–5.
[67] Carroll SB. EvoDevo and an expanding evolutionary synthesis: a genetic theory of morphological evolution. Cell 2008;134:25–36.
[68] Sommer RJ. The future of evo-devo: model systems and evolutionary theory. Nat Rev Genet 2009;10(6):416–22.
[69] Müller GB. Evo-devo: extending the evolutionary synthesis. Nat Rev Genet 2007;8:943–9.

8.2. Parte II:

Artículo:

“Antelope": a hybrid-logic model checker for branching-time Boolean GRN analysis

Gustavo Arellano, Julián Argil, Eugenio Azpeitia, Mariana Benítez, Miguel Carrillo, Pedro Góngora, David A Rosenblueth, Elena R Alvarez-Buylla

BMC Bioinformatics

BMC Bioinformatics

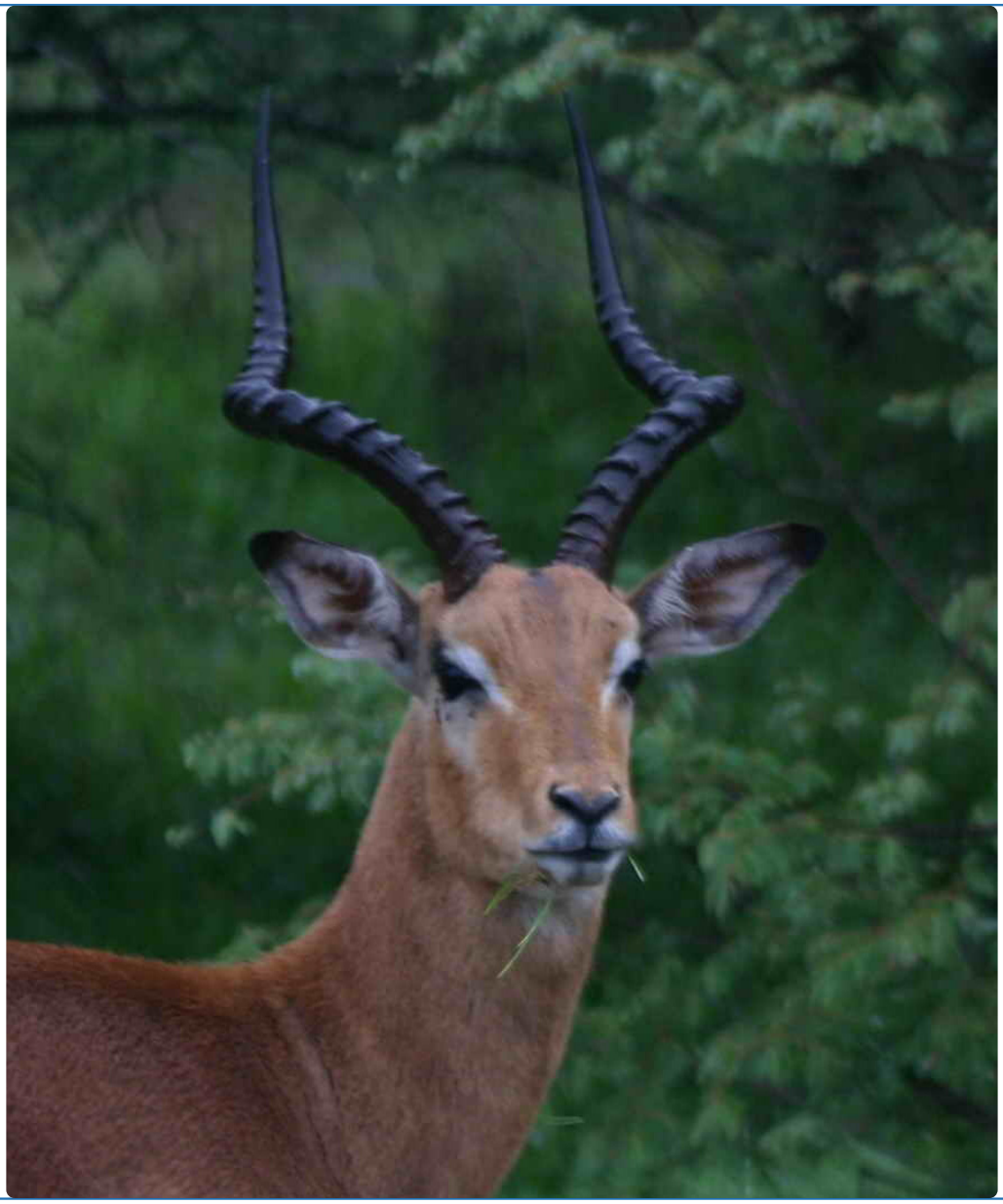

"Antelope": a hybrid-logic model checker for branching-time Boolean GRN analysis

Arellano *et al.*

BioMed Central

Arellano *et al. BMC Bioinformatics* 2011, **12**:490
http://www.biomedcentral.com/1471-2105/12/490 (22 December 2011)

BMC Bioinformatics

SOFTWARE Open Access

"Antelope": a hybrid-logic model checker for branching-time Boolean GRN analysis

Gustavo Arellano[5], Julián Argil[5], Eugenio Azpeitia[1,2], Mariana Benítez[1,3,4], Miguel Carrillo[5], Pedro Góngora[5], David A Rosenblueth[1,5*] and Elena R Alvarez-Buylla[1,2]

Abstract

Background: In Thomas' formalism for modeling gene regulatory networks (GRNs), *branching time*, where a state can have *more than one possible future*, plays a prominent role. By representing a certain degree of unpredictability, branching time can model several important phenomena, such as (a) asynchrony, (b) incompletely specified behavior, and (c) interaction with the environment. Introducing more than one possible future for a state, however, creates a difficulty for ordinary simulators, because *infinitely many* paths may appear, limiting ordinary simulators to statistical conclusions. *Model checkers* for branching time, by contrast, are able to prove properties in the presence of infinitely many paths.

Results: We have developed *Antelope* ("Analysis of Networks through TEmporal-LOgic sPEcifications", http://turing.iimas.unam.mx:8080/AntelopeWEB/), a model checker for analyzing and constructing Boolean GRNs. Currently, software systems for Boolean GRNs use branching time almost exclusively for asynchrony. *Antelope*, by contrast, also uses branching time for incompletely specified behavior and environment interaction. We show the usefulness of modeling these two phenomena in the development of a Boolean GRN of the *Arabidopsis thaliana* root stem cell niche.

There are two obstacles to a direct approach when applying model checking to Boolean GRN analysis. First, ordinary model checkers normally only verify whether or not a *given* set of model states has a given property. In comparison, a model checker for Boolean GRNs is preferable if it *reports* the set of states having a desired property. Second, for efficiency, the expressiveness of many model checkers is limited, resulting in the inability to express some interesting properties of Boolean GRNs.

Antelope tries to overcome these two drawbacks: Apart from reporting the set of all states having a given property, our model checker can express, at the expense of efficiency, some properties that ordinary model checkers (e.g., NuSMV) cannot. This additional expressiveness is achieved by employing a logic extending the standard Computation-Tree Logic (CTL) with hybrid-logic operators.

Conclusions: We illustrate the advantages of *Antelope* when (a) modeling incomplete networks and environment interaction, (b) exhibiting the set of all states having a given property, and (c) representing Boolean GRN properties with hybrid CTL.

Background

Gene regulatory network models

A major challenge in current biology is relating spatio-temporal gene expression patterns to phenotypic traits of an organism. These patterns result partly from complex regulatory interactions sustained principally by genes and encoded proteins. The complexity of such interactions exceeds the human capacity for analysis. Thus, mathematical and computational models of gene regulatory networks (GRNs) are indispensable tools for tackling the problem of mapping the genotype into the phenotype. These models have been fruitfully applied in numerous biological systems (e.g., [1-4]).

Within the various kinds of GRN models [5], Boolean GRNs are especially valuable for their simplicity and for

* Correspondence: drosenbl@servidor.unam.mx
[1]Centro de Ciencias de la Complejidad, piso 6, ala norte, Torre de Ingeniería, Universidad Nacional Autónoma de México, Coyoacán, 04510 México D.F., México
Full list of author information is available at the end of the article

nonetheless having a rich behavior yielding meaningful biological information [6,7]. Examples where Boolean GRNs have been successfully used are: the segment polarity gene network of *Drosophila melanogaster* [4,8], the flower organ determination GRN of *Arabidopsis thaliana* [9], the mammalian cell cycle [10], and the yeast cell cycle [11,12].

In a Boolean GRN, each gene has only two possible activation values: active (1) or inactive (0); intermediate expression levels are neglected. A *network state* at time t is a vector containing the activation values of all the genes in the GRN at time t. In addition, time is viewed as proceeding in discrete steps. The value of every gene X at time $t + 1$ is specified by a Boolean function of the values of its regulators $g_1, g_2, \ldots, g_{n_X}$ at time t.

Branching time

Boolean GRNs are closely related to the formalism developed by Thomas and his collaborators [13-15]. Thus, computer systems for Boolean GRNs are often influenced by Thomas' formalism, which employs GRN models with branching time, allowing states with *more than one immediate future* [[13], p. 33]. A network state with more than one immediate future represents the fact that the next state of the regulatory system modeled by such a GRN can be any one of several states. Hence, the next state of the modeled system is only partially determined. Let us then say that there is an *indetermination* in the network. This indetermination in the system's behavior reflects a certain degree of unpredictability that can be identified with several important phenomena.

Asynchrony

One such phenomenon is *asynchrony* [[13], p. 33]. Experiments for inferring gene interaction do not normally establish the length of time between state changes. Hence, when such experiments indicate the change in value of two genes, say, it is preferable to model such a situation with a single state having two successors, one for each change, as illustrated in Figure 1. The reasons are that we do not know the relative values of both delays in real biological systems [[13], p. 44] and that complete synchrony might be practically impossible [[13], pp. 33, 55].

Many computer systems based on, or inspired by, Thomas' formalism (such as BooleanNet [16], BoolNet [17], GINsim [18-20], GNBox [21,22], SMBioNet [23,24], and SQUAD [25-27]) employ asynchronous models. Thomas' formalism, however, incorporates *two additional phenomena* with indeterminations, that are typically excluded in such systems.

Incompletely specified behavior

One such additional phenomenon is *incompletely specified behavior* [[13], p. 24]. This behavior may emerge, first, from a "synthetic" approach [[13], pp. 60-67], where we are interested in all Boolean GRNs having certain properties (e.g., a certain set of steady states) regardless of other properties. The tables specifying the network behavior would then have outputs whose value "does not matter" [[13], p. 24]. Second, lack of some of the experimental information of a regulatory system also emerges as incompletely specified behavior. In this case, the behavior tables would have outputs whose value we *do not know*.

Interaction with the environment

Another phenomenon usually neglected in computer systems for GRN analysis and that can be modeled with branching time is that of *interaction with the environment*. Assume that the next state of a regulatory system depends on the temperature: If the temperature is low, the system's next state will be one, but if the temperature is high, the system's next state will be different. Another example is the unpredictability of radiation-induced apoptosis [28]. In this case, for the same degree of radiation some cells will initiate apoptosis while others will not. Thomas and D'Ari reflect such an unpredictability with an "input variable" [[13], pp. 33-35] of an unknown value. This phenomenon can be readily incorporated with indeterminations.

Simulators

Boolean GRNs are sometimes studied with *simulators* (e.g., Atalia [9], BooleanNet [16], and BoolNet [17]). A simulator attempts to replicate the behavior of a system

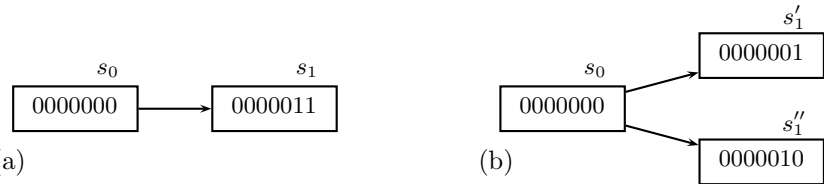

Figure 1 A fragment of the state-transition graph of a Boolean GRN exemplifying asynchrony. Assume that the behavior of a network specifies a simultaneous transition of the value of the two rightmost genes from 0 to 1 (panel (a)). If we exclude the possibility of simultaneous changes, it might be more realistic to model such a phenomenon with an indetermination (panel (b)).

by performing state changes in the *same order* as they occur in the system being modeled. Hence, network paths are traversed forward from one state to the next. In the presence of a state with more than one successor, such a straightforward approach must be complemented with additional mechanisms. Two of such mechanisms are: (a) a random device (randomly selecting one successor) and (b) backtracking (systematically selecting one successor after another by remembering which successors of each state have already been selected) coupled with a cycle-detection mechanism.

A random device, on the one hand, allows for only drawing statistical conclusions. The reason is that in the presence of a state with more than one successor, the number of paths may be infinite [6], as depicted in Figure 2. Backtracking and cycle detection, on the other hand, can be inefficient (taking, in the worst case, an exponential amount of time in the size of the network [[29], p. 82]).

There are two important approaches for circumventing these difficulties. One of these techniques is an elaboration of backtracking so as to increase its efficiency by requiring certain *constraints* to be satisfied as the network is traversed [30]. The work by Corblin et al. [21,22] uses this approach. Another relevant method is model checking.

Model checking

Model checking [31,32] is a collection of techniques for automatically verifying properties especially of discrete systems. The main ideas of model checking appeared 30 years ago [31,32]. At present, numerous model-checking tools exist. Model checking is routinely used, mainly for hardware verification, but also for software verification [33], and was distinguished with the A. M. Turing award in 2007. Model checking has been advocated for analyzing biological systems with increasing interest [6,24,34-43].

A model checker normally has as input (1) a "Kripke structure" representing a discrete system (comprising a finite number of states), (2) a distinguished "initial" state (or set of states) in the Kripke structure, and (3) a "temporal-logic" formula expressing a desirable property, that may or may not hold (i.e., be true) at a state. The output of the model checker is either a confirmation or a denial that the formula holds at the initial state(s) (given by the user as part of the input).

In a Kripke structure time is branching, so that there may be more than one possible future of a given state. The introduction of branching time may produce infinitely many forward traversals (see Figure 2). Model checkers, however, unlike simulators randomly selecting a successor state, can systematically analyze such infinitely many possibilities [6]. Intuitively, this is often done by traversing the Kripke structure in reverse and accumulating the set of all states at which a subformula holds. Model checking amounts, thus, to performing an exhaustive search (in the presence of branching time). Such a search plays the role of a *mathematical proof* establishing a property for infinitely many paths.

Programming vs. formula writing

By being based on properties formalized in temporal logic, model checkers have another advantage over simulators. The decision of whether or not a state satisfies a property of interest is programmed in the simulator itself. Therefore, if an unforeseen property appears during the usage of a Boolean GRN simulator, such a property must be incorporated in the simulator by modifying program code. This renders simulators rigid: either the user's needs are anticipated or reprogramming must be done.

Compared with simulators, model checkers exhibit the benefit of having replaced programming with temporal-logic formula writing. Instead of having to modify the computer program of a simulator, many new queries can be dealt with by writing new temporal-logic formulas (as long as the queries can be expressed in the selected logic), which (unlike large programs and their modifications) are concise and self-contained.

Organization of this paper

In the Implementation section, we first illustrate both Computation-Tree Logic (CTL) [31] and its hybrid extension, Hybrid CTL (which we based on [44,45]), chosen to be able to express interesting properties for

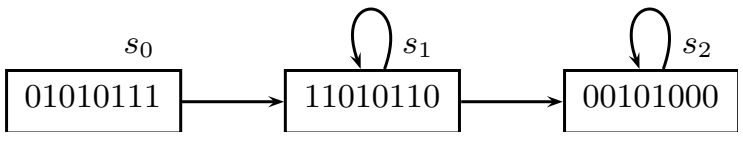

Figure 2 A fragment of the state-transition graph of a Boolean GRN showing the appearance of infinitely many paths. Infinitely many paths appear in this Boolean GRN because of one state (s_1) having more than one future and occurring in a cycle. Some paths are: ($s_0s_1s_2$ ...), ($s_0s_1s_1s_2$ ...), ($s_0s_1s_1s_1s_2$ ...), ... A simulator using a random device traverses the model forward, state by state, following a single path of the state graph, limiting the use of such a tool to drawing only statistical conclusions about all paths in models such as this one. Model checkers, by contrast, can prove precise properties, even in the presence of infinitely many paths resulting from states having more than one future.

Boolean GRN analysis and construction. The term "hybrid" here means a combination of propositional modal logic with classical predicate logic, and should not to be confused with hybrid model checking, combining discrete with continuous variables. The Implementation section subsequently covers the model-checking algorithms and some implementation details. Next we show, in the Results section, the use of the *Antelope* model checker in the presence of indeterminations either caused by environment interaction or by an incompletely specified behavior. Finally, the Discussion section reviews other similar software systems, compares *Antelope* with such systems, and outlines features planned for the future.

Implementation

This section first covers the temporal logics used by *Antelope*. After explaining CTL, we turn our attention to its hybrid extension. Next, we cover the model-checking algorithms, as well as additional implementation issues.

Computation-Tree Logic

We now give a short account of CTL and refer the reader to additional file 1 of this paper for a gentle introduction and to additional file 2 for a formal definition of CTL. More thorough treatments can be found in [46-50].

Boolean and temporal operators

Formulas in CTL can have Boolean operators, such as **not** and **or**. In addition, such formulas can have "temporal operators", allowing us to refer to formulas holding in the future of a particular state. In this case, we must indicate whether we mean some future or all futures. Hence, it is possible to refer either (1) to *some* path starting in the present with the "modality" **E**, or (2) to *all* paths starting in the present with the modality **A**. Similarly, it is possible to refer (a) to the immediate future with the modality **X**, (b) to any state in the present or any point in the future with the modality **F**, or (c) to all states in the present and in the future with the modality **G**. Table 1 summarizes these modalities.

A *temporal operator* is composed of a modality in the upper part together with a modality in the lower part of this table, which results in six temporal operators. (Often more temporal operators are included in CTL [49].) For example, a formula asserting that there exists a path such that in the present or in the future g_0 does not hold (i.e., g_0 is inactive) and g_1 does hold (i.e., g_1 is active) would be: "**EF**((**not** g_0) **and** g_1)". Hence, assuming that there is a single state s in which g_0 does not hold and g_1 does hold, this formula can be used to obtain the basin of attraction of such a state, with a model checker computing all states at which a given formula holds. The formula "**AX** ((**not** g_0) **and** g_1)" holds at all states from which it is *necessary* to reach s in one step, i. e., states which have s as their only next state. The formula "**EX** ((**not** g_0) **and** g_1)" holds at all states from which it is *possible* to reach s in one step, i.e., states which have s as a next state (and possibly other next states because of indeterminations). Other CTL formulas can characterize, for instance, whether or not it is necessary to go through a state s_1 to reach another state s_2. See [51] for a list of CTL formulas specifying various biological properties.

Table 1 CTL modalities

modality	meaning
E	some path (i.e., there Exists a path)
A	All paths
X	neXt state (i.e., immediate future)
F	any state either in the present or in the Future
G	all states in the present and in the future (Global)

Some properties not expressible in CTL

There do not exist, however, CTL formulas for characterizing steady states (i.e., a formula holding exactly at the set of all steady states of an arbitrary Boolean GRN) [51], or oscillations. This motivates the use of a more expressive logic than CTL. *Antelope* provides a "hybrid" extension of CTL.

Hybrid Computation-Tree Logic

This subsection is devoted to Hybrid CTL. We refer the reader to additional file 1 of this paper for a gentle introduction and to additional file 2 for a formal definition of Hybrid CTL. Deeper treatments of hybrid logics are in [52,53].

State variables

The main idea behind the hybrid extension of a temporal logic consists in the addition of variables allowing us to refer to states (i.e., state variables). The downarrow binder "$\downarrow\sigma$" sets the state variable σ to the current state of evaluation. The formula "$\downarrow\sigma$.**AX** σ", for example, characterizes the set of states which have themselves as their only next state. Hence, Hybrid CTL allows us to characterize the set of steady states. Moreover, by employing branching time, we are able to distinguish between two kinds of steady state. When a state has only one transition from and to itself, following Thomas and D'Ari [13], we will call it a *stable steady state*. When a state has, in addition to a self-loop, other transitions going to other states, following [13], we will call it an *unstable steady state* (named "stationary" state in [51]). Hybrid CTL formulas for calculating both these sets of states are: "$\downarrow\sigma$.**AX** σ", for the set of stable steady states, and "$\downarrow\sigma$.**EX**σ", for the union of the sets of stable and unstable steady states.

Other formulas

Attractors of various sizes and oscillations

The notion of a steady state can be generalized in an *attractor*, possibly involving more than one state. A

steady state would then be a one-state attractor. A formula characterizing attractors of any size would be: "$\downarrow\sigma$. **EX EF** σ".

Another interesting formula would be "$\downarrow\sigma$.**EX**((**not** σ) **and EX** σ)", which holds at states belonging to a size-two attractor. Oscillations, where a gene is alternatively active and inactive, can also be characterized in Hybrid CTL: Additional file 1 explains a formula for the basin of attraction of possible oscillations. We refer the reader to the *Antelope* web site http://turing.iimas.unam.mx:8080/AntelopeWEB/ for more formulas.

Algorithms

CTL

Antelope uses a standard "labeling" algorithm [46] for ordinary CTL formulas. Labeling algorithms for model checking are so called because we can think of each state as being labeled with the subformulas holding at that state.

Say that the formula given by the user is ϕ. The labeling algorithm starts by considering the simplest subformulas of ϕ, that is, the names of the genes. For each gene *g*, labeling all states at which the formula "*g*" holds is easy, as that information is already present in the Kripke structure.

Next, the labeling algorithm proceeds to more complex subformulas, until ϕ is reached, by treating the operator of each such subformula by cases. For instance, if the subformula is of the form "ψ_1 **and** ψ_2", then the labeling algorithm computes the set of states at which such a subformula holds as the intersection of the set of states at which ψ_1 holds with the set of states at which ψ_2 holds. All Boolean operators can be treated by combining set operations, like union, intersection, and set difference.

The labeling algorithm treats some temporal operators, such as **AX**, by using equivalences. For example, "**AX** ψ" is equivalent to "**not EX not** ψ". The rest of the temporal operators, however, must be dealt with explicitly. For all such primitive operators the labeling algorithm traverses the Kripke structure in *reverse*. Take for instance "**EX** ψ", which holds if there Exists a neXt state at which ψ holds. Given the set of states at which ψ holds, the labeling algorithm treats "**EX** ψ" by obtaining all states which have an immediate successor in such a set, i.e., all the *predecessors* of the states in such a set. The labeling algorithm processes operators such as **EG** by repetitively traversing the Kripke structure in reverse.

Hybrid CTL

The labeling algorithm is efficient (taking polynomial time in the size of the Kripke structure). The additional expressiveness of hybrid operators, such as "$\downarrow$" comes at a price, however. Given a CTL formula ϕ, the computation of the set of states at which a formula of the form "$\downarrow\sigma.\phi$" holds involves calling the labeling algorithm with ϕ *once for each state*. The decrease in efficiency is even more if the "$\downarrow$" operator appears nested. *Antelope*, however, treats certain patterns in special ways, requiring less time than a direct approach.

More implementation issues

Antelope is a symbolic model checker [54], representing state sets by Reduced, Ordered Binary-Decision Diagrams (BDDs) [55]. (In particular, *Antelope* employs JavaBDD [56], which in turn uses BuDDy [57].)

Representation of a set of states

A BDD is a representation of a Boolean function. Thus, to use a BDD for representing a set of states in a Kripke structure we must view such a set as a Boolean function. This is possible if each row of the truth table of the Boolean function corresponds to an element which may or may not belong to such a set. The value of such a function will be 1 at exactly those states belonging to the set.

Representation of a set of transitions

In addition to representing sets of states, BDDs are used for representing the set of transitions of Kripke structures. In this case, the Boolean function has twice as many variables as there are genes. The reason is that each transition (corresponding to a row in the truth table of such a function) has both a source and a terminating state. BDDs are often surprisingly concise, allowing the verification of many large Kripke structures, with more than 10^{20} states [54]. We refer the reader to [49] for a detailed description of BDDs and their use in symbolic model checking.

Optimizations

Apart from the use of BDDs, *Antelope* has several "optimizations" (i.e., special treatment of particular patterns so as to increase the efficiency). For example, a straightforward formula characterizing the states with more than one successor has the pattern "$\downarrow\sigma$.**EX** $\downarrow\tau.\phi$". If evaluated as described in the Algorithms section, this formula would call the labeling algorithm a number of times proportional to the square of the number of states ($O(|S|^2)$, where $|S|$ is the number of states). To find the set of states with more than one successor, however, it is not necessary to visit all states for each state of the Kripke structure. It suffices to be able to enumerate the successors of each state. *Antelope* treats the formula for characterizing the states with more than one successor as a special case so that the CTL model-checking algorithm is called with ϕ as input a number of times linear in the size of the Kripke structure ($O(|S| + |R|)$, where $|R|$ is the number of transitions).

Another optimization is that of the operator **EY** (for "Exists Yesterday"), which is the converse of **EX**. Although this operator need not be primitive, *Antelope*

does treat it as primitive by simply traversing the transitions forward. This operator allows the user to view *Antelope* as a kind of simulator.

Additional file 3 has a table comparing the verification times for a few models with respect to some properties of increasing complexity.

Input formats

Antelope accepts two formats for describing the Boolean GRN: tables and equations. In both cases, the values of a gene (at the current time step) are specified as a Boolean *relation* which depends on the values of (some) genes (at the previous time step). A table can be viewed as an extension of an ordinary truth table, where stars are allowed on the right-hand side, denoting indeterminations. Sometimes, however, it may be more convenient to use a logical formula instead of a truth table. Hence, *Antelope* accepts equations, each of which is of the form:

$$X := f_X(g_1, g_2, \ldots, g_{n_X})$$

where the left-hand side represents the value of the gene X at the current time step, and the right-hand side is an arbitrary Boolean function (defined employing the usual Boolean operators, such as conjunction, disjunction, or negation) on the values of genes at the previous time step. To be able to represent indeterminations, we need *two* equations with the same left-hand side. We refer the reader to the *Antelope* user's manual, which appears in additional file 4, and in the URL http://turing.iimas.unam.mx:8080/AntelopeWEB/.

Results

We now exemplify the use of Antelope for analyzing Boolean variants of the *A. thaliana* root stem cell niche GRN. Stem cells or initials are undifferentiated cells from which particular cell types of the organisms are generated; the microenvironment in which stem cells are located is called the stem cell niche.

Anatomically, stem cell niches are conformed by two different cell types, the stem cells themselves, and another cell or group of cells sometimes generically called organizer cells [58]. The organizer cells maintain the stem cells in the undifferentiated state through short-range signals. Understanding how the different cells conforming stem cell niches are specified, as well as how the balance between cell division and cell differentiation is maintained in the niches, is central for understanding the development, growth and regeneration processes occurring in plants and animals. In particular, plant stem cell niches constitute valuable model systems for studying regenerative and plastic developmental processes, as these organisms grow new organs and structures throughout their life [58,59].

We focus on the root stem cell niche of *A. thaliana*, that is located near the root tip and is well characterized at the anatomical and molecular level (see the recent review in [60]). This niche is conformed by the so-called quiescent center (QC), which is in turn conformed by the organizer cells of the root SCN, and is surrounded by four different stem cell types [59]. Each of these four types of stem cell will give rise to a different cell lineage: vascular, cortex/endodermal, epidermal, and columella/root-cap cells. However, in this contribution two of the stem cell types (epidermal and root-cap cells) are considered as only one since the available experimental evidence is not enough to distinguish between them at the gene expression level (see more details in [61]), leaving only four types of initial cells (QC, vascular, cortex/endodermal (CEI), and epidermal/root-cap (CEpI) initials).

Besides being thoroughly characterized at the anatomical level, the root stem cell niche of *A. thaliana* has been relatively well described from a molecular and genetic perspective. Indeed, some of the molecular components that are necessary to establish and maintain the root SCN cellular patterning have been recently uncovered. Among these components are the genes *SHORTROOT* (*SHR*) and its target gene *SCARECROW* (*SCR*), the immediately downstream genes of the dimer SHR/SCR, and other genes that interact with them. Another set of relevant genes includes the *PLETHORA* (*PLT*) genes, which have been proposed to be key components of the molecular readout of the plant hormone auxin. Finally, the QC specific gene *WUSCHEL RELATED HOMEOBOX5* (*WOX5*) is fundamental for root SCN organization [60,62-64]; see the graphical representation of the interactions between these genes in Figure 3. Moreover, the expression patterns of these genes and the localization of their corresponding proteins have been described. Thus, it is possible to postulate a gene expression profile that characterizes each of the SCN cell types mentioned above according to the Table 2.

In order to define the rules for a Boolean GRN model for this system, we considered all the genes that have been reported to play a relevant role in the specification of the root stem cells and gathered the available experimental information for the regulation of their expression [60,61]; see Figure 3. These data included mostly molecular genetics experiments, such as experiments with plants containing a mutant allele of a gene. The resulting rules can be summarized in the following logical statements (uploaded in *Antelope* under the name 'Root gene regulatory network"):

```
// SHR; without regulators
// Auxin; without regulators
PLT: = ARF;
```

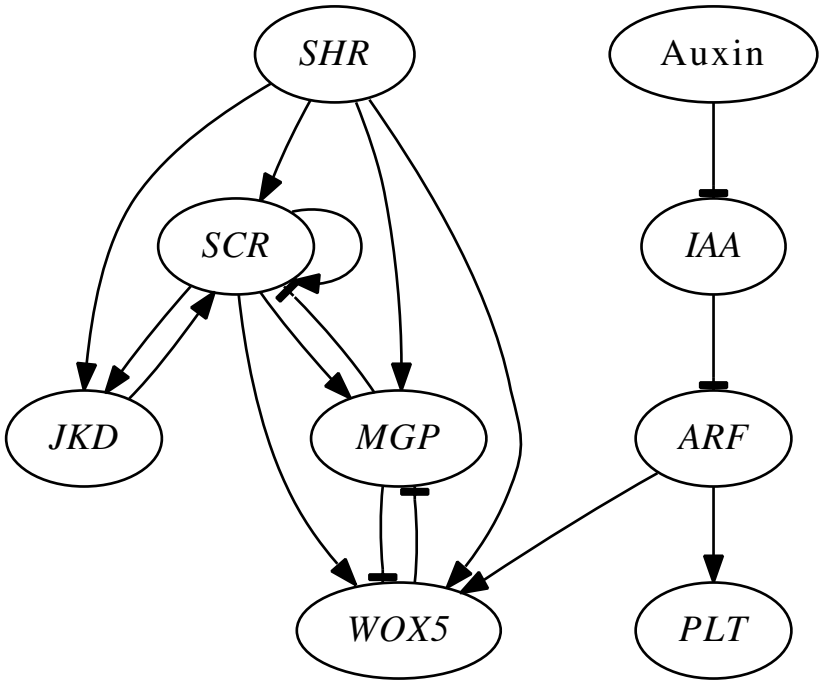

Figure 3 The interaction diagram of the GRN underlying cell type determination in the root stem cell niche of the model plant A. thaliana. The abbreviated names of the genes are inside ellipses and the edges correspond to the regulatory interactions. Auxin is a morphogene. The genes are: *Auxin/INDOLE-3-ACETIC ACID* (*Aux/IAA*), *AUXIN RESPONSE FACTOR* (*ARF*), *JACKDAW* (*JKD*), *MAGPIE* (*MGP*), *PLETHORA* (*PLT*), *SCARECROW* (*SCR*), *SHORTROOT* (*SHR*), and *WUSCHEL-RELATED HOMEBOX5* (*WOX5*). Ordinary arrow heads denote activation; T-bar arrow heads denote inhibition.

```
AUXINS: = AUXINS;
IAA: = ~ AUXINS;
ARF: = ~ IAA;
SHR: = SHR;
SCR: = SHR & SCR & (JKD | ~MGP);
JKD: = SHR & SCR;
MGP: = SHR & SCR &~ WOX;
WOX: = ARF & SHR & SCR & (~ MGP | WOX);
```

As has been proposed for other systems (e.g., [1,9]), we expected the stable steady states of our GRN model to correspond to the gene expression profiles characterizing the different stem cells within the root niche of *A. thaliana* (table above). Thus, from our knowledge of the system, we expected four stable steady states. The expected steady states are indeed obtained after postulating a mutual negative interaction between *WOX5* and *MGP*, which gives rise to a new testable prediction [61].

Table 2 Expected expression profiles for the cells conforming the A. thaliana root stem cell niche

Cell type	PLT	Auxin	ARF	Aux/IAA	SHR	SCR	JKD	MGP	WOX5
QC	1	1	1	0	1	1	1	0	1
Vascular	1	1	1	0	1	0	0	0	0
CEI	1	1	1	0	1	1	1	1	0
Cepl	1	1	1	0	0	0	0	0	0

Using this GRN model, we first illustrate the use of indeterminations representing incomplete experimental data. Next, we use indeterminations for modeling the influence of unpredictable external signals.

Experimental gap

Steady states and SCARECROW

While developing the truth tables for this GRN, we detected an experimental gap. We know that *SCARECROW* (*SCR*), a target gene of the dimer SHORTROOT (SHR)/SCR [62,63], either loses or diminishes its own expression in the *JACKDAW* single mutant (*jkd*) in the stem cell niche [64]. The same is true for *SCR*-dependent quiescent-center marker *QC25* [65]. The *MAGPIE* mutant (*mgp*), by contrast, has no visible phenotype. Finally, the *mgp jkd* double mutant recovers the *SCR* expression [64] (but see [66] for different results).

Based on this information, we established the truth table for *SCR*, which appears in Table 3. Observe the indetermination, reflecting the fact that activity could or could not be lost in a *jkd* background. *Antelope* produced three stable steady states, but four unstable steady

Table 3 Truth table for SCR

SHR	*SCR*	*JKD*	*MGP*	*SCR'*
0	0	0	0	0
0	0	0	1	0
0	0	1	0	0
0	0	1	1	0
0	1	0	0	0
0	1	0	1	0
0	1	1	0	0
0	1	1	1	0
1	0	0	0	0
1	0	0	1	0
1	0	1	0	0
1	0	1	1	0
1	1	0	0	1
1	1	0	1	*
1	1	1	0	1
1	1	1	1	1

states (see the Hybrid Computation-Tree Logic subsection for definitions of stable and unstable steady states). Hence, removing the indetermination in the above table may recover the four expected stable steady states. We performed the *jkd* loss-of-function simulation in our models to distinguish which of the two possibilities (i.e., no *SCR* transcription in *jkd* or *SCR* transcription in *jkd*) recovered the expected states. Interestingly, following the GRN state transitions *backwards*, using the **EX** operator, we noted that if *SCR* is unable to be expressed in *jkd*, then neither the *WUSCHEL-RELATED HOMEBOX5* (*WOX5*) (another quiescent-center marker, dependent on *SCR* [60]) expression nor the *SCR* expression disappeared at the quiescent-center.

Furthermore, our *jkd* mutant does cause a loss of the cortex-endodermis initials attractor, contrary to what is observed in experimental *jkd* mutants [64], suggesting that *jkd* only diminishes *SCR* expression. Again, following the GRN transitions backwards for the case in which *jkd* loss-of-function does not lose *SCR* expression, we found that the system was able to recover the *jkd* loss-of-function mutant. Based on the result found with the system including indeterminations, we replaced the star by a 1 in the table for *SCR*. Once the indetermination was so removed, we obtained four stable steady states.

External signals

FAS and SCR

Let us now exemplify *Antelope* as used for modeling the effect of external signals that affect one or more GRN nodes. The root stem cell niche of *A. thaliana* is affected by several external signals, such as genes and molecules from modules involved in other processes in the organism. For example, Kaya and collaborators [67] reported that *FASCIATA1* (*FAS1*) and *FASCIATA2* (*FAS2*), hereafter collectively called *FAS*, affect *SCR* expression. In the *fas* mutant, *SCR* expression is deregulated and can be either expressed or not expressed in almost any cell of the root stem cell niche. Similarly, Inagaki and collaborators [68] reported the *TECHBI* (*TEB*) mutants also affecting *SCR* expression. Again, when *TEB* is mutated, *SCR* may or may not be expressed through the endodermal layer, the cortex-endodermis initial cells, and the quiescent center.

We incorporated *FAS* by adding a variable *FAS* to the truth table for *SCR*. For *FAS* = 1, the truth table obtained in the "Experimental gap" subsection was used. For *FAS* = 0, by contrast, *all the right-hand sides* of the new truth table had indeterminations. In the case of *TEB*, we only used indeterminations for the right-hand side of the *SCR* table where the output was 1 for the *teb* mutant. We found that under these conditions the original four attractors were preserved in both cases. We also found that in the *fas* mutant, *SCR* could be expressed in any of the four original attractors, while in the *teb* mutant *SCR* could or could not be expressed either in the quiescent center or in the cortex-endodermis attractor. It is worth noting that in both cases the basins of attraction changed. For instance, consider the states that without any indetermination originally led to the cortex-endodermis attractor. Such states could now lead to vascular initials due to *SCR* indeterminations, as expected given the experimental evidence. It is also important to note that even though *SCR* expression is clearly affected in real roots, cells may not switch among cell types. However, the results derived from modeling the GRN using *Antelope* are consistent with data currently available and demonstrate the utility of this tool when we deal with networks in which the truth tables for some genes are not completely known. Figures 4 and 5 show screenshots of this analysis.

Other properties

These two analyses were based on indeterminations, stable and unstable steady states, and basins of attraction of such states. When designing and analyzing larger GRNs, more complex state attributes, such as global properties or conditional reachability may be useful.

For example, all the states occurring in either one-state or two-state attractors (which may be either stable or unstable) satisfy the formula "$\downarrow\sigma.\mathbf{EX}\ \mathbf{EX}\ \sigma$". The formula "$\mathbf{EF}(\downarrow\sigma.\mathbf{EX}\ \mathbf{EX}\ \sigma)$", in turn, can be used to calculate the basins of attraction of all such attractors. Hence, the formula "$\mathbf{not}(\mathbf{EF}\ (\downarrow\sigma.\mathbf{EX}\ \mathbf{EX}\ \sigma))$" would characterize the complement of all such basins of attraction. This is equivalent to the set of all states in the basins of attraction of attractors with more than two states. Similarly,

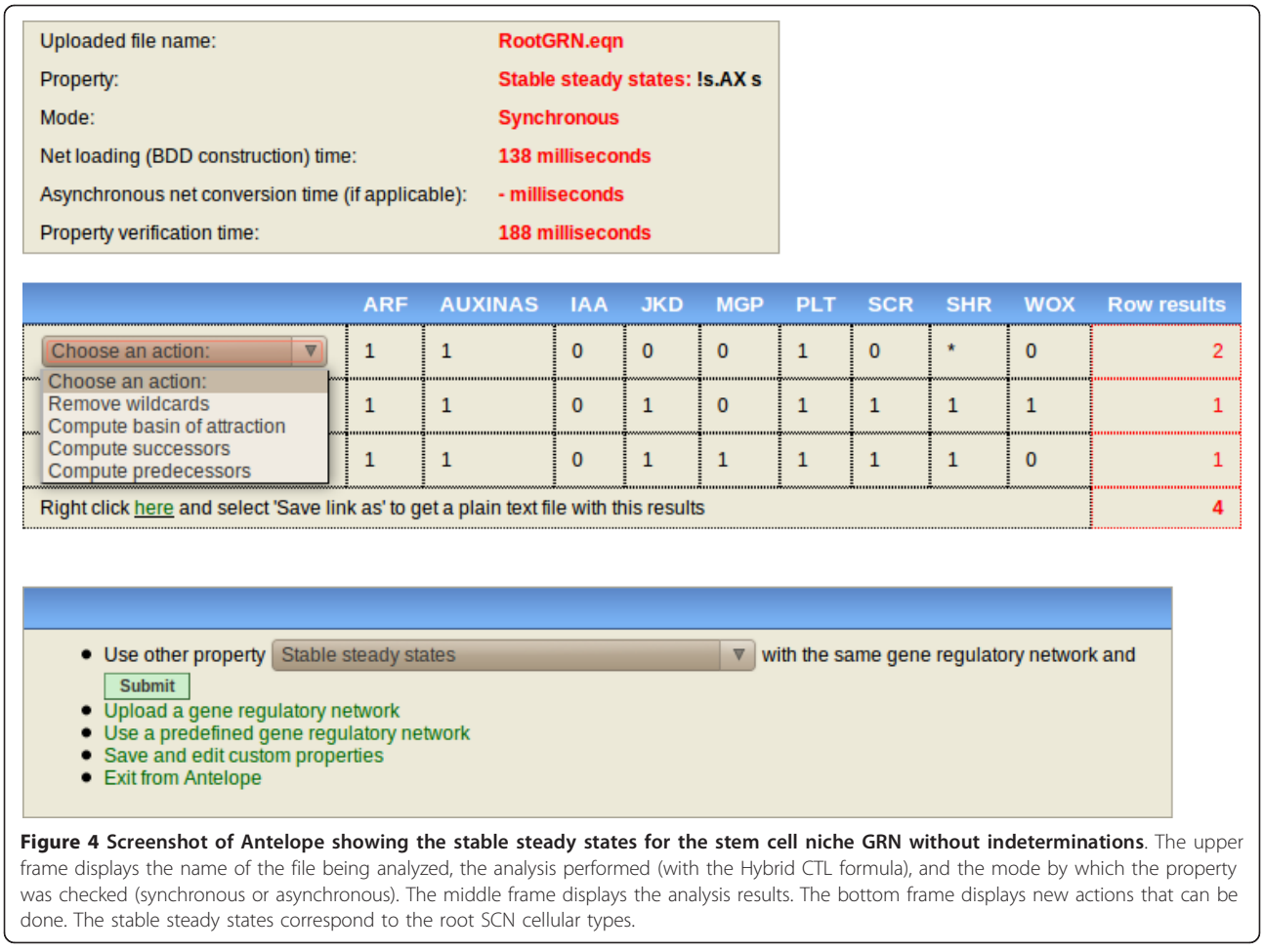

Figure 4 Screenshot of Antelope showing the stable steady states for the stem cell niche GRN without indeterminations. The upper frame displays the name of the file being analyzed, the analysis performed (with the Hybrid CTL formula), and the mode by which the property was checked (synchronous or asynchronous). The middle frame displays the analysis results. The bottom frame displays new actions that can be done. The stable steady states correspond to the root SCN cellular types.

the set of states occurring in exactly two-state attractors can be calculated with the formula "$\downarrow\sigma$.**EX** ((**not** σ) **and EX** σ)". These global properties cannot be expressed by CTL formulas.

Conditional reachability can be expressed with the **EU** operator (for "Exists Until"), a generalization of **EF**. Whereas "**EF**s_2" holds at all states from which it is possible to reach state s_2, "**E**[ϕ **U** s_2]" holds at all states from which it is possible to reach s_2 by going only through states at which the formula ϕ holds. For instance, the set of states from which it is possible to reach s_2 without going through s_1 corresponds to the formula "**E**[(**not** s_1) **U** s_2]". By contrast, the set of states from which it is possible to reach s_2 only by going through s_1 at least once is the complement of the previous set of states with respect to the basin of attraction of s_2: "**not**(**E**[(**not** s_1) **U** s_2]) **and EF** s_2". In formulas having such schemata, we would need to name states. Such a naming is possible in CTL by identifying a state with the conjunction of its nonnegated active genes and its negated inactive genes. *Antelope*, by contrast, provides more concise ways of referring to a state, with a number which, if written in binary, follows the lexicographic order of the names of the genes. We refer the reader to the *Antelope* user's manual and site.

Discussion

Other related systems

We now describe other systems relevant for us. For brevity, we have to exclude certain works: First, we leave out Boolean GRN simulators, such as Atalia [9], BooleanNet [16], and BoolNet [17]. Second, we omit research based on structures other than Kripke structures; examples are: a work utilizing the LTL (Linear-time Temporal Logic) model checker of the Maude system [34], works using reactive modules with the Mocha model checker [42,43], and those employing probabilistic model checking with PRISM [35,37,38]. We start with systems based on Thomas' formalism and proceed with systems using continuous approaches.

GNBox

GNBox [21,22] applies constraint logic programming techniques [30] to Thomas' formalism [13]. Such a formalism establishes a search space resulting from

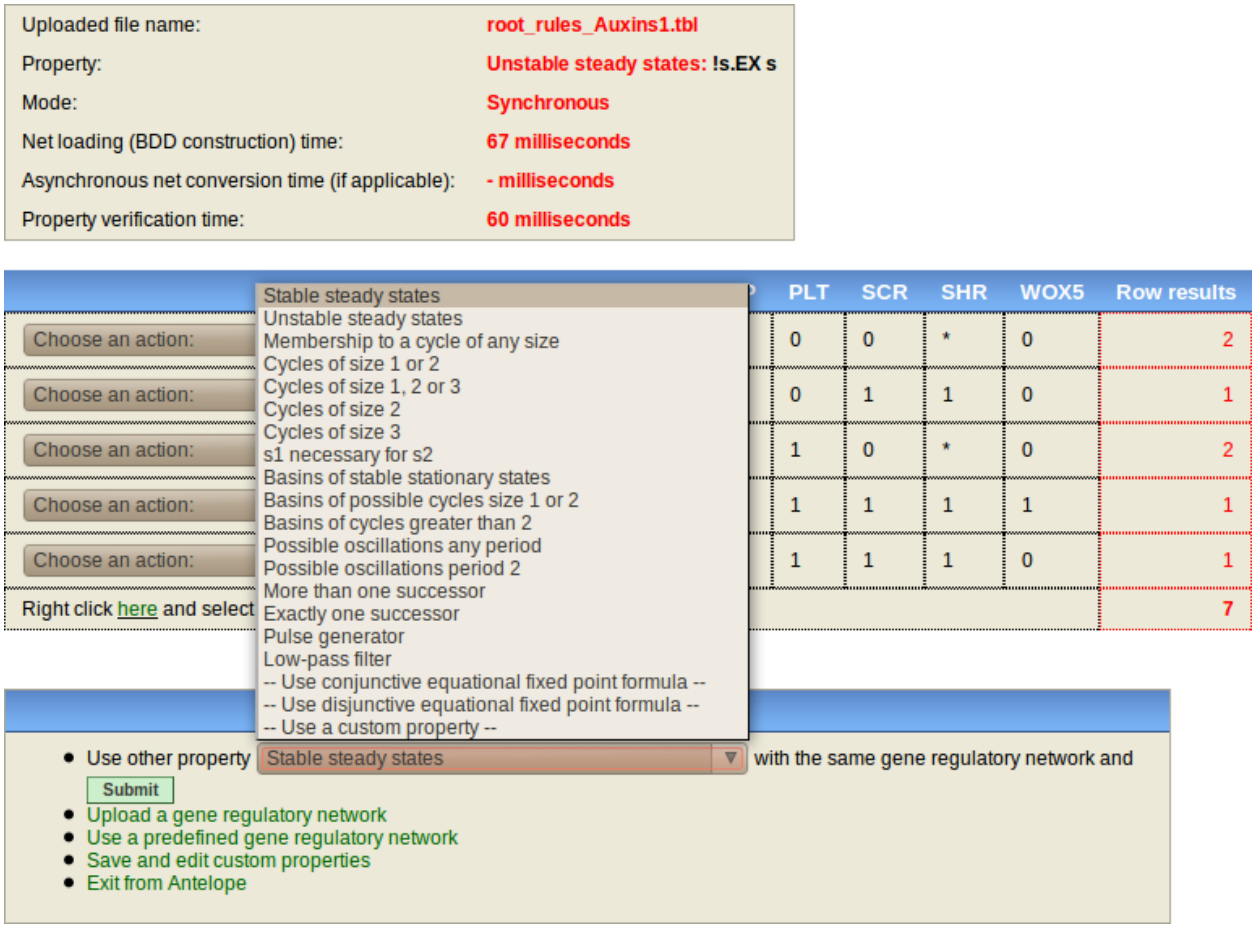

Figure 5 Screenshot of Antelope showing the results for unstable steady state search for the stem cell niche GRN with an indetermination in the SCR logical rule. This indetermination represents a mutation in *FAS*. As observed, *SCR* activity is present even in the absence of *SHR*, which is indispensable for *SCR* activity. It is important to note that some of the changes can only be observed analyzing the basins of attraction. For instance, the steady states for QC and CEI (two different cell types) are not possible without *SCR* presence; hence, a change of one steady state for another is only observable through their basins of attraction.

states possibly having more than one successor. A straightforward implementation of a logic programming language (without constraints) typically traverses a search space following a depth-first, top-down discipline in the same way as an ordinary simulator. Unlike a simulator employing a random device, however, such an implementation utilizes *backtracking*. Observe that a depth-first, top-down discipline together with backtracking can take an exponential amount of time in the size of the model [[29], p. 82]. Constraint logic programming languages, nevertheless, use constraints to efficiently traverse the search space. In particular, GNBox expresses constraints as a Boolean satisfiability (SAT) problem that is turned over to a dedicated SAT solver. This approach is able to model many possible GRNs, thereby pruning the search space and eliminating the need for performing numerous simulations. By expressing desired properties as constraints, GNBox can find parameter values of GRNs represented in Thomas' framework.

GINsim

GINsim [18-20] also uses a variant of Thomas' formalism. As in such a formalism, networks in GINsim have indeterminations representing asynchrony. GINsim computes the state transition graph of the GRN (presumably with forward traversal together with backtracking because of the indeterminations) before proceeding to analyze a trajectory selected by the user. GINsim can also classify circuits in the interaction diagram (i.e., can identify "functional" circuits) and can compute the set of all (stable) steady states of GRNs which do not have indeterminations using MDDs, a multi-value generalization of BDDs. Finally, GINsim can find the strongly connected components of the state-transition graph or the interaction graph.

SMBioNet and Mateus et al.'s system

SMBioNet [23,24] employs a variant of Thomas' formalism as well. The input is an interaction diagram of the GRN under study, together with desired properties expressed as CTL formulas. The output is a set of all the models conforming to the given interaction diagram and which also satisfy the given formulas. Candidate models are generated by instantiating parameters and then tested with a model checker.

Another system also using both Thomas' formalism and temporal logic is that by Mateus et al. [39]. Inequalities over the parameters of the model are obtained from the interaction diagram. These inequalities are augmented with LTL formulas specifying desirable properties of the model. The model is traversed forward and paths that do not satisfy the constraints are eliminated, so that only paths satisfying the constraints are retained.

SQUAD

SQUAD [25-27] combines a continuous model, employing ordinary differential equations, with a Boolean model of the network. The user provides the interaction diagram of the network, from which SQUAD obtains a continuous model. To find steady states of the continuous model, SQUAD first converts such a model into an approximate Boolean asynchronous model. (Thomas' formalism is not used because such a formalism has "proved to scale badly for large networks" [26].) In the Boolean model, SQUAD then computes, using BDDs and a random device, the set of states probably belonging to attractors of any size and occurring in attractors without indeterminations (called "steady" states in [26,27]). Next, SQUAD repetitively uses such states as initial states in a continuous simulator to search for steady states in the continuous model. Perturbations may be introduced to confirm that such steady states are stable and to identify the effect of specific genes.

GNA

GNA [40,69-72] is based on piecewise-linear differential equations. Unlike other systems using this formalism, the user need not specify precise values of parameters. Instead, less precise *intervals* are employed. States are qualitative and represent ranges of concentrations of proteins, so that simulations are also qualitative. In addition, GNA computes a discrete abstraction [73] of the continuous model, that can be verified with standard model checkers (NuSMV and CADP). The user in this case can express simple properties in CTL. For more complex properties, the GNA group has developed its own logic, called Computation Tree Regular Logic [74]. This logic extends CTL with regular expressions and fairness operators, allowing the expression of properties such as multistability and oscillations. Finally, GNA has a formula editor, guiding the user in writing new formulas.

BIOCHAM

BIOCHAM [41] can analyze and simulate *biochemical* networks using Boolean, kinetic, and stochastic models. In addition, properties can be formalized in temporal logic (CTL or LTL with numerical constraints), so that a model checker can be used to validate such properties. BIOCHAM models a network of protein interactions as a set of biochemical reaction rules, such as A+B = > C. Indeterminations appear because such a rule, for instance, is translated into four transitions going out of the same state, resulting from the four combinations of either reactant A or reactant B being completely or incompletely consumed. In addition, BIOCHAM has a model-update module, repairing models that do not satisfy the formalized properties.

Comparison and planned features

On the one hand, compared with systems employing constraints, *Antelope*, by using BDDs, can compute large sets of states having a certain CTL property (e.g., a basin of attraction). On the other hand, compared with simulators, in addition to this benefit, *Antelope* can prove assertions about infinitely many paths, as opposed to only drawing statistical conclusions. It is interesting to observe, though, that some systems built around a simulator (e.g., GINsim and SQUAD) leave the simulation technique for BDDs when calculating steady states (or approximations to such states).

We also find differences between *Antelope* and other systems using model checking. For instance, SMBioNet, Mateus et al.'s system, GNA, and BIOCHAM perform model checking for *verification*, using a model checker to confirm or deny that a certain formula is satisfied. *Antelope*, by comparison, employs model checking for *calculating* sets of states.

A first clear limitation of *Antelope* when compared with systems based on Thomas' formalism (GNBox, GINsim, SMBioNet, and Mateus et al.'s system) is its being restricted to Boolean genes. We thus plan to extend *Antelope* with multi-valued genes. In this case, it would be interesting to try to incorporate into *Antelope* techniques using constraints, like those of GNBox, for determining parameter values.

Currently, *Antelope*'s GRNs are only either completely synchronous or completely asynchronous. Another improvement would then be the possibility of representing partially asynchronous GRNs, as employed in [10]. Many of the systems we reviewed allow the user to draw the GRN, whereas currently *Antelope* only accepts textual formats for describing the GRN. Clearly, future versions of *Antelope* should also have such drawing capabilities. In addition, GNA, for instance, has a formula editor, which would be desirable in *Antelope* as well. By contrast, *Antelope* is a web application, requiring no

installation of any local software from the user other than a standard web browser. Moreover, *Antelope* can also run locally, exhibiting advantages of both web and local applications.

We can mention two further additions requiring more substantial work. BIOCHAM has an update module, repairing faulty models. A similar update module would also enhance *Antelope*'s features.

Another improvement, as with any model checker, would be the addition of more powerful methods for approaching the state-explosion problem. Currently, *Antelope* only has BDDs for representing large sets of states, but new techniques, such as CEGAR (Counterexample-guided abstraction refinement) [75] would enable *Antelope* to deal with larger GRNs.

Conclusions

Systems for analyzing and building Boolean GRNs employ branching time almost exclusively for representing asynchronous transitions. Thomas' work, however, represents two other important phenomena with branching time, namely incomplete specifications and environment interaction. A consequence of including these two other kinds of indetermination is that unstable steady states may appear. We have shown how having both stable and unstable steady states is useful for developing Boolean GRNs.

In addition, we reviewed and extended the advantages of model checking, as compared with simulation, in the presence of indeterminations. In particular, we observed that model checkers, unlike simulators randomly selecting a successor, can prove properties of a set of infinitely many paths. Another advantage we reviewed is that of handling new, unforeseen properties: While model checkers can often represent new properties with additional temporal-logic formulas, simulators require the incorporation of such properties in their program code.

We illustrated the advantages of two extensions to ordinary model checking. First, we noted that ordinary model checkers would only confirm or deny that all the states in a *given* set of states have a certain property. By contrast, we claimed that model checkers are more useful for reasoning about Boolean GRN when *exhibiting* the set of states that have a property of interest. Second, we observed that the logics (e.g., CTL and LTL) underlying many model checkers are not expressive enough for representing many interesting properties of Boolean GRNs. *Antelope* tries to overcome these two limitations by showing the set of states satisfying a given formula, and by employing a hybrid extension of CTL.

It is important to remark that model checkers for hybrid logics are both relevant and neglected. As pointed out in [76], "The implementation of model checkers for hybrid logics still remains a quite unexplored field of research". Other than *Antelope*, we only know of two hybrid model checkers [52,76]. These, however, employ a basic modal logic instead of CTL, and their implementations do not use BDDs. This makes *Antelope* the first symbolic model checker for Hybrid CTL (as far as we know) with which to experiment in the development of Boolean GRNs.

Availability and requirements

- **Project name:** *Antelope*
- **Project home page:** http://turing.iimas.unam.mx:8080/AntelopeWEB/
- **Operating system(s):** Platform independent
- **Programming language:** Java
- **Other requirements:** Any standard web browser
- **License:** GPL
- **Any restrictions to use by non-academics:** none other than those in GPL

Additional material

Additional file 1: A gentle introduction to (Hybrid) Computation-Tree Logic. This additional file has gentle introductions to Computation-Tree Logic and Hybrid Computation-Tree Logic.

Additional file 2: (Hybrid) Computation-Tree Logic. This additional file has formal definitions of Computation-Tree Logic and Hybrid Computation-Tree Logic.

Additional file 3: Benchmarks. This additional file shows the execution time for several examples.

Additional file 4: Antelope User's Manual. This additional file has the *Antelope* user's manual.

Acknowledgments

This paper owes much to Pablo Padilla-Longoria, who carefully read a previous version of this paper and subsequently had valuable discussions with us. We also thank Carlos Velarde, who patiently helped us with LATEX, Montserrat Alvarado, who helped us translating the first version of *Antelope*'s manual and generating the figures, and who is in charge of turing.iimas.unam.mx, Gabriel Muñoz-Carrillo and Jorge Hernández, who helped us translating the first version of *Antelope*'s windows and menus, Carlos Gershenson and Nathan Weinstein, who gave us useful suggestions, and Michael Dent and Michael Scott White, who proposed English changes. We gratefully acknowledge the facilities provided by the IIMAS, the Instituto de Ecología, and the Centro de Ciencias de la Complejidad. MB participated in this paper through the Centro de Ciencias de la Complejidad, by means of the "Red de Conacyt Complejidad, Ciencia y Sociedad". MB was also supported by the Czech Ministry of Education, Youth and Sports (grant LC06034). ERAB acknowledges the financial support from Conacyt grants 81433, 81542, and 90565, and PAPIIT grants IN210408, IN229009-3, and IN223607-3. DAR acknowledges the financial support from PAPIIT grant IN120509-3. Finally, we are grateful to the referees whose comments helped improve the previous version of this paper.

Author details

[1]Centro de Ciencias de la Complejidad, piso 6, ala norte, Torre de Ingeniería, Universidad Nacional Autónoma de México, Coyoacán, 04510 México D.F., México. [2]Laboratorio de Genética Molecular, Desarrollo y Evolución de Plantas, Instituto de Ecología, Universidad Nacional Autónoma de México, 3er Circuito Universitario Exterior, Junto al Jardín Botánico, Coyoacán, 04510

México D.F., México. [3]Department of Functional Genomics and Proteomics, Masaryk University, Kotlářská 2, CZ-61137 Brno, Czech Republic. [4]CEITEC-Central European Institute of Technology, Masaryk University, Žerotínovo nám. 9, CZ-60177 Brno, Czech Republic. [5]Instituto de Investigaciones en Matemáticas Aplicadas y en Sistemas, Universidad Nacional Autónoma de México, Apdo. Postal 20-726, 01000 México D.F., México.

Authors' contributions

GA did most of the web interface. JA participated in the design of, and wrote the code for, the previous version of *Antelope*'s model checker. EA contributed to the design of the stem cell niche GRN from the literature data, used *Antelope*, and participated in writing the biology part of this paper, as well as the manual. MB also contributed to the design of the stem cell niche GRN from the literature data and wrote the rest of the biology part of this paper, as well as the manual. MC suggested using Hybrid CTL to overcome CTL limitations, participated in the design of *Antelope*, contributed to the presentation of these results, and wrote the formal definitions of CTL and Hybrid CTL (additional file 2). PG wrote the code for *Antelope*'s model checker, connected the model checker with the web interface, embedded *Antelope* and *Apache Tomcat* in a single file, did the rest of the web interface, and added numerous features to *Antelope*. DAR participated in the design of *Antelope* and wrote the model-checking part of this paper. ERAB put forward the idea of testing Kauffman's hypothesis that Boolean GRNs can recover experimental gene expression profiles, and led the translation of actual data into the the stem cell niche GRN. All authors read and approved the final manuscript.

Received: 31 May 2011 Accepted: 22 December 2011
Published: 22 December 2011

References

1. von Dassow G, Meir E, Munro E, Odell G: **The segment polarity network is a robust developmental module.** *Nature* 2000, **406**:188-192.
2. Espinosa-Soto C, Padilla-Longoria P, Alvarez-Buylla E: **A gene regulatory network model for cell-fate determination during *Arabidopsis thaliana* flower development that is robust and recovers experimental gene expression profiles.** *The Plant Cell* 2004, **16**:2923-2939.
3. Li S, Assmann SM, Albert R: **Predicting essential components of signal transduction networks: a dynamic model of guard cell abscisic acid signaling.** *PLoS Biology* 2006, **4(10)**:1732-1748.
4. Albert R: **Boolean modeling of genetic regulatory networks.** In *Complex Networks.* Edited by: Ben-Naim E, Frauenfelder H, Toroczkai Z. Springer; 2004:459-481, [Lecture Notes in Physics Vol. 650].
5. de Jong H: **Modeling and simulation of genetic regulatory systems: a literature review.** *Journal of Computational Biology* 2002, **9**:67-103.
6. Fisher J, Henzinger TA: **Executable cell biology.** *Nature Biotechnology* 2007, **25(11)**:1239-1249.
7. Bornholdt S: **Boolean network models of cellular regulation: prospects and limitations.** *J R Soc Interface* 2008, **5**:S85-S94.
8. Albert R, Othmer HG: **The topology of the regulatory interactions predicts the expression pattern of the segment polarity genes in Drosophila melanogaster.** *J Theor Biol* 2003, **223**:1-18.
9. Alvarez-Buylla ER, Benítez M, Corvera-Poiré A, Candor AC, de Folter S, de Buen AG, Garay-Arroyo A, García-Ponce B, Jaimes-Miranda F, Pérez-Ruiz RV, Pineiro-Nelson A, Sánchez-Corrales YE: **Flower development.** *The Arabidopsis Book* 2010, **8**:e0999, [Doi:10.1199/tab.0999].
10. Fauré A, Naldi A, Chaouiya C, Thieffry D: **Dynamical analysis of a genetic Boolean model for the control of the mammalian cell cycle.** *Bioinformatics* 2006, **22(14)**:e124-e131.
11. Li F, Long T, Lu Y, Ouyang Q, Tang C: **The yeast cell-cycle network is robustly designed.** *Proc Natl Acad Sci USA* 2004, **101(14)**:4781-4786.
12. Davidich MI, Bornholdt S: **Boolean network model predicts cell cycle sequence of fission yeast.** *PLoS One* 2008, **3(2)**:e1672, [Doi:10.1371/journal.pone.0001672].
13. Thomas R, D'Ari R: *Biological Feedback* CRC Press; 1990.
14. Thomas R: **Regulatory networks seen as asynchronous automata.** *J Theor Biol* 1991, 1-23.
15. Thomas R, Thieffry D, Kaufman M: **Dynamical behaviour of biological regulatory networks–I. Biological role of feedback loops and practical use of the concept of the loop-characteristic state.** *Bull Math Biol* 1995, **57(2)**:247-276.
16. Albert I, Thakar J, Li S, Zhang R, Albert R: **Boolean networks simulations for life scientists.** *Source Code Biol Med* 2008, **3(16)**, [Doi: 10.1186/1751-0473-3-16].
17. Müssel C, Hopfensitz M, Kestler HA: **BoolNet–an R package for generation, reconstruction and analysis of Boolean networks.** *Bioinformatics* 2010, **26(10)**:1378-1380, [Applications Note].
18. Chaouiya C, Remy E, Mossé B, Thieffry D: **Qualitative analysis of regulatory graphs: a computational tool based on a discrete formal framework.** *Positive Systems, LNCIS* 2003, **294**:119-126.
19. Gonzalez AG, Naldia A, Sánchez L, Thieffry D, Chaouiya C: **GINsim: A software suite for the qualitative modelling, simulation and analysis of regulatory networks.** *BioSystems* 2006, **84**:91-100.
20. Naldi A, Berenguier D, Fauré A, Lopez F, Thieffry D, Chaouiya C: **Logical modelling of regulatory networks with GINsim 2.3.** *BioSystems* 2009, **97**:134-139.
21. Corblin F, Tripodi S, Fanchon E, Ropers D, Trilling L: **A declarative constraint-based method for analyzing discrete genetic regulatory networks.** *BioSystems* 2009, **98**:91-104.
22. Corblin F, Fanchon E, Trilling L: **Applications of a formal approach to decipher discrete genetic networks.** *BMC Bioinfomatics* 2010, **11**:385.
23. Bernot G, Comet JP, Richard A, Guespin J: **Application of formal methods to biological regulatory networks: extending Thomas' asynchronous logical approach with temporal logic.** *Journal of Theoretical Biology* 2004, **229**:339-347.
24. Khalis Z, Comet JP, Richard A, Bernot G: **The SMBioNet method for discovering models of gene regulatory networks.** *Genes, Genomes and Genomics* 2009, **3**:15-22.
25. Mendoza L, Xenarios I: **A method for the generation of standardized qualitative dynamical systems of regulatory networks.** *Theoretical Biology and Medical Modelling* 2006, **3**:13.
26. Cara AD, Garg A, Micheli BD, Xenarios I, Mendoza L: **Dynamic simulation of regulatory networks using SQUAD.** *BMC Bioinformatics* 2007, **8**:462.
27. Garg A, Xenarios I, Mendoza L, DeMicheli G: **An efficient method for dynamic analysis of gene regulatory networks and *in silico* gene perturbation experiments.** *Proc Research in Computational Molecular Biology* 2007, 62-76, [Lecture Notes in Computer Science No. 4453].
28. Feinendegen LE: **Significance of basic and clinical research in radiation medicine: challenges for the future.** *British Institute of Radiology supplement* 2005, **27**:185-195.
29. Poole DL, Mackworth AK: *Artificial Intelligence. Foundations of Computational Agents* Cambridge University Press; 2010.
30. Cohen J: **Constraint logic programming languages.** *Communications of the ACM* 1990, **33(7)**:52-68.
31. Clarke EM, Emerson EA: **Design and synthesis of synchronization skeletons using branching time temporal logic.** *Proc Workshop on Logics of Programs* IBM Watson Research Center; 1981, 52-71, [Lecture Notes in Computer Science No. 131].
32. Quielle JP, Sifakis J: **Specification and verification of concurrent systems in CESAR.** *Proc 5th International Symposium on Programming* 1981, 337-350.
33. Emerson EA: **The beginning of model checking: a personal perspective.** *25 Years of Model Checking* Springer; 2008, 27-45, [Lecture Notes in Computer Science No. 5000, DOI: 10.1007/978-3-540-69850-0_2].
34. Eker S, Knapp M, Laderoute K, Lincoln P, Meseguer J, Sonmez K: **Pathway logic: symbolic analysis of biological signaling.** *Proc Pacific Symposium on Biocomputing* 2002, 400-412.
35. Calder M, Vyshemirsky V, Gilbert D, Orton R: **Analysis of signalling pathways using the PRISM model checker.** *Proc Computational Methods in Systems Biology* 2005, 179-190, [Lecture Notes in Computer Science No. 4416].
36. Ahmad J, Bernot G, Comet JP, Lime D, Roux O: **Hybrid modelling and dynamical analysis of gene regulatory networks with delays.** *Complexus* 2006, **3**:231-251.
37. Heath J, Kwiatkowska M, Norman G, Parker D, Tymchyshyn O: **Probabilistic model checking of complex biological pathways.** *Theoretical Computer Science* 2008, **391(3)**:239-257.
38. Ciocchetta F, Gilmore S, Guerriero ML, Hillston J: **Integrated simulation and model-checking for the analysis of biochemical systems.** *Electronic Notes in Theoretical Computer Science* 2009, **232**:17-38.
39. Mateus D, Gallois JP, Comet JP, Gall PL: **Symbolic modeling of genetic regulatory networks.** *Journal of Bioinformatics and Computational Biology* 2007, **5(2b)**:627-640.

40. Batt G, Ropers D, de Jong H, Geiselmann J, Mateescu R, Page M, Schneider D: **Validation of qualitative models of genetic regulatory networks by model checking: analysis of the nutritional stress response in *Escherichia coli*.** *Bioinformatics* 2005, **21(Suppl 1)**:i19-i28.
41. Calzone L, Fages F, Soliman S: **BIOCHAM: An environment for modeling biological systems and formalizing experimental knowledge.** *Bioinformatics* 2006, **22(14)**:1805-1807.
42. Li C, Nagasaki M, Ueno K, Miyano S: **Simulation-based model checking approach to cell fate specification during Caenorhabditis elegans vulval development by hybrid functional Petri net with extension.** *BMC Systems Biology* 2009, **3(42)**, [Doi:10.1186/1752-0509-3-42].
43. Fisher J, Piterman N, Hajnal A, Henzinger TA: **Predictive modeling of signaling crosstalk during *C. elegans* vulval development.** *PLoS Computational Biology* 2007, **3(5)**:e92, [Doi:10.1371/journal.pcbi.0030092].
44. Prior A: *Past, Present and Future. Clarendon* 1967.
45. Blackburn P, Seligman J: **Hybrid languages.** *Journal of Logic, Language and Information* 1995, **4**:251-272.
46. Clarke EM, Emerson EA, Sistla AP: **Automatic verification of finite-state concurrent systems using temporal logic specifications.** *ACM Transactions of Programming Languages and Systems* 1986, **8(2)**:244-263.
47. Clarke EM, Grumberg O, Peled DA: *Model Checking* MIT Press; 1999.
48. Bérard B, Bidoit M, Finkel A, Laroussinie F, Petit A, Petrucci L, Schnoebelen P, McKenzie P: *Systems and Software Verification. Model-Checking Techniques and Tools* Springer; 2001.
49. Huth MRA, Ryan MD: *Logic in Computer Science. Modelling and reasoning about systems.* 2 edition. Cambridge University Press; 2004.
50. Baier C, Katoen JP: *Principles of Model Checking* MIT Press; 2008.
51. Chabrier-Rivier N, Chiaverini M, Danos V, Fages F, Schächter V: **Modeling and querying biomolecular interaction networks.** *Theoretical Computer Science* 2004, **325**:25-44.
52. Franceschet M, de Rijke M: **Model checking hybrid logics (with an application to semistructured data).** *Journal of Applied Logic* 2006, **4(3)**:279-304.
53. Areces C, ten Cate B: **Hybrid logics.** In *Handbook of Modal Logics.* Edited by: Blackburn P, Wolter F, van Benthem J. Elsevier; 2006:821-868.
54. Burch J, Clarke E, McMillan K, Dill DL, Hwang LJ: **Symbolic model checking: 10^{20} states and beyond.** *Information and Computation* 1992, **98**:142-170.
55. Bryant RE: **Graph-based algorithms for Boolean function manipulation.** *IEEE Transactions on Computers* 1986, **C-35(8)**:1035-1044.
56. Whaley J: **JavaBDD 1.0b2.** 2007 [http://javabdd.sourceforge.net/].
57. Lind-Nielsen J: **BuDDy 2.4.** 2004 [http://sourceforge.net/projects/buddy/].
58. Scheres B: **Stem-cell niches: nursery rhymes across kingdoms.** *Nat Rev Mol Cell Biol* 2007, **8(5)**:345-354.
59. Dolan L, Janmaat K, Willemsen V, Linstead P, Poethig S, Roberts K, Scheres B: **Cellular organisation of the *Arabidopsis thaliana* root.** *Development* 1993, **119**:71-84.
60. Sarkar AK, Luijten M, Miyashima S, Lenhard M, Hashimoto T, Nakajima K, Scheres B, Heidstra R, Laux T: **Conserved factors regulate signalling in *Arabidopsis thaliana* shoot and root stem cell organizers.** *Nature* 2007, **446(7137)**:811-814.
61. Azpeitia E, Benítez M, Vega I, Villarreal C, Alvarez-Buylla ER: **Single-cell and coupled GRN models of cell patterning in the *Arabidopsis thaliana* root stem cell niche.** *BMC Syst Biol* 2010, **4(135)**.
62. Levesque M, Vernoux T, Busch W, Cui H, Wang J, Blilou I, Hassan H, Nakajima K, Matsumoto N, Lohmann J, Scheres B, Benfey P: **Whole-genome analysis of the SHORT-ROOT developmental pathway in *Arabidopsis*.** *PLoS Biol* 2006, **4(5)**:e143.
63. Cui H, Levesque M, Vernoux T, Jung J, Paquette A, Gallagher K, Wang J, Blilou I, Scheres B, Benfey P: **An evolutionarily conserved mechanism delimiting SHR movement defines a single layer of endodermis in plants.** *Science* 2007, **316(5823)**:421-425.
64. Welch D, Hassan H, Blilou I, Immink R, Heidstra R, Scheres B: ***Arabidopsis* JACKDAW and MAGPIE zinc finger proteins delimit asymmetric cell division and stabilize tissue boundaries by restricting SHORT-ROOT action.** *Genes Dev* 2007, **21(17)**:2196-2204.
65. Sabatini S, Heidstra R, Wildwater M, Scheres B: **SCARECROW is involved in positioning the stem cell niche in the Arabidopsis root meristem.** *Genes Dev* 2003, **17(3)**:354-358.
66. Ogasawara H, Kaimi R, Colasanti J, Kozaki A: **Activity of transcription factor JACKDAW is essential for SHR/SCR-dependent activation of SCARECROW and MAGPIE and is modulated by reciprocal interactions with MAGPIE, SCARECROW and SHORT ROOT.** *Plant Mol Biol* 2011.
67. Kaya H, Shibahara K, Taoka K, Iwabuchi M, Stillman B, Araki T: **FASCIATA genes for chromatin assembly factor-1 in *Arabidopsis* maintain the cellular organization of apical meristems.** *Cell* 2001, **104**:131-142.
68. Inagaki S, Suzuki T, Ohto M, Urawa H, Horiuchi T, Nakamura K, Morikami A: **Arabidopsis TEBICHI, with helicase and DNA polymerase domains, is required for regulated cell division and differentiation in meristems.** *Plant Cell* 2006, **18(4)**:879-892.
69. de Jong H, Geiselmann J, Hernández C, Page M: **Genetic Network Analyzer: qualitative simulation of genetic regulatory networks.** *Bioinformatics* 2003, **19(3)**:336-344.
70. Batt G, Ropers D, de Jong H, Geiselmann J, Mateescu R, Page M, Schneider D: **Analysis and verification of qualitative models of genetic regulatory networks: a model-checking approach.** *IJCAI* 2005, 370-375.
71. Ropers D, de Jong H, Page M, Schneider D, Geiselmann J: **Qualitative simulation of the carbon starvation response in Escherichia coli.** *BioSystems* 2006, **84**:124-152.
72. Monteiro PT, Dumas E, Besson B, Mateescu R, Page M, Freitas AT, de Jong H: **A service-oriented architecture for integrating the modeling and formal verification of genetic regulatory networks.** *BMC Bioinformatics* 2009, **10(450)**[http://www.biomedcentral.com/1471-2105/10/450].
73. Batt G, de Jong H, Page M, Geiselmann J: **Symbolic reachability analysis of genetic regulatory networks using discrete abstractions.** *Automatica* 2008, **44**:982-989.
74. Mateescu R, Monteiro PT, Dumas E, de Jong H: **Computation Tree Regular Logic for genetic regulatory networks.** In *Proc Automated Technology for Verification and Analysis (ATVA)* Edited by: Cha SS, Choi JY, Kim M, Lee I, Viswanathan M 2008, 48-63, [Lecture Notes in Computer Science No. 5311, Seoul, Korea].
75. Clarke E, Grumberg O, Jha S, Lu Y, Veith H: **Counterexample-guided abstraction refinement for symbolic model checking.** *Journal of the ACM* 2003, **50(5)**:752-794.
76. Mosca A, Manzoni L, Codecasa D: **HyLMoC a model checker for hybrid logic.** *Proc 24th Italian Congress on Computational Logic (CILC-09)* 2009.

doi:10.1186/1471-2105-12-490
Cite this article as: Arellano *et al.*: "Antelope": a hybrid-logic model checker for branching-time Boolean GRN analysis. *BMC Bioinformatics* 2011 **12**:490.

8.3. Parte III:

Artículo:

Hormone Symphony During Root Growth and Development

Adriana Garay-Arroyo, María De La Paz Sánchez, Berenice García-Ponce, Eugenio Azpeitia, Elena R. Álvarez-Buylla

Developmental Dynamics

DEVELOPMENTAL DYNAMICS 241:1867–1885, 2012

SPECIAL ISSUE REVIEWS–A PEER REVIEWED FORUM

Developmental Dynamics

Hormone Symphony During Root Growth and Development

Adriana Garay-Arroyo,[1,2†*] María De La Paz Sánchez,[1,2†] Berenice García-Ponce,[1,2] Eugenio Azpeitia,[1,2] and Elena R. Álvarez-Buylla[1,2,3*]

Hormones regulate plant growth and development in response to external environmental stimuli via complex signal transduction pathways, which in turn form complex networks of interaction. Several classes of hormones have been reported, and their activity depends on their biosynthesis, transport, conjugation, accumulation in the vacuole, and degradation. However, the activity of a given hormone is also dependent on its interaction with other hormones. Indeed, there is a complex crosstalk between hormones that regulates their biosynthesis, transport, and/or signaling functionality, although some hormones have overlapping or opposite functions. The plant root is a particularly useful system in which to study the complex role of plant hormones in the plastic control of plant development. Physiological, cellular, and molecular genetic approaches have been used to study the role of plant hormones in root meristem homeostasis. In this review, we discuss recent findings on the synthesis, signaling, transport of hormones and role during root development and examine the role of hormone crosstalk in maintaining homeostasis in the apical root meristem. *Developmental Dynamics 241:1867–1885, 2012.* © 2012 Wiley Periodicals, Inc.

Key words: hormones; root growth; plant development

Accepted 17 September 2012

INTRODUCTION

Normal cell growth and morphogenesis result from the concerted modulation of cell proliferation and cell elongation, which in turn respond and feed back to a complex combination of environmental and endogenous stimuli. Hormones are key endogenous stimuli in plant development that affect plant growth in small concentrations. Thus far, eight different plant hormones have been identified and isolated: auxins, gibberellins, cytokinins, ethylene, abscisic acid, brassinosteroids, strigolactones, and jasmonic acid (Santner et al., 2009; Santner and Estelle, 2009; Wolters and Jurgens, 2009). Plant hormones are small, naturally occurring substances with very diverse chemical natures and structures. These compounds regulate plant growth and development in response to external environmental stimuli via complex signal transduction pathways, which in turn exhibit feedback regulation of networks controlling cell differentiation and proliferation (Santner et al., 2009; Santner and Estelle, 2009; Wolters and Jurgens, 2009; Depuydt and Hardtke, 2011).

The activity of a given hormone depends on its biosynthesis, transport, conjugation, accumulation in the vacuole, and degradation. All hormones regulate several processes independently, and recent studies indicate that there is a complex crosstalk between hormones that regulates their biosynthesis, transport, and/or signaling functionality, although some hormones have overlapping or opposite functions (Benková and Hejatko, 2009; Galinha et al., 2009; Santner et al., 2009; Santner and Estelle, 2009; Wolters and Jurgens, 2009).

The size of meristems results from the balance between cell proliferation

[1]Laboratorio de Genética Molecular, Desarrollo y Evolución de Plantas, Instituto de Ecología, Universidad Nacional Autónoma de México, México D.F., México
[2]Centro de Ciencias de la Complejidad, Universidad Nacional Autónoma de México, México City, Mexico
[3]University of California, Berkeley. College of Natural Resources. Department of Plant and Microbial Biology, Berkeley, California
[†]**Adriana Garay-Arroyo and María de la Paz Sánchez contributed equally to this work.**
***Correspondence to: Adriana Garay Arroyo and Elena R. Alvarez-Buylla, Laboratorio de Genética Molecular, Desarrollo y Evolución de Plantas, Instituto de Ecología, Universidad Nacional Autónoma de México, 3er Circuito Ext. Junto a J. Botánico, Ciudad Universitaria, UNAM, México D.F. 04510, México. E-mail: garay.adriana@gmail.com; eabuylla@gmail.com**

DOI 10.1002/dvdy.23878
Published online 1 October 2012 in Wiley Online Library (wileyonlinelibrary.com).

Fig. 1. Longitudinal confocal section of Arabidopsis root tip showing two of the three root zones. The proliferation zone (MZ) includes the stem cell niche and the zone in which cells divide actively. The elongation zone (EZ) is the region in which cells stop dividing and elongate. When elongation terminates, the cells attain their final fates. E, epidermis; C, cortex; En, endodermis; St, stele; Col, columella.

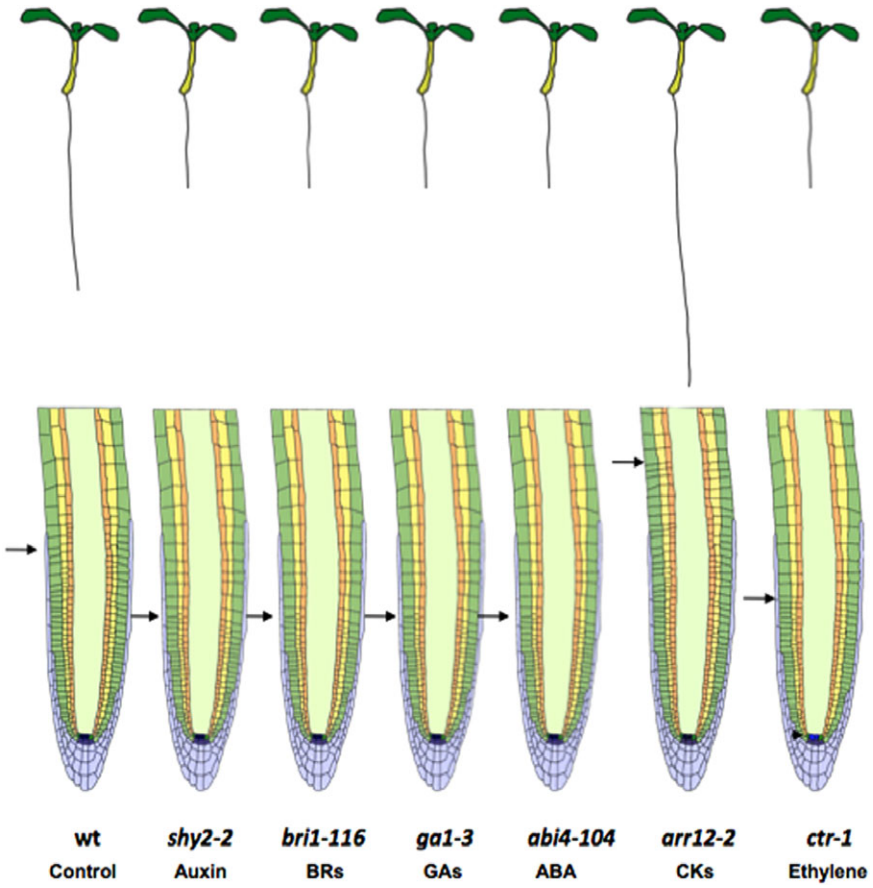

Fig. 2. Schematic representations of mutant root phenotypes for hormone pathways components. Loss- or gain-of-function mutants (top) and meristem sizes (bottom) are shown. The black arrows indicate the boundary between proliferation and elongation zones. Repression of auxin, Brassinosteroids (BRs), and Gibberelins (GAs) signaling causes short root phenotypes and a reduction in meristem size as observed in *shy2-2* gain-of-function and *bri1-116* loss-of-function mutants that repress auxin signaling (Dello Ioio et al., 2008b) and BR signaling (Gonzalez-Garcia et al., 2011), respectively; the same root growth phenotype is observed in *ga1-3* (GA) and *abi4-104* (Abscisic Acid; ABA) -deficient mutants (Achard et al., 2009; Cui et al., 2012). However, *arr12-2* loss-of-function mutants that repress Cytokinins (CKs) signaling have longer roots and meristems (Dello Ioio et al., 2007). The constitutive triple response *ctr-1* mutants exhibit enhanced ethylene signaling and short roots with smaller meristems as well as ectopic QC cell division (Ortega-Martinez et al., 2007; Negi et al., 2008; Thomann et al., 2009).

and differentiation rates. Meristem size regulation, which is clearly affected by plant hormones, is fundamental for normal development (Dharmasiri et al., 2005; Dello Ioio et al., 2007, 2008a; Benková and Hejatko, 2009; Galinha et al., 2009; Ubeda-Tomas et al., 2009). The root meristem is a particularly useful system in which to study such balance as the result, among others, of the complex role of plant hormones in the plastic control of plant development and physiology; both molecular genetic and cellular approaches have been used to study the role of plant hormones in root meristem homeostasis (Dharmasiri et al., 2005; Dello Ioio et al., 2007, 2008a; Benková and Hejatko, 2009; Galinha et al., 2009; Ubeda-Tomas et al., 2009). However, an integrated view of the independent and concerted action of all plant hormones in root meristem homeostasis has not been provided in previous reviews (Dello Ioio et al., 2007, 2008a; Benková and Hejatko, 2009; Galinha et al., 2009).

ROOT DEVELOPMENT

During embryogenesis, plant meristems are established and provide most of the post-embryonic cells that constitute the organs of plants throughout their life cycle. There are two main meristems: an aerial meristem at the growing tip of the shoot (shoot apical meristem; SAM) and an underground meristem at the root apex (root apical meristem; RAM). The *Arabidopsis thaliana* RAM contains a self-renewal stem-cell niche (SCN) with a central organizer termed the quiescent center (QC) because it comprises four cells with a very low division rate. The QC is surrounded by the stem (or initial) cells, which yield the cells of all the major tissues that compose the root. The initial cells divide asymmetrically with an intermediate proliferation rate. One of the daughter cells of each of the stem cells remains close to the QC and retains its stem cell identity,

TABLE 1. Summarized Characterization of Six Plant Hormones and Their Role During Root Development

HORMONE	Site of synthesis in the plant	Precursors	Conjugates (reversible storage)	Inactivation	Movement	Receptor and subcellular localization	Signal transduction components	DNA binding motif	Role in root development	Root mutant phenotype
AUXIN	In the shoot apical meristem and young leaves. In the roots along the meristem and, very importantly, in the QC.	Tryptophan and indole-3-glycerol phosphate.	Ester or amide linkages to sugars, amino acids, or peptides.	Oxindole-3-acetic acid.	Passive and active (influx carriers: AUX and LAX and efflux carriers: PIN and ABCB).	TIR-like and ABP1. Nuclear localization.	AUX/IAA and ARF.	5′-GTGCGC-3′	It has a central role in the establishment, organization and maintenance of the RAM, also affects root proliferation and elongation.	*shy2-2*, the triple mutant *tir1-1*/*afb2-1*/*afb3-1* and the quadruple *tir1-1*/*afb1-1*/*afb2-1*/*afb3-1* mutants have short roots.
CYTOKININ	Abundant in proliferating tissues, such as root and shoot apical meristems, young leaves, and immature seeds.	Adenine.	Cytokinins exist in plants not only as free bases but also in the form of nucleosides and nucleotides.	Depends on the activity of the CKX proteins.	Passive: tZ-type has been found on the xylem sap and iP-type in leaf exudates.	AHK2, AHK3 and AHK4. Plasma membrane localization.	AHP, A-ARR, B-ARR and CRF.	5′-(A/G)GGAT(T/C)-3′	Affects the rate of cell differentiation in the vascular tissues.	The triple mutant *ahk2*/*ahk3*/*ahk4* showed reduced root meristem. *ahk3* or (*ipt3*/*ipt5*/*ipt7*) have longer roots and meristems than *wt*.
GIBBERELLINS	In rapidly growing tissues such as the shoot and root tips, developing flowers and seeds.	Terpenoids.	GA-O-glucosyl ether or GA-glucosyl ester. There are many biosynthetic intermediates or catabolites.	2β-hydroxylation by GA 2-oxidases (GA2oxs).	Transport of intermediate pathway compounds between cells.	GID1a, GID1b and GID1c. Nuclear localization.	DELLA.	5′-TAACAAA/G-3′	Regulates root growth controlling cell proliferation and elongation (only in the endodermis).	Only one of the double mutant receptor combinations (*atgid1a*/*atgid1c*) shows a dwarf phenotype. *ga1-3* and *ga3ox1*/*ga3ox2* have smaller roots and root meristems.
BRASSINOSTEROIDS	In young aerial tissues, such as apical shoots, pollen and siliques.	Steroids.	Glycosylation and sterefication (myristate, palmitate and laurate).	25 and 26 hydroxylation.	Probably by short-distance that involves unknown carrier.	BRI1, BRL1 and BRL3. Plasma membrane localization.	BZR1 and BZR2/BES1.	5′-CGTG(T/C)G-3′ and 5′-CANNTG-3′	Affects root cell expansion and root cell division.	*bak1-1, dwf1-6, cbb3, bri1-116* mutants and *bak1-4*/*bkk1-1*/*serk1-8* triple mutant have short roots; *bri1-116* also has short meristems.
ETHYLENE	Leaves, roots, shoots and flowers.	Methionine.	N-malonyl-ACC.	Ethylene oxide.	Diffusion freely through membranes. The gas is distributed through intracellular spaces.	ETR1, ETR2, ERS1, ERS2, EIN4. Plasma membrane localization.	EIN2, EIN3.	5′-TAAGAGC CGCC-3′	Regulates root cell elongation and root hair differentiation. In the QC can promote cell division.	Mutants that increase the levels of ethylene as *ctr1-1* and *eto1-2* have short roots and QC ectopic cell division.
ABSCISIC ACID	In all tissues; in vascular parenchyma cells.	Zeaxanthin.	ABA-glucosyl esters (ABA-GE).	8′-OH-ABA.	Transported via xylem and phloem. Efflux by ABCG25 and iflux by ABCG40.	PYR and RCAR are soluble receptors.	ABI1 to ABI5 and ABFs.	ABREs (5′-ACGTGG/TC-3′) and CE1 (5′-CCACC-3′) or CE3 (5′-GCGTGTC-3′)	Regulates root elongation, quiescence and cell differentiation.	*abi4-104 mutant* has smaller roots. Several mutants are deficient in SCN differentiation such as *ba1-1, aba2-3, aba2-4, aba3-2, abi1-1, abi2-1, abi3-1 and abi5-5*.

whereas the other cell divides anticlinally, attains a maximum proliferation rate, and eventually elongates and differentiates into a specific root cell type (Dolan et al., 1993; van den Berg et al., 1995, 1997). After 4 to 6 division cycles in the meristematic or proliferation zone (MZ), the cells commence elongation and form the elongation zone (EZ) (V. Ivanov, personal communication; Bennett and Scheres, 2010). The cells then attain their ultimate fate in the differentiation zone (DZ). The Arabidopsis primary root has a simple radial structure of concentric cylinders of different cell types including (from outermost to innermost layer) a lateral root cap that extends as an outermost sheath of the root tip in the meristematic zone, epidermis, cortex, endodermis, and stele (pericycle and vasculature) (Dolan et al., 1993) (Fig. 1).

In this review, we examine recent findings on the synthesis, signaling, and transport of hormones that regulate homeostasis in the apical root meristem, and we review findings regarding the transcriptional activation of major genes involved in hormone pathways during root meristem development.

AUXIN

Auxin is involved at nearly all stages of plant growth and development in all organs (reviewed in (Woodward and Bartel, 2005; Benková and Hejatko, 2009; Galinha et al., 2009; Santner et al., 2009; Santner and Estelle, 2009; Wolters and Jurgens, 2009).

The most bioactive form of auxin in plants is indole-3-acetic acid (IAA), which is synthesized in Arabidopsis by tryptophan-dependent (TAM and IAN) and tryptophan-independent pathways (reviewed in Woodward and Bartel, 2005). Similar to most hormones, auxin can form inactive conjugates (Table 1) that may function in the storage of IAA, as intermediates in degradative processes or as protection against oxidative degradation; indeed, once IAA is oxidized to oxindole-3-acetic acid (OxIAA), it is broken down irreversibly (Ostin et al., 1998).

Auxin is mainly synthesized in young leaves and in the SAM, and it is transported to the root via the phloem (Ljung et al., 2001). However, recent studies have demonstrated that it is also synthesized in the root, and such synthesis is indispensable for maintaining the observed patterns of auxin gradients in the root meristem (Ljung et al., 2005; Ikeda et al., 2009; Petersson et al., 2009).

Auxin perception in plant cells begins when auxin binds to one of its multiple nuclear receptors including TRANSPORT INHIBITOR RESPONSE 1 (TIR1; Dharmasiri et al., 2005; Kepinski and Leyser, 2005), the TIR1-like proteins AUXIN SIGNALING F-BOX PROTEIN 1 to 5 (AFB1-AFB5; Dharmasiri et al., 2005; Parry et al., 2009), and the AUXIN BINDING PROTEIN (ABP1; Hertel et al., 1972; Jones, 1998). TIR1 and AFB1-AFB5 are F-box subunits of the ubiquitin ligase complex SCF^{TIR1}. Interaction with auxin does not appear to induce a conformational change in the complex; however, it does appear to stabilize the affinity of the receptors for AUX/IAA proteins, which are transcriptional repressors of *AUXIN RESPONSE FACTOR* (*ARF*) transcription factors. When AUX/IAA proteins interact with auxin receptors, the AUX/IAA proteins become ubiquitinated and targeted for degradation by the proteosome. This degradation effectively releases ARF proteins, which form dimers and regulate their target genes (reviewed in Calderon Villalobos et al., 2012). ARF family members bind to a sequence within the regulatory regions of target genes known as the AUXIN RESPONSE ELEMENT (ARE; 5′-TGTCTC-3′).

Auxin moves within Arabidopsis using two types of transport mechanisms. One of these mechanisms functions over long distances (termed long-range transport), is dependent on the phloem, and moves auxin mainly from the aerial part of the plant to the root. The other mechanism functions over short distances and is responsible for transport through plasma membranes via import-export mechanisms such as membrane diffusion, secretion, and receptor- or transporter-mediated systems (reviewed in Paponov et al., 2005; Petrásek and Friml, 2009; Vanneste and Friml, 2009). This cell-to-cell transport system complements vasculature translocation and is used mainly to load and unload substances from the phloem and to distribute short-range signals within tissues (Swarup et al., 2001; Marchant et al., 2002). When this short-range transport involves influx and efflux carriers that are distributed asymmetrically in the plasma membrane, it is referred to as polar auxin transport (PAT) and gives directionality to auxin distribution. PAT is dependent on influx carriers such as *AUXIN RESISTANCE 1* (*AUX1*) and *LIKE AUX* (*LAX*) family members as well as efflux transporters such as *PIN FORMED* (*PIN*) and *ATP-BINDING CASSETTE GROUP B* (*ABCB*/*MDRPGP*) family members (Bennett et al., 1996; Galweiler et al., 1998; Luschnig et al., 1998; Noh et al., 2001; Friml et al., 2002, 2003; Swarup et al., 2008; Verrier et al., 2008; Mravec et al., 2009).

PIN proteins mainly control the direction of auxin flux and the PIN family in Arabidopsis consists of eight members (Vieten et al., 2007; Zazímalová et al., 2007). The PIN proteins have a polar distribution in cell membranes, which causes a directed flux of auxin from one cell to another (Petrásek et al., 2006; Wisniewska et al., 2006; Mravec et al., 2008). Newly synthesized PIN proteins pass through the cell endomembrane system and are targeted to the apical, basal, or lateral plasma membrane (Feraru and Friml, 2008; Grunewald and Friml, 2010). Additionally, these proteins are continuously internalized by endocytosis from the plasma membrane and participate in constant cycles of endocytosis and exocytosis (Geldner et al., 2001; Marhavy et al., 2011).

AUXIN AND ROOT DEVELOPMENT

Auxin concentration varies among different plant tissues and organs, and such graded distribution is correlated with different cellular behaviors (Sabatini et al., 1999; Friml et al., 2002; Benková et al., 2003). In the root, graded auxin distribution is clearly associated with patterns of cell proliferation and elongation observed

along the apical-basal axis. High levels of auxin are found in the QC where there is little mitotic activity, intermediate auxin levels promote an intermediate level of mitotic activity in stem cells. Whereas in meristematic zone lower auxin levels are correlated with rapid cell proliferation, and the lowest levels of auxin are correlated with proliferation arrest and cell elongation/differentiation (Grieneisen et al., 2007). The *PLETHORA* (*PLT*) genes, which encode transcriptional regulators, have been postulated to be key components of the read-out mechanisms of auxin gradients. Indeed, the *PLT* genes that respond to auxin are also expressed along the RAM in a graded manner that resembles that of auxin (Aida et al., 2004; Galinha et al., 2007). Importantly, *PLT* genes, in conjunction with *SCARECROW* (*SCR*) and *SHORTROOT* (*SHR*) genes, are a fundamental part of the network that specifies the SCN (Helariutta et al., 2000; Sabatini et al., 2003; Azpeitia and Alvarez-Buylla, 2012; Aida et al., 2004). Auxin also regulates *WUSCHEL-RELATED HOMEOBOX 5* (*WOX5*), which is expressed in the QC and is necessary for maintaining the stem cells of the columella in an undifferentiated state (Ding and Friml, 2010; Sarkar et al., 2007).

The graded distribution of auxin along the root depends largely on the polar localization of its PIN transporters. At least five PIN proteins localize to the plasma membrane and create a "reflux" loop that controls auxin distribution in the growing root meristem (Blilou et al., 2005; Vieten et al., 2005). The PIN transporters appear to be functionally redundant, and only their multiple mutants show severe growth and differentiation defects (Blilou et al., 2005). These proteins localize to different areas of the root (Vieten et al., 2005) where they control the flux of recirculating auxin in the root meristem and could operate partially independently of auxin coming from the shoot (Blilou et al., 2005; Ljung et al., 2005; Vieten et al., 2005). The acropetal auxin flow in the stele toward the root tip seems to be maintained by PIN1, PIN3, PIN4, and PIN7; PIN4 then distributes this auxin to the columella where PIN3 and PIN7 redistribute it laterally to the lateral root cap and epidermis. PIN2, with the assistance of AUX1 and ABCB4, mediates basipetal auxin transport toward the elongation zone, whereas PIN1, PIN3, PIN4, and PIN7 recycle some auxin from the epidermis back to the vasculature. PIN2 transports auxin acropetally through the cortex cells (Blilou et al., 2005; Vieten et al., 2005). It has been shown that the modulation of PIN activity can independently affect meristem size, elongation rate, and final cell size (Blilou et al., 2005; Vieten et al., 2005).

Auxin also has a central role in the establishment, organization, and maintenance of the RAM (Reed et al., 1998; Sabatini et al., 1999; Benjamins et al., 2001; Friml et al., 2002; Lewis et al., 2007; Benjamins and Scheres, 2008). Mutants with defects in auxin activity fail to initiate roots and exhibit premature arrest of the root meristem and root stem cell function (Hardtke and Berleth, 1998). Exogenously applied auxin may have positive or negative effects on root growth depending on the concentration; the application of 0.1 nM IAA to wild-type Arabidopsis roots causes an increase in both meristem size (Dello Ioio et al., 2007) and root growth via modulation of the cellular response to gibberellins (see Root Cell Proliferation section in this review; Fu and Harberd, 2003).

In addition to its role in cell proliferation, auxin controls the transition from cell proliferation to cell differentiation in the root meristem via inhibition of the endoreduplication cycle (Ishida et al., 2010). Moreover, auxin also inhibits root cell elongation in non-stem cells at a concentration of 10^{-6} M, whereas at lower concentrations (10^{-10} M), root cell elongation is maintained (Evans et al., 1994).

When auxin transport is blocked, root regeneration (Sena et al., 2009) and lateral root formation are inhibited, root hair initiation and elongation are decreased (Quint et al., 2009), and the production of ectopic QC and stem cells is induced (Sabatini et al., 1999). Moreover, the triple *tir1-1/afb2-1/afb3-1* and quadruple *tir1-1/afb1-1/afb2-1/afb3-1* auxin receptor mutants exhibit various root phenotypes, with some plants displaying shortened roots whereas others entirely lack roots (Dharmasiri et al., 2005).

CYTOKININS

Cytokinins (CKs) play roles in many aspects of plant growth and development including apical dominance, the repression of leaf senescence, root cell differentiation, vascular tissue development, pathogen responses, nutrient mobilization, seed germination, and SAM maintenance (reviewed in Klee and Lanahan, 1995; Kieber, 2002). Many of these processes are controlled in coordination with other hormones, particularly auxin. Although CKs regulate many processes, they mainly function to control proliferation in the shoot and differentiation in the root (Ferreira and Kieber, 2005; Dello Ioio et al., 2007, 2008b; Kyozuka, 2007).

CKs are adenine derivatives that are abundant in proliferating tissues such as shoot apical meristems, young leaves, and immature seeds. Interestingly, one of the major regions in which cytokinin biosynthesis occurs is the columella of the root tip (reviewed in Aloni et al., 2004). CKs can act within the region where they are synthesized or they can move, e.g., from the root tip to the aerial tissues of the plant via the xylem (Takei et al., 2004; Hirose et al., 2008).

The synthesis of CK is initiated in a rate-limiting step catalyzed by *ATP/ADP-ISOPENTYL-TRANSFERASE* (*IPT*; Miyawaki et al., 2004; Takei et al., 2004), which transfers an isopentenyl group to an adenine nucleotide (iP nucleotide). In Arabidopsis, iP nucleotides are converted to tZ nucleotides by the cytochrome P450 monooxygenases CYP735A1 and CYP735A2 (Takei et al., 2004; Hirose et al., 2008). Inactive CK nucleotides such as iPRMP and tZRMP can be activated by *LONELY GUY* (*LOG*) proteins that directly convert these compounds to the bioactive freebase (Kyozuka, 2007), whereas most metabolic CK inactivation depends on the activity of the CYTOKININ OXIDASE/DEHYDROGENASE (CKX) protein family (Werner et al., 2001, 2003). All these genes and proteins are regulated differently, which suggests that they play important roles in coordinating cytokinins both spatially and

temporally during growth and development (Werner et al., 2003; Hirose et al., 2008; Frebort et al., 2011).

CKs are classified into 4 groups (isopentenyladenine (iP)-type, trans-zeatin-type (tZ-type), cis-zeatin-type, and aromatic cytokinins) according to the structure of their side chain. Although only the iP-type cytokinin (N^6-(Δ2-isopentenyl) adenine and its hydroxylated derivative trans-zeatin (tZ) are active in Arabidopsis, a variety of conjugates may form, which allows the plant to fine-tune the level of active hormone (Matsumoto-Kitano et al., 2008).

CKs are transported through the vasculature in a compartmentalized way; the tZ-type has been observed in the xylem sap and the iP-type was found in leaf exudates (Hirose et al., 2007; Matsumoto-Kitano et al., 2008). Thus far, no differences in the physiological roles of these two types of CKs have been observed; however, the translocation of cytokinins is apparently mediated by subsets of purine permeases and nucleoside transporters (Gillissen et al., 2000; Burkle et al., 2003; Hirose et al., 2005).

In Arabidopsis, CKs are perceived by a two-component system that involves a histidine kinase receptor located in the plasma membrane that induces a phosphorylation cascade and subsequently activates transcription factors in the nucleus (Muller and Sheen, 2007). Three independent histidine kinase receptors (*AHK2, AHK3*, and *CRE1*/*WOL*/*AHK4*) bind to cytokinin, autophosphorylate, and subsequently transfer the phosphoryl group to a histidine phosphotransfer protein that translocates to the nucleus and phosphorylates ARABIDOPSIS RESPONSE REGULATORS (ARR). Type-B ARRs are positive regulators that initiate the transcription of CK-responsive genes; among the targets of type *B-ARR* genes are a group of negative regulators termed type-A *ARRs* (To et al., 2004). Type-A ARRs are repressors that lack a DNA-binding domain and predominantly localize to the nucleus; there, it is likely that they act in conjunction with other transcription factors to regulate genes (Argueso et al., 2010). Certain members of the AP2 family of transcription factors, renamed CYTOKININ RESPONSE FACTORS (CRFs), are upregulated by cytokinin through the two-component system pathway. CRFs are also activated by AHPs, and it was proposed that they mediate cytokinin-regulated gene expression in tandem with B-type ARRs (Rashotte et al., 2006). B-ARR proteins bind to a core sequence within the regulatory regions of their target genes (5′-(G/A)GGAT(T/C)-3′).

THE ROLE OF CYTOKININS IN ROOT MERISTEM DEVELOPMENT

CKs negatively regulate the size of the RAM and primarily affect the meristematic cell differentiation rate. Exogenously applied cytokinin reduces the root meristem size (Dello Ioio et al., 2007), and CK-deficient mutants (e.g., *arr12-2* or the biosynthetic triple mutant *ipt3*/*ipt5*/*ipt7*; see Fig. 2) as well as plants overexpressing CKX display longer roots with longer meristems (Werner et al., 2003). The application of cytokinins does not appear to alter SCN activity or meristematic cell proliferation in the root; CKs affect the cell differentiation rate only when applied to the vascular tissue at the MZ/EZ transition zone in the presence of auxin (Dello Ioio et al., 2007). Furthermore, using mutant analysis, it was shown that only the AHK3 receptor and the ARR1 and ARR12 transcription factors mediated this effect (Dello Ioio et al., 2007, 2008b). It is important to emphasize that root meristem size and root growth are mediated mainly by the interplay between cytokinin and auxin (see Root Cell Proliferation and Root Cell Elongation sections in this review).

As expected, the over-expression of CKX in Arabidopsis induces many developmental changes in the root including a larger root meristem, a thicker columella cell layer, enhanced radial expansion with additional cell files, an enhanced vascular system, increased root branching, and additional adventitious roots (Schmülling et al., 2003). Interestingly, studies on CK receptor mutants revealed a positive role for CK in the root meristem: the triple receptor mutant (*ahk2*/*ahk3*/*ahk4*) exhibits a strong reduction in shoot and root growth (Nishimura et al., 2004). These results imply that the root response to CK is not linear; a small reduction in cytokinin levels or signaling increases root growth, but reduction beyond a threshold results in decreased growth.

GIBBERELLINS

Gibberellins (GAs) are important regulators of diverse aspects of plant growth and development including seed germination, stem and root elongation, leaf expansion, flower and seed development, and the size of the RAM. GAs promote cell division in the proliferation zone but have no effect on SCN activity (Taiz and Zeiger, 2006), and although they form a large family, only a small number of GAs are biologically active (e.g., GA_1, GA_3, GA_4, and GA_7, with GA_4 being the most active GA in Arabidopsis; reviewed in Hedden and Phillips, 2000). Consequently, many of the other GAs are biosynthetic intermediates or catabolites of bioactive GAs, and the final concentration of biologically active GAs depends on biosynthesis, catabolism and metabolic deactivation (reviewed in Yamaguchi, 2008).

GAs are synthesized and act mainly in rapidly growing tissues such as the shoot and root tips as well as developing flowers and seeds (Silverstone et al., 1997). GAs are biosynthesized from geranylgeranyl diphosphate (GGDP), a common C20 precursor of diterpenoids, and bioactive GAs in plants are synthesized by three different classes of enzymes: terpene synthases (TPSs), cytochrome P450 monooxygenases (P450s), and 2-oxoglutarate–dependent dioxygenases (2ODDs). GAs are deactivated in several different ways; the best characterized of these is 2β-hydroxylation catalyzed by a class of 2ODDs, the GA 2-oxidases (GA2oxs). However, other deactivation reactions have been reported including epoxidation in *Oryza sativa* and methylation in Arabidopsis (reviewed in Yamaguchi, 2008).

Another level of GA biosynthesis regulation in Arabidopsis might depend on (1) the subcellular compartmentalization of the pathway, which is similar to the biosynthesis of ent-kaurene in proplastids, the

conversion of ent-kaurene to GA_{12} in the endoplasmic reticulum, and other reactions that take place in the cytoplasm (Spray et al., 1996; Aach et al., 1997; Helliwell et al., 2001; Itoh et al., 2001; Nelson et al., 2004; Appleford et al., 2006) or (2) the physical separation of early and late GA biosynthetic steps in flowers, roots, and developing seeds, suggesting the transport of intermediate pathway compounds between cells (Yamaguchi et al., 2001; Kaneko et al., 2002, 2003; Mitchum et al., 2006). GAs influence their own metabolism via a feedback mechanism: GA downregulates the expression of enzymes that participate in its biosynthesis and upregulates enzymes that inactivate GAs (reviewed by Bethke and Jones, 1998; Williams et al., 1998; Hedden and Phillips, 2000). Some of the target genes of GA signaling have an element in their regulatory regions that is characterized as a GA-responsive element (GARE; 5′-TAACAAA/G-3′; see Table 1).

The soluble GA receptor was first discovered in rice and since then has been observed in many other plants including Arabidopsis, which has three redundant *GIBBERELIN INSENSITIVE DWARF1* (*GID1*) receptors termed *AtGID1a, AtGID1b*, and *AtGID1c* (Nakajima et al., 2006). Bioactive GA binds to the *GID1* receptor with high affinity, whereas inactive GAs exhibit low or nonexistent affinity for this receptor. This interaction allows for the destruction of DELLA proteins, which are repressors of transcription factors that mediate GA responses (Pysh et al., 1999; Chandler et al., 2002; Cao et al., 2005). The GA-GID-DELLA complexes are thought to perform two roles that are important for GA action. First, they induce a conformational change in DELLA that provokes its recognition and degradation through the $SCF^{GID2/SLY1}$ proteasome pathway (Fu et al., 2002; McGinnis et al., 2003; Sasaki et al., 2003). Second, they sequester DELLA proteins, thus reducing their ability to interact with growth-promoting transcription factors (Ueguchi-Tanaka et al., 2005; Nakajima et al., 2006). Because only double mutant plants (*atgid1a/atgid1c*) show a dwarf phenotype (Suzuki et al., 2009), there is some redundancy among the receptors.

Arabidopsis has five genes that encode DELLA proteins (GAI, RGA, RGL1, RGL2, and RGL3). These proteins are part of the GRAS protein family and may restrict the growth of organs and affect proliferation by upregulating the cell cycle inhibitors Kip-related protein 2 (KRP2) and SIAMESE (SIM). Additionally, they may alter the elongation rate of differentiated cells (Silverstone et al., 2001; Ubeda-Tomas et al., 2008; Achard et al., 2009).

GIBBERELLIN AND ROOT MERISTEM DEVELOPMENT

GA promotes root development and regulates root growth by controlling cell proliferation and elongation through the degradation of DELLA proteins (Fu and Harberd, 2003; Ubeda-Tomas et al., 2008, 2009; Achard et al., 2009). A reduction in the endogenous GA levels, either via genetic or chemical approaches, results in plants with shorter roots and smaller root meristems compared with wild type (Achard et al., 2009; Ubeda-Tomas et al., 2009). The *gai* mutant has a stabilized DELLA that cannot be marked for degradation, and affects cell elongation only when it is expressed in the RAM endodermis. However, the restriction of endodermal cell expansion affects the extension of all other cell files and thus affects total root growth (Ubeda-Tomas et al., 2008). Additionally, this mutant illustrates that bioactive GAs promote cell proliferation by affecting cell production rate and meristem size without interfering with SCN specification or activity (Ubeda-Tomas et al., 2009). Moreover, biosynthetic mutants of GA (*ga1-3* and *ga3ox1/ga3ox2*) have shorter roots and a smaller root meristem size compared with wild-type plants (Fig. 2; Ubeda-Tomas et al., 2009).

BRASSINOSTEROIDS

Brassinosteroids (BRs) are steroids that are essential for normal plant development and participate in the regulation of cell elongation, cell division, bending, reproductive and vascular development, photomorphogenesis, root development, and various stress responses (reviewed in Clouse and Sasse, 1998; Divi and Krishna, 2009). Over 70 types of BRs have been identified in plants, but Brassinolide (BL) has the highest biological activity among BRs (reviewed in Fujioka and Yokota, 2003; Bajguz, 2007). BRs also form conjugates with sugars and fatty acids (Bajguz and Tretyn, 2003); however, the relevance (biological or otherwise) of these conjugates remains unknown (see Table 1).

BRs are synthesized in the cytoplasm by the mevalonate and isoprenoid pathways and are used to generate cycloartenol, the primary precursor of plant sterols (reviewed in Clouse and Sasse, 1998; Divi and Krishna, 2009). Several genes have been implicated in BR biosynthesis including *DET2* (Fujioka et al., 1997, 2002), *DWFA, CPD* (Szekeres et al., 1996; Choe et al., 1998, 1999), and BR6ox (Shimada et al., 2001).

Information regarding the site of BR synthesis is limited. Nevertheless, based on expression analyses of genes involved in their synthesis and analyses of where they are accumulated, it has been suggested that BRs are most actively synthesized and likely used in young developing aerial tissues (e.g., apical shoots, pollen, and siliques) and roots. Interestingly, although BR synthesis is more active in root tissues compared with shoot tissues, the concentration of BRs is lower in roots, which likely occurs because BRs are catabolized more rapidly in the root than in the shoot (Friedrichsen et al., 2000; Bancos et al., 2002; Shimada et al., 2003).

BRs are detected by the membrane-bound receptor BRI1 (BRASSINOSTEROID INSENSITIVE 1), which is a member of the leucine-rich repeat receptor-like kinase (LRR-RLK) receptor family (Belkhadir and Chory, 2006; Shiu et al., 2004). There are three BRI1 homologs in Arabidopsis, and at least two of these (BRL1 and BRL3) bind to BRs and apparently mediate the cell-type-specific BR response in vascular tissues (Cano-Delgado et al., 2004). BRI1 homodimerizes, and it is not clear whether BRs stabilize BRI1 homodimers or cause a conformational change that favors homodimerization in a manner similar to auxin-induced TIR1-IAA protein dimerization (see Auxin section in this review; Kim and Wang,

2010). This homodimerization is not sufficient for the activation of BRI1, and the receptor must first associate with BRs and subsequently with co-receptors such as BAK1 (BRI1-Associated Receptor Kinase 1), SERK1, and BKK1 (Wang et al., 2008; Gou et al., 2012). When a BR binds to its receptor, BRI1 autophosphorylation is induced, BKI1 (BRI1 KINASE INHIBITOR 1) dissociates, and BRI1 associates with BAK1 (Wang and Chory, 2006; Wang et al., 2008). Both BRI1 and BAK1 are serine/threonine and tyrosine kinases, and their association increases their level of autophosphorylation and sequential trans-phosphorylation (Oh et al., 2009a,b, 2010, 2012; Jaillais et al., 2011). The BRI1-BAK1 phosphorylation cascade triggers a downstream signaling cascade that activates BZR1 and BZR2/BES1, two transcription factors that regulate the expression of hundreds of genes. BZR1 is a transcriptional repressor that is able to recognize the BR-response element (BRRE; CGTG(T/C)G), whereas BZR2/BES1-BIM is a transcriptional activator that is able to bind to the E-box element (CANNTG) of a BR-inducible promoter (Wang et al., 2002; He et al., 2005; Yin et al., 2005; Sun et al., 2010). Recent reports indicate that both BZR1 and BZR2/BES1-BIM can bind to BR-repressible and BR-inducible genes. Nevertheless, BRRE and E-box (CACGTG) sequences are highly enriched in BR-repressible genes, whereas the CATGTG motif is highly enriched in BR-inducible genes (Sun et al., 2010).

Another important protein involved in the BR signal transduction pathway is BIN2 (BRASSINOSTEROID INSENSITIVE 2; Kim and Wang, 2010). In the absence of BRs, this GSK3-like kinase phosphorylates and inactivates BZR2/BES1 and BZR1 via several mechanisms that include protein degradation and reduced DNA binding (He et al., 2002; Li et al., 2002; Peng et al., 2008). In the presence of BRs, the activated BRI1-BAK1 complex initiates a signal cascade that blocks the activity of BIN2. Recent studies suggest that BIN2 is also targeted for protein degradation in response to BR signaling through the protein phosphatase BSU1 (BRI1 SUPPRESSOR 1; Kim and Wang, 2010).

BRASSINOSTEROIDS AND ROOT MERISTEM DEVELOPMENT

The expression of genes involved in BR biosynthesis and the detection of BRs in root tissues (Friedrichsen et al., 2000; Bancos et al., 2002; Shimada et al., 2003) suggest that BRs play an important role in roots. In fact, BRs promote root growth as indicated by studies of BR-related mutants (e.g., *dwf1-6, cbb3, bri1-116*, and the *bak1-4/bkk1-1/serk1-8* triple mutant) that exhibit a short root phenotype (Li et al., 2002; Mussig et al., 2003; Mouchel et al., 2006; Hacham et al., 2011; Du et al., 2012) and the exogenous application of BRs at low concentrations that promotes root growth. However, as is the case for all hormones, high concentrations inhibit root growth (Mussig et al., 2003). Root growth inhibition in mutants with low levels of BRs (*bri1* mutants) revealed that BRs are required for the promotion of cell expansion and cell division in meristematic root cells (Fig. 2; Gonzalez-Garcia et al., 2011; Hacham et al., 2011). In this case, the size of the root meristem is controlled by BRI1 activation in epidermal cells (Fig. 3), where this gene induces signals that allow for communication with the inner cells. In turn, these signals may be controlled through BES1 and BZR1 (Hacham et al., 2011). The role of BRs in root growth has been further demonstrated by the short root phenotype of the *bak1-4/bkk1-1/serk1-8* triple mutant, in which BR signal transduction is blocked (Du et al., 2012).

The function of BRs in stem cells remains unknown; however, several studies have recently indicated that BR signaling might enhance cell division and participate in gene expression in QC cells. The specific expression of BRI1 in the epidermis and its absence in other cell types (QC, endodermis and stele) non-autonomously activates the expression of *AGL42*, a member of the MADS box gene family (Hacham et al., 2011) with an unknown function that is mainly expressed in the root QC. Additionally, the *WUSCHEL-RELATED HOMEOBOX 5* (*WOX5*), *SCR*, and *SHR* transcription factors, which are required for the maintenance of root stem cells, are also upregulated by BRs and downregulated in the absence of BR signaling (Gonzalez-Garcia et al., 2011; Du et al., 2012), although it is unclear whether these genes are direct targets of this hormone. The mechanism by which BRs are able to regulate various processes during root development is thus far largely unknown.

ETHYLENE

Ethylene is a volatile compound that is soluble in both aqueous and lipid environments and plays roles in the regulation of seed germination, cell elongation, fruit ripening, leaf senescence, resistance to pathogens, root and flower growth (Bleecker and Kende, 2000). Ethylene is synthesized in all plant organs, including leaves, roots, shoots, and flowers; however, the highest rates of ethylene synthesis are observed in meristematic, stressed, or ripening tissues (Lin et al., 2009).

S-adenosylmethionine (S-AdoMet) is a precursor in ethylene biosynthesis and is converted to ethylene by 1-CARBOXYLIC ACID (ACC) SYNTHASE (ACS) and ACC OXIDASE (Kende, 1993). In this pathway, the rate-limiting step is the conversion of S-AdoMet to ACC. In Arabidopsis, seven ACS genes have been characterized, and their transcription is differentially regulated during development and in response to stressful stimuli (Liang et al., 1992; Van der Straeten et al., 1992; Arteca and Arteca, 1999; Lin et al., 2009).

The ethylene signaling pathway is complex and not fully understood; however, mutants affected in the ethylene triple response (i.e., inhibition of elongation growth of dark-grown seedlings, induction of stem swelling, and the closure of the apical hook) have been isolated. Five putative endoplasmatic reticulum (ER) membrane-bound ethylene receptors, all of which are His-kinase two-component regulators, have been described: ETHYLENE RESPONSE1 (ETR1), ETR2, ETHYLENE RESPONSE SENSOR1 (ERS1), ERS2, and ETHYLENE INSENSITIVE4 (EIN4) (Hua et al., 1995, 1998; Bleecker et al., 1998; Sakai et al., 1998). In the absence of ethylene, CONSTITUTIVE

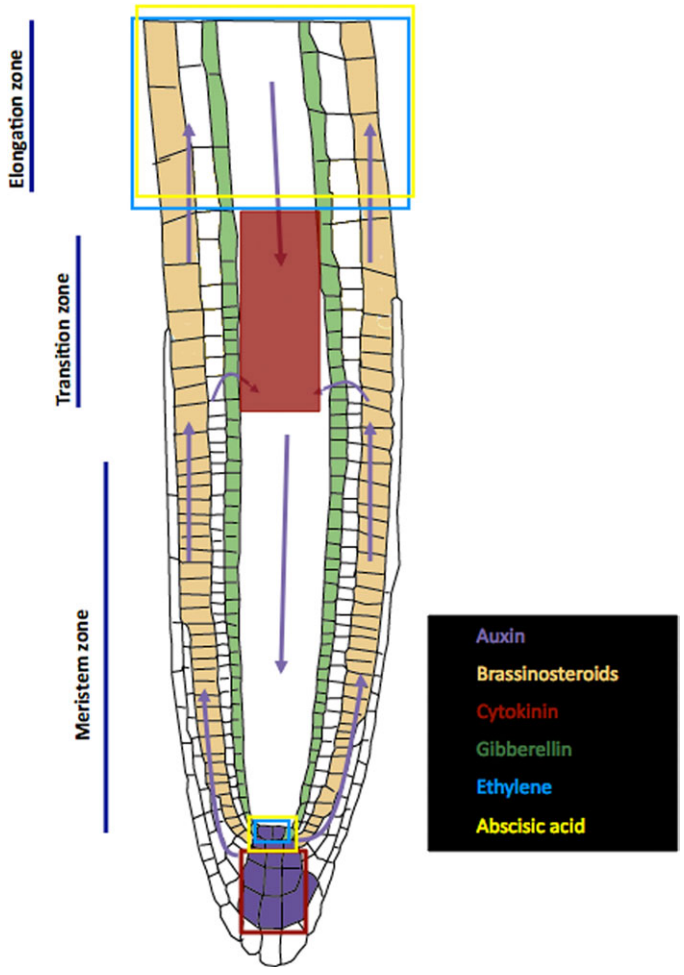

Fig. 3. Schematic representation of main tissue-specific concentration/function of different hormones in the root meristem. Auxin mainly accumulates in the stem and columella cells (purple color and arrows indicate auxin distribution). Brassinosteroids (BRs) mainly function in the epidermal cells to control meristem size (peach). Cytokinins (CKs) acts in the transition zone and columella cells (red). Gibberelins (GAs) acts in the endodermal cells to control meristem size and cell elongation (green). Ethylene accumulates in the QC and elongation zone (blue) and Abscisic Acid (ABA) functions in the elongation zone and QC cells (yellow).

TRIPLE RESPONSE 1 (CTR1) is active and represses ETHYLENE INSENSITIVE 2 (EIN2) as well as all the downstream components of the ethylene signaling pathway; CTR1 also localizes to the ER membrane. The transcription factor ETHYLENE INSENSITIVE 3 (EIN3) is constantly degraded through the action of EIN3 BINDING F-BOX 1 and 2 (EBF1 and EBF2) via the proteasome-mediated degradation pathway (Etheridge et al., 2005). Upon binding ethylene, the histidine-kinase domain of its receptor interacts with and inactivates CTR1, thus relieving the repression of downstream signaling. The newly activated EIN2 then promotes the activation of EIN3 and EIN3-like (EIL) transcription factors, which induces the expression of ETHYLENE RESPONSE FACTOR (ERF), which is another transcription factor implicated in the activation of a subset of ethylene response genes (reviewed in Bleecker and Kende, 2000). Ethylene also promotes the accumulation of EIN3 by repressing the action of EBF1 and EBF2 (Potuschak et al., 2003; Binder et al., 2007). It was previously thought that ethylene receptors only form homodimers to facilitate interaction with CTR1; however, all the ethylene receptors were recently shown to be capable of forming homo- and heterodimers in vitro in any combination, although their role in ethylene signaling has not yet been demonstrated (Lin et al., 2009).

The ethylene biosynthesis and signaling pathways are post-transcriptionally regulated. Some ACS isoforms and the transcription factor EIN3 are regulated by ubiquitin/26S proteasome-mediated degradation (Etheridge et al., 2005). Additionally, ETR1 gain-of-function and loss-of-function mutations affect the expression of ETR1 at the post-transcriptional level (Zhao et al., 2002).

ETHYLENE AND ROOT MERISTEM DEVELOPMENT

During root development, ethylene promotes root hair differentiation and inhibits cell elongation (Tanimoto et al., 1995; Pitts et al., 1998; Ruzicka et al., 2007). Ethylene also affects other aspects of root growth via the induction of certain genes involved in auxin biosynthesis including *ASA1/WE12/TIR7, ASB1/WE17* (alpha and beta subunits of ANTHRANILATE SYNTHASE), *TAA1/WE18* (TRYPTOPHAN AMINOTRANSFERASE), and *TARs* (*TAA1*-related genes) (Ruzicka et al., 2007; Swarup et al., 2007; Stepanova et al., 2008). The interaction between ethylene and auxin will be discussed in Root Cell Elongation section in this review.

Additionally, ethylene affects cell division in QC cells and is likely to be involved in root meristem maintenance. First, the high level of ethylene in *eto1* mutants promotes QC cell division independently of auxin and without interfering with QC cell fate, and, second, the constitutive activation of the ethylene response in *ctr* mutants generates additional QC cells and smaller root meristems (Fig. 2; Ortega-Martinez et al., 2007; Thomann et al., 2009).

ABSCISIC ACID (ABA)

Abscisic acid (ABA) is an isoprenoid hormone that is involved in the regulation of seed development and dormancy as well as plant responses to various environmental stresses, particularly stress due to water deficit. This hormone is present in all plant tissues from the apical bud to the root tip (reviewed in Finkelstein et al., 2002).

ABA is synthesized in nearly every cell that contains plastids; however, vascular tissues are likely to be the

main sites of ABA biosynthesis in non-stressed plants (Nambara and Marion-Poll, 2005). ABA is derived from the C_{15} compound farnesyl pyrophosphate or C_{40} carotenoids synthesized by the plastid 2C-methyl-D-erythritol-4-phosphate (MEP) pathway, and is predominantly found in vascular parenchyma cells (Nambara and Marion-Poll, 2005). Genes involved in ABA biosynthesis include a ZEAXANTHIN EPOXIDASE PROTEIN (ZEP), a 9-CIS-EPOXYCAROTENOID DIOXYGENASE (NCED), a SHORT-CHAIN ALCOHOL DEHYDROGENASE/REDUCTASE (SDR), and an ALDEHYDE OXIDASE (AAO). ABA is also synthesized indirectly through the cleavage of a C_{40} carotenoid precursor (reviewed in Xiong and Zhu, 2003). ABA is ubiquitous in vascular tissues and is transported via the xylem and phloem.

ABA may be inactivated by oxidation or by covalent conjugation with other molecules such as glucose to form ABA-glucose ester (ABA-GE). The three ABA hydroxylation pathways that oxidize ABA produce compounds that could carry out biological activities; however, hydroxylation triggers further inactivation steps (Nambara and Marion-Poll, 2005). It has also been shown that conjugation not only inactivates ABA but also causes an alteration in cellular distribution such that some conjugated ABA localizes in vacuoles and may serve as a storage form of the hormone. Moreover, these conjugates could be important for long-distance transport of ABA from the root to the shoot because ABA-GE has been found in high concentrations in the xylem sap (Verslues et al., 2007).

Recent biochemical and genetic approaches have uncovered several soluble ABA receptors including 14 proteins of the PYRABACTIN RESISTANCE/PYRABACTIN-LIKE or REGULATORY COMPONENTS OF ABA RECEPTOR family (collectively known as the PYR/PYL/RCAR family). Signaling commences when ABA binds to PYR/PYL/RCAR receptors, which promotes the inhibition of protein phosphatases of type 2C (PP2Cs). Because PP2Cs act as negative regulators of SnRK2, this inhibition allows for SnRK2 activation and subsequent phosphorylation of target proteins (Ma et al., 2009; Park et al., 2009). Several SnRK2 targets have been reported both at the plasma membrane and in the nucleus; these include ABA-responsive element binding factors (ABFs/AREBs) and the ion channels responsible for turgor-mediated stomatal closure (Melcher et al., 2010). SnRK2s also recognize ABA-responsive elements (ABRE) in the promoter regions of ABA-inducible genes. Six homologs of PP2C have been described (ABI1, ABI2, HAB1, HAB2, AHG1, and AHG3; Leung et al., 1997; Leonhardt et al., 2004; Saez et al., 2004; Yoshida et al., 2006; Nishimura et al., 2007), and several transcription factors (ABI3, ABI4, ABI5, and the ABFs) that regulate downstream ABA-inducible genes have also been characterized (reviewed in Finkelstein and Rock, 2002; Finkelstein et al., 2005; Fujita et al., 2005).

ABA AND ROOT DEVELOPMENT

ABA promotes root elongation in a dose-dependent manner when it is exogenously applied at 0.1 μM, whereas root growth is inhibited when the hormone is applied at concentrations above 1.0 μM (Ghassemian et al., 2000). This inhibition of the primary root requires *SnRK 2.2* and *SnRK 2.3* because mutations in these genes confer resistance to ABA (Fujii et al., 2007). It is likely that other ABA regulators are repressed during normal root development. For example, *SCR* inhibits *ABI4* (a transcription factor induced in response to ABA signaling) specifically in the endodermis. *scr-1* mutants have short roots and high levels of *ABI4*, and overexpression of ABI4 in the endodermis (where *SCR* is normally expressed) also yields shorter roots (Fig. 2). However, *abi4-104* loss-of-function mutants also have shorter roots, indicating that the expression level of ABI4 and the specific tissue where it is expressed have other root growth effects (Cui et al., 2012). ABA also acts as a root-to-shoot signal that controls the closure of stomata and affects root architecture in response to drought (Sharp, 2002; De Smet et al., 2003).

Additionally, ABA induces QC quiescence and suppresses cell differentiation in the SCN. Extra QC divisions were observed in mutants that are ABA-deficient (*aba1-1, aba2-3, aba2-4*, and *aba3-2*) or ABA-insensitive (*abi1-1, abi2-1, abi3-1*, and *abi5-1*). The inhibition of ABA biosynthesis also promotes stem cell differentiation (Zhang et al., 2010).

HORMONE CROSSTALK DURING ROOT DEVELOPMENT

For each plant hormone, knowledge regarding its metabolism, region of action, and function is important; however, hormones do not act independently of each other. In fact, hormone action depends on the relative concentrations of multiple hormones rather than only on their individual concentrations. Their signal transduction and biosynthetic pathways are interlinked, and this interdependence is known as hormone crosstalk. Thus, hormones form a complex network that underlies their net role during different developmental processes including root development.

The integrated role of plant hormones in the SCN as well as in cell proliferation, elongation, and departure from the RAM (i.e., entrance into the elongation and differentiation zones) will be discussed in the Root Cell Proliferation, Root Cell Elongation and Hormone crosstalk and SCN Patterning sections in this review.

ROOT CELL PROLIFERATION

The auxin/CK ratio is important for determining cell behavior along the apical-basal axis in the root because it maintains root meristem size and controls the transition from cell proliferation to cell elongation. A high level of auxin activity relative to CK action or concentration is required for the maintenance of cell proliferation, thus preventing cell expansion and differentiation. In contrast, relatively high levels of CK are important for the transition from the proliferative meristematic zone to the differentiation zone. In this antagonistic relationship, genes that are responsive to both hormones are cross-regulated. CK upregulates *SHORT HYPOCOTYL 2* (*SHY2*), which corresponds to

IAA3, an ARF repressor that decreases the expression of *PIN1, PIN3*, and *PIN7* (among other genes) in the vascular tissue of the transition zone (Dello Ioio et al., 2007, 2008b; Ruzicka et al., 2009; Moubayidin et al., 2010). Additionally, CK signaling negatively regulates PIN genes at the post-transcriptional level (Zhang et al., 2011). However, in the proliferation zone, auxin mediates the degradation of the SHY2 protein, which allows for PIN expression, proper auxin distribution, and normal cell division (Dello Ioio et al., 2007, 2008b). Auxin can inhibit CK metabolic inactivation by inducing CK oxidases, whereas CK locally promotes auxin synthesis (Zhou et al., 2011; Jones et al., 2010). Thus, CK not only represses polar auxin transport but also promotes local auxin biosynthesis in the proliferation zone (Zhou et al., 2011). However, the function of CK is complex, and although the overexpression of CKX in Arabidopsis leads to larger root meristems, CK receptor mutants exhibit short root phenotypes. GA indirectly promotes *PIN* expression by inhibiting ARR1, and GAs also target PIN proteins for vacuolar degradation (Moubayidin et al., 2010; Willige et al., 2011). The means by which these two processes are stabilized is not clear.

GA is also involved in RAM size regulation via its effects on the auxin/CK balance (Vanstraelen and Benková, 2012). In this balance, various downstream genes are regulated. Concurrently, auxin promotes GA synthesis (Frigerio et al., 2006) and enhances the degradation of RGA and GAI DELLA proteins (Fu and Harberd, 2003). Therefore, mutants that accumulate DELLAs typically have very small RAMs (Achard and Genschik, 2009; Ubeda-Tomas et al., 2009). Additionally, GA can act independently of the auxin-CK pathway and regulate cell proliferation and meristem size by downregulating the cell cycle inhibitor KRP2 via DELLA degradation (Achard and Genschik, 2009; Ubeda-Tomas et al., 2009).

BRs have also been implicated in the relationship between auxin and CK. *BREVIS RADIX* (*BRX*) is a putative transcriptional co-regulator that promotes root growth primarily by affecting meristem size (Mouchel et al., 2004). The *brx* mutant is deficient in BRs, and most of its auxin-responsive genes are globally impaired, which demonstrates the requirement for BRs in auxin-responsive transcription (Mouchel et al., 2006). In young roots, BRX is a direct target of ARF5/MONOPTEROS (MP), which transiently enhances *PIN3* expression to promote meristem growth. At later stages, cytokinin induction of *SHY2* in the vascular transition zone restricts *BRX* and *PIN3* expression, limiting meristem growth (Scacchi et al., 2010). Theoretical and experimental results suggest that BRX forms a complex with ARFs and that this interaction amplifies the transcriptional activity of ARFs. Alternatively, BRX may compete with Aux/IAA for interaction with ARFs (Scacchi et al., 2010; Sankar et al., 2011). It is unclear whether BRX/ARF complexes play a role in controlling meristem size because the BRI receptor is expressed in the epidermis and a BR-mediated signal has been demonstrated to originate from the epidermis (Gonzalez-Garcia et al., 2011; Hacham et al., 2011).

Taken together, these data indicate that cell proliferation and RAM size are regulated by the collective action of auxin, CKs, Gas, and BRs, all of which exhibit regulatory interdependency at the levels of biosynthesis, signaling, and transport.

JA and ABA also participates in root cell Proliferation antagonizing auxin. It has been documented that JA directly represses the expression of PLT or PIN, thus inhibiting RAM growth (Chen et al., 2011). However, a feedback mechanism occurs between these hormones. JA promotes auxin biosynthesis by inducing the expression of *ASA1*/*WE12*/*TIR7* (Stepanova et al., 2005; Sun et al., 2009), and auxin reduces JA signaling by upregulating the JAZ1 repressor (Grunewald et al., 2009). In addition, ABA and CK regulate ABI4, which in turn represses PIN1 expression (Shkolnik-Inbar and Bar-Zvi, 2011; Vanstraelen and Benková, 2012). A synergistic effect of ABA and auxin has also been reported. The exogenous application of ABA upregulates certain auxin response genes (e.g., *MP* and *PLT2*) (Zhang et al., 2010). Interestingly, unlike GA and BRs, ABA inhibits cell division via upregulation of *KRP1* (Wang et al., 1998).

ROOT CELL ELONGATION

Auxin and GA pathways converge during root elongation and tissue differentiation; auxin is required for GA-induced degradation of RGA to mediate root elongation (Fu and Harberd, 2003). However, the GA-induced degradation of DELLA proteins is inhibited by ethylene (Achard et al., 2003). Thus, it is very interesting that certain regulatory effects of ethylene and auxin on growth are mediated via DELLA proteins (Achard et al., 2003; Fu and Harberd, 2003). DELLA proteins appear to be integrators of at least three different hormone pathways that orchestrate the response of the plant to different stimuli.

Auxin may induce BRs and, together or in parallel, these two hormones promote cell elongation (Hacham et al., 2011). However, BRs are known to stimulate the production of ethylene in roots (Mussig et al., 2003; Benková and Hejatko, 2009), indicating potential negative feedback regulation among these two hormones.

Auxin, GA, and BRs induce cell elongation; however, ethylene and auxin synergistically inhibit this process, and they reciprocally induce their biosynthesis and response. Ethylene stimulates auxin biosynthesis in root tips through the induction of *ASA1, ASB1, TAA1*, and *TAR* genes (Stepanova et al., 2005, 2008) and also stimulates basipetal auxin transport to the elongation zone, thus inhibiting cell elongation via regulation of polar auxin transporters (AUX1 and PIN2; Luschnig et al., 1998; Ruzicka et al., 2007; Swarup et al., 2007; Negi et al., 2008). However, elevated auxin levels lead to increased ethylene synthesis, which facilitates the inhibitory effect of ethylene on cell elongation (Swarup et al., 2007). Moreover, a whole-genome analysis revealed that auxin and ethylene function both independently and in concert, and the two hormones regulate each other at the levels of synthesis, transport, and signaling (Stepanova et al., 2007). CK also inhibits cell elongation, and this regulation depends on ETR1 and EIN2, two

components of the ethylene signaling pathway (Ruzicka et al., 2009; Kushwah et al., 2011). Interestingly, the repressive effect of ethylene on elongation does not affect the meristematic zone (Galinha et al., 2009).

Understanding how all these hormones pathways feed back and together underlie the modulation of cell proliferation and cell elongation/differentiation during root development will require integrative formal approaches (see "Theoretical approaches to the study of hormones in the root" section in this review).

HORMONE CROSSTALK AND SCN PATTERNING

As described above, several hormones affect SCN establishment and cellular patterning in the root. However, little is known about hormone crosstalk in the SCN. In fact, many of the hormone interactions observed in the proliferation and elongation zones (e.g., the synergistic relationship between auxin and BR at the signaling level) are not present in the SCN (Gonzalez-Garcia et al., 2011). Moreover, an effort to detect the interaction of ABA with ethylene in the regulation of the SCN indicated that ABA regulation is ethylene-independent (Zhang et al., 2010) even when ABA promotes ethylene biosynthesis (Ghassemian et al., 2000). There are only three documented examples of crosstalk in the SCN. The first of these is the induction of *MP* and *WOX5* expression by ABA, suggesting that auxin and ABA interact in the regulation of the SCN (Zhang et al., 2010). The second example is the auxin-mediated suppression of CK signaling during embryonic development, which determines the SCN of the primary root as a result of PIN-mediated auxin accumulation and the expression of *WOX5* and *PLT* (Friml et al., 2003; Weijers et al., 2006; Muller and Sheen, 2008). The third example is the upregulation of *TAA1* expression by ethylene in the QC (Stepanova et al., 2008). *TAA1* is an auxin biosynthesis gene that is also induced by CK and is necessary for maintaining proper auxin levels in the root. Contrary to these results, it has been reported that the effect of ethylene on QC cells is auxin independent, and it was suggested that auxin itself is not sufficient to induce cell division in the QC (Ortega-Martinez et al., 2007). Further experiments will be needed to clarify this apparent discrepancy.

Unraveling the means by which hormones communicate to regulate SCN maintenance, development, and patterning remains a challenge that needs to be addressed in future research. However, it is clear that hormone interactions at the levels of synthesis, metabolism, and distribution are being uncovered. Additionally, hormone interactions during the transcriptional or post-transcriptional regulation of key molecular components in signal transduction pathways and hormone interactions with many target genes in several developmental-specific contexts are slowly being clarified. Thus, a complex network of interactions and crosstalk between hormone pathways is emerging.

THEORETICAL APPROACHES TO THE STUDY OF HORMONES IN THE ROOT

Hormonal regulation is a complex process, and due to the non-linear nature of their interactions, hormones exhibit non-intuitive behaviors that necessitate theoretical and computational tools for their analysis. Some researchers have begun to use these tools, and auxin transport in the root has been the subject of theoretical analyses. An earlier study demonstrated that auxin transport mediated by PIN proteins is sufficient to robustly generate the auxin gradient observed along the root (Grieneisen et al., 2007), and a recent study illustrated how this mechanism, when coupled to the auxin-regulated PIN expression and degradation process, was able to recover the self-organizing properties of the auxin gradient observed in the root (Mironova et al., 2012), which is similar to what occurs during the root regeneration process (Sena et al., 2009).

Ethylene signaling has also been studied using theoretical tools. In this work, the communication channel conformed by the ethylene signal transduction pathway was studied in Arabidopsis root cells, and the Shannon entropy (H), or degree of uncertainty that the signal transduction pathway has during the decoding of the message received by ethylene receptors, was computed. These models showed that the amount of information managed by the root cells could be correlated with the frequency of the input signal. Indeed, it was shown that if one "master" gene (*ERF1*) and one "slave" gene (*HLS1*) are considered, then the total H is determined by the uncertainty associated with the expression of the "master" gene. Additionally, the H associated with *HLS1* expression determines the information content of the system that is related to the interaction of the antagonistic *ARF1,2* and *HLS1* genes (Diaz and Alvarez-Buylla, 2006, 2009).

Importantly, similar types of theoretical approximations have been used to formally evaluate the role of integrated hormone signaling pathways. The crosstalk between the auxin, ethylene, and CK signaling pathways was modeled using the same approximation as in Diaz and Alvarez-Buylla (2006). The model indicated how the *POLARIS* gene controls the ethylene-dependent regulation of auxin at the transport and biosynthesis levels, consequently regulating the auxin concentration at the root tip. This work also demonstrated how variations in the model parameters generate different auxin responses (Liu et al., 2010). The crosstalk between auxin and BRs was studied with a qualitative continuous approximation, which suggested the possible role of BRX in mediating communication between auxin and BRs (Sankar et al., 2011). Importantly, this hypothesis was experimentally verified (Scacchi et al., 2010). The crosstalk between auxin and CKs observed at the transition zone and the means by which auxin regulates the pattern and maintenance of the root SCN in conjunction with other transcription factors have also been studied with theoretical tools (Muraro et al., 2011; Azpeitia et al., 2010). This body of research has provided important clues about hormone function and highlights how the combined use of experimental and

theoretical approaches can improve our understanding of the crosstalk among hormones.

PERSPECTIVES

As data on plant hormone biosynthesis, metabolism, signal transduction pathways, transport, and overall function are uncovered, a complex network of interactions is revealed. However, we are still far from understanding how plant cells and whole plants dynamically integrate environmental and endogenous signals to control cell function and status (e.g., proliferative vs. elongating/differentiating). Previous views of hierarchical unidirectional pathways acting independently of each other are being discarded. Current knowledge regarding hormone pathways suggests that: (1) several hormones regulate genes in the signaling pathways of other hormones (Nemhauser et al., 2006); (2) proteosome protein degradation occurs in most hormone pathways (auxin, ethylene, BRs, and GAs); and (3) DELLA proteins function as central molecular components of a growth-repressing mechanism that integrates the action of most hormones (Achard et al., 2003, 2006).

Hormone pathways also converge in the regulation of common targets. Interestingly, however, transcriptomic analysis using GA, IAA, and BRs has suggested that the exogenous application of each hormone regulates a set of specific target genes independently (Nemhauser et al., 2006). This finding suggests that the direct targets of plant hormones may be specific; however, the same experiments suggest that different members of the same family are regulated by different hormones (Nemhauser et al., 2006).

We propose that integrative dynamic models such as those used to understand gene regulatory networks (Alvarez-Buylla et al., 2010) or single hormone signaling pathways (Diaz and Alvarez-Buylla, 2006, 2009) could be used to integrate and better understand the complex interactions that underlie hormone biosynthesis, metabolism, signaling, transport, and action, as well as their integrated role in cell proliferation and differentiation during root growth.

ACKNOWLEDGMENTS

Rigoberto Vicencio Pérez-Ruiz helped with various laboratory tasks and Diana Romo with logistical support. Grant sponsor: "Programa de Apoyo a Proyectos de Investigación e Innovación Tecnológica", Universidad Nacional Autónoma de México (UNAM; IN204011-3; IN229009-3; IN226510-3; IB201212; IN204011-3), and Consejo Nacional de Ciencia y Tecnología "Complejidad, Ciencia y Sociedad" (CONACYT): 81542; 167705; 152649; 105678; 180098 and Red Temática de Investigación CONACYT: "Complejidad, Ciencia y Sociedad" (124909) and UC-MEXUS CN.12-623; CN.12-571. E.R.A.B. is supported by the Miller Institute for Basic Research in Science, University of California, Berkeley.

REFERENCES

Aach H, Bode H, Robinson DG, Graebe JE. 1997. ent-Kaurene synthase is located in proplastids of meristematic shoot tissues. Planta 202:211–219.

Achard P, Genschik P. 2009. Releasing the brakes of plant growth: how GAs shutdown DELLA proteins. J Exp Bot 60:1085–1092.

Achard P, Vriezen WH, Van Der Straeten D, Harberd NP. 2003. Ethylene regulates arabidopsis development via the modulation of DELLA protein growth repressor function. Plant Cell 15: 2816–2825.

Achard P, Cheng H, De Grauwe L, Decat J, Schoutteten H, Moritz T, Van Der Straeten D, Peng J, Harberd NP. 2006. Integration of plant responses to environmentally activated phytohormonal signals. Science 311:91–94.

Achard P, Gusti A, Cheminant S, Alioua M, Dhondt S, Coppens F, Beemster GT, Genschik P. 2009. Gibberellin signaling controls cell proliferation rate in Arabidopsis. Curr Biol 19:1188–1193.

Aida M, Beis D, Heidstra R, Willemsen V, Blilou I, Galinha C, Nussaume L, Noh YS, Amasino R, Scheres B. 2004. The PLETHORA genes mediate patterning of the Arabidopsis root stem cell niche. Cell 119:109–120.

Aloni R, Langhans M, Aloni E, Ullrich CI. 2004. Role of cytokinin in the regulation of root gravitropism. Planta 220: 177–182.

Alvarez-Buylla ER, Azpeitia E, Barrio R, Benitez M, Padilla-Longoria P. 2010. From ABC genes to regulatory networks, epigenetic landscapes and flower morphogenesis: making biological sense of theoretical approaches. Semin Cell Dev Biol 21:108–117.

Appleford NE, Evans DJ, Lenton JR, Gaskin P, Croker SJ, Devos KM, Phillips AL, Hedden P. 2006. Function and transcript analysis of gibberellin-biosynthetic enzymes in wheat. Planta 223:568–582.

Argueso CT, Raines T, Kieber JJ. 2010. Cytokinin signaling and transcriptional networks. Curr Opin Plant Biol 13: 533–539.

Arteca JM, Arteca RN. 1999. A multi-responsive gene encoding 1-aminocyclopropane-1-carboxylate synthase (ACS6) in mature Arabidopsis leaves. Plant Mol Biol 39:209–219.

Azpeitia E, Alvarez-Buylla ER. 2012. A complex systems approach to Arabidopsis root stem-cell niche developmental mechanisms: from molecules, to networks, to morphogenesis. Plant Mol Biol 80:351–363.

Azpeitia E, Benitez M, Vega I, Villarreal C, Alvarez-Buylla ER. 2010. Single-cell and coupled GRN models of cell patterning in the Arabidopsis thaliana root stem cell niche. BMC Syst Biol 4:134.

Bajguz A. 2007. Metabolism of brassinosteroids in plants. Plant Physiol Biochem 45:95–107.

Bajguz A, Tretyn A. 2003. The chemical characteristic and distribution of brassinosteroids in plants. Phytochemistry 62:1027–1046.

Bancos S, Nomura T, Sato T, Molnar G, Bishop GJ, Koncz C, Yokota T, Nagy F, Szekeres M. 2002. Regulation of transcript levels of the Arabidopsis cytochrome p450 genes involved in brassinosteroid biosynthesis. Plant Physiol 130:504–513.

Belkhadir Y, Chory J. 2006. Brassinosteroid signaling: a paradigm for steroid hormone signaling from the cell surface. Science 314:1410–1411.

Benjamins R, Scheres B. 2008. Auxin: the looping star in plant development. Annu Rev Plant Biol 59:443–465.

Benjamins R, Quint A, Weijers D, Hooykaas P, Offringa R. 2001. The PINOID protein kinase regulates organ development in Arabidopsis by enhancing polar auxin transport. Development 128: 4057–4067.

Benková E, Hejatko J. 2009. Hormone interactions at the root apical meristem. Plant Mol Biol 69:383–396.

Benková E, Michniewicz M, Sauer M, Teichmann T, Seifertova D, Jurgens G, Friml J. 2003. Local, efflux-dependent auxin gradients as a common module for plant organ formation. Cell 115: 591–602.

Bennett PA, Levy A, Carmignac DF, Robinson IC, Lightman SL. 1996. Differential regulation of the growth hormone receptor gene: effects of dexamethasone and estradiol. Endocrinology 137: 3891–3896.

Bennett T, Scheres B. 2010. Root development-two meristems for the price of one? Curr Top Dev Biol 91:67–102.

Bethke PC, Jones RL. 1998. Gibberellin signaling. Curr Opin Plant Biol 1: 440–446.

Binder BM, Walker JM, Gagne JM, Emborg TJ, Hemmann G, Bleecker AB, Vierstra RD. 2007. The Arabidopsis EIN3 binding F-Box proteins EBF1 and

EBF2 have distinct but overlapping roles in ethylene signaling. Plant Cell 19:509–523.
Bleecker AB, Kende H. 2000. Ethylene: a gaseous signal molecule in plants. Annu Rev Cell Dev Biol 16:1–18.
Bleecker AB, Esch JJ, Hall AE, Rodriguez FI, Binder BM. 1998. The ethylene-receptor family from Arabidopsis: structure and function. Phil Trans R Soc Lond B Biol Sci 353:1405–1412.
Blilou I, Xu J, Wildwater M, Willemsen V, Paponov I, Friml J, Heidstra R, Aida M, Palme K, Scheres B. 2005. The PIN auxin efflux facilitator network controls growth and patterning in Arabidopsis roots. Nature 433:39–44.
Burkle L, Cedzich A, Dopke C, Stransky H, Okumoto S, Gillissen B, Kuhn C, Frommer WB. 2003. Transport of cytokinins mediated by purine transporters of the PUP family expressed in phloem, hydathodes, and pollen of Arabidopsis. Plant J 34:13–26.
Calderon Villalobos LI, Lee S, De Oliveira C, Ivetac A, Brandt W, Armitage L, Sheard LB, Tan X, Parry G, Mao H, Zheng N, Napier R, Kepinski S, Estelle M. 2012. A combinatorial TIR1/AFB-Aux/IAA co-receptor system for differential sensing of auxin. Nat Chem Biol 8:477–485.
Cano-Delgado A, Yin Y, Yu C, Vafeados D, Mora-Garcia S, Cheng JC, Nam KH, Li J, Chory J. 2004. BRL1 and BRL3 are novel brassinosteroid receptors that function in vascular differentiation in Arabidopsis. Development 131: 5341–5351.
Cao D, Hussain A, Cheng H, Peng J. 2005. Loss of function of four DELLA genes leads to light- and gibberellin-independent seed germination in Arabidopsis. Planta 223:105–113.
Chandler PM, Marion-Poll A, Ellis M, Gubler F. 2002. Mutants at the Slender1 locus of barley cv Himalaya. Molecular and physiological characterization. Plant Physiol 129:181–190.
Chen Q, Sun J, Zhai Q, Zhou W, Qi L, Xu L, Wang B, Chen R, Jiang H, Qi J, Li X, Palme K, Li C. 2011. The basic helix-loop-helix transcription factor MYC2 directly represses PLETHORA expression during jasmonate-mediated modulation of the root stem cell niche in Arabidopsis. Plant Cell 23:3335–3352.
Choe S, Dilkes BP, Fujioka S, Takatsuto S, Sakurai A, Feldmann KA. 1998. The DWF4 gene of Arabidopsis encodes a cytochrome P450 that mediates multiple 22alpha-hydroxylation steps in brassinosteroid biosynthesis. Plant Cell 10: 231–243.
Choe S, Noguchi T, Fujioka S, Takatsuto S, Tissier CP, Gregory BD, Ross AS, Tanaka A, Yoshida S, Tax FE, Feldmann KA. 1999. The Arabidopsis dwf7/ste1 mutant is defective in the delta7 sterol C-5 desaturation step leading to brassinosteroid biosynthesis. Plant Cell 11:207–221.
Clouse SD, Sasse JM. 1998. BRASSINOSTEROIDS: essential regulators of plant growth and development. Annu Rev Plant Physiol Plant Mol Biol 49:427–451.
Cui H, Hao Y, Kong D. 2012. SCARECROW has a SHORT-ROOT-independent role in modulating the sugar response1. Plant Physiol 158:1769–1778.
De Smet I, Signora L, Beeckman T, Inze D, Foyer CH, Zhang H. 2003. An abscisic acid-sensitive checkpoint in lateral root development of Arabidopsis. Plant J 33:543–555.
Dello Ioio R, Linhares FS, Scacchi E, Casamitjana-Martinez E, Heidstra R, Costantino P, Sabatini S. 2007. Cytokinins determine Arabidopsis root-meristem size by controlling cell differentiation. Curr Biol 17:678–682.
Dello Ioio R, Linhares FS, Sabatini S. 2008a. Emerging role of cytokinin as a regulator of cellular differentiation. Curr Opin Plant Biol 11:23–27.
Dello Ioio R, Nakamura K, Moubayidin L, Perilli S, Taniguchi M, Morita MT, Aoyama T, Costantino P, Sabatini S. 2008b. A genetic framework for the control of cell division and differentiation in the root meristem. Science 322: 1380–1384.
Depuydt S, Hardtke CS. 2011. Hormone signalling crosstalk in plant growth regulation. Curr Biol 21:R365–373.
Dharmasiri N, Dharmasiri S, Estelle M. 2005. The F-box protein TIR1 is an auxin receptor. Nature 435:441–445.
Diaz J, Alvarez-Buylla ER. 2006. A model of the ethylene signaling pathway and its gene response in Arabidopsis thaliana: pathway cross-talk and noise-filtering properties. Chaos 16:023112.
Diaz J, Alvarez-Buylla ER. 2009. Information flow during gene activation by signaling molecules: ethylene transduction in Arabidopsis cells as a study system. BMC Syst Biol 3:48.
Ding Z, Friml J. 2010. Auxin regulates distal stem cell differentiation in Arabidopsis roots. Proc Natl Acad Sci USA 107:12046–12051.
Divi UK, Krishna P. 2009. Brassinosteroid: a biotechnological target for enhancing crop yield and stress tolerance. N Biotechnol 26:131–136.
Dolan L, Janmaat K, Willemsen V, Linstead P, Poethig S, Roberts K, Scheres B. 1993. Cellular organisation of the Arabidopsis thaliana root. Development 119:71–84.
Du J, Yin H, Zhang S, Wei Z, Zhao B, Zhang J, Gou X, Lin H, Li J. 2012. Somatic embryogenesis receptor kinases control root development mainly via brassinosteroid-independent actions in Arabidopsis thaliana. J Integr Plant Biol 54:388–399.
Etheridge N, Chen YF, Schaller GE. 2005. Dissecting the ethylene pathway of Arabidopsis. Brief Funct Genomic Proteomic 3:372–381.
Evans ML, Ishikawa H, Estelle MA. 1994. Responses of Arabidopsis roots to auxin studied with high temporal resolution: comparison of wild-type and auxin-response mutants. Planta 194:215–222.
Feraru E, Friml J. 2008. PIN polar targeting. Plant Physiol 147:1553–1559.
Ferreira FJ, Kieber JJ. 2005. Cytokinin signaling. Curr Opin Plant Biol 8:518–525.
Finkelstein RR, Rock CD. 2002. Abscisic Acid biosynthesis and response. Arabidopsis Book 1:e0058.
Finkelstein RR, Gampala SS, Rock CD. 2002. Abscisic acid signaling in seeds and seedlings. Plant Cell 14(Supp): S15–45.
Finkelstein R, Gampala SS, Lynch TJ, Thomas TL, Rock CD. 2005. Redundant and distinct functions of the ABA response loci ABA-INSENSITIVE(ABI)5 and ABRE-BINDING FACTOR (ABF)3. Plant Mol Biol 59:253–267.
Frebort I, Kowalska M, Hluska T, Frebortova J, Galuszka P. 2011. Evolution of cytokinin biosynthesis and degradation. J Exp Bot 62:2431–2452.
Friedrichsen DM, Joazeiro CA, Li J, Hunter T, Chory J. 2000. Brassinosteroid-insensitive-1 is a ubiquitously expressed leucine-rich repeat receptor serine/threonine kinase. Plant Physiol 123:1247–1256.
Frigerio M, Alabadi D, Perez-Gomez J, Garcia-Carcel L, Phillips AL, Hedden P, Blazquez MA. 2006. Transcriptional regulation of gibberellin metabolism genes by auxin signaling in Arabidopsis. Plant Physiol 142:553–563.
Friml J, Wisniewska J, Benkova E, Mendgen K, Palme K. 2002. Lateral relocation of auxin efflux regulator PIN3 mediates tropism in Arabidopsis. Nature 415:806–809.
Friml J, Vieten A, Sauer M, Weijers D, Schwarz H, Hamann T, Offringa R, Jurgens G. 2003. Efflux-dependent auxin gradients establish the apical-basal axis of Arabidopsis. Nature 426:147–153.
Fu X, Harberd NP. 2003. Auxin promotes Arabidopsis root growth by modulating gibberellin response. Nature 421:740–743.
Fu X, Richards DE, Ait-Ali T, Hynes LW, Ougham H, Peng J, Harberd NP. 2002. Gibberellin-mediated proteasome-dependent degradation of the barley DELLA protein SLN1 repressor. Plant Cell 14:3191–3200.
Fujii H, Verslues PE, Zhu JK. 2007. Identification of two protein kinases required for abscisic acid regulation of seed germination, root growth, and gene expression in Arabidopsis. Plant Cell 19:485–494.
Fujioka S, Yokota T. 2003. Biosynthesis and metabolism of brassinosteroids. Annu Rev Plant Biol 54:137–164.
Fujioka S, Li J, Choi YH, Seto H, Takatsuto S, Noguchi T, Watanabe T, Kuriyama H, Yokota T, Chory J, Sakurai A. 1997. The Arabidopsis deetiolated2 mutant is blocked early in brassinosteroid biosynthesis. Plant Cell 9:1951–1962.
Fujioka S, Takatsuto S, Yoshida S. 2002. An early C-22 oxidation branch in the brassinosteroid biosynthetic pathway. Plant Physiol 130:930–939.
Fujita Y, Fujita M, Satoh R, Maruyama K, Parvez MM, Seki M, Hiratsu K, Ohme-Takagi M, Shinozaki K, Yamaguchi-Shinozaki K. 2005. AREB1 is a transcription activator of novel ABRE-

dependent ABA signaling that enhances drought stress tolerance in Arabidopsis. Plant Cell 17:3470–3488.
Galinha C, Hofhuis H, Luijten M, Willemsen V, Blilou I, Heidstra R, Scheres B. 2007. PLETHORA proteins as dose-dependent master regulators of Arabidopsis root development. Nature 449: 1053–1057.
Galinha C, Bilsborough G, Tsiantis M. 2009. Hormonal input in plant meristems: a balancing act. Semin Cell Dev Biol 20:1149–1156.
Galweiler L, Guan C, Muller A, Wisman E, Mendgen K, Yephremov A, Palme K. 1998. Regulation of polar auxin transport by AtPIN1 in Arabidopsis vascular tissue. Science 282:2226–2230.
Geldner N, Friml J, Stierhof YD, Jurgens G, Palme K. 2001. Auxin transport inhibitors block PIN1 cycling and vesicle trafficking. Nature 413:425–428.
Ghassemian M, Nambara E, Cutler S, Kawaide H, Kamiya Y, McCourt P. 2000. Regulation of abscisic acid signaling by the ethylene response pathway in Arabidopsis. Plant Cell 12: 1117–1126.
Gillissen B, Burkle L, Andre B, Kuhn C, Rentsch D, Brandl B, Frommer WB. 2000. A new family of high-affinity transporters for adenine, cytosine, and purine derivatives in Arabidopsis. Plant Cell 12:291–300.
Gonzalez-Garcia MP, Vilarrasa-Blasi J, Zhiponova M, Divol F, Mora-Garcia S, Russinova E, Cano-Delgado AI. 2011. Brassinosteroids control meristem size by promoting cell cycle progression in Arabidopsis roots. Development 138:849–859.
Gou X, Yin H, He K, Du J, Yi J, Xu S, Lin H, Clouse SD, Li J. 2012. Genetic evidence for an indispensable role of somatic embryogenesis receptor kinases in brassinosteroid signaling. PLoS Genet 8:e1002452.
Grieneisen VA, Xu J, Maree AF, Hogeweg P, Scheres B. 2007. Auxin transport is sufficient to generate a maximum and gradient guiding root growth. Nature 449:1008–1013.
Grunewald W, Friml J. 2010. The march of the PINs: developmental plasticity by dynamic polar targeting in plant cells. EMBO J 29:2700–2714.
Grunewald W, Vanholme B, Pauwels L, Plovie E, Inze D, Gheysen G, Goossens A. 2009. Expression of the Arabidopsis jasmonate signalling repressor JAZ1/TIFY10A is stimulated by auxin. EMBO Rep 10:923–928.
Hacham Y, Holland N, Butterfield C, Ubeda-Tomas S, Bennett MJ, Chory J, Savaldi-Goldstein S. 2011. Brassinosteroid perception in the epidermis controls root meristem size. Development 138:839–848.
Hardtke CS, Berleth T. 1998. The Arabidopsis gene MONOPTEROS encodes a transcription factor mediating embryo axis formation and vascular development. EMBO J 17:1405–1411.
He JX, Gendron JM, Yang Y, Li J, Wang ZY. 2002. The GSK3-like kinase BIN2 phosphorylates and destabilizes BZR1, a positive regulator of the brassinosteroid signaling pathway in Arabidopsis. Proc Natl Acad Sci USA 99: 10185–10190.
He JX, Gendron JM, Sun Y, Gampala SS, Gendron N, Sun CQ, Wang ZY. 2005. BZR1 is a transcriptional repressor with dual roles in brassinosteroid homeostasis and growth responses. Science 307:1634–1638.
Hedden P, Phillips AL. 2000. Gibberellin metabolism: new insights revealed by the genes. Trends Plant Sci 5:523–530.
Helariutta Y, Fukaki H, Wysocka-Diller J, Nakajima K, Jung J, Sena G, Hauser MT, Benfey PN. 2000. The SHORT-ROOT gene controls radial patterning of the Arabidopsis root through radial signaling. Cell 101:555–567.
Helliwell CA, Sullivan JA, Mould RM, Gray JC, Peacock WJ, Dennis ES. 2001. A plastid envelope location of Arabidopsis ent-kaurene oxidase links the plastid and endoplasmic reticulum steps of the gibberellin biosynthesis pathway. Plant J 28:201–208.
Hertel R, Thomsom K, Russo VEA. 1972. In vitro auxin binding to particulate cell fractions from corn coleoptiles Planta 107:325–340.
Hirose N, Makita N, Yamaya T, Sakakibara H. 2005. Functional characterization and expression analysis of a gene, OsENT2, encoding an equilibrative nucleoside transporter in rice suggest a function in cytokinin transport. Plant Physiol 138:196–206.
Hirose N, Makita N, Kojima M, Kamada-Nobusada T, Sakakibara H. 2007. Overexpression of a type-A response regulator alters rice morphology and cytokinin metabolism. Plant Cell Physiol 48:523–539.
Hirose N, Takei K, Kuroha T, Kamada-Nobusada T, Hayashi H, Sakakibara H. 2008. Regulation of cytokinin biosynthesis, compartmentalization and translocation. J Exp Bot 59:75–83.
Hua J, Chang C, Sun Q, Meyerowitz EM. 1995. Ethylene insensitivity conferred by Arabidopsis ERS gene. Science 269: 1712–1714.
Hua J, Sakai H, Nourizadeh S, Chen QG, Bleecker AB, Ecker JR, Meyerowitz EM. 1998. EIN4 and ERS2 are members of the putative ethylene receptor gene family in Arabidopsis. Plant Cell 10:1321–1332.
Ikeda Y, Men S, Fischer U, Stepanova AN, Alonso JM, Ljung K, Grebe M. 2009. Local auxin biosynthesis modulates gradient-directed planar polarity in Arabidopsis. Nat Cell Biol 11: 731–738.
Ishida T, Adachi S, Yoshimura M, Shimizu K, Umeda M, Sugimoto K. 2010. Auxin modulates the transition from the mitotic cycle to the endocycle in Arabidopsis. Development 137:63–71.
Itoh H, Ueguchi-Tanaka M, Sentoku N, Kitano H, Matsuoka M, Kobayashi M. 2001. Cloning and functional analysis of two gibberellin 3 beta -hydroxylase genes that are differently expressed during the growth of rice. Proc Natl Acad Sci USA 98:8909–8914.
Jaillais Y, Hothorn M, Belkhadir Y, Dabi T, Nimchuk ZL, Meyerowitz EM, Chory J. 2011. Tyrosine phosphorylation controls brassinosteroid receptor activation by triggering membrane release of its kinase inhibitor. Genes Dev 25: 232–237.
Jones AM. 1998. Auxin transport: down and out and up again. Science 282: 2201–2203.
Jones B, Gunneras SA, Petersson SV, Tarkowski P, Graham N, May S, Dolezal K, Sandberg G, Ljung K. 2010. Cytokinin regulation of auxin synthesis in Arabidopsis involves a homeostatic feedback loop regulated via auxin and cytokinin signal transduction. Plant Cell 22: 2956–2969.
Kaneko M, Itoh H, Ueguchi-Tanaka M, Ashikari M, Matsuoka M. 2002. The alpha-amylase induction in endosperm during rice seed germination is caused by gibberellin synthesized in epithelium. Plant Physiol 128:1264–1270.
Kaneko M, Itoh H, Inukai Y, Sakamoto T, Ueguchi-Tanaka M, Ashikari M, Matsuoka M. 2003. Where do gibberellin biosynthesis and gibberellin signaling occur in rice plants? Plant J 35: 104–115.
Kende H. 1993. Ethylene biosynthesis. Annu Rev Cell Plant Physiol 44: 283–207.
Kepinski S, Leyser O. 2005. The Arabidopsis F-box protein TIR1 is an auxin receptor. Nature 435:446–451.
Kieber JJ. 2002. Cytokinins. Arabidopsis Book 1:e0063.
Kim TW, Wang ZY. 2010. Brassinosteroid signal transduction from receptor kinases to transcription factors. Annu Rev Plant Biol 61:681–704.
Klee HJ, Lanahan MB. 1995. Transgenic plants in hormones biology. In: Davies PJ, editor. Dordrecht: Kluwer Academic Publisher.
Kushwah S, Jones AM, Laxmi A. 2011. Cytokinin interplay with ethylene, auxin, and glucose signaling controls Arabidopsis seedling root directional growth. Plant Physiol 156:1851–1866.
Kyozuka J. 2007. Control of shoot and root meristem function by cytokinin. Curr Opin Plant Biol 10:442–446.
Leonhardt N, Kwak JM, Robert N, Waner D, Leonhardt G, Schroeder JI. 2004. Microarray expression analyses of Arabidopsis guard cells and isolation of a recessive abscisic acid hypersensitive protein phosphatase 2C mutant. Plant Cell 16:596–615.
Leung J, Merlot S, Giraudat J. 1997. The Arabidopsis ABSCISIC ACID-INSENSITIVE2 (ABI2) and ABI1 genes encode homologous protein phosphatases 2C involved in abscisic acid signal transduction. Plant Cell 9:759–771.
Lewis DR, Miller ND, Splitt BL, Wu G, Spalding EP. 2007. Separating the roles of acropetal and basipetal auxin transport on gravitropism with mutations in

two Arabidopsis multidrug resistance-like ABC transporter genes. Plant Cell 19:1838–1850.
Li J, Wen J, Lease KA, Doke JT, Tax FE, Walker JC. 2002. BAK1, an Arabidopsis LRR receptor-like protein kinase, interacts with BRI1 and modulates brassinosteroid signaling. Cell 110:213–222.
Liang X, Abel S, Keller JA, Shen NF, Theologis A. 1992. The 1-aminocyclopropane-1-carboxylate synthase gene family of Arabidopsis thaliana. Proc Natl Acad Sci USA 89:11046–11050.
Lin Z, Zhong S, Grierson D. 2009. Recent advances in ethylene research. J Exp Bot 60:3311–3336.
Liu J, Mehdi S, Topping J, Tarkowski P, Lindsey K. 2010. Modelling and experimental analysis of hormonal crosstalk in Arabidopsis. Mol Syst Biol 6:373.
Ljung K, Bhalerao RP, Sandberg G. 2001. Sites and homeostatic control of auxin biosynthesis in Arabidopsis during vegetative growth. Plant J 28:465–474.
Ljung K, Hull AK, Celenza J, Yamada M, Estelle M, Normanly J, Sandberg G. 2005. Sites and regulation of auxin biosynthesis in Arabidopsis roots. Plant Cell 17:1090–1104.
Luschnig C, Gaxiola RA, Grisafi P, Fink GR. 1998. EIR1, a root-specific protein involved in auxin transport, is required for gravitropism in Arabidopsis thaliana. Genes Dev 12:2175–2187.
Ma Y, Szostkiewicz I, Korte A, Moes D, Yang Y, Christmann A, Grill E. 2009. Regulators of PP2C phosphatase activity function as abscisic acid sensors. Science 324:1064–1068.
Marchant A, Bhalerao R, Casimiro I, Eklof J, Casero PJ, Bennett M, Sandberg G. 2002. AUX1 promotes lateral root formation by facilitating indole-3-acetic acid distribution between sink and source tissues in the Arabidopsis seedling. Plant Cell 14:589–597.
Marhavy P, Bielach A, Abas L, Abuzeineh A, Duclercq J, Tanaka H, Parezova M, Petrasek J, Friml J, Kleine-Vehn J, Benkova E. 2011. Cytokinin modulates endocytic trafficking of PIN1 auxin efflux carrier to control plant organogenesis. Dev Cell 21:796–804.
Matsumoto-Kitano M, Kusumoto T, Tarkowski P, Kinoshita-Tsujimura K, Vaclavikova K, Miyawaki K, Kakimoto T. 2008. Cytokinins are central regulators of cambial activity. Proc Natl Acad Sci USA 105:20027–20031.
McGinnis KM, Thomas SG, Soule JD, Strader LC, Zale JM, Sun TP, Steber CM. 2003. The Arabidopsis SLEEPY1 gene encodes a putative F-box subunit of an SCF E3 ubiquitin ligase. Plant Cell 15:1120–1130.
Melcher K, Zhou XE, Xu HE. 2010. Thirsty plants and beyond: structural mechanisms of abscisic acid perception and signaling. Curr Opin Struct Biol 20:722–729.
Mironova VV, Omelyanchuk NA, Novoselova ES, Doroshkov AV, Kazantsev FV, Kochetov AV, Kolchanov NA, Mjolsness E, Likhoshvai VA. 2012. Combined in silico/in vivo analysis of mechanisms providing for root apical meristem self-organization and maintenance. Ann Bot 110:349–360.
Mitchum MG, Yamaguchi S, Hanada A, Kuwahara A, Yoshioka Y, Kato T, Tabata S, Kamiya Y, Sun TP. 2006. Distinct and overlapping roles of two gibberellin 3-oxidases in Arabidopsis development. Plant J 45:804–818.
Miyawaki K, Matsumoto-Kitano M, Kakimoto T. 2004. Expression of cytokinin biosynthetic isopentenyltransferase genes in Arabidopsis: tissue specificity and regulation by auxin, cytokinin, and nitrate. Plant J 37:128–138.
Moubayidin L, Perilli S, Dello Ioio R, Di Mambro R, Costantino P, Sabatini S. 2010. The rate of cell differentiation controls the Arabidopsis root meristem growth phase. Curr Biol 20:1138–1143.
Mouchel CF, Briggs GC, Hardtke CS. 2004. Natural genetic variation in Arabidopsis identifies BREVIS RADIX, a novel regulator of cell proliferation and elongation in the root. Genes Dev 18:700–714.
Mouchel CF, Osmont KS, Hardtke CS. 2006. BRX mediates feedback between brassinosteroid levels and auxin signalling in root growth. Nature 443:458–461.
Mravec J, Kubes M, Bielach A, Gaykova V, Petrasek J, Skupa P, Chand S, Benkova E, Zazimalova E, Friml J. 2008. Interaction of PIN and PGP transport mechanisms in auxin distribution-dependent development. Development 135:3345–3354.
Mravec J, Skupa P, Bailly A, Hoyerova K, Krecek P, Bielach A, Petrasek J, Zhang J, Gaykova V, Stierhof YD, Dobrev PI, Schwarzerova K, Rolcik J, Seifertova D, Luschnig C, Benkova E, Zazimalova E, Geisler M, Friml J. 2009. Subcellular homeostasis of phytohormone auxin is mediated by the ER-localized PIN5 transporter. Nature 459:1136–1140.
Muller B, Sheen J. 2007. Advances in cytokinin signaling. Science 318:68–69.
Muller B, Sheen J. 2008. Cytokinin and auxin interaction in root stem-cell specification during early embryogenesis. Nature 453:1094–1097.
Muraro D, Byrne H, King J, Voss U, Kieber J, Bennett M. 2011. The influence of cytokinin-auxin cross-regulation on cell-fate determination in Arabidopsis thaliana root development. J Theor Biol 283:152–167.
Mussig C, Shin GH, Altmann T. 2003. Brassinosteroids promote root growth in Arabidopsis. Plant Physiol 133:1261–1271.
Nakajima M, Shimada A, Takashi Y, Kim YC, Park SH, Ueguchi-Tanaka M, Suzuki H, Katoh E, Iuchi S, Kobayashi M, Maeda T, Matsuoka M, Yamaguchi I. 2006. Identification and characterization of Arabidopsis gibberellin receptors. Plant J 46:880–889.
Nambara E, Marion-Poll A. 2005. Abscisic acid biosynthesis and catabolism. Annu Rev Plant Biol 56:165–185.
Negi S, Ivanchenko MG, Muday GK. 2008. Ethylene regulates lateral root formation and auxin transport in Arabidopsis thaliana. Plant J 55:175–187.
Nelson DR, Schuler MA, Paquette SM, Werck-Reichhart D, Bak S. 2004. Comparative genomics of rice and Arabidopsis. Analysis of 727 cytochrome P450 genes and pseudogenes from a monocot and a dicot. Plant Physiol 135:756–772.
Nemhauser JL, Hong F, Chory J. 2006. Different plant hormones regulate similar processes through largely nonoverlapping transcriptional responses. Cell 126:467–475.
Nishimura C, Ohashi Y, Sato S, Kato T, Tabata S, Ueguchi C. 2004. Histidine kinase homologs that act as cytokinin receptors possess overlapping functions in the regulation of shoot and root growth in Arabidopsis. Plant Cell 16:1365–1377.
Nishimura N, Yoshida T, Kitahata N, Asami T, Shinozaki K, Hirayama T. 2007. ABA-Hypersensitive Germination1 encodes a protein phosphatase 2C, an essential component of abscisic acid signaling in Arabidopsis seed. Plant J 50:935–949.
Noh B, Murphy AS, Spalding EP. 2001. Multidrug resistance-like genes of Arabidopsis required for auxin transport and auxin-mediated development. Plant Cell 13:2441–2454.
Oh MH, Clouse SD, Huber SC. 2009a. Tyrosine phosphorylation in brassinosteroid signaling. Plant Signal Behav 4:1182–1185.
Oh MH, Wang X, Kota U, Goshe MB, Clouse SD, Huber SC. 2009b. Tyrosine phosphorylation of the BRI1 receptor kinase emerges as a component of brassinosteroid signaling in Arabidopsis. Proc Natl Acad Sci USA 106:658–663.
Oh MH, Wang X, Wu X, Zhao Y, Clouse SD, Huber SC. 2010. Autophosphorylation of Tyr-610 in the receptor kinase BAK1 plays a role in brassinosteroid signaling and basal defense gene expression. Proc Natl Acad Sci USA 107:17827–17832.
Oh MH, Wang X, Clouse SD, Huber SC. 2012. Deactivation of the Arabidopsis BRASSINOSTEROID INSENSITIVE 1 (BRI1) receptor kinase by autophosphorylation within the glycine-rich loop. Proc Natl Acad Sci USA 109:327–332.
Ortega-Martinez O, Pernas M, Carol RJ, Dolan L. 2007. Ethylene modulates stem cell division in the Arabidopsis thaliana root. Science 317:507–510.
Ostin A, Kowalyczk M, Bhalerao RP, Sandberg G. 1998. Metabolism of indole-3-acetic acid in Arabidopsis. Plant Physiol 118:285–296.
Paponov IA, Teale WD, Trebar M, Blilou I, Palme K. 2005. The PIN auxin efflux facilitators: evolutionary and functional perspectives. Trends Plant Sci 10:170–177.
Park SY, Fung P, Nishimura N, Jensen DR, Fujii H, Zhao Y, Lumba S, Santiago J, Rodrigues A, Chow TF, Alfred SE, Bonetta D, Finkelstein R, Provart NJ, Desveaux D, Rodriguez PL, McCourt P, Zhu JK, Schroeder JI, Volkman BF,

Cutler SR. 2009. Abscisic acid inhibits type 2C protein phosphatases via the PYR/PYL family of START proteins. Science 324:1068–1071.

Parry G, Calderon-Villalobos LI, Prigge M, Peret B, Dharmasiri S, Itoh H, Lechner E, Gray WM, Bennett M, Estelle M. 2009. Complex regulation of the TIR1/AFB family of auxin receptors. Proc Natl Acad Sci USA 106: 22540–22545.

Peng P, Yan Z, Zhu Y, Li J. 2008. Regulation of the Arabidopsis GSK3-like kinase BRASSINOSTEROID-INSENSITIVE 2 through proteasome-mediated protein degradation. Mol Plant 1:338–346.

Petersson SV, Johansson AI, Kowalczyk M, Makoveychuk A, Wang JY, Moritz T, Grebe M, Benfey PN, Sandberg G, Ljung K. 2009. An auxin gradient and maximum in the Arabidopsis root apex shown by high-resolution cell-specific analysis of IAA distribution and synthesis. Plant Cell 21:1659–1668.

Petrásek J, Friml J. 2009. Auxin transport routes in plant development. Development 136:2675–2688.

Petrásek J, Mravec J, Bouchard R, Blakeslee JJ, Abas M, Seifertova D, Wisniewska J, Tadele Z, Kubes M, Covanova M, Dhonukshe P, Skupa P, Benkova E, Perry L, Krecek P, Lee OR, Fink GR, Geisler M, Murphy AS, Luschnig C, Zazimalova E, Friml J. 2006. PIN proteins perform a rate-limiting function in cellular auxin efflux. Science 312: 914–918.

Pitts RJ, Cernac A, Estelle M. 1998. Auxin and ethylene promote root hair elongation in Arabidopsis. Plant J 16: 553–560.

Potuschak T, Lechner E, Parmentier Y, Yanagisawa S, Grava S, Koncz C, Genschik P. 2003. EIN3-dependent regulation of plant ethylene hormone signaling by two arabidopsis F box proteins: EBF1 and EBF2. Cell 115: 679–689.

Pysh LD, Wysocka-Diller JW, Camilleri C, Bouchez D, Benfey PN. 1999. The GRAS gene family in Arabidopsis: sequence characterization and basic expression analysis of the SCARECROW-LIKE genes. Plant J 18:111–119.

Quint M, Barkawi LS, Fan KT, Cohen JD, Gray WM. 2009. Arabidopsis IAR4 modulates auxin response by regulating auxin homeostasis. Plant Physiol 150: 748–758.

Rashotte AM, Mason MG, Hutchison CE, Ferreira FJ, Schaller GE, Kieber JJ. 2006. A subset of Arabidopsis AP2 transcription factors mediates cytokinin responses in concert with a two-component pathway. Proc Natl Acad Sci USA 103:11081–11085.

Reed RC, Brady SR, Muday GK. 1998. Inhibition of auxin movement from the shoot into the root inhibits lateral root development in Arabidopsis. Plant Physiol 118:1369–1378.

Ruzicka K, Ljung K, Vanneste S, Podhorska R, Beeckman T, Friml J, Benkova E. 2007. Ethylene regulates root growth through effects on auxin biosynthesis and transport-dependent auxin distribution. Plant Cell 19:2197–2212.

Ruzicka K, Simaskova M, Duclercq J, Petrasek J, Zazimalova E, Simon S, Friml J, Van Montagu MC, Benkova E. 2009. Cytokinin regulates root meristem activity via modulation of the polar auxin transport. Proc Natl Acad Sci USA 106: 4284–4289.

Sabatini S, Beis D, Wolkenfelt H, Murfett J, Guilfoyle T, Malamy J, Benfey P, Leyser O, Bechtold N, Weisbeek P, Scheres B. 1999. An auxin-dependent distal organizer of pattern and polarity in the Arabidopsis root. Cell 99:463–472.

Sabatini S, Heidstra R, Wildwater M, Scheres B. 2003. SCARECROW is involved in positioning the stem cell niche in the Arabidopsis root meristem. Genes Dev 17:354–358.

Saez A, Apostolova N, Gonzalez-Guzman M, Gonzalez-Garcia MP, Nicolas C, Lorenzo O, Rodriguez PL. 2004. Gain-of-function and loss-of-function phenotypes of the protein phosphatase 2C HAB1 reveal its role as a negative regulator of abscisic acid signalling. Plant J 37:354–369.

Sakai H, Hua J, Chen QG, Chang C, Medrano LJ, Bleecker AB, Meyerowitz EM. 1998. ETR2 is an ETR1-like gene involved in ethylene signaling in Arabidopsis. Proc Natl Acad Sci USA 95: 5812–5817.

Sankar M, Osmont KS, Rolcik J, Gujas B, Tarkowska D, Strnad M, Xenarios I, Hardtke CS. 2011. A qualitative continuous model of cellular auxin and brassinosteroid signaling and their crosstalk. Bioinformatics 27:1404–1412.

Santner A, Estelle M. 2009. Recent advances and emerging trends in plant hormone signalling. Nature 459: 1071–1078.

Santner A, Calderon-Villalobos LI, Estelle M. 2009. Plant hormones are versatile chemical regulators of plant growth. Nat Chem Biol 5:301–307.

Sarkar AK, Luijten M, Miyashima S, Lenhard M, Hashimoto T, Nakajima K, Scheres B, Heidstra R, Laux T. 2007. Conserved factors regulate signalling in Arabidopsis thaliana shoot and root stem cell organizers. Nature 446: 811–814.

Sasaki A, Itoh H, Gomi K, Ueguchi-Tanaka M, Ishiyama K, Kobayashi M, Jeong DH, An G, Kitano H, Ashikari M, Matsuoka M. 2003. Accumulation of phosphorylated repressor for gibberellin signaling in an F-box mutant. Science 299:1896–1898.

Scacchi E, Salinas P, Gujas B, Santuari L, Krogan N, Ragni L, Berleth T, Hardtke CS. 2010. Spatio-temporal sequence of cross-regulatory events in root meristem growth. Proc Natl Acad Sci USA 107:22734–22739.

Schmülling T, Werner T, Riefler M, Krupkova E, Bartrina y Manns I. 2003. Structure and function of cytokinin oxidase/dehydrogenase genes of maize, rice, Arabidopsis and other species. J Plant Res 116:241–252.

Sena G, Wang X, Liu HY, Hofhuis H, Birnbaum KD. 2009. Organ regeneration does not require a functional stem cell niche in plants. Nature 457: 1150–1153.

Sharp RE. 2002. Interaction with ethylene: changing views on the role of ABA in root and shoot growth responses to water stress. Plant, Cell Environ 25: 211–222.

Shimada Y, Fujioka S, Miyauchi N, Kushiro M, Takatsuto S, Nomura T, Yokota T, Kamiya Y, Bishop GJ, Yoshida S. 2001. Brassinosteroid-6-oxidases from Arabidopsis and tomato catalyze multiple C-6 oxidations in brassinosteroid biosynthesis. Plant Physiol 126: 770–779.

Shimada Y, Goda H, Nakamura A, Takatsuto S, Fujioka S, Yoshida S. 2003. Organ-specific expression of brassinosteroid-biosynthetic genes and distribution of endogenous brassinosteroids in Arabidopsis. Plant Physiol 131:287–297.

Shiu SH, Karlowski WM, Pan R, Tzeng YH, Mayer KF, Li WH. 2004. Comparative analysis of the receptor-like kinase family in Arabidopsis and rice. Plant Cell 16:1220–1234.

Shkolnik-Inbar D, Bar-Zvi D. 2011. ABI4 mediates abscisic acid and cytokinin inhibition of lateral root formation by reducing polar auxin transport in Arabidopsis. Plant Cell 22:3560–3573.

Silverstone AL, Chang C, Krol E, Sun TP. 1997. Developmental regulation of the gibberellin biosynthetic gene GA1 in Arabidopsis thaliana. Plant J 12:9–19.

Silverstone AL, Jung HS, Dill A, Kawaide H, Kamiya Y, Sun TP. 2001. Repressing a repressor: gibberellin-induced rapid reduction of the RGA protein in Arabidopsis. Plant Cell 13:1555–1566.

Spray CR, Kobayashi M, Suzuki Y, Phinney BO, Gaskin P, MacMillan J. 1996. The dwarf-1 (dt) Mutant of Zea mays blocks three steps in the gibberellin-biosynthetic pathway. Proc Natl Acad Sci USA 93:10515–10518.

Stepanova AN, Hoyt JM, Hamilton AA, Alonso JM. 2005. A Link between ethylene and auxin uncovered by the characterization of two root-specific ethylene-insensitive mutants in Arabidopsis. Plant Cell 17:2230–2242.

Stepanova AN, Yun J, Likhacheva AV, Alonso JM. 2007. Multilevel interactions between ethylene and auxin in Arabidopsis roots. Plant Cell 19: 2169–2185.

Stepanova AN, Robertson-Hoyt J, Yun J, Benavente LM, Xie DY, Dolezal K, Schlereth A, Jurgens G, Alonso JM. 2008. TAA1-mediated auxin biosynthesis is essential for hormone crosstalk and plant development. Cell 133: 177–191.

Sun J, Xu Y, Ye S, Jiang H, Chen Q, Liu F, Zhou W, Chen R, Li X, Tietz O, Wu X, Cohen JD, Palme K, Li C. 2009. Arabidopsis ASA1 is important for jasmonate-mediated regulation of auxin

biosynthesis and transport during lateral root formation. Plant Cell 21: 1495–1511.
Sun Y, Fan XY, Cao DM, Tang W, He K, Zhu JY, He JX, Bai MY, Zhu S, Oh E, Patil S, Kim TW, Ji H, Wong WH, Rhee SY, Wang ZY. 2010. Integration of brassinosteroid signal transduction with the transcription network for plant growth regulation in Arabidopsis. Dev Cell 19: 765–777.
Suzuki H, Park SH, Okubo K, Kitamura J, Ueguchi-Tanaka M, Iuchi S, Katoh E, Kobayashi M, Yamaguchi I, Matsuoka M, Asami T, Nakajima M. 2009. Differential expression and affinities of Arabidopsis gibberellin receptors can explain variation in phenotypes of multiple knock-out mutants. Plant J 60: 48–55.
Swarup K, Benkova E, Swarup R, Casimiro I, Peret B, Yang Y, Parry G, Nielsen E, De Smet I, Vanneste S, Levesque MP, Carrier D, James N, Calvo V, Ljung K, Kramer E, Roberts R, Graham N, Marillonnet S, Patel K, Jones JD, Taylor CG, Schachtman DP, May S, Sandberg G, Benfey P, Friml J, Kerr I, Beeckman T, Laplaze L, Bennett MJ. 2008. The auxin influx carrier LAX3 promotes lateral root emergence. Nat Cell Biol 10:946–954.
Swarup R, Friml J, Marchant A, Ljung K, Sandberg G, Palme K, Bennett M. 2001. Localization of the auxin permease AUX1 suggests two functionally distinct hormone transport pathways operate in the Arabidopsis root apex. Genes Dev 15:2648–2653.
Swarup R, Perry P, Hagenbeek D, Van Der Straeten D, Beemster GT, Sandberg G, Bhalerao R, Ljung K, Bennett MJ. 2007. Ethylene upregulates auxin biosynthesis in Arabidopsis seedlings to enhance inhibition of root cell elongation. Plant Cell 19:2186–2196.
Szekeres M, Nemeth K, Koncz-Kalman Z, Mathur J, Kauschmann A, Altmann T, Redei GP, Nagy F, Schell J, Koncz C. 1996. Brassinosteroids rescue the deficiency of CYP90, a cytochrome P450, controlling cell elongation and de-etiolation in Arabidopsis. Cell 85:171–182.
Taiz L, Zeiger E. 2006. Plant physiology. Sunderland, MA: Sinauer Associates, Inc., 764 p.
Takei K, Yamaya T, Sakakibara H. 2004. Arabidopsis CYP735A1 and CYP735A2 encode cytokinin hydroxylases that catalyze the biosynthesis of trans-Zeatin. J Biol Chem 279:41866–41872.
Tanimoto M, Roberts K, Dolan L. 1995. Ethylene is a positive regulator of root hair development in Arabidopsis thaliana. Plant J 8:943–948.
Thomann A, Lechner E, Hansen M, Dumbliauskas E, Parmentier Y, Kieber J, Scheres B, Genschik P. 2009. Arabidopsis CULLIN3 genes regulate primary root growth and patterning by ethylene-dependent and -independent mechanisms. PLoS Genet 5:e1000328.
To JP, Haberer G, Ferreira FJ, Deruere J, Mason MG, Schaller GE, Alonso JM, Ecker JR, Kieber JJ. 2004. Type-A Arabidopsis response regulators are partially redundant negative regulators of cytokinin signaling. Plant Cell 16: 658–671.
Ubeda-Tomas S, Swarup R, Coates J, Swarup K, Laplaze L, Beemster GT, Hedden P, Bhalerao R, Bennett MJ. 2008. Root growth in Arabidopsis requires gibberellin/DELLA signalling in the endodermis. Nat Cell Biol 10: 625–628.
Ubeda-Tomas S, Federici F, Casimiro I, Beemster GT, Bhalerao R, Swarup R, Doerner P, Haseloff J, Bennett MJ. 2009. Gibberellin signaling in the endodermis controls Arabidopsis root meristem size. Curr Biol 19:1194–1199.
Ueguchi-Tanaka M, Ashikari M, Nakajima M, Itoh H, Katoh E, Kobayashi M, Chow TY, Hsing YI, Kitano H, Yamaguchi I, Matsuoka M. 2005. GIBBERELLIN INSENSITIVE DWARF1 encodes a soluble receptor for gibberellin. Nature 437:693–698.
van den Berg C, Willemsen V, Hage W, Weisbeek P, Scheres B. 1995. Cell fate in the Arabidopsis root meristem determined by directional signalling. Nature 378:62–65.
van den Berg C, Willemsen V, Hendriks G, Weisbeek P, Scheres B. 1997. Short-range control of cell differentiation in the Arabidopsis root meristem. Nature 390:287–289.
Van der Straeten D, Rodrigues-Pousada RA, Villarroel R, Hanley S, Goodman HM, Van Montagu M. 1992. Cloning, genetic mapping, and expression analysis of an Arabidopsis thaliana gene that encodes 1-aminocyclopropane-1-carboxylate synthase. Proc Natl Acad Sci US 89:9969–9973.
Vanneste S, Friml J. 2009. Auxin: a trigger for change in plant development. Cell 136:1005–1016.
Vanstraelen M, Benková E. 2012. Hormonal interactions in the regulation of plant development. Annu Rev Cell Dev Biol 28:22.1–22.25.
Verrier PJ, Bird D, Burla B, Dassa E, Forestier C, Geisler M, Klein M, Kolukisaoglu U, Lee Y, Martinoia E, Murphy A, Rea PA, Samuels L, Schulz B, Spalding EJ, Yazaki K, Theodoulou FL. 2008. Plant ABC proteins–a unified nomenclature and updated inventory. Trends Plant Sci 13:151–159.
Verslues PE, Kim YS, Zhu JK. 2007. Altered ABA, proline and hydrogen peroxide in an Arabidopsis glutamate:-glyoxylate aminotransferase mutant. Plant Mol Biol 64:205–217.
Vieten A, Vanneste S, Wisniewska J, Benkova E, Benjamins R, Beeckman T, Luschnig C, Friml J. 2005. Functional redundancy of PIN proteins is accompanied by auxin-dependent cross-regulation of PIN expression. Development 132:4521–4531.
Vieten A, Sauer M, Brewer PB, Friml J. 2007. Molecular and cellular aspects of auxin-transport-mediated development. Trends Plant Sci 12:160–168.
Wang H, Qi Q, Schorr P, Cutler AJ, Crosby WL, Fowke LC. 1998. ICK1, a cyclin-dependent protein kinase inhibitor from Arabidopsis thaliana interacts with both Cdc2a and CycD3, and its expression is induced by abscisic acid. Plant J 15:501–510.
Wang X, Chory J. 2006. Brassinosteroids regulate dissociation of BKI1, a negative regulator of BRI1 signaling, from the plasma membrane. Science 313: 1118–1122.
Wang X, Kota U, He K, Blackburn K, Li J, Goshe MB, Huber SC, Clouse SD. 2008. Sequential transphosphorylation of the BRI1/BAK1 receptor kinase complex impacts early events in brassinosteroid signaling. Dev Cell 15: 220–235.
Wang ZY, Nakano T, Gendron J, He J, Chen M, Vafeados D, Yang Y, Fujioka S, Yoshida S, Asami T, Chory J. 2002. Nuclear-localized BZR1 mediates brassinosteroid-induced growth and feedback suppression of brassinosteroid biosynthesis. Dev Cell 2:505–513.
Weijers D, Schlereth A, Ehrismann JS, Schwank G, Kientz M, Jurgens G. 2006. Auxin triggers transient local signaling for cell specification in Arabidopsis embryogenesis. Dev Cell 10:265–270.
Werner T, Motyka V, Strnad M, Schmulling T. 2001. Regulation of plant growth by cytokinin. Proc Natl Acad Sci USA 98:10487–10492.
Werner T, Motyka V, Laucou V, Smets R, Van Onckelen H, Schmulling T. 2003. Cytokinin-deficient transgenic Arabidopsis plants show multiple developmental alterations indicating opposite functions of cytokinins in the regulation of shoot and root meristem activity. Plant Cell 15:2532–2550.
Williams J, Phillips AL, Gaskin P, Hedden P. 1998. Function and substrate specificity of the gibberellin 3beta-hydroxylase encoded by the Arabidopsis GA4 gene. Plant Physiol 117: 559–563.
Willige BC, Isono E, Richter R, Zourelidou M, Schwechheimer C. 2011. Gibberellin regulates PIN-FORMED abundance and is required for auxin transport-dependent growth and development in Arabidopsis thaliana. Plant Cell 23: 2184–2195.
Wisniewska J, Xu J, Seifertova D, Brewer PB, Ruzicka K, Blilou I, Rouquie D, Benkova E, Scheres B, Friml J. 2006. Polar PIN localization directs auxin flow in plants. Science 312:883.
Wolters H, Jurgens G. 2009. Survival of the flexible: hormonal growth control and adaptation in plant development. Nat Rev Genet 10:305–317.
Woodward AW, Bartel B. 2005. Auxin: regulation, action, and interaction. Ann Bot 95:707–735.
Xiong L, Zhu JK. 2003. Regulation of abscisic acid biosynthesis. Plant Physiol 133:29–36.
Yamaguchi S. 2008. Gibberellin metabolism and its regulation. Annu Rev Plant Biol 59:225–251.

Yamaguchi S, Kamiya Y, Sun T. 2001. Distinct cell-specific expression patterns of early and late gibberellin biosynthetic genes during Arabidopsis seed germination. Plant J 28:443–453.

Yin Y, Vafeados D, Tao Y, Yoshida S, Asami T, Chory J. 2005. A new class of transcription factors mediates brassinosteroid-regulated gene expression in Arabidopsis. Cell 120:249–259.

Yoshida T, Nishimura N, Kitahata N, Kuromori T, Ito T, Asami T, Shinozaki K, Hirayama T. 2006. ABA-hypersensitive germination3 encodes a protein phosphatase 2C (AtPP2CA) that strongly regulates abscisic acid signaling during germination among Arabidopsis protein phosphatase 2Cs. Plant Physiol 140:115–126.

Zazímalová E, Krecek P, Skupa P, Hoyerova K, Petrasek J. 2007. Polar transport of the plant hormone auxin: the role of PIN-FORMED (PIN) proteins. Cell Mol Life Sci 64:1621–1637.

Zhang H, Han W, De Smet I, Talboys P, Loya R, Hassan A, Rong H, Jurgens G, Paul Knox J, Wang MH. 2010. ABA promotes quiescence of the quiescent centre and suppresses stem cell differentiation in the Arabidopsis primary root meristem. Plant J 64: 764–774.

Zhang W, To JP, Cheng CY, Eric Schaller G, Kieber JJ. 2011. Type-A response regulators are required for proper root apical meristem function through post-transcriptional regulation of PIN auxin efflux carriers. Plant J 68:1–10.

Zhao XC, Qu X, Mathews DE, Schaller GE. 2002. Effect of ethylene pathway mutations upon expression of the ethylene receptor ETR1 from Arabidopsis. Plant Physiol 130:1983–1991.

Zhou ZY, Zhang CG, Wu L, Chai J, Wang M, Jha A, Jia PF, Cui SJ, Yang M, Chen R, Guo GQ. 2011. Functional characterization of the CKRC1/TAA1 gene and dissection of hormonal actions in the Arabidopsis root. Plant J 66: 516–527.

Developmental Dynamics

8.4. Parte IV:

Artículo:

Dynamic models of epidermal patterning as an approach to plant eco-evo-devo

Mariana Benítez, Eugenio Azpeitia, Elena R Álvarez-Buylla

Current Opinion in Plant Biology

Available online at www.sciencedirect.com

SciVerse ScienceDirect

Current Opinion in Plant Biology

Dynamic models of epidermal patterning as an approach to plant eco-evo-devo

Mariana Benítez[1,2], Eugenio Azpeitia[2,3] and Elena R Alvarez-Buylla[2,3,*]

Epidermal patterning in *Arabidopsis thaliana* leaves and root has become a model system for experimental and theoretical developmental studies, yielding well-characterized regulatory networks. We succinctly review the dynamic models proposed for this system and then argue that it provides an excellent instance to integrate and further study the role of non-genetic factors in plant development and evolution. Then, we set up to review the role of phytohormones and environmental stimuli in the regulation of cell-fate determination and patterning in this system. We conclude that dynamic modeling of complex regulatory networks can help understand the plasticity and variability of cellular patterns, and hence, such modeling approaches can be expanded to advance in the consolidation of plant Evolutionary and Ecological Developmental Biology (eco-evo-devo).

Addresses
[1] Departamento de Ecología de la Biodiversidad, Instituto de Ecologa, Universidad Nacional Autónoma de México, Ciudad Universitaria, 3er circuito exterior junto al Jardn Botanico, Del. Coyoacan, México D.F. 04510, Mexico
[2] C3, Centro de Ciencias de la Complejidad, Universidad Nacional Autónoma de México, Apartado postal 70-725, México D.F., C.P. 04510, Mexico
[3] Laboratorio de Genética Molecular, Desarrollo y Evolución de Plantas, Departamento de Ecología Funcional, Instituto de Ecología, Universidad Nacional Autónoma de México, Ciudad Universitaria, 3er circuito exterior junto al Jardín Botánico, Del. Coyoacán, México D.F. 04510, Mexico

Corresponding author: Alvarez-Buylla, Elena R (eabuylla@gmail.com)
* Present Address: Miller Institute for Basic Research in Science, University of California Berkeley, United States.

Current Opinion in Plant Biology 2012, **16**:xx–yy

This review comes from a themed issue on **Growth and Development**

Edited by **Marja Timmermans** and **Michael J. Scanlon**

1369-5266/$ – see front matter,

http://dx.doi.org/10.1016/j.pbi.2012.11.005

Epidermal patterning system: molecular genetics and systems biology approaches

The differentiation of the leaf and root epidermal cells in *Arabidopsis thaliana* (Arabidopsis) has become a model system for the study of cell fate determination and pattern emergence. Vast work on molecular genetics and modeling has shown that the distribution of epidermal hairs (trichomes in the leaves, and trichoblasts in the root) emerge from similar gene regulatory networks (GRNs) [1–3], even though the spatial distribution of hair cells differs between these two systems; trichomes tend to appear away from each other (Figure 1), while trichoblasts are arranged in cell files that alternate with atrichoblast cell files.

Briefly summarized, epidermal cell identities depend mainly on the presence of a complex formed by a MYB protein – WEREWOLF (WER) in the root and GLABRA1 (GL1) in the shoot–, the bHLH proteins GLABRA3 (GL3) and ENHANCER OF GLABRA3 (EGL3), and the WD40 protein TRANSPARENT TEST GLABRA1 (TTG1). In turn, TRIPTYCHON (TRY), CAPRICE (CPC), and ENHANCER OF TRY AND CPC 1,2,3 (ETC1,2,3), all of them R3 single repeat MYB transcription factors, prevent the formation of the MYB-BHLH-WD40 complex and act as inhibitors of trichome and atrichoblast cell fate (recent reviews in [3,4]; Figure 2a, b). However, other proteins involved in the regulation of epidermal patterning have been identified and further characterized. TRICHOMLESS1 and 2 (TCL1,2) have been shown to interact with GL3 and to inhibit the trichome fate by directly suppressing the expression of GL1 [5,6]. *MYB23* acts in a partially redundant way with *WER* and is able to substitute for the function of *WER* and to induce its own expression [7,8]. Additionally, high-throughput experiments have yielded valuable insight into new components of these GRNs, identifying for example other bHLH genes involved in root hair determination and differentiation [9••].

Mathematical and computational dynamic models have been used to integrate available experimental data and test the sufficiency of regulatory modules for epidermal cell differentiation and patterning in leaves and roots (Figure 2c–f). The fact that cell determination occurs on the surface of leaves and roots, and cells maintain their relative positions during this process has facilitated the postulation of spatiotemporal models as a fixed two-dimensional domain with emphasis in different processes ([10–15]; e.g. Figure 2). Overall, these efforts have provided novel predictions and hypotheses for further experimental studies. For example, these models have enabled to test the hypothesis sustaining that epidermal patterning is generated by an activator–inhibitor mechanism, a class of reaction–difussion system [16] conformed by a self-activating substance (activator) that acts at short distances and that upregulates a long-range acting antagonist (inhibitor), that can spontaneously generate spatial patterns of activator concentration [17]. Models

Please cite this article in press as: Benítez M, et al.: Dynamic models of epidermal patterning as an approach to plant eco-evo-devo, Curr Opin Plant Biol (2012), http://dx.doi.org/10.1016/j.pbi.2012.11.005

Figure 1

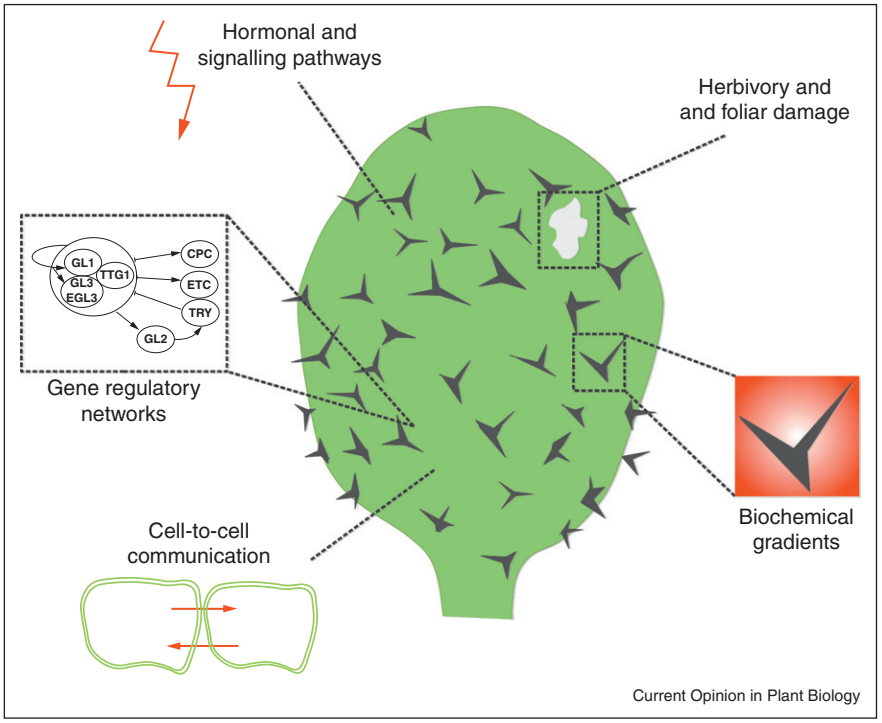

Factors involved in leaf epidermal patterning in Arabidopsis. As other developmental processes, epidermal cell determination and patterning emerges from the complex interactions among several genetic and non-genetic factors. In the case of leaves, this process is affected by intercellular communication, the formation of biochemical gradients, abiotic and biotic ecological interactions that may involve other organisms such as herbivores, and gene regulatory networks, which in turn establish mutual regulation with hormonal and signaling pathways.

have revealed that an activator–inhibitor mechanism conformed by the MYB/bHLH/WD40 complex and its inhibitors CPC and TRY seems to stabilize pattern formation, but that such regulatory motif is coupled to other partially redundant patterning motifs in a larger and dynamically-richer system [18–20]. Indeed, models of epidermal patterning add up to other integrative efforts in diverse systems suggesting that redundancy at the circuit or dynamic level contributes to the robustness of patterning processes during plant and animal development [21,22].

Dynamical models of epidermal patterning have also been successfully used to formulate predictions that would have been difficult (if not impossible) to conceive without the use of models. These include predictions regarding the phenotypic effect of changes in a wide range of parameter values [11], as well as predictions considering the role of cell geometry on the overall cellular patterns in the root [11]. Moreover, some of these predictions have been experimentally tested and have contributed with new data to the existing set of empirical evidence and to the understanding of developmental patterning processes in general (reviewed in [3]). For instance, Digiuni *et al.* [14] used a combination of modeling and experiments to uncover the nature of the competition between the members of the MYB/bHLH/WD40 complex and their inhibitors. Using a continuous model, three possible forms of TRY-mediated inhibition of the complex were explored and simulations demonstrated that while all three mechanisms were compatible with the wild type spacing pattern, only one of them was able to account for the results of overexpression experiments. Based on the simulation results, focused experiments showed that the binding of TRY to free GL3 was the most likely competitive inhibition mechanism. Bouyer *et al.* [15] also followed a combined experimental and theoretical approach to explore the role of TTG1 mobility in trichome pattern formation. Using a continuous model of a highly reduced GRN, the authors demonstrated that local self-activation of the complex together with TTG1 diffusion could alone generate a pattern similar to that observed in the leaf epidermis. Then, they went on to show that fluorescent TTG1 fusion proteins accumulate in developing trichomes while being depleted in their closest neighbors, providing the community with new experimental data that help validate the proposed models.

Finally, some of the theoretical studies revised here have explored the mechanisms by which certain phytohormones [12] or nutrient conditions [23•] could alter cell

Please cite this article in press as: Benítez M, et al.: Dynamic models of epidermal patterning as an approach to plant eco-evo-devo, Curr Opin Plant Biol (2012), http://dx.doi.org/10.1016/j.pbi.2012.11.005

Figure 2

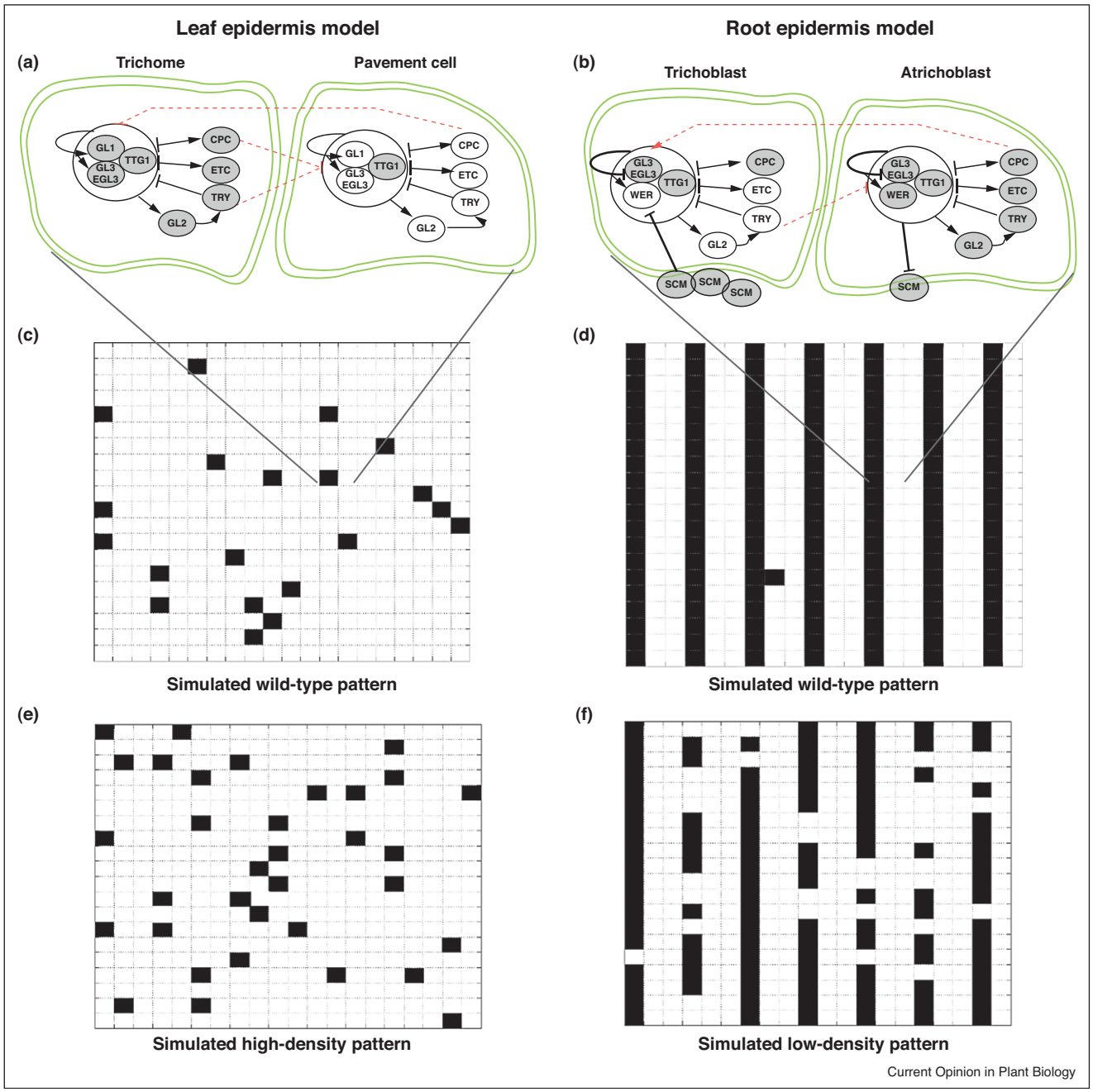

Data-based dynamical models may reproduce wild-type patterns and suggest possible mechanisms behind pattern plasticity. **(a, b)** The spatiotemporal model of cellular determination and patterning postulated by Benítez *et al.* (2008) considers the epidermis of leaves and roots as a two-dimensional domain conformed by cells, each of which contains a gene regulatory network (GRN). In this figure the network's components that are stably expressed in each cell type are shaded in grey. But note that overall GRN topology is the same in both cell types of the leaf and root epidermis. Since it has been shown that some molecular components of these networks can move to neighboring cells via plasmodesmata, the GRNs are coupled by these mobile elements. **(c, d)** The dynamics of the coupled networks are sufficient to reproduce the generation of the leaf and root wild-type patterns of hair and nonhair cells. **(e, f)** Altered patters of trichomes and trichoblasts can be generated by modified versions of the simulated GRNs, providing a tool to simulate the precise effect of genetic alterations (e.g. *GL3* overexpression in **(e)**, and *CPC* loss of function in **(f)**). Similarly, these models can help postulate specific ways in which signaling and hormonal pathways affect the GRNs and regulate the plastic epidermal patterns that are observed.

Please cite this article in press as: Benítez M, et al.: Dynamic models of epidermal patterning as an approach to plant eco-evo-devo, Curr Opin Plant Biol (2012), http://dx.doi.org/10.1016/j.pbi.2012.11.005

patterning. Nevertheless, modeling efforts have focused mainly on the transcription factors involved in epidermal patterning and still face the challenge of integrating the growing evidence for hormonal, environmental and biophysical regulation of cellular determination and patterning [24•].

Pattern variability in response to internal and external signals

Dynamic network models and experimental evidence have suggested that cell patterning is sensitive to a wide range of regulatory processes at the cellular, organismal and ecological scale. Such processes involve non-genetic DNA modifications (e.g. methylation), the interactions constituting complex GRNs, physical and chemical fields, and environmental factors that contribute to the generation of spatio-temporal patterns [25,26] (Figure 1). These processes in certain ways constrain – while in others drive – the emergence of patterns and shapes during development, and are therefore key to understanding the emergence, variability and evolution of cell patterns.

Indeed epidermal cellular identities and densities plastically change during development [27,28] and in response to diverse types of stimuli and conditions [6,29–33] (Table 1; Figure 2). The GRNs involved in epidermal patterning respond to and integrate various signaling and hormonal systems. In the leaf epidermis, it has been described that Gibberellin (GA) signaling upregulates *GL1* and promotes trichome development [30,34,35], which could account for the changes in trichome density during plant maturation and after flowering [27,28]. Interestingly, both GA and cytokinins, which act as antagonists in other contexts [36], stimulate the development of trichoblasts via transcription factors related to *GLABROUS INFLORESCENCE STEMS* (*GIS*) [35]. Jasmonates (JA) also promote trichome development and increase trichome density by inhibiting the action of JAZ proteins, which in turn inhibit *GL3*, *EGL3*, and *GL1* [33,37••], while salicylic acid (SA) produces a reduced-trichome density phenotype [6,31].

In the root epidermis, ethylene appears to mediate Fe-deficiency-induced root hair formation. Roots treated with the ethylene precursor ACC exhibit ectopic root hairs, as do roots under –Fe conditions and ethylene-overproducing mutant seedlings [38]. Finally, it was recently reported that reduction in the expression of a C2H2 zinc finger protein *ZINC FINGER PROTEIN 5* (*ZFP5*), which is induced by cytokinins, leads to fewer and shorter root hairs as compared to wild type by directly promoting the expression of *CPC* [39•]. Adding to the complexity of the developmental system under discussion, cross talk between hormonal signaling systems that affect the epidermal cellular patterning GRN appears to be ubiquitous in plant development [6,31,40].

Environmental factors that induce modifications on epidermal patterning, particularly on hair density are also important. Such modifications may be ecologically significant to contend with various types of abiotic and biotic factors. For example, salt stress reduces trichoblast density and size, and extremely high salt concentrations transform root hair pattern [41], while CO2 increases trichoblast density and size [42]. It is not clear how these signals are integrated by the GRN involved in epidermal patterning, but it is likely that hormonal signaling pathways mediate this response, as hormonal signaling systems often mediate the response to diverse environmental signals. For instance, JA mediates plant responses to insect attack, wounding, pathogen infection, stress, and UV damage, and at the same time induces the formation of trichomes on the leaf epidermis [33].

Importantly, the components of networks involved in epidermal patterning do not only sense environmental signals, but also affect the organism's plastic response and establish feedbacks in the organism–environment interactions. For instance, *gl1*, *gl3* and *try* single mutants have a defective cuticle formation. Cuticle is important for the systemic acquired resistance, which is a defensive response against pathogens. Consequently, these mutants have a reduced or compromised resistance against pathogen infection, a phenotype that can be partially rescued with GA addition [43].

Table 1

Summary of the environmental, signaling and hormonal factors involved in epidermal patterning in the leaf and root of Arabidopsis

	Phenotypic effect on the cellular patterns	Hormonal, environmental or organismal stimuli	References
Leaf epidermal patterning	Increased density of trichomes	Gibberellins	[30,34]
		Jasmonates	[33,37••]
		Cytokinins	[35]
		Plant maturation, flowering	[27,28]
	Decreased trichome density	Salicylic acid	[6,31]
Root epidermal patterning	Increased number of trichoblasts	Nutrient deficiency	[23,32,38]
		Ethylene	[38,66]
		CO_2	[42]
	Decreased number and size of trichoblasts	Cytokinin	[6,39•]
		Salt stress	[41]

Please cite this article in press as: Benítez M, et al.: Dynamic models of epidermal patterning as an approach to plant eco-evo-devo, Curr Opin Plant Biol (2012), http://dx.doi.org/10.1016/j.pbi.2012.11.005

Furthermore, the regulatory networks associated to root and leaf epidermal patterning are tightly coupled to other developmental modules, which could account for spatial and temporal regulation of epidermal patterning along the life cycle of Arabidopsis. For instance, early experiments showing that *GL3* reduces endoreduplication, while *TRY* increases it [44], demonstrated that epidermal hair patterns and cell cycle are coupled. More recent evidence is beginning to clarify this link, in which CYCLIN B1;2 and D3;1 [45], SIAMESE (SIM) [46,47], CDKA and CC52A1 [4,47,48] and other molecules are involved. As a matter of interest, the reduction of endoreduplication levels can induce trichomes to lose their fate and transdifferentiate as epidermal pavement cells [49], which further points to a complex and bidirectional link between the modules of epidermal patterning and cell cycle regulation (review in [4]). Epidermal cell determination is also coupled to stem cell development and maintenance via *JACKDAW* (*JKD*), which was initially characterized as a transcription factor involved in root stem-cell maintenance and later shown to act in a non-cell autonomous manner during root hair determination [50••]. Indeed, *jkd* loss of function produces randomized epidermal hair distribution instead of the typical bands, and epistasis analyses revealed that it acts upstream of the root hair GRN.

Figure 3

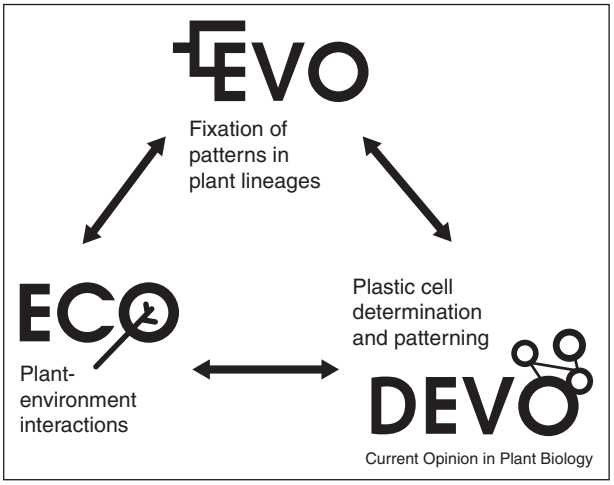

The system of epidermal patterning in Arabidopsis leaves and roots as a model system in eco-evo-devo. Environmental cues and conditions may elicit signal transduction mechanisms, often involving hormone systems, that feedback with complex regulatory networks and other developmental mechanisms to give rise to plastic patterns of trichomes and trichoblasts. Variation in such patterns can in turn affect the plant-environment interactions. Finally, pattern variation may be inherited by genetic or epigenetic mechanisms and may thus be fixed in certain lineages and impact organismal evolution.

Epidermal patterning as a model in eco-evo-devo

Eco-evo-devo, or ecological and evolutionary developmental biology has resulted from three disciplines coming together in the need to fully understand the origin, variation, and thus evolution, of phenotypes [51–53]. Such integrative discipline has been largely motivated by the wealth of empirical data showing that phenotypes and their evolution cannot be reduced to the evolution of genes and that, besides regulatory interactions within and among GRNs, other factors are central to the generation and variation of organismal shapes, physiology, phenology, and so on [25,54–56]. Then, among the issues that this field aims to investigate is the role of environmental factors in the generation of new phenotypes and, in turn, the effect of developmental variability in the modification of ecological interactions, and the potential for transgenerational inheritance of phenotypic changes induced by environmental stimuli (Figure 3). Importantly, addressing the issues identified by the eco-evo-devo program requires dynamical and mechanistic explanations of the relationship between developmental modules, environmental factors and phenotype construction [53]. Mathematical and computational models constitute an indispensable tool to dynamically integrate data corresponding to these three areas, as well as for providing a mechanistic account of the relationship among different types of genetic and non-genetic factors during development and evolution. Modeling approaches as those that have been used to study the evolution of gene and molecular networks (e.g. [57,58]) can also shed light on the evolutionary processes giving rise to key features of regulatory networks involved in development. Additionally, integrative models will be necessary to perform comparative analyses of the dynamics of whole developmental modules [26].

Plant post-embryonary development underlies the generation of new tissues and structures throughout their whole lives. In contrast to animal development, plant cell fates and morphogenesis are constantly adjusted in response to organismal and environmental stimuli. This makes plants excellent models to study developmental plasticity – the phenotypic variability generated during development in close interaction with the environment – as well as the constraining (or driving) role of organism–environment interactions in the origin and evolution of phenotypes. In particular, epidermal patterning in Arabidopsis constitutes an ideal system to assess the effect of these interactions in the generation and modification of cellular patterns. Much as the research on other developmental systems, the study of epidermal patterning has focused mainly on uncovering the genetic factors involved in this process, and more recently on the regulatory interactions that give rise to GRNs. This has greatly contributed to our understanding of plant development and has set a solid basis on which theoretical and systemic studies have to be carried out in the future. But now it will be necessary to postulate mechanisms that couple such networks with

Please cite this article in press as: Benítez M, et al.: Dynamic models of epidermal patterning as an approach to plant eco-evo-devo, Curr Opin Plant Biol (2012), http://dx.doi.org/10.1016/j.pbi.2012.11.005

other aspects of development that also appear to play a central role in epidermal patterning.

Another key issue will be to address if the patterns of epidermal cells have been fixed by natural selection, or are byproducts of adaptive processes involving other traits. The latter could be possible given that the regulatory module involved in epidermal cell patterning is linked to other developmental modules, as stated above. However, it has been documented that some of the contrasting patterns of epidermal cell patterning are fixed within specific varieties or ecotypes [27], suggesting that adaptive diversification could have played a role in fixing such patterns in some cases. Moreover, the fact that trichomes increase herbivore resistance [59•] reveals links between this developmental system, plant ecology, and possibly plant evolution. Then, an interesting eco-evo-devo challenge is to address which specific molecular mechanisms are the target of positive selection. This goal first implies uncovering the molecular mechanisms involved in responding to specific environmental factors or selection forces.

Furthermore, in two plant species (*Mimulus guttatus* and *Raphanus raphanistrum*) it has been shown that modifications in the trichome patterning induced by leaf damage or herbivory can be inherited transgenerationally [60–62,63••]. These and other studies (e.g. [64•]) open new and exciting avenues in the use of this system to explore the role of the environment in the modification of developmental patterns that can be passed on to the following generations, and that could then be relevant in evolutionary terms. Work in this line could help evaluate and further develop theoretical frameworks in which developmental plasticity is key to phenotypic evolution, such as those of genetic accommodation [54] and genetic assimilation [65].

Conclusions

Being epidermal patterning in the leaf and root of Arabidopsis a plastic developmental process that integrates hormonal, environmental and cellular signals, and at the same time is amenable to molecular genetic and morphogenetic studies, it may constitute an excellent model to pursue joint experimental and modeling efforts to address open questions in eco-evo-devo, such as what are the genetic and non-genetic mechanisms behind the plasticity of cell fate determination and patterning during development. Data-based dynamical models will help to assess the relative contribution of complex genetic interactions and other non-genetic factors in the generation and phenotypic variability of epidermal patterning, will enable comparative analyses at the developmental-module level, and may inform current theoretical proposals regarding the role of non-genetic mechanisms in the evolution of phenotypes.

Acknowledgements

The authors would like to thank Carlos Espinosa-Soto for valuable comments and discussions. ERAB is supported by the Miller Institute for Basic Research in Science, University of California Berkeley, and by the projects CONACyT (81542, 81433, 167705, 152649, 180380, 180098), PAPIIT (IN229003-3, IN204011-3, 226510-3, IB201212-2), UC-MEXUS (CN.12-623, CN.12-571), and REDES TEMÁTICAS DE INVESTIGACIÓN CONACyT: Red Complejidad, Ciencia y Sociedad. We apologize to the authors whose work was not included in this review owing to lack of space.

References and recommended reading

Papers of particular interest, published within the period of review, have been highlighted as:

- • of special interest
- •• of outstanding interest

1. Lee MM, Schiefelbein J: **Developmentally distinct MYB genes encode functionally equivalent proteins in Arabidopsis**. *Development* 2001, **128**:1539-1546.

2. Schiefelbein J: **Cell-fate specification in the epidermis: a common patterning mechanism in the root and shoot**. *Curr Opin Plant Biol* 2003, **6**:74-78.

3. Benítez M, Monk NM, Alvarez-Buylla ER: **Epidermal patterning in Arabidopsis: models make a difference**. *J Exp Zool B Mol Dev Evol* 2011, **316**:241-253.

4. Grebe M: **The patterning of epidermal hairs in Arabidopsis-updated**. *Curr Opin Plant Biol* 2011, **15**:31-37.

5. Wang S, Kwak SH, Zeng Q, Ellis BE, Chen XY, Schiefelbein J, Chen JG: **TRICHOMELESS1 regulates trichome patterning by suppressing GLABRA1 in Arabidopsis**. *Development* 2007, **134**:3873-3882.

6. An L, Zhou Z, Yan A, Gan Y: **Progress on trichome development regulated by phytohormone signaling**. *Plant Signal Behav* 2011, **6**:1959-1962.

7. Kang YH, Kirik V, Hulskamp M, Nam KH, Hagely K, Lee MM, Schiefelbein J: **The MYB23 gene provides a positive feedback loop for cell fate specification in the Arabidopsis root epidermis**. *Plant Cell* 2009, **21**:1080-1094.

8. Tominaga-Wada R, Ukumizu YN, Ato SS, Ato TK, Abata ST, Ada TW: **Functional divergence of MYB-related genes, WEREWOLF and AtMYB23 in Arabidopsis**. *Biosci Biotechnol Biochem* 2012, **76**:883-887.

9. •• Bruex A, Kainkaryam RM, Wieckowski Y, Kang YH, Bernhardt C, Xia Y, Zheng X, Wang JY, Lee MM, Benfey P *et al.*: **A gene regulatory network for root epidermis cell differentiation in Arabidopsis**. *PLoS Genet* 2011, **8**:e1002446.
This work constitutes a comprehensive transcriptomic exploration that uncovers new genes involved in epidermal patterning and trichome differentiation in Arabidopsis, opening novel avenues in this field and providing possible links between this and other developmental systems.

10. Mendoza L, Alvarez-Buylla ER: **Genetic regulation of root hair development in *Arabidopsis thaliana*: a network model**. *J Theor Biol* 2000, **204**:311-326.

11. Benítez M, Espinosa-Soto C, Padilla-Longoria P, Díaz J, Alvarez-Buylla ER: **Equivalent genetic regulatory networks in different contexts recover contrasting spatial cell patterns that resemble those in Arabidopsis root and leaf epidermis: a dynamic model**. *Int J Dev Biol* 2007, **51**:139-155.

12. Benítez M, Espinosa-Soto C, Padilla-Longoria P, Alvarez-Buylla ER: **Interlinked nonlinear subnetworks underlie the formation of robust cellular patterns in Arabidopsis epidermis: a dynamic spatial model**. *BMC Syst Biol* 2008, **16**:1-16.

13. Savage NS, Walker T, Wieckowski Y, Schiefelbein J, Dolan L, Monk NAM: **Mutual support mechanism through intercellular movement of CAPRICE and GLABRA3 can pattern the Arabidopsis root epidermis**. *PLoS Biol* 2008, **6**:e235.

14. Digiuni S, Schellmann S, Geier F, Greese B, Pesch M, Wester K, Dartan B, Mach V, Srinivas BP, Timmer J *et al.*: **A competitive**

Please cite this article in press as: Benítez M, et al.: Dynamic models of epidermal patterning as an approach to plant eco-evo-devo, Curr Opin Plant Biol (2012), http://dx.doi.org/10.1016/j.pbi.2012.11.005

complex formation mechanism underlies trichome patterning on Arabidopsis leaves. *Mol Syst Biol* 2008, **4**:217.

15. Bouyer D, Geier F, Kragler F, Schnittger A, Pesch M, Wester K, Balkunde R, Timmer J, Fleck C, Hülskamp M: **Two-dimensional patterning by a trapping/depletion mechanism: the role of TTG1 and GL3 in Arabidopsis trichome formation**. *PLoS Biol* 2008, **6**:e141.

16. Turing AM: **The chemical basis of morphogenesis**. *Philos Trans R Soc Lond B Biol Sci* 1952, **237**:37-72.

17. Meinhardt H, Gierer A: **Pattern formation by local self-activation and lateral inhibition**. *Bioessays* 2000, **22**:753-760.

18. Balkunde R, Pesch M, Hulskamp M: **Trichome patterning in *Arabidopsis thaliana* from genetic to molecular models**. *Curr Top Dev Biol* 2010, **91**:299-321.

19. Benítez M, Alvarez-Buylla ER: **Dynamic-module redundancy confers robustness to the gene regulatory network involved in hair patterning of Arabidopsis epidermis**. *Biosystems* 2010, **4**:134.

20. Alvarez-Buylla ER, Benítez M, Espinosa-Soto C: **Mutually reinforcing patterning mechanisms**. *Nat Rev Mol Cell Biol* 2011, **316**:2011.

21. Kitano H: **Biological robustness**. *Nat Rev Genet* 2004, **5**:826-837.

22. Kwon YK, Cho KH: **Coherent coupling of feedback loops: a design principle of cell signaling networks**. *Bioinformatics* 2008, **24**:1926-1932.

23. • Savage NS, Schmidt W: **From priming to plasticity: the changing fate of rhizodermic cells**. *Bioessays* 2007, **30**:75-81.
This constitutes the first modeling effort to study the mechanisms behind the plasticity of root hair patterning in response to environmental stimuli, mainly nutrient depletion.

24. • Niklas KJ, Kutschera U: **Plant development, auxin, and the subsystem incompleteness theorem**. *Front Plant Sci* 2012, **3**:37.
This work provides a valuable conceptual framework to study developmental subsystems and emphasizes the need to adopt a whole-organism perspective in the study of plant morphogenesis.

25. Newman SA, Muller GB: **Epigenetic mechanisms of character origination**. *J Exp Zool Part B* 2000, **288**:304-317.

26. Hernández Hernández V, Niklas KJ, Newman SA, Benítez M: **Dynamic patterning modules in plant development and evolution**. *Int J Dev Biol* 2012, **56**:661-674.

27. Telfer A, Bollman KM, Poethig RS: **Phase change and the regulation of trichome distribution in *Arabidopsis thaliana***. *Development* 1997, **124**:645-654.

28. Tsukaya H, Shoda K, Kim GT, Uchimiya H: **Heteroblasty in *Arabidopsis thaliana* (L.) Heynh**. *Planta* 2000, **210**:536-542.

29. Chien JC, Sussex M: **Differential regulation of trichome formation on the adaxial and abaxial leaf surfaces by gibberellins and photoperiod in *Arabidopsis thaliana* (L.) Heynh**. *Plant Phys* 1995, **92**:1321-1328.

30. Perazza, Vachon, Herzog: **Gibberellins promote trichome formation by Up-regulating GLABROUS1 in Arabidopsis**. *Plant Physiol* 1998, **117**:375-383.

31. Traw MB, Bergelson J: **Interactive effects of jasmonic acid, salicylic acid, and gibberellin on induction of trichomes in Arabidopsis**. *Plant Physiol* 2003, **133**:1367-1375.

32. Perry P, Linke B, Schmidt W: **Reprogramming of root epidermal cells in response to nutrient deficiency**. *Biochem Soc Trans* 2007, **35**:161-163.

33. Yoshida Y, Sano R, Wada T, Takabayashi J, Okada K: **Jasmonic acid control of GLABRA3 links inducible defense and trichome patterning in Arabidopsis**. *Development* 2009, **136**:1039-1048.

34. Gan Y, Kumimoto R, Liu C, Ratcliffe O, Yu H, Broun P: **GLABROUS INFLORESCENCE STEMS modulates the regulation by gibberellins of epidermal differentiation and shoot maturation in Arabidopsis**. *Plant Cell* 2006, **18**:1383-1395.

35. Gan Y, Liu C, Yu H, Broun P: **Integration of cytokinin and gibberellin signalling by Arabidopsis transcription factors GIS, ZFP8 and GIS2 in the regulation of epidermal cell fate**. *Development* 2007, **134**:2073-2081.

36. Taiz L, Zeiger E: *Plant Physiology*. edn 5. Sinauer Associates, Inc.; 2010.

37. •• Qi T, Song S, Ren Q, Wu D, Huang H, Chen Y, Fan M, Peng W, Ren C, Xie D: **The Jasmonate-ZIM-domain proteins interact with the WD-Repeat/bHLH/MYB complexes to regulate Jasmonate-mediated anthocyanin accumulation and trichome initiation in *Arabidopsis thaliana***. *Plant Cell* 2011, **23**:1795-1814.
This work describes a clear molecular mechanism linking diverse environmental stimuli with hormonal signaling pathways and the gene network associated to leaf epidermal patterning.

38. Schmidt W, Tittel J, Schikora A: **Role of hormones in the induction of iron deficiency responses in Arabidopsis roots**. *Plant Phys* 2000, **122**:1109-1118.

39. • An L, Zhou Z, Sun L, Yan A, Xi W, Yu N, Cai W, Chen X, Yu H, Schiefelbein J, Gan Y: **A zinc finger protein gene ZFP5 integrates phytohormone signaling to control root hair development in Arabidopsis**. *Plant J* 2012, **72**:474-490.
This work reveals the role of a zinc-finger protein as a molecular link between hormonal signaling and trichoblast patterning, opening new avenues in the study of root hair plasticity in response to environmental stimuli.

40. Depuydt S, Hardtke CS: **Hormone signalling crosstalk in plant growth regulation**. *Curr Biol* 2011, **21**:R365-R373.

41. Wang Y, Li X: **Salt stress-induced cell reprogramming, cell fate switch and adaptive plasticity during root hair development in Arabidopsis**. *Plant Signal Behav* 2008, **3**:436-438.

42. Niu Y, Jin C, Jin G, Zhou Q, Lin X, Tang C, Zhang Y: **Auxin modulates the enhanced development of root hairs in *Arabidopsis thaliana* (L.) Heynh. under elevated CO(2)**. *Plant Cell Environ* 2011, **34**:1304-1317.

43. Xia Y, Yu K, Navarre D, Seebold K, Kachroo A, Kachroo P: **The glabra1 mutation affects cuticle formation and plant responses to microbes**. *Plant Phys* 2012, **154**:833-846.

44. Hulskamp MMS, Jurgens G: **Genetic dissection of trichome cell development in Arabidopsis**. *Cell* 1994, **76**:555-566.

45. Schnittger A, Weinl C, Bouyer D, Schöbinger U, Hülskamp M: **Misexpression of the cyclin-dependent kinase inhibitor ICK1/KRP1 in single-celled Arabidopsis trichomes reduces endoreduplication and cell size and induces cell death**. *Plant Cell* 2003, **15**:303-315.

46. Morohashi K, Grotewold E: **A systems approach reveals regulatory circuitry for Arabidopsis trichome initiation by the GL3 and GL1 selectors**. *PLoS Genet* 2009, **5**:e1000396.

47. Churchman ML, Brown ML, Kato N, Kirik V, Hülskamp M, Inzé D, De Veylder L, Walker JD, Zheng Z, Oppenheimer DG *et al.*: **SIAMESE, a plant-specific cell cycle regulator, controls endoreplication onset in *Arabidopsis thaliana***. *Plant Cell* 2006, **18**:3145-3157.

48. Kasili R, Huang CC, Walker JD, Simmons LA, Zhou J, Faulk C, Hülskamp M, Larkin JC: **BRANCHLESS TRICHOMES links cell shape and cell cycle control in Arabidopsis trichomes**. *Development* 2011, **138**:2379-2388.

49. Bramsiepe J, Wester K, Weinl C, Roodbarkelari F, Kasili R, Larkin JC, Hülskamp M, Schnittger A: **Endoreplication controls cell fate maintenance**. *PLoS Genet* 2010, **6**:e1000996.

50. •• Hassan H, Scheres B, Blilou I: **JACKDAW controls epidermal patterning in the Arabidopsis root meristem through a non-cell-autonomous mechanism**. *Development* 2010, **137**:1523-1529.
This paper reveals JACKDAW as a link between two well-characterized developmental modules, those of stem-cell specification in the root and epidermal patterning.

51. Gilbert SF: **The morphogenesis of evolutionary developmental biology**. *Int J Dev Biol* 2003, **47**:467-477.

52. Pigliucci M: **Do we need an extended evolutionary synthesis?** *Evolution* 2007, **61**:2743-2749.

Please cite this article in press as: Benítez M, et al.: Dynamic models of epidermal patterning as an approach to plant eco-evo-devo, Curr Opin Plant Biol (2012), http://dx.doi.org/10.1016/j.pbi.2012.11.005

53. Müller GB: **Evo-devo: extending the evolutionary synthesis**. *Nat Rev Genet* 2007, **8**:943-949.

54. West-Eberhard MJ: **Developmental plasticity and the origin of species differences**. *Proc Natl Acad Sci USA* 2005, **102**:6543-6549.

55. Jablonka E, Lamb MJ: **Précis of evolution in four dimensions**. *Behav Brain Sci* 2007, **30**:353-389.

56. Waddington CH: *The Strategy of the Genes. A Discussion of Some Aspects of Theoretical Biology*. New York, NY: MacMillan; 1957.

57. Siegal-Gaskins D, Grotewold E, Smith GD: **The capacity for multistability in small gene regulatory networks**. *BMC Syst Biol* 2009, **3**:96.

58. Espinosa-Soto C, Martin OC, Wagner A: **Phenotypic plasticity can facilitate adaptive evolution in gene regulatory circuits**. *BMC Evol Biol* 2011, **11**:5.

59. • Kivimäki M, Kärkkäinen K, Gaudeul M, Løe G, Agren J: **Gene, phenotype and function: GLABROUS1 and resistance to herbivory in natural populations of Arabidopsis lyrata**. *Mol Ecol* 2007, **16**:453-462.
This paper shows that the density of trichomes is correlated with reduced damage from insect herbivores in natural populations of *Arabidopsis lyrata*, and identify *GLABRA1* as a relevant gene in the generation of natural variation of this trait.

60. Holeski LM: **Within and between generation phenotypic plasticity in trichome density of *Mimulus guttatus***. *J Evol Biol* 2007, **20**:2092-2100.

61. Holeski LM, Jander G, Agrawal A: **Transgenerational defense induction and epigenetic inheritance in plants**. *Trends Ecol Evol* 2012, **27**:1-9.

62. Herman JJ, Sultan SE: **Adaptive transgenerational plasticity in plants: case studies, mechanisms, and implications for natural populations**. *Front Plant Sci* 2011, **2**:1-10.

63. •• Scoville AG, Barnett LL, Bodbyl-Roels S, Kelly JK, Lena C: **Differential regulation of a MYB transcription factor is correlated with transgenerational epigenetic inheritance of trichome density in *Mimulus guttatus***. *New Phytol* 2012, **191**:251-263.
The authors identify a MYB gene as a possible negative regulator of trichome development and find that parental leaf damage induces its downregulation progeny, linking epigenetic transmission of an ecologically important trait with differential gene expression states in a plant of the Phrymaceae family.

64. • Latzel V, Zhang Y, Karlsson Moritz K, Fischer M, Bossdorf O: **Epigenetic variation in plant responses to defence hormones**. *Ann Bot* 2012, **110**:1-6.
This study suggests that epigenetic variation can cause heritable variation in the responses to defence hormones, and that some of the variation of plant defences observed in natural populations may be due to underlying epigenetic variation.

65. Waddington CH: **Canalization of development and the inheritance of acquired characters**. *Nature* 1942, **150**:563-565.

66. Pitts RJ, Cernac A, Estelle M: **Auxin and ethylene promote root hair elongation in Arabidopsis**. *Plant J* 1998, **16**:553-560.

Please cite this article in press as: Benítez M, et al.: Dynamic models of epidermal patterning as an approach to plant eco-evo-devo, Curr Opin Plant Biol (2012), http://dx.doi.org/10.1016/j.pbi.2012.11.005

8.5. Parte V:

Artículo:

Cell Patterns Emerge from Coupled Chemical and Physical Fields with Cell Proliferation Dynamics: The Arabidopsis thaliana Root as a Study System

Rafael A. Barrio, José Roberto Romero-Arias, Marco A. Noguez, Eugenio Azpeitia, Elizabeth Ortiz-Gutiérrez, Valeria Hernández-Hernández, Yuriria Cortes-Poza, Elena R. Álvarez-Buylla

PLOS Computation Biology

OPEN ACCESS Freely available online

PLOS | COMPUTATIONAL BIOLOGY

Cell Patterns Emerge from Coupled Chemical and Physical Fields with Cell Proliferation Dynamics: The *Arabidopsis thaliana* Root as a Study System

Rafael A. Barrio[1]*, José Roberto Romero-Arias[1], Marco A. Noguez[2], Eugenio Azpeitia[3,4], Elizabeth Ortiz-Gutiérrez[3,4], Valeria Hernández-Hernández[3,4], Yuriria Cortes-Poza[4], Elena R. Álvarez-Buylla[3,4]*

1 Instituto de Física, Universidad Nacional Autónoma de México (UNAM), México, Distrito Federal, México, **2** Universidad Autónoma de la Ciudad de México, Mexico, Distrito Federal, México, **3** Instituto de Ecología, Universidad Nacional Autónoma de México, México, Distrito Federal, México, **4** Centro de Ciencias de la Complejidad-C3, Universidad Nacional Autónoma de México, Distrito Federal, México

Abstract

A central issue in developmental biology is to uncover the mechanisms by which stem cells maintain their capacity to regenerate, yet at the same time produce daughter cells that differentiate and attain their ultimate fate as a functional part of a tissue or an organ. In this paper we propose that, during development, cells within growing organs obtain positional information from a macroscopic physical field that is produced in space while cells are proliferating. This dynamical interaction triggers and responds to chemical and genetic processes that are specific to each biological system. We chose the root apical meristem of *Arabidopsis thaliana* to develop our dynamical model because this system is well studied at the molecular, genetic and cellular levels and has the key traits of multicellular stem-cell niches. We built a dynamical model that couples fundamental molecular mechanisms of the cell cycle to a tension physical field and to auxin dynamics, both of which are known to play a role in root development. We perform extensive numerical calculations that allow for quantitative comparison with experimental measurements that consider the cellular patterns at the root tip. Our model recovers, as an emergent pattern, the transition from proliferative to transition and elongation domains, characteristic of stem-cell niches in multicellular organisms. In addition, we successfully predict altered cellular patterns that are expected under various applied auxin treatments or modified physical growth conditions. Our modeling platform may be extended to explicitly consider gene regulatory networks or to treat other developmental systems.

Citation: Barrio RA, Romero-Arias JR, Noguez MA, Azpeitia E, Ortiz-Gutiérrez E, et al. (2013) Cell Patterns Emerge from Coupled Chemical and Physical Fields with Cell Proliferation Dynamics: The *Arabidopsis thaliana* Root as a Study System. PLoS Comput Biol 9(5): e1003026. doi:10.1371/journal.pcbi.1003026

Editor: Anand R. Asthagiri, Northeastern University, United States of America

Received August 2, 2012; **Accepted** February 25, 2013; **Published** May 2, 2013

Funding: JRRA, EA and EOG were supported by scholarships from CONACYT and Universidad Nacional Autonoma de Mexico Graduate Programmes. ERAB was funded by CONACYT 81542, 180380, 180098 and PAPIIT IN229009-3 grants, and by the Miller Institute for Basic Research in Science, University of California, Berkeley (UCB). RAB acknowledges financial support from CONACYT through project No. 179616. The funders had no role in study design, data collection and analysis, decision to publish, or preparation of the manuscript.

Competing Interests: The authors have declared that no competing interests exist.

* E-mail: barrio.rafael@gmail.com (RAB); eabuylla@gmail.com (ERAB)

Introduction

The study of stem-cell niche patterns, and specifically how stem cells can maintain their totipotent state while simultaneously giving rise to daughter cells that obtain distinct fates to form differentiated tissues and organs, is fundamental to understanding the development of multicellular organisms [1]. Although plants and animals have key differences in their development (e.g. lack of cell migration in plant development), the cellular organization of stem-cell niches in both lineages reveals striking similarities [1,2]. In both plants and animals, stem-cell niches are formed by an organizer group of cells with low rates of division, surrounded by stem cells with slightly higher division rates. Moving distally from the organizer and stem cells, cells proliferate at high rates. This proliferation domain (also called amplification domain) is bordered by the elongation and then the differentiation domains where proliferation stops and expansion and differentiation, respectively, take place [1,3].

Gene interactions within intracellular complex regulatory networks (GRN) [4,5] or from morphogen dynamics at supracellular scales (see [6,7]) are fundamental for proper growth and development. Indeed organ and tissue development, as well as stem cell maintenance relies to a great extent on complex transcriptional regulatory networks and chemical fields. However, these are not the only components of pattern formation. It is now recognized that physical fields are also critical to explain developmental patterns, as they may provide positional information that modifies cell behavior and differentiation (see [6,7]). At the cellular level, the simplest physical constraint is space. Cell expansion is driven by turgidity, which is an important force acting on the cell wall [8]. The cell wall is a network of rigid cellulose microfibrils cross-linked by polysaccharides and proteins, that confer stiffness to the wall and allows it to resist turgidity [9]. Expansion of the cell is opposed by the rigidity of the cell wall, producing a real stress field. Recent evidence shows that these kind of mechanical cues are transmitted to the nucleus and, directly or indirectly, regulate transcription factors (see for instance [10] and references therein).

Given the complexity of the processes involved in the coupling of developmental restrictions, mathematical and computational tools have become indispensable in our efforts to understand the network of interactions involved in cellular differentiation and

Author Summary

The emergence of tumors results from altered cell differentiation and proliferation during organ and tissue development. Understanding how such altered or normal patterns are established is still a challenge. Molecular genetic approaches to understanding pattern formation have searched for key central genetic controllers. However, biological patterns emerge as a consequence of coupled complex genetic and non-genetic sub-systems operating at various spatial and temporal scales and levels of organization. We present a two-dimensional model and simulation benchmark that considers the integrated dynamics of physical and chemical fields that result from cell proliferation. We aim at understanding how the cellular patterns of stem-cell niches emerge. In these, organizer cells with very low rates of proliferation are surrounded by stem cells with slightly higher proliferation rates that transit to a domain of active proliferation and then of elongation and differentiation. We quantified such cellular patterns in the *Arabidopsis thaliana* root to test our theoretical propositions. The results of our simulations closely mimic observed root cellular patterns, thus providing a proof of principle that coupled physical fields and chemical processes under active cell proliferation give rise to stem-cell patterns. Our framework may be extended to other developmental systems and to consider gene regulatory networks.

organ development. Previously [11] we demonstrated that a simplified version of the originally proposed GRN [12,13] involved in floral development, could be coupled with a mesoscopic physical field. This provides positional information to cells in the floral meristem which is required to produce the overall spatial pattern of cells observed during early flower development. This and other similar studies [14] suggest that robust morphogenetic patterns in multicellular organisms emerge from complex interconnected dynamical processes, acting at different levels of organization and spatio-temporal scales. However, models that include such dynamical processes into the dynamics of pattern formation in multicellular organs are in their infancy [15,16]. Here we use the *Arabidopsis thaliana* (*A. thaliana*) root apical meristem as a study system to propose a model that couples cell proliferation and growth with chemical-physical dynamical processes to predict the emergence of patterns in a multicellular and multi-scale system.

The *A. thaliana* root has become an important experimental model for understanding the molecular, cellular and biophysical basis of morphogenesis in complex organs. This is due to its relatively simple cellular structure and its indeterminate growth, which gives rise to a multicellular structure with distinct cell proliferation and elongation domains. Importantly, the root apical meristem exhibits the typical cellular organization of stem cells described above (see Fig. 1). At the tip of roots stem cells are located surrounding the quiescent centre cells or the organizer cells (green cells in Fig. 1); together, they constitute the stem-cell niche (SCN) of the Arabidopsis root. Towards the base of the plant, the stem cells transit to a cell proliferation domain (CPD) where cells have high rates of cell division (also called proximal meristem by some authors, for example: [17]), then they enter a transition domain (TD), where cells have low or no probability of dividing, but they have not started to elongate [18]. The SCN, the CPD and the TD comprise the root apical meristem (RAM). More distally from the organizer center, cells cease to proliferate and start to grow in the elongation domain (EZ). Upon expanding to their maximum length, cells attain their final fate in the differentiation domain and produce the different tissues of the root.

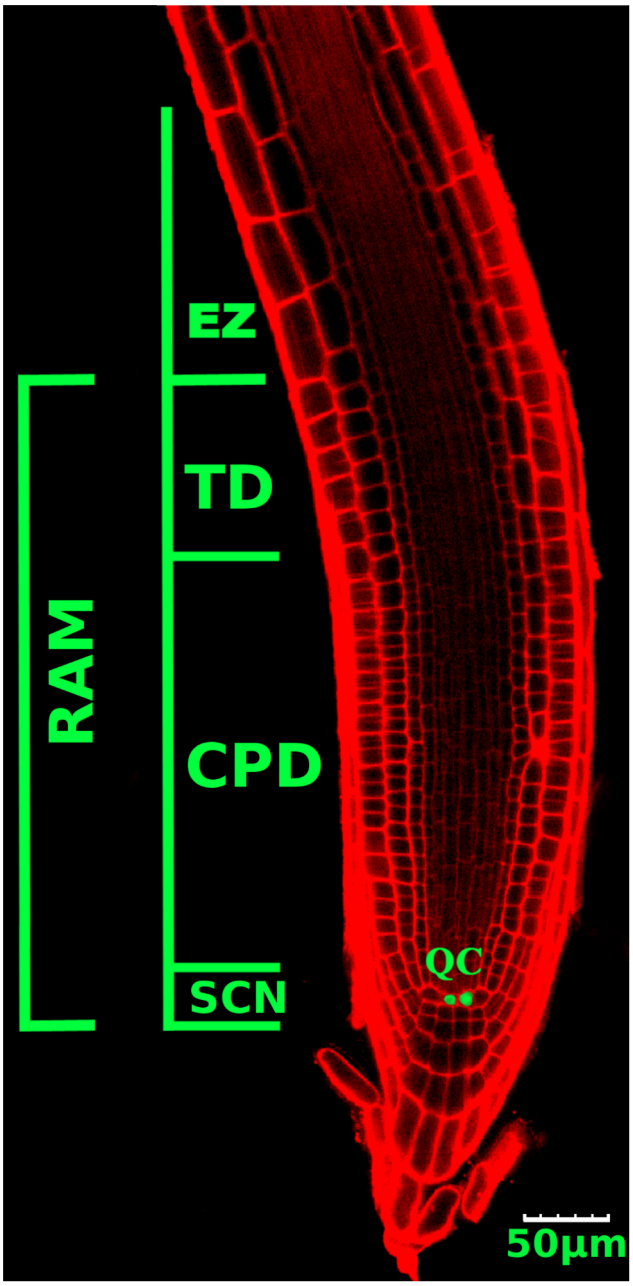

Figure 1. Confocal microscopy image of the *A. thaliana* root tip. The stem-cell niche (SCN) with the quiescent cells (QC, in green) and surrounding stem cells, the cell proliferation domain (CPD) with actively proliferating cells, the transition domain (TD) and the elongation zone (EZ), where cells do not proliferate, are indicated. The SCN, CPD and TD comprise the RAM.
doi:10.1371/journal.pcbi.1003026.g001

Key experimental data on cell cycle regulation and auxin behavior in the root are used to develop our model. Patterns of cell proliferation along the root longitudinal (apical-basal) axis are greatly affected by the dynamics of the cell cycle itself and by the concentration of several plant hormones, including auxin [19–23]. Cells in the root proliferation domain of the RAM undergo several

rounds of division before starting to elongate in the elongation domain. A complex network of regulatory interactions controls the cell cycle, in which cyclin proteins are key regulators. As their name suggests, the expression of cyclins oscillates during each cell cycle. At the beginning of each cell cycle, D-type cyclins (CYCD) induce the expression of the RETINOBLASTOMA-RELATED (RBR) gene through E2F-RBR pathway. RBR is a negative regulator of E2F transcription factors, which activate the transcription of mitotic cyclin CYCB. Later, CYCB cyclins are degraded by the Anaphase-promoting complex/cyclosome, thus completing the cycle and returning to the beginning of the cell cycle (see reviews in: [24,25]). For the present study, the oscillatory and time differential expressions of CYCD and CYCB are sufficient to represent the cell cycle dynamics. The cell cycle phases and main regulators are illustrated in Fig. 2.

Auxin is a phytohormone involved in almost every aspect of plant development (see [26–32]). Auxin is a key regulator of cell proliferation and cell elongation, and also modulates cell cycle progression and cyclins [33–35]. Auxin has been shown to upregulate mitotic cyclin (CYCA and CYCB) expression, and the over-expression of CYCA can partially recover the phenotype caused by low auxin levels, thus suggesting that auxin promotes cell cycle progression [35]. It is also well-documented that auxin gradients correlate with apical-basal patterns of cell proliferation and elongation along the root (see [35–41]). There is an auxin concentration gradient along the longitudinal axis of the root, with the maximum concentration detected at the stem-cell niche, specifically in the quiescent center [41,42]. While other hormones are important in root growth and development, we exclusively consider auxin due to its clear role in regulating cell cycle dynamics and its measurable concentration gradient that correlates with root developmental patterning [26].

Theoretical and experimental studies suggest that such auxin gradients depend critically on the polar localization of the auxin efflux transporter proteins, belonging to the *PINFORMED* gene family (*PIN*) (see [43–47]). Five *PIN* members are expressed throughout the root, namely *PIN1*, *2*, *3*, *4* and *7*. The proteins PIN1, 3, 4, and 7 maintain a continuous auxin flow from the base to the apex along the central tissues of the root. At the most apical zone, below the QC, auxin is laterally redistributed to the peripheral tissues by PIN3, 4, and 7. Finally, PIN2 directs flow from the root apex to the base in addition to lateral auxin flow in peripheral tissues. In conjunction, all PIN proteins create a reverse fountain mechanism that maintains an auxin gradient along the root [43,46,48].

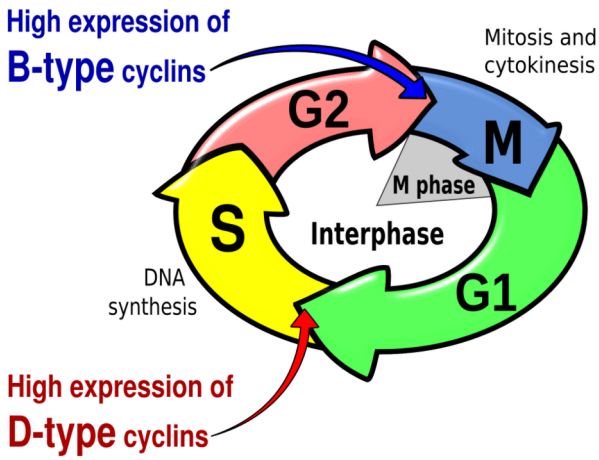

Figure 2. Simplified scheme of the cell cycle. The four main phases and the expression of two key cyclins are indicated.
doi:10.1371/journal.pcbi.1003026.g002

Physical signals have been shown to affect auxin distribution, for instance auxin gradients can be modified by mechanically-induced root bending [49,50], or by changes in gravitational fields [51,52]. Polar auxin transport and microtubule orientation also respond to mechanical forces in the shoot apical meristem [53,54]. Such evidence suggests that auxin transport is affected by and tightly coupled to physical forces. Furthermore, there is increasing evidence that mechanical stress is extremely important for plant morphogenesis; for instance, experiments show that differentiation of mesenchymal cells is influenced by the rigidity of the intracellular matrix [55].

In this paper we propose a simple model to study the interaction between cell proliferation dynamics, local auxin concentration (that in turn depends on the polar localization of PIN transporters in the cell membranes), and an elastic physical field arising from the inherent growth dynamics of the root. Our model provides a formal tool that can be used to understand and predict the emergence of the cellular patterns in the root tip. This type of model can be extended to explore similarities in stem-cell niche organization and subsequent cellular behaviors (proliferation, elongation and differentiation) of plants and animals, and to predict if such cellular organization might be explained by the coupling of generic non-linear physical and chemical fields relevant to cell proliferation dynamics. Our model is validated with experimental measurements on cell size and proliferation patterns along *A. thaliana* root, and sets the stage for developing similar approaches in other systems.

Model

Roots are three-dimensional structures. However, the root tip presents a consistent cylindrical symmetry that allows one to ignore changes in the transverse plane of the root when considering growth models. It is therefore possible to use a two-dimensional domain consisting of undifferentiated cells to represent the shape of the root tip. This approximation allows for numerical analysis of the model in 2D space. The model can be validated by comparing the patterns obtained with those observed experimentally in longitudinal histological or optical sections as the ones readily used in experimental assays done with *A. thaliana* roots. In some cases we have also compared our results obtained from 3D roots.

Based on the shape and spatial arrangement of the root, we conclude that cell reproduction in the early stages of root development involves mainly three chained dynamics of cell proliferation and resulting elastic field, and of the pattern of auxin concentration, whose co-occurrence provides the spatial information necessary to regulate the proliferation rate of each cell and to ultimately determine its future fate during differentiation (see Fig. 3 for a schematic summary of the processes to be modeled and the region of the root in which they take place).

Our first hypothesis is that a macroscopic physical field along the root tip results from cell growth and proliferation within this tissue in addition to constrained conditions imposed by the root cap and the epidermal cells surrounding the root. We propose that this field is elastic in nature and can be characterized by point functions of stress, pressure, or local mechanical forces that stem from the symplastic nature of plant tissues that are formed by interconnected cells surrounded by cellulose cell walls. Perfect equilibrium represents a state in which there are no mechanical forces acting anywhere in the system. In practice, this equilibrium

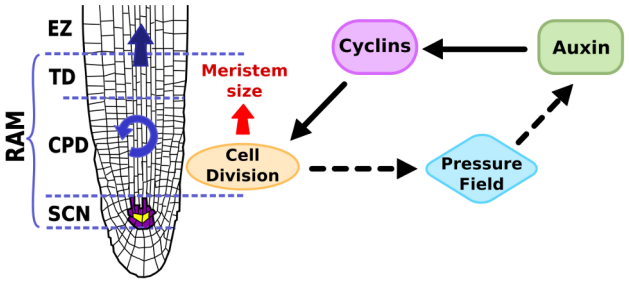

Figure 3. Histological drawing of the *A. thaliana* root tip. Here we show the SCN and the same domains as shown in Fig. 1 are indicated along the root apical-basal axis, as well as an schematic representation of the processes that are included in the cellular model and their interactions.
doi:10.1371/journal.pcbi.1003026.g003

cannot be completely achieved because of the geometric hindrances that impede the macroscopic system to reach a global minimum in the energy landscape, trapping it in a local minimum. In this situation there are remnant forces, and consequently the field is not uniform. Our model considers this lack of uniformity as a source of spatial information.

Our second hypothesis is that the synthesis, degradation and transportation of auxin respond to the local elastic field in a direct way, producing a dynamic pattern of auxin concentration along the longitudinal axis of the root tip. This is important, since the dynamical behavior of the formation of an auxin gradient should be very different from the relaxation dynamics of the elastic field, and it should occur at a different spatio-temporal scale.

Our third hypothesis proposes a direct relationship between auxin concentration and cell cycle regulation that determines cell proliferation rate. In the locations where cells divide and expand, the elastic field is greatly modified and, in fact, it is reinforced locally. This, in turn, affects the cell proliferation dynamics.

In short, we propose that the interaction among three different coupled dynamics (the relaxation of the physical field, the transport and concentration gradient of auxins and the oscillations of the cell cycle regulators, i.e., the cyclins) capture the key aspects underlying the overall emergent patterns of cell proliferation/elongation, as well as the macroscopic appearance and overall shape of the root. Our model includes the three dynamical processes (cell proliferation, auxin spatio-temporal concentration patterns and the elastic field) and their couplings in a two-dimensional domain that represents a longitudinal section of the root.

Cell dynamics and physical fields

We start by modeling the space occupied by a cell. Expansion of the cell volume, whether by turgidity or growth, is opposed by the rigidity of the cell wall producing a real stress field [9,56]. This field is also present at the larger scale of a group of cells, such as within the root apical meristem, since the increase in volume required by cell growth and division is opposed by the surface forces exerted by the root cap and epidermal cells surrounding it [57]. From this perspective, it is logical to assume that this stress field is self-regulated, that is, the accumulation of local stress (or pressure) triggers mechanisms that prevent (or enhance) cell division and growth. This assumption of self-regulation has been incorporated into previous models of cellular interactions: Dupuy and collaborators [58] used a rigidity matrix to model the relationship between cell displacement and implied forces. A form of potential energy has likewise been proposed as a way of describing the equilibrium between turgor and cell wall resistance [59]. Finally, in a recent paper investigating the floral meristem of *A. thaliana*, potential energy was proposed as the means of regulating auxin transport [15].

In our model for the root apex, we define a spatial domain in which a potential function acts. The spatial derivatives of this function render the mechanical force as a function of time and space. Taking advantage of the radial symmetry of the region of the root tip, we consider a two-dimensional space and divide it into cells. We simulate cells by a Voronoi diagram obtained from a collection of generating points that represent the position assigned to each cell.

Voronoi diagrams

A Voronoi diagram, or tessellation, associated with a collection of points assigns to each point a limited region of space in the form of a convex polygon (polyhedron in three dimensions). Voronoi cells are used nowadays in many fields of science, however it was Honda [60] who first proposed the use of 2D Voronoi to model cells in a biological context.

Our domain is defined as follows: 1) We construct a regular shape with points on a rectangle and a parabolic tip. The exterior points are fixed and represent the epidermal cells surrounding the ground tissue of the root (See Videos S1 and S2). 2) These points in the border cannot define a convex polygon, so the corresponding cells have a point at infinity. 3) We create N points with random coordinates in the interior of this domain and perform a Voronoi tessellation using a Delaunay triangulation algorithm.

A typical configuration is shown in Fig. 4. Observe that the areas of the cells (A_i) vary in size and shape, and that the generating points shown in the figure ($\vec{r}_i$) do not correspond, in general, to the centre of mass of the cells ($\vec{r}_{0_i}$).

The average $\bar{A}_0 = \sum_{i=1}^{N} A_i/N$ is the space that each cell would occupy in a regular hexagonal lattice. Analogously, the distance is $d_i = |\vec{r}_i - \vec{r}_{0_i}| = 0 \forall i$ in the regular array. In two dimensions the array of cells with minimal surface energy is the hexagonal lattice, and we use this fact to define a potential function around this equilibrium configuration.

Elastic fields

Previous studies have used springs to simulate the interactions among cells [61], and the elements of the cellular walls [62,63]. In our case the equilibrium area $\bar{A}_0$ could be used to fix the size of mature cells, so deviations from this value would represent immature cells. If the cells in the tissue tend to be isotropic in shape, then a value of d_i different from zero would represent cells with the wrong shape and, consequently, largely stressed.

Regardless of the actual functional form of the energy potential, it is possible to make a Taylor expansion around the equilibrium state retaining only the first non-zero terms, provided one considers small deviations from equilibrium. The first non-trivial contributions correspond to a quadratic form, whose coefficients can be interpreted as force constants.

Therefore, we propose a harmonic potential acting on each cell i

$$V(x_i,y_i,t) = \frac{K_v}{2}(A_i(t) - \bar{A}_0(t))^2 + \frac{K_c}{2}(\vec{r}_i(t) - \vec{r}_{0_i}(t))^2 \qquad (1)$$

where the first term tends to uniformize the size, and the second term is related with the shape of the cells. K_v and K_c are elastic constants.

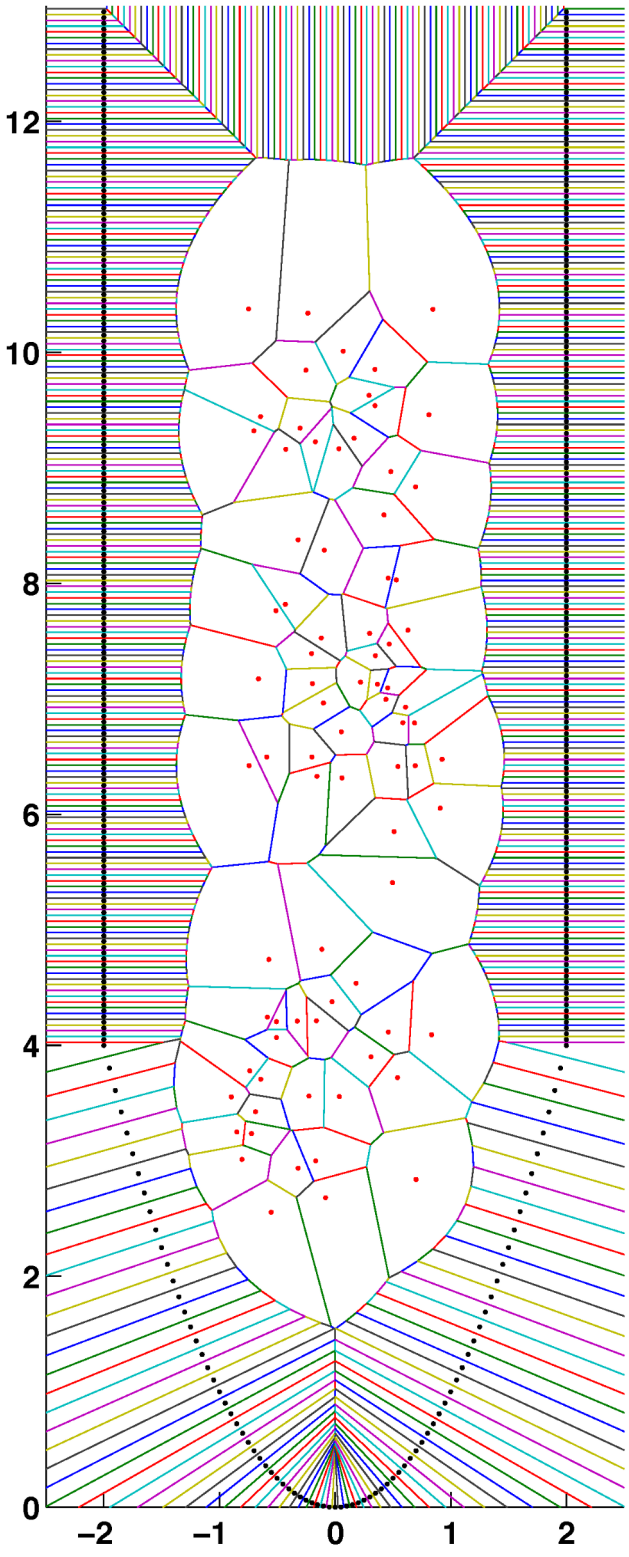

Figure 4. Typical initial configuration of cells after the Voronoi tessellation of random generating points.
doi:10.1371/journal.pcbi.1003026.g004

The expressions for the components of the force are:

$$\begin{aligned} F_x(x_i,t) &= -\frac{K_v}{2}\left[\frac{1}{2}\sum_{m=1}^{M}\frac{(x_i-x_m)\cdot l_{i,m}}{|\vec{r}_i-\vec{r}_m|}\{A_i-\tilde{A}_0\}\right] \\ &\quad -K_c(x_i-x_{0_i}) \\ F_y(y_i,t) &= -\frac{K_v}{2}\left[\frac{1}{2}\sum_{m=1}^{M}\frac{(y_i-y_m)\cdot l_{i,m}}{|\vec{r}_i-\vec{r}_m|}\{A_i-\tilde{A}_0\}\right] \\ &\quad -K_c(y_i-y_{0_i}) \end{aligned} \tag{2}$$

where $l_{i,m}$ is the length of the edge shared between neighboring cells, and we have omitted the time dependence of the variables on the right hand side. All quantities in Eqs. 1 and 2 can be readily calculated with the algorithm used to define the Voronoi diagram.

Since this is a conservative system, and there is no reason to assume conservation in the root system, we include dissipation in the form of friction that simulates losses due to the inability of cells to make drastic elastic changes of shape or size. Therefore, the total force should be:

$$\vec{F}_T(x_i,y_i,t) = -\nabla V(x_i,y_i,t) - k\vec{v}(x_i,y_i,t) \tag{3}$$

where $\vec{v}$ is the velocity and k is a friction coefficient. The N coupled dynamical equations of this newtonian system

$$\begin{aligned} \frac{\partial \vec{v}}{\partial t} &= \vec{F}_T \\ \frac{\partial \vec{r}}{\partial t} &= \vec{v} \end{aligned} \tag{4}$$

can be integrated numerically by using a simple Euler method, imposing fixed boundary conditions on the fixed surface points.

As an example of the relaxation process with this scheme, in Fig. 5 we show the configuration of points in Fig. 4 after 2000 time iterations. The numerical calculation was stopped when the relative changes of the positions and velocities was less than 10^{-10}. The magnitude of the constants K_c, K_v and k sets the units of the time variations of the dynamical behavior of the system, and should be adjusted to physical units when modeling the growth of the RAM. One should consider the number of cell divisions per unit time (2.6 events/hr), the cell production rate (between 0 and 6 $\text{cells}\times\text{mm}^{-1}\text{hr}^{-1}$) and the cell proliferation rate distribution (between 0 and 50 $\mu\text{m/hr}$) in the RAM [64]. The final form of the relaxed field suggests that it could be used to transfer positional information to the cells in the meristem. In order to achieve the latter, the auxin concentration must be coupled to the local value of the potential.

We introduced the process of cell division and proliferation into the simulation by defining two points inside a cell when it undergoes mitosis. The resulting Voronoi cells then locally alter the field, and the extra space needed for the two daughter cells is obtained by moving the upper border of the domain a proper distance to provide the exact extra space required. We show details of this process below.

Auxin transport

It is assumed that the field V is involved in the processes of auxin transport. In any transport equation there are basically two aspects to be considered: the hydrodynamic forces compelling a fluid to move, and the diffusion phenomena. Both are important for the case of auxins. Furthermore, the process of auxin transport

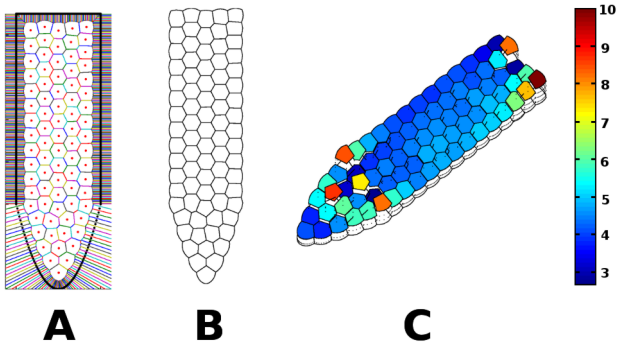

Figure 5. Configuration of cells after 2000 time iterations. (A) The points in Fig. 4 once they have attained equilibrium using the potential (See Video S3). (B) Final configuration of the cells in the RAM. Observe the regularity of the shapes and sizes of the cells. (C) 2D profile of the field after relaxation. Observe that it is not constant, but there are three well defined sections (See Video S4).
doi:10.1371/journal.pcbi.1003026.g005

is recognized to be active, meaning that the transfer of matter through the cell membranes could go against the concentration gradient of auxin molecules due to the action of PIN proteins. We propose that the amount of matter Q transported per unit time from cell i to a neighbor cell m is proportional to the gradient of the field V:

$$Q_{i,m} = -P_{i,m} \cdot A_{i,m} \cdot |V_i - V_m|, \tag{5}$$

where $P_{i,m}$ represents the permeability of the membrane and $A_{i,m}$ is the contact surface between the cells i and m (the line $l_{i,m}$ in 2D).

Observe that if the values of the $P_{i,m}$'s were constant, this equation would reduce to the well known Darcy's Law in hydraulics, which is analogous to Fourier's law in heat conduction, or Ohm's law in electrical networks. However this is not the case, because of the action of the PIN proteins which are critical. Therefore, the permeability is:

$$P_{i,m} = \alpha(c_i - c_m)\mathcal{F}_{i,m}, \tag{6}$$

where α is a constant related with the time scale of the dynamics, and the direction of the flux with respect to the concentration gradient $(c_i - c_m)$ (diffusion term) is given by the logical function $\mathcal{F}_{i,m}$. This latter function mimics the action of the PIN molecules, which attach to the membrane according to orientation and position in the domain.

We can simplify this action by considering "gates", which could be opened (1) or closed (0) according to specified simple rules. Let $\mathcal{S}$ be the set of cells at the surface, i.e. in contact with the immobile epidermal cells. We have set the following rules: All gates are closed, except

1. when $i,m \in \mathcal{S}$ and i is above m,
2. or if $i,m \notin \mathcal{S}$ and i is below m,
3. or if $i \notin \mathcal{S}$ and $m \in \mathcal{S}$ and i is above m.

The dynamical equation for the concentration of auxins in cell i is then:

$$\frac{1}{\alpha}\frac{\partial c_i}{\partial t} = \sum_{m=1}^{M} l_{im}(c_i - c_m)|V_i - V_m|, \tag{7}$$

where the sum is over all neighboring cells. This expression can be readily integrated numerically in parallel with Eq. 4, once the parameter α has been properly adjusted.

In Fig. 6 we show the effect of the logical rules on the formation of auxin gradients. On the left we show a calculation without these rules, that is, maintaining all the membranes permeable. In (B) we incorporate the PIN action into the model. Observe that the distribution of the concentration of auxins (normalized with its maximum value) is similar to the one observed in real roots [42].

Cell division cycle

We shall assume that the period of the cell division cycle is regulated by the local concentration of auxins c_i. We are aware that this is an oversimplification of the complex hormonal regulation of the cell cycle in plants, but auxin has been shown to be an important component of such regulation [65]. We therefore need a model for the oscillations of cyclin concentrations. The robustness of these oscillations suggests that a non-linear oscillator would be a good model. We consider a two-component system for simplicity, considering CYCD and CYCB as the two key players. Since both undergo regular out-of phase oscillations with maxima related to the transitions between the G1-S and G2-M phases, respectively (See Fig. 2), we choose a simple Lotka-Volterra non-linear system with two components, generally used in ecology to model the predator-prey dynamics. This system presents all characteristics required for the observed time behavior of the concentration of cyclins [66]. The adimensional activator-inhibitor dynamical equations are:

$$\begin{aligned} \frac{\partial u}{\partial \tau} &= u(1-v) \\ \frac{\partial v}{\partial \tau} &= \beta v(u-1), \end{aligned} \tag{8}$$

where u and v represent CYCD and CYCB, respectively. This system presents an oscillatory behavior, provided β is within a certain range, whose period (T) and wave shape depend only on β and on the boundary conditions. It is easily shown that the period is:

$$T = \frac{2\pi}{\sqrt{\beta}}, \tag{9}$$

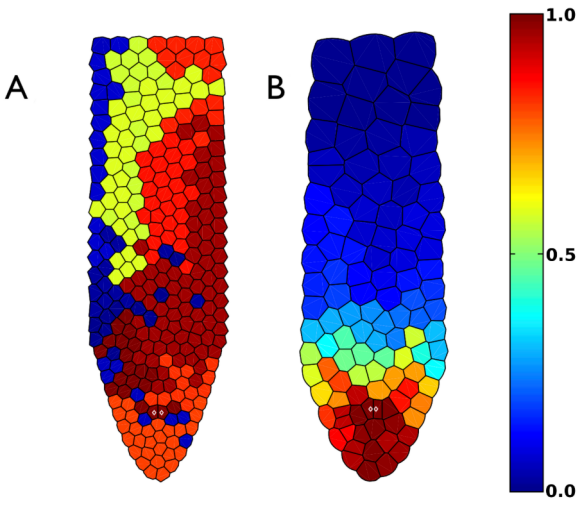

Figure 6. Typical numerical integration of Eq. 7 showing the formation of auxin gradients. (A) All gates are open (no PIN action). (B) Including the logical rules to open the gates to model the PIN action.
doi:10.1371/journal.pcbi.1003026.g006

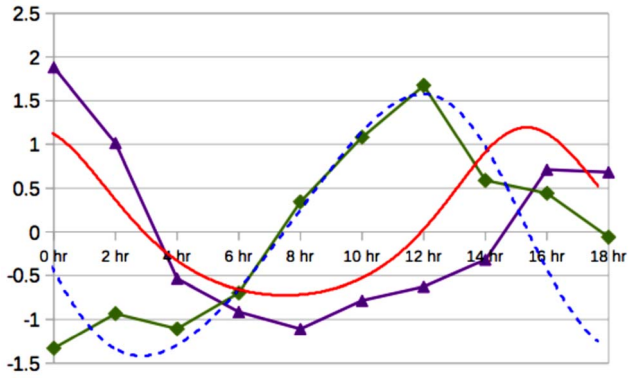

Figure 7. Variation of two-type cyclins concentrations and typical oscillations from the Lotka-Volterra model. Relative expression data of D-type cyclins (purple triangles) and B-type cyclins (green rhombuses) were taken from analysis of gene expression profiles using aphidicolin synchronization on Ref. [76], and are available on GENEVESTIGATOR web page. The oscillations from the Lotka-Volterra model of the inhibitor (blue dashed line) and the activator (red line) are also shown.
doi:10.1371/journal.pcbi.1003026.g007

which is inversely proportional to the square root of the ratio of the linear growth rate of the "prey" (u) to the death rate of the "predator" (v). In Fig. 7 we illustrate the oscillations of both variables.

Experimental data has shown that the cell cycle is arrested if the auxin concentration is below or above certain threshold values, and that the cycle period increases with auxin concentration [65]. Therefore, we simply assume that the auxin concentration is linearly related to the only parameter of this dynamical system: $\beta=\gamma c(i)$. Hence, each cell has its individual clock, which runs faster or slower depending on the auxin concentration in the model under consideration. We couple this dynamical feature into the numerical calculation of the model by performing a division of cell i when $t=\delta(n\Delta t-T_i[\tau])$ (where the $\delta-$function is one when the number of iterations $n\Delta t$, used in the Euler integration, surpasses the period). Therefore, γ is another constant that relates the time scale of reproduction (τ) to the time step used for relaxation dynamics. Parameters α and γ should be fitted according to the observed time scales for each of the three dynamics. Time step Δt (in seconds) should be obtained as well.

In practice, the act of cellular division is performed in the following manner:

1. At each time step, advance the internal clock of all cells according to the value of the local auxin concentration given by the cell life-cycle model.
2. Detect the cells in which the internal clock completes one period (a single division event occurs every cycle), and set the clock of these cells to zero.
3. In each one of these cells, $\vec{r}_i$ is substituted by two points, oriented at random and at equal distances of $\vec{r}_i$. This distance is typically of the order of a quarter of the radius of the cell.
4. The kinetic energy ($v_i^2/2$) of the mother cell is equally divided between mother and daughter cells.
5. The upper boundary of the domain is shifted upwards to increase the area by the exact amount required by these new cells to grow eventually to adult size.

The changes in the domain size and the size of the new cells produce a rearrangement of all cells, and this changes the local value of the elastic field, which, at the same time, drives the auxin concentration that, in turn, regulates the division rate of all cells. We hypothesize that coupling among such three dynamics at different time scales is sufficient to produce the growth of the root with cellular patterns that mimic those of real systems in a wide region of the parameter space. We verified that the process is extremely robust against changes of initial conditions.

Results

In Fig. 8 we show the dynamical loop that integrates the dynamical equations with an Euler method. The program is initiated by choosing the values of the number of cells (N), the position of each cell (r_i), their proliferation rate (v_i), the gates given by the PIN action between two cells ($\mathcal{F}_{i,m}$) and the concentration of auxins (c_i) at time $t=0$.

It is important to note that we normalize the auxin concentration function c with its maximum value at every time step. This allows our model to take into account the role of possible sources and sinks of auxin, since c is not a conserved quantity. The final distribution of auxin is insensitive to the initial conditions, but we start with a random distribution of auxin with a maximum at the quiescent centre in accordance with experimental observations. We recovered the same results if auxin concentrations were random at initial conditions (data not shown). The cycle clocks of each cell are set to zero at $t=0$ and reset after a successful cell division.

The shape and color of the boxes (Fig. 8) represent the action of the different dynamics as described in experimental systems (see Fig. 3). The red square indicates a subroutine that includes the logical rules $\mathcal{F}_{i,m}$ of the PIN action and the red circles represent points of logical decisions at appropriate times. Black arrows represent the direction of flux of the simulation and the black-dash arrow indicates a decision related to the time condition for the dynamics of the cyclins. Eq. 4 is implemented in the blue diamond

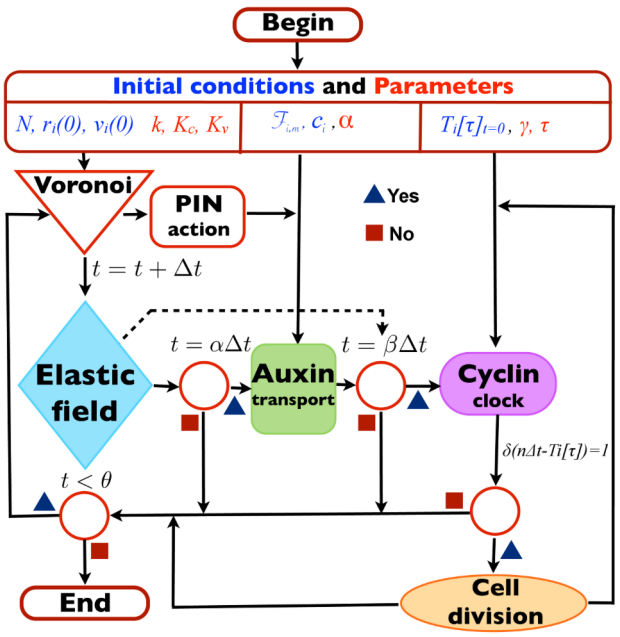

Figure 8. Flow-chart diagram of the program used for the numerical simulations. We show the parameters in red and the initial conditions in blue at the top of the diagram.
doi:10.1371/journal.pcbi.1003026.g008

block that represents the elastic field with time scale Δt. The loop is performed while the time t is less than the final time θ. Eq. 7 is implemented in the green block. The cyclin period is calculated for each cell at the violet block using Eqs. 8 and 9 and the threshold $\beta=\gamma c(i)$. Cellular divisions are performed as a subroutine represented by the orange block, and cell proliferation alters the conditions of all three dynamics.

The first step is to estimate the values of the parameters of the system. The adjustable parameters are the quantities indicated in red in Fig. 8. We start with the kinematical parameters. The constant K_c is related to the elastic modulus E of the cells. This quantity is measured when studying the mechanics of walls, cells, and tissues and is of the order of $E\sim 10\mathrm{MPa}$, as reported in [67].

For simplicity let us consider hexagonal cells in equilibrium. The magnitude of the elastic force is $|F_E|=ES_0\Delta L/L_0$, where S_0 is the contact area between two cells, $\Delta L=|A-A_0|^{1/2}$ is the change in length just after division, where $A_0=\sqrt{3}L_0^2$ is the area of the hexagon, if L_0 is the distance between centroids of two contiguous cells. This should be equal to the corresponding force magnitude in our model $|F_{K_c}|=K_c|\vec{r}_i-\vec{r}_{0_i}|$. Just after a cell division, $A=A_0/2$, thus $\Delta L=\sqrt{\sqrt{3}L_0^2/2}$, $|\vec{r}_i-\vec{r}_{0_i}|\simeq L_0/2$ and $S_0=A_0/6$. Equating the two forces we obtain

$$K_c\simeq\frac{L_0}{\sqrt{2\sqrt{3}}}E.$$

Taking the average diameter of a mature cell as $L_0=15\ \mu\mathrm{m}$ [64] and the experimental value $E=10\ \mathrm{MPa}$ we obtain $K_c\sim 80\ \mathrm{Pa-m}$.

At this stage, K_v should be related to the properties of the cell membrane, the metabolism of cell growth and the turgor pressure. It is difficult to associate the action of the first term of Eq.(1) to a single biological property. However, the dynamics of this term should produce a restoring force of the same order of magnitude as the second term, if the form and geometry of the domain are to be maintained during the growth dynamics. Therefore, if we use a value of $K_v=80\ \mathrm{Pa/m}$ the system should relax to a set of cells with roughly the same size and shape, as shown in the calculation of Fig. 5B. We found numerically that this produces results for the dynamics of growth that are comparable to the experimental quantities measured.

Parameter k is related to the viscous damping of the cell motion. The dynamical friction constant k can be estimated by observing that the amplitude of the oscillatory motion $e^{-i\omega t}$, caused by the harmonic forces should be reduced, to avoid oscillations, by a factor of $1/e$ in a lapse of at most one period $T=2\pi/\omega$, that is $k\geq m/T$. Note that in Eq. (4) the mass of the cell (m) is considered to be one. This gives $\omega=2\sqrt{K_c/m}\approx 18\ \mathrm{sec}^{-1}$, and $k=m\omega/2\pi=2.84\ \mathrm{Pa-m-sec}$.

The values used in the calculations are $K_c=80$, $K_v=80$ and $k=3$. With these values we obtain the real time scale of an iteration step Δt in the numerical calculations, by finding the number of iterations needed to obtain the experimental number of cell divisions in that lapse. In seven days, our observations showed (see Fig. 1) that the number of cells in the meristem is about 350. In averaged calculations we reproduce this number in 3400 iterations by using $\gamma=100$ and $\alpha=8$. This means that the lapse representing one iteration is the number of minutes in 7 days over the number of iterations, that is $\Delta t=(7\times 24\times 60)/3400=3$ min. Considering that the average auxin concentration is $\langle c\rangle=0.5$, the value of β is ≈ 50 in units of τ, which is about 100 times Δt. These values produce a single cell cycle period on the order of 12 hr, as shown in Fig. 7 [66].

In Fig. 9 (and Video S5) we provide an example of the growth of the system. We start with eight points at random in the parabolic tip of the domain, and fix the position of two additional points that represent the quiescent cells in the centre of the domain, marked with a white symbol. These cells reproduce at a rate ten times lower than the others; they divide after ten divisions per cell on average (in the right panel of the figure these quiescent cells have just divided). The auxin concentration in these cells is set to the maximum initially, and this is represented by a dark red color in the figure. The cell's position, shape, and proliferation rate are calculated every time step and the auxin is transported between cells. After 400 time steps the cells are attaining a uniform shape and size (Fig. 9), and the auxin gradient is already formed. This gradient will dictate the time in which a complete cell proliferation cycle is accomplished locally, followed by a cell division event that produces a sudden increase of the local potential that, in turn, governs auxin transport.

Despite these complicated dynamical interactions, the auxin gradient is preserved throughout and the process of growth and cell patterning is by no means random. This can be seen in Fig. 10. The overall pattern that emerges after some cycles of coupled dynamics is very similar to the apical-basal pattern of cell proliferation and elongation observed in RAM and along the length of the root tip. Such dynamics and emergent pattern are robust to initial conditions.

It is interesting to note that the region around the quiescent center in the stem-cell niche shows the greatest concentration of auxin, and a maximum in the potential. Also, the cell division cycle is minimum at this location. An intermediate region in which the auxin concentration diminishes and the potential is very small, but the cell proliferation rate is roughly constant, surrounds the quiescent cells. Finally, the most distal part from the tip (towards the base of the plant) is characterized by a very small concentration of auxin, causing the cell proliferation rate to be very small, and the potential to increase enormously. The combination of these effects results in the arrest of cell proliferation and in the formation of the elongation zone at a defined distance from the root tip. The emergent patterns recovered in the model are similar to those observed for the distribution of auxin as reported in Ref. [68], and the pattern of cell proliferation along the root longitudinal axis reported in Ref. [69]. Our results are also in agreement with the qualitative patterns of cell proliferation and elongation that are observed along the apical-basal, longitudinal axis of the growing *A. thaliana* root.

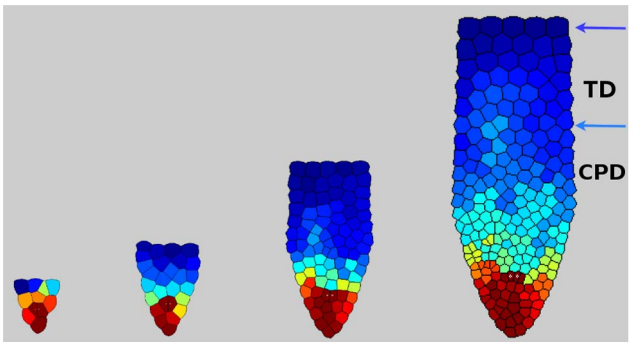

Figure 9. Typical calculation of the dynamical growth of the root using the model described. We show four snapshots of the configuration at 400, 1400, 2400 and 3400 time steps. The color code represents the concentration of auxins, red for the maximum and blue for the minimum. See Video S5.
doi:10.1371/journal.pcbi.1003026.g009

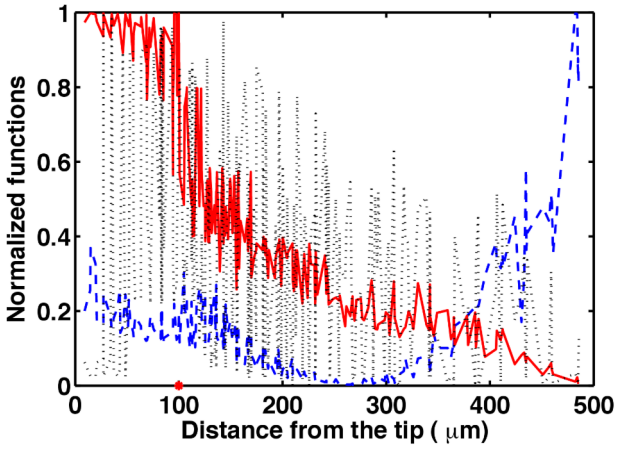

Figure 10. Plots of local potential, auxin concentration and cell cycle, after coupling dynamics. The normalized local potential (dashed-blue), the auxin concentration (red) and the advance of the cycle clock (dotted-black) as functions of the distance from the tip (μm), at $t = 3400$ time steps, corresponding to seven days.
doi:10.1371/journal.pcbi.1003026.g010

We can use this model to predict what patterns are expected under different growth conditions. In Fig. 11 we show a histogram of the number of cell divisions occurring at a given distance from tip, as obtained from an example calculation in which we fixed the parameter $\alpha = 8$. Interestingly, we observe that the length of the RAM does not surpass a certain value, which depends on α, because the modeled coupled dynamics prevents cells far from the tip to divide. Such types of coupled dynamics could explain the emergence of the transition from proliferation to the elongation cellular states in real roots, as well as the limited ranges or domain sizes of actively proliferating cells in stem-cell niches of plants and animals [1,3].

Hence, our model can be used to generate novel predictions concerning the role of the parameters considered in the model, and in determining RAM size and cell proliferation and elongation patterns along the root apical-basal axis for *A. thaliana* under different environmental or growth conditions. Our general model

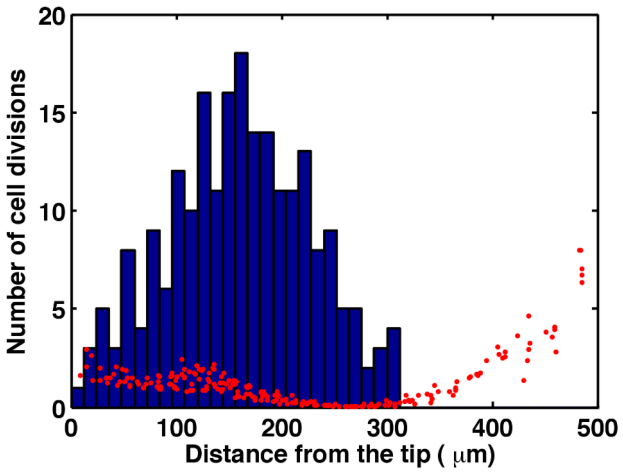

Figure 11. Histogram of the number of cell divisions obtained along the root when $\alpha = 8$. The potential profile is shown as red dots. Observe that there are no cell divisions beyond ~ 300 μm, meaning that the meristem has attained a stationary length.
doi:10.1371/journal.pcbi.1003026.g011

could eventually be adjusted to model stem-cell niches in other plants and animal systems, as well as modeling growth and differentiation in communities of unicellular organisms if similar physical fields can be postulated in such latter cases.

In order to examine the quantitative behavior of the model and validate it with published experimental data, we compared our model's predictions to measurements of the proliferation rates along the axis of the *A. thaliana* root as a function of the distance from the quiescent centre [64]. We ran numerous iterations of the model in order to obtain a reasonable statistical sample. We show a typical result from the simulations run to the experimental data in Fig. 12. Panel (A) shows the available experimental results for cell proliferation rates along the apical-basal axis of the root reported in Ref. [64] as a continuous red curve. The numerical results from our model are shown in blue. These results were obtained using the estimated parameter values that give the time in hours and the sizes in μm. We shifted the origin to account for the fact that all quantities in our calculations were measured from the tip of the domain and not from the quiescent centre. Notice that the simulated and experimentally generated curves are very similar.

In Fig. 12(B) we show an histogram of the frequency distribution of cell size. This histogram varies with different iterations because of the stochastic nature of cell proliferation and growth dynamics [70]. However, all calculations share the same qualitative characteristics; namely an unimodal distribution between ~ 10 and ~ 35 μm, with a maximum around 15 μm. This result was already recovered by Verbelen and collaborators Ref. [71]. The red curve was obtained by measuring the cell size in an Arabidopsis root Fig. 1. Similar curves have been obtained for many different plant species, including wheat [70].

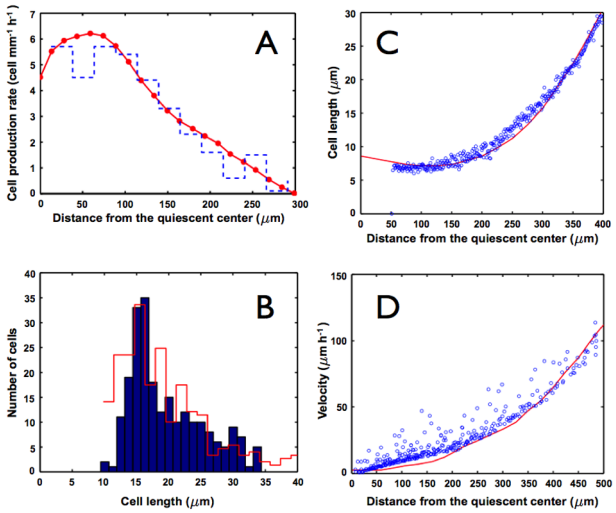

Figure 12. Comparisons between results obtained with the model and experimental data. (A) Cell proliferation rate as a function of the distance from the quiescent centre; calculation from Fig. 9 after six days of growth. The red line and dots are the experimental points reported in Ref. [64]. (B) Frequency distribution for cell length. Experimental data were taken from our laser microscope image of Fig. 1. (C) Average cell length as a function of the distance from the quiescent centre; calculation from Fig. 9 after six days of growth. The red line is the experimental result reported in Ref. [64]. (D) Average cell proliferation velocity as a function of the distance from the quiescent centre; calculation from Fig. 9 after six days of growth. The red line is the experimental result reported in Ref. [64].
doi:10.1371/journal.pcbi.1003026.g012

In Fig. 12(C) we show the variation of cell length along the longitudinal axis of the root. The red curve is the experimental result from Ref. [64]. It should be pointed out that the experiment was obtained by measuring the cell flux in a fixed point and by counting along the axis of the root in two dimensions, which is very convenient when comparing with our two-dimensional model. In order to mimic the experimental procedures, our numerical results were obtained by spotting the centroids of the Voronoi cells in the final time, which corresponds to six days. We calculated the length (l) by assigning an area of $A_i = \pi(l/2)^2$ to each cell. Again, a shift of 10 μm in the horizontal axis was needed to account for the difference in the origin, and the results for each cell are displayed as blue dots in the figure. Once again, the agreement between our simulated results and the experimental data are clear.

Finally, in Fig. 12(D) we show the average cell proliferation velocity, as defined in Ref. [64], as a function of the distance from the quiescent centre (red line), and compare it with our results (blue dots). In the experiment, Beemster and collaborators measured the difference in position of each cell for two subsequent times, averaged over time. In our calculation we measured the difference in position of each cell with respect to the apex of the root, which is itself being displaced every time a cell division takes place. By changing the frame of reference, we can compare the reported experiment with our results. The agreement is also remarkable when one compares the simulation results recovered with our model and the experimental data. This is more significant than the previous validations, since this result reflects the totality of the dynamical behavior in time and not only in a frozen snapshot, as in the previous cases.

Discussion

We present a dynamical model that couples auxin concentration gradients, cell proliferation and a physical tension field in a two-dimensional spatial domain that mimics the *A. thaliana* root tip. We have validated our model with both static and dynamic cellular empirical data, and have shown that our model recovers the pattern of rates of cell proliferation observed in the apical-basal axis of roots. The model also recovers the discrete transition from the proliferative to the elongation domains. Thus, our model puts forward a novel theoretical framework to test hypothesis concerning the coupled roles of auxin, cell proliferation, and physical fields dynamics in the emergence of the cellular pattern observed along the *A. thaliana* root tip. Ultimately, we have postulated a complex system in which the main emergent property of the coupled dynamics is at the appropriate spatial and cellular structure for the intracellular genetic networks to express differentially along the root. However, the explicit consideration of complex gene regulatory networks is out of the scope of this paper.

Our model and analysis suggest that the size of the RAM depends on the value of the parameter α (Fig. 13) in a rather defined manner. This parameter represents the ratio between the time scales of the potential relaxation and the auxin transport mechanisms. The length of the RAM decreases as the auxin transport parameter α increases as a power law. Therefore, this quantitative prediction can be verified experimentally, as auxin concentrations and transport along the root can be modified by manipulating the conditions of root growth (e.g. adding NPA to the growth medium to block auxin transport). Previous experimental work has suggested that the size of the RAM varies depending on growth conditions and is altered with external supplementation of auxin [39].

Given that plant growth is influenced by the mechanical behavior of the cell wall, measurements of the mechanical properties of living cell walls are important to fully understand how cellular organization is achieved. Like most biological materials, material properties of cell walls change as a function of age, the magnitude of forces they are subjected to, and immediate physiological conditions [67,72]. This confers spatial and temporal heterogeneity on cell wall constituents, complicating measurements of the mechanical properties of plant living walls even with present-day instrumentation. Furthermore, a single modulus of elasticity is not sufficient because of the structural anisotropy of the cell wall [67]. Therefore, comparisons between the predicted values of Kv and Kc of our model and the values reported for the modulus of elasticity of real cell walls are far from being straightforward. However, the fact that we reproduced the root tip pattern with the selected values suggests that they are likely to be biologically meaningful.

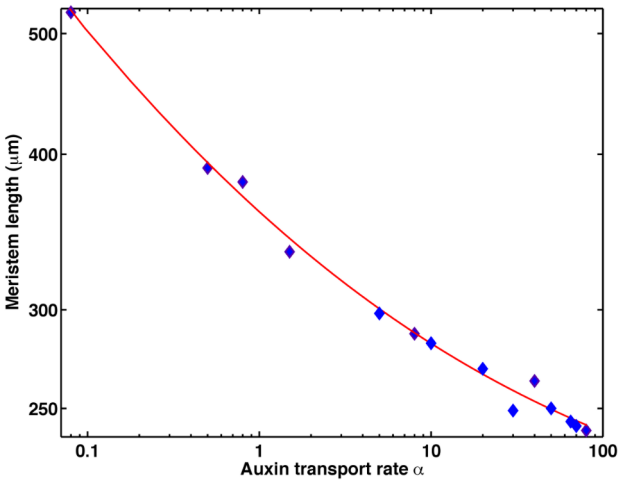

Figure 13. Log-log plot of the maximum RAM as a function of the parameter α. Numerical results are blue rhombuses, and the red line is the best fit with a function of the form $f(x) = 1.7x^{-0.26} + 1.88$ with $R^2 = .993$.
doi:10.1371/journal.pcbi.1003026.g013

More generally, our work reinforces conclusions from recent studies that experimentally demonstrate the importance of physical forces in the regulation of root apical-basal patterning [49,53], such as the mechanical induction of lateral roots or the coordination between auxin concentration and microtubule orientation [49,53,54]. It is remarkable that simple arguments concerning uniform size, shape and geometry of cell disposition is sufficient to produce a non-uniform field that provides sufficient spatial information to recover the overall dynamical growth pattern observed along the root. It is thus predicted that modification of physical forces would change the size and the pattern of these zones, an issue that could in principle be further explored theoretically and experimentally.

Auxin response is modulated not only by auxin concentration, but also by the auxin signaling pathway, which includes many components of different gene families, and which interact through several feedback loops, creating non-linear behaviors. Consequently, auxin concentration at any location does not necessarily coincide with auxin response. Even if this is not the case in the root [68], it could be important to include an explicit model of the auxin signaling pathway in future extensions of our model. In addition, in our model we considered the polar PIN configuration as fixed, as in Ref. [46]. However, in reality a more robust dynamic auxin transport is observed when the PIN expression is regulated by auxin [73].

In our model we fixed the position and number of the quiescent cells. We are aware that the root stem-cell niches are regulated by a complex regulatory network [74]. WUSCHEL RELATED HOMEOBOX5 (WOX5) is a Quiescent Center identity gene indispensable for the maintenance of the undifferentiated state of stem cells and niche size regulation, and it is part of the proposed root stem-cell niche regulatory network [74,75]. Recent theoretical and experimental work has suggested that WOX5 regulates and is regulated by auxin [36,74]. In our calculations we input several initial conditions for auxin concentration, and demonstrated that the model is fairly robust to these changes. However, as shown in Fig. 6, neglecting the action of PIN polarization destroys the auxin gradient along the root. Including these and other regulatory interactions in a future model would enable us to explicitly consider intracellular complex gene regulatory networks, which are likely coupled among cells by physical and hormone fields.

The complex network underlying the cell cycle was also reduced to consider two basic components, because for our purposes, only the phases of the oscillations of the concentrations matter. Since CYCA and CYCB oscillate in phase, we consider them as a single variable; and because CYCD oscillates in anti phase, we take this to mean that there is an activator-inhibitor interaction between these two groups of proteins. In our model we stressed the importance of the relationship between auxin concentration and the regulation of cell proliferation, and we neglected the details of the known regulatory processes of the cell cycle, which although important, do not directly affect the overall results of our simulation. Nonetheless, such details of the gene regulatory network underlying the cell cycle, cell differentiation and auxin dynamics should be incorporated in future developments of the model.

In conclusion, we have put forward a minimal mathematical model that considers the essential dynamical coupling of cell proliferation with a physical field and chemical (hormone) gradients, in order to explore if such processes are sufficient to obtain the emergence of cellular organization during stem-cell niche patterning and organ growth. We have used the *A. thaliana* root as our study system.

Despite the simplification of many biological details, our model is able to recover patterns that greatly resemble those observed in stem-cell niches of plants and animals, and particularly those in the *A. thaliana* root tip. The remarkable coincidence between the simulated cellular characteristics along the model root apical-basal axis (shown in Fig. 12), with those that have been observed and quantified in actual roots, validates the qualitative features and utility of our model for understanding the emergence of cellular patterns in such a multicellular organ. Furthermore, the cellular patterns of stem-cells among multicellular plants and animals have generic traits. Our model provides a formal tool to explore if such traits may be explained by the generic non-linear coupling of relevant physical and chemical fields to discover emergent properties of cell proliferation dynamics across biological systems.

Supporting Information

Video S1 Dynamical growth and proliferation of cells and boundary.
(MP4)

Video S2 Dynamical behavior of stem cells only.
(MP4)

Video S3 Relaxation process for a fixed number of cells.
(MP4)

Video S4 Dynamical changes of the local cell potential.
(MP4)

Video S5 Dynamical development of auxin concentration.
(MP4)

Acknowledgments

Technical assistance from Mariana Benítez, Adriana Garay, Juan Carlos Martínez-García, Rigoberto Vicencio Pérez Ruiz, Diana Romo and Karina Jiménez Durán is appreciated, and Chelsea Spetch for overall support while at University of California, Berkeley, as well as meaningful discussions and careful revisions of previous versions of this paper.

Author Contributions

Conceived and designed the experiments: RAB EA EOG ERAB. Performed the experiments: RAB JRRA MAN YCP. Analyzed the data: RAB JRRA MAN EA EOG VHH YCP ERAB. Contributed reagents/materials/analysis tools: RAB JRRA MAN EA YCP ERAB. Wrote the paper: RAB JRRA MAN EA EOG ERAB.

References

1. Scheres B (2007) Stem-cell niches: nursery rhymes across kingdoms. Nat Rev Mol Cell Biol 8: 345–54.
2. Sablowski R (2004) Plant and animal stem cells: conceptually similar, molecularly distinct? Trends Cell Biol 14: 605–11.
3. Li L, Xie T (2005) Stem cell niche: structure and function. Annu Rev Cell Dev Biol 21: 605–31.
4. Huang S (2012) The molecular and mathematical basis of Waddington's epigenetic landscape: A framework for post-Darwinian biology? Bio Essays 34: 149–157.
5. Álvarez-Buylla E, Chaos A, Aldana M, Benítez M, Cortes-Poza Y, et al. (2008) Floral morphogenesis: Stochastic explorations of a gene network epigenetic landscape. PLoS ONE 3: e3626.
6. Newman S, Bhat R (2008) Dynamical patterning modules: physico-genetic determinants of morphological development and evolution. Phys Biol 5: 015008.
7. Newman S, Bhat R (2009) Dynamical patterning modules: a "pattern language" for development and evolution of multicellular form. Int J Dev Biol 53: 693–705.
8. Fernandes AN, Chen X, Scotchford CA, Walker J, Wells DM, et al. (2012) Mechanical properties of epidermal cells of whole living roots of Arabidopsis thaliana : An atomic force microscopy study. Phys Rev E Stat Nonlin Soft Matter Phys 85: 021916.
9. Hamant O, Traas J, Boudaoud A (2010) Regulation of shape and patterning in plant development. Curr Opin Genet Dev 20: 454–9.
10. Mammoto A, Mammoto T, Ingber DE (2012) Mechanosensitive mechanisms in transcriptional regulation. J Cell Sci 125: 3061–73.
11. Barrio RA, Hernández-Machado A, Varea C, Romero-Arias JR, Álvarez-Buylla E (2010) Flower development as an interplay between dynamical physical fields and genetic networks. PLoS ONE 5: e13523.
12. Espinosa-Soto C, Padilla-Longoria P, Alvarez-Buylla ER (2004) A gene regulatory network model for cell-fate determination during Arabodopsis thaliana ower development that is robust and recovers experimental gene expression profiles. Plant Cell 16: 2923–2939.
13. Alvarez-Buylla ER, Azpeitia E, Barrio R, Benitez M, Padilla-Longoria P (2010) From ABC genes to regulatory networks, epigenetic landscapes and ower morphogenesis: Making biological sense of theoretical approaches. Semin Cell Dev Biology 21: 108–117.
14. Kwiatkowska D (2008) Flowering and apical meristem growth dynamics. J Exp Bot 59: 187–201.
15. van Mourik S, Kaufmann K, van Dijk ADJ, Angenent GC, Merks RMH, et al. (2012) Simulation of organ patterning on the oral meristem using a polar auxin transport model. PLoS ONE 7: e28762.
16. Hester S, Belmonte J, Gens JS, Clendenon SG, Glazier J (2011) A multi-cell, multi-scale model of vertebrate segmentation and somite formation. PLoS Comput Biol 7: e1002155, doi:10.1371/journal.pcbi.1002155.
17. Perilli S, Mambro RD, Sabatini S (2012) Growth and development of the root apical meristem. Curr Opin Plant Biol 15: 17–23.
18. Ivanov VB, Dubrovsky JG (2012) Longitudinal zonation pattern in plant roots: conicts and solutions. Trends Plant Sci 00219-1: S1360–1385.
19. Benková E, Hejátko J (2009) Hormone interactions at the root apical meristem. Plant Mol Biol 69: 383–96.

20. Garay-Arroyo A, De La Paz Sánchez M, García-Ponce B, Azpeitia E, Álvarez Buylla ER (2012) Hormone symphony during root growth and development. Dev Dyn 241: 1867–1885.
21. Sanz L, Murray JA, Dewitte W (2012) To divide and to rule; regulating cell division in roots during post-embryonic growth. In: Lüttge U, Beyschlag W, Büdel B, Francis D, editors. Progress in Botany. Volume 73. Berlin Heidelberg: Springer. pp. 57–80.
22. Moubayidin L, Perilli S, Ioio RD, Mambro RD, Costantino P, et al. (2010) The rate of cell differentiation controls the Arabidopsis root meristem growth phase. Curr Biol 20: 1138–43.
23. Ivanov VB (1997) Relationship between cell proliferation and transition to elongation in plant roots. Int J Dev Biol 41: 907–15.
24. Inzé D, De Veylder L (2006) Cell cycle regulation in plant development. Annu Rev Genet 40: 77–105.
25. De Veylder L, Beeckman T, Inzé D (2007) The ins and outs of the plant cell cycle. Nat Rev Mol Cell Biol 8: 655–65.
26. Overvoorde P, Fukaki H, Beeckman T (2010) Auxin control of root development. Cold Spring Harb Perspect Biol 2: a001537.
27. Woodward A, Bartel B (2005) Auxin: regulation, action, and interaction. Ann Bot 95: 707–735.
28. Guilfoyle T, Hagen G (2007) Auxin response factors. Curr Opin Plant Biol 10: 453–460.
29. Kleine-Vehn J, Friml J (2008) Polar targeting and endocytic recycling in auxin-dependent plant development. Annu Rev Cell Dev Biol 24: 447–473.
30. Mockaitis K, Estelle M (2008) Auxin receptors and plant development: a new signaling paradigm. Annu Rev Cell Dev Biol 24: 55–80.
31. Lau S, Jürgens G, De Smet I (2008) The evolving complexity of the auxin pathway. Plant Cell 20: 1738–1746.
32. Vanneste S, Friml J (2009) Auxin: a trigger for change in plant development. Cell 136: 1005–1016.
33. Himanen K, Boucheron E, Vanneste S, de Almeida Engler J, Inzé D, et al. (2002) Auxin-mediated cell cycle activation during early lateral root initiation. Plant cell 14: 2339–51.
34. Oakenfull EA, Riou-Khamlichi C, Murray JAH (2002) Plant D-type cyclins and the control of G1 progression. Philos Trans R Soc Lond B Biol Sci 357: 749–60.
35. Ishida T, Adachi S, Yoshimura M, Shimizu K, Umeda M, et al. (2010) Auxin modulates the transition from the mitotic cycle to the endocycle in Arabodopsis. Development 137: 63–71.
36. Ding Z, Friml JL (2010) Auxin regulates distal stem cell differentiation in Arabodopsis roots. Proc Natl Acad Sci U S A 107: 12046–51.
37. Jurado S, Abraham Z, Manzano C, López-Torrejón G, Pacios L, et al. (2010) The Arabodopsis cell cycle F-box protein SKP2A binds to auxin. Plant Cell 22: 3891–904.
38. Tromas A, Braun N, Muller P, Khodus T, Paponov IA, et al. (2009) The AUXIN BINDING PROTEIN 1 is required for differential auxin responses mediating root growth. PLoS ONE 4: e6648.
39. Ioio RD, Nakamura K, Moubayidin L, Perilli S, Taniguchi M, et al. (2008) A genetic framework for the control of cell division and differentiation in the root meristem. Science 322: 1380–1384.
40. Friml J, Benková E, Blilou I, Wisniewska J, Hamann T, et al. (2002) AtPIN4 mediates sink-driven auxin gradients and root patterning in Arabidopsis. Cell 108: 661–673.
41. Sabatini S, Beis D, Wolkenfelt H, Murfett J, Guilfoyle T, et al. (1999) An auxin-dependent distal organizer of pattern and polarity in the Arabodopsis root. Cell 99: 463–472.
42. Petersson S, Johansson A, Kowalczyk M, Makoveychuk A, Wang J, et al. (2009) An auxin gradient and maximum in the Arabodopsis root apex shown by high-resolution cell-specific analysis of IAA distribution and synthesis. Plant Cell 21: 1659–1668.
43. Blilou I, Xu J, Wildwater M, Willemsen V, Paponov I, et al. (2005) The PIN auxin efflux facilitator network controls growth and patterning in Arabodopsis roots. Nature 433: 39–44.
44. Vieten A, Vanneste S, Wisniewska J, Benková E, Benjamins R, et al. (2005) Functional redundancy of PIN proteins is accompanied by auxin-dependent cross-regulation of PIN expression. Development 132: 4521–4531.
45. Petrásek J, Mravec J, Bouchard R, Blakeslee J, Abas M, et al. (2006) PIN proteins perform a rate-limiting function in cellular auxin efflux. Science 312: 914–918.
46. Grieneisen V, Xu J, Marée P AFand Hogeweg, Scheres B (2007) Auxin transport is sufficient to generate a maximum and gradient guiding root growth. Nature 449: 1008–1013.
47. Mironova V, Omelyanchuk N, Yosiphon G, Fadeev S, Kolchanov N, et al. (2010) A plausible mechanism for auxin patterning along the developing root. BMC Syst Biol 4: 98.
48. Swarup R, Bennett M (2003) Auxin transport: the fountain of life in plants? Dev Cell 5: 824–826.
49. Ditengou FA, Teale WD, Kochersperger P, Flittner KA, Kneuper I, et al. (2008) Mechanical induction of lateral root initiation in Arabidopsis thaliana. Proc Natl Acad Sci U S A 105: 18818–18823.
50. Laskowski M, Grieneisen V, Hofhuis H, Hove C, Hogeweg P, et al. (2008) Root system architecture from coupling cell shape to auxin transport. PLoS Biol 16: e307.
51. Kleine-Vehn J, Ding Z, Jones A, Tasaka M, Morita M, et al. (2010) Gravity-induced PIN transcytosis for polarization of auxin uxes in gravity-sensing root cells. Proc Natl Acad Sci U S A 107: 22344–22349.
52. Palme K, Dovzhenko A, Ditengou F (2006) Auxin transport and gravitational research: perspectives. Protoplasma 229: 175–181.
53. Heisler M, Hamant O, Krupinski P, Uyttewaal M, Ohno C, et al. (2010) Alignment between PIN1 polarity and microtubule orientation in the shoot apical meristem reveals a tight coupling between morphogenesis and auxin transport. PLoS Biol 8: e1000516.
54. Nakayama N, Smith RS, Mandel T, Robinson S, Kimura S, et al. (2012) Mechanical regulation of auxin-mediated growth. Curr Biol 22: 1468–76.
55. Engler AJ, Sen S, Sweeney HL, Disher DE (2006) Matrix elasticity directs stem cell lineage specification. Cell 126: 677–689.
56. Hamant O, Heisler MG, Jonsson H, Krupinski P, Uyttewaal M, et al. (2008) Developmental patterning by mechanical signals in Arabidopsis. Science 322: 1650–1655.
57. Kutschera U, Niklas KJ (2007) The epidermal-growth-control theory of stem elongation: an old and a new perspective. J Plant Physiol 164: 1395–409.
58. Dupuy L, Mackenzie J, Haseloff J (2010) Coordination of plant cell division and expansion in a simple morphogentetic system. Proc Natl Acad Sci U S A 107: 2711–2716.
59. Merks RM, Guravage M, Inzé D, Beemster GT (2011) VirtualLeaf: An open-source framework for cell-based modeling of plant tissue growth and development. Plant Physiol 155: 656–666.
60. Honda H (1978) Description of cellular patterns by Dirichlet domains: the two-dimensional case. J Theor Biol 72: 523–543.
61. Prusinkiewicz P, Lindenmayer A (1990) The algorithmic beauty of plants. New York: Springer-Verlag.
62. Jönsson H, Heisler MG, Shapiro BE, Meyerowitz EM, Mjolsness E (2006) An auxin-driven polarized transport model por phyllotaxis. Proc Natl Acad Sci U S A 103: 1633–1638.
63. Rudge T, Haseloff J (2005) A computational model of cellular morphogenesis in plants. Lect Notes Comput Sci 3630: 78–87.
64. Beemster GT, Baskin TI (1998) Analysis of cell division and elongation underlying the developmental acceleration of root growth in Arabidopsis thaliana. Plant Physiol 116: 1515–1526.
65. Perrot-Rechenmann C (2010) Cellular responses to auxin: division versus expansion. Cold Spring Harb Perspect Biol 2: a001446.
66. Menges M, De Jager SM, Gruissem W, Murray JA (2005) Global analysis of the core cell cycle regulators of Arabidopsis identifies novel genes, reveals multiple and highly specific profiles of expression and provides a coherent model for plant cell cycle control. Plant Cell 41: 546–566.
67. Mirabet V, Das P, Boudaoud A, Hamant O (2011) The role of mechanical forces in plant morphogenesis. Annu Rev Plant Biol 62: 365–85.
68. Brunoud G, Wells D, Oliva M, Larrieu A, Mirabet V, et al. (2012) A novel sensor to map auxin response and distribution at high spatio-temporal resolution. Nature 482: 103–106.
69. Baskin TI (2000) On the constancy of cell division rate in the root meristem. Plant Mol Biol 43: 545–554.
70. Ivanov VB, Dobrochaev AE, Baskin TI (2002) What the distribution of cell lengths in the root meristem does and does not reveal about cell division. J Plant Growth Regul 21: 60–67.
71. Verbelen JP, Cnodder TD, Le J, Vissenberg K, Baluska F (2006) The root apex of Arabidopsis thaliana consists of four distinct zones of growth activites. Plant Signal Behav 1: 296–304.
72. Niklas K, Spatz H (2012) Plant physics. Chicago: University of Chicago Press. 447 pp.
73. Mironova V, Omelyanchuk N, Novoselova E, Doroshkov A, Kazantsev F, et al. (2012) Combined in silico/in vivo analysis of mechanisms providing for root apical meristem self-organization and maintenance. Ann Bot 110:349–360.
74. Azpeitia E, Benitez M, Vega I, Villarreal C, Alvarez-Buylla E (2010) Single-cell and coupled GRN models of cell patterning in the Arabidopsis thaliana root stem cell niche. BMC Syst Biol 4: 134.
75. Sarkar A, Luijten M, Miyashima S, Lenhard M, Hashimoto T, et al. (2007) Conserved factors regulate signalling in Arabidopsis thaliana shoot and root stem cell organizers. Nature 446: 811–814.
76. Menges M, Hennig L, Gruissem W, Murray JAH (2003) Genome-wide gene expression in an Arabidopsis cell suspension. Plant molecular biology 53: 423–442.